Résilience des écosystèmes hydrothermaux : résultats d'une expérience de perturbation au sein du champ hydrothermal Lucky Strike (dorsale médio-Atlantique)

Julien Marticorena

DOCTORAT SCIENCES BRETAGNE DE LA MER LOIRE ET DU LITTORAL

UBO
Université de Bretagne Occidentale

THESE DE DOCTORAT DE

L'UNIVERSITE
DE BRETAGNE OCCIDENTALE

ECOLE DOCTORALE N° 598
Sciences de la Mer et du littoral
Spécialité : Ecologie marine

Par

Julien MARTICORENA

Résilience des écosystèmes hydrothermaux : résultats d'une expérience de perturbation au sein du champ hydrothermal Lucky Strike (dorsale médio-Atlantique)

Thèse présentée et soutenue à Plouzané, le 12 février 2021
Unité de recherche : Unité Étude des Écosystèmes Profonds (EEP) au laboratoire LEP (Ifremer)

Rapporteurs avant soutenance :

Lauren MULLINEAUX
Department Chair, Woods Hole Oceanographic Institution

Eric THIEBAUT
Professeur, Sorbonne Université, CNRS

Composition du Jury :

Lauren MULLINEAUX (Rapporteur)
Department Chair, Woods Hole Oceanographic Institution

Eric THIEBAUT (Rapporteur)
Professeur, Sorbonne Université, CNRS

François LE LOC'H (Président du jury)
Directeur de recherche, Université de Bretagne Occidentale
IRD, UMR LEMAR

Ana HILARIO (Examinateur)
Assistant researcher, Universidade de Aveiro

Thierry COMTET (Examinateur)
Cadre de recherche, Sorbonne Université, CNRS

Jozée SARRAZIN (Directrice de thèse)
Cadre de recherche, Ifremer, LEP

Invitées :
Marjolaine MATABOS (Co-directrice de thèse)
Cadre de recherche, Ifremer, LEP

Eva RAMIREZ-LLODRA (Co-directrice de thèse)
Senior researcher, Norwegian Institute for Water Research, REV Ocean

« Pendant la majeure partie de l'histoire, l'Homme a dû combattre la nature pour survivre ; dans ce siècle, il commence à comprendre que pour survivre, il doit la protéger »

Jacques-Yves Cousteau

Remerciements

Ces 4 années passées à Brest sont pour moi non seulement une expérience enrichissante, mais également un superbe tremplin pour entrer dans l'impitoyable monde du travail ! Il me paraît ambitieux de faire des remerciements exhaustifs, tant cette thèse a constitué un travail d'échange et d'entraide aussi bien sur le plan professionnel que personnel, mais je vais essayer…

En premier lieu, je souhaite remercier chaleureusement mes trois directrices de thèse, **Jozée Sarrazin**, **Marjolaine Matabos** et **Eva Ramirez-Llodra,** de m'avoir offert l'opportunité de réaliser cette thèse et de s'être montrées disponibles et à l'écoute tout au long de ce travail riche en émotions. Je vous serai éternellement reconnaissant de m'avoir permis d'embarquer sur ces 2 missions hauturières, de voyager en Norvège, en Espagne, aux États-Unis, aux Açores et même à 1 700 mètres de fond sur l'édifice Montségur pour apprendre de nouvelles choses, partager mes travaux ou récolter des échantillons. Une Québécoise, une Landaise, une Catalane et un Basque, ça ressemble au début d'une mauvaise blague mais c'est en réalité la clôture d'une magnifique aventure.

Je tiens également à remercier **Pierre-Marie Sarradin** de m'avoir accueilli au sein du Laboratoire Environnement Profond, d'abord en tant que stagiaire puis en tant que thésard. Sa bienveillance et ses conseils avisés ont largement contribué à l'aboutissement cette thèse.

Je profite de cette occasion pour remercier également tous les membres du LEP pour tous les instants partagés au laboratoire, en mer, mais aussi souvent à la salle café. Nos échanges quotidiens et la bonne humeur ambiante ont constitué un véritable moteur pour moi et je regrette déjà ces bons moments. Je ne peux cependant pas m'abstenir de citer mes merveilleux colocataires de bureau, en commençant par **Pauline** qui m'a aidé à garder le cap malgré les appels répétés du tartare, **Joan** « la Maquina » avec qui j'ai énormément échangé pendant toute cette thèse et de qui j'ai énormément appris, je n'oublierai jamais notre session de pêche sous des trombes d'eau au Dellec et nos nombreuses marrades au bureau. Plus récemment **Mélissa**, à qui j'ai légué le bureau des docteurs ; nous avons beaucoup discuté et

je m'excuse de t'avoir tant de fois empêchée de travailler en te submergeant d'âneries ! Cette escapade écossaise restera aussi gravée dans ma mémoire et elle m'aura permis d'en apprendre beaucoup sur la Roumanie et les Carpates ahahah. Enfin le petit dernier, **Loïc,** je me souviendrai toujours des piña colada sirotées ensemble sur les plages brésiliennes pendant le DSBS … À moins que je ne confonde avec les pintes de grosse bertha aux fauvettes ... Je suis aussi très heureux d'avoir croisé la route de **Paulo**. Entre nous, tout a commencé par un polychète inconnu qui, sous son regard expert et après un parcours chaotique à travers une clé de détermination, a retrouvé une identité sous forme de nomenclature binomiale chère à ce brave Carl von Linné ! Merci également à **Fanny** et **Pierre** pour tous ces bons moments partagés et cette magnifique escapade en Californie ☺. Comment ne pas également citer **Marie-Ève-Julie Arsenault Pernet de Gaspésie** (j'espère ne rien avoir oublié ☺) et **Sandra** aka **ZouBi**, mes deux confidentes du labo, pour ces tant d'heures passées à papoter de tout et de rien et pour votre soutien dans les moments difficiles, je vous dois beaucoup. Rien n'aurait été possible sans l'aide des instrum' **Philippe**, **Nico** et **Lolo** qui ont respectivement érigé des pyramides d'acier super-connectées (du moins pendant 12 jours), manié PEPITO aux 4 coins des quadrats et équipé les bols d'aspi sur le Nautile alors que je prolongeais ma nuit sur le PP. A huge thank you also to all the postdocs, students or researchers that I have met during this PhD, **Dominique**, **Nuria**, **Mauricio**, **Adriana**, **Elisa**, **Gina**, **Mark**, **Raffaele** and so many others ! Pour clôturer ce petit tour du labo, je voulais aussi remercier tous les étudiants que j'ai eu le plaisir d'encadrer de près ou de loin, **Thomas**, **Abel**, **Fanny**, **Maureen**, **Baptiste**, **Axel**, **Mathilde** et l'apprenti chercheur **Riwan** qui m'ont énormément aidé au labo, que ce soit pour le tri, les pesées, la tamisage ou la biométrie des individus !

Je tiens spécifiquement à remercier l'ensemble de mes co-auteurs et membres de mon comité de thèse, **Loïc Michel**, **Gauthier Schaal**, **Cécile Cathalot**, **Agathe Laes-Huon**, **Stéphane Hourdez**, **Ana Colaço**, **Florence Pradillon** et **Jacques Grall** d'avoir donné de leur temps pour m'accompagner dans l'analyse de données, l'interprétation des résultats et la rédaction des différents chapitres de cette thèse.

À tous les copains de l'IUEM de l'Ifremer ou autre, **Yann**, **Val**, **David**, **Natalia**, **Aurélien**, **Kevin, Marc**, **N'Goulot, Fanny**, **Justine**, **Pauline, Anaïs**, **Felifish**, **Camille**, **Nico**, **Jules, Will, Margaux, Elyne, Gabin, Chloé** et tous les autres, votre compagnie au cours de ces 4 dernières années a

été pour moi un vrai bol d'air et j'espère qu'on restera en contact à la fin de cette épopée. Merci aux membres de la team **Suze** de m'avoir accordé leur confiance malgré des performances médiocres de ma part… Erzurumspor dans nos cœurs !

Enfin, je tiens à remercier tout particulièrement ma famille, la chose la plus importante à mes yeux, de m'avoir transmis de bonnes valeurs et un goût prononcé de l'effort et de la persévérance. Ma **mère**, d'avoir toujours prêté une oreille attentive aux petits tracas de la vie et partagé tant de fous-rires malgré la distance qui nous séparait. Mon **père**, pour ses conseils avisés et son soutien sans faille tout au long de mes études. **Gat**, de m'avoir transmis son amour de la nature et de l'océan, et sans qui je n'aurais sûrement pas choisi la biologie marine comme point d'arrivée. Mon frère, **Pierre**, qui compte énormément pour moi ! Nous avons trop souvent été séparés ces dernières années, maintenant que son parcours valenciennois se termine avec brio, il me tarde que l'on puisse profiter à l'eau, à la montagne ou sur un fronton ! Mon frère d'adoption, **Alpha**, qui malgré son jeune âge, représente un véritable modèle pour moi et je suis fier de pouvoir le compter parmi notre famille. Enfin **Richard** et **Odette**, les Marseillais au grand cœur, toujours ravis de nous accueillir dans la plus belle ville du monde (sans ironie aucune ☺). Merci beaucoup d'avoir relu et corrigé mon manuscrit dans les ultimes moments et de nous avoir accompagnés en direct pour la soutenance !

Enfin, mention spéciale pour celle qui partage ma vie depuis 7 ans, **Sarah**, chasseuse de pokémon émérite, boxeuse un jour, grimpeuse de renom toujours, merci pour tous ces moments, pour le soutien, pour l'amour ... Notre couple a survécu à un rendu de manuscrit le même jour et à une soutenance à 3 jours d'intervalle, donc je ne vois pas ce qui pourrait nous arriver de pire !

Table des matières

Remerciements 3

Liste des figures 10

Liste des tableaux 12

Avant-propos 14

I. Introduction 17

I.1. Les écosystèmes hydrothermaux 18

I.1.1. Formation et distribution des sources hydrothermales 18

I.1.2. La production primaire chimiosynthétique 22

I.1.3. Structure des communautés de faune hydrothermale 24

I.1.4. Dynamique temporelle des communautés hydrothermales 28

I.2. Concept de résilience 30

I.2.1. Qu'est-ce que la résilience en écologie ? 30

I.2.2. Comment mesurer la résilience d'un écosystème ? 35

I.2.3. Minimiser les impacts et assister le rétablissement des écosystèmes impactés 35

I.3. Résilience des écosystèmes hydrothermaux 39

I.3.1. Colonisation et succession écologique 39

I.3.2. Taux de rétablissement des écosystèmes hydrothermaux 41

I.3.3. Estimation indirecte de la résilience des communautés hydrothermales 42

I.3.4. Potentiels impacts de l'exploitation minière profonde 47

I.4. Objectifs de la thèse 50

II. Matériel et méthodes 52

II.1. Site d'étude: le champ hydrothermal Lucky Strike 53

II.2. La faune hydrothermale du champ Lucky Strike 54

II.3. Design expérimental 56

II.4. Caractérisation physico-chimique 60

II.5. Échantillonnage et préservation des échantillons 60

II.6. Analyse de la structure des communautés 61

II.7. Analyse de la structure du réseau trophique 63

II.8. Structure des populations et biologie de la reproduction des gastéropodes 66

III. Rétablissement de la structure des communautés en réponse à une perturbation 70

III.1. Introduction 75

III.2. Material and methods 78

III.2.1. Study site 78

III.2.2. Experimental setup 79

III.2.3. Environmental characterisation 81

III.2.4. Faunal sampling and identification 81

III.2.5. Population size structure 82

III.2.6. Data analyses 83

III.3. Results 86

III.3.1. Environmental conditions 86

III.3.2. Pre-disturbed communities 87

III.3.3. Recovery patterns of benthic communities 90

III.4. Discussion 97

III.4.1. Habitat characterisation 97

III.4.2. Pre-disturbed communities and natural variability 99

III.4.3. Recolonisation processes and recovery 101

III.4.4. From small-scale to large scale disturbance 106

III.5. References 109

III.6. Supplementary files 119

III.7. Synthèse des résultats 124

IV. Rétablissement de la structure du réseau trophique en réponse à une perturbation *127*

IV.1. Introduction 128

IV.2. Materials and methods 130

IV.2.1. Experimental design and faunal sampling 130

IV.2.2. Laboratory analyses 132

IV.2.3. Data analyses 133

IV.3. Results 136

IV.3.1. Diversity among trophic guild 136

IV.3.2. Biomass recovery 136

IV.3.3. $\delta^{13}C$ – $\delta^{15}N$ isotopic composition 140

IV.3.4. Community-wide food web structure 142

IV.4. Discussion 142

IV.4.1. Taxonomic diversity and biomass along recovery 143

IV.4.2. Trophic structure 146

IV.5. Conclusion 150

IV.6. References 152

IV.7. Supplementary files 159

IV.8. Synthèse des résultats 161

V. Biologie de la reproduction des gastéropodes *163*

V.1. Introduction 166

V.2. Material and Methods 168

V.2.1. Field sampling 168

V.2.2. Population structure 171

V.2.3. Reproductive biology 172

V.3. Results 174

V.3.1. Environmental conditions 174

V.3.2. Gonad morphology and gametogenesis 174

V.3.3. Oocyte size-frequency distribution 175

V.3.4. Fecundity 177

V.3.5. Population structure 179

V.4. Discussion 181

V.4.1. Reproductive anatomy 181

V.4.2. Gametogenesis 181

V.4.3. Reproductive output 184

V.4.4. Recruitment and population structure 186

V.4.5. Implications for the resilience of vent communities 187

V.5. References 190

V.6. Supplementary files 198

VI. Discussion générale *201*

VI.1. Limites de l'expérience 203

VI.2. Processus de colonisation des communautés actives 206

VI.3. Rétablissement des communautés à petite échelle 208

VI.4. Résilience des écosystèmes hydrothermaux : de nouvelles connaissances essentielles à la mise en place de plans de gestion 212

VI.5. Perspectives 215

*Bibliographie*_____ *218*

*Annexes*_____ *234*

Annexe 1. Tableau d'interprétation de la roue de rétablissement _____ **235**

Annexe 2. Article ADN environnemental _____ **236**

Annexe. 3 Article récupération de la diversité _____ **258**

Liste des figures

Chapitre I : Introduction

Figure I.1. Carte générale de la répartition des sites hydrothermaux découverts et suspectés à ce jour 18
Figure I.2. Carte générale des vitesses d'expansion au sein des différents systèmes tectoniques 19
Figure I.3. Schéma général illustrant la mise en place de la circulation hydrothermale 20
Figure I.4. Schéma général des différentes formes d'émission des sources hydrothermales 22
Figure I.5. Caractérisation générale de la production primaire chimiosynthétique en milieu hydrothermal 23
Figure I.6. Distribution des provinces biogéographiques des écosystèmes hydrothermaux 25
Figure I.7. Modèle conceptuel de zonation des assemblages sur l'édifice Tour Eiffel 27
Figure I.8. Distribution spatio-temporelle des communautés hydrothermales sur l'édifice Tour Eiffel 30
Figure I.9. Schémas conceptuel illustrant les différents aspects de la résilience en écologie 32
Figure I.10. Roue de rétablissement permettant de suivre l'avancement du projet de restauration 37
Figure I.11. Modèle conceptuel de succession des communautés hydrothermales sur la dorsale Est-Pacifique 40
Figure I.12. Cycle de vie des invertébrés benthiques 44
Figure I.13. Temps de rétablissement des communautés hydrothermales des bassins arrières-arc du Pacifique Ouest 46
Figure I.14. Extraction des sulfures polymétalliques à proximité des sites inactifs hydrothermaux 49

Chapitre II : Matériel et méthodes

Figure II.1. Carte bathymétrique de la dorsale médio-Atlantique 53
Figure II.2. Les trois sites étudiés au sein du champ hydrothermal Lucky Strike 54
Figure II.3. Quadrat expérimental C1acg avant/ après défaunation 56
Figure II.4. Résumé du plan d'expérience mis en place pour le suivi de la structure des communautés hydrothermales en réponse à une perturbation induite 58
Figure II.5. Méthodes d'échantillonnage et de caractérisation chimique 61
Figure II.6. Illustration des descripteurs de taille utilisés pour les espèces dominantes 63

Chapitre III : Rétablissement de la structure des communautés en réponse à une perturbation

Figure III.1. Location of the Lucky Strike vent field along the Mid-Atlantic Ridge and the three study sites 78
Figure III.2. The C1a-cg experimental quadrat before/after disturbance 80
Figure III.3. Principal component analysis of environmental variables 87
Figure III.4. Canonical redundancy analysis of macrofaunal densities in the baseline community of the Montségur 91
Figure III.5. Principal component analysis of macrofaunal composition on the three sampling sites 91
Figure III.6. Histograms and boxplots of size frequency distribution of *Bathymodiolus azoricus* 93
Figure III.7. Canonical redundancy analysis of macrofaunal densities during the recolonisation process 94
Figure III.8. Densities of most abundant species along recovery process on Montségur 95
Figure III.9. Observed and proposed model of community succession after a disturbance on the Lucky Strike vent assemblages 103
Figure III.S1. Quadrats were deployed on three sampling sites 119
Figure III.S2. Temperatures monitored by within the experimental quadrats on the Montségur edifice 119

Figure III.S3. Rarefaction curves for macrofaunal communities in the baseline communities of the three habitats 120
Figure III.S4. Recolonisation dynamics of *Bathymodiolus azoricus* on the Montségur edifice along the recovery process 120
Figure III.S5. Alpha diversity descriptors of macrofaunal communities on Montségur along recovery 121
Figure III.S6. Size frequency distribution of the most dominant species on Montségur along recovery 122

Chapitre IV : Rétablissement de la structure du réseau trophique en réponse à une perturbation

Figure IV.1. A. Location of the Lucky Strike vent field along the Mid-Atlantic Ridge 131
Figure IV.2. Summary of the experimental design on Montségur to follow the recovery of trophic structure 131
Figure IV.3. Biomass of the macrofauna per trophic guild on Montségur along recovery 138
Figure IV.4. Stable isotope bi-plots showing vent consumers' isotope composition weighted by biomass 139
Figure IV.5. Isotopic space of the different assemblages along the recolonisation process 141
Figure IV.6. Layman metrics associated with the small-scale disturbance experiment on the active edifice Montségur at the Lucky Strike vent field 141
Figure IV.S1. Biomass of *Bathymodiolus azoricus* among all the assemblages of the experiment 159
Figure IV.S2. Stable isotope relationship between the engineer species *Bathymodiolus azoricus* and its commensal worm *Branchipolynoe seepensis* 159

Chapitre V. Biologie de la reproduction des gastéropodes

Figure V.1. Location of the Lucky Strike vent field on the Mid-Atlantic ridge, south of the Azores 170
Figure V.2. Morphology of reproductive structures of *Protolira valvatoides* and *Pseudorimula midatlantica* 173
Figure V.3. Oocyte size–frequency histograms of pooled individuals of *P. valvatoides* 176
Figure V.4. Oocyte size–frequency histograms of pooled individuals of *P. midatlantica* 176
Figure V.5. Box plot of the oocyte size distribution of *P. valvatoides* and *P. midatlantica* 178
Figure V.6. Relationship between animal shell length and proportion of vitellogenic oocytes 178
Figure V.7. Size–frequency distribution of shell length of *P. valvatoides* and *P. midatlantica* 180
Figure V.S1. Oocyte size-frequency histograms of pooled individuals of *P. valvatoides* 198
Figure V.S2. Oocyte size-frequency histograms of pooled individuals of *P. midatlantica* 199

Chapitre VI. Discussion générale

Figure VI.1. Schéma illustrant la progression du rétablissement des assemblages de macrofaune 209

Liste des tableaux

Chapitre III : Rétablissement de la structure des communautés en réponse à une perturbation

Table III.1. Details of each quadrat deployed as part of the disturbance experiment on Montségur_80
Table III.2. Information about size structure on the most dominant species on Montségur_____83
Table III.3. Environmental conditions on the baseline communities on Montségur _____85
Table III.4. Univariate measures of macrofaunal community structure among the different quadrats sampled on the Lucky Strike vent field _____89
Table III.S1. Biological characteristics of pre- and post-disturbed communities on the Montségur_123

Chapitre IV : Rétablissement de la structure du réseau trophique en réponse à une perturbation

Table IV.1. Trophic guild and nutritional modes of macrofaunal species on Montségur_____135
Table IV.2. Taxonomic richness among trophic guilds before/after disturbance_____137
Table IV.3. Range of $\delta^{13}C$ ratio of the dominant basal sources of hydrothermal vent food web ___ 146
Table IV.S1. Stable isotope composition of the different before /after disturbance_____160

Chapitre V. Biologie de la reproduction des gastéropodes

Table V.1. Summary of vent sites and stations, time of sampling, number of individuals and shell size range of all individuals of the two species used for histological analyses in this study _____170
Table V.2. Matrix of p-value of the Nemenyi and Dunn multiple range test used to compare the shell length distribution of *Protolira valvatoides* and *Pseudorimula midatlantica*_____180
Table V.3. Summary of reproductive traits of vent limpets from the *Lepetodrilidae* family _____183
Table V.4. Summary of known reproductive traits of dominant species of the Lucky Strike vent field _____ 183
Table S1. Results of Kruskal–Wallis multisample tests and the Nemenyi and Dunn multiple range tests comparing oocyte size distributions _____200

« Voici ma thèse, avec un « T » comme t'es là… T'es là ou t'es pas là ? T'es pas là mais où c'est que t'es, ah t'es là, avec un « T » comme Thèse »

Adapté de Jeff Tuche

Avant-propos

Les travaux présentés dans ce manuscrit de thèse ont principalement été financés par l'Ifremer, la compagnie d'énergie Equinor et le projet européen H2020 MERCES (Marine Ecosystem Restoration in Changing European Seas, Project ID 689518). Ce projet fait également partie du nœud régional EMSO-Açores (http://www.emso-fr.org), de l'infrastructure de recherche EMSO ERIC (http://emso.eu). Durant ces trois années, j'ai été accueilli au sein du Laboratoire Environnement Profond (LEP) de l'unité de recherche Étude des Écosystèmes Profonds (EEP) sur le site Bretagne de l'Ifremer. Dans le cadre d'une codirection avec Dr Eva Ramirez-Llodra de l'Institut Norvégien de recherche sur le milieu aquatique (NIVA), j'ai eu l'opportunité de réaliser deux séjours de deux mois, en février 2018 et mars 2019 à Oslo (Norvège). Ces séjours m'ont permis de me former aux analyses histologiques au sein du laboratoire NIVA, sous la direction de Dr Ramirez-Llodra, en collaboration avec l'Institut Vétérinaire d'Oslo. Ils ont également été l'occasion de présenter l'avancement des résultats du projet au siège social de la compagnie Equinor à Fornebu (Norvège). Ces séjours ont été financés par une bourse de mobilité étudiante ISblue.

Les résultats présentés sont issus de données acquises au cours des campagnes annuelles MOMARSAT : Monitoring The Mid Atlantic Ridge [https://doi.org/10.18142/130] (en 2017, 2018 et 2019) au niveau du champ hydrothermal Lucky Strike (dorsale médio-Atlantique) à 1 700 m de fond. J'ai eu la chance d'embarquer sur MOMARSAT 2018, du 08 au 27 août 2018 à bord du N/O *Atalante* équipé du ROV *Victor6000* ainsi que MOMARSAT 2019, du 11 juin au 7 juillet 2019 à bord du N/O *Pourquoi Pas ?* équipé du HOV *Nautile.* J'ai même eu l'immense privilège de prendre part à la plongée 1949-11 du Nautile pour l'échantillonnage des assemblages étudiés dans ce travail.

Le chapitre V de ce manuscrit a fait l'objet d'un article publié en mars 2020 dans la revue *Marine Biology* et le chapitre III est actuellement en révision dans la revue *Marine Environnemental Research* en tant que premier auteur. J'ai également travaillé en collaboration avec Dr Dominique Cowart dans le cadre de son post-doctorat au laboratoire, dont l'objectif était d'évaluer l'apport des analyses moléculaires basées sur des échantillons d'ADN environnemental dans l'étude de la diversité des sources hydrothermales et des

habitats inactifs adjacents dans un contexte de recolonisation. Ce travail a abouti sur une publication dans la revue *Frontiers in Marine Science* en tant que co-auteur.

J'ai également présenté mes résultats dans le cadre de plusieurs conférences nationales et internationales :

- Marticorena et al. (2018) « Toward restoration of deep-sea ecosystems » Présentation orale – Marine Ecosystem Restoration in Changing European Seas (MERCES meeting) – Barcelone, Espagne

- Marticorena et al. (2018) « Suivi de la dynamique de recolonisation de la macrofaune benthique en réponse à une perturbation majeure » Présentation orale – LuckyScales Workshop – Brest

- Marticorena et al. (2018) « Towards a restoration approach in the deep sea: first results of a disturbance experiment in the Lucky Strike hydrothermal vent field» Présentation orale – Colloque National sur la Biologie et l'Ecologie des Ecosystèmes à Base de Chimiosynthèse – CONNECT 3 – Roscoff

- Marticorena et al. (2019) « Recovery of hydrothermal communities in response to an induced disturbance at the Lucky Strike vent field (Mid-Atlantic Ridge)» Présentation orale – Réunion annuelle avec les financeurs de la thèse (Statoil) – Fornebu – Norvège

- Marticorena et al. (2018) « Restoration in the deep sea: results of a disturbance experiment » Poster – 15ème Deep Sea Biology Symposium – Monterey, California, Etats-Unis

- Marticorena et al. (2020) « Recovery of hydrothermal communities in response to an induced disturbance at the Lucky Strike vent field (Mid-Atlantic Ridge)» Présentation orale - Online Deep Sea Biology Symposium (eDSBS)

D’autre part, j’ai participé à la rédaction de délivrables, sous forme de rapports trimestriels dans le cadre de la collaboration avec Equinor, ainsi que de rapports annuels pour le projet européen MERCES.

L’une des missions principales de l’Ifremer, au-delà de la recherche, vise à informer le grand public sur les enjeux de l’étude du milieu marin en participant à des événements de vulgarisation. À ce titre, j’ai été sollicité pour animer une présentation grand public en février 2020 à la cité de l’océan à Biarritz et ai également participé à différents événements impliquant d’autres membres du laboratoire : La nuit des chercheurs (Océanopolis, Brest), Immersion sciences (île Tudy), Le festival du centre de la terre (Crozon), Forum pédagogique (Saint Renan).

Enfin, les étroites relations entre l’Ifremer et l’Université de Bretagne Occidentale m’ont permis de réaliser 80 h (heures équivalent travaux dirigés) d’enseignement réparties entre des travaux dirigés en biologie animale à destination d’étudiants de Licence Sciences de la vie et de cours magistraux à destination d’étudiants du Master Sciences de la Mer (Institut Universitaire Européen de la Mer).

I. Introduction

I.1. Les écosystèmes hydrothermaux

I.1.1. Formation et distribution des sources hydrothermales

En 2020, l'inventaire global des champs hydrothermaux répertorie 613 sites situés au niveau des zones d'expansion de la croûte océanique, le long des dorsales médio-océaniques, dans les bassins d'arrière-arc, aux abords des zones de subduction et le long d'arcs volcaniques et sur des points chauds intra-plaques (Figure I.1 ; Beaulieu et Szafrański 2020). Il existe une grande diversité morphologique et géologique entre les différents systèmes hydrothermaux en fonction de la vitesse d'expansion océanique. Cette vitesse fait référence au taux d'accrétion de la croûte océanique formée en une année. Les rides médio-océaniques sont généralement séparées en 5 grandes catégories en fonction de leur vitesse d'expansion : ultra lente, lente, intermédiaire, rapide et très rapide (Figure I.2).

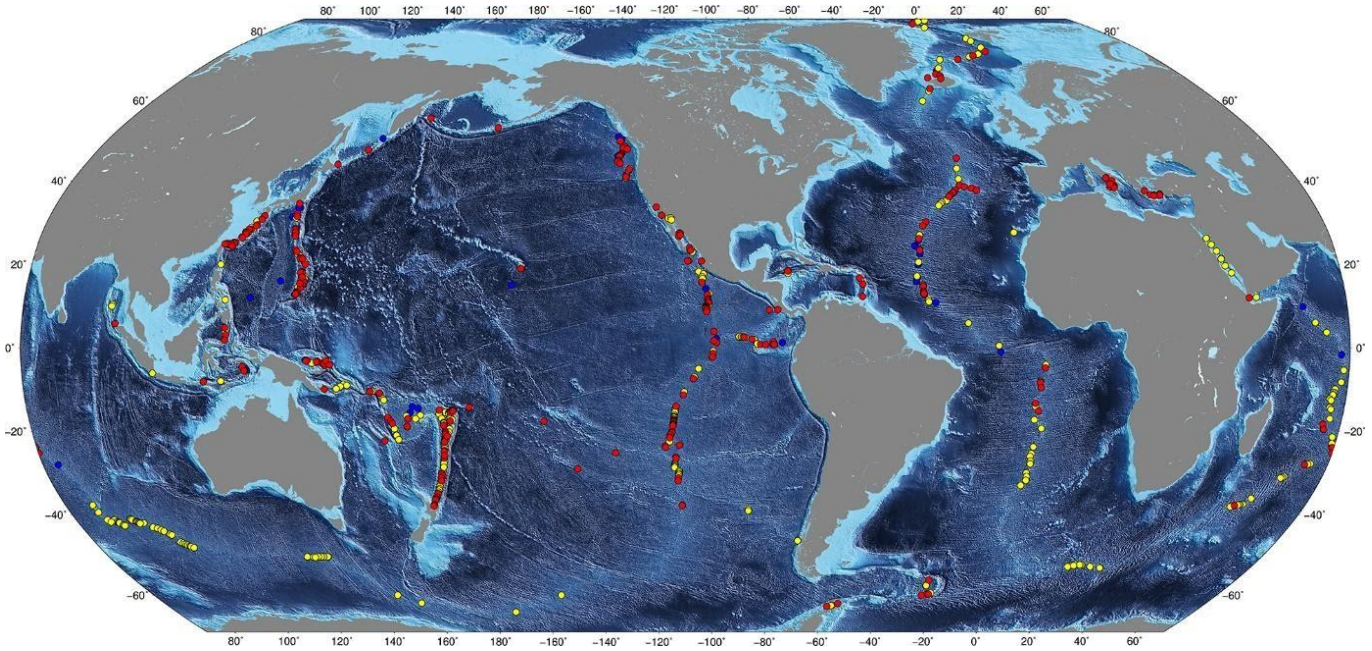

Figure I.1. Carte générale de la répartition des sites hydrothermaux découverts et suspectés à ce jour. Tirée de Beaulieu et al. 2020.

Les centres d'expansion rapides et très rapides, tels que la dorsale du Pacifique oriental, présentent une vitesse d'expansion supérieure à 80 mm.an^{-1} et sont caractérisés par d'importants apports magmatiques et une forte fréquence d'éruptions volcaniques (de l'ordre de la décennie ; (Rubin et al. 2012)). Les sites hydrothermaux présents au sein de ces systèmes d'expansion disposent d'une morphologie majoritairement sculptée par l'activité volcanique et se trouvent généralement proches de la zone d'expansion. Leur durée d'activité est relativement faible et n'excède généralement pas 100 ans (Lalou et al. 1993). À l'inverse, les

centres d'expansion ultra-lents et lents sont caractérisés par des vitesses d'expansion respectives de <20 mm.an^{-1} et entre 20 et 50 mm.an^{-1} (Karson et al. 2015). Ils incluent notamment la dorsale médio-Atlantique, arctique et les bassins d'arrière-arc de l'ouest Pacifique et sont caractérisés par des apports magmatiques sporadiques et moins importants (Kelley et al. 2002). La formation des sites hydrothermaux y résulte principalement de l'activité tectonique (i.e. failles transformantes, formation de vallées axiales ; Karson et al. 1987; Cannat et al. 1997) et la fréquence d'éruption y est très faible, pouvant atteindre 1 éruption tous les 10 000 ans (Perfit et Chadwick 1998). Ces sites sont en moyenne plus espacés entre eux (de plusieurs dizaines à plusieurs centaines de kilomètres) et présentent une importante longévité (plusieurs milliers d'années d'activité ; (Druffel et al. 1990 ; German et Parson 1998). Les sites caractérisés par une vitesse d'expansion intermédiaire (entre 50 et 80 mm.an^{-1}) présentent une structure et une morphologie de transition entre les centres lents et rapides. Cette catégorie regroupe des systèmes hydrothermaux comme la dorsale Juan de Fuca, la dorsale sud-est indienne ou encore la dorsale des Galápagos. Les caractéristiques géologiques contrastées des différents systèmes hydrothermaux jouent un rôle primordial sur la composition du fluide hydrothermal, la diversité de la faune ainsi que sur la dynamique spatiale et temporelle des communautés (Tunnicliffe 1991).

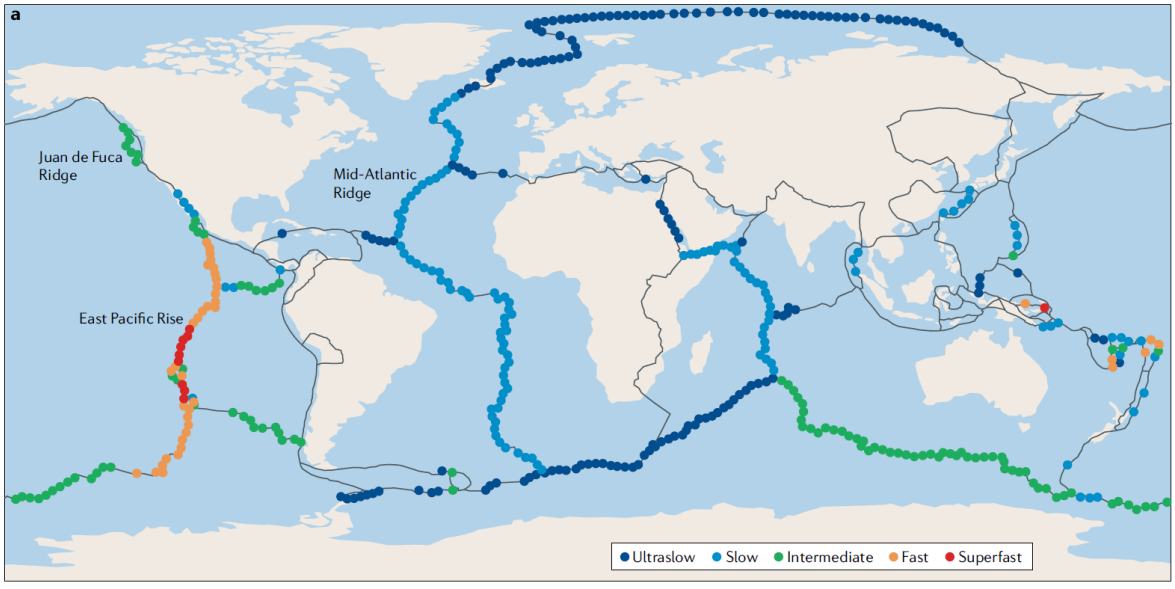

Figure I.2. Carte générale des vitesses d'expansion au sein des différents systèmes tectoniques.Tirée de Dick et al. 2019.

La formation d'une source hydrothermale résulte de la circulation d'eau de mer dans le plancher océanique à proximité d'une chambre magmatique (Figure I.3 ; Tivey 2007). En effet,

dans un premier temps, de l'eau de mer froide (0 – 4 °C) s'infiltre dans le plancher océanique à travers des fissures formées par l'activité tectonique. Elle entame alors une descente de plusieurs kilomètres à travers les interstices de la croûte océanique et se réchauffe progressivement à l'approche de la chambre magmatique. Lorsque la température du fluide augmente, une modification de sa composition chimique s'opère à la suite d'interactions avec les roches environnantes. Ce processus appelé « métamorphisme hydrothermal » entraîne une décharge du fluide en éléments oxydants et un enrichissement en métaux tels que le fer, le manganèse, le zinc ou le cuivre ainsi qu'en gaz tel que l'hydrogène sulfuré, le dihydrogène et le méthane, en partie issus de processus de dégazage du magma (Figure I.3). Le fluide chauffé, devenu acide (pH compris entre 2 et 3) et anoxique, entame, sous l'effet de la densité, une remontée vers le plancher océanique avant d'être expulsé à la surface sous différentes formes d'émissions en fonction du degré de mélange avec l'eau de mer froide (Figure I.4).

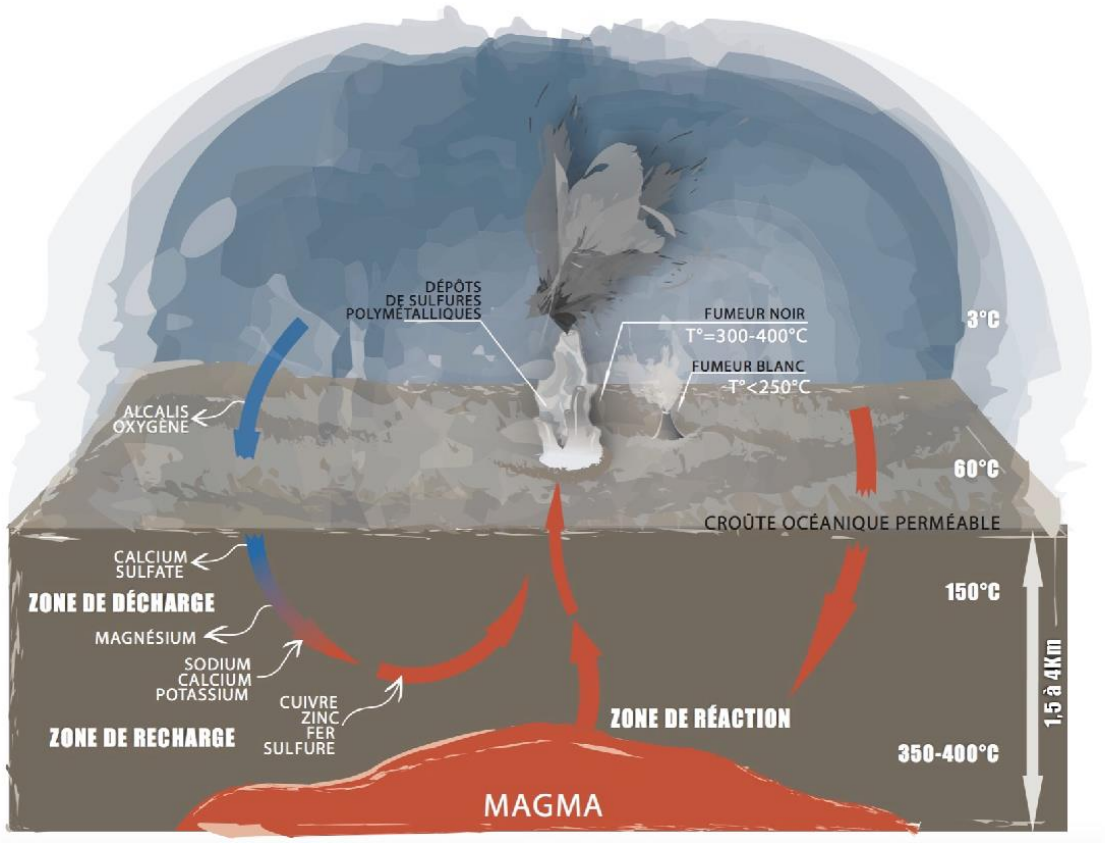

Figure I.3. Schéma général illustrant la mise en place de la circulation hydrothermale ainsi que les interactions eau-roche en subsurface. Tiré de Sarrazin et Desbruyères 2015.

Lorsque le fluide pur (i.e non dilué en sub-surface) jaillit du plancher océanique, il forme un panache vertical rapide – pouvant atteindre 120 $cm.s^{-1}$ (Mittelstaedt et al. 2012) – appelé fumeur noir en raison de sa couleur (Figure I.4B ; Alt 1995). Les fumeurs noirs sont caractérisés

par des températures très élevées, généralement supérieures à 300 °C et pouvant atteindre 400 °C (Lilley et al. 1995) ainsi que de fortes concentrations en éléments réduits et métaux dissous. Cette couleur noire provient de la précipitation de sulfures polymétalliques (Hannington et al. 1995). Les fumeurs blancs (Figure I.4C), d'aspect laiteux en raison de la présence de sulfate de calcium, présentent des températures moins élevées (entre 100 °C et 200 °C). Ils sont également alimentés par du fluide pur, légèrement dilué avec de l'eau de mer à travers la matrice poreuse du plancher océanique (Barreyre et al. 2014). L'accumulation des métaux qui précipitent à la sortie du fluide hydrothermal, conduit avec le temps à la formation de dépôts polymétalliques qui constituent les édifices hydrothermaux (Lilley et al. 1995). Le dernier type d'émission correspond aux flux diffus (Figure I.4D) dont la température n'excède généralement pas 100 °C (Figure I.6D, Bemis et al. 2012). Leur formation peut résulter de la dilution en sub-surface du fluide hydrothermal avec l'eau de mer qui s'infiltre à travers des anfractuosités de la roche (Figure I.4), ou de l'infiltration d'eau de mer qui se charge en éléments volatiles, par l'intermédiaire de la diffusion moléculaire et se réchauffe par conduction avec les conduits de circulation secondaire du fluide hydrothermal présent à proximité (Figure I.4 ; Barreyre et al. 2014).

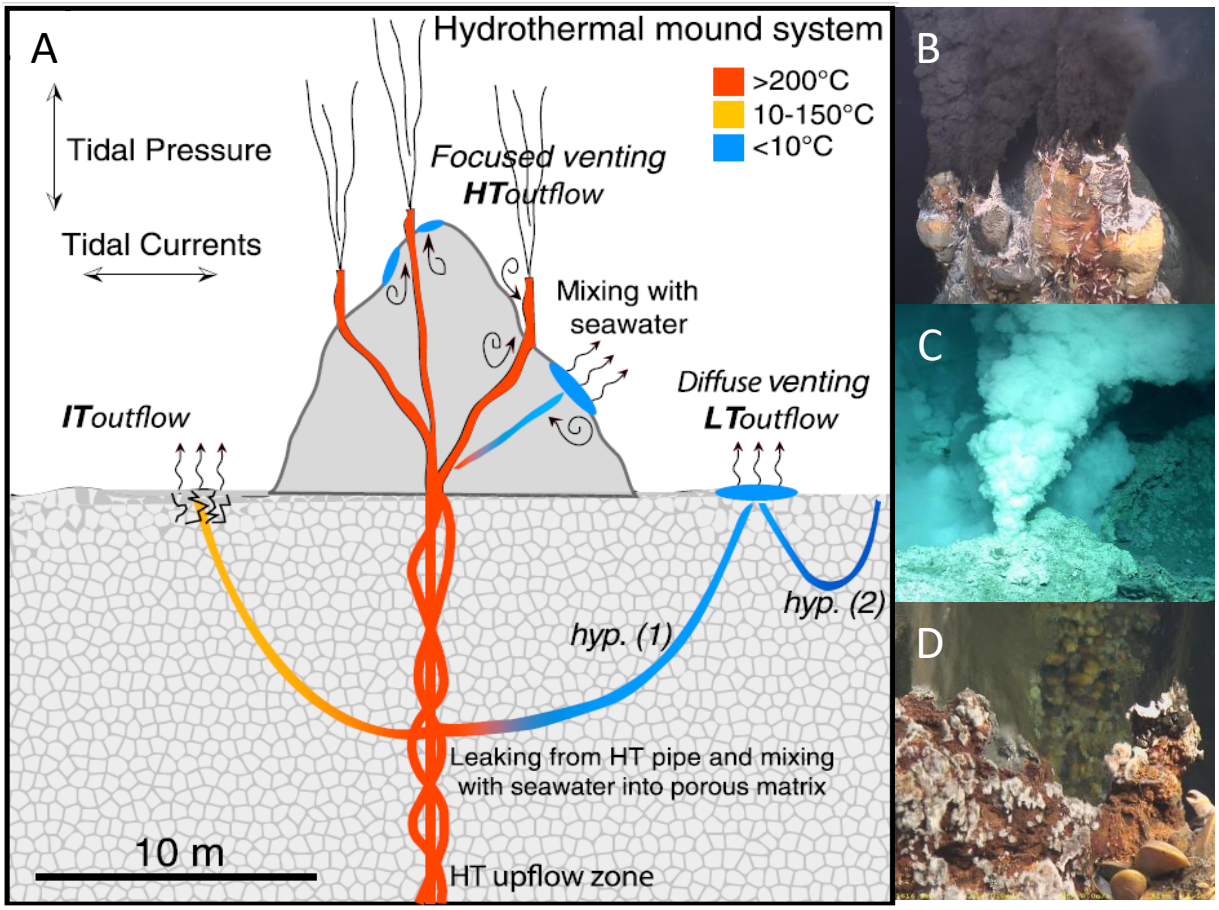

Figure I.4. A) Schéma général des différentes formes d'émission des sources hydrothermales (Barreyre et al. 2014) **B)** fumeur noir, **C)** fumeur blanc et **D**) fluide diffus.

I.1.2. La production primaire chimiosynthétique

La découverte des écosystèmes hydrothermaux sur la dorsale des Galápagos en 1977 (Lonsdale 1977), et de la profusion de vie associée, a constitué une avancée majeure non seulement sur la connaissance du fonctionnement des écosystèmes profonds mais aussi pour la biologie en général. En effet, jusqu'alors considérés comme des déserts de vie en raison de la faible quantité d'apports organiques en provenance de la production photosynthétique de surface, la découverte de denses assemblages de faune aux abords d'une cheminée hydrothermale à 2 500 mètres de profondeur a permis de mettre en avant l'existence d'un écosystème basé sur une source d'énergie alternative (Corliss et al. 1979).

Rapidement, la présence de micro-organismes (bactéries et archées), capables d'oxyder des composés réduits et d'en retirer de l'énergie afin de produire de la matière organique, a été mise en évidence (Jannasch 1985). Au cours d'une réaction d'oxydo-réduction, les organismes chimio-autotrophes utilisent des éléments oxydants présents dans l'eau de mer en tant qu'accepteurs d'électrons, pour oxyder les éléments réduits contenus dans le fluide

hydrothermal anoxique afin de produire de l'énergie sous forme d'ATP. Une grande variété d'éléments réduits et oxydants sont présents au niveau des zones de mélange entre le fluide hydrothermal chaud et l'eau de mer froide, offrant des conditions favorables à l'utilisation d'une grande diversité de réactions d'oxydo-réduction par des micro-organismes chimiosynthétiques (Fisher et al. 2007). En effet, les différentes espèces de micro-organismes sont susceptibles d'utiliser une grande variété de donneurs d'électrons, telle que des sulfures (H_2S), du méthane (CH_4), du dihydrogène (H_2), de l'ammonium (NH_4^+) ou encore du fer (Fe^{2+}), mais également différents accepteurs d'électrons, comme l'oxygène (O_2), les nitrates (NO_3^-) ou les sulfates (SO_4^{2-}) de manière à produire l'énergie sous forme d'ATP, en fonction de leur optimum de croissance et de leurs capacités métaboliques (Figure I.5 ; Childress et al. 1986 ; Childress et Fisher 1992 ; Takai et al. 2004, 2013 ; Edwards et al. 2004 ; Fisher et al. 2007 ; Nakagawa et Takai 2008 ; Petersen et al. 2011 ; Dick 2019). Cependant, en raison de la forte concentration en composés soufrés au niveau des sources hydrothermales, l'oxydation de l'hydrogène sulfuré (H_2S) par des microorganismes thiotrophes représente la voie de biosynthèse la plus utilisée (Akerman et al. 2013 ; Fortunato et al. 2018). Ce mode de production primaire, appelé chimiosynthèse, est à la base des réseaux trophiques associés aux sources hydrothermales, mais aussi des écosystèmes des sources froides ainsi que ceux liés aux substrats organiques comme les carcasses de baleines et les bois coulés (Dubilier et al. 2008).

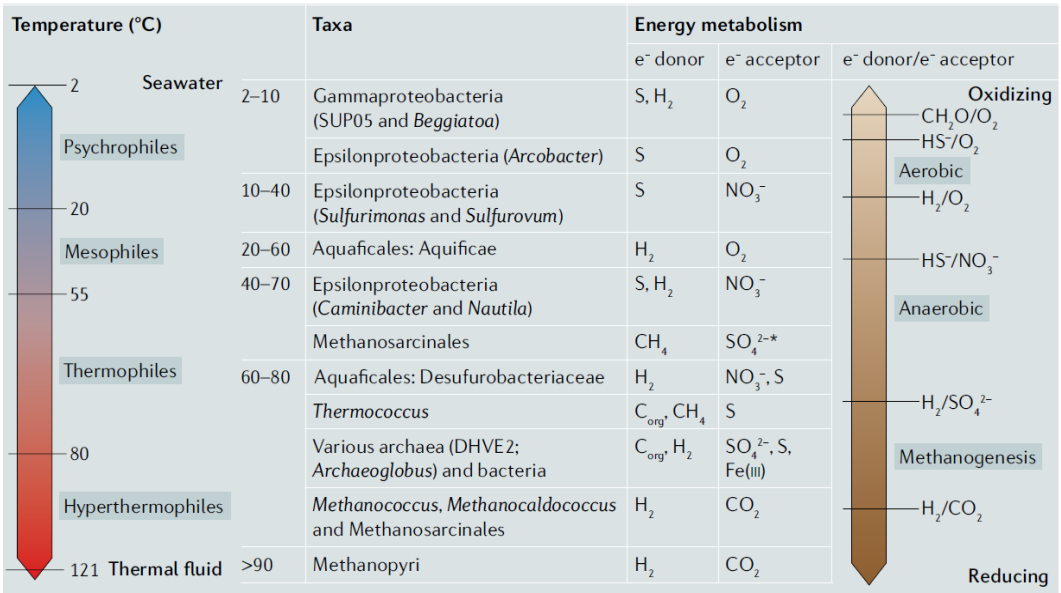

Figure I.5. Caractérisation générale de la production primaire chimiosynthétique en milieu hydrothermal en fonction des conditions environnementales (Dick et al. 2019)

Dans le milieu hydrothermal, les microorganismes occupent une grande variété d'habitats - flux diffus, panache, anfractuosités du plancher océanique, sédiments ou cheminées inactives – en fonction de leurs besoins énergétiques et des conditions environnementales idéales à leur optimum de croissance (Dick 2019). Leur forte productivité s'exporte aux échelons trophiques supérieurs et permet de supporter une importante biomasse. Ces microorganismes peuvent être utilisés par des consommateurs primaires bactérivores qui se nourrissent en broutant les tapis microbiens, ou en filtrant les bactéries libres dans l'eau où ils vivent en association symbiotique avec des invertébrés (Dubilier et al. 2008). Des symbioses ont été identifiées chez un grand nombre de phyla, parmi lesquels des annélides, des mollusques – aussi bien des bivalves que des gastéropodes –, des crustacés et des nématodes (Dubilier et al. 2008 ; Bellec et al. 2018). Ces invertébrés manifestent une grande variété d'adaptations morphologiques qui leur permettent d'héberger et de tirer profit des microorganismes. En fonction de la localisation des symbiontes, on distingue l'ectosymbiose – pour laquelle les symbiontes se répartissent à l'extérieur des tissus de l'animal – et l'endosymbiose – lorsqu'ils sont hébergés à l'intérieur des tissus de l'hôte.

I.1.3. Structure des communautés de faune hydrothermale

Les écosystèmes hydrothermaux sont considérés comme des « hotspots » de productivité et de biomasse principalement en raison de la forte abondance d'espèces ingénieures, le plus souvent symbiotiques, qui structurent l'habitat et permettent une diversification des niches écologiques. La faune hydrothermale est également caractérisée par une relativement faible diversité spécifique en comparaison aux communautés des plaines abyssales ou des habitats côtiers, ainsi qu'un fort taux d'endémisme (Tunnicliffe 1991). Ces particularités peuvent être expliquées par le fait que la plupart des espèces hydrothermales disposent d'adaptations anatomiques, physiologiques et comportementales spécifiques qui leur permettent de faire face aux conditions particulières de ces environnements (i.e. anoxie, forts gradients de température, toxicité du fluide hydrothermal, etc. ; Powell et Somero 1986 ; Johnson et al. 1988 ; Sarrazin et al. 1999 ; McMullin et al. 2000 ; Hourdez et Lallier 2006 ; Govenar 2010 ; Bates et al. 2010 ; Gollner et al. 2015b).

Bio-régionalisation des communautés hydrothermales

À l'échelle globale, la composition des communautés hydrothermales varie entre les différents systèmes, et une « bio-régionalisation » des communautés en différentes grandes provinces est observée. Plusieurs études ont permis de mettre en évidence l'existence de 5 à 11 provinces biogéographiques, caractérisées par des divergences plus ou moins marquées en termes de diversité faunistique (Ramirez-Llodra et al. 2007 ; Bachraty et al. 2009 ; Moalic et al. 2012 ; Rogers et al. 2012 ; Thaler et Amon 2019). L'étude la plus récente, et compilant les données du plus grand nombre de campagnes océanographiques, fait état de 8 provinces majeures (Figure I.6 ; Thaler et Amon 2019). Ces provinces se distinguent notamment par la nature des espèces dominantes, souvent symbiotiques (Figure I.6).

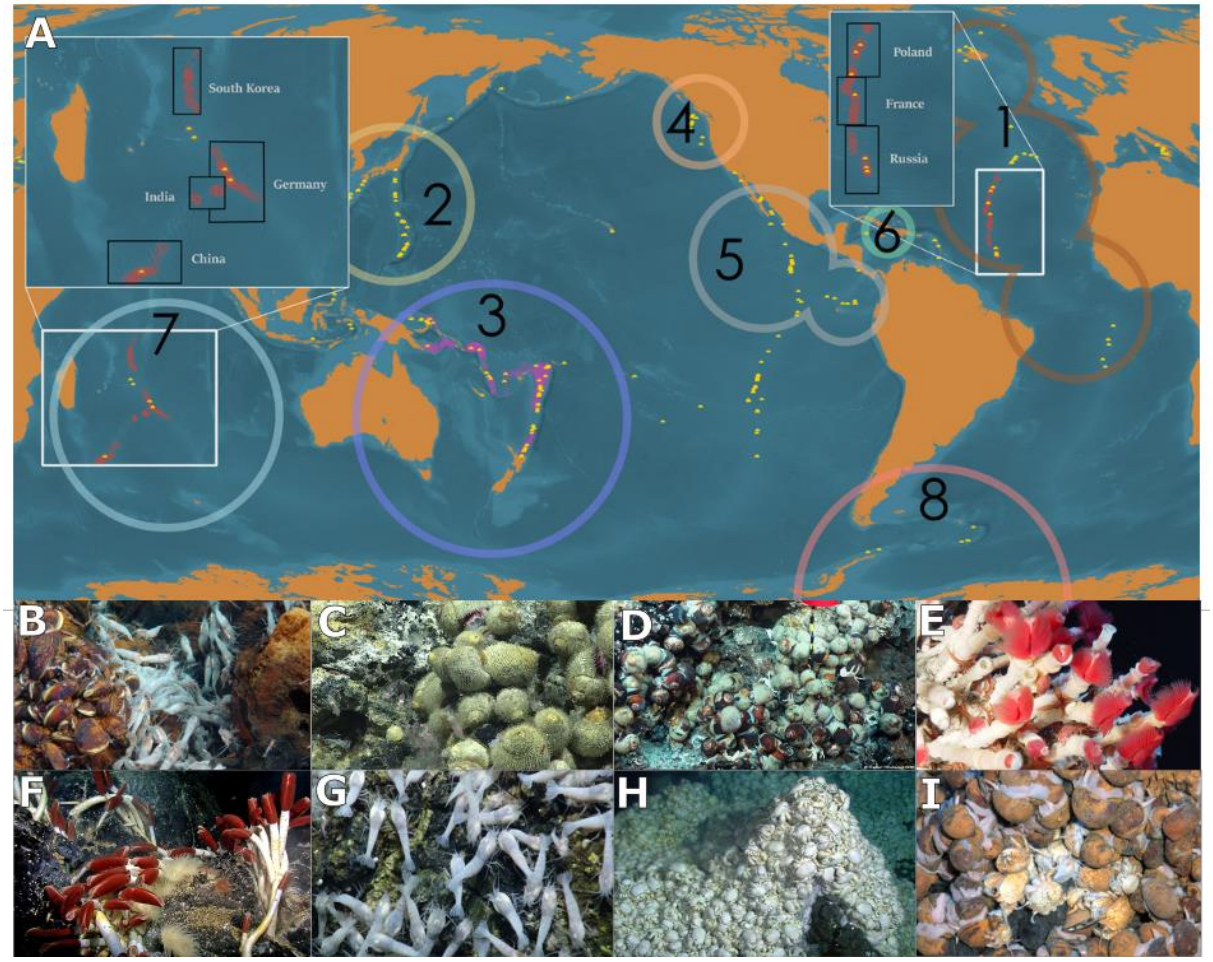

Figure I.6. A) Distribution des 8 grandes provinces biogéographiques des écosystèmes hydrothermaux à l'échelle du globe (Thaler et Amon 2019). Illustration des assemblages caractéristiques de **B)** la ride Médio-Atlantique ; **C)** les bassins arrière-arc du Nord-Ouest Pacifique ; **D)** des bassins arrière-arc du Sud-Ouest Pacifique ; **E)** de la dorsale Juan de Fuca ; **F)** de la dorsale Est pacifique ; **G)** de la dorsale indienne ; **H)** de la dorsale de Scotia et **I)** de la ride des Caymans.

Les divergences observées en termes de composition faunistique entre les grandes provinces biogéographiques sont liées à l'histoire évolutive des différents systèmes de dorsales, qui a entraîné des événements de spéciation par allopatrie de part et d'autre de barrières géographiques (Vrijenhoek 1998 ; Van Dover et al. 2002 ; Hurtado et al. 2004). Ce phénomène est intimement lié aux caractéristiques géologiques et hydrodynamiques qui forment des barrières topographiques et des fronts, limitant la dispersion larvaire et le flux de gènes entre les différentes provinces (Tunnicliffe et Bone 1988 ; Tunnicliffe et Fowler 1996 ; Tyler et al. 2002 ; Thomson et al. 2003 ; Ramirez-Llodra et al. 2007 ; Plouviez et al. 2013 ; Matabos et Jollivet 2019). Les capacités de dispersion des espèces sont déterminées par leur cycle de vie, c'est-à-dire leur mode de reproduction, leur fécondité, le comportement et le mode de nutrition des larves ainsi que leur succès de recrutement (Tyler et Young 1999). En raison de l'importante fragmentation des habitats hydrothermaux, les concepts de métapopulations et métacommunautés ont été évoqués pour décrire la répartition et la dynamique des assemblages de faune (Jollivet et al. 1999 ; Neubert et al. 2006 ; Mullineaux et al. 2018). L'étude de la dynamique de ces métapopulations et métacommunautés, à différentes échelles spatiales, semble être la plus pertinente pour mieux comprendre les mécanismes d'extinction et de recolonisation des habitats hydrothermaux (Mullineaux et al. 2018).

Facteurs responsables de la distribution des assemblages à l'échelle locale

À l'échelle des édifices, la distribution des différentes espèces hydrothermales est principalement régie par leur tolérance à la toxicité du fluide, à la température ainsi qu'à leurs besoins nutritionnels (Tunnicliffe 1991 ; Sarrazin et al. 1997 ; 1999 ; Luther et al. 2001 ; Micheli et al. 2002 ; Mullineaux et al. 2003 ; Govenar et al. 2005). Ce filtre environnemental, créé par l'étroit gradient physico-chimique au niveau de la zone de mélange entre fluide hydrothermal et eau de mer, entraîne une zonation des assemblages de faune le long de cette zone dite critique (Figure I.7 ; Shank et al. 1998 ; Sarrazin et al. 1999 ; Cuvelier et al. 2009). La complexité topographique des zones d'émission, la nature du substrat et des variations de la porosité de la roche conduisent à une distribution en mosaïque des assemblages sur les édifices actifs (Sarrazin et al. 1999, 2002 ; Cuvelier et al. 2009 ; Girard et al. 2020). L'interaction des courants benthiques avec la topographie et la position des sorties de fluides jouent également un rôle primordial sur la distribution des espèces en contrôlant localement l'apport en particules (Girard et al. 2020). D'autre part, les interactions biotiques, bien que difficiles à quantifier, semblent jouer un rôle prépondérant dans la structure des communautés (Micheli et al. 2002 ; Hunt et al. 2004 ; Govenar et Fisher 2007). En effet, plusieurs études ont mis en évidence

différents types d'interactions entre les espèces, telles que la facilitation (Sarrazin et al. 1997 ; Mullineaux et al. 2000, 2003 ; Gollner et al. 2015a), la prédation (Micheli et al. 2002 ; Hunt et al. 2004), le partage des ressources trophiques (Levesque et al. 2003, 2006 ; Bergquist et al. 2007 ; Lelièvre et al. 2018) et la compétition (Lenihan et al. 2008) qui façonnent la distribution des espèces au sein d'un habitat. Il a également été suggéré que les espèces ingénieures peuvent à la fois moduler les conditions environnementales en faisant office de tampon au niveau des zones d'émissions diffuses (Johnson et al. 1988 ; Le Bris et Gaill 2006), mais également augmenter la complexité de l'habitat grâce à leur structure tridimensionnelle et ainsi diversifier les niches écologiques et augmenter la diversité locale (Van Dover et al. 2002 ; Govenar et Fisher 2007 ; Lelièvre et al. 2018). Une forte hétérogénéité spatiale des conditions environnementales est également observée avec des variations à l'échelle du centimètre, qui peuvent impacter les organismes hydrothermaux depuis l'échelle moléculaire (e.g. possible modification de l'activité enzymatique jusqu'au comportement des espèces), influençant ainsi la structure des communautés (Bates et al. 2010)

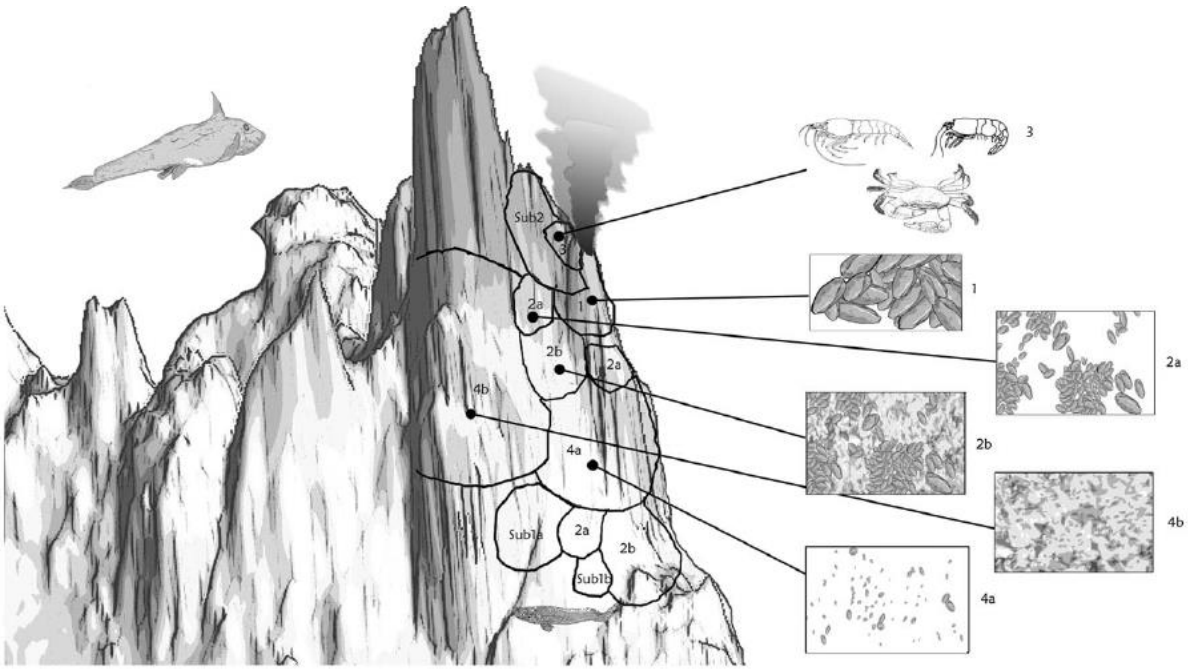

Figure I.7. Modèle conceptuel de zonation des assemblages de faune et des différents types de substrats sur l'édifice Tour Eiffel (champ hydrothermal Lucky-Strike, MAR). L'assemblage 1 est constitué d'une forte densité de *Bathymodiolus azoricus* de grande taille (> 4cm) ; l'assemblage 2, par des patchs de *B. azoricus* de taille moyenne (< 4cm) séparés par du substrat nu ; l'assemblage 3 désigne une surface nue colonisée par des crevettes (*Mirocaris fortunata* et/ou *Rimicaris chacei*) ; et l'assemblage 4 est constitué de surfaces nues avec les présences de recrues de B. azoricus. La présence ou non de mattes microbiennes sur les substrats nus, des sous-assemblages (notés « a » sans mattes microbiennes et « b » présence de mattes microbiennes) ont également été définis. (Tiré de Cuvelier et al. 2009)

Les forts gradients de stress et de productivité jouent également un rôle important sur la biologie des organismes et donc la structure des assemblages. En effet, la variation des conditions environnementales peut influencer certains traits reproductifs des espèces en affectant notamment leur fécondité, la taille des œufs ainsi que la taille et l'âge de maturité sexuelle (Eckelbarger et Watling 1995 ; Ramirez Llodra 2002 ; Kelly et Metaxas 2007). D'autre part, les conditions environnementales jouent un rôle sur la structure des populations de certaines espèces (Matabos et al. 2008). Plusieurs études font également état d'une ségrégation des individus d'une même espèce en fonction de leur taille le long d'un gradient d'activité hydrothermale (Comtet et Desbruyères 1998 ; Desbruyères et al. 2001 ; Marcus et Tunnicliffe 2002). Ainsi, chez le modioles *Bathymodiolus azoricus*, espèce ingénieure dominante des sites hydrothermaux de la dorsale médio-Atlantique nord, les individus de grande taille (> 6 cm) sont associés aux microhabitats « chauds », avec des températures maximales pouvant atteindre ~ 20 °C (Desbruyères et al. 2001 ; De Busserolles et al. 2009 ; Cuvelier et al. 2009 ; Sarrazin et al. 2015, Husson et al. 2017) alors que les individus de plus petite taille (< 1,5 cm) sont présents dans le pôle « froid », avec des températures proches de celles de l'eau de mer ambiante (De Busserolles et al. 2009 ; Cuvelier et al. 2009, 2011b ; Sarrazin et al. 2015, Husson et al. 2017). Les mécanismes qui régissent la zonation des espèces au sein des écosystèmes hydrothermaux sont toujours sujets à discussion et leur rôle relatif demeure difficile à départager car la distribution de la faune résulte d'une combinaison de facteurs biotiques et abiotiques.

I.1.4. Dynamique temporelle des communautés hydrothermales

Les écosystèmes hydrothermaux sont décrits comme des systèmes dynamiques et affichent une forte variabilité temporelle à différentes échelles, de l'ordre de la seconde à plusieurs millions d'années. Les variations des assemblages faunistiques sont associées à la forte variabilité des conditions environnementales, et de plus en plus d'études montrent des liens étroits entre ces facteurs et la biologie des espèces hydrothermales. Par exemple, il a été démontré que certains organismes répondent à des fluctuations à l'échelle de quelques heures, comme c'est le cas de *B. azoricus*, qui alterne des phases d'ouverture et de fermeture de ses valves en cohérence avec le cycle de la marée (Mat et al. 2020). Des études sclérochronologiques ont permis de mettre en évidence une croissance discontinue répondant à un rythme circadien chez une autre espèce de bivalve appartenant au même genre (Schöne et Giere 2005 ; Nedoncelle et al. 2013). Sur la dorsale Juan de Fuca, un rythme

tidal a également été observé dans le comportement du ver siboglinidé *Ridgeia piscesae* (Cuvelier et al. 2014) et les espèces mobiles qui y sont associées ajusteraient leur position dans le buisson en fonction de l'apport en fluide dépendant des variations des courants benthiques (Lelièvre et al. 2017). En effet, les mécanismes qui sous-tendent ces comportements restent à définir ; mais ces études ont émis l'hypothèse du rôle de la modulation du flux hydrothermal diffus par des variations des courants de fonds (Tivey et al. 2002 ; Scheirer et al. 2006 ; Khripounoff et al. 2008 ; Barreyre et al. 2014) et par une augmentation de la pression hydrostatique exercée sur le plancher océanique (Barreyre et al. 2014), tous deux liés aux rythmes des marées.

Localement, des modifications de la circulation en sub-surface ou de porosité du substrat ou des obstructions de sorties du fluide peuvent intervenir et affecter la distribution des communautés (Tunnicliffe et Kim Juniper 1990 ; Sarrazin et al. 1997 ; Cuvelier et al. 2011a). Cependant, on observe une grande divergence d'un système hydrothermal à un autre en termes de variabilité spatio-temporelle des conditions environnementales, variations liées à leurs spécificités géologiques et à l'activité tectonique (Du Preez et Fisher 2018). Par exemple, le suivi temporel à partir d'analyses vidéo de la distribution des communautés au sein d'un édifice de la dorsale Juan de Fuca (dorsale intermédiaire) a montré d'importants changements de communautés en réponse à des perturbations environnementales en l'espace de 4 ans (Sarrazin et al. 1997). En contraste, le même type de suivi sur la dorsale médio-Atlantique (dorsale lente) a révélé une forte stabilité des communautés, même après 14 années de suivi (Figure I.8 ; Cuvelier et al. 2011). De la même façon, Du Preez et Fisher (2018) ont constaté une importante longévité des assemblages et une stabilité décennale des communautés hydrothermales au sein des bassins arrière-arc du sud-ouest Pacifique. En effet, la vitesse d'expansion des différents systèmes a une influence sur la survenue d'événements géodynamiques et donc, sur la stabilité des habitats (Juniper et Tunnicliffe 1997). Les éruptions volcaniques ou les séismes, responsables de la création ou de la disparition d'habitats hydrothermaux (Juniper et Tunnicliffe 1997) vont affecter la distribution des communautés. C'est d'ailleurs à la suite d'éruptions volcaniques que les premières études sur la colonisation de nouveaux substrats et la succession écologique des communautés hydrothermales ont vu le jour (Tunnicliffe et al. 1997 ; Shank et al. 1998 ; Marcus et al. 2009 ; Mullineaux et al. 2010 ; Gollner et al. 2015a).

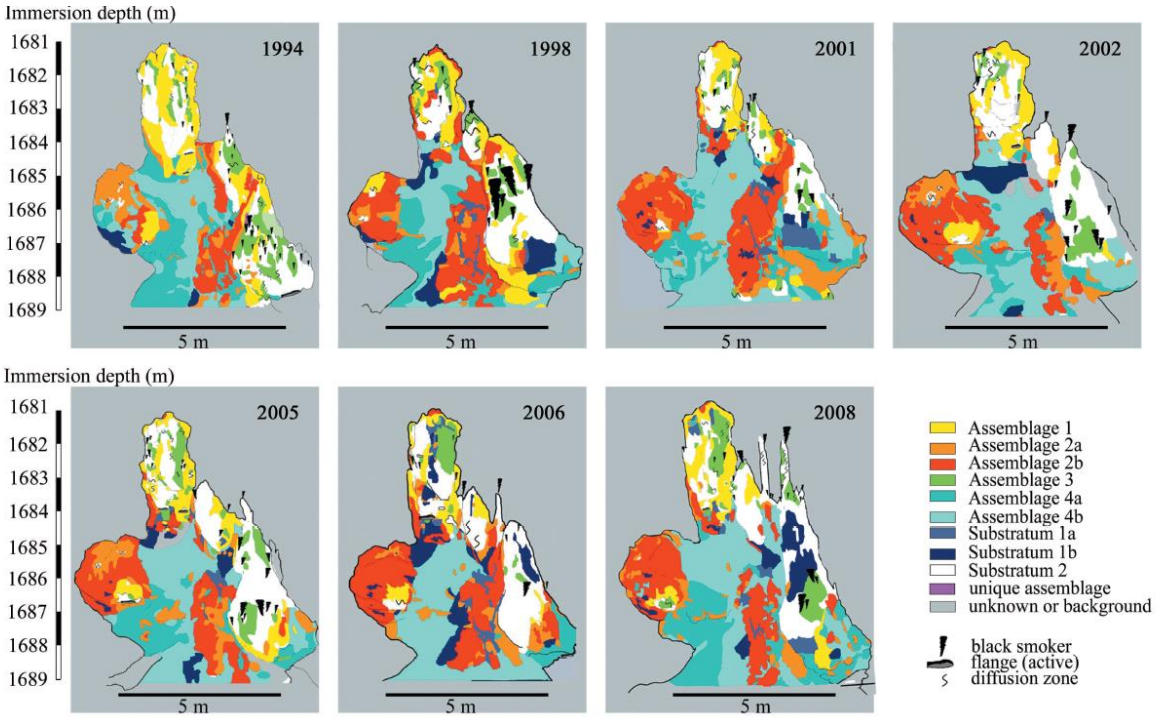

Figure I.8 Distribution spatio-temporelle des communautés hydrothermales sur la face Est de l'édifice Tour Eiffel (MAR) au cours d'un suivi temporel de 14 années.

I.2. Concept de résilience

I.2.1. Qu'est-ce que la résilience en écologie ?

Le concept de **résilience**[1] est aujourd'hui entré dans le langage courant et employé dans une multitude de domaines de manière plus ou moins rigoureuse. Au début du XVIII^{e} siècle, il est employé comme synonyme du terme « rebond ». Conformément à son étymologie, il vient du latin « resilere » (de « salire », sauter et « re », indiquant un mouvement en arrière). Il est, pour la première fois, utilisé au sein du milieu académique dans le domaine de la physique des matériaux, où apparaît la notion de « module de résilience » qui désigne le degré de résistance d'un matériau déterminé en fonction de son comportement élastique (Tredgold 1818). Le concept de résilience a, par la suite, été repris et redéfini dans de nombreuses disciplines telles que la médecine (Carson et al. 1820), l'écologie (Holling 1973), la psychologie (Tugade et Fredrickson 2004) ou encore l'économie (Barrett et Constas 2014).

Le concept de résilience, introduit par le professeur en sciences écologiques Crawford Stanley Holling (1973) et utilisé en écologie, n'a pas vocation à s'appliquer à des éléments individuels

[1] Tous les termes en gras, utilisés dans cette section sont définis dans l'Encart 1

comme c'était le cas en science des matériaux mais à des systèmes complexes composés de plusieurs entités/populations qui interagissent entre elles. Dès lors, il propose d'analyser en détail les processus écologiques qui régissent l'hétérogénéité temporelle des écosystèmes autour de son point d'équilibre en tenant compte des événements aléatoires qui affectent sa stabilité. Deux comportements distincts sont identifiés, avec d'un côté la stabilité qui désigne le temps qu'un écosystème met à retourner à son état d'équilibre à la suite d'une **perturbation** temporaire (assimilé à une forme d'élasticité du système), et de l'autre la résilience qui correspond à la mesure de la persistance du système et à sa capacité à absorber les perturbations pour demeurer dans un même domaine d'équilibre (Holling 1973). Ces deux propriétés ont par la suite été redéfinies et nommées par Holling en 1996 comme «**engineering resilience**» et «**ecological resilience**» respectivement. La définition de l' «*engineering resilience»,* plus traditionnellement utilisée*,* permet alors de décrire le comportement d'un système et sa stabilité proche d'un état d'équilibre unique (Pimm 1984 ; O'Neill et al. 1986). *A contrario*, l'« *ecological resilience* » s'intéresse aux conditions éloignées de l'état d'équilibre pour lesquelles le système est toujours en mesure de retourner à son état d'équilibre avant d'atteindre un certain **seuil**, au-delà duquel il bascule vers un autre domaine de stabilité pour atteindre un équilibre différent. L'une des principales distinctions entre ces deux définitions repose sur l'existence d'un ou plusieurs états d'équilibre (Gunderson 2000). Ces deux aspects sont régulièrement illustrés schématiquement par le comportement mécanique d'une boule - symbolisant le système écologique - dans une topologie de vallées - qui représentent les multiples domaines de stabilité que le système est susceptible d'atteindre (Figure I.9 ; Carpenter et Cottingham 1997 ; Gunderson 2000 ; Carpenter et al. 2001 ; Walker et al. 2004 ; Standish et al. 2014 ; Desjardins et al. 2015). L'état d'équilibre est atteint lorsque la boule se trouve au fond du domaine de stabilité (Gunderson 2000). La flèche symbolise alors l'impact d'une perturbation qui fait dévier le système de son état d'équilibre. Dans cette représentation, l' « engineering resilience », ou rétablissement, peut être assimilée à la pente de la vallée (i.e. plus la pente est importante, plus le système regagne son état d'équilibre rapidement après une perturbation) (Figure I.9B) alors que «l'ecological resilience », ou résistance, est décrite comme la largeur au sommet de la vallée (Figure I.9C). Face à une perturbation majeure entraînant de fortes modifications du système au-delà d'un certain seuil, celui-ci peut être en mesure de se réorganiser pour atteindre un nouvel état d'équilibre

au sein d'un nouveau domaine de stabilité (Figure I.9A). Cette aptitude correspond à la **capacité adaptative** d'un système (Angeler et Allen 2016)**.**

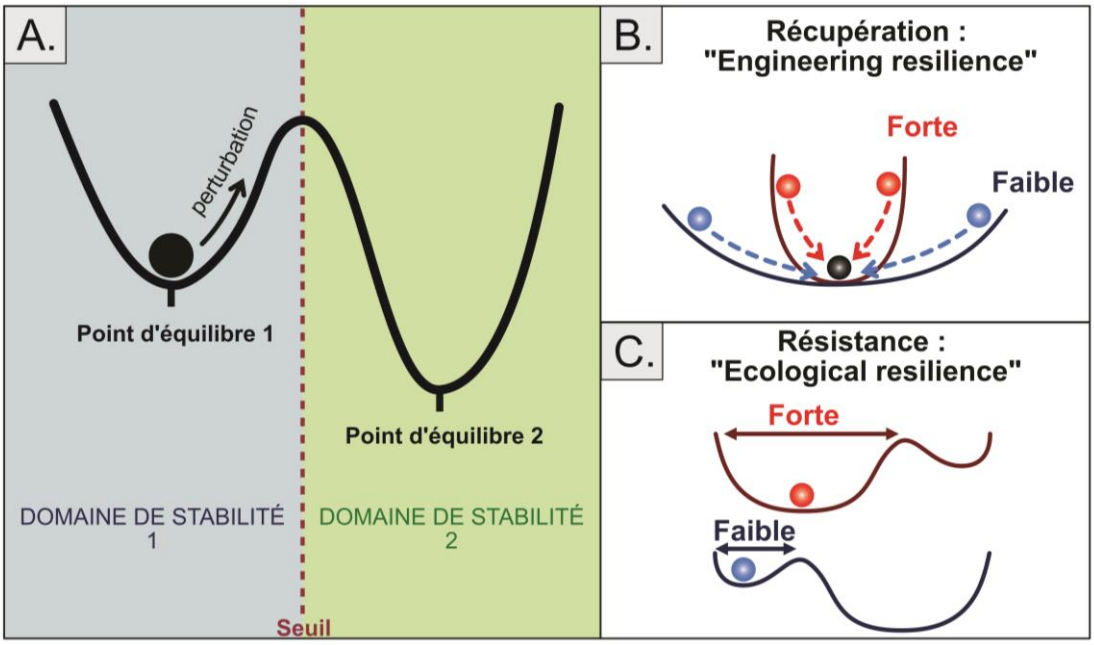

Figure I.9. Schéma conceptuel illustrant les différents aspects de la résilience en écologie. **A)** Les vallées représentent les domaines de stabilité que l'écosystème peut atteindre, la balle schématise l'écosystème et la flèche symbolise l'effet d'une perturbation sur le système. **B)** La récupération fait référence à la vitesse que met le système à retrouver son état d'équilibre et **C)** La résistance correspond à la quantité de stress que le système peut absorber avant de changer de domaine de stabilité.

Par la suite, les définitions du terme résilience et leurs applications dans les différents domaines de l'écologie se sont multipliées, faisant parfois l'objet de nombreux débats sémantiques au sein de la communauté scientifique depuis les années 1970, comme en témoignent les récentes discussions dans *Trends in Ecology and Evolution* (Connell et Ghedini 2015 ; Hodgson et al. 2015, 2016 ; Yeung et Richardson 2016, 2018 ; Oliver et al. 2016 ; Connell et al. 2016 ; Sundstrom et al. 2016 ; Ingrisch et Bahn 2018). Dans la présente thèse, à l'instar d'autres études en écologie marine, la résilience se définit comme la capacité d'un système de conserver sa structure principale et d'assurer les mêmes fonctions en réponse à des changements induits par une perturbation (Gollner et al. 2017 ; Gladstone-Gallagher et al. 2019). Ce concept-clé de résilience dépend principalement de deux processus sous-jacents interconnectés (Côté et Darling 2010 ; McClanahan et al. 2012) : (1) la résistance dérivée de la notion « d'ecological resilience » (*sensus* Holling et al. 1996) fait référence à la quantité de stress et de perturbation qu'un système est capable d'absorber avant de subir des changements d'ordre structurel ou fonctionnel (Folke et al. 2004) et (2) le **rétablissement** (i.e.

« recovery »), hérité du concept « d'engineering resilience » (*sensus* Holling et al. 1996) qui désigne la capacité d'un écosystème à retrouver les mêmes conditions que l'**état de référence** lorsque celles-ci ont été affectées par une perturbation (Lotze et al. 2011).

Encart 1 | Définitions utilisées pour caractériser le concept de résilience dans cette thèse

Capacité adaptative : habilité d'un système à maintenir des fonctions et processus essentiels au cours d'un changement de domaine d'équilibre ou en réponse à de nouvelles conditions environnementales (Angeler et Allen 2016).

Diversité fonctionnelle : valeur et gamme des traits fonctionnels des organismes présents dans un écosystème (Tilman 2001). Les traits fonctionnels sont des caractéristiques de l'organisme qui déterminent sa réponse à l'environnement et/ou ses effets sur le fonctionnement de l'écosystème (Díaz et Cabido 2001). Des exemples de traits fonctionnels, couramment utilisés pour mesurer la diversité fonctionnelle, sont la taille des organismes, leur mode de dispersion, leur guilde trophique, etc.

Diversité réponse : diversité d'espèces qui contribuent de manière similaire aux fonctions de l'écosystème mais qui répondent différemment à une perturbation (Mori et al. 2013).

Diversité structurelle : organisation physique d'un écosystème, comprenant la densité d'organismes, la distribution des espèces, la configuration et la fragmentation de l'habitat ainsi que les conditions abiotiques.

État de référence : l'état de référence d'une communauté considérée comme non-dégradée est défini par une diversité taxonomique, un ensemble de conditions abiotiques et de fonctions répondant à des processus et une succession écologique naturelle.

Perturbation : force ou processus qui affecte directement ou indirectement un écosystème, une communauté, une population ou un individu et qui induit une réponse en termes de diversité et/ou de fonctions écosystémiques ; par exemple réduction de l'abondance, de la richesse spécifique ou disparition de certaines fonctions de l'écosystème. Chaque perturbation est caractérisée le long d'un continuum de temps (persistance et fréquence de la perturbation), d'espace (étendue spatiale des effets directs et indirects) et d'intensité (magnitude de l'impact qu'une perturbation engendre).

Redondance fonctionnelle : la redondance fonctionnelle correspond au nombre d'espèces appartenant à un même groupe fonctionnel et contribuant ainsi de manière similaire aux fonctions de l'écosystème (Walker 1992).

Restauration écologique : processus qui consiste à assister le rétablissement d'un écosystème dégradé ou détruit par le biais de la mise en place d'actions ciblées (Société pour la restauration écologique – SER – 2016).

Résilience : capacité d'un écosystème à conserver sa structure principale et à assurer les mêmes fonctions en réponse à des changements induits par une perturbation. Ce concept dépend principalement de la résistance et du rétablissement d'un écosystème en réponse à une perturbation.

Résistance (cf. « Ecological resilience ») : dans le contexte de cette étude, la résistance représente un aspect de la résilience qui se définit comme la quantité de stress et de perturbation qu'un système est capable d'absorber avant de subir des changements d'ordre structurel ou fonctionnel (Folke et al. 2004).

Rétablissement (cf. « Engineering resilience » et « Recovery ») : capacité d'un écosystème à retrouver la même structure ou les mêmes conditions que l'état de référence à la suite d'une perturbation ayant affecté sa composition, sa structure et ses fonctions (Lotze et al. 2011).

Seuil : point à partir duquel un infime changement des conditions environnementales, dû à une perturbation, induit un changement de domaine de stabilité et une réorganisation de la structure et de la fonction d'un écosystème (Suding et Hobbs 2009)

I.2.2. Comment mesurer la résilience d'un écosystème ?

À ce jour, une grande partie de la littérature sur la résilience en écologie s'est concentrée sur l'aspect théorique, les définitions et la conceptualisation générale concernant l'application de ce concept (e.g. Gunderson 2000 ; Folke et al. 2004, 2010 ; Walker et al. 2004 ; Desjardins et al. 2015). Plus récemment, plusieurs études ont cherché à déterminer l'importance de la **diversité structurelle** et **fonctionnelle** dans l'optique de quantifier la résilience de différents écosystèmes en réponse à des perturbations (Angeler et Allen 2016 ; Baho et al. 2017 ; Roberts et al. 2018). Ces travaux ont permis de faire émerger un consensus sur le fait que la biodiversité est étroitement liée aux fonctions présentes dans un écosystème (Hooper et al. 2005 ; Gagic et al. 2015 ; Chambers et al. 2019). En effet, la contribution d'une espèce aux fonctions de l'écosystème dépend essentiellement des traits biologiques qui la caractérisent (mode de nutrition, stratégie de reproduction, mobilité, modification de l'habitat ; Villnäs et al. 2018). Plusieurs indices, basés sur l'étude des traits fonctionnels, ont d'ailleurs récemment émergé (Mouillot et al. 2013). Deux d'entre eux apparaissent comme particulièrement pertinents pour l'étude de la résilience, à savoir la **redondance fonctionnelle** et la **diversité réponse**. En effet, les espèces qui partagent la même combinaison de traits fonctionnels sont considérées comme redondantes d'un point de vue fonctionnel. Cette redondance fonctionnelle peut jouer un rôle majeur en termes de résilience des écosystèmes (Standish et al. 2014) en permettant de maintenir certaines fonctions en dépit d'une éventuelle perte de diversité spécifique (Walker 1992). Certains travaux ont d'ailleurs permis de mettre en évidence une perte de redondance fonctionnelle dans des écosystèmes dégradés (Balvanera et al. 2006 ; Flynn et al. 2009 ; Laliberté et al. 2010). D'autre part, la diversité réponse correspond à la manière différente que peuvent avoir des espèces d'un même groupe fonctionnel de répondre à une même perturbation (Elmqvist et al. 2003). Dans le cadre de l'évaluation et de la quantification de la résilience d'un écosystème, il s'avère donc primordial d'allier les approches complémentaires du suivi de la diversité structurelle en association avec l'étude des traits fonctionnels des différentes espèces.

I.2.3. Minimiser les impacts et assister le rétablissement des écosystèmes impactés

Aujourd'hui, face au dérèglement global et à l'intensification des activités anthropiques, on constate une nette augmentation du taux d'extinction des espèces (Vitousek et al. 1997) et à

une déstructuration des communautés, conduisant à l'appauvrissement des fonctions au sein des écosystèmes et à une réduction des services écosystémiques (Balvanera et al. 2006 ; Cardinale et al. 2012). C'est dans ce contexte, que de nombreux acteurs scientifiques, des agences de gestion ainsi que des organisations internationales (e.g. UICN, la société pour la restauration écologique, les objectifs d'Aichi pour la biodiversité portés par l'ONU) ont cherché à définir un cadre de gestion afin de mieux caractériser la résilience des écosystèmes et mettre en place des mesures de restauration écologique afin de minimiser l'impact des perturbations et favoriser le rétablissement des écosystèmes endommagés. La société internationale de restauration écologique (« Society for Ecological Restoration » SER) a ainsi publié en 2016, suite à un gros effort de standardisation, un guide pratique permettant de suivre la résilience d'un écosystème endommagé. Ce document définit les standards, les indicateurs et les attributs, applicables à n'importe quel écosystème (terrestre, lacustre, côtier ou marin), à investiguer pour quantifier la résilience et envisager des actions ciblées pour assister la restauration naturelle.

La base de travail de ce type d'approche consiste à caractériser l'état de référence de l'écosystème. Cet état de référence (baseline) constituera la cible à atteindre pour le projet de restauration. Cela implique une description détaillée de la structure et de la diversité fonctionnelle de l'écosystème à partir de sites de référence non impactés. Pour cela, de nombreux facteurs tels que les paramètres abiotiques (type de substrat, hydrodynamisme, chimie de l'habitat), la structure taxonomique (richesse spécifique, densité d'organismes, composition faunistique), la diversité fonctionnelle (étendue du réseau trophique, capacité de dispersion) ainsi que des informations concernant la succession naturelle des communautés doivent être pris en considération. Par la suite, six catégories comprenant des attributs clés des écosystèmes ont été identifiées pour mesurer la progression du rétablissement de l'écosystème au cours projet de restauration : 1) la cessation de la menace, 2) les conditions physico-chimiques, 3) la composition spécifique, 4) la structure de la diversité, 5) les fonctions écosystémiques et 6) les échanges externes (Figure I.10). Conformément aux objectifs fixés au début du projet de restauration, l'état d'avancement peut être suivi au fil du temps grâce à la représentation d'une roue de rétablissement (Figure I.10). Ce schéma permet d'illustrer le niveau de rétablissement de l'écosystème (graduation allant de 1 à 5) pour chacun des attributs, et de cibler les actions de restauration à mettre en place pour faciliter le retour à

l'état de référence. Il est également possible d'adapter la roue de rétablissement aux spécificités de l'écosystème en ajoutant des sous-attributs qui permettent une meilleure définition de l'avancement du rétablissement de l'écosystème. L'encart 2 regroupe les attributs identifiés pour le suivi du rétablissement des écosystèmes hydrothermaux en réponse à une perturbation naturelle ou anthropique.

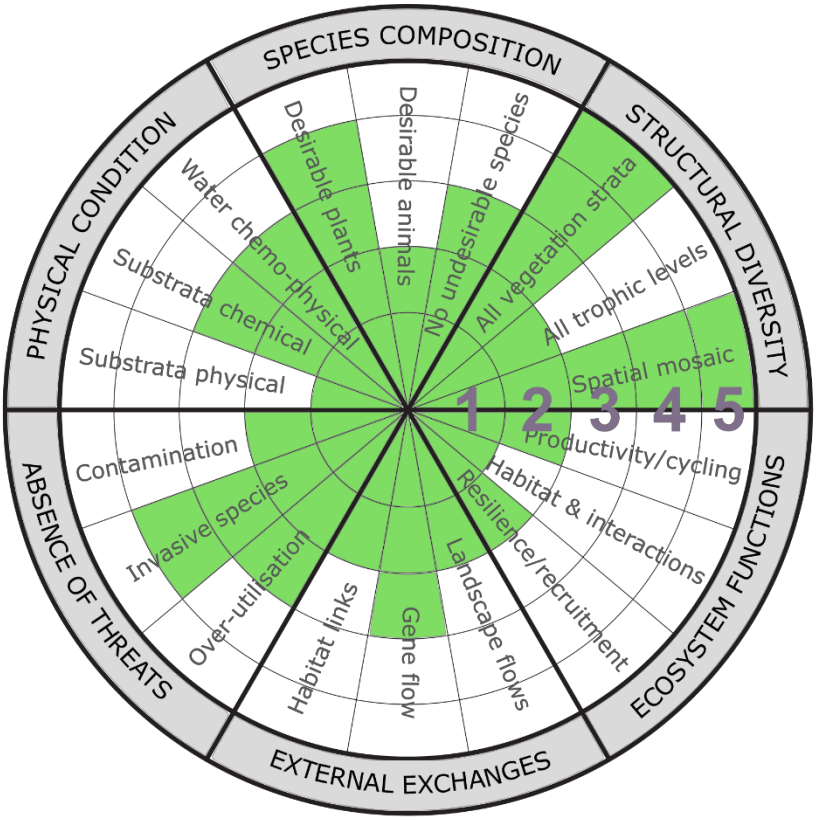

Figure I.10. Roue de rétablissement permettant de suivre l'avancement du projet de restauration, conformément aux objectifs fixés. La roue est divisée en 6 catégories clés afin de rendre compte de l'évolution du rétablissement de l'écosystème dans son ensemble grâce à une gradation allant de 1 à 5. Les sous-catégories peuvent être adaptées pour ajuster le modèle aux spécificités de l'écosystème. Il s'agit ici d'un exemple appliqué à des prairies. Tiré de SER 2016

La quantification des capacités de résilience d'un système nécessite donc une approche multifacette pouvant aboutir à la définition d'actions de mitigation spécifiques pour favoriser le retour à un point d'équilibre à la suite d'une perturbation.

Encart 2 | Evaluation du rétablissement des écosystèmes hydrothermaux

Les six attributs clés et les dix-huit sous-attributs listés dans le Tableau A permettent de rendre compte de l'évolution des multiples facettes caractéristiques des écosystèmes hydrothermaux. Le rétablissement au cours du temps peut être échelonné selon un système à cinq niveaux (ou 5 étoiles), représentant un gradient cumulatif allant d'un très faible rétablissement (1 étoile) à des conditions comparables à l'écosystème de référence (5 étoiles). L'annexe 1 définit les caractéristiques nécessaires pour atteindre ces différents niveaux pour l'ensemble des attributs.

Dans le cadre de ce travail, les scientifiques doivent également mettre en place des indicateurs et/ou des métriques afin de quantifier le rétablissement de chaque attribut au cours du temps. Par exemple, la comparaison de la richesse taxonomique, à un instant donné du rétablissement, avec les valeurs de l'état de référence, permet de renseigner sur le niveau de rétablissement de l'attribut « Composition spécifique ». D'autre part, la mesure des facteurs environnementaux donnent généralement des indications sur le rétablissement des « conditions de l'habitat ».

Tableau A. Liste des attributs et des sous-attributs identifiés pour estimer le rétablissement des communautés hydrothermales à la suite d'une perturbation

ATTRIBUTE	SUB-ATTRIBUTE	DEFINITION
Habitat conditions	Substrata physical	General characteristic of substrata (porosity, composition etc.)
	3D topography	Tridimentionnal structure complexity of substrata, (cracks, chimneys etc.)
	Water chemo-physical	Temperature regime, chemicals (CH_4, H_2S, Fe, O_2 etc.)
Species composition	Native communities	Diversity of typical dominant vent fauna
	Opportunistic mobile fauna	Diversity of mobile fauna dependant of vent species
	Microbial diversity	Community composition of microbial mats and symbiotic microorganisms
Structural diversity	3D biogenic structure	Habitat complexity provided by engineer species (Bivalves shell, tubeworms etc.)
	Densities and biomass	Total densities and biomass of organisms within assemblages
	Population demography	Presence of a large range of organisms size, multiples cohorts
Ecosystem functioning	Trophic diversity	Diversity of basal sources of food-web
	Trophic interactions	Presence of all trophic levels and trophic complexity
	Reproduction	Sufficient number of mature individuals to reproduce and maintain population
External exchanges	Larval dispersal	Ability to spawn and disperse larvae toward other habitats
	Larval recruitment	Arrival and settlement of larvae from local or far areas
	Local migration	Migration of organisms from adjacent habitats
Absence of threats	Science sampling impact	Specimen removed or disturbed by sampling
	Natural disturbance	Variability of abiotic factors or major disturbance events (e.g. volcanic eruption)
	Light and noise	Light and noise induced by scientific activities

I.3. Résilience des écosystèmes hydrothermaux

À l'échelle du globe, les écosystèmes hydrothermaux affichent des caractéristiques faunistiques et géologiques divergentes d'une zone géographique à une autre. Les différences observées en termes de biologie des espèces, de stabilité des conditions environnementales, et de fréquences d'occurrence de perturbations naturelles majeures peuvent se traduire par différentes capacités de résilience des communautés (Gollner et al. 2017). La caractérisation des aptitudes de rétablissement des communautés hydrothermales, en réponse à une perturbation, passe notamment par une bonne compréhension des mécanismes de recolonisation et de succession écologique.

I.3.1. Colonisation et succession écologique

Le succès de colonisation et la dynamique temporelle des communautés hydrothermales résultent de mécanismes complexes qui demeurent à ce jour mal compris. Les connaissances actuelles sont le résultat d'études menées à la suite d'éruptions volcaniques dans l'océan Pacifique (Tunnicliffe et al. 1997, Nees et al. 2008 ; Marcus et al. 2009 ; Mullineaux et al. 2010 ; Gollner et al. 2013, Gollner et al. 2015a), par le suivi temporel des communautés lors de retour sur zone (Sarrazin et al. 1997, Cuvelier et al. 2011, Sen et al. 2014), ou via le déploiement de substrats de colonisation (Van Dover et al. 1988 ; Mullineaux et al. 2003 ; Kelly et Metaxas 2007 ; Cuvelier et al. 2014a ; Gollner et al. 2015b ; Zeppilli et al. 2015 ; Plum et al. 2017 ; Baldrighi et al. 2018, Alfaro-Lucas et al. 2020). Les communautés microbiennes sont les premiers colonisateurs de ces environnements à la suite de la création d'un nouvel habitat (Shank et al. 1998, Figure I.11). La dispersion et le recrutement de différentes espèces de métazoaires à partir de communautés adjacentes constituent ensuite des étapes-clés dans la colonisation de ces habitats et des facteurs critiques de la viabilité des populations qui s'y installent (Van Dover et al. 1988 ; Mullineaux et al. 2000, 2010 ; Adams et al. 2012). L'établissement d'assemblages faunistiques plus complexes est dépendant de la stabilisation des conditions environnementales qui rendent l'habitat soutenable et influencent les différentes étapes de la succession écologique (Tunnicliffe et al. 1997 ; Sarrazin et al. 1997, Shank et al. 1998, Sarrazin et al. 2002 ; Marcus et al. 2009). Dans l'océan Pacifique, des études ont montré que l'installation des espèces symbiotiques s'effectue entre un et deux ans après l'ouverture d'un nouvel habitat et concorde avec une réduction de la couverture des biofilms microbiens (Tunnicliffe et al. 1997 ; Shank et al. 1998 ; Sarrazin et al. 2002 ; Mullineaux et al.

2010, 2012). Au cours des trois années suivantes, une phase de transition s'opère et les interactions biotiques (i.e. compétition, prédation, facilitation, etc.) entraînent un déclin progressif de l'abondance des espèces pionnières au profit d'une forte augmentation de la biomasse des espèces symbiotiques qui deviennent visuellement dominantes. La prolifération de ces espèces structurantes permet d'augmenter considérablement la surface tridimensionnelle et l'hétérogénéité de l'habitat, favorisant ainsi l'établissement d'autres espèces associées (Bergquist et al. 2003 ; Govenar et Fisher 2007 ; Lelièvre et al. 2018). Contrairement aux dorsales rapides, les systèmes hydrothermaux, caractérisés par une faible vitesse d'expansion, disposent d'un environnement plus stable et d'une faible fréquence d'éruptions volcaniques, si bien qu'à ce jour, peu d'événements de grande envergure ont été enregistrés (Copley et al. 2007 ; Cuvelier et al. 2011). De plus, aucun d'entre eux n'a réinitialisé ses communautés hydrothermales comme cela a pu être le cas dans l'Est Pacifique, si bien que de telles données sur la colonisation et succession écologique sont absentes au niveau de ces systèmes.

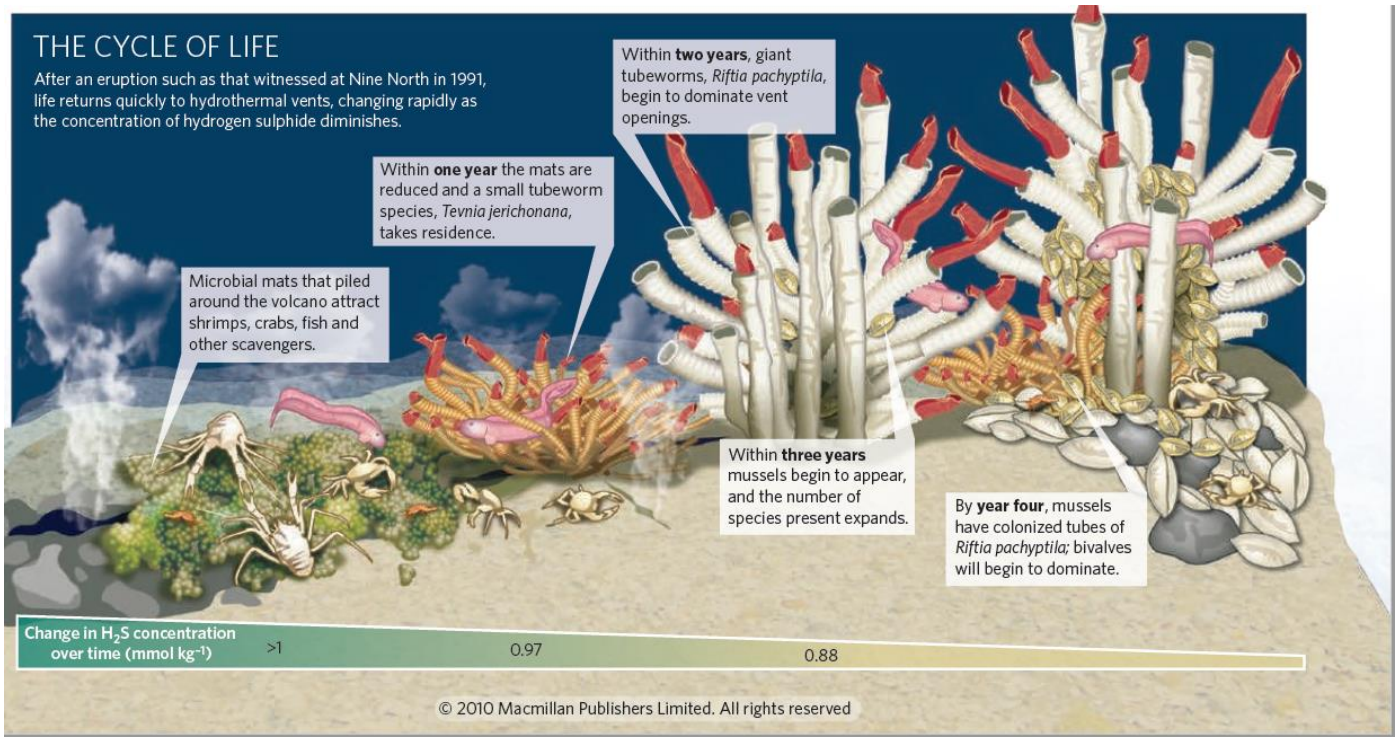

Figure I.11. Modèle conceptuel de succession des communautés hydrothermales sur la dorsale Est-Pacifique à la suite d'une éruption volcanique. Tiré de Qiu, 2010

I.3.2. Taux de rétablissement des écosystèmes hydrothermaux

À ce jour, l'essentiel des connaissances acquises sur le rétablissement des écosystèmes hydrothermaux à la suite de perturbations, se limite à des études réalisées au sein de systèmes d'expansion rapide. En effet, en raison de la forte dynamique temporelle qui les caractérise, plusieurs événements catastrophiques à grande échelle, principalement des éruptions volcaniques, ont été enregistrés et ont permis de suivre la dynamique de rétablissement des communautés dans les années suivantes. Ces événements peuvent entraîner l'éradication complète de la faune et induire des modifications de débit et de composition du fluide à l'échelle locale (Mullineaux et al. 2012). Des suivis temporels ont notamment été menés sur deux sites : entre 1993 et 1998 sur la dorsale Juan de Fuca (JdF, Tunnicliffe et al. 1997 ; Marcus et al. 2009) et entre 1991 et 2006 sur des édifices de la dorsale est Pacifique (East Pacific Rise (EPR), Shank et al. 1998 ; Nees et al. 2008 ; Mullineaux et al. 2010 ; Gollner et al. 2013 ; Gollner et al. 2015a). Ces études ont mis en évidence un rapide rétablissement de la densité d'organismes de macrofaune (17 % de la valeur pré-perturbation 1 an après l'éruption et 290 % après 2 ans) et de biomasse (12 % après 1 an et 102 % après 2 ans) sur la dorsale JdF (Marcus et al. 2009). Sur l'EPR, l'abondance totale a atteint une valeur comparable à l'état de référence, 4 ans après l'éruption de 2006 (Gollner et al. 2015a). En termes de diversité de macrofaune, la dorsale JdF affiche également un rapide rétablissement (75 % de rétablissement, 3 ans après l'éruption de 1998 et 90 % après celle de 1993 ; Tunnicliffe et al. 1997 ; Marcus et al. 2009), alors qu'elle semble plus lente sur l'EPR (69 % de rétablissement, 4 ans après l'éruption de 1991 et 55 %, 4 ans après celle de 2006) (Shank et al. 1998 ; Gollner et al. 2015a). L'étude de la composition faunistique au cours de la recolonisation a permis d'identifier des espèces pionnières généralement peu ou pas représentées au sein des assemblages de référence, comme c'est le cas pour le gastéropode *Ctenopelta porifera*, premier colonisateur sur l'EPR (Mullineaux et al. 2012). Au niveau de la dorsale JdF, les premiers organismes colonisateurs s'établissant 1 an après l'éruption volcanique de 1998 sont des vers polychètes brouteurs des familles des Polynoidae et des Dorvilleidae. Ces vers se nourrissent des mattes microbiennes présentes sur le substrat nu (Marcus et al. 2009). Au sein de ces deux systèmes de dorsale, la recolonisation et l'évolution temporelle des communautés, suite à une perturbation majeure, semblent être principalement influencées par la dispersion larvaire et le recrutement d'espèces en provenance des communautés environnantes (Van Dover et al. 1988 ; Mullineaux et al. 2010, 2012), la variabilité des

conditions physico-chimiques du milieu (Tunnicliffe et al. 1997 ; Marcus et al. 2009 ; Gollner et al. 2015a, 2017) ainsi que par les interactions biotiques telles que la facilitation, la compétition et la prédation (Shank et al. 1998 ; Mullineaux et al. 2003, 2012 ; Govenar et Fisher 2007 ; Kelly et Metaxas 2007 ; Marcus et al. 2009).

Par ailleurs des divergences méthodologiques apparaissent entre les différentes études évoquées précédemment, rendant toute comparaison du taux de rétablissement délicate. En effet, elles présentent des différences dans leur définition des communautés de référence (souvent non-échantillonnées et déduites d'études antérieures sur des sites voisins), les compartiments faunistiques étudiés (méga-, macro- et méiofaune) ou encore l'étendue spatiale considérée (tenant plus ou moins compte de l'hétérogénéité spatiale des assemblages au sein de microhabitats).

I.3.3. Estimation indirecte de la résilience des communautés hydrothermales

Le potentiel de recolonisation, et donc de rétablissement des communautés après une perturbation, peut aussi être décrit en étudiant la connectivité des populations (Lowe et Allendorf 2010 ; Baco et al. 2016 ; Boschen et al. 2016). Deux méthodes complémentaires peuvent être utilisées pour estimer cette connectivité : 1) des modèles biophysiques qui tiennent compte de la circulation océanique et des stratégies de reproduction des espèces afin de caractériser leur capacité de dispersion (Pradillon et al. 2001 ; Hilario 2005 ; Metaxas et Saunders 2009 ; Vic et al. 2018) et 2) des modèles basés sur la génétique des populations qui permettent d'estimer les flux géniques au sein des espèces et de détecter de potentielles populations-sources. Ces approches sont particulièrement informatives pour des systèmes qui ne sont pas, ou très peu, sujets à des perturbations naturelles et pour lesquels le suivi des processus de recolonisation est impossible.

Reproduction et dispersion des espèces hydrothermales

Dans un environnement où les sites peuvent être espacés de plusieurs centaines de mètres, voire des kilomètres, les capacités de dispersion et de colonisation des espèces jouent un rôle essentiel dans leur capacité de (re)coloniser de nouveaux sites. Le développement larvaire et le recrutement des individus sont des processus majeurs du cycle de vie des organismes hydrothermaux et jouent un rôle primordial d'un point de vue écologique et biogéographique. Cette capacité de dispersion est dépendante d'un grand nombre de processus reproductifs

intervenant en amont, depuis la gamétogénèse jusqu'à l'émission des larves (Figure I.12). Étant donné la difficulté de conserver les organismes hydrothermaux vivant en laboratoire, les principales descriptions du mode de reproduction et de la dispersion larvaire des espèces découlent d'observations anatomiques et histologiques des organes reproducteurs.

Certains processus reproducteurs semblent phylogénétiquement contraints (Tyler et Young 1999 ; Hilàrio 2005). C'est le cas de la gamétogénèse, qui englobe les processus de germination et de différenciation des gamètes et de la vitellogénèse, qui désigne le processus de maturation et de stockage des ovocytes. La fécondité, correspondant au nombre d'ovocytes produits par une femelle à chaque événement de ponte, conditionne le succès reproducteur des espèces. Certaines études ont montré une importante flexibilité de la fécondité au sein d'une même espèce en fonction des facteurs environnementaux tels que la température, la salinité ou la disponibilité de la nourriture (Stearn, 1992 ; Eckelbarger, 1994 ; Ramirez Llodra 2002).

Une fois les ovocytes fécondés, les embryons et les larves se développent dans la colonne d'eau et adoptent différents modes de nutrition en fonction des espèces. On distingue, en effet, les larves planctotrophes, capables de se nourrir activement de matière organique en suspension dans la colonne d'eau, des larves lécithotrophes, qui dépendent des réserves de vitellus présentes dans l'œuf. Le déploiement de pompes à larves et de trappes à sédiment à proximité des zones d'émission permet de quantifier et caractériser le pool larvaire et donc d'inférer sur le potentiel de dispersion et les mécanismes de colonisation de nouveaux habitats (Mullineaux et al. 2005 ; Metaxas 2011). Cependant, l'efficacité de ces outils est limitée et hautement dépendante des courants de fonds et la collection de larves reste difficile (Beaulieu et al. 2009). Le suivi de la distribution des larves d'organismes hydrothermaux aux abords d'édifices de l'EPR a mis en évidence une décroissance de leur abondance en s'éloignant des zones d'émission (Mullineaux et al. 2005). Ces résultats suggèrent une forte rétention des larves au sein de leur habitat d'origine et une dispersion relativement faible à destination des champs hydrothermaux voisins. Bien que le panache hydrothermal ait été considéré comme un mode de transport potentiel des larves sur de grandes distances dans la colonne d'eau (Mullineaux et al. 1995), l'abondance des larves s'est avérée plus importante près du fond que dans les couches supérieures de la colonne d'eau (Metaxas 2004 ; Mullineaux et al. 2005). En revanche, des modifications dans l'approvisionnement larvaire ont été

identifiées à la suite d'une éruption volcanique éradiquant les communautés locales, ce qui a permis de mettre en évidence une colonisation à partir de sites hydrothermaux potentiellement éloignés de plusieurs centaines de kilomètres (Mullineaux et al. 2010). En comparant la distribution larvaire avec un modèle théorique, Mullineaux et al. (2013) suggèrent que les larves de certaines espèces sont capables de se positionner, de manière active, au niveau du plancher océanique. Les larves subissent, par la suite, différentes métamorphoses au cours de leur vie planctonique jusqu'à devenir prêtes pour une implantation au sein d'un nouvel habitat, à condition que ce dernier dispose de conditions environnementales soutenables. Certaines études suggèrent que les larves seraient capables de détecter des signaux chimiques en provenance des émissions de fluide hydrothermal et de s'installer dans un habitat favorable à leur développement (Rittschof et al. 1998). D'autres travaux ont également mis en évidence la capacité pour certaines espèces de détecter des signaux chimiques émis par d'autres espèces (Mullineaux et al. 2000 ; Dattagupta et al. 2007). Le cycle de vie des espèces hydrothermales comprend donc un grand nombre de processus cruciaux qui jouent un rôle primordial dans leur capacité à maintenir une population effective au sein d'un habitat ainsi qu'à coloniser de nouveaux sites à plus ou moins grande échelle spatiale (Figure I.12).

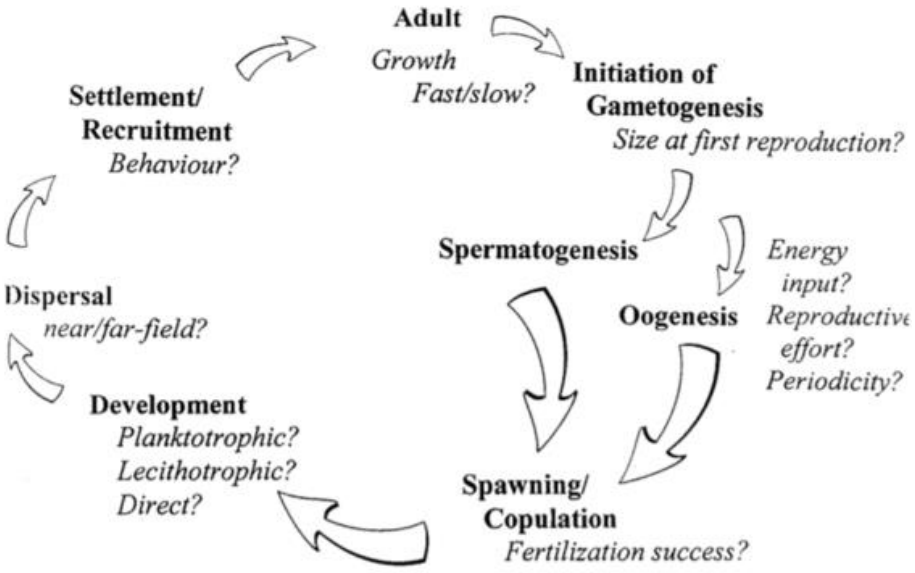

Figure I.12. Cycle de vie des invertébrés benthiques. Les différentes étapes sont représentées en gras et les questions relatives à chaque étape sont en italique. Tiré de Tyler et Young 1999

Connectivité des populations

D'autres études utilisent des modèles biophysiques de dispersion larvaire entre différents champs hydrothermaux pour évaluer le potentiel de résilience des communautés en réponse à une perturbation. Par exemple, Suzuki et al. (2018) ont combiné un modèle de dynamique de population et de dispersion larvaire des espèces-clés des communautés des bassins d'arrière-arc de l'ouest Pacifique au sein de 131 champs hydrothermaux afin d'estimer leur potentiel de rétablissement. Malgré la forte variabilité estimée du taux de rétablissement entre les sites, le temps évalué pour que les communautés retrouvent des abondances semblables aux assemblages de référence sont relativement longs (entre 6 et 130 années ; Figure I.13).

La génétique des populations, permettant d'inférer les flux géniques et les processus démographiques des espèces, constitue une autre approche indirecte pour étudier les modalités de dispersion des organismes et d'ainsi inférer la capacité de recolonisation des communautés. Par exemple, le long de la dorsale Est Pacifique, plusieurs espèces cryptiques - présentant plusieurs lignées évolutives - ont été identifiées suggérant une forte structuration spatiale et un faible flux génique le long de la dorsale (Hurtado et al. 2004 ; Matabos et al. 2008 ; Matabos et Jollivet, 2019 ; Vrijenhoek, 2009). En revanche, les populations *de Riftia pachyptila* et de *Bathymodiolus thermophilus* apparaissent comme relativement homogènes entre la dorsale Est Pacifique et celle des Galapagos (Hurtado et al. 2004 ; Won et al. 2003). Les différences observées entre ces espèces au sein d'un même environnement peuvent être expliquées par des divergences de traits d'histoire de vie (Hurtado et al. 2004). De nombreuses études font également état d'une importante homogénéité génétique sur des distances de plusieurs milliers de kilomètres, suggérant une forte connectivité pouvant permettre la recolonisation de milieux perturbés selon le concept de métapopulations (Beedessee et al. 2013 ; Roterman et al. 2016 ; Teixeira et al. 2013 ; Yahagi et al. 2015).

Ces approches indirectes permettent de contribuer à l'évaluation de la résilience de communautés peu impactées par des perturbations naturelles, mais disposent également de certaines limites (Breusing et al. 2016 ; Cowen et Sponaugle, 2009). En effet, les marqueurs génétiques utilisés pour les études moléculaires ne permettent pas toujours d'obtenir une résolution suffisante pour détecter des événements de dispersion récents. Par ailleurs, le réseau de connectivité entre deux sites peut être biaisé dans le cas où un site intermédiaire,

jouant un rôle dans la dispersion larvaire, n'est pas pris en compte. En ce qui concerne les modèles biophysiques, les principales limites sont dues à un manque de données pour la paramétrisation de la partie biologique, notamment à propos de la flottabilité et la durée de vie planctonique des larves (Hilário et al. 2015 ; Metaxas et Saunders, 2009). De plus, ces méthodes indirectes ne permettent pas d'identifier les différentes étapes de la recolonisation, ni d'estimer le rôle des facteurs biotiques et abiotiques au cours de ce processus. Il est donc primordial de les coupler avec des expérimentations *in situ* qui permettent l'obtention de données sur l'évolution de la diversité, de la densité, de la composition faunistique ainsi que d'identifier les espèces pionnières avec une meilleure résolution spatiale et temporelle. Ceci est d'autant plus essentiel dans un contexte où les environnements marins profonds sont de plus en plus sollicités par les activités anthropiques

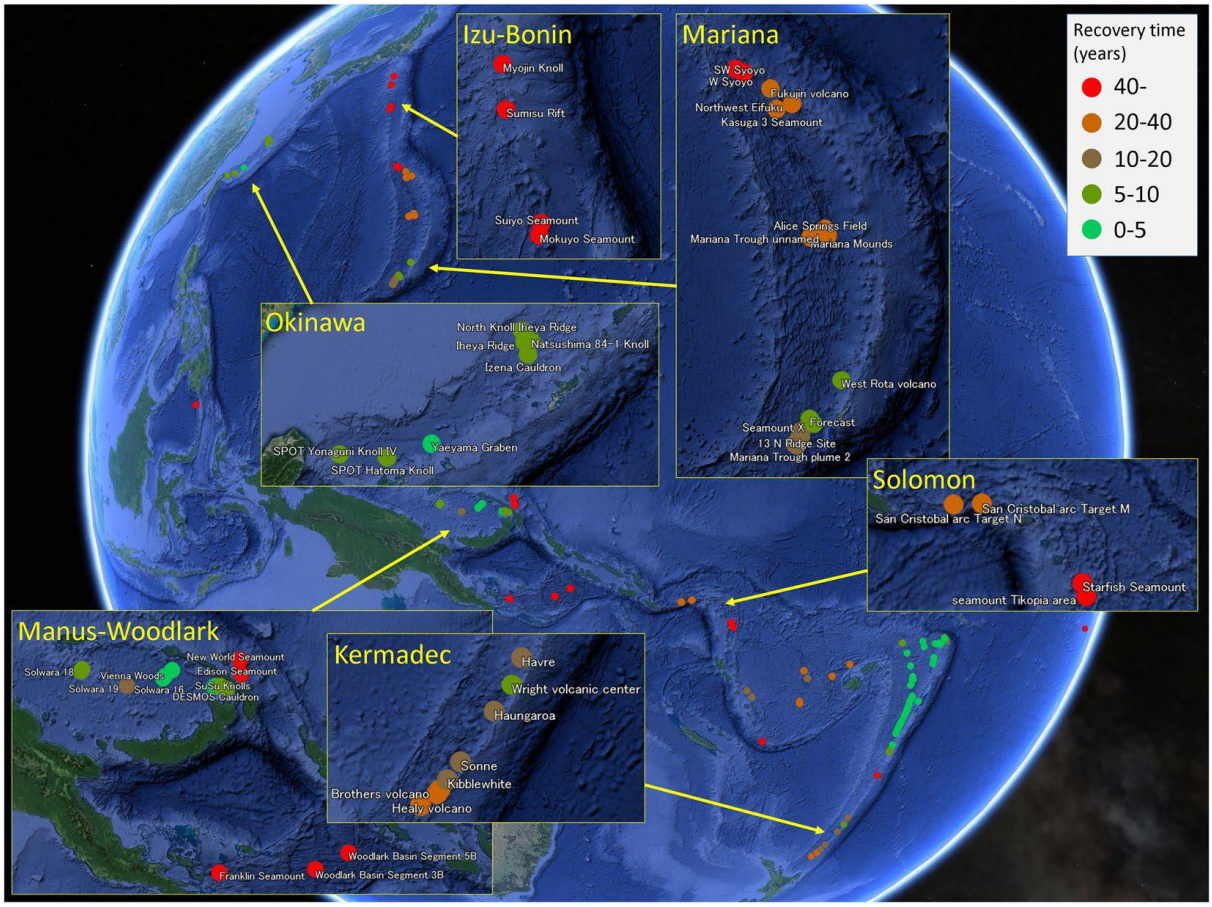

Figure I.13. Temps de rétablissement des communautés hydrothermales au sein de 131 champs hydrothermaux des bassins arrière-arc du Pacifique Ouest. Tiré de Suzuki et al. 2018

I.3.4. Potentiels impacts de l'exploitation minière profonde

Depuis quelques années, les compagnies minières affichent un intérêt de plus en plus grand pour l'exploitation minière des ressources minérales profondes (Wedding et al. 2015). Trois ressources minérales potentielles sont particulièrement ciblées : il s'agit des dépôts massifs de sulfures polymétalliques (SMS) associés aux sources hydrothermales (Hoagland et al. 2010), des encroûtements cobaltifères présents sur les monts sous-marins (Glasby 2000) et des nodules polymétalliques des plaines abyssales (Margolis et Burns 1976). La mise en application de l'extraction minière profonde aura pour conséquence d'induire des perturbations à grande échelle, auxquelles les communautés marines devront faire face (Van Dover 2011 ; Ramirez-Llodra et al. 2011 ; Boschen et al. 2013 ; Van Dover 2014 ; Levin et al. 2016 ; Gollner et al. 2017). La régulation des licences d'exploration et d'exploitation est gérée par un organisme onusien, l'Agence Internationale des Fonds Marins (AIFM), dans les eaux internationales (la Zone) et elle revient aux juridictions nationales dans les Zones Économiques Exclusives (ZEE) situées dans les eaux territoriales. Ainsi, la première licence d'exploitation des SMS a été délivrée à la compagnie *Nautilus Minerals* par le gouvernement de la Papouasie-Nouvelle-Guinée et concerne une superficie d'exploitation d'environ 10 hectares (Van Dover 2014). Cependant, l'entreprise ayant subi une faillite, aucune activité d'exploitation minière ne devrait avoir lieu sur ce site à court terme.

Les dépôts de sulfures polymétalliques des dorsales lentes, s'accumulent depuis plusieurs milliers d'années en raison de la faible activité tectonique, et constituent donc une cible privilégiée des compagnies d'exploitation minières (Hannington et al. 2011), par rapport aux dorsales rapides où les accumulations sont moindres. Les conséquences de l'exploitation minière des dépôts massifs de sulfures sur les communautés hydrothermales restent pour le moment incertaines, car il existe peu de connaissances sur les méthodes employées, leur étendue spatiale et temporelle, leur persistance et leur intensité. Cependant, plusieurs études se sont penchées sur les impacts qui pourraient être générés par de telles activités d'extraction et de collecte. Les impacts directs sur les écosystèmes incluent une éradication des communautés par destruction, fragmentation ou modification de l'habitat sur le site même de l'exploitation (Glover et Smith 2003 ; Van Dover 2011 ; Ramirez-Llodra et al. 2011 ; Hein et al. 2013). Une modification de l'activité hydrothermale ou de la composition du fluide risque d'impacter lourdement les communautés benthiques qui dépendent de la production

primaire chimiosynthétique aux abords des sources hydrothermales actives (Van den Hove et Moreau 2007 ; Coffey Natural Systems 2008 ; Baker et al. 2010). Les impacts indirects évoqués concernent notamment la production sonore, les vibrations et le rayonnement électromagnétique des engins déployés au fond (Gollner et al. 2017). La formation d'un panache de sédiment pourrait s'étendre nettement au-delà de la zone d'exploitation et impacter aussi bien les systèmes pélagiques que benthiques (Thiel 2003 ; Halfar et Fujita 2007 ; Coffey Natural Systems 2008 ; Baker et al. 2010 ; Van Dover 2011 ; Ramirez-Llodra et al. 2011 ; Van Dover 2014). En effet, l'action des chenilles ainsi que du broyage et de la collecte de la roche peut induire la dispersion du panache au fond, mais également dans la colonne d'eau le long des conduits d'extraction ainsi qu'en surface au moment du traitement des minerais à bord du navire (Glover et Smith 2003 ; Blake et al. 2009 ; Ramirez-Llodra et al. 2011 ; Boschen et al. 2013 ; Van Dover 2014 ; Figure 14). Le panache généré pourrait présenter de fortes concentrations en métaux lourds et avoir des impacts sur des organismes non-adaptés à ce type de sédiment (Natulis Minerals 2008 ; Boschen et al. 2013).

Dans le contexte d'une exploitation imminente de ces ressources, il apparaît urgent d'acquérir des connaissances fondamentales sur la résilience des écosystèmes hydrothermaux face à des perturbations naturelles ou anthropiques de grande envergure, afin de mettre en place des mesures pour minimiser les impacts potentiels, proposer des stratégies de mitigation et des plans de conservation, et évaluer le potentiel de restauration des communautés impactées.

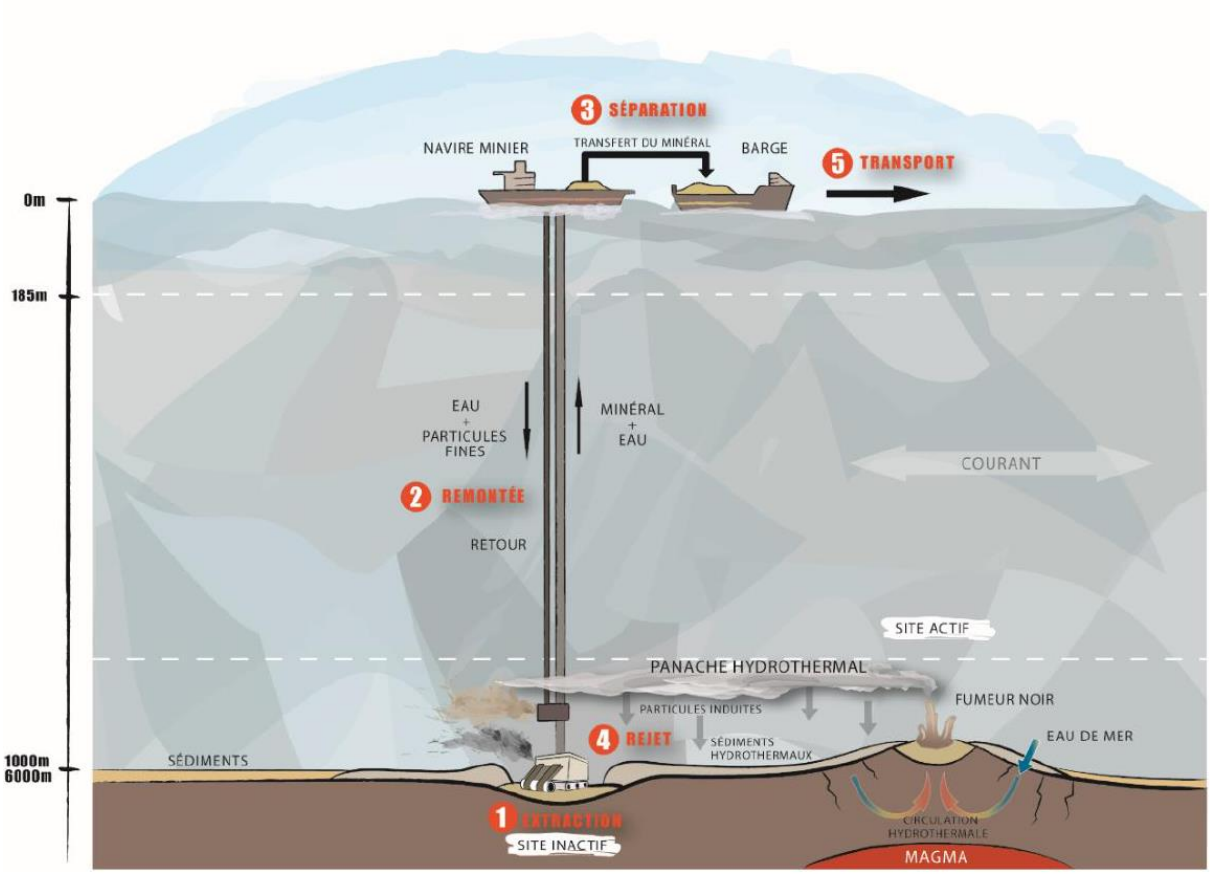

Figure I.14. Extraction des sulfures polymétalliques à proximité des sites inactifs hydrothermaux. Tirée de Sarrazin et Desbruyères, 2015.

I.4. Objectifs de la thèse

Cette thèse s'inscrit dans le projet européen H2020 MERCES (Marine Ecosystem Restoration in Changing European Seas) qui vise à comprendre le processus de restauration écologique de différents habitats marins dégradés afin de définir les cadres juridiques et de gouvernance nécessaires pour optimiser l'efficacité de différentes approches de restauration. L'objectif principal de cette thèse est de contribuer à l'évaluation de la capacité de résilience des communautés benthiques des sources hydrothermales, en réponse à une perturbation induite de défaunation. Plus spécifiquement, nous avons cherché à :

1) Caractériser la diversité et la structure des communautés de macrofaune des moulières à *Bathymodiolus azoricus* sur l'édifice hydrothermal actif Montségur (champ hydrothermal Lucky Strike, dorsale médio-Atlantique) en fonction des conditions environnementales.
2) Réaliser une première caractérisation quantitative des communautés adjacentes à Montségur au sein d'habitats sédimentaires en périphérie et d'une structure hydrothermale inactive.
3) Suivre, pendant 2 ans, le processus de recolonisation à la suite d'une perturbation en termes de structure des communautés (diversité, densité, structure démographique des populations) et d'écologie fonctionnelle (réseaux trophiques et reproduction des espèces dominantes) des communautés associées aux trois habitats.
4) Évaluer le rôle des facteurs environnementaux ainsi que des interactions biotiques sur ces processus de recolonisation.
5) Décrire la gamétogénèse de deux espèces hydrothermales clés, établir les liens avec la structure démographique des communautés et son rôle dans la dispersion des espèces hydrothermales dans un contexte de résilience.

Afin de répondre au mieux à l'ensemble des objectifs fixés dans ce projet de thèse, le plan du manuscrit se décline en 6 chapitres. À la suite de cette introduction, le **deuxième chapitre** visera à décrire l'expérience mise en place ainsi que les méthodes d'échantillonnage et d'analyse employées pour répondre à la problématique de la thèse. Le **troisième chapitre** aura pour objectif de caractériser la diversité et de décrire la composition faunistique des communautés de macrofaune benthique associées à l'édifice actif Montségur, une zone périphérique et un édifice inactif du champ hydrothermal Lucky Strike. Ce chapitre comprend

également le suivi du rétablissement de ces communautés en termes de diversité et de structure des populations, à la suite d'une perturbation de défaunation. Le **quatrième chapitre** porte sur la résilience fonctionnelle des communautés hydrothermales par le biais de l'étude de l'évolution du réseau trophique, de la composition biochimique et d'indices de conditions pour les espèces dominantes à différentes étapes du processus de recolonisation. Le **cinquième chapitre** est consacré à la description de la gamétogénèse et des traits d'histoire de vie de deux espèces abondantes de gastéropodes et à leur implication dans un contexte de résilience des communautés hydrothermales. Un chapitre de **synthèse et de perspectives** finalisera ce travail.

II. Matériel et méthodes

II.1. Site d'étude: le champ hydrothermal Lucky Strike

Le champ hydrothermal Lucky Strike (LS), situé sur la dorsale médio-Atlantique, se trouve au sud du point de jonction triple des Açores, où se rencontrent les plaques tectoniques nord-américaine, africaine et eurasienne (Desbruyères et al. 2001). Situé à environ 1 700 mètres de profondeur, LS se compose d'un lac de lave fossilisé entouré d'une vingtaine d'édifices hydrothermaux actifs (Figure II.1 ; Ondreas et al. 2009). Ce champ hydrothermal a fait l'objet de nombreuses campagnes océanographiques et abrite depuis 2010 un observatoire grand fond pluridisciplinaire, déployé dans le cadre du programme européen EMSO (*European Multidisciplinary Seafloor and water Column Observatory*). Cet observatoire, appelé EMSO-Açores, permet de récolter des données géophysiques, chimiques et biologiques en continu et de les transmettre par satellite grâce à une bouée située en surface.

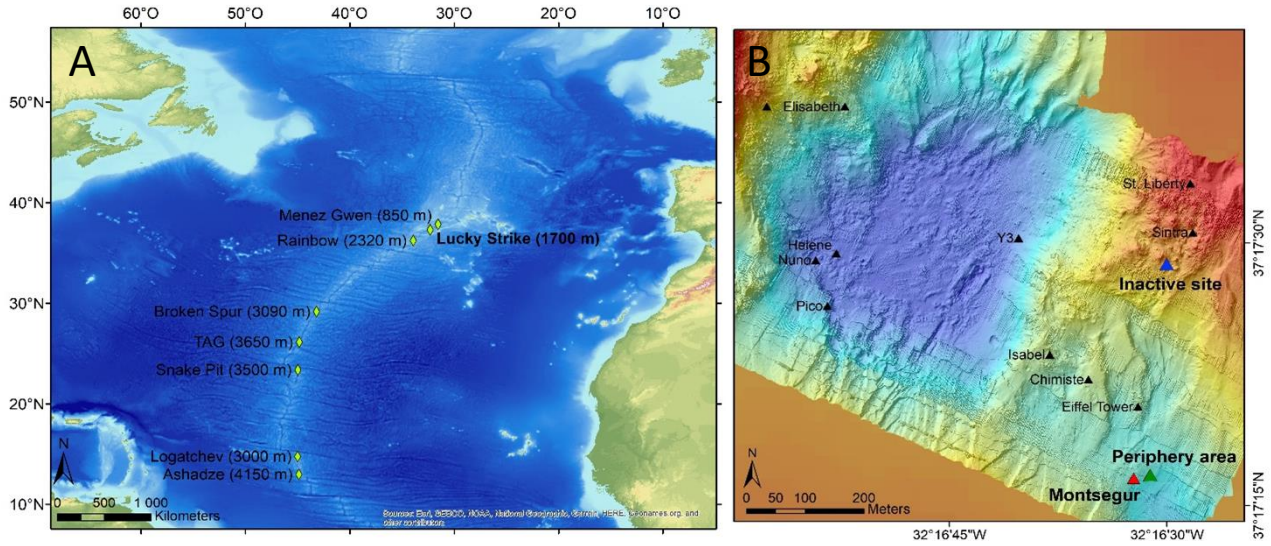

Figure II.1. A) Carte bathymétrique de la dorsale médio-Atlantique avec la position des différents champs hydrothermaux connus ; **B)** position des édifices hydrothermaux autour du lac de lave (triangles noirs) et des 3 sites d'étude : l'édifice actif Montségur (triangle rouge), une zone périphérique de cet édifice (triangle vert) et une cheminée inactive (triangle bleu).

Le principal site d'étude de ce travail est l'édifice Montségur, situé au sud-est du champ hydrothermal Lucky Strike (Figure II.1B). Montségur est un mont de sulfures d'environ 5 – 7

mètres de haut qui s'étend sur une surface de 24 m x 16 m sur du « slab[2] » hydrothermal (Langmuir et al. 1997). Au moins sept fumeurs noirs ont été identifiés sur ce mont et de nombreuses zones de flux diffus sont présentes au niveau de fissures sur le plancher océanique, à la base de l'édifice (Barreyre et al. 2014). Plus de la moitié de la structure est recouverte de denses populations de modioles *Bathymodiolus azoricus* abritant une faune associée (Figure II.2A). Une partie de l'expérience a également été conduite au sein de deux autres habitats considérés comme inactifs : 1) une zone en périphérie de Montségur (environ 30 mètres) caractérisée par une fine couche de sédiments meubles recouvrant le slab hydrothermal (Figures II.1B et II.2B) ; 2) une cheminée de sulfure inactive d'environ 5 mètres de haut située à 400 mètres au nord de Montségur et recouverte à sa base d'une fine couche noire d'oxyhydroxydes de manganèse (Figures II.1B et II.2C).

Figure II.2. Les trois sites étudiés au sein du champ hydrothermal Lucky Strike. **A)** Édifice actif Monségur ; **B)** Zone périphérique inactive ; **C)** Cheminée inactive**.**

II.2. La faune hydrothermale du champ Lucky Strike

De nombreuses études réalisées sur l'édifice hydrothermal Tour Eiffel, situé à 100 mètres au nord de Montségur, ont permis de décrire les patrons de biodiversité de la faune en fonction des paramètres environnementaux et des facteurs biotiques (Van Dover et al. 1996 ; Van Dover et Trask 2000 ; Desbruyères et al. 2001 ; Cuvelier et al. 2009, 2011b ; Sarrazin et al. 2015 ; Husson et al. 2017 ; Alfaro-Lucas et al. 2020 ; Girard et al. 2020, Sarrazin et al. 2020)

[2] Le slab est composé d'une consolidation de matériel volcanique et hydrothermal. Il comprend des fragments de verre basaltique et des cristaux de plagioclase, incrustés dans de la barytine et de la silice (Langmuir et al. 1997)

ainsi que leur dynamique spatio-temporelle (Cuvelier et al. 2011a ; Sarrazin et al. 2014). Les communautés faunistiques de Tour Eiffel sont visuellement dominées par l'espèce ingénieure *Bathymodiolus azoricus* accompagnée de plusieurs espèces associées. Au total, près de 79 espèces de méio- et macrofaune ont été identifiées à la suite d'échantillonnages sur l'édifice (Husson et al. 2017). Une relation positive a été mise en évidence entre la taille de *B. azoricus* et la température du fluide au sein de leur habitat, créant ainsi une zonation des populations (Sarradin et al. 1998 ; Comtet et Desbruyères 1998 ; Cuvelier et al. 2011b). Les modioles de grande taille (> 6 cm) occupent la partie haute du gradient environnemental et peuvent résister à des températures allant jusqu'à 20 °C (Desbruyères et al. 2001 ; De Busserolles et al. 2009 ; Husson et al. 2017). Les modioles de tailles intermédiaires (1,5 cm - 6 cm) colonisent préférentiellement le milieu du gradient, alors que les individus de plus petite taille (< 1,5 cm) s'établissent dans des environnements où la température est proche de celle de l'eau de mer ambiante, soit 4,6 °C (De Busserolles et al. 2009 ; Cuvelier et al. 2009).

Par ailleurs, une étude de la distribution des assemblages d'espèces associées a permis d'identifier trois types d'habitats distincts en fonction des conditions environnementales (Sarrazin et al. 2015) : 1) Un habitat chaud et variable, caractérisé par des températures supérieures à 6 °C, un faible pH et de fortes concentrations en fer et sulfures dissous, 2) un habitat froid et plus stable dont les températures n'excèdent pas 6 °C et avec de faibles concentrations en fer et sulfures dissous, et 3) un habitat aux caractéristiques intermédiaires. Ces conditions abiotiques peuvent varier très fortement dans l'espace, générant des différences dans les patrons faunistiques observés à l'échelle de quelques centimètres. Le pôle chaud est caractérisé par une faible richesse taxonomique et est préférentiellement colonisé par des crevettes *Rimicaris chacei* et *Mirocaris fortunata* ainsi que par des modioles de grande taille (Cuvelier et al. 2009 ; Sarrazin et al. 2015). Le pôle froid est, quant à lui, caractérisé par une plus grande diversité taxonomique et une répartition plus équitable des différentes espèces. Associées à l'espèce ingénieure *B. azoricus*, sept espèces indicatrices du pôle froid ont été identifiées : les polychètes *Branchipolynoe seepensis* et *Amphisamytha lutzi*, les gastéropodes *Lepetodrilus atlanticus* et *Protolira valvatoides* pour la macrofaune et les nématodes *Paracanthonchus*, *Microlaimus sp*. et *Cephalochaetosoma sp*. pour la méiofaune (Sarrazin et al. 2015). Une étude comparative de la distribution des assemblages a permis de

mettre en évidence une forte similarité de composition faunistique entre les édifices Tour Eiffel et Montségur (Sarrazin et al. 2020).

Les habitats périphériques autour des sites actifs demeurent très peu investigués et la caractérisation des communautés se résume principalement à des observations visuelles et/ou au déploiement de substrats de colonisation (Zeppilli et al. 2015 ; Plum et al. 2017 ; Baldrighi et al. 2018 ; Alfaro-Lucas et al. 2020). Les espèces observées en périphérie des zones actives comprennent principalement des filtreurs (hydraires, cirripèdes), de petits carnivores mobiles (amphipodes, isopodes, polychètes) ainsi que certaines espèces de poissons qui font également irruption au sein des habitats actifs pour se nourrir (Desbruyères et al. 2001 ; Alfaro-Lucas 2019). Les expériences de déploiement de substrats de colonisation en périphérie des zones actives ont mis en évidence de faibles densités d'organismes, une forte richesse spécifique chez les copépodes et les nématodes et la présence de plusieurs espèces « rares » (Zeppilli et al. 2015 ; Plum et al. 2017 ; Baldrighi et al. 2018).

II.3. Design expérimental

Afin de répondre aux objectifs de la thèse, une expérimentation *in situ* d'une durée de 2 ans a été mise en place sur l'édifice actif Montségur ainsi qu'au sein de deux habitats inactifs (zone périphérique et cheminée inactive). Le but de cette expérience a été d'induire pour la première fois une perturbation de défaunation à petite échelle (Figure II.3) et de suivre le processus naturel de recolonisation des assemblages de faune en ré-échantillonnant 1 an et 2 ans après la défaunation.

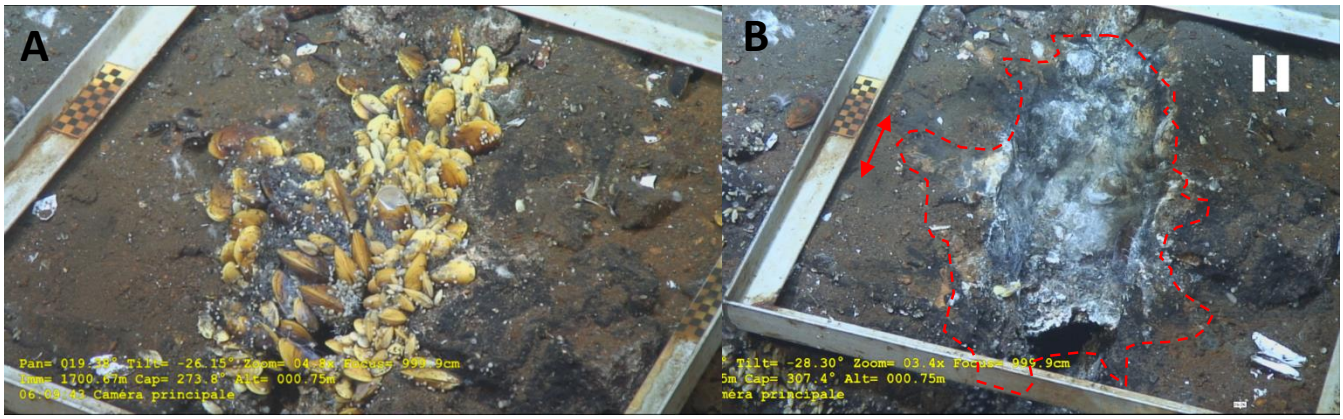

Figure II.3. Quadrat expérimental C1acg **A)** colonisé par un assemblage de *Bathymodiolus azoricus* avant la perturbation et **B)** dénudé après l'opération de défaunation. La flèche rouge illustre le damier utilisé pour calibrer le logiciel d'imagerie et estimer la surface d'échantillonnage (pointillés rouges)

Ce dispositif expérimental a été déployé en 2017 sur l'édifice Montségur au cours de la campagne Momarsat, à bord du N/O *Pourquoi pas ?* avec le sous-marin téléguidé *Victor6000*. Le plan d'expérience a été schématisé dans la Figure II.4 pour plus de clarté. Au total, 13 quadrats (50 cm x 50 cm) ont été installés au sein d'assemblages de *Bathymodiolus azoricus* (Figure II.2A) sur les flancs de l'édifice Montségur et dans des fissures à sa base. Comme le relief est escarpé, l'emplacement des quadrats a été choisi de façon aléatoire, en fonction des capacités d'accès du ROV et de la possibilité de déposer des quadrats. Parmi eux, huit quadrats appelés « quadrats expérimentaux » et notés « C » étaient dédiés au suivi des processus de recolonisation de la faune 1 an (quadrats notés « C1 ») et 2 ans (quadrats notés « C2 ») après la perturbation (Figure II.4). Pour chaque année, deux quadrats réplicats (notés « a » et « b ») ont été utilisés pour caractériser la variabilité de la dynamique de recolonisation. Les huit quadrats expérimentaux ont subi une opération de défaunation en 2017 et leur surface a été entièrement nettoyée à l'aide de la pince et de l'aspirateur du ROV (Figure II.3). Au-delà de l'objectif d'induire une perturbation, la faune de chaque quadrat a été récupérée et nous a permis de caractériser la structure initiale des communautés avant perturbation. À la suite de la perturbation, 4 des 8 quadrats expérimentaux ont été recouverts avec un grillage en plastique de maille 1 cm afin d'exclure les grands prédateurs mobiles (poissons, crabes, crevettes) et d'évaluer leur rôle sur le processus de recolonisation (Figure II.5D). Ces quadrats « cagés » sont notés « cg ». La faune des quadrats expérimentaux a, par la suite, été ré-échantillonnée 1 an (« C1 ») et 2 ans (« C2 ») après la perturbation pour évaluer le taux de rétablissement et comparer la structure des communautés et l'évolution du réseau trophique. L'ensemble des quadrats expérimentaux est représenté aux cours du processus de recolonisation sur la planche 1. En parallèle, des échantillons additionnels dits de « référence » (noté R) ont été réalisés sur l'édifice au cours des trois années d'échantillonnage afin de caractériser la dynamique naturelle des communautés sur Montségur et de la comparer à la recolonisation des communautés impactées (Figure II.4).

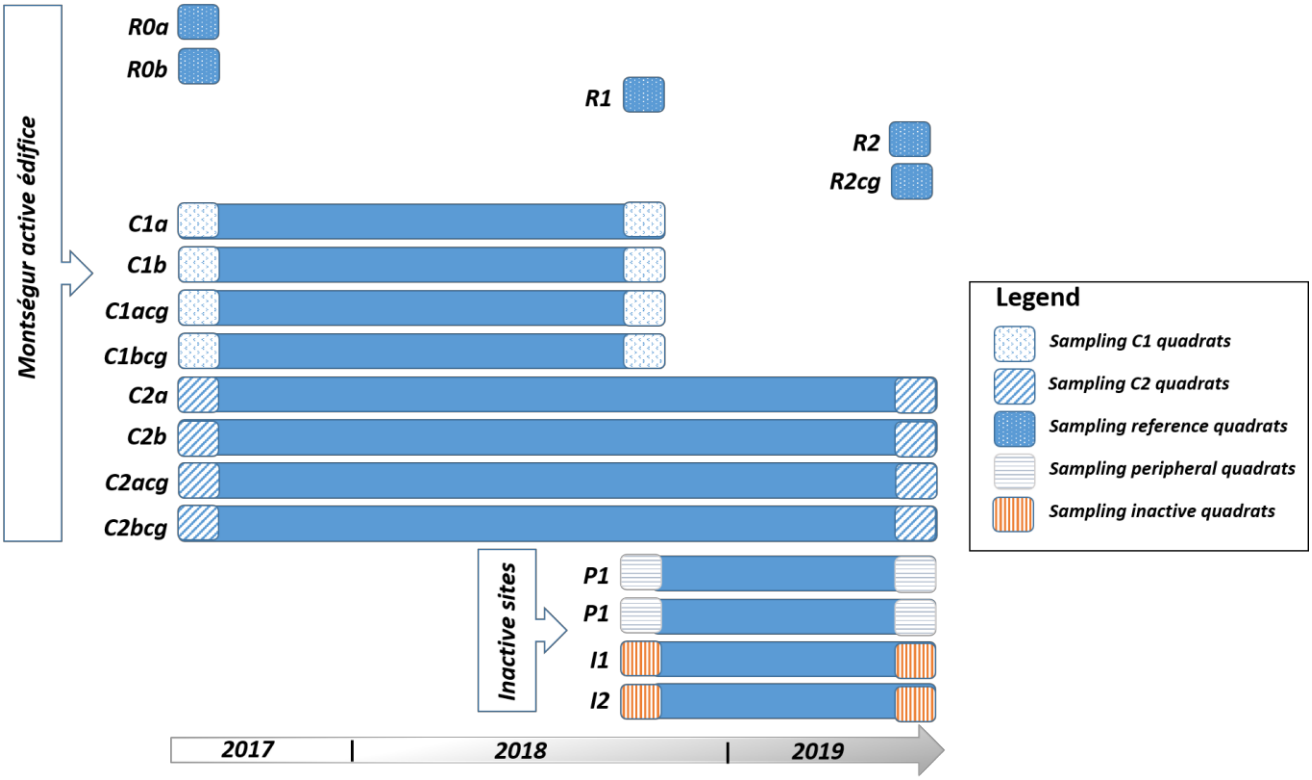

Figure II.4. Résumé du plan d'expérience mis en place pour le suivi de la structure des communautés hydrothermales en réponse à une perturbation induite. Les quadrats notés « R » représentent des échantillons de référence sur l'édifice Montségur. Les figurés représentent l'échantillonnage des quadrats et les rectangles bleus la période de recolonisation étudiée pour chaque quadrat. Les quadrats nommés C1 et C2 (quadrats expérimentaux) ont subi une défaunation en 2017 et ont été ré-échantillonnés respectivement 1 an et 2 ans après cette perturbation. Les quadrats déployés au sein des deux habitats inactifs ont subi une défaunation en 2018 et la dynamique de recolonisation n'a été étudiée que durant un an. Les quadrats notés « cg » ont été équipés de cages à l'issue de la perturbation afin d'exclure les prédateurs.

En 2018, l'expérience a été étendue à deux habitats inactifs via l'installation de 4 nouveaux quadrats : 2 réplicats en zone périphérique de l'édifice Montségur (P1 et P2, Figures II.1B et II.2B) et 2 réplicats sur un site inactif (I1 et I2, Figures II.1B et II.2C). Pour ces derniers, l'opération de défaunation a été menée en 2018 et les assemblages n'ont été ré-échantillonnés qu'en 2019 (Figure II.4).

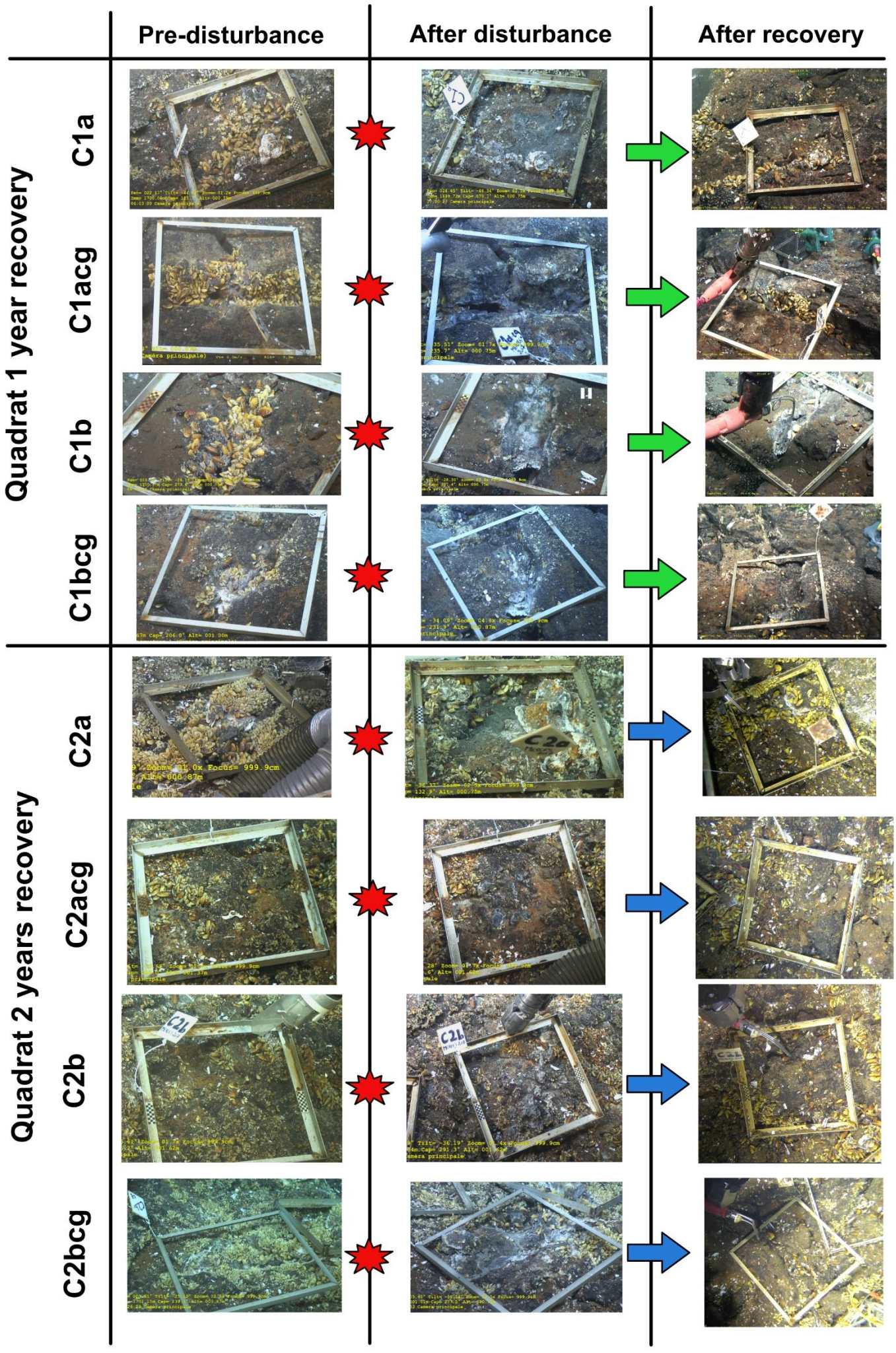
Pre-disturbance
After disturbance
After recovery
Quadrat 1 year recovery
C1a
C1acg
C1b
C1bcg
Quadrat 2 years recovery
C2a
C2acg
C2b
C2bcg

Planche 1. Ensemble des quadrats expérimentaux photographiés avant la perturbation (état de référence), juste après la perturbation et à l'issue de la recolonisation. La défaunation est schématisée par l'étoile rouge. Les flèches vertes représentent le processus de recolonisation durant une année et les flèches bleues durant deux années.

II.4. Caractérisation physico-chimique

Une caractérisation physico-chimique des habitats a été réalisée sur chacun des quadrats en collaboration avec Cécile Cathalot et Agathe Laës-Huon, toutes deux chercheures chimistes à l'Ifremer. L'analyseur chimique CHEMINI a permis de réaliser des mesures *in situ* du dioxygène (O_2), du fer total dissous (TdFe) ainsi que des sulfures totaux dissous (TdS). Le système de prélèvement d'eau PEPITO a permis d'échantillonner du fluide et de le filtrer avant une estimation en laboratoire des concentrations en cuivre (Cu), zinc (Zn) et méthane (CH_4). Chaque quadrat était également équipé de 2 sondes de température (iButtons^{TM}) séparées d'une dizaine de centimètres qui ont permis, grâce à des mesures en continu, de suivre l'évolution spatiale et temporelle de la température au cours des deux années de l'expérience. Des descripteurs simples de la température tels que la moyenne (T.avg), la variance (T.sd) le maximum (T.max) et le minimum (T.min) ont été utilisés pour caractériser l'habitat sur l'ensemble des assemblages échantillonnés.

II.5. Échantillonnage et préservation des échantillons

L'ensemble des échantillons a été récolté grâce à l'utilisation de la pince hydraulique des engins submersibles Victor6000 (ROV) et Nautile (sous-marin habitable) ainsi que de leurs aspirateurs à faune, plus efficaces pour échantillonner la faune mobile (Figure II.5). Par la suite, des images haute définition de la surface échantillonnée ont été réalisées afin de calculer l'aire d'échantillonnage pour chaque assemblage via l'utilisation du logiciel d'analyse d'images Image J © (Figure II.6, Schneider et al 2012). Ces mesures ont par la suite été utilisées pour estimer la densité d'organismes pour chaque assemblage. Une fois à bord, les échantillons ont été rincés et tamisés sur des mailles de 300 µm et 63 µm, permettant la séparation des groupes taxonomiques de la macrofaune de ceux de la méiofaune. En règle générale, il est considéré que les individus qui passent la maille de 1 mm appartiennent à la méiofaune (Giere 2008) mais l'utilisation de tamis à mailles plus petites (500 µm ou 300 µm) est courante dans les études des écosystèmes profonds (Montagna et al. 2017). Par ailleurs, il est commun que des individus plus gros appartenant à des groupes typiques de la méiofaune (nématodes/copépodes) se retrouvent dans les échantillons > 300 µm, particulièrement au

niveau des écosystèmes chimiosynthétiques. Dans cette étude, tous les organismes > 300 µm ont été considérés. Un premier tri des individus en grand groupe taxonomique a été réalisé à bord afin d'isoler quelques spécimens d'espèces cibles dans une solution de formol 4% pour des analyses histologiques et à - 80 °C pour les analyses isotopiques. Les autres spécimens ont été conservés dans une solution d'éthanol à 96 % qui permet une bonne conservation des tissus pour l'identification tout en assurant l'intégrité de l'ADN. Les échantillons de méiofaune sensu stricto (< 63 µm) ont été conservés au formol 4 % pour des analyses ultérieures.

Figure II.5. A) Caractérisation chimique à l'aide de la canule du submersible, réalisée avant et après l'échantillonnage, **B**) Aspiration de la faune à l'aide de l'échantillonneur de substrat dur, **C**) Collecte de la faune à l'aide de la pince du submersible, **D**) Quadrats cagés et non-cagés déployés au cours du processus de recolonisation.

II.6. Analyse de la structure des communautés

Au cours de ce travail, uniquement les assemblages de macrofaune (> 300 µm) et quelques individus appartenant à des taxa de la méiofaune de grande taille (nématodes et copépodes) ont été traités. Au total, l'ensemble des individus des 29 assemblages échantillonnés ont été triés et identifiés sous loupe binoculaire jusqu'au plus bas niveau taxonomique avec l'aide de spécialistes internationaux. Certains spécimens ont été sélectionnés par Dominique Cowart, post-doctorante du laboratoire, afin de réaliser des analyses moléculaires et de créer une banque génétique des espèces dominantes. La structure des communautés a été étudiée au

sein de chaque assemblage grâce à l'utilisation de descripteurs simples (richesse taxonomique, densité d'organismes, courbe de raréfaction) ainsi que d'indices de diversité α (indice de Shannon, et de régularité de Pielou). Des analyses multivariées (analyses en composante principale et analyses canoniques de redondance) ont également permis d'appréhender les patrons de distribution de la faune au sein des trois habitats étudiés et de caractériser la dynamique de recolonisation à la suite de la perturbation. L'ensemble des analyses ont été réalisées à l'aide du package « vegan » (Oksanen et al. 2019) du logiciel de traitement de données R (R Core Team, 2020).

D'autre part, des analyses de la structure démographique des 6 espèces dominantes au sein des assemblages de modioles ont été réalisées, comprenant : l'espèce ingénieure *Bathymodiolus azoricus* (Figure II.6A) et son ver commensal *Branchipolynoe seepensis* (Figure 21F), ainsi que le polychète *Amphisamytha lutzi* (Figure II.6E) et les gastéropodes *Protolira valvatoides* (Figure II.6B), *Lepetodrilus atlanticus* (Figure II.6C) et *Pseudorimula midatlantica* (Figure II.6D). Chaque individu a été mesuré de manière différente en fonction de l'espèce (Figure II.6). Les plus gros individus ont été mesurés à l'aide d'un pied à coulisse alors que les plus petits ont été traités grâce au logiciel de mesure intégré à la loupe binoculaire, avec une précision de 0,001 mm. La structure des populations a été décrite pour ces 5 espèces dans chaque échantillon à l'aide d'une représentation sous forme d'histogrammes de classes de tailles. L'erreur de mesure a été définie pour chaque espèce en mesurant 10 fois 10 individus. Des comparaisons de moyennes de tailles (test non-paramétrique de Wilcoxon-Mann-Whitney) ainsi que de distributions (test de Kolmogorov Smirnov) ont été réalisées entre les assemblages de référence et ceux échantillonnés 1 et 2 ans après la perturbation afin d'identifier les différents processus écologiques impliqués au cours de la recolonisation i.e. migration d'organismes adultes depuis les communautés environnantes ou recrutement de post larves issues d'une dispersion à plus grande échelle.

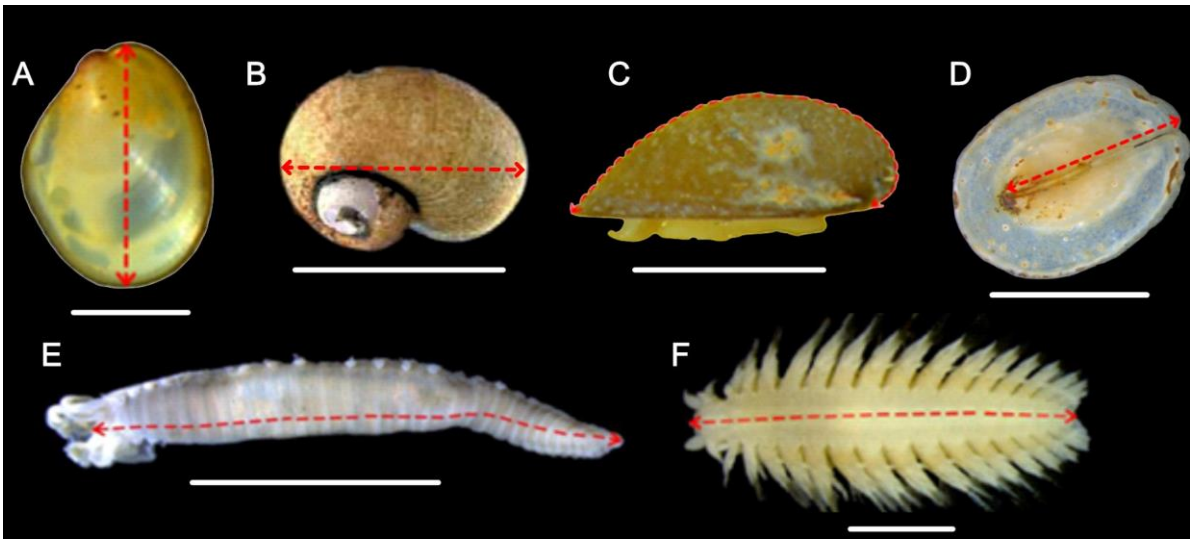

Figure II.6. Illustration des descripteurs de taille utilisés pour les espèces dominantes pour les analyses de structure des populations (flèches en pointillés rouge). **A**) *Bathymodiolus azoricus* : longueur maximale de la coquille ; **B**) *Protolira valvatoides* : largeur maximale de la coquille ; **C**) *Lepetodrilus atlanticus* : distance curvilinéaire, du bord antérieur de la coquille à l'apex ; **D**) *Pseudorimula midatlantica* : distance curvilinéaire **E**) *Amphisamytha lutzi* : longueur totale du corps *;* **F**) *Branchipolynoe* seepensis : longueur totale du corps. L'échelle blanche en dessous de chaque individu représente une mesure de 2 mm.

II.7. Analyse de la structure du réseau trophique

Afin de suivre l'évolution de la structure du réseau trophique au cours du processus de rétablissement, des analyses de biomasse ainsi que de compositions isotopiques ont été réalisées sur les différentes guildes trophiques et l'ensemble des espèces.

Le poids sec libre de cendres, ou perte au feu, équivaut à la masse de matière organique contenue dans un individu, et a donc été utilisé comme descripteur de la biomasse des différentes espèces au sein des assemblages. Pour *B. azoricus* et *B. seepensis*, une centaine d'individus ont été mesurés et pesés individuellement afin de tester la relation Longueur (L) / Biomasse (B). Pour ces deux espèces, une relation « puissance » significative a été établie selon : $B = 10^{-4,26} \times L^{2,39}$ pour *B. azoricus* ($R^2 = 0,98$) et $B = 10^{-6,31} \times L^{2,64}$, pour *B. seepensis* ($R^2 = 0,83$). Ces équations ont été utilisées pour estimer la biomasse totale de ces deux espèces pour lesquelles tous les individus ont été mesurés. Pour l'ensemble des autres espèces, en raison de leur faible biomasse et compte tenu de la précision de la balance, une biomasse individuelle a été obtenue en groupant plusieurs spécimens. Celle-ci a, par la suite, été multipliée par la densité d'organismes dans chaque échantillon pour obtenir une valeur de

biomasse totale. Les informations obtenues dans la littérature nous ont permis d'assigner les différentes guildes trophiques (symbiotiques, brouteurs, détritivores et prédateurs/charognards) à chacune des espèces.

Des analyses isotopiques du carbone ($\delta^{13}C$) et de l'azote ($\delta^{15}N$) ont été réalisées via la plateforme isotopes stables de l'IUEM afin d'obtenir des informations sur les relations trophiques entre les différentes espèces des assemblages. La structure du réseau trophique a été étudiée au cours du processus de rétablissement grâce à l'utilisation de métriques isotopiques à l'échelle de la communauté (Encart 3). Ces métriques sont basées sur la position relative des différentes espèces au sein de l'espace isotopique ($\delta^{13}C$- $\delta^{15}N$) de chaque assemblage (Layman et al. 2007 ; Jackson et al. 2011). Elles permettent notamment de quantifier la complexité du réseau trophique en estimant à la fois diversité trophique et redondance trophique au sein des différents assemblages. Ces métriques constituent également un moyen de comparer quantitativement les assemblages avant/après perturbation, et cagés/non-cagés, afin d'identifier des changements et de les relier aux patrons de diversité déjà décrits.

Encart 3 | Métriques isotopiques à l'échelle des communautés

L'espace isotopique $\delta^{13}C$- $\delta^{15}N$ occupé par l'ensemble des espèces d'une communauté peut être assimilé à la niche trophique réalisée (Bearhop et al. 2004). Récemment, de nouvelles approches analytiques, à l'échelle des communautés, ont été développées pour mesurer différentes facettes de la structure du réseau trophique à partir du bi-plot isotopique (Layman et al. 2007 ; Jackson et al. 2011 ; Cucherousset et Villéger 2015). Principalement, sept métriques ont été analysées dans ce travail afin de comparer la structure du réseau trophique des différents assemblages. Elles sont représentées de manière illustrative sur le bi-plot $\delta^{13}C$ - $\delta^{15}N$ de démonstration suivant. Sur ce graphique, les ressources basales sont représentées par des cercles, les consommateurs primaires par des triangles et les prédateurs par des losanges.

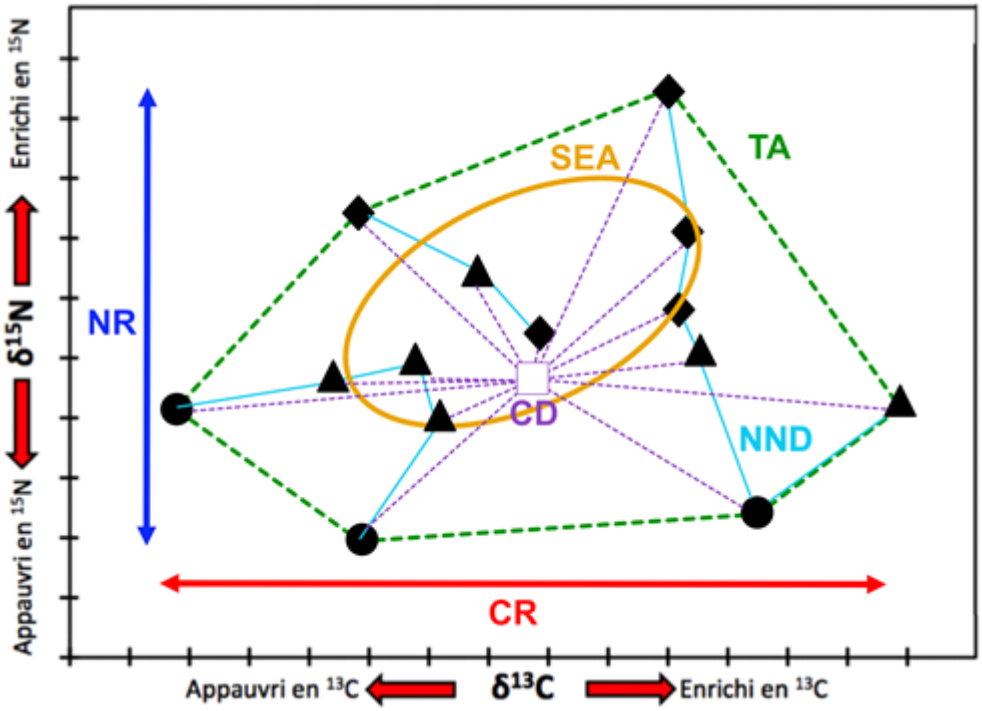

⟩⟩ **La gamme de $\delta^{13}C$** (**CR**) correspond à la distance entre les deux espèces avec les valeurs les plus enrichies et appauvries en ^{13}C et permet de rendre compte de la diversification des sources basales.

⟩⟩ **La gamme de $\delta^{15}N$** (**NR**) correspond à la distance entre les deux espèces avec les valeurs les plus enrichies et appauvries en ^{15}N et informe sur la longueur du réseau trophique

⟩⟩ **L'aire totale de l'enveloppe convexe** (**TA**) indique l'étendue de la niche occupée par l'ensemble des espèces et correspond à une mesure de la diversité trophique.

⟩⟩ **L'aire de l'ellipse isotopique** (**SEA**) correspond également à une mesure de l'étendue de la niche isotopique mais est moins sensible à la taille de l'échantillon et aux différences de richesse taxonomique

⟩⟩ **La distance au centroïde** (**CD**) correspond à la moyenne de la distance des différents points par rapport au centroïde du nuage de points. Elle informe sur le degré moyen de diversité trophique au sein d'un assemblage.

⟩⟩ **La moyenne et l'écart-type de la distance aux plus proches voisins** (**MNND** et **SDNND**) sont calculés à partir de la distance entre l'individu le plus proche de chaque espèce. MNND donne une information de la redondance trophique au sein de l'assemblage et SDNND correspond plutôt à une mesure de l'uniformité de répartition des différentes espèces dans l'espace isotopique.

II.8. Structure des populations et biologie de la reproduction des gastéropodes

Dans un premier temps, la structure démographique des deux espèces dominantes de gastéropodes *Protolira valvatoides* et *Pseudorimula midatlantica* a été étudiée dans chaque échantillon grâce à des mesures réalisées sur la coquille des individus (voir section II.6. Analyse de la structure des communautés). Le but de ces analyses est de déterminer l'existence de différentes cohortes dans la population établie, qui pourrait être une indication d'un recrutement discontinu. Pour chaque échantillon, la structure des populations a été présentée sous forme d'histogrammes de classes de taille d'intervalle 0,3 mm pour *P. midatlantica* et de 0,2 mm pour *P. valvatoides*. Ces intervalles de taille ont été choisis selon trois critères (Jollivet et al. 2000) : 1) la plupart des classes de taille doivent contenir au moins 5 individus ; 2) le nombre de classes vides adjacentes doit être réduit au maximum ; et 3) l'intervalle doit être nettement plus grand que l'erreur de mesure.

La gamétogénèse de ces deux espèces a été décrite à partir d'analyses histologiques effectuées sur les gonades en collaboration avec l'institut Norvégien de recherche sur le milieu aquatique (NIVA) et l'institut vétérinaire d'Oslo. Tous les individus utilisés pour ces analyses ont été préalablement mesurés et leur coquille retirée sous loupe binoculaire. Pour la patelle *P. midatlantica*, le corps mou a simplement été délicatement détaché de la coquille à l'aide d'une pince fine. Pour le gastéropode enroulé *P. valvatoides,* une décalcification des coquilles a été réalisée en plongeant les individus dans une solution d'acide chlorhydrique (HCl) à 10 % pendant 1 minute, puis le corps mou a été séparé du reste de la coquille à l'aide d'une pince et conservé dans du formol. Le corps mou des individus a ensuite été déshydraté dans des bains successifs d'éthanol pendant 8 h (70 %, 96 %, 100 %), puis passé dans un bain d'isopropanol pendant 2 h avant d'être rincé dans une solution d'*histoclear* et inclus dans un bloc de paraffine. Des coupes histologiques sériées d'une épaisseur de 7 µm ont été réalisées à l'aide d'un microtome sur les gonades de 58 individus de l'espèce *P. valvatoides* et 34 femelles de l'espèce *P. midatlantica* sélectionnés dans différents assemblages de l'édifice Montségur, de manière à étudier la variabilité spatiale en fonction des conditions environnementales. Une coloration des coupes à l'éosine et à l'hématoxyline, permettant de discriminer le cytoplasme (rose pâle) des noyaux (violet) de cellules en fonction de leur acidité, a été réalisée (**Encart 4**). Les gonades ont été observées au microscope et des images ont été

Encart 4 | Analyses histologiques de la gamétogenèse

Les coupes histologiques réalisées dans les gonades et la coloration à l'éosine et à l'hématoxyline nous ont permis de mettre en évidence les différents types d'ovocytes :

1) Les **ovogonies** (détourées en **vert**), qui sont le premier stade de développement des ovocytes, se différencient dans l'épithélium germinal. Sur les coupes histologiques, elles apparaissent comme de petites cellules avec un gros noyau coloré en violet, qui occupe la totalité de celles-ci.
2) Les ovogonies se développent ensuite en **ovocytes prévitellogéniques** (détourés en **bleu**). Ceux-ci sont plus gros et se différencient par la présence d'un cytoplasme basique (coloré en rose) plus volumineux.
3) Ces ovocytes vont ensuite subir la **vitellogenèse** (détourés en **rouge**), qui correspond à l'accumulation et au stockage de réserves nutritives, essentiellement composées de lipides, protéines, carbohydrates, d'acides aminés et d'acides nucléiques (Eckelbarger, 1994). Ces ovocytes se distinguent par leur apparence granuleuse visible sur l'ensemble de la cellule et par un faible ratio noyau/cytoplasme.

Chaque type d'ovocytes a été compté et mesuré sur plusieurs coupes histologiques (entre 3 et 10) de chaque individu. En effet, un minimum de 100 ovocytes a été nécessaire pour estimer leur distribution en classe de tailles au sein de la gonade et déterminer la présence de différentes cohortes, témoignant d'une production de gamètes quasi-continue (avec de très courtes périodes de pause). Uniquement les ovocytes sectionnés à travers le noyau ont été mesurés pour s'assurer qu'un ovocyte n'a pas été mesuré plusieurs fois sur des coupes différentes. La mesure utilisée est le diamètre de Feret, qui a été calculé par le logiciel Image J ® à partir du détourage de la surface totale de chaque ovocyte. Le diamètre de Feret est une mesure utilisée pour les objets ovoïdes irréguliers et correspond à une estimation du diamètre hypothétique qu'aurait cette forme si elle était un disque.

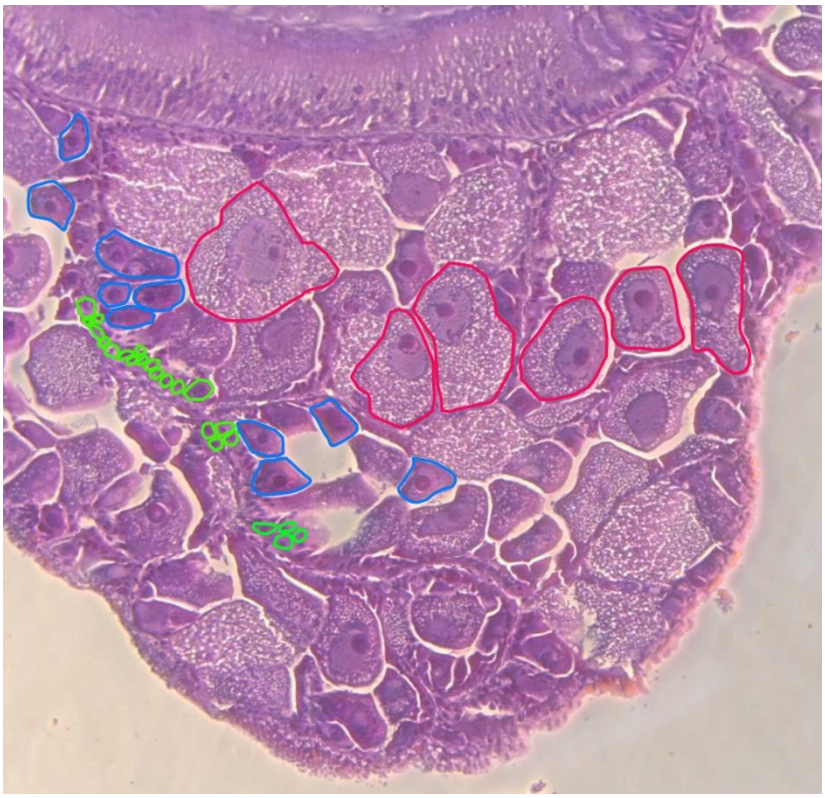

Coupe histologique dans la gonade d'une femelle de l'espèce *Pseudorimula midatlantica*. Les ovocytes sont détourés en fonction de leur stade de développement :

- **ovogonies (vert)**
- **pré-vitellogéniques (bleu)**
- **vitellogéniques (rouge)**

réalisées pour permettre de réaliser des mesures sur le logiciel de traitement d'image ImageJ© (Schneider et al 2012).

Les analyses histologiques nous ont permis d'obtenir des informations sur :

1) Le mode de reproduction des espèces, à savoir si les individus sont gonochoriques (i.e. individus mâles et femelles séparés) ou hermaphrodites (i.e. un même individu dispose à la fois de gonades mâle et femelle). Il est également important d'analyser plusieurs individus de tailles variables au sein d'une même espèce pour éventuellement identifier un hermaphrodisme successif (protandrie ou protérogynie).

2) La taille de maturité, définie comme la taille à partir de laquelle l'individu possède des ovocytes, afin d'identifier le moment à partir duquel les individus sont en mesure de se reproduire.

3) La période de ponte, pour savoir si la production de gamètes est continue au cours de l'année ou si une pause périodique est observée en fonction de la saisonnalité. La façon la plus précise de répondre à cette question serait d'échantillonner des individus d'une même espèce à différentes périodes de l'année et de mettre en évidence la présence ou l'absence d'ovocytes matures. Cependant, en raison de contraintes météo liées au déploiement des engins submersibles, une grande majorité des campagnes d'échantillonnage au niveau des Açores sont réalisées à la saison la plus propice rendant ainsi impossible l'utilisation de cette méthode. Dans ce cas, une approche alternative est mise en place. Cette méthode consiste à étudier la distribution des tailles d'ovocytes au sein d'un même individu. On considère que la production de gamètes est continue lorsque tous les stades de maturation des ovocytes (ovogonie, prévitellogéniques et vitellogéniques) sont présents au sein d'un même individu (**Encart 3**). Pour cela, un minimum de 100 ovocytes a été mesuré pour chaque individu en utilisant le diamètre de Féret et des histogrammes de fréquence de taille des ovocytes ont été construits. Des comparaisons de taille moyenne d'ovocytes et de synchronie du développement reproducteur entre les individus intra- et inter-échantillons ont été menées à l'aide de tests de Kruskall-Walllis.

4) La fécondité instantanée a été évaluée en comptant le nombre total d'ovocytes matures (i.e. vitellogéniques) et prêts à être expulsés au prochain événement de ponte

dans toute la gonade d'un individu. Cette mesure a été réalisée sur 10 individus de chaque espèce.

5) Le mode de nutrition des larves au cours de leur développement, à savoir si elles sont planctotrophiques et se nourrissent activement dans la colonne d'eau ou plutôt lécitotrophiques et dépendent des réserves contenues dans l'œuf pour se développer. En effet, la taille des ovocytes matures est couramment utilisée comme indicateur de mode de développement larvaire. Cela suppose que les ovocytes de plus grande taille accumulent plus de réserves permettant ainsi de fournir les ressources énergétiques nécessaires aux larves pour se développer lorsqu'elles sont dispersées dans la colonne d'eau. *A contrario*, lorsque les œufs vitellogéniques sont de plus petites tailles, il est considéré qu'ils ne permettent pas de subvenir aux besoins énergétiques des larves, au cours de la dispersion et que ces dernières se nourrissent de phytoplancton, de bactéries ou de détritus directement dans la colonne d'eau.

III. Rétablissement de la structure des communautés en réponse à une perturbation

Notre capacité à prédire la résilience des écosystèmes passe par la compréhension des mécanismes impliqués dans la structuration et le fonctionnement des communautés à différentes échelles spatiales et temporelles. Dans le cadre de l'évaluation du rétablissement d'un écosystème en réponse à une perturbation, la compréhension des processus de recolonisation revêt une importance capitale car ils conditionnent les modalités d'un retour à l'état d'équilibre. Les communautés hydrothermales sont naturellement soumises à des perturbations de grande envergure (e.g. éruption volcanique, séismes) pouvant conduire à la destruction de l'habitat et à l'éradication des assemblages qui s'y établissent (Juniper et Tunnicliffe 1997). À ce jour, l'essentiel des connaissances concernant le rétablissement des écosystèmes hydrothermaux ont été évaluées à la suite d'éruptions volcaniques au sein de systèmes de dorsales rapides (i.e. dorsale Juan de Fuca et est-Pacifique, Shank et al. 1998 ; Tunnicliffe et al. 1997 ; Marcus et al. 2009 ; Gollner et al. 2015). *A contrario*, en raison de l'importante stabilité des conditions environnementales et de la faible fréquence d'occurrence de perturbations naturelles au sein des systèmes d'expansion lente (Perfit et Chadwick 1998), la capacité de rétablissement des communautés associées reste méconnue et demeure difficile à quantifier (Gollner et al. 2017). Sur la dorsale médio-Atlantique, et particulièrement sur le champ hydrothermal Lucky Strike, plusieurs études se sont intéressées aux mécanismes de colonisation d'un nouvel habitat grâce à des déploiements de substrats de colonisation (Cuvelier et al. 2014 ; Zeppilli et al. 2015 ; Plum et al. 2017 ; Baldrighi et al. 2018 ; Alfaro-Lucas et al. 2020). Ces études ont mis en évidence une forte influence des conditions environnementales sur la colonisation de la méga- et macrofaune au sein d'habitats actifs (Cuvelier et al. 2014 ; Alfaro 2020). En revanche, des patrons différents ont été observés pour les organismes de la méiofaune et d'importantes différences de composition des communautés ont été rapportées en fonction de la nature du substrat (i.e. substrat organique ou inorganique ; Zeppilli et al. 2015 ; Plum et al. 2017). D'autre part, le suivi à long terme des communautés hydrothermales sur un site actif du champ hydrothermal LS a mis en évidence une forte stabilité des assemblages à l'échelle de l'édifice sur une période d'une dizaine d'années (Cuvelier et al. 2011). Pour autant, à ce jour, aucune étude n'a permis de caractériser la dynamique de colonisation de ces communautés sur leur substrat naturel, ni de décrire les différentes étapes de la succession écologique qui aboutissent à l'atteinte d'un état d'équilibre.

Dans ce chapitre, nous avons utilisé une nouvelle approche expérimentale pour évaluer les processus de recolonisation et de succession écologique des communautés hydrothermales au sein du champ hydrothermal Lucky Strike, avec un focus sur la macrofaune (> 300 um). La mise en place de l'expérience de défaunation présentée précédemment (voir II.4 Design expérimental) nous a permis, dans un premier temps, de caractériser les assemblages de référence sur un édifice actif ainsi qu'au sein de deux habitats inactifs. Par la suite, la dynamique de rétablissement des assemblages en termes de diversité taxonomique, de densité d'organismes et de structure des populations a été décrite au cours de deux années consécutives à la perturbation induite. Le suivi des conditions environnementales et la mise en place d'une expérience d'exclusion des prédateurs nous ont également permis d'identifier le rôle des facteurs biotiques et abiotiques tout au long du processus de rétablissement. Les résultats de cette étude nous ont permis de proposer un premier modèle de succession des communautés hydrothermales au sein du champ Lucky Strike à la suite d'une perturbation.

Recovery of hydrothermal vent communities in response to an induced disturbance at the Lucky Strike vent field (Mid-Atlantic Ridge)

Marticorena J.[1]*, Matabos M.[1]*, Ramirez-Llodra E.[2,3], Cathalot, C.[4], Laes-Huon, A.[5], Leroux R.[6], Hourdez S. [7], Donval J-P. [4], Sarrazin J.[1]*

[1] *Ifremer, REM/EEP, F-29280 Plouzané, France*

[2] *Norwegian Institute for Water Research, Gaustadalleen 21, 0349 Oslo, Norway*

[3]*REV Ocean, Oksenøyveien 10, 1366 Lysaker, Norway*

[4] *Ifremer, REM/GM/LCG, F-29280 Plouzané, France*

[5] *Ifremer, REM/RDT/LDCM, F-29280 Plouzané, France*

[6] *Research Centre for Watershed-Aquatic Ecosystem Interactions, Université du Québec à Trois-Rivières, Trois-Rivières, QC G9A 5H7, Canada*

[7] *Observatoire Oceanologique de Banyuls-sur-Mer, UMR 8222 CNRS-SU, 1 avenue Pierre Fabre, 66650, Banyuls-sur-Mer, France.*

*Corresponding authors : Julien Marticorena (julienmarticorena@gmail.fr), Jozée Sarrazin (Jozee.sarrazin@ifremer.fr), Marjolaine Matabos (Marjolaine.matabos@ifremer.fr)

Graphical abstract

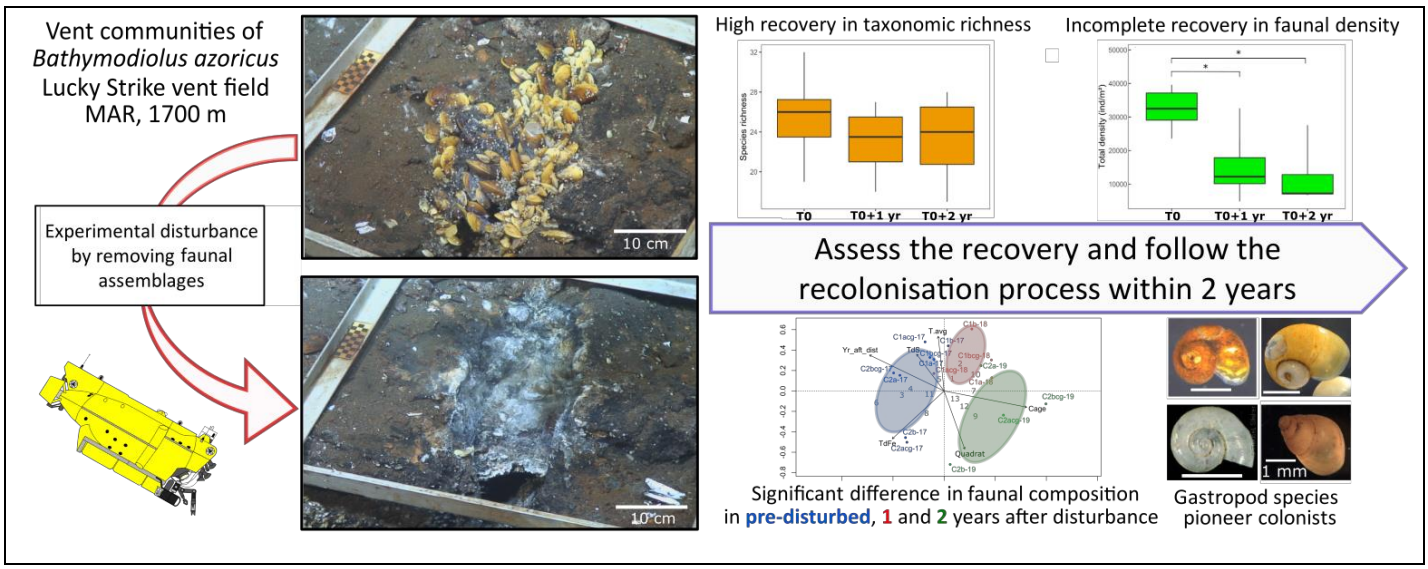

Abstract

Deep-sea hydrothermal communities experience large-scale natural disturbances such as volcanic eruptions, but might be soon impacted by anthropogenic activities related to mining. So far, the natural recovery of vent communities has only been evaluated at fast spreading centres, by monitoring faunal recolonisation after volcanic eruptions. In this study, we implemented a novel experimental approach by inducing a small-scale disturbance to assess the recovery potential of vent communities at a slow-spreading site along the Mid-Atlantic Ridge (MAR). We followed the recovery patterns of 17 macrofaunal assemblages among an active vent edifice, a peripheral area and an inactive structure at the Lucky Strike vent field. Within 2 years after the disturbance, almost all taxonomic richness had recovered, with the exception of a few rare species. However, we observed only a partial recovery of faunal densities and a change in faunal composition characterised by an increase in abundance of gastropod species, which are considered as the pioneer colonists of these habitats. A model of post-disturbance succession from habitat opening to climax assemblages for MAR vent communities highlights numerous knowledge gaps. This type of experimental approach, combined with dispersal and connectivity analyses, will contribute to fully assess the resilience of active vent communities after a major disturbance, especially along slow spreading centres targeted for seafloor massive sulphide extraction.

Key words: Hydrothermal vent; *Bathymodiolus azoricus*; Disturbance; Colonisation; Recovery; Deep-sea mining; Ecological succession; Benthic ecology; Mid-Atlantic Ridge

III.1. Introduction

Since the first discovery of hydrothermal vents and associated seafloor massive sulphide (SMS) deposits, more than 40 years ago, the interest of mining companies for commercial exploitation of their high metal content is increasing (Corliss et al. 1979; Spiess et al. 1980; Van Dover 2011). The recent development of deep-sea mining technologies (Nautilus Mineral 2008) and the rising number of exploration licenses in international waters (https://www.isa.org.jm) and within the Exclusive Economic zone (EEZ) of certain countries (e.g. Japan, Papua New Guinea) raise the question of the impacts of potential large-scale disturbances on benthic communities (Gollner et al. 2017). Active hydrothermal vent communities are considered as productivity hotspots with a high level of endemic fauna (Tunnicliffe 1991) that thrives mainly on chemoautotrophic primary production (Childress and Fisher 1992). Vent faunal assemblages are often dominated by symbiotic foundation species such as siboglinid tubeworms, mytilid mussels, large provannid gastropods or alvinocaridid shrimps, which promote local diversity by providing 3D structures and enhancing habitat heterogeneity (Dreyer et al. 2005; Govenar and Fisher 2007). Different levels of impacts due to SMS extraction are predicted on all faunal compartments, from those of inactive and surrounding peripheral areas to active vent communities (Boschen et al. 2013; Cuvelier et al. 2018; Orcutt et al. 2020). On the mining site, the main impact would be the physical destruction of habitats and the complete eradication of their faunal communities (Van Dover 2007). In addition, potential indirect impacts may affect different biological processes, such as reproduction, dispersal, mobility and feeding strategies (Van Dover, 2010; Boschen et al., 2013; Gollner et al., 2017; Suzuki et al., 2018; Washburn et al., 2019). However, there are still many uncertainties about faunal response and resilience, and the time-scale needed for a possible recovery of the impacted ecosystems (Cuvelier et al. 2018).

At active vents, the few examples of recovery are based on studies linked to large-scale natural disturbances caused by volcanic and tectonic activities (Butterfield et al., 1997; Tunnicliffe et al., 1997; Shank et al., 1998; Marcus et al., 2009; Gollner et al., 2015a). The frequency of such disturbances is highly variable among vent systems, depending on their geological settings. At fast-spreading ridges, where vent sites are separated by a few kilometers, volcanic eruptions occurs with time intervals of a decade (Tolstoy et al. 2006) and

macrofaunal communities are able to reach pre-disturbed diversity and densities within four years following the eruption (Tunnicliffe et al. 1997; Shank et al. 1998; Marcus et al. 2009; Gollner et al. 2015a, 2017, 2020). However, differences in community composition after re-colonisation are observed (Mullineaux et al. 2012). At slow spreading ridges, vent sites are separated by hundreds of kilometers (Beaulieu et al. 2015) and opportunities to observe natural disturbances are rare. Therefore, assessing the recovery ability of communities requires the use of alternative indirect approaches. One way is to use population connectivity data to estimate the recolonisation potential of key species, and thus infer vent community recovery rates (Baco et al. 2016; Breusing et al. 2016) as it was done by Suzuki et al. (2018). Their dispersal network analysis on species from 131 vent fields of the western Pacific Ocean estimated that a full recovery to original communities would take from 6 to 130 years. Another approach is with disturbance experiments designed to mimic mining activity as it was done on nodules from the Clarion-Clipperton zone (Jones et al. 2017) and at active vents in the Japanese EEZ (Toyohara et al. 2011).

Quantitative data on communities from vent peripheral areas and inactive vents remain scarce and are often limited to visual surveys and image analyses (Collins et al. 2012; Sen et al. 2014; Van Dover 2019). These habitats are characterised by lower densities of visible organisms as a result of lower energy inputs (Levin et al. 2016a; Van Dover 2019), but higher species richness compared to active hydrothermal edifices (Cowart et al. 2020). Peripheral and inactive megafaunal communities mainly consist of sessile, filter-feeding and slow-growing taxa, including sponges, corals, hydroids and holothurians, typical of deep-sea hard substratum habitats (Galkin 1997; Colaço et al. 1998; Collins et al. 2012; Sen et al. 2014; Van Dover 2019). The presence of vent endemic species with microbial symbionts on inactive chimneys has also been marginally reported (Desbruyères et al., 2001; Kouris et al., 2007, 2010; Soule et al., 2018). It was attributed to a recent cessation of venting, unreliable temperature measurements or to the presence of facultative nutritional mode (Van Dover 2019). However, with the exception of a few studies, almost no data is available on the smaller faunal compartments (macro- and meiofauna) of either peripheral or inactive structures. Van Dover et al. (2007) hypothesised that some taxa might be endemic to inactive vents, with specific adaptations to the unique chemical environment of weathering inactive deposits. Moreover, the presence of juveniles of typical vent species on peripheral areas near active

edifices in the Mid-Atlantic Ridge (MAR) (Plum et al. 2017, Alfaro-Lucas et al. 2020) and on the East Pacific Rise (EPR) (Gollner et al. 2015a) suggests a connection between active vent communities and those in surrounding areas. Evidence of organic matter consumption from chemoautotrophic origin has been reported at the periphery of vents (Alfaro-Lucas et al. 2020) as well as in inactive habitats of the Manus Basin (Erickson et al. 2009), highlighting the key link between active vents and their surroundings (Levin et al. 2016a). While inactive sites with massive deposits are preferentially targeted by mining companies (Van Dover et al. 2020), we cannot exclude that some impacts may reach active vent communities located in the vicinity.

In the present study, we provide an early evaluation of the recovery potential of active vent communities to a small-scale (< 1 m²) disturbance experiment initiated in 2017 on the Lucky Strike (LS) vent field, Mid-Atlantic Ridge (MAR). After removing the fauna, we followed during 2 years the recolonisation dynamics of *Bathymodiolus azoricus* mussel assemblages and their habitats on a series of experimental quadrats. The recolonisation dynamics of macrofauna at a peripheral site and inactive structure was also monitored over a year. This experimental setting allowed us to describe the pre-disturbed structure of vent communities on the Montségur edifice (LS) and to monitor the recolonisation of benthic communities after the disturbance. We also investigated the role of biotic and abiotic conditions on recolonisation dynamics, respectively, through the use of cages and measurements of environmental conditions. We anticipated only a partial recovery of the density and diversity of active vent communities two years after the induced disturbance. As observed at Pacific vent sites, we expected that microbial communities would first colonise the bare substratum, followed by grazers (Shank et al. 1998). The engineer species *B. azoricus* would take a few years to fully occupy the space, its presence facilitating the establishment of associated taxa and contributing to increasing diversity. We postulated that active vent communities colonising habitats with higher food inputs (active vents) should exhibit a faster recovery rate than those from the peripheral and inactive sites. Although the scale and target of this experiment strongly differ from the reality of large-scale mining, our results provide critical knowledge on recolonisation patterns of active and inactive hydrothermal vent habitats.

III.2. Material and methods

III.2.1. Study site

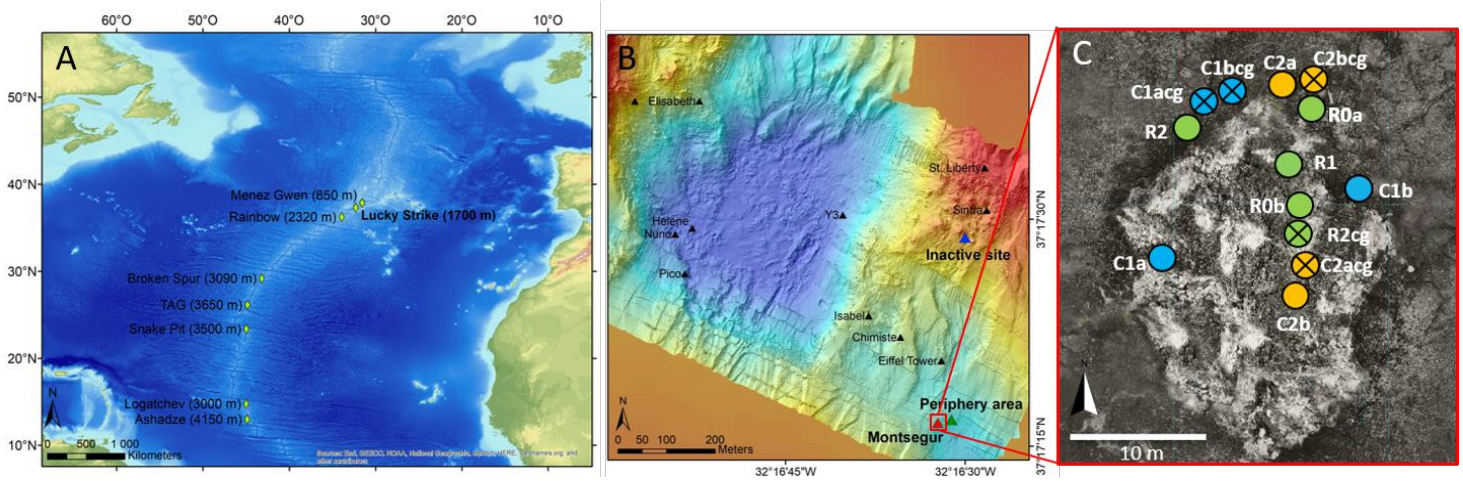

Figure III.1. A. Location of the Lucky Strike (LS) vent field along the Mid-Atlantic Ridge. **B**. Bathymetric chart of LS with the three study sites: (▲) the Montségur edifice, (▲) the extended peripheral area and (▲) the inactive site. **C**. Position of the experimental and reference quadrats on and around the Montségur edifice. Green circles represent the reference quadrats, blue circles represent the experimental quadrats used to study the recolonisation after 1 year, and orange circles represent the experimental quadrats used to study the recolonisation after 2 years. Crossed off circles represent "caged" quadrats while empty circles represent quadrats without cage.

The Lucky Strike (LS) vent field is a basalt-hosted vent field situated close to the Azores Triple Junction on the northern part of the Mid Atlantic Ridge (MAR) (Langmuir et al. 1997) (Figure III.1A). LS contains over twenty active hydrothermal edifices distributed around a circular fossil lava lake at an average depth of 1700 m (Ondreas et al. 2009). Montségur is a small active sulphide edifice that extends over a surface of 24 m x 16 m. It is located on a flat hydrothermal slab at the south-east of LS (Figure III.1B). At least seven black smokers have been identified on the edifice, in addition to the extensive diffuse low-temperature discharges through cracks at its base and on its flanks (Barreyre et al. 2014). Montségur is covered by dense mussel assemblages of the engineer species *Bathymodiolus azoricus* (Figure S1A). Vent faunal communities inhabiting diffuse flow areas on and around the edifice are characterised by high-density populations of gastropods (*Protolira valvatoides, Lepetodrilus atlanticus, Pseudorimula midatlantica*), polychaetes (*Branchipolynoe seepensis, Amphisamytha lutzi*) and shrimps (*Mirocaris fortunata*) (Sarrazin et al. 2020). In the present study, we also consider the macrofauna from a soft sediment pocket covering the slab at the extended peripheral area of Montségur (Figure III.1B, Figure S1B) and from a ~5 m height inactive structure (Figure III.1B) consisting of indurated sulphides. A yellowish low temperature precipitate formed by iron oxy-

hydroxides and amorphous silica and covered by a thin black layer of manganese oxy-hydroxides was present at its base (E. Pelleter, pers. com.; Figure 1B, Figure S1C). No hydrothermal activity or vent macrofauna were visible at the extended periphery nor at the inactive structure (Figure S1B and S1C).

III.2.2. Experimental setup

In 2017, an experimental setup was deployed during the Momarsat cruise on board the R/V "*Pourquoi pas ?*" using the Remotely Operated Vehicle (ROV) *Victor6000*. Thirteen stainless steel quadrats (50 x 50 cm), along with pyramidal structures aside, were installed over *Bathymodiolus azoricus* assemblages (Figure III.2), on the steep walls of the Montségur edifice or in cracks at its base (Figure III.1C). Eight of them, named "experimental quadrats", were devoted to the study of recolonisation processes following faunal clearance after 1 (C1) and 2 (C2) years (2018 and 2019 respectively). Replicate samples for each year were denoted as "a" or "b" (Figure III.1C). In addition to the experimental quadrats, five "reference" quadrats (R) were deployed and sampled in 2017 (R0a, R0b), 2018 (R1) and 2019 (R2, R2cg) to characterise the natural dynamics of faunal communities on Montségur throughout the experiment. The role of large mobile predators (crabs, shrimp or fish) on local recolonisation was examined by covering some of the pyramidal structures with a 1 cm plastic mesh; these specific quadrats were denoted as "cg" for caged (Figure III.2C). This experimental design is summarised in Table III.1.

In 2018, the experiment was extended to two additional habitats, first to describe the unknown macrofauna associated with peripheral and hydrothermally-inactive habitats, and, second to compare the recovery rates one year after faunal clearance between active vents, peripheral habitat and an inactive chimney. To do so, four new quadrats were deployed during the Momarsat 2018 cruise on-board the R/V *L'Atalante* with the ROV *Victor6000.* Two replicate quadrats were placed on a sedimented peripheral area (denoted as "P"), located ~30 m east of Montségur (Figure III.1B), and two others were placed on a small inactive structure (noted as "I"), 400 m north of Montségur and 70 m from the closest active edifice Sintra (Figure III.1B, Table III.1). Due to time constraints, there were no reference quadrats for these sites.

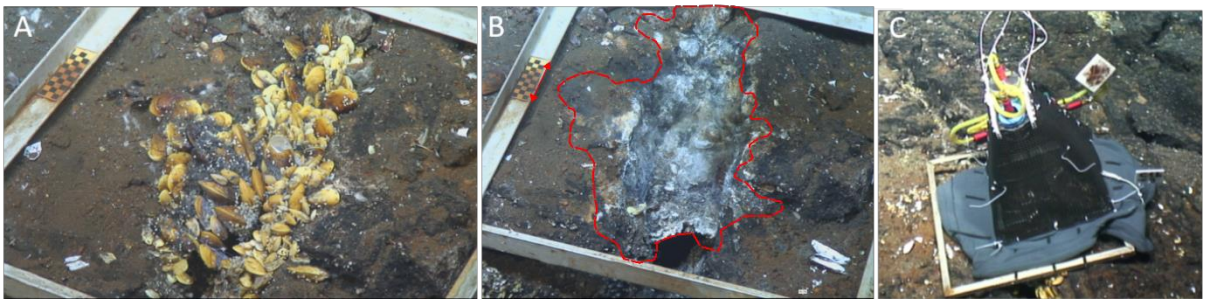

Figure III.2. The C1a-cg experimental quadrat in 2017, (**A**) before faunal clearance (baseline community) and ; (**B**) after the induced disturbance. Red arrow highlights the check board used to calibrate imagery analysis and estimate the sampling surface area (dotted line). (**C**) The C1bcg "caged" experimental quadrat used to exclude large (> 1 cm) mobile predators.

Table III.1. Details of each quadrat deployed as part of the disturbance experiment on the Montségur active hydrothermal edifice, at a peripheral area and at one small inactive structure on the Lucky Strike vent field (Mid-Atlantic Ridge). "FS-baseline": reference faunal sample to characterize baseline community on all years, "FS-disturbance": Induced disturbance by removing faunal assemblages and characterization of the baseline community; "FS-recovery": Faunal sampling after the disturbance to study recolonisation dynamics.

Quadrat	Type of quadrat	ROV operations			Cage
		2017	2018	2019	
Montségur active edifice					
R0a	Reference	FS-baseline			No
R0b	Reference	FS-baseline			No
R1	Reference		FS-baseline		No
R2	Reference			FS-baseline	No
R2cg	Reference			FS-baseline	Yes
C1a	Experimental – 1 year	FS-disturbance	FS-recovery		No
C1b	Experimental – 1 year	FS-disturbance	FS-recovery		No
C1acg	Experimental – 1 year	FS-disturbance	FS-recovery		Yes
C1bcg	Experimental – 1 year	FS-disturbance	FS-recovery		Yes
C2a	Experimental – 2 years	FS-disturbance		FS-recovery	No
C2b	Experimental – 2 years	FS-disturbance		FS-recovery	No
C2acg	Experimental – 2 years	FS-disturbance		FS-recovery	Yes
C2bcg	Experimental – 2 years	FS-disturbance		FS-recovery	Yes
Periphery					
P1	Experimental – 1 year		FS-disturbance	FS-recovery	No
P2	Experimental – 1 year		FS-disturbance	FS-recovery	No
Inactive structure					
I1	Experimental – 1 year		FS-disturbance	FS-recovery	No
I2	Experimental – 1 year		FS-disturbance	FS-recovery	No

III.2.3. Environmental characterisation

Temperature and key chemical parameters were assessed from *in situ* measurements on all quadrats before and after faunal sampling and this, for each year of the study (2017 to 2019). Our objectives were to identify the spatial and temporal variability of these factors and evaluate their role in the recolonisation processes. The *in situ* chemical analysers CHEMINI (Vuillemin et al. 2009) were used on three replicate points in each quadrat to measure dissolved concentration of total sulphides [TdS : $H_2S+HS^-+S_2$] and dissolved iron [TdFe : Fe (II)]. To complete the chemical characterisation, water samples were collected with the PEPITO water sampler at each quadrat prior to sampling (Sarradin et al. 2009). Oxygen concentrations were measured using an Aanderaa optode probe (Tengberg et al. 2006) connected to the outlet of the PEPITO sampler. Methane [CH_4], was analysed back in the laboratory by GC-FID and HID (Donval et al. 2008). Temperature was also monitored every 2 hours over the deployment period using two iButtons^{TM} probes attached to each quadrat and deployed directly on the mussel assemblages. Measurement resolution of these probes is 0.5°C. Finally, a reversing thermometer RMT 4002 X, with a measurement resolution of 10^{-4}°C, was used to obtain the sea water temperature of the bottom and make sure that the ROV probe was well calibrated. A total of 16 measures are made during a 3 second interval to estimate the mean and the standard deviation of temperature.

III.2.4. Faunal sampling and identification

During the Momarsat 2017 cruise, all eight experimental quadrats -noted “C”- were cleared of their fauna using both the suction sampler and the claw of of *Victor6000* mechanical arm (Figure III.2A, III.2B). R0a and R0b reference quadrats were also sampled, leading to a total of 10 quadrats used to describe the pre-disturbed vent community of Montségur (Table III.1). During Momarsat 2018, the four experimental quadrats dedicated to the “one-year after disturbance recolonisation study” -noted “C1”- and the reference quadrat R1 were sampled (5 quadrats in total; Table III.1). Moreover, the four quadrats deployed in the surrounding habitats (2 at the peripheral area, 2 on the inactive chimney) were cleared and their faunal communities removed. During the Momarsat 2019 cruise, the four experimental quadrats dedicated to the “two-year after disturbance recolonisation study” noted “C2”-and reference quadrats R2 and R2-cg were sampled (6 quadrats, Table III.1). In addition, the fauna from the four experimental quadrats on the peripheral area and inactive chimney were also sampled,

one year after the disturbance, leading to a total of 10 quadrats sampled in 2019 (Table III.1). The surface area of each quadrat was filmed before and after faunal sampling with the ROV high definition cameras to estimate the sampled surfaces using imagery analysis (Figure III.2A, III.2B). A target with 7 mm check board squares was fixed on each quadrat, providing scaling in the field of view (Figure III.2B).

On board, all faunal samples were washed on a 300 µm mesh sieve to recover all macrofauna species, and the samples were preserved in 96% ethanol. All individuals collected were identified to the lowest possible taxonomic level under a stereomicroscope and counted.

III.2.5. Population size structure

Size-frequency distributions of the six most dominant species were analysed for each sample of the Montségur edifice. Each individual was measured, using different measurements depending on the species (see details in Table III.2). The biggest individuals were measured using a calliper while small individuals were measured on screen to the nearest 0.001 mm, using the Leica Application Suite software. Measurement error was calculated as the maximum difference among 10 measurements of the same individual on 10 specimens comprising a range of all sizes for each species (Table III.2). For each assemblage sampled, length-frequency distribution was plotted for the six species. The size class intervals were chosen according to three criteria: i) most size-classes must have at least five individuals; ii) the number of adjacent empty classes must be minimized; and iii) the interval has to be greater than the measurement error (see Jollivet et al. 2000). Size-frequency distributions were compared to a normal distribution using a one-sample Kolmogorov-Smirnov test and differences between the pre-disturbed and post-disturbance communities were identified using a pairwise Kolmogorov-Smirnov test. Non-parametric Wilcoxon-Mann-Whitney tests were performed to identify differences in mean individual size between the pre-disturbed community and the novel one, after the recolonisation processes in each location.

Table III.2. Information about size structure measurements on the six most dominant species of the Montségur edifice, Lucky Strike vent field on the Mid-Atlantic Ridge.

Species	Measurement used	Measurement error (mm)	Interval of the size classes (mm)
Bathymodiolus azoricus	Maximum shell length	0.135	3
Protolira valvatoides	Maximum shell length	0.029	3
Amphisamytha lutzi	Maximum longitudinal body size	0.602	1
Branchipolynoe seepensis	Maximum longitudinal body size	0.193	1
Lepetodrilus atlanticus	Curvilinear distance	0.052	0.5
Pseudorimula midatlantica	Curvilinear distance	0.092	0.5

III.2.6. Data analyses

All analyses were computed in R environment (R Core Team, 2018). Species rarefaction curves were computed for each sample, habitat and year to verify the robustness of the sampling effort and characterise the overall diversity. Local diversity was estimated for each assemblage by computing α diversity indices such as species richness (S), Shannon entropy (H) and the Pielou's evenness index (J') using the vegan package in R (Oksanen et al. 2019). Contingency tables were pondered by the sampling surface for each quadrat for comparison purposes. The resulting density data were used for all subsequent analyses.

Environmental conditions – The temperature measured by the iButtons^{TM} probes were used to characterise each assemblage/quadrat. Four temperature parameters were compiled, including the average (T.avg), minimum (T.min), maximum (T.max) and standard deviation (T.sd). In addition, average concentrations of oxygen (O_2), methane (CH_4), dissolved iron (TdFe) and total sulphides (TdS) as well as standard deviations of TdFe and TdS were used to characterise the spatial variability of abiotic factors among the different quadrats of Montségur. A principal component analysis (PCA) was built with all environmental variables (packages FactoMineR and factoextra - Kassambara and Mundt 2019) to identify patterns in environmental conditions among quadrats and determine which variables accounted for most of the observed variance. Finally, Whittaker-Robinson periodograms, programmed in the R package *adespatial* (Dray et al., 2020) were used to screen for significant periodicities in temperature time series.

Community structure – A Principal Component Analysis (PCA) was performed to visualise differences in species composition between pre-disturbed communities of the three study sites: the active and inactive structures and the peripheral area. Therefore, for Montségur,

only the fauna from the experimental and reference quadrats sampled in 2017 was considered for this analysis. The pre-disturbed communities for the peripheral area and inactive structure are represented by the 2018 samples. The PCA was computed on Hellinger-transformed density data (Legendre and Gallagher, 2001). In addition, a canonical redundancy analysis (RDA) was used on Hellinger-transformed densities and environmental variables retained by a forward selection (vegan package - Oksanen et al. 2019) to evaluate how environmental conditions accounted for differences in species composition among and across habitats.

Recovery patterns – Faunal recovery patterns were assessed from experimental quadrats on the three sites. Differences in faunal composition among quadrats along the recolonisation processes were tested using an a non-parametric analysis of similarity (ANOSIM; Anderson 2001). The ANOSIM R value is based on differences in average ranking of dissimilarity indices (i.e., Bray-Curtis dissimilarity matrix) between and within the different predefined groups (here each recovery stage, i.e.: pre-disturbed state, one year and two years after disturbance). A RDA on Hellinger-transformed densities data was also used to identify the role of environmental conditions and biotic interactions (i.e. by testing the cage effect) on the structure of macrofaunal assemblages during the recolonisation processes. A variable named "quadrat" was used to evaluate the independence of the samples from the same quadrat over the years in the explanatory environmental matrix. Moreover, to test for the effect of time after disturbance, we coded a quantitative variable named "Yr-aft-dist" (i.e. year after disturbance). In this framework, pre-disturbed reference samples were considered as baseline communities at an equilibrium state and thus were coded with a value greater than 2 years. As the age of the natural community is unknown, analyses were run with different values [3 years, 10 years and 100 years] but they all yielded to similar results. Based on previous studies about the temporal stability of these communities (more than 14 years on Eiffel Tower, Cuvelier et al. 2011b) and data about recovery time in other vent system after a major disturbance (4/5 years, Gollner et al. 2017), we considered 10 years as a good compromise to be used for the analysis.

Table III.3. Environmental conditions on the baseline communities of the different quadrats deployed on the Montségur edifice (Lucky Strike vent field, Mid-Atlantic Ridge). Temperature: average: T.avg., standard deviation: T.std. maximum: T.max and minimum: T.min. from iButtons™. Oxygen (O_2). Total dissolved sulphide (TdS) and Total dissolved iron (TdFe) measured with the *in situ* analyser CHEMINI. Methane (CH_4) and pH were measured through quantitative analyses from samples collected with the PEPITO water sampler (Sarradin et al. 2009). Highest values are highlighted in bold and lowest values in grey.

Quadrat	T.avg	T.std	T.min	T.max	O_2 (µM)	TdS (µM)	TdFe (µM)	CH_4 (µM)	pH
					Mean ± SD				
Montségur									
R0a	*5.2*	*0.2*	*4.6*	*6.1*	*208.2 ± 0.1*	2.7 ± 0.2	0.2 ± 0.1	0.4	**7.8**
R0b	6.9	0.8	5.1	11.5	207.2 ± 0.4	3.1 ± 1.0	1.1 ± 0.3	0.5	7.6
R1	**9.5**	**2.7**	**6.1**	**22.1**	206.1 ± 1.1	2.3 ± 0.2	**2.2 ± 0.2**	**2.1**	7.2
R2	5.5	0.4	5.1	11.4	206.9 ± 1.3	3.2 ± 2.7	0.2 ± 0.1	0.9	7.5
R2cg	5.3	0.2	4.6	7.1	205.6 ± 0.6	0.9 ± 0.2	0.6 ± 1.1	*0.2*	7.9
C1a	6.1	0.3	5.1	7.1	207.4 ± 0.1	3.2 ± 0.8	0.2 ± 0.1	0.7	7.6
C1acg	5.8	1.2	4.6	12.1	204.3 ± 1.5	3.9 ± 2.6	0.3 ± 0.1	**2.1**	7.2
C1b	6.4	0.4	4.6	10.6	206.2 ± 1	**10.8 ± 14.7**	0.3 ± 0.3	1.1	7.4
C1bcg	5.7	0.42	4.6	8.1	207.9 ± 0.4	2.5 ± 0.6	0.2 ± 0.1	0.8	7.7
C2a	**7.6**	**1.12**	**6.1**	**16.1**	203.8 ± 2.1	**23.2 ± 26.3**	1.1 ± 0.3	**15.2**	6.1
C2acg	6.3	0.5	5	8.6	207.4 ± 0.8	1.3 ± 0.1	0.9 ± 0.8	0.7	7.7
C2b	5.3	0.2	5	*6.1*	205.2 ± 0.5	3.8 ± 3.8	0.9 ± 0.4	0.4	7.8
C2bcg	5.3	0.3	4.6	6.6	206.6 ± 0.3	5.6 ± 1.2	0.2 ± 0.1	**2.0**	7.2
Periphery									
P1	4.6	0.02	4.6	5.1	**224.1 ± 0.2**	0.40 ± 0.04	0.20 ± 0.02	0.08	**7.9**
P2	4.7	0.02	4.6	5.1	**223.7 ± 0.3**	0.40 ± 0.20	0.20 ± 0.04	0.03	**7.9**
Inactive structure									
I1	4.8	0.01	4.6	5.1	na	na	na	5.24	**7.9**
I2	4.8	0.02	4.6	5.1	na	na	na	0.24	**7.8**

III.3. Results

III.3.1. Environmental conditions

Mean temperature among the different quadrats of Montségur varied between 5.2°C and 9.5°C (Table III.3). R1 and C2a exhibited the highest maximum temperature, sulphide, iron and methane concentrations as well as the lowest pH and oxygen concentrations, while the reference quadrats R0a and R2cg displayed the opposite trend. Temperatures measured in the peripheral area and inactive structure (4.6 - 4.8°C) were close to that of the bottom seawater measured at LS (4.8°C ± 0.1°C). Similarly, the sulphide and iron concentration values were very low and close to the detection limit on the peripheral area. These environmental conditions are consistent with the absence of hydrothermal activity among these quadrats, except for quadrat I1 at the inactive site that displayed a relatively high concentration of methane compared to all other quadrats (Table III.3). This distinction between the inactive habitats (e.g. periphery and inactive chimney) and the Montségur quadrats was confirmed by the PCA constructed with environmental variables. The first axis accounted for 53.3% and the second axis for 17.3% of the total variance of abiotic conditions for the 17 studied quadrats (Figure III.3). The correlation circle of the PCA showed that the first axis was mainly correlated with the vent fluid influence with TdFe, TdS and CH_4 concentrations positively correlated with maximum temperature, while pH and O_2 concentrations were negatively correlated with temperature (Figure III.3A). However, due to an absence of sulphide, iron and oxygen measurements on the inactive chimney samples, we observe a discrepancy with the peripheral samples in the PCA. At the active site, the C2a and R1 quadrats were well separated on the PCA along the first and second axes (Figure III.3B) and were characterised by higher temperatures that reached respectively 16.1°C and 22.1°C but also higher concentration in TdFe and CH_4 associated with a more acidic pH (Table III.3, Figure III.3).

The two temperature probes separated by ± 10 cm deployed on each quadrat were used to characterise the spatial variability of abiotic conditions at fine scales. While homogeneous temperatures are observed within some quadrats (e.g. C1a, C1bcg, C2b, C2bcg), others showed a high variability of temperatures in the narrow spatial gradient (few centimetres, e.g. C1b, C2acg); (Figure III.S2). On the contrary, temperatures were homogeneous and extremely stable over time on both the peripheral site and inactive chimney (Table III.3).

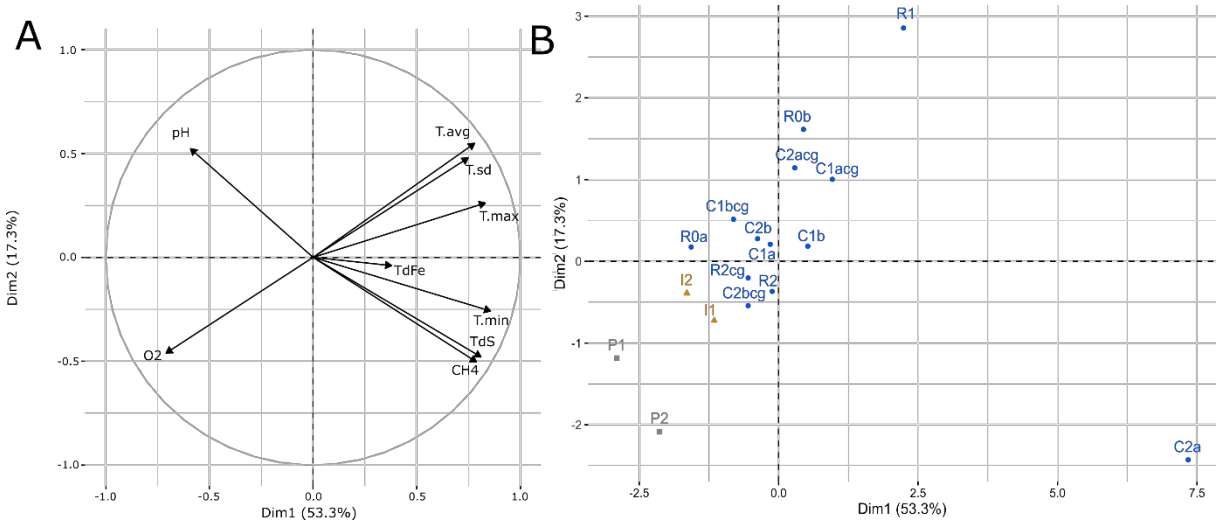

Figure III.3. Principal component analysis (PCA) of environmental variables measured on the 17 quadrats studied at the Lucky Strike vent field (Mid-Atlantic Ridge) from 2017 to 2019. The first axis explains 53.3 % of total variance of environmental factors while axis 2 explains 17.3 %. **A**. Correlation circle of variables used to build the PCA **B**. Projection of the different samples studied on the Montségur active edifice (blue), peripheral area (grey) and inactive site (orange). Environmental variables: Minimum temperature (T.min), maximum temperature (T.max), temperature average (T.avg), standard deviation of temperature (T.sd), mean concentration of total dissolved iron (TdFe), mean concentration of total dissolved sulphides (TdS), mean concentration of methane (CH4), mean concentration of oxygen (O2) and pH.

At the active site, notable differences in temperature on single quadrats between the two years were observed. C1b, C1acg and C2a quadrats showed a sharp decrease in mean and variability of temperatures at different times during the first year of deployment (Figure III.S2). Periodogram analyses carried out on temperature time series revealed significant periods of 12 h for most quadrats. In addition, significant periods of 24 h were also identified on all quadrats except C1acg. Additional periodic signals, possibly harmonics related to the tidal signal, with periods of 36 h and 48 h, were also revealed for C1a, C1acg and C1bcg.

III.3.2. Pre-disturbed communities

In total, more than 60% of the macrofaunal taxonomic richness (26 taxa over 43) was restricted to the active edifice, while 25% and 35% of taxa were exclusive to the periphery and inactive structure respectively. Four taxa were found in all environments, including the gastropod *Lurifax vitreus* and specimens which have only been identified to a higher taxonomic level (*Ostracoda sp.*, *Oncholaimus dyvae*, *Harpacticoida sp.*). Active vent communities shared 9 taxa exclusively with the peripheral area (*Glycera tesselata*, *Pseudorimula midatlantica*, *Lepetodrilus atlanticus*, *Lurifax vitreus*, *Xylodiscula analoga*, *Protolira valvatoides*, *Bathymodiolus azoricus*, *Aphotopontius sp.* and *Halacaridae sp.*) and 3

with the inactive structure (*Pseudotanais sp.*, *Sipuncula sp*. and *Cumacea sp.*). The peripheral site shared 8 taxa with the inactive structure (*Polynoidae sp*., *Haploniscidae sp*., *Epicaridae sp*., *Munnopsidae cf. Ilyarachna sp.*, *Tanaidacae sp.*, *Bythocypris sp.* and *Trachyleberididae sp*.)

Active vent community – The rarefaction curves built for each pre-disturbed sample of Montségur (Figure III.S3A) nearly reached an asymptote showing that the sampling effort was sufficient to capture the overall taxonomic diversity of macrofaunal benthic communities of the Montségur active edifice. In total, 43 taxa were identified among a total of 34 158 individuals in the different samples. Most assemblages were characterised by a taxonomic richness varying between 19 and 28 (Table III.4). The C1a sample, which is the only quadrat located on the west side of the edifice, displayed the highest taxonomic richness with the occurrence of 32 taxa, while R2 showed only 12 taxa among 133 identified specimens (Table III.4). Macrofaunal communities were dominated by six taxa: the engineer species *Bathymodiolus azoricus* and its commensal worm *Branchipolynoe seepensis*, the polychaete *Amphisamytha lutzi* and three species of gastropods *Lepetodrilus atlanticus*, *Protolira valvatoides* and *Pseudorimula midatlantica*. Together, they accounted for 68.3 ± 15.7% of the total abundance. The nematode *Oncholaimus dyvae* and copepod *Aphotopontius sp*., which are typical meiofaunal species, were also abundant in the > 300 µm fraction of most samples. In the pre-disturbed community, ~74% of taxa (e.g. 29 taxa over 43) can be considered as "rare" because of their low occurrence and abundance in the different samples (i.e. below 1% frequency).

Environmental conditions significantly explained the variance in macrofaunal community structure at Montségur. The RDA model performed on Hellinger-transformed species densities accounted for 49.6% (adjusted R^2: 25.1%, p = 0.008) of the total inertia in macrofaunal species assemblage structure (Figure III.4). The overall RDA model was significant (*p-value* = 0.004) and only the first axis was significant (p = 0.05), accounting for 20% of the variation in community structure. Maximum temperature (T.max) and sulphide concentrations (TdS) were the significant environmental factors influencing macrofaunal composition (p = 0.009 and 0.021, respectively). The years at which the samples were collected did not explain the differences between quadrats. R2cg sample stood out from the other sampling locations and was characterised by a high relative density of the gastropod

Table III.4. Univariate measures of macrofaunal community structure among the different quadrats sampled on the Lucky Strike vent field on the Mid-Atlantic Ridge

Habitat	Type	Year of sampling	Quadrat	Taxonomic Richness	Total density (ind.m^{-2})	Shannon index	Pielou's evenness
Montségur active edifice	Reference	2017	R0a	27	21 120	2.65	0.3
			R0b	26	68 960	2.9	0.33
		2018	R1	24	38 520	3.13	0.36
		2019	R2	12	3 330	2.59	0.38
			R2cg	23	17 980	3	0.35
	Baseline community	2017	C1a-17	32	36 350	2.77	0.29
			C1b-17	24	30 770	2.9	0.34
			C1acg-17	27	39 630	3.1	0.34
			C1bcg-17	25	49 420	2.47	0.28
			C2a-17	27	34 240	2.68	0.3
			C2b-17	22	24 610	2.21	0.26
			C2acg-17	19	29 630	2.53	0.32
			C2bcg-17	28	30 570	2.78	0.31
	1 year post disturbance	**2018**	**C1a-18**	**27**	**12 580**	**3.01**	**0.33**
			C1b-18	**18**	**4 850**	**2.98**	**0.38**
			C1acg-18	**22**	**11 890**	**2.96**	**0.35**
			C1bcg-18	**24**	**33 750**	**3.37**	**0.38**
	2 years post disturbance	**2019**	**C2a-19**	**28**	**7 180**	**3.52**	**0.38**
			C2b-19	**17**	**7 260**	**2.33**	**0.30**
			C2acg-19	**22**	**23 590**	**3.01**	**0.36**
			C2bcg-19	**26**	**6 730**	**3.49**	**0.38**
Periphery	Baseline community	2018	P1-18	16	6 440	3.45	0.45
			P2-18	17	2 440	3.36	0.43
	1 year post disturbance	**2019**	**P1-19**	**9**	**1 530**	**2.70**	**0.45**
			P2-19	**11**	**1 520**	**2.86**	**0.44**
Inactive edifice	Baseline community	2018	I1-18	14	3 330	3.38	0.46
			I2-18	14	4 520	3.19	0.44
	1 year post disturbance	**2019**	**I1-19**	**10**	**1 580**	**2.76**	**0.44**
			I2-19	**13**	**2 500**	**2.85**	**0.41**

Lurifax vitreus, contrasting with a low density of *B. azoricus* (Figure III.4). Moreover, the C2acg and R0b samples, characterised by a high density of amphipods (*Luckia striki*), formed a distinct group (Figure III.4). All other samples showed a quite homogeneous macrofaunal composition.

Peripheral area and inactive structure – The rarefaction curves of the peripheral area and inactive structure were far from reaching a plateau (Figure III.S3A), suggesting that the total diversity of those environments was underestimated. The pre-disturbed taxonomic richness of communities from the two samples from the peripheral area were 16 and 17 taxa, and 14 taxa for the inactive structure, much lower than that from the active vent edifice (Table III.4). The total density of organisms was also lower on the periphery and inactive structure than at Montségur, reaching 2 440 and 6 440 ind.m^{-2} on the periphery and 3 330 and 4 520 ind.m^{-2} on the inactive structure (Table III.4). The PCA computed on Hellinger-transformed macrofaunal densities showed distinct community composition in the two sampled habitats (Figure III.5). The first axis explained 30.2% of total variance in macrofaunal species densities. The community from the active Montségur site, characterised by *B. seepensis*, *B. azoricus, L. atlanticus* and *A. lutzi*, is well separated from those of the peripheral area and inactive structure, mainly characterised by isopod and tanaid species. The second axis explained 16.9% of total variance and clearly separated the peripheral samples from those collected on the inactive structure. The main taxa contributing to this axis were Harpacticoida copepods, characteristic of Inactive structure while polychaetes belonging to the Glyceridae and Syllidae families but also hydroids characterised peripheral area. The community composition of the periphery site appears to be more variable than that of the inactive structure (Figure III.5).

III.3.3. Recovery patterns of benthic communities

Recolonisation dynamics of the foundation species – The recovery rate of *Bathymodiolus azoricus*, in terms of density, varied between 9.7% and 37.6% on the different quadrats one year after disturbance, and from 1.9% to 33% two years after disturbance (Figure III.S4). No significant difference can be noticed between the mean recovery rate after 1 year (19.8 ± 13%) and 2 years of recolonisation (14.4 ± 13.5%) (Student test: t = 0.59, *p-value* = 0.58). However, with the exception of the C2bcg quadrat, the percentage of recovery was slightly higher in the quadrats that were caged during the recolonisation process (>20%) compared to the uncaged quadrats (<15%) (Figure III.S4). The size population structure analyses of *B. azoricus* showed

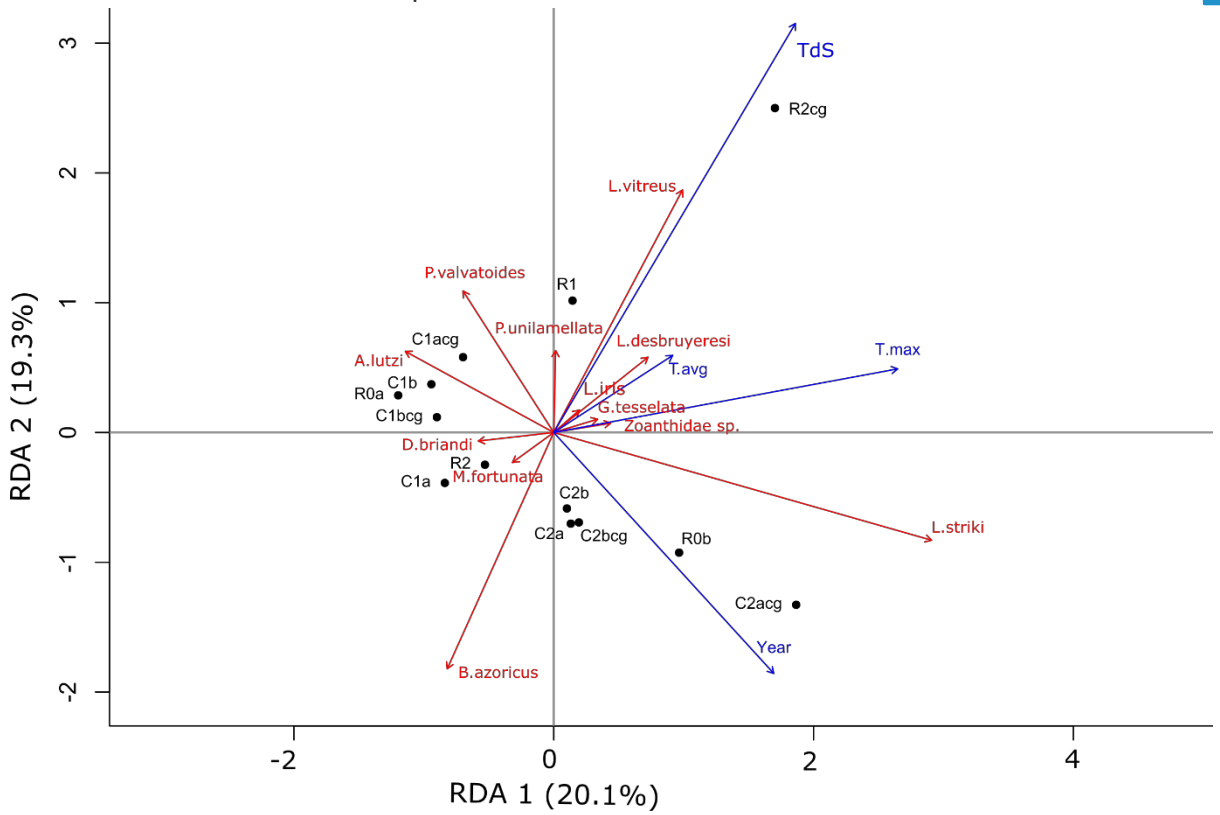

Figure III.4. Canonical redundancy analysis (RDA, scaling 2) of Hellinger-transformed macrofaunal densities observed in the baseline community of the Montségur active edifice at the Lucky Strike vent field (Mid-Atlantic Ridge). The first canonical axis represents 20.1 % of the total variance in macrofaunal densities while the second axis represents 19.3% (adj R^2 = 25.1%, p = 0.004). The first axis is significant (p = 0.05). Only species that accounted for more than 50% of cumulative inertia on the two first axis are represented.

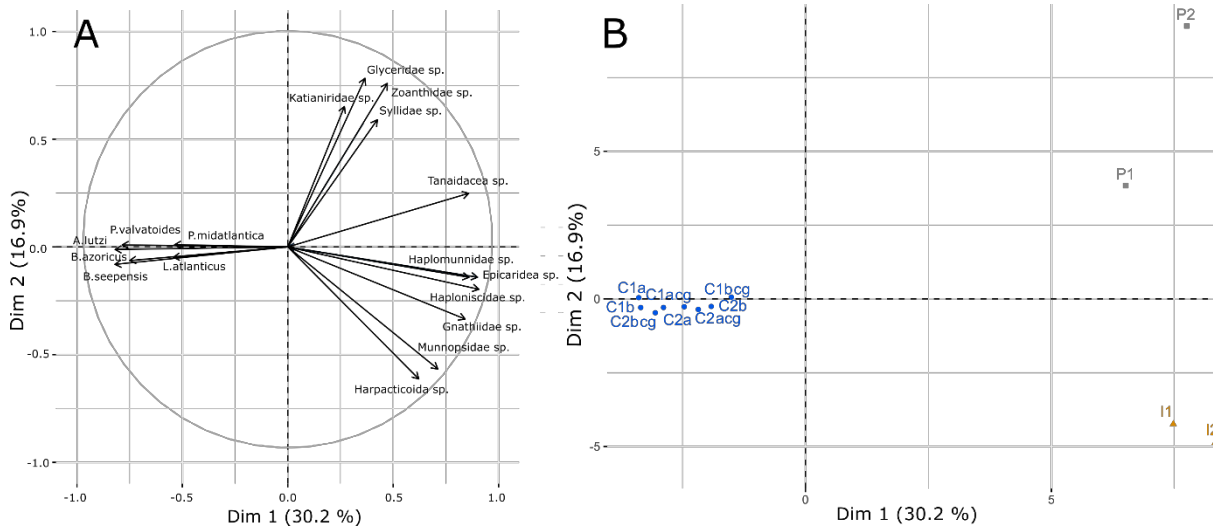

Figure III.5. Principal component analysis (PCA) of Hellinger-transformed densities of macrofaunal composition of the baseline communities of the three sampling sites. Colors indicate the sample sites: Montségur active edifice (blue); peripheral area (grey) and inactive site (orange).

individuals ranging from 251 µm to 8.5 cm length within the different assemblages (Figure III.6). The pre-disturbed structure of the community on Montségur showed a polymodal size distribution dominated by a large proportion (i.e. 52% of the overall population) of small individuals below 5 mm in shell-length and a tail of distribution in larger sizes containing several cohorts (Figure III.6). Pairwise Kolmogorov-Smirnov distribution tests showed significant differences in size structure population between the pre-disturbed and the post-disturbance communities in all samples (*p-value* < 0.001), except C2b (D = 0.10, *p-value* = 0.13) (Figure III.6). Furthermore, Wilcoxon-Mann-Whitney tests highlighted that the mean shell length of *B. azoricus* was smaller 1 and 2 years after the disturbance compared to that of the pre-disturbed community for all samples except C1acg and C2b (Figure III.6). Furthermore, the proportion of juveniles of *B. azoricus* (< 5 mm) in the overall population was higher in assemblages sampled 1 year (67%) and two years (70%) after the disturbance in comparison to pre-disturbed populations (52%) (Table III.S1).

Recolonisation dynamics of the active vent communities – The rarefaction curves did not level off for most of the post-disturbance samples on Montségur, but they show similar trends than that of the pre-disturbed communities (Figure III.S3B). The shape of the curves indicate that they should reach a plateau earlier, highlighting a higher evenness in the recovering communities. Species richness (S) is lower (from 1 to 6 less species) in the post-disturbance assemblages compared to the pre-disturbed communities 1 year after the induced disturbance (Table III.4). On the other hand, two years after, the C2a and C2acg quadrats showed a higher species richness than pre-disturbed quadrats, while C2b and C2bcg exhibited lower values after the disturbance (Table III.4). Overall, species richness was homogeneous between all samples and was not significantly different along the recolonisation process (Kruskal-Wallis test: P= 1.17, *p-value* = 0.56, Figure III.S5A). However, macrofaunal densities were significantly lower after 1 year (15 768 ± 12 487 ind.m^{-2}) and 2 years (11 190 ± 8 270 ind.m^{-2}) after the disturbance, in comparison to the pre-disturbed community (34 402 ± 7 590 ind.m^{-2}) (Kruskal-Wallis test: P= 7.65, *p-value* = 0.021 and Post hoc Dunn test: *p-value* < 0.05, Figure III.S5A) with a density recovery rate ranging from 15.7% on C1b after 1 year to 79.6% on C2acg 2 years after the disturbance (Table III.4, Figure III.S5A). The Shannon index and Pielou's evenness were highly variable across samples in the pre-disturbed communities, but always higher 1 year and 2 years after the disturbance (Table III.4, Figure III.S5C and III.S5D).

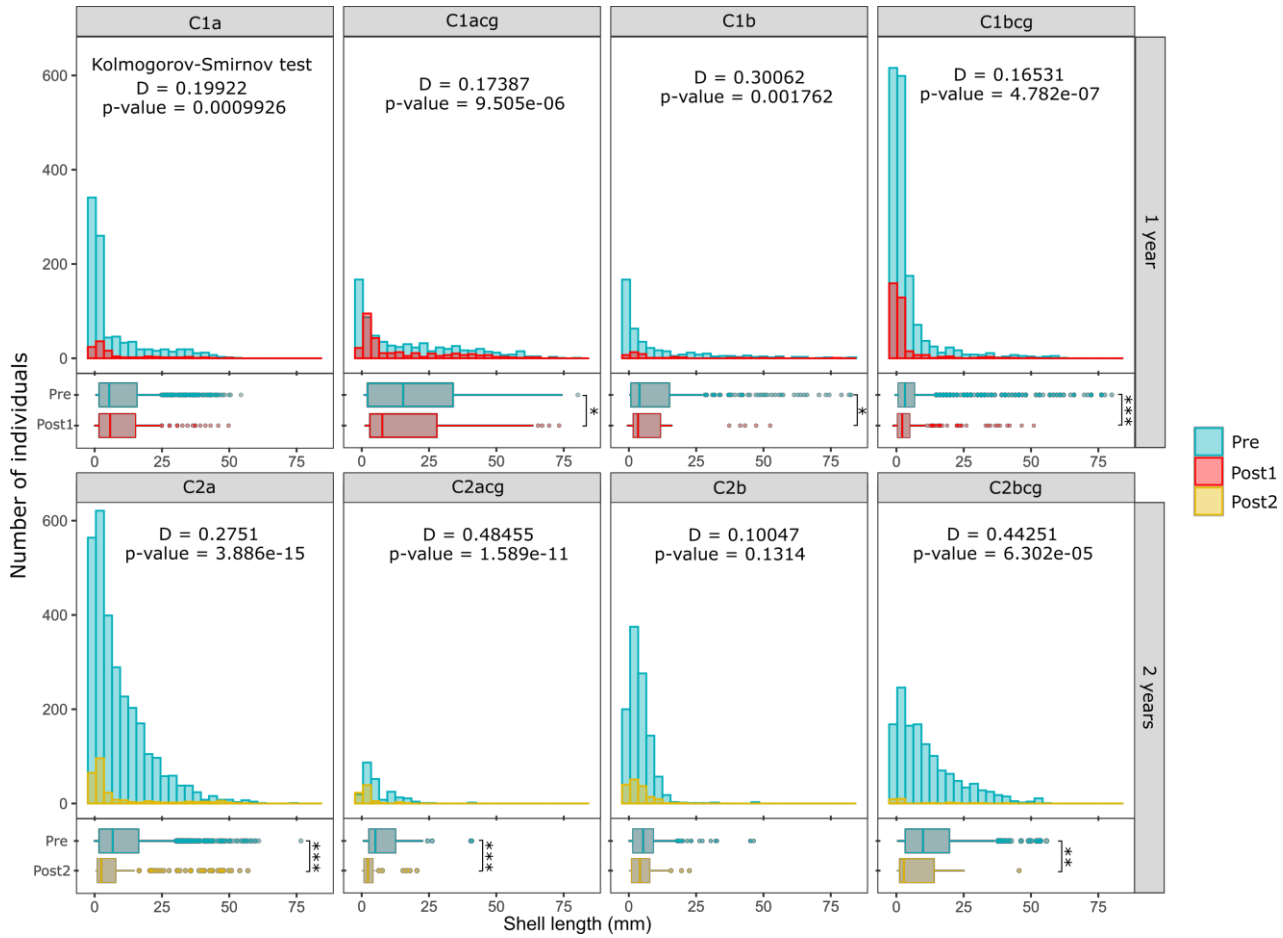

Figure III.6. Histograms and boxplots of size frequency distribution of *Bathymodiolus azoricus* for each quadrat sampled at the Montségur active edifice at the Lucky Strike vent field (Mid-Atlantic Ridge) including the pre-disturbed community (blue) and the community one (red) and 2 (yellow) years after disturbance. Pairwise Kolmogorov-Smirnov tests were performed to account for differences in length distributions between the pre-disturbed communities and the one-or two-year post-disturbance communities. Statistics and p-values of these tests are presented on top of each histogram. Wilcoxon-Mann-Whitney tests were performed to identify differences in mean individual size between the baseline community and in post-disturbance communities. Asterisks indicate significant differences in mean shell length. (*p-value<0.05; ** p-value <0.01; *** p-value <0.001)

Overall Pielou's evenness index is significantly higher in post-disturbance communities compared to pre-disturbed communities (Kruskal-Wallis test: P= 7.34, *p-value* = 0.026 and Post hoc Dunn test: *p-value* < 0.05, Figure III.S5D). In the same way, the proportion of 'rare' species is lower in post-disturbance communities (60% after 1 year and 58% after 2 years) than prior to the induced disturbance (74%) (Table III.S1).

The output of the RDA computed on Hellinger-transformed densities of the different species along the recolonisation process showed a significant difference in faunal composition between the pre-disturbed community and the post-disturbance assemblages at Montségur

(Figure III.7). The RDA model explained 42% (Adjusted R^2 = 20.5%) of the total inertia in species assemblage structure (*p-value* = 0.006). The main driver of this observed difference is time after the induced disturbance (*p-value* = 0.001), whereas no significant cage effect or dependence between sites were observed (p-values = 0.300 and 0.262, respectively). The analysis of similarity (ANOSIM) on Bray-Curtis dissimilarity matrix suggests a major change in macrofaunal composition between pre-disturbed assemblages and those after 1 and 2 years of recolonisation (R = 0.712, *p-value* = 0.001). However, no significant difference in faunal composition was identified between the assemblages collected 1 year and those collected 2 years after the disturbance.

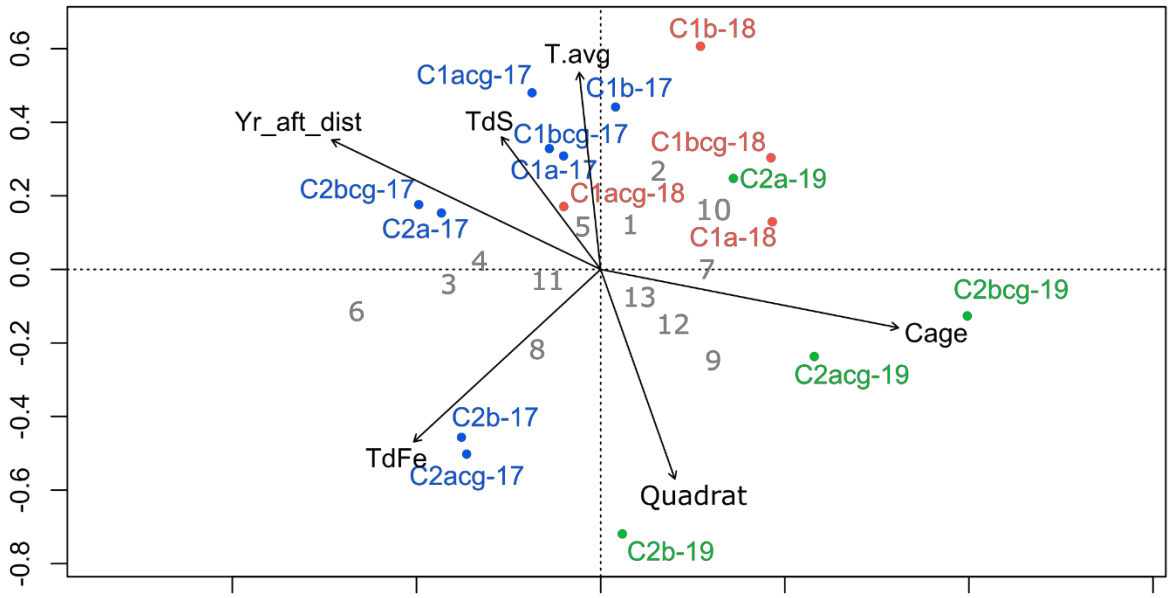

Figure III.7. Canonical redundancy analysis (RDA, scaling 2) of Hellinger-transformed macrofaunal densities observed in the different assemblages during the recolonisation process at the Montségur active edifice (Lucky Strike vent field, Mid-Atlantic Ridge). The first canonical axis represents 20.8% of the total variance in macrofaunal densities while the second axis represents 10.8% (with an adjusted R^2 of 20.5%). The RDA and the first axis are significant (p-values =0.006 and 0.023, respectively). Only species showing good fit with the first two canonical axes are represented. Colors refer to the time after disturbance: baseline communities (blue); 1 year after disturbance (red); two years after disturbance (green). Explanatory variables: Years after disturbance (*Yr_aft_dist*), average temperature measured before sampling (*T.avg*), mean concentration of total dissolved sulphides (*TdS*), mean concentration of total dissolved iron (*TdFe*), if quadrats are caged or uncaged (*Cage*), identification of quadrats to test the dependence of the same location over the years of experiment (*Quadrat*). Response variables, each species is designated by a number: 1 – *Amphisamytha lutzi*; 2 – *Aphotopontius sp.*; 3 – *Bathymodiolus azoricus*; 4 – *Branchipolynoe seepensis*; 5 – *Lepetodrilus atlanticus*; 6 – *Lirapex costellata*; 7 – *Laeviphitus desbruyeresi*; 8 – *Luckia striki*; 9 – *Lurifax vitreus*; 10 – *Oncholaimus dyvae*; 11 – *Paralepetopsis ferrugivora*; 12 – *Protolira valvatoides*; 13 – *Xylodiscula analoga*.

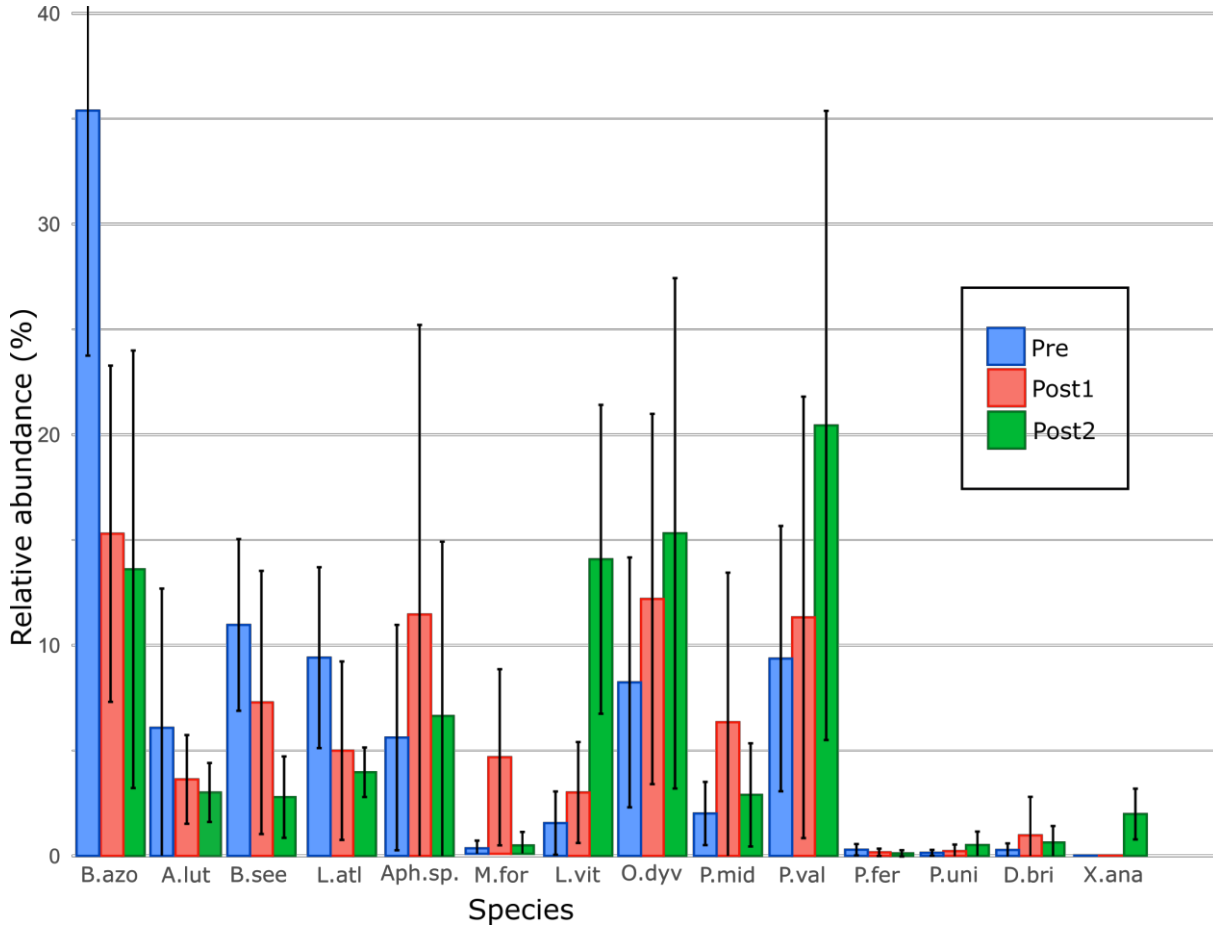

Figure III.8. Mean and standard deviations of densities for the most abundant species among the experimental quadrats on the active Montségur edifice before the disturbance (Pre) and one/two years after the disturbance (Post1 and Post2). Species acronyms: B.azo – *Bathymodiolus azoricus*, A.lut – *Amphisamytha lutzi*; B.see – *Branchipolynoe seepensis*; L.atl – *Lepetodrilus atlanticus*; Aph.sp. – *Aphotopontius sp.*; M.for – *Mirocaris fortunata*; L.vit – *Lurifax vitreus*; O.dyv – *Oncholaimus dyvae*; P.mid – *Pseudorimula midatlantica*; P.val – *Protolira valvatoides*; P.uni – *Prionospio unilamellata*; D.bri – *Divia briandi*; X.ana – *Xylodiscula analoga*.

Some species appeared to play a major role in the observed differences along the recolonisation process (Figure III.8). Indeed, a decrease in the abundance of the typical vent species (*Bathymodiolus azoricus*, *Branchipolynoe seepensis*, *Amphisamytha lutzi* and *Lepetodrilus atlanticus)* was observed in the post-disturbance communities, while small gastropod species (i.e. *Lurifax vitreus*, *Protolira valvatoides*, *Laeviphitus desbruyeresi*, *Xylodiscula analoga*) and nematodes (*Oncholaimus dyvae*) showed a significant increase in the post-disturbance communities (Figure III.8, Figure III.S6). *Pseudorimula midatlantica* and the copepod *Aphotopontius sp.* displayed higher relative abundances in the first year after the disturbance in comparison to the pre-disturbed community and returned to lower values 2 years after the disturbance. As observed for *B. azoricus,* the other dominant species displayed a polymodal structure of size distribution and differences have been identified between the pre-disturbed community and post disturbance state (pairwise Kolmogorov-Smirnov test) (Figure III.S6). Furthermore, individuals of *A. lutzi*, *B. seepensis, L. lepetodrilus* and *P. valvatoides* were overall smaller within the communities after disturbance in comparison to those of the pre-disturbed community in most quadrats (Figure III.S6). For *P. midatlantica*, only 1 quadrat showed significant (Figure III.S6).

Recolonisation dynamics of the peripheral and inactive benthic communities – The recovery of macrofaunal densities 1 year after the disturbance was variable across samples collected in the periphery (25% for P1 and 62% for P2) and the inactive structure (47% for I1 and 55% for I2), but the percentage of recovery was overall higher compared to that on the active Montségur edifice (34% for C1a, 16% for C1b, 30% for C1acg and 68% for C1bcg). Our results show that approximately 60% of the macrofaunal species richness recovered at the peripheral area after 1 year of recolonisation (9 out of 16 taxa for P1; 11 out of 17 taxa for P2). On the inactive structure, the recovery of macrofaunal species richness reached approximately 71% of the initial value for I1 (10 out of 14 taxa) and 93% for I2 (13 out of 14 taxa; Table III.4). Compared to the active area, the diversity, as measured by the Shannon index, is lower one year after disturbance than in pre-disturbed community. In terms of faunal composition, no difference has been observed between the pre-disturbed communities and post-disturbance at the periphery area and at the inactive structure after one year. No data are available after 2 years for these habitats.

III.4. Discussion

In this study, we provide an early evaluation of the recovery of deep-sea benthic communities to a small-scale (<1 m²) disturbance experiment at three sites characterised by different levels of hydrothermal activity: an active edifice, a peripheral site and an inactive structure located on the Lucky Strike vent field. The structure of pre-disturbed communities and their recovery patterns were characterised through the analysis of faunal composition, diversity, population size structure and environmental factors at the Montségur active edifice and vent proximate habitats. This experimental design represents an innovative approach to assess the recovery of vent communities in areas where opportunities to observe natural disturbances are rare. They provide significant insights about colonisation patterns in the deep sea, data that are essential to the elaboration of conservation strategies in the context of potential deep-sea mining activities on seafloor massive sulphides.

III.4.1. Habitat characterisation

In active vent ecosystems, environmental factors are strongly linked to the output flux and chemistry of hydrothermal fluids and the resulting physico-chemical conditions along the mixing gradient between vent fluids and surrounding sea water. Within the active habitats sampled in this study, mean temperature among *Bathymodiolus azoricus* faunal assemblages varied from 5.2 to 9.5°C with a maximum of 22.1°C, which corresponds to the temperature ranges of Eiffel Tower habitats (Husson et al. 2017, Sarrazin et al. 2020). We identified two microhabitats hosting *B. azoricus* assemblages, described as cold and warm habitats in Sarrazin et al. (2015). However, while in our study these habitats are colonised by mussels, in the previous study warm habitats were rather reported to be associated with shrimp assemblages. This discrepancy could be related to temperature measurements: in the present study, temperature was measured using iButtons™ deployed on or within the mussels while most measurements reported previously were conducted using the ROV probe placed a few millimeters above the faunal assemblages (Cuvelier et al. 2014a, Husson et al. 2017, Sarrazin et al. 2015, 2020).

Similar to previous studies, most samples belonging to the cold habitat showed small variability in environmental conditions and were associated with low temperature, low concentrations of iron and sulphides, high pH and high concentrations of dissolved oxygen

(Cuvelier et al. 2011a; Sarrazin et al. 2015). However, a few quadrats (R1, C2a and R0b) were characterised by higher temperatures, total sulphide and dissolved iron concentrations as well as lower dissolved oxygen concentrations with acidic pH, which are more representative of warm habitats.

The continuous bi-hourly monitoring of temperature revealed a high spatial variability in temperature regime (up to 3°C across 10 cm) suggesting the occurrence of multiple microhabitats within a single quadrat. This was supported by high standard deviation values of replicate measurements for sulphides and iron performed every year. This small-scale temporal variability of temperature can be a result of several processes including the interplay between sulphide and oxygen biological uptake (Johnson et al. 1988), the formation of diffuse fluids in the subsurface, the chemical reactivity of the mixing zone, the porosity of the substratum in active habitats (Butterfield et al. 1990; Sarrazin et al. 2002, Le Bris et al. 2006) or tidal oscillations (Barreyre et al. 2014). Our results show significant semi-diurnal and diurnal periods and harmonics supporting the presence of periodic oscillations related to tidal processes. Tidal modulation of diffused-flow has been reported in many vent systems (Scheirer et al. 2006; Cuvelier et al. 2014b; Sarrazin et al. 2014). These variations are mainly caused by tidally induced currents (Khripounoff et al. 2008; Barreyre et al. 2014) and changes in hydrostatic pressure on the seafloor (Davis and Becker 1999). This periodicity could be beneficial for symbiotic sessile species that need alternative inputs of reduced compounds and oxygen to insure chemosynthesis (Scheirer et al. 2006, Mat et al. 2020) but can also play a role in the behaviour of mobile species (Lelièvre et al. 2017).

The temperature range at the peripheral and inactive habitats corresponded to those of the LS bottom seawater. They are consistent with the absence of hydrothermal activity, except for the I1 quadrat that displayed one high methane value and may suggest diffuse flow seeping. The absence of replicate measurements and the low amount of parameters available for this site, prevent us from driving further conclusions.

III.4.2. Pre-disturbed communities and natural variability

On the active Montségur edifice, all experimental quadrats were visually dominated by medium-sized *B. azoricus* mussels from 5.2 ± 8.8 mm to 24.4 ± 14.3 mm. These sizes are consistent with the mean lengths reported by Comtet and Desbruyères (1998) on different edifices of Lucky Strike (between 5.63 ± 5.67 mm and 49.63 ± 31.41 mm), but smaller than those measured by Sarrazin et al. (2015) on the nearby Eiffel Tower edifice (between 22.7 ± 18.07 and 74.7 ± 2.57 mm). Indeed, we observed a high proportion (between 52 and 96%) of very small individuals -below 3 mm- in each sample, sizes that correspond to post larval and juvenile stages. The presence of several successive cohorts suggests the occurrence of a massive recruitment event around June, just before sampling. These results are consistent with the lifecycle of *B. azoricus*, with an annual spawning event in January followed by a planktotrophic larval development and the settlement of post-larvae in May-June (Comtet and Desbruyères 1998; Colaço et al. 2006; Dixon et al. 2006). Furthermore, the differences in mean shell length of *B. azoricus* observed among samples on pre-disturbed communities may be due to spatial segregation of sizes related to environmental factors (Husson et al., 2017; Sarrazin et al., 2015) or to biotic interactions (e.g. competition, predation) that may play an important role in recruitment success and survival of post-larvae (Sancho et al. 2005; Lenihan et al. 2008).

All samples collected at the active Montségur edifice were dominated by the same macrofaunal species (e.g. *B. azoricus*, *B. seepensis*, *A. lutzi*, *P. valvatoides* and *L. atlanticus*), which have been previously described as indicator species of cold microhabitats on the Eiffel Tower edifice situated ~ 50 m from Montségur (Sarrazin et al. 2015b). The high similarity between the fauna from the two edifices may be related to their belonging to the same chemistry domain (Chavagnac et al. 2018, Sarrazin et al. 2020). Among the 43 macrofaunal species identified on Montségur, approximately 74% exhibit a low frequency of abundance (<1%) and can be considered as “rare” taxa. Total densities of organisms in the pre-disturbed communities ranged from 3 330 to 68 960 ind.m^{-2} across the different samples, and is much lower than the values reported by Sarrazin et al. (2020) on the same edifice (between 62 253 and 126 437). In several studies, small mussel assemblages, inhabiting cold microhabitats, harbour higher density and diversity of associated species than large mussel assemblages,

found in warmer microhabitats (Cuvelier et al., 2009; Dreyer et al., 2005; Sarrazin et al., 2015). Surprisingly, in this study the highest densities of organisms have been observed in the warmest and more variable habitats.

As expected, macrofaunal distribution was significantly influenced by environmental conditions, especially by mean temperature and mean concentrations in total sulphides and methane, in addition to slightly acidic conditions (pH <7.3). However, biotic factors such as competition for space and food resource, but also predation or facilitation, may also play an important role in faunal distribution in diffuse flow habitats (Sarrazin et al. 1997, Sen et al. 2013; Gollner et al. 2015b; Husson et al. 2017). On the other hand, faunal composition within reference quadrats did not differ over the three years of the experiment, suggesting a relative stability of assemblages over time. This supports the observed high stability of mussel communities on the nearby Eiffel Tower edifice, which led to the assumption that *B. azoricus* assemblages at Lucky Strike can be considered as a “climax” community (Cuvelier et al. 2011a). The absence of natural changes in faunal assemblages, at the edifice scale, during the experiment allow us to use them as a baseline to test the effect of the induced disturbance on benthic communities.

Inactive and peripheral macrofaunal communities were mainly characterised by isopods, amphipods, hydroids and polychaetes. These non-symbiotic taxa are described as predators or scavengers and rely on detrital organic matter from the surface photosynthetic primary production. They may also consume chemosynthetic-based organic matter exported from nearby active vent habitats (Erickson et al. 2009; Levin et al. 2016b; Sen et al. 2016). The low diversity observed in these samples could be due to different biases. First, the low taxonomic resolution might account for the small number of species reported. In addition, this study only focuses on macrofauna while the higher proportion of diversity at peripheral and inactive sites is expected to lie in the meiofaunal (Gollner et al. 2015a) and microeukaryote (Cowart et al. 2020) compartments. Finally, the sampling protocol, designed for the collection of vent assemblages, might not have been optimal for the inactive and periphery sites. The use of the ROV suction device, especially at the peripheral site, led to a rapid clogging of the inlet filter resulting in a small collection volume. Such limitation may have resulted in an underestimation of the diversity of these low-density, food-limited, habitats associated communities.

Communities inhabiting active vent and inactive proximate sites were distinct in terms of macrofaunal species composition, as reported by Cowart et al. (2020). In addition, even if species richness was lower in samples collected at the peripheral area and inactive site, the rarefaction curves suggest that only a small part of the overall diversity have been recorded and that these habitats could potentially harbour a higher diversity than active sites. This assumption is supported by the recent environmental DNA results acquired from the same experimental quadrats, in which the number of Operational Taxonomic Units OTUs were 2 times higher at inactive structure compared to the active edifice (Cowart et al. 2020). Indeed, hydrothermal communities associated to active venting are described as patchy and transitory due to the high spatial and temporal variability of environmental factors (Lutz and Kennish, 1993; Sarrazin et al., 1999, 1997; Copley et al., 1997, 2007; Cuvelier et al., 2011a) that limit the colonisation to a low number of well-adapted species. Conversely, vent periphery and the deep seafloor in general are characterised by more stable environmental conditions, allowing for the presence of a higher diversity contrasting with a lower productivity (Tunnicliffe 1992; Zeppilli et al. 2015; Gollner et al. 2015a; Plum et al. 2017, Alfaro-Lucas et al. 2020). Despite its limitations, this study provides one of the first quantitative data of macrofaunal communities inhabiting the surrounding habitats of active vents at Lucky Strike. Additional sampling effort is needed to fully describe these ecosystems and better understand the interplay between active vents and their proximate habitats.

III.4.3. Recolonisation processes and recovery

In this experiment, we hypothesised that the limited scale of the induced disturbance would not lead to changes in environmental factors. Indeed, the main abiotic characteristics monitored over time (temperature, sulphides, iron, methane, oxygen and pH) were not notably different after the disturbance compared to values measured prior to it. However, only a partial recovery (between 1.9% and 37.6%) of *B. azoricus* density occurred during the experiment with no significant differences in the recovery rate 1 or 2 years after disturbance. Thereby, despite the presence of mature assemblages of *B. azoricus* and its associated fauna only few centimetres from the experimental quadrats, the recovery rate of the engineer species remained relatively low. This contrasts with what was observed at vents from the Pacific Ocean, where a rapid colonisation was observed following volcanic eruptions (Tunnicliffe et al. 1997; Marcus et al. 2009; Gollner et al. 2015a). Indeed, the most mature communities, harbouring engineer species, were observed in the first years after the

disturbance on the Juan de Fuca (Tunnicliffe et al. 1997; Marcus et al. 2009) and East Pacific Rise (Gollner et al., 2015a) vent fields. This suggests that the recovery ability of foundation species is higher at vents situated at fast spreading ridges, probably because their faunal communities are naturally subjected to a higher temporal variability and instability of environmental conditions (Tunnicliffe et al. 1991, Boschen et al. 2013; Gollner et al. 2015b, 2017; Suzuki et al. 2018; Smith et al. 2020).

Recolonisation of *B. azoricus* can occur through recruitment events and settlement of post-larvae and juveniles or by immigration of mobile adults from nearby assemblages (Comtet and Desbruyères 1998). Since the growth rate of *B. azoricus* juveniles has been estimated to reach ~2 mm per year on the Eiffel Tower edifice (from imagery analyses, Sarrazin and Matabos unpublished data), we can assume that the presence of mussels larger than 1 cm after 1 and 2 years of recolonisation is most probably a result of adult migration. On the other hand, the mean shell length of *B. azoricus* was significantly lower and a higher proportion of juveniles were observed on post-disturbance assemblages compared to pre-disturbed communities. This suggests that within our study, the recruitment and settlement of young mussels were the main drivers of recolonisation after the disturbance, rather than migration.

Interestingly, the recovery of *B. azoricus* densities was higher in quadrats equipped with cages than in uncaged ones. This result suggests that the exclusion of large predators (>1 cm) enhanced the recolonisation of *B. azoricus.* Indeed, a higher number of small recruits, rather than adults, were observed in caged quadrats one year after recovery. A similar caging experiment conducted during 8 months on an active hydrothermal vent of the EPR also described an increase of small gastropod abundance when large predators were excluded (Micheli et al. 2002). The impact of predation on the entire benthic community is even more significant when predators specifically feed on preys that play a key role in the community and interact widely with other species (Paine 1966). We also observed that the cages led to the formation of a thick microbial mats on their surfaces, implying that the pyramidal structure may have modified the input of hydrothermal fluids. Our cage experiment also has some limitations as the choice of a 1 cm grid was not optimal to avoid smaller predators. Such an experiment with different grid sizes would give additional insights into the role of predators on recolonisation processes.

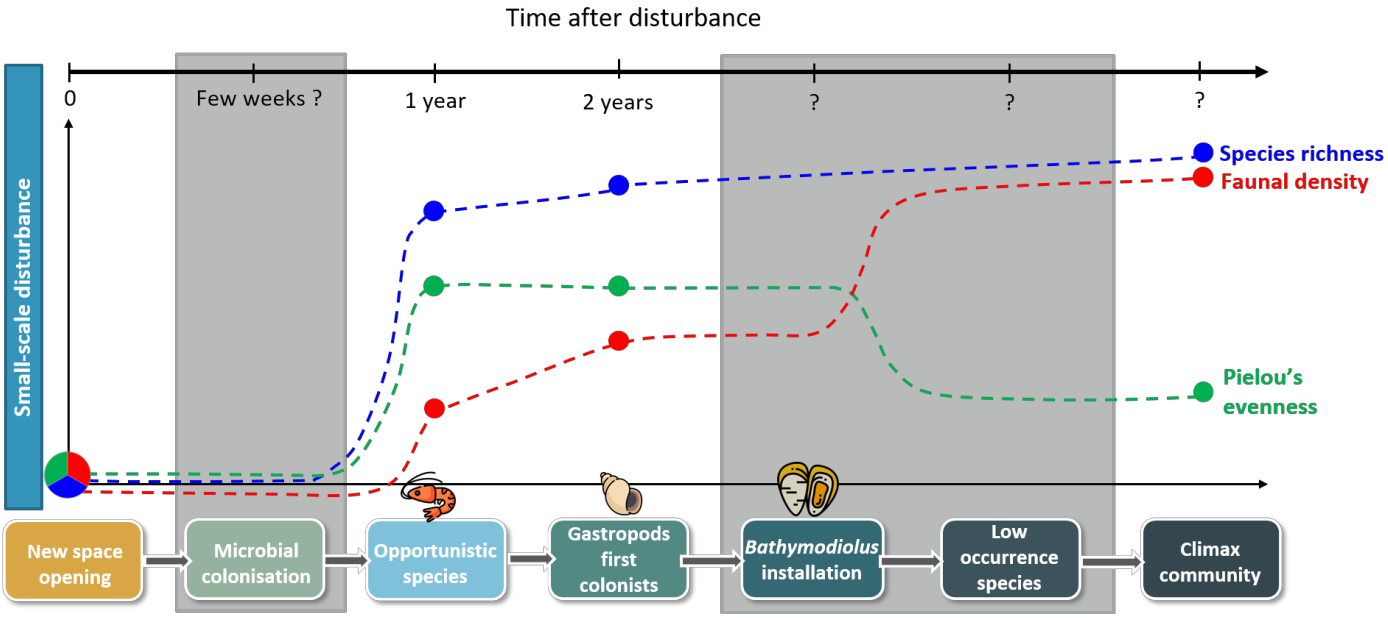

Figure III.9. Conceptual model of colonisation and ecological succession until climax after a small-scale disturbance on the Lucky Strike vent field assemblages (MAR). Evolution of species richness, faunal densities and Pielou's evenness index during the recovery process, based on the main results of our disturbance experiment (solid dots) and inferred from the literature (grey boxes).

Several factors can come into play to favour the recovery of vent communities (Gollner et al. 2017). Faunal colonisation and ecological succession at vents are strongly affected by environmental conditions and their spatio-temporal variability, which may lead to local extinction or creation of new suitable habitats (Sarrazin et al. 1997; Shank et al. 1998, Marcus et al. 2009; Sen et al. 2014). In addition, biological traits including reproduction (Kelly and Metaxas 2007), larval dispersal modes and recruitment abilities (Levin et al., 1996; Levin, 2006; Mullineaux et al., 2003, 2012) represent key factors that influence faunal colonisation processes and subsequent successional patterns (Adams et al. 2012; Nakamura et al. 2014). Feeding strategies (Van Audenhaege et al. 2019) and biotic interactions (i.e. competition for space, facilitation or predation) have also been identified as important drivers of faunal succession (Sarrazin et al. 1997, Micheli et al. 2002; Hunt et al. 2004; Govenar and Fisher 2007; Cuvelier et al. 2014a). Furthermore, under stable environmental conditions, as observed on the MAR or in back-arc basins, biological interactions are more likely to play a predominant role in faunal succession (Sen et al. 2014).

In Figure III.9, we propose a succession model of vent communities based on the present experiment at the Lucky Strike vent field. The first step after the disturbance relies on the creation of a sustainable habitat, including stabilisation of environmental conditions, especially of temperature and reduced compounds to allow chemoautotrophic primary production and proliferation of microbial mats, as observed in Pacific studies (Tunnicliffe et al. 1997; Shank et al. 1998; Marcus et al. 2009). In this experiment, the induced disturbance opened a new space available and already sustainable for colonisation (Figure III.9A). This was followed, within a few months, by a rapid colonisation by grazers. However, our sampling procedure did not allow for a total removal of microbial communities (authors pers. obs.), and we observed an increase in abundance of gastropod grazers one year after the disturbance. This step could take longer depending on the microbial colonisation processes involved and further studies are required to understand this initial step. The next step includes the arrival of larvae and recruitment of pioneer macrofaunal species from surrounding larval and adult communities. The time scale of this process will depend on the degree of connectivity with the undisturbed communities, based on the distance from remote populations, dispersal capacity of colonisers and regional oceanographic currents (Mullineaux et al. 2010). In our study, the adult populations surrounded the impacted area, allowing for a quick recolonisation

by migration or through recruitment by the local larval pool. The establishment of the main engineer species (*B. azoricus*) would then promote the recruitment of the rest of the community. Ultimately, the mussel assemblages would reach a climax stage, as suggested by Cuvelier et al. (2011a).

Gastropods have already been described as main pioneer colonists at 9°N EPR after the 2006 volcanic eruption (Mullineaux et al. 2010, 2012). These organisms are described as grazers or detritivores, feeding on free-living microbial communities (De Busserolles et al. 2009; Portail et al. 2018). In addition, despite contrasting reproductive characteristics, some of them are able to maintain an important effective population size and support high abundances, especially through an early maturity and continuous gametogenesis (Marticorena et al. 2020). These specific traits may explain rapid recovery observed in terms of faunal densities, even one or two years after the disturbance (Figure III.9A). Furthermore, the pioneer taxa *Lurifax vitreus* and *Xylodiscula analoga*, absent or in low abundance before the disturbance, were dominant within the post-disturbance communities. The same observation has been reported after the EPR eruption where high abundances of *Lepetodrilus tevnianus* were observed at the early stages of recovery, before a shift in dominance with the ubiquitous *L. elevatus,* which became more abundant in latter successional stages (Gollner et al., 2015a; Mullineaux et al., 2010, 2012). These authors suggested that the pioneer species *L. tevnianus* may outcompete its congener *L. elevatus* in the first period after the eruption, but that changes in habitat availability and biotic interactions would later favour *L. elevatus* in the successional sequence (Mullineaux et al. 2010). In our model, we hypothesise a later settlement of the foundation species *B. azoricus* due to its seasonal reproduction, which leads to a single recruitment event in June (Colaço et al. 2006; Dixon et al. 2006). Moreover, our results suggest that the recruitment success of *B. azoricus* might depend on predation pressure on post-larval individuals by large and mobile predators. The establishment and growth of *B. azoricus* may then promote macrofaunal species richness (Figure III.9) through the creation of a three dimensional habitat that contribute to reduce fluid flux, making the habitat more suitable for other species (Johnson et al. 1988; Sarrazin et al. 1997, Shank et al. 1998). However, this successional step might take more time compared to other vent systems because of the low growth rates of *B. azoricus*, which is the main engineer species of the northern MAR assemblages, in comparison to other symbiont-containing faunal groups (e.g. Siboglinid

worms, *Alviniconcha* and *Ifremeria* gastropods; Thiébaut et al. 2002; Urcuyo et al. 2003; Sen et al. 2014). With the increase in species richness, we expect an increase in trophic food web complexity with the colonisation by secondary consumers and predator species. Finally, biotic interactions including predation, competition for space and nutritional resources but also facilitation may lead to changes in faunal relative abundance and dominance before reaching an equilibrium. All these mechanisms contribute to reduce the evenness among assemblages and enhance the dominance of a few taxa (Figure III.9). Once this equilibrium is achieved, we can consider that these assemblages reach their climax. The climax community of Montségur appears to be similar to that of the neighbour Eiffel tower edifice (Cuvelier et al. 2011b) and some other active edifices of the vent field (Sarrazin pers. obs.). These communities are characterised by the dominance of a few vent taxa and a high proportion of 'rare' species with low relative abundances. Natural or anthropogenic disturbance events that can occur at each step of this successional model may lead to significant changes in faunal assemblages and even provoke community collapse, depending on their spatial breadth.

III.4.4. From small-scale to large scale disturbance

In this study, we provide novel data that contributes to a better understanding of recovery processes and ecological succession of active vent communities following a disturbance. However, the disturbance that was induced was implemented at a very small scale (< 0.1 m^2), making it difficult to compare with potential environmental consequences of deep-sea mining activities. In fact, unlike large-scale disturbance events that can lead to the entire destruction of habitats and eradication of all faunal communities (Van Dover 2014), here the habitat was still sustainable for microbial and vent faunal communities as shown by the stability of environmental factors during the two-year experiment. Furthermore, the experimental quadrats used to estimate the recovery rate of vent communities were deployed on an active edifice surrounded by mature faunal assemblages allowing migration of adult individuals. However, despite the close proximity of similar communities, the studied faunal assemblages showed a lower recovery rate than those located in the eastern Pacific (Tunnicliffe et al. 1997; Shank et al. 1998; Marcus et al. 2009; Gollner et al. 2015a). This is similar to what was observed at vents from back-arc basins in the western Pacific where community succession appeared to be much slower (Sen et al. 2014). Slow successional patterns may be characteristic of slow-spreading rate ecosystems as hypothesised by many authors (Tunnicliffe et al. 1997; Cuvelier

et al. 2011a; Sen et al. 2014; Gollner et al. 2017), suggesting that their communities might take a long time to recover from large-scale disturbance. Therefore, recovery patterns may be of a different order of magnitude in these systems compared to those observed naturally at fast spreading ridges (but still unknown). Unfortunately, these slow-spreading systems are especially targeted because of the much larger size and richer composition of their SMS (Levin et al. 2016a). Consequently, the impact of large-scale anthropogenic disturbances, such as those caused by seabed mining, may have a more profound impact on these communities than previously considered. Another difference of industrial-scale mining with the present study is that most of the economically viable mining sites result from past hydrothermal activity and are thus inactive (Van Dover 2019; Orcutt et al. 2020; Van Dover et al. 2020). This implies that their benthic communities are different from those at active sites, as supported by our results on the inactive structure (Cowart et al. 2020 and this study).

Despite these limitations, we propose a tentative model building from the knowledge gathered in the present study coupled to the information available in the literature. It has been mentioned by several authors that mining may cause direct (habitat destruction, eradication of fauna) and indirect (plume extent, light and noise) impacts that may affect faunal communities at the vent-field scale (Ramirez-Llodra et al. 2011; Boschen et al. 2013; Van Dover 2014; Gollner et al. 2017). Our model starts by “habitat creation” instead of the “space opening” found in the small-scale disturbance one and finishes with a potential climax community. However, most of the recovery steps, from the initial microbial colonisation to the climax community, including the diversity of pioneer species, the time scale at which succession occurs and the role of biotic and abiotic factors, are still unknown, highlighting the multiple knowledge gaps (Figure III.9B). This type of experimental approach is essential to gather information on colonisation processes. Combined with investigation on the biology of key species as well as faunal dispersal abilities and connectivity, they will contribute to determining the potential recovery of communities in response to large-scale deep-sea mining. These data are essential to inform industry and authorities so specific measures can be defined to limit and mitigate long-term harmful effects on hydrothermal vent ecosystems from seabed mining.

DOI of cruises involved

SARRADIN Pierre-Marie, CANNAT Mathilde (2017) MOMARSAT2017 cruise, RV Pourquoi pas ?, https://doi.org/10.17600/17000500

CANNAT Mathilde (2018) MOMARSAT2018 cruise, RV L'Atalante, https://doi.org/10.17600/18000514

SARRADIN Pierre-Marie, LEGRAND Julien (2019) MOMARSAT2019 cruise, RV Pourquoi pas ?, https://doi.org/10.17600/18001110

Author contributions

JM, MM and JS conceived the ideas and designed the methodology. JM, MM, JS, ALH and CC collected the samples on board during oceanographic cruises. JM, MM, JS, ALH, CC, JPD and SH processed and analysed the data. JM and RL did the statistical analyses. JM wrote the first draft of the manuscript and all authors commented on previous versions of the manuscript. All authors read and approved the final manuscript

Acknowledgements

We would like to thank the captains and crews of the oceanographic cruises Momarsat 2017, 2018 and 2019 aboard the vessels N/O Pourquoi pas? and L'Atalante, as well as the ROV Victor6000 and Nautile team. We are particularly grateful to Pierre-Marie Sarradin and Mathilde Cannat, chief scientists of the cruises who greatly supported our sampling program. We are also sincerely thankful to Philippe Rodier for instrumental design of pyramidal structure and cage experiment but also for the deployment of the reversing thermometer and the data acquisition of bottom sea water temperature. We would like to offer our special thanks to Sandra Fuchs and Fanny Girard for sample collection during the cruise and Julie Tourolle for providing the map captions. We are particularly grateful for the assistance given by Thomas Day, Mathilde Le Pans, Maureen Lapalme and Fanny Volage in sorting and morphometrical measurement of specimens. Finally, we wish to acknowledge the help provided for specimen identification by the taxonomists Dr Paulo Bonifácio and Dr Maurício Shimabukuro for polychaetes, Dr Anders Warén for gastropods, Dr Inmaculada Frutos for isopods, Dr Magdalena Błażewicz for tanaids and Dr Hayato Tanaka for ostracods. This research was supported by the European H2020 MERCES (Project ID 689518) and by the eCOREF project funded by Equinor (Norway). Julien Marticorena PhD project was funded by Ifremer and Equinor. This project is part of the EMSO-Azores (https://www.emso-fr.org) regional node and EMSO ERIC Research Infrastructure (https://emso.eu/). ERLL was supported by the European H2020 MERCES (Project ID 689518).

III.5. References

Adams DK, Arellano SM, Govenar B (2012) Larval dispersal : vent life in the water column. *Oceanography*, 25:256–268.

Anderson MJ (2001) A new method for non-parametric multivariate analysis of variance. Austral *Ecology* 26:32–46.

Baco AR, Etter RJ, Ribeiro PA, Heyden S von der, Beerli P, Kinlan BP (2016) A synthesis of genetic connectivity in deep-sea fauna and implications for marine reserve design. *Molecular Ecology* 25:3276–3298.

Barreyre T, Escartín J, Sohn RA, Cannat M, Ballu V, Crawford WC (2014) Temporal variability and tidal modulation of hydrothermal exit-fluid temperatures at the Lucky Strike deep-sea vent field, Mid-Atlantic Ridge. J*ournal of Geophysical Research: Solid Earth* 119:2543–2566.

Beaulieu SE, Szafrański KM (2020) InterRidge Global Database of Active Submarine Hydrothermal Vent Fields Version 3.4.

Beaulieu SE, Baker ET, German CR (2015) Where are the undiscovered hydrothermal vents on oceanic spreading ridges? *Deep Sea Research Part II: Topical Studies in Oceanography* 121:202–212.

Bergquist DC, Eckner JT, Urcuyo IA, Cordes EE, Hourdez S, Macko SA, Fisher CR (2007) Using stable isotopes and quantitative community characteristics to determine a local hydrothermal vent food web. *Marine Ecology Progress Series* 330:49–65.

Blake JA (1985) Polychaeta from the vicinity of deep-sea geothermal vents in the eastern Pacific. I. Euphrosinidae, Phyllodocidae, Hesionidae, Nereididae, Glyceridae, Dorvilleidae, Orbiniidae, and Maldanidae. *Bulletin of the Biological Society of Washington* 6:67–101.

Blake JA, Hilbig B (1990) Polychaeta from the vicinity of deep-sea hydrothermal vents in the eastern Pacific. II. New species and records from the Juan de Fuca and Explorer Ridge systems. *Pacific Science* 44.

Boschen RE, Rowden AA, Clark MR, Gardner JPA (2013) Mining of deep-sea seafloor massive sulfides: A review of the deposits, their benthic communities, impacts from mining, regulatory frameworks and management strategies. *Ocean & Coastal Management* 84:54–67.

Brescia LA, Tunnicliffe V (1998) Population biology of two pycnogonid species (Ammotheidae) at hydrothermal vents in the northeast Pacific. *Cah Biol Mar* 39:233–236.

Breusing C, Biastoch A, Drews A, Metaxas A, Jollivet D, Vrijenhoek RC, Bayer T, Melzner F, Sayavedra L, Petersen JM, Dubilier N, Schilhabel MB, Rosenstiel P, Reusch TBH (2016) Biophysical and Population Genetic Models Predict the Presence of “Phantom” Stepping Stones Connecting Mid-Atlantic Ridge Vent Ecosystems. *Curr Biol* 26:2257–2267.

Britayev TA, Martin D, Krylova EM, Von Cosel R, Aksiuk TS (2007) Life-history traits of the symbiotic scale-worm Branchipolynoe seepensis and its relationships with host mussels of the genus Bathymodiolus from hydrothermal vents. *Marine Ecology* 28:36–48.

Butterfield DA, Massoth GJ, McDuff RE, Lupton JE, Lilley MD (1990) Geochemistry of hydrothermal fluids from Axial Seamount hydrothermal emissions study vent field, Juan de Fuca Ridge:

Subseafloor boiling and subsequent fluid-rock interaction. *Journal of Geophysical Research: Solid Earth* 95:12895–12921.

Butterfield DA, Jonasson IR, Massoth GJ, Feely RA, Roe KK, Embley RE, Holden JF, McDuff RE, Lilley MD, Delaney JR (1997) Seafloor eruptions and evolution of hydrothermal fluid chemistry. *Philosophical Transactions of the Royal Society of London Series A: Mathematical, Physical and Engineering Sciences* 355:369–386.

Cannat M, Lagabrielle Y, Bougault H, Casey J, de Coutures N, Dmitriev L, Fouquet Y (1997) Ultramafic and gabbroic exposures at the Mid-Atlantic Ridge: geological mapping in the 15°N region. *Tectonophysics* 279:193–213.

Childress JJ, Fisher CR (1992) The biology of hydrothermal vent animals: physiology, biochemistry, and autotrophic symbioses. *Oceanography and Marine Biology* 30:337–441.

Colaco, A., Desbruyeres, D., Comtet, T., & Alayse, A. M. (1998). Ecology of the Menez gwen hydrothermal vent field (Mid-Atlantic Ridge Azores triple junction). Cahiers de Biologie Marine, 39(3-4), 237-240.Colaço A, Dehairs F, Desbruyères D (2002) Nutritional relations of deep-sea hydrothermal fields at the Mid-Atlantic Ridge: a stable isotope approach. *Deep Sea Research Part I: Oceanographic Research Papers* 49:395–412.

Colaço A, Martins I, Laranjo M, Pires L, Leal C, Prieto C, Costa V, Lopes H, Rosa D, Dando PR, Serrão-Santos R (2006) Annual spawning of the hydrothermal vent mussel, Bathymodiolus azoricus, under controlled aquarium, conditions at atmospheric pressure. *Journal of Experimental Marine Biology and Ecology* 333:166–171.

Colaço A, Desbruyères D, Guezennec J (2007) Polar lipid fatty acids as indicators of trophic associations in a deep-sea vent system community. *Marine Ecology* 28:15–24.

Collins PC, Kennedy R, Van Dover CL (2012) A biological survey method applied to seafloor massive sulphides (sms) with contagiously distributed hydrothermal-vent fauna. *Marine Ecology Progress Series*, 452:89-107.

Comtet T, Desbruyères D (1998) Population structure and recruitment in mytilid bivalves from the Lucky Strike and Menez Gwen hydrothermal vent fields (37°17\'N and 37°50\'N on the Mid-Atlantic Ridge). *Marine Ecology Progress Series* 163:165–177.

Copley JTP, Tyler PA, Murton BJ, Van Dover CL (1997) Spatial and interannual variation in the faunal distribution at Broken Spur vent field (29°N, Mid-Atlantic Ridge). *Marine Biology* 129:723–733.

Copley JTP, Jorgensen PBK, Sohn RA (2007) Assessment of decadal-scale ecological change at a deep Mid-Atlantic hydrothermal vent and reproductive time-series in the shrimp Rimicaris exoculata. *Journal of the Marine Biological Association of the United Kingdom* 87:859–867.

Corliss JB, Dymond J, Gordon LI, Edmond JM, Herzen RP von, Ballard RD, Green K, Williams D, Bainbridge A, Crane K, Andel TH van (1979) Submarine Thermal Springs on the Galápagos Rift. *Science* 203:1073–1083.

Cowart DA, Matabos M, Brandt MI, Marticorena J, Sarrazin J (2020) Exploring Environmental DNA (eDNA) to Assess Biodiversity of Hard Substratum Faunal Communities on the Lucky Strike Vent Field (Mid-Atlantic Ridge) and Investigate Recolonisation Dynamics After an Induced Disturbance. *Front Mar Sci* 6:783.

Cuvelier D, Sarrazin J, Colaço A, Copley J, Desbruyères D, Glover AG, Tyler P, Serrão Santos R (2009) Distribution and spatial variation of hydrothermal faunal assemblages at Lucky Strike (Mid-Atlantic Ridge) revealed by high-resolution video image analysis. *Deep Sea Research Part I: Oceanographic Research Papers* 56:2026–2040.

Cuvelier D, Sarrazin J, Colaço A, Copley JT, Glover AG, Tyler PA, Santos RS, Desbruyères D (2011a) Community dynamics over 14 years at the Eiffel Tower hydrothermal edifice on the Mid-Atlantic Ridge. *Limnology and Oceanography* 56:1624–1640.

Cuvelier D, Sarradin P-M, Sarrazin J, Colaço A, Copley JT, Desbruyères D, Glover AG, Santos RS, Tyler PA (2011b) Hydrothermal faunal assemblages and habitat characterisation at the Eiffel Tower edifice (Lucky Strike, Mid-Atlantic Ridge). *Marine Ecology* 32:243–255.

Cuvelier D, Beesau J, Ivanenko VN, Zeppilli D, Sarradin P-M, Sarrazin J (2014a) First insights into macro- and meiofaunal colonisation patterns on paired wood/slate substrata at Atlantic deep-sea hydrothermal vents. *Deep Sea Research Part I: Oceanographic Research Papers* 87:70–81.

Cuvelier D, Legendre P, Laes A, Sarradin P-M, Sarrazin J (2014b) Rhythms and Community Dynamics of a Hydrothermal Tubeworm Assemblage at Main Endeavour Field – A Multidisciplinary Deep-Sea Observatory Approach. *PLOS ONE* 9:e96924.

Cuvelier D, Gollner S, Jones DOB, Kaiser S, Arbizu PM, Menzel L, Mestre NC, Morato T, Pham C, Pradillon F, Purser A, Raschka U, Sarrazin J, Simon-Lledó E, Stewart IM, Stuckas H, Sweetman AK, Colaço A (2018) Potential Mitigation and Restoration Actions in Ecosystems Impacted by Seabed Mining. *Front Mar Sci.* 5:146

Davis E, Becker K (1999) Tidal pumping of fluids within and from the oceanic crust: New observations and opportunities for sampling the crustal hydrosphere. *Earth & planet sci lett* 172:141–149.

De Busserolles F, Sarrazin J, Gauthier O, Gélinas Y, Fabri MC, Sarradin PM, Desbruyères D (2009) Are spatial variations in the diets of hydrothermal fauna linked to local environmental conditions? *Deep Sea Research Part II: Topical Studies in Oceanography* 56:1649–1664.

Desbruyères D, Almeida A, Biscoito M, Comtet T, Khripounoff A, Bris NL, Sarradin PM, Segonzac M (2000) A review of the distribution of hydrothermal vent communities along the northern Mid-Atlantic Ridge: Dispersal vs. environmental controls. *Hydrobiologia* 440:201–216.

Desbruyères D, Biscoito M, Caprais JC, Colaço A, Comtet T, Crassous P, Fouquet Y, Khripounoff A, Bris NL, Olu K, Riso R, Sarradin PM, Segonzac M, Vangriesheim A (2001) Variations in deep-sea hydrothermal vent communities on the Mid-Atlantic Ridge near the Azores plateau. *Deep-Sea Research Part I: Oceanographic Research Papers* 48:1325–1346.

Desbruyères D, Segonzac M, Bright M, Biologiezentrum OL, Desbruyeres D, Segonzac M, Bright M (2006) Handbook of deep-sea hydrothermal vent fauna, 2nd completely rev. ed. / editors, Daniel Desbruyères, Michel Segonzac&Monika Bright. Linz, Austria : *Land Oberösterreich, Biologiezentrum der Oberösterreichische Landesmuseen*

Dixon DR, Lowe DM, Miller PI, Villemin GR, Colaço A, Serrão-Santos R, Dixon LRJ (2006) Evidence of seasonal reproduction in the Atlantic vent mussel Bathymodiolus azoricus, and an apparent link with the timing of photosynthetic primary production. *Journal of the Marine Biological Association of the United Kingdom* 86:1363–1371.

Dreyer JC, Knick KE, Flickinger WB, Dover CLV (2005) Development of macrofaunal community structure in mussel beds on the northern East Pacific Rise. *Marine Ecology Progress Series* 302:121–134.

Druffel ER, Lalou C, Thompson G, Arnold M, Brichet E, Druffel E, Rona PA (1990) Geochronology of TAG and Snakepit hydrothermal fields, Mid-Atlantic Ridge: witness to a long, complex hydrothermal history. *Earth and Planetary Science Letters* 97:113–128.

Erickson KL, Macko SA, Van Dover CL (2009) Evidence for a chemoautotrophically based food web at inactive hydrothermal vents (Manus Basin). *Deep Sea Research Part II: Topical Studies in Oceanography* 56:1577–1585.

Fisher CR (1990) Chemoautotrophic and methanotrophic symbioses in marine invertebrates. *Reviews in Aquatic Sciences* 2:399–436.

Galkin SV (1997) Megafauna associated with hydrothermal vents in the Manus Back-Arc Basin (Bismarck Sea). *Marine Geology* 142:197–206.

German CR, Parson LM (1998) Distributions of hydrothermal activity along the Mid-Atlantic Ridge: interplay of magmatic and tectonic controls. *Earth and Planetary Science Letters* 160:327–341.

Goffredi SK, Warén A, Orphan VJ, Van Dover CL, Vrijenhoek RC (2004) Novel forms of structural integration between microbes and a hydrothermal vent gastropod from the Indian Ocean. *Applied and Environmental Microbiology* 70:3082–3090.

Gollner S, Govenar B, Arbizu PM, Mills S, Le Bris N, Weinbauer M, Shank TM, Bright M (2015a) Differences in recovery between deep-sea hydrothermal vent and vent-proximate communities after a volcanic eruption. *Deep Sea Research Part I: Oceanographic Research Papers* 106:167–182.

Gollner S, Govenar B, Arbizu PM, Mills S, Le Bris N, Weinbauer M, Shank TM, Bright M (2015b) Differences in recovery between deep-sea hydrothermal vent and vent-proximate communities after a volcanic eruption. *Deep Sea Research Part I: Oceanographic Research Papers* 106:167–182.

Gollner S, Govenar B, Fisher CR, Bright M (2015c) Size matters at deep-sea hydrothermal vents: different diversity and habitat fidelity patterns of meio- and macrofauna. *Marine Ecology Progress Series* 520:57–66.

Gollner S, Kaiser S, Menzel L, Jones DOB, Brown A, Mestre NC, van Oevelen D, Menot L, Colaço A, Canals M, Cuvelier D, Durden JM, Gebruk A, Egho GA, Haeckel M, Marcon Y, Mevenkamp L, Morato T, Pham CK, Purser A, Sanchez-Vidal A, Vanreusel A, Vink A, Martinez Arbizu P (2017) Resilience of benthic deep-sea fauna to mining activities. *Marine Environmental Research* 129:76–101.

Govenar B, Fisher CR (2007) Experimental evidence of habitat provision by aggregations of Riftia pachyptila at hydrothermal vents on the East Pacific Rise. *Marine Ecology* 28:3–14.

Hourdez S, Desbruyeres D (2003) A new species of scale-worm (Polychaeta: Polynoidae), Levensteiniella iris sp nov., from the Rainbow and Lucky Strike vent fields (Mid-Atlantic Ridge). *CBM-Cahiers de Biologie Marine* 44:13–21.

Hunt HL, Metaxas A, Jennings RM, Halanych KM, Mullineaux LS (2004) Testing biological control of colonisation by vestimentiferan tubeworms at deep-sea hydrothermal vents (East Pacific Rise, 9°50'N). *Deep Sea Research Part I: Oceanographic Research Papers* 51:225–234.

Husson B, Sarradin P-M, Zeppilli D, Sarrazin J (2017) Picturing thermal niches and biomass of hydrothermal vent species. *Deep Sea Research Part II: Topical Studies in Oceanography* 137:6–25.

Johnson KS, Childress JJ, Beehler CL (1988) Short-term temperature variability in the Rose Garden hydrothermal vent field: an unstable deep-sea environment. *Deep Sea Research Part A Oceanographic Research Papers* 35:1711–1721.

Jones DOB, Kaiser S, Sweetman AK, Smith CR, Menot L, Vink A, Trueblood D, Greinert J, Billett DSM, Arbizu PM, Radziejewska T, Singh R, Ingole B, Stratmann T, Simon-Lledó E, Durden JM, Clark MR (2017) Biological responses to disturbance from simulated deep-sea polymetallic nodule mining. Plose One. e0171750

Jumars PA, Dorgan KM, Lindsay SM (2015) Diet of worms emended: an update of polychaete feeding guilds. *Annual Review of Marine Science.* 7

Karson JA, Thompson G, Humphris SE, Edmond JM, Bryan WB, Brown JR, Winters AT, Pockalny RA, Casey JF, Campbell AC, Klinkhammer G, Palmer MR, Kinzler RJ, Sulanowska MM (1987) Along-axis variations in seafloor spreading in the MARK area. *Nature* 328:681–685.

Karson JA, Kelley DS, Fornari DJ, Perfit MR, Shank TM (2015) Discovering the Deep: A Photographic Atlas of the Seafloor and Ocean Crust. *Cambridge University Press*

Kelley DS, Baross JA, Delaney JR (2002) Volcanoes, Fluids, and Life at Mid-Ocean Ridge Spreading Centers. *Annual Review of Earth and Planetary Sciences* 30:385–491.

Kelly NE, Metaxas A (2007) Influence of habitat on the reproductive biology of the deep-sea hydrothermal vent limpet Lepetodrilus fucensis (Vetigastropoda: Mollusca) from the Northeast Pacific. *Mar Biol* 151:649–662.

Khripounoff A, Vangriesheim A, Crassous P, Segonzac M, Lafon V, Warén A (2008) Temporal variation of currents, particulate flux and organism supply at two deep-sea hydrothermal fields of the Azores Triple Junction. *Deep Sea Research Part I: Oceanographic Research Papers* 55:532–551.

Kouris A, Juniper SK, Frébourg G, Gaill F (2007) Protozoan–bacterial symbiosis in a deep-sea hydrothermal vent folliculinid ciliate (Folliculinopsis sp.) from the Juan de Fuca Ridge. *Marine Ecology* 28:63–71.

Kouris A, Limén H, Stevens C, Juniper S (2010) Blue mats: faunal composition and food web structure in colonial ciliate (Folliculinopsis sp.) mats at Northeast Pacific hydrothermal vents. *Marine Ecology Progress Series* 412:93–101.

Lalou C, Reyss J-L, Brichet E, Arnold M, Thompson G, Fouquet Y, Rona PA (1993) New age data for Mid-Atlantic Ridge hydrothermal sites: TAG and Snakepit chronology revisited. *Journal of Geophysical Research: Solid Earth* 98:9705–9713.

Langmuir C, Humphris S, Fornari D, Van Dover C, Von Damm K, Tivey MK, Colodner D, Charlou J-L, Desonie D, Wilson C, Fouquet Y, Klinkhammer G, Bougault H (1997) Hydrothermal vents near

a mantle hot spot: the Lucky Strike vent field at 37°N on the Mid-Atlantic Ridge. *Earth and Planetary Science Letters* 148:69–91.

Le Bris N, Govenar B, Le Gall C, Fisher CR (2006) Variability of physico-chemical conditions in 9°50'N EPR diffuse flow vent habitats. *Marine Chemistry* 98:167–182.

Lelièvre Y, Legendre P, Matabos M, Mihály S, Lee RW, Sarradin P-M, Arango CP, Sarrazin J (2017) Astronomical and atmospheric impacts on deep-sea hydrothermal vent invertebrates. Proceedings of the Royal Society B: *Biological Sciences* 284:319–407.

Lelièvre Y, Sarrazin J, Marticorena J, Schaal G, Day T, Legendre P, Hourdez S, Matabos M (2018) Biodiversity and trophic ecology of hydrothermal vent fauna associated with tubeworm assemblages on the Juan de Fuca Ridge. *Biogeosciences* 15:2629–2647.

Lenihan HS, Mills SW, Mullineaux LS, Peterson CH, Fisher CR, Micheli F (2008) Biotic interactions at hydrothermal vents: Recruitment inhibition by the mussel Bathymodiolus thermophilus. *Deep Sea Research Part I: Oceanographic Research Papers* 55:1707–1717.

Levin LA (2006) Recent progress in understanding larval dispersal: new directions and digressions. *Integr Comp Bio*l 46:282–297.

Levin LA, D T, G T (1996) Succession of macrobenthos in a created salt marsh. *Marine Ecology Progress Series* 141:67–82.

Levin LA, Mengerink K, Gjerde KM, Rowden AA, Van Dover CL, Clark MR, Ramirez-Llodra E, Currie B, Smith CR, Sato KN, Gallo N, Sweetman AK, Lily H, Armstrong CW, Brider J (2016a) Defining "serious harm" to the marine environment in the context of deep-seabed mining. *Marine Policy* 74:245–259.

Levin LA, Baco AR, Bowden DA, Colaco A, Cordes EE, Cunha MR, Demopoulos AWJ, Gobin J, Grupe BM, Le J, Metaxas A, Netburn AN, Rouse GW, Thurber AR, Tunnicliffe V, Van Dover CL, Vanreusel A, Watling L (2016b) Hydrothermal Vents and Methane Seeps: Rethinking the Sphere of Influence. *Front Mar Sci*. 3:72

Lutz RA, Kennish MJ (1993) Ecology of deep-sea hydrothermal vent communities: A review. *Reviews of Geophysics* 31:211–242.

Marcus J, Tunnicliffe V, Butterfield DA (2009) Post-eruption succession of macrofaunal communities at diffuse flow hydrothermal vents on Axial Volcano, Juan de Fuca Ridge, Northeast Pacific. *Deep Sea Research Part II: Topical Studies in Oceanography* 56:1586–1598.

Marticorena J, Matabos M, Sarrazin J, Ramirez-Llodra E (2020) Contrasting reproductive biology of two hydrothermal gastropods from the Mid-Atlantic Ridge: implications for resilience of vent communities. *Mar Biol* 167:109.

Micheli F, Peterson CH, Mullineaux LS, Fisher CR, Mills SW, Sancho G, Johnson GA, Lenihan HS (2002) Predation Structures Communities at Deep-Sea Hydrothermal Vents. *Ecological Monographs* 72:365–382.

Mullineaux LS, Peterson CH, Micheli F, Mills SW (2003) Successional Mechanism Varies Along a Gradient in Hydrothermal Fluid Flux at Deep-Sea Vents. *Ecological Monographs* 73:523–542. doi: 10.1890/02-0674

Mullineaux LS, Adams DK, Mills SW, Beaulieu SE (2010) Larvae from afar colonise deep-sea hydrothermal vents after a catastrophic eruption. *PNAS* 107:7829–7834.

Mullineaux LS, Bris NL, Mills SW, Henri P, Bayer SR, Secrist RG, Siu N (2012) Detecting the Influence of Initial Pioneers on Succession at Deep-Sea Vents. *PloS One 7:*e50015.

Nakamura M, Watanabe H, Sasaki T, Ishibashi J, Fujikura K, Mitarai S (2014) Life history traits of Lepetodrilus nux in the Okinawa Trough, based upon gametogenesis, shell size, and genetic variability. *Marine Ecology Progress Series* 505:119–130.

Oksanen J, Blanchet FG, Friendly M, Kindt R, Legendre P, McGlinn D, Minchin PR, O'Hara RB, Simpson GL, Solymos P, Stevens MHH, Szoecs E, Wagner H (2019) vegan: Community Ecology Package.

Ondreas H, Cannat M, Fouquet Y, Normand A, Sarradin P, Sarrazin J (2009) Recent volcanic events and the distribution of hydrothermal venting at the Lucky Strike hydrothermal field, Mid-Atlantic Ridge. Recent volcanic events and the distribution of hydrothermal venting at the Lucky Strike hydrothermal field, Mid-Atlantic Ridge. *Geochemistry, Geophysics, Geosystems*, 10

Orcutt BN, Bradley JA, Brazelton WJ, Estes ER, Goordial JM, Huber JA, Jones RM, Mahmoudi N, Marlow JJ, Murdock S, Pachiadaki M (2020) Impacts of deep-sea mining on microbial ecosystem services. *Limnology and Oceanography*. 65:1489-1510

Paine RT (1966) Food Web Complexity and Species Diversity. *The American Naturalist* 100:65–75.

Perfit MR, Chadwick WW (1998) Magmatism at Mid-Ocean Ridges: Constraints from Volcanological and Geochemical Investigations. In: Faulting and Magmatism at Mid-Ocean Ridges. *American Geophysical Union (AGU)* 59–115

Pettibone MH (1988) New species and new records of scaled polychaetes (Polychaeta: Polynoidae) from hydrothermal vents of the Northeast Pacific Explorer and Juan de Fuca Ridges. *Proceedings of the Biological Society of Washington.*

Pettibone MH (1997) Revision of the Scaleworm Genus Eulagisca Mcintosh (Polychaeta: Polynoidae) with the Erection of the Subfamily Eugaliscinae and the New Genus Pareula Gisca. *Proceedings of the Biological Society of Washington*

Plum C, Pradillon F, Fujiwara Y, Sarrazin J (2017) Copepod colonisation of organic and inorganic substrata at a deep-sea hydrothermal vent site on the Mid-Atlantic Ridge. *Deep Sea Research Part II: Topical Studies in Oceanography* 137:335–348.

Portail M, Brandily C, Cathalot C, Colaço A, Gélinas Y, Husson B, Sarradin P-M, Sarrazin J (2018) Food-web complexity across hydrothermal vents on the Azores triple junction. *Deep Sea Research Part I: Oceanographic Research Papers* 131:101–120.

Qiu J (2010) Oceanography: Death and rebirth in the deep. *Nature* 465:284–286.

Ramirez-Llodra E, Tyler PA, Baker MC, Bergstad OA, Clark MR, Escobar E, Levin LA, Menot L, Rowden AA, Smith CR, Dover CLV (2011) Man and the Last Great Wilderness: Human Impact on the Deep Sea. *PLOS ONE* 6:e22588.

Rubin KH, Soule SA, Chadwick WW, Fornari DJ, Clague DA, Embley RW, Baker ET, Perfit MR, Caress DW, Dziak RP (2012) Volcanic Eruptions in the Deep Sea. *Oceanography* 25:142–157.

Sancho G, Fisher CR, Mills S, Micheli F, Johnson GA, Lenihan HS, Peterson CH, Mullineaux LS (2005) Selective predation by the zoarcid fish Thermarces cerberus at hydrothermal vents. *Deep Sea Research Part I: Oceanographic Research Papers* 52:837–844.

Sarradin P-M, Waeles M, Bernagout S, Le Gall C, Sarrazin J, Riso R (2009) Speciation of dissolved copper within an active hydrothermal edifice on the Lucky Strike vent field (MAR, 37°N). *Science of The Total Environment* 407:869–878.

Sarrazin J, V R, Sk J, Jr D (1997) Biological and geological dynamics over four years on a high-temperature sulfide structure at the Juan de Fuca Ridge hydrothermal observatory. *Marine Ecology Progress Series* 153:5–24.

Sarrazin J, Juniper SK, Massoth G, Legendre P (1999) Physical and chemical factors influencing species distributions on hydrothermal sulfide edifices of the Juan de Fuca Ridge, northeast Pacific. *Marine Ecology Progress Series* 190:89–112.

Sarrazin J, Cuvelier D, Peton L, Legendre P, Sarradin PM (2014) High-resolution dynamics of a deep-sea hydrothermal mussel assemblage monitored by the EMSO-Açores MoMAR observatory. *Deep Sea Research Part I: Oceanographic Research Papers* 90:62–75.

Sarrazin J, Legendre P, de Busserolles F, Fabri M-C, Guilini K, Ivanenko VN, Morineaux M, Vanreusel A, Sarradin P-M (2015a) Biodiversity patterns, environmental drivers and indicator species on a high-temperature hydrothermal edifice, Mid-Atlantic Ridge. *Deep Sea Research Part II: Topical Studies in Oceanography* 121:177–192.

Sarrazin J, Legendre P, de Busserolles F, Fabri M-C, Guilini K, Ivanenko VN, Morineaux M, Vanreusel A, Sarradin P-M (2015b) Biodiversity patterns, environmental drivers and indicator species on a high-temperature hydrothermal edifice, Mid-Atlantic Ridge. *Deep Sea Research Part II: Topical Studies in Oceanography* 121:177–192.

Sarrazin J, Portail M, Legrand E, Cathalot C, Laes A, Lahaye N, Sarradin PM, Husson B (2020) Endogenous versus exogenous factors: What matters for vent mussel communities? *Deep Sea Research Part I: Oceanographic Research Papers* 103260.

Scheirer DS, Shank TM, Fornari DJ (2006) Temperature variations at diffuse and focused flow hydrothermal vent sites along the northern East Pacific Rise. *Geochemistry, Geophysics, Geosystems* 7 (3).

Sen A, Becker EL, Podowski EL, Wickes LN, Ma S, Mullaugh KM, Hourdez S, Luther GW, Fisher CR (2013) Distribution of mega fauna on sulfide edifices on the Eastern Lau Spreading Center and Valu Fa Ridge. *Deep Sea Research Part I: Oceanographic Research* 72:48–60.

Sen A, Podowski EL, Becker EL, Shearer EA, Gartman A, Yücel M, Hourdez S, Luther GW III, Fisher CR (2014) Community succession in hydrothermal vent habitats of the Eastern Lau Spreading Center and Valu Fa Ridge, Tonga. *Limnology and Oceanography* 59:1510–1528.

Sen A, Kim S, Miller AJ, Hovey KJ, Hourdez S, Luther GW, Fisher CR (2016) Peripheral communities of the Eastern Lau Spreading Center and Valu Fa Ridge: community composition, temporal change and comparison to near-vent communities. *Marine Ecology* 37:599–617.

Shank TM, Fornari DJ, Von Damm KL, Lilley MD, Haymon RM, Lutz RA (1998) Temporal and spatial patterns of biological community development at nascent deep-sea hydrothermal vents

(9°50'N, East Pacific Rise). *Deep Sea Research Part II: Topical Studies in Oceanography* 45:465–515.

Smith CR, Tunnicliffe V, Colaço A, Drazen JC, Gollner S, Levin LA, Mestre NC, Metaxas A, Molodtsova TN, Morato T, Sweetman AK, Washburn T, Amon DJ (2020) Deep-Sea Misconceptions Cause Underestimation of Seabed-Mining Impacts. *Trends in Ecology & Evolution* 35: 853–857.

Spiess FN, Macdonald KC, Atwater T, Ballard R, Carranza A, Cordoba D, Cox C, Garcia VM, Francheteau J, Guerrero J, Hawkins J, Haymon R, Hessler R, Juteau T, Kastner M, Larson R, Luyendyk B, Macdougall JD, Miller S, Normark W, Orcutt J, Rangin C (1980) East pacific rise: hot springs and geophysical experiments. *Science* 207:1421–1433.

Suzuki K, Yoshida K, Watanabe H, Yamamoto H (2018) Mapping the resilience of chemosynthetic communities in hydrothermal vent fields. *Sci Rep* 8:9364.

Thiébaut É, Huther X, Shillito B, Jollivet D, Gaill F (2002) Spatial and temporal variations of recruitment in the tube worm Riftia pachyptila on the East Pacific Rise (9°50[1]N and 13°N). *Mar Ecol Prog Ser* 234:147-157

Tolstoy M, Cowen JP, Baker ET, Fornari DJ, Rubin KH, Shank TM, Waldhauser F, Bohnenstiehl DR, Forsyth DW, Holmes RC, Love B, Perfit MR, Weekly RT, Soule SA, Glazer B (2006) A Sea-Floor Spreading Event Captured by Seismometers. *Science* 314:1920–1922.

Toyohara T, Okamoto N, Kawai T, Kodama T, Shibasaki H (2011) Environmental Research for Assessing the Impacts of Mining Seafloor Massive Sulfides in Japan. *American Society of Mechanical Engineers Digital Collection*, 135–140

Tunnicliffe V (1991) The biology of hydrothermal vents : ecology and evolution. *Oceanogr Mar Biol* 29:319–407.

Tunnicliffe V (1992) The Nature and Origin of the Modern Hydrothermal Vent Fauna. *PALAIOS* 7:338–350.

Tunnicliffe V, Embley RW, Holden JF, Butterfield DA, Massoth GJ, Juniper SK (1997) Biological colonisation of new hydrothermal vents following an eruption on Juan de Fuca Ridge. *Deep Sea Research Part I: Oceanographic Research Papers* 44:1627–1644.

Urcuyo IA, Massoth GJ, Julian D, Fisher CR (2003) Habitat, growth and physiological ecology of a basaltic community of Ridgeia piscesae from the Juan de Fuca Ridge. *Deep Sea Research Part I: Oceanographic Research Papers* 50:763–780.

Van Audenhaege L, Fariñas-Bermejo A, Schultz T, Lee Van Dover C (2019) An environmental baseline for food webs at deep-sea hydrothermal vents in Manus Basin (Papua New Guinea). *Deep Sea Research Part I: Oceanographic Research Papers* 148:88–99.

Van Dover CL (2010) Mining seafloor massive sulphides and biodiversity: what is at risk? *ICES J Mar Sci* 68:341–348.

Van Dover CL (2014) Impacts of anthropogenic disturbances at deep-sea hydrothermal vent ecosystems: A review. *Marine Environmental Research* 102:59–72.

Van Dover CL (2019) Inactive Sulfide Ecosystems in the Deep Sea: A Review. *Front Mar Sci.*,6, 461

Van Dover CL, Fry B (1989) Stable isotopic compositions of hydrothermal vent organisms. *Marine Biology* 102:257–263.

Van Dover CL, Trask J, Gross J, Knowlton A (1999) Reproductive biology of free-living and commensal polynoid polychaetes at the Lucky Strike hydrothermal vent field (Mid-Atlantic Ridge). *Marine Ecology Progress Series* 181:201–214.

Van Dover CL, Colaço A, Collins PC, Croot P, Metaxas A, Murton BJ, Swaddling A, Boschen-Rose RE, Carlsson J, Cuyvers L, Fukushima T, Gartman A, Kennedy R, Kriete C, Mestre NC, Molodtsova T, Myhrvold A, Pelleter E, Popoola SO, Qian P-Y, Sarrazin J, Sharma R, Suh YJ, Sylvan JB, Tao C, Tomczak M, Vermilye J (2020) Research is needed to inform environmental management of hydrothermally inactive and extinct polymetallic sulfide (PMS) deposits. *Marine Policy* 104183.

Vuillemin R, Le Roux D, Dorval P, Bucas K, Sudreau JP, Hamon M, Le Gall C, Sarradin PM (2009) CHEMINI: A new in situ CHEmical MINIaturized analyzer. *Deep Sea Research Part I: Oceanographic Research Papers* 56:1391–1399.

Ward ME, Jenkins CD, Dover CLM (2003) Functional morphology and feeding strategy of the hydrothermal-vent polychaete Archinome rosacea (family Archinomidae). *Canadian Journal of zoology* 81:582–590.

WAREN A (2001) Gastropoda and Monoplacophora from hydrothermal vents and seeps ; new taxa and records. *The Veliger* 44:116–231.

Warèn A, Bouchet P (1993) New records, species, genera, and a new family of gastropods from hydrothermal vents and hydrocarbon seeps. *Zoologica Scripta* 22:1–90.

Washburn TW, Turner PJ, Durden JM, Jones DOB, Weaver P, Van Dover CL (2019) Ecological risk assessment for deep-sea mining. *Ocean & Coastal Management* 176:24–39.

Zeppilli D, Vanreusel A, Pradillon F, Fuchs S, Mandon P, James T, Sarrazin J (2015) Rapid colonisation by nematodes on organic and inorganic substrata deployed at the deep-sea Lucky Strike hydrothermal vent field (Mid-Atlantic Ridge). *Mar Biodiv* 45:489–504.

Zeppilli D, Bellec L, Cambon-Bonavita M-A, Decraemer W, Fontaneto D, Fuchs S, Gayet N, Mandon P, Michel LN, Portail M, Smol N, Sørensen MV, Vanreusel A, Sarrazin J (2019) Ecology and trophic role of Oncholaimus dyvae sp. nov. (Nematoda: Oncholaimidae) from the lucky strike hydrothermal vent field (Mid-Atlantic Ridge). *BMC Zoology* 4:6.

(2019) factoextra: Extract and Visualize the Results of Multivariate Data Analyses.

III.6. Supplementary files

Figure III.S1. Quadrats were deployed on three sampling sites: (**A**) at the base of the active Montségur edifice, (**B**) at the extended periphery located ~30 m east of the Montségur edifice, (**C**) on a small inactive structure, north of the Lucky Strike vent field.

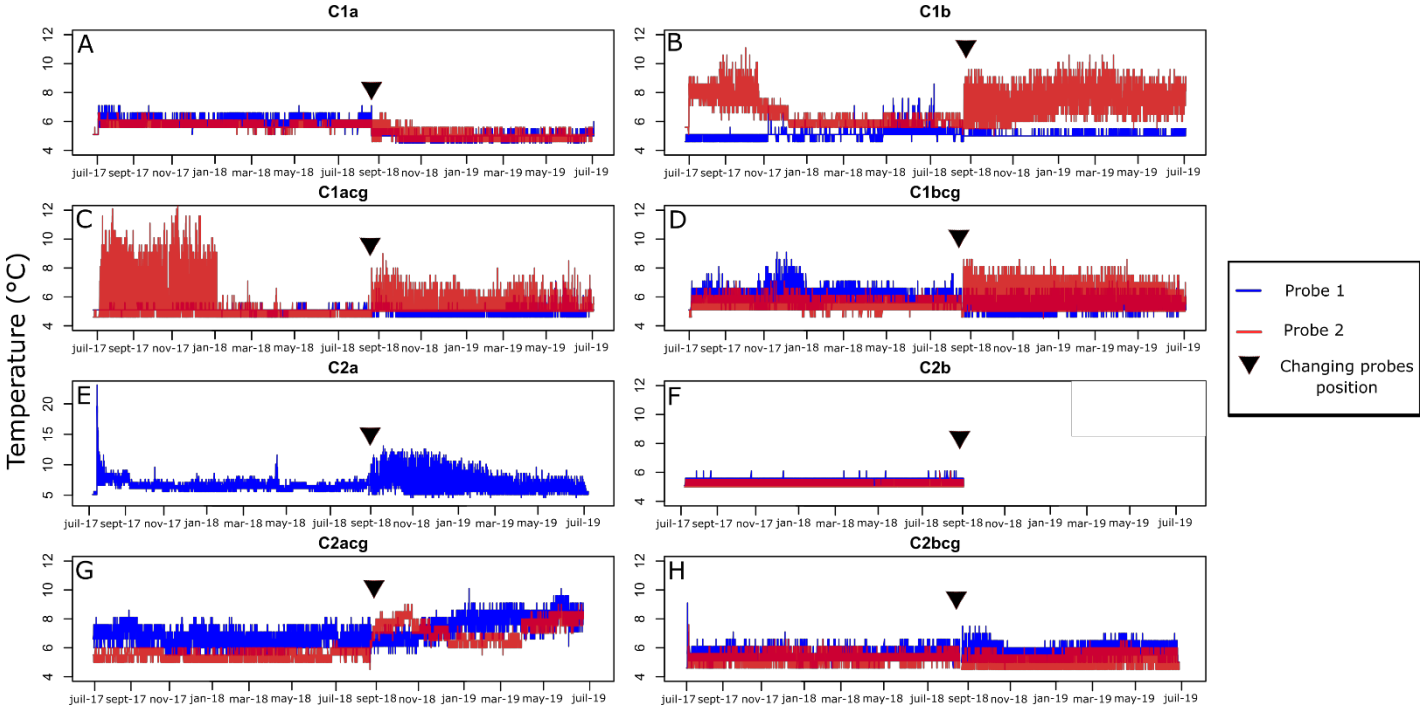

Figure III.S2. Temperatures monitored by iButtonsTM within the experimental quadrats on the Montségur edifice between July 2017 and July 2019. Quadrats A. C1a; B. C1b; C. C1acg; D. C1bcg ; E. C2a ; F. C2b. G. C2acg ; H. C2bcg. Colors: measurements of probe n°1 in blue and measurements of probe n°2 in red. The black triangle represent the replacement time of the probes during the Momarsat 2018 cruise. No data is available for C2b during the second sampling period.

a

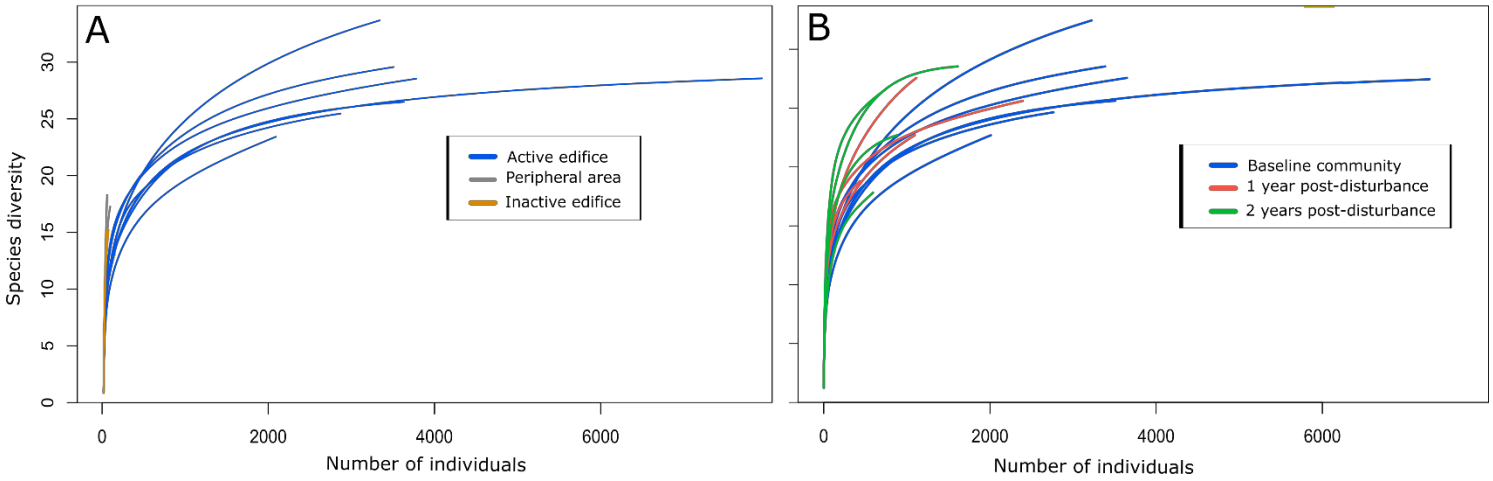

Figure III.S3. Rarefaction curves for macrofaunal communities in the baseline communities of the three habitats sampled (**A**) and across the recolonisation process at the Montségur edifice (**B**).

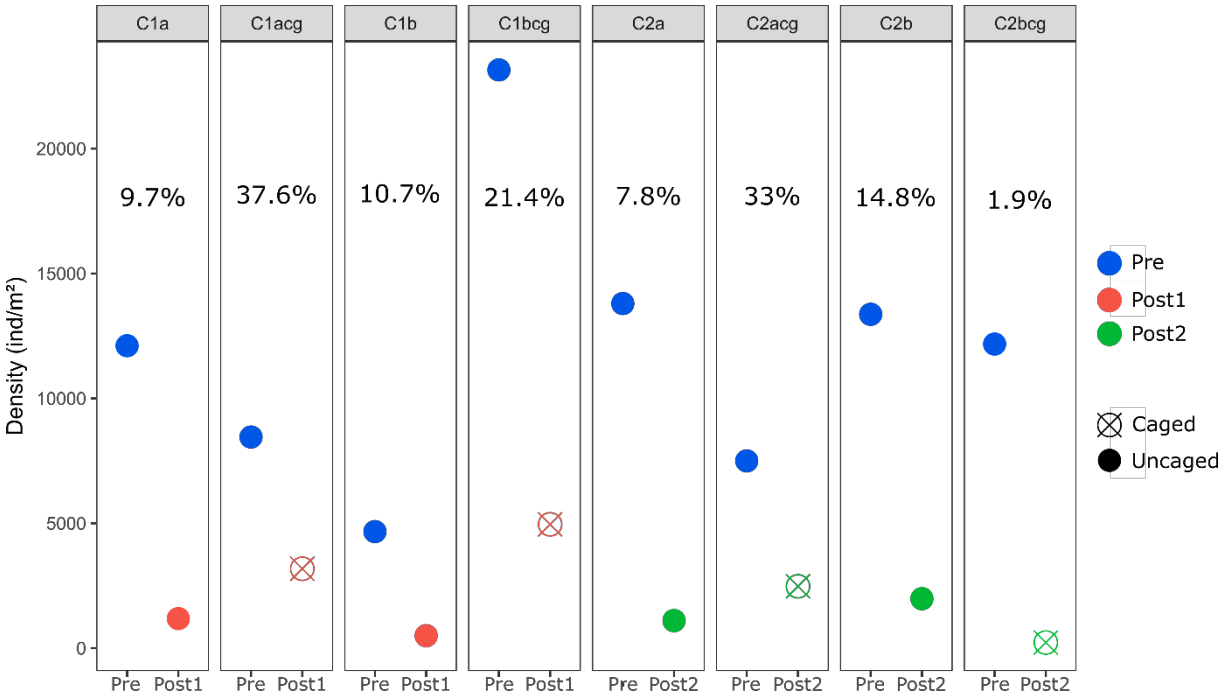

Figure III.S4. Recolonisation dynamics of *Bathymodiolus azoricus* in terms of density on the experimental quadrats of the Montségur edifice along the recovery process. Red circles represent the baseline community before the disturbance. Green circles represent the community 1 year after the disturbance and blue circles represent the community 2 years after the disturbance. Solid circles symbolize the uncaged quadrats while crossed circles represent the caged ones. Percentage represent the proportion of *B. azoricus* density which recovered in comparison of the pre-disturbed value in each quadrat.

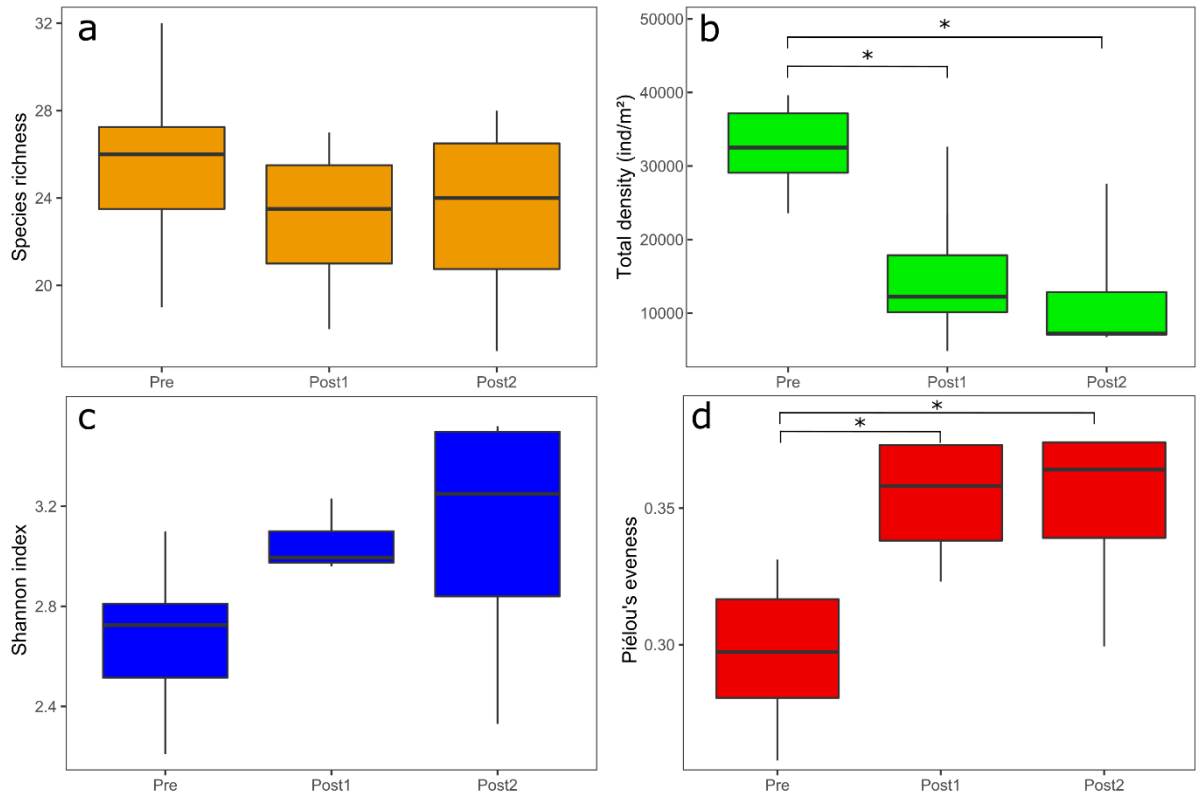

Figure III.S5. Species richness (**a**), total density (**b**), Shannon index (**c**) and Pielou's eveness index (**d**) of macrofaunal communities on the baseline communities and during the recolonisation process on the active Montségur edifice. Pre: assemblages sampled before the disturbance; Post1: assemblages sampled 1 year after the disturbance; Post2: assemblages sampled 2 years after the disturbance. Significance of Kruskall-Wallis multisample tests and post-hoc Dunn's tests are represented on the top of the boxplots.

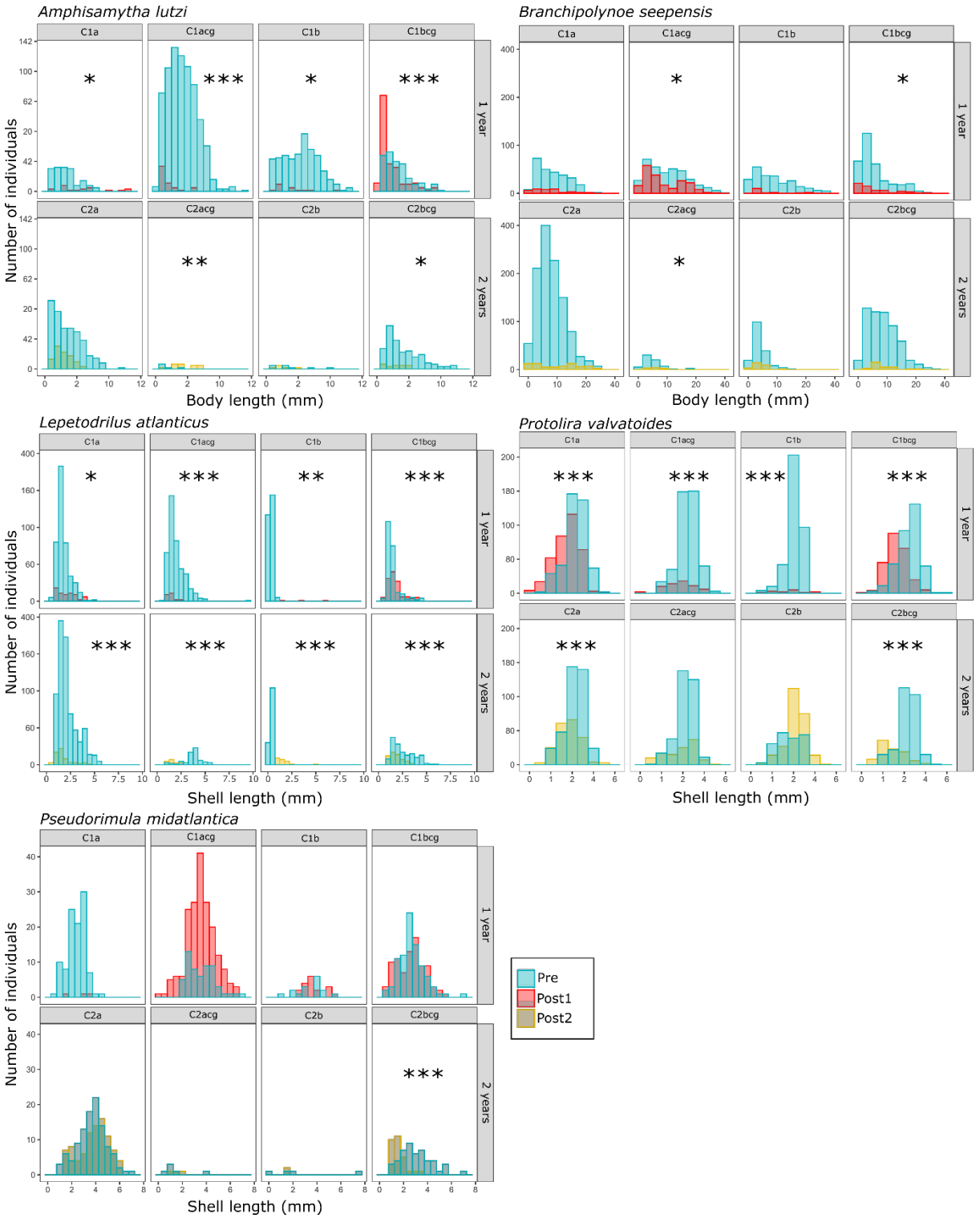

Figure III.S6. Size frequency distribution of the most dominant species for each quadrat sampled at the Montségur active edifice at the Lucky Strike vent field (Mid-Atlantic Ridge) including the pre-disturbed community (blue) and the community one (red) and two (yellow) years after disturbance. Wilcoxon-Mann-Whitney tests were performed to identify differences in mean individual size between the baseline community and in post-disturbance communities. Asterisks indicate significant differences in mean length. (*p-value<0.05; ** p-value <0.01; *** p-value <0.001)

Table III.S1. Biological characteristics of pre- and post-disturbed communities on the Montségur edifice, extended periphery and inactive structure. * Rare taxa represents species with total frequency bellow 1% in the overall community.

Biological characteristics	Pre-disturbed	1 year post-disturbance	2 years post-disturbance
Montségur			
Range mussel size (mean ± sd)	288 µm to 8.5 cm (9.3 ± 11.7 mm)	251 µm to 7.8 cm (8.4 ± 13.9 mm)	393 µm to 5.7 cm (6.5 ± 10.3 mm)
% juvenile (< 5mm)	52 %	67%	70%
B. azoricus recovery rate	Baseline	9.7 % - 37.6 %	1.9 % - 33 %
5most dominant taxa	*B. azoricus* *B. seepensis* *L. atlanticus* *P. valvatoides* *A. Lutzi*	*B. azoricus* *P. valvatoides* *O. dyvae* *Aphotoponthus sp.* *L. atlanticus*	*P. valvatoides* *L. vitreus* *B. azoricus* *L. desbruyeresi* *O. dyvae*
Faunal densities	34 402 ± 7 590 ind.m^{-2}	15 768 ± 12 487 ind.m^{-2}	11 190 ± 8 270 ind.m^{-2}
% of rare taxa*	29/40 (74%)	20/33 (60%)	19/33 (58%)
Taxonomic richness	19-28	18-27	17-28
Total density recovery	Baseline	15.8-68.3 %	21-79.6 %
Environmental drivers	Maximum temperature Sulphide concentrations		
Extended periphery			
5 most dominant taxa	*Tanaidacae sp2* *G. tesselata* *Harpacticoida sp.* *Haplomunnidae sp.* *Syllidae sp.*	*Harpacticoida sp.* *Syllidae sp.* *Bythocypris sp.* *O. dyvae* *L. vitreus*	
Faunal densities	2 440 and 6 440 ind.m^{-2}	1 530 and 1 520 ind.m^{-2}	
Taxonomic richness	18 and 17	9 and 11	
Total density recovery	Baseline	25 and 62%	
Environmental drivers	Oxygen, pH		
Inactive structure			
5 most dominant taxa	*Harpacticoida sp.* *Bythocypris sp.* *Tanaidacae sp2* *Munnopsidae sp.* *Epicaridea sp.*	*Harpacticoida sp.* *O. dyvae* *Bythocypris sp.* *L. vitreus* *Halacaridae sp.*	
Faunal densities	3 330 and 4 510 ind.m^{-2}	1 580 and 2500 ind.m^{-2}	
Taxonomic richness	14	10 and 13	
Total density recovery	Baseline	47 and 55 %	
Environmental drivers	Oxygen, pH		

III.7. Synthèse des résultats

Ce travail a permis d'effectuer une description complète des assemblages de macrofaune à l'état de référence au sein de l'édifice actif Montségur. Ces assemblages présentent de fortes similitudes avec les communautés décrites sur l'édifice voisin Tour Eiffel confirmant une forte connectivité à l'échelle du champ hydrothermal Lucky Strike (Sarrazin et al. 2020).

La dynamique de recolonisation sur Montségur, à la suite de cette perturbation de défaunation, semble gouvernée à la fois par le recrutement et l'installation post-larvaire mais également par la migration d'individus adultes en provenance des assemblages adjacents. Le suivi de la structure des assemblages a mis en évidence un bon rétablissement de la richesse taxonomique à l'exception de quelques espèces « rares » au cours des deux années consécutives à la perturbation. Ces résultats contrastent avec un faible retour des densités d'organismes et un réarrangement de la composition des assemblages. En effet, malgré une bonne stabilité des conditions environnementales, l'espèce ingénieure *Bathymodiolus azoricus* n'a que partiellement réinvesti l'espace libéré par la perturbation. Or cette espèce, au même titre que d'autres espèces ingénieures de l'écosystème hydrothermal, est reconnue pour jouer un rôle important dans la structuration de l'habitat et la régulation des conditions environnementales (Johnson et al. 1988 ; Le Bris et Gaill 2006) favorisant ainsi la richesse taxonomique des espèces associées (Van Dover et al. 2002 ; Govenar et Fisher 2007 ; Lelièvre et al. 2018). D'importantes modifications de la composition des assemblages ont été mises en évidence au cours du processus de rétablissement, notamment caractérisées par une répartition plus uniforme des différentes espèces et une forte augmentation des densités relatives de plusieurs espèces de gastéropodes (*Protolira valvatoides, Lurifax vitreus, Pseudorimula midatlantica, Xylophaga analoga*). Le modèle de succession, proposé à l'issue de ce travail, suppose d'ailleurs que ces gastéropodes constituent les premiers colonisateurs de macrofaune des habitats impactés par une perturbation à petite échelle sur le champ hydrothermal Lucky Strike. Enfin, l'expérience d'exclusion des grands prédateurs mobiles (poissons, crabes, crevettes) montre qu'ils jouent un rôle sur le rétablissement des assemblages au sein de l'édifice actif Montségur. En se nourrissant de recrues, ils semblent influer sur le recrutement des espèces et plus particulièrement sur l'installation de l'espèce ingénieure *Bathymodiolus azoricus*.

L'appréciation de la résilience d'un écosystème passe par l'évaluation du rétablissement en réponse à une perturbation aussi bien d'un point de vue structurel que fonctionnel (Folke et al. 2004). En effet, il a été établi que l'étude des traits fonctionnels est plus informative sur le fonctionnement d'un écosystème que la simple utilisation de la richesse spécifique (Hooper et al. 2005). Bien qu'en règle générale, une augmentation de la richesse taxonomique aboutit à une augmentation de la diversité fonctionnelle, favorisant ainsi la coexistence des espèces (Hooper et al. 2005 ; Micheli et Halpern 2005 ; Alfaro et al. 2020), la force de cette relation est susceptible de varier. Par exemple, dans certains écosystèmes très diversifiés, il n'est pas rare d'assister à une forte redondance fonctionnelle induisant un décalage entre l'augmentation de la richesse taxonomique et de la diversité fonctionnelle qui tend vers une asymptote à l'approche de sa valeur maximale (Micheli et Halpern 2005). Dans ce contexte, il paraît nécessaire de se focaliser ici sur la diversité fonctionnelle des assemblages afin d'établir le lien avec la richesse taxonomique mais également d'être en mesure de prédire leur capacité de résilience en réponse à des perturbations.

Bearhop et al. (2004) ont développé le concept de niche isotopique, proposant ainsi d'utiliser la variation des ratios isotopiques au sein de communautés (ou de populations) pour comparer l'étendue de leur niche isotopique. De plus, Rigolet et al. (2015) ont déclaré que l'espace bidimensionnel constitué par les ratios isotopiques du carbone ($\delta^{13}C$) et de l'azote ($\delta^{15}N$) reflétait à la fois certains traits biologiques (comportement de nutrition, caractéristiques morphologiques) mais également les relations interspécifiques (compétition pour la ressource, prédation, etc.) au sein du réseau trophique. Les analyses isotopiques permettent donc d'obtenir des informations sur la diversité fonctionnelle au sein d'une communauté. Dans le chapitre suivant, nous avons donc étudié l'évolution de la structure du réseau trophique des assemblages de macrofaune sur l'édifice actif Montségur, au cours du processus de rétablissement. L'approche combinée des analyses isotopiques ($\delta^{13}C$ et $\delta^{13}N$) et de l'estimation de la biomasse nous a permis d'estimer des caractéristiques clés du réseau trophique (i.e. étendue du réseau trophique, diversité des ressources, redondance et spécialisation du régime trophique des espèces, etc.) et de quantifier les principales voies de transfert de matière organique des assemblages. Le rétablissement de la structure du réseau trophique a été quantifié grâce à l'utilisation de métriques isotopiques à l'échelle des communautés (Layman et al. 2007) tout au long du processus de recolonisation. Enfin, la

distribution des différentes guildes trophiques au cours des deux années qui ont suivi la perturbation nous a permis de mieux appréhender le rôle des interactions biotiques sur le rétablissement des assemblages.

IV. Rétablissement de la structure du réseau trophique en réponse à une perturbation

Hydrothermal food web recovery after small-scale disturbance: an experimental approach

Marticorena J., Sarrazin J., Schaal G., Michel N.L., Leroux R., Matabos M.

IV.1. Introduction

In the global context of climate change and intensification of anthropogenic disturbances, ecosystems are facing habitat loss and fragmentation, resulting in a decline of species diversity, abundances and modifications of ecosystem functions and services (Hoekstra et al., 2005; Cardinale et al., 2012; Ceballos et al., 2015). One of the main concerns of ecologists has been to assess the ecosystem's response to these changes and evaluate their resilience potential to natural or anthropogenic disturbances. Resilience can be defined as the ability of an ecosystem to persist or maintain its overall structure and functions in the face of external disturbance (Holling, 1973; Walker et al., 2004). Understanding the relationship between community structure and functional diversity is critical to predict ecosystem response and propose effective environmental management plans (Hooper et al., 2005).

The deep sea, considered as the largest biome on Earth, is increasingly threatened by direct and indirect impacts of anthropogenic activities (Ramirez-Llodra et al., 2011; Mengerink et al., 2014). As a result, a recent deep-sea expert elicitation revealed a wide consensus about the necessity to assess ecosystem damage and recovery, with a particular focus on ecosystem functioning through estimation of food-web structure and biomass transfer (Danovaro et al., 2020), which have been identified as major components of ecosystem functioning (Govenar, 2012). Stable isotope and functional trait analyses are useful approaches to describe food-web structure and identify trophic interactions as they provide a time-integrated overview of animal’s diet over a long timescale (Peterson and Fry, 1987; Post, 2002).

Deep-sea hydrothermal vent food webs are mainly supported by chemosynthetic primary production, performed by free-living and symbiotic chemoautotrophic microorganisms (Childress and Fisher, 1992; Jannasch, 1985). This autochthonous primary production may involve different chemosynthetic pathways depending on the carbon sources but also on which electron donors and acceptors are used by the microorganisms for autotrophic

reactions (Hügler and Sievert, 2011; Karl, 1995). Most vent communities are dominated by dense assemblages of engineer symbiotic species (e.g. bathymodiolin mussels, siboglinid tubeworms, gastropods), which promote local diversity by providing additional colonisation substratum, increasing habitat complexity and multiplying potential ecological niches (Dreyer et al., 2005; Govenar and Fisher, 2007). However, despite their high productivity, few species appear to directly feed on them and to contribute to the export of this biomass to upper trophic levels (Bergquist et al., 2007; De Busserolles et al., 2009; Lelièvre et al., 2018). Vent assemblages are often characterized by high abundances of bacterivore primary consumers, including grazers and deposit feeders, feeding on free-living microbial communities, (Govenar, 2012; Lelièvre et al., 2018; Portail et al., 2018). Secondary consumers include local predators and scavengers feeding on primary consumers and dead animals but also a few abyssal opportunistic species attracted by the high productivity of vent systems (Levin et al., 2016). Some species are described as specialists but generalism is most common in vent assemblages. Moreover, many species exhibit an important trophic flexibility which may be an advantage in such a variable environment (Bell et al., 2016; Bergquist et al., 2007; Levin et al., 2016, 2009; Portail et al., 2016). Habitat selection and trophic partitioning are also described as major factors structuring vent communities (Beinart et al., 2012; Govenar et al., 2015; Levesque et al., 2003; Levin et al., 2013; Portail et al., 2016).

Hydrothermal habitats are characterized by a high spatial and temporal variability of abiotic factors, which plays an important role on faunal distribution at local scales (Husson et al., 2017; Le Bris et al., 2019; Mullineaux et al., 2018; Tunnicliffe, 1991), and affects carbon fluxes within the food web (De Busserolles et al., 2009; Govenar, 2012; Limen and Juniper, 2006).

At larger scales, hydrothermal ecosystems may be subject to natural disturbance events such as volcanic eruptions that can eradicate faunal assemblages and reshape community composition and functional diversity through recovery. New potential anthropogenic activities in the deep sea may also impact the structure and dynamics of these communities. Indeed, deep-sea mineral resources have been considered for commercial exploitation that could directly or indirectly impact faunal communities (Van Dover et al., 2011; Ramirez-Llodra et al., 2011). In this context, fundamental knowledge about the recovery dynamics of vent communities and a description of community structure and functional diversity post-

disturbance are needed to start gaining insights about the resilience of these communities (Boschen et al., 2013).

In this study, we investigate the evolution of the trophic structure in eight vent assemblages after an experimental small-scale disturbance, compare this structure to the pre-disturbance (baseline) state and assess the role of predators in the recovery process. The combined stable isotopes/biomass approach will be used to estimate several food web features, including source diversification, food-chain length as well as trophic specialization and redundancy within each assemblage (Layman et al., 2007; Portail et al., 2018; Rigolet et al., 2015). Therefore, we aim at answering the following questions: (1) What is the trophic structure of baseline communities at Montsegur? (2) How does the trophic structure recover 2 years after a disturbance in relation to the pre-disturbed communities? (3) What is the role of large mobile predators in food-web structure during the recovery? (4) How does the engineer species *Bathymodiolus azoricus* contribute to the associated macrofaunal food web and can they influence the recovery of the trophic structure? We expect an incomplete recovery of the food-web structure in the two years following the disturbance due to a decrease of habitat heterogeneity and faunal diversity in response to absence of large *B. azoricus* individuals. We also hypothesize that the presence of large predators will slow down the recovery of the food-web structure through a top-down control.

IV.2. Materials and methods

IV.2.1. Experimental design and faunal sampling

This study was conducted on an active hydrothermal vent edifice, situated at the Lucky Strike (LS) vent field on the Mid-Atlantic Ridge (MAR; Figure IV.1). It is part of a defaunation experiment that was set up in 2017 and to evaluate the recovery rate and recolonisation dynamics of vent communities after an experimental small-scale disturbance (Marticorena et al. 2021). Faunal clearance sampling was carried out on eight (50 x 50 cm) quadrats deployed over Bathymodiolus azoricus assemblages colonising the Montségur edifice. Faunal removal was performed using the claw of the hydraulic arm and the suction device of the Victor6000 ROV onboard the R/V Pourquoi pas ? and aimed to 1) provide a reference state of the community at Montsegur and 2) open a new surface for colonisation and follow recolonisation and recovery processes. Among those eight quadrats sampled in 2017, four were resampled one year later, in August 2018 (quadrats noted “C1”; Figs. IV.1 & IV.2) and the other four,

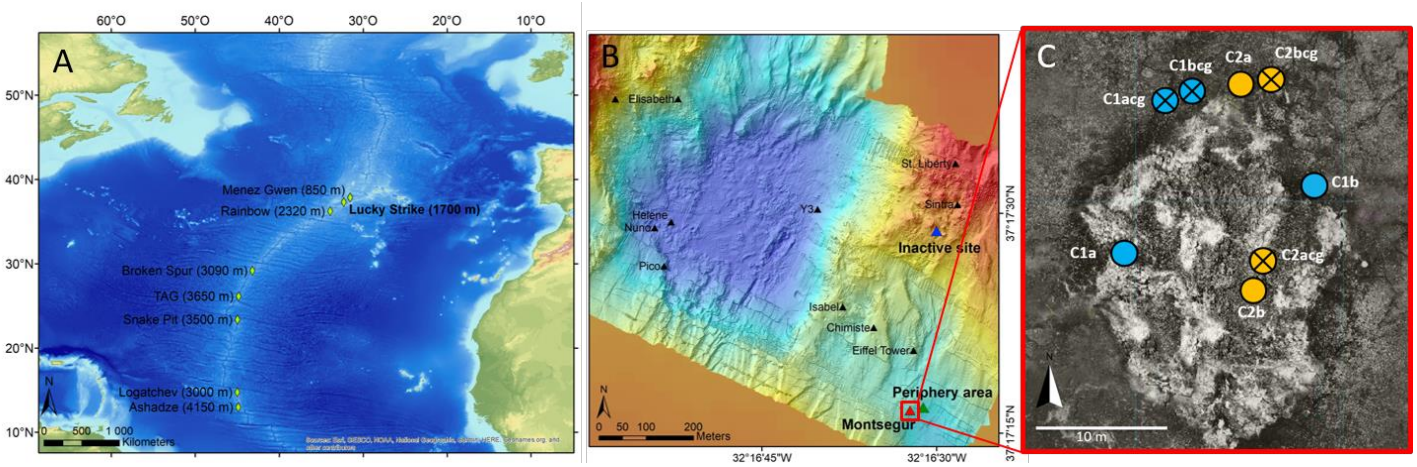

Figure IV.1. A. Location of the Lucky Strike (LS) vent field along the Mid-Atlantic Ridge. **B**. Bathymetric chart of LS with the Montségur edifice (▲) **C**. Position of the experimental and reference quadrats on and around Montségur. Blue circles represent those used to study the recolonisation after 1 year, and orange circles represent the experimental quadrats used to study the recolonisation after 2 years. Crossed off circles represent "caged" quadrats while empty circles represent those without cage.

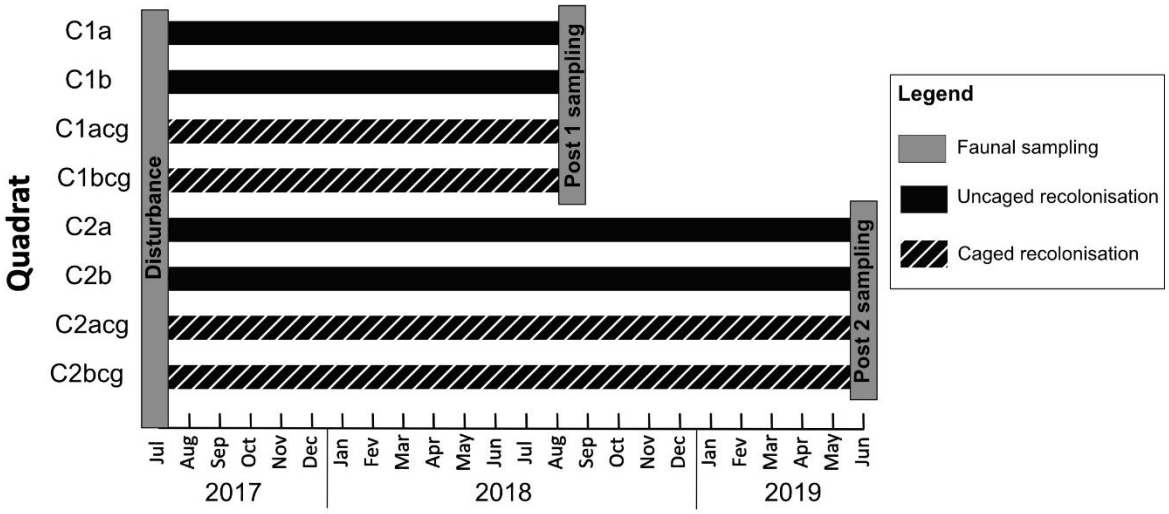

Figure IV.2. Summary of the experimental design used to follow the food web structure of vent faunal assemblages after an induced disturbance on the MAR. Each ~ 50 x 50 cm quadrat (named C1 or C2) has been sampled in 2017 to assess pre-disturbed trophic structure. A disturbance was then induced by clearing the substrata within each quadrat, opening a new available surface. The "C1" assemblages were resampled one year after the disturbance in August 2018 (Post 1) and the "C2" assemblages two years after the disturbance in June 2019 (Post 2). In addition quadrat names ending with "cg" and represented by hatched rectangles were equipped with cages to exclude large predators, those in black were left uncaged.

two years after the disturbance, in June 2019 (quadrats noted “C2”; Figs. IV.1 & IV.2). In addition, we deployed a predator exclusion experiment aiming at identifying the role of large predators on food-web structure along the recovery process. Indeed, half of the quadrats were protected by caged pyramidal structures surrounded by a 1 cm plastic mesh to exclude large mobile predators such as crabs, shrimps or fish (quadrats denoted “cg”).

IV.2.2. Laboratory analyses

Faunal identification

On board, all faunal samples were washed on a 300 µm mesh sieve to recover macrofaunal organisms and large meiofaunal individuals. Each specimen was then identified to the lowest taxonomic level (i.e. generally down to species level) under a stereomicroscope and preserved in 96 % ethanol.

Stable isotope analyses

Sample preparation for stable isotopes analyses were different depending on specimen size. For large organisms, the measurement was performed on muscle tissue while for small specimens the entire body or a pool of several individuals were used to reach sufficient mass for isotope analyses. When possible, 5 replicate measurements for each species of each sample were made to account for intraspecific variability in isotopic composition. Animal tissues were oven-dried at least 48 h at 60°C and ground into homogeneous powder using a mortar and a pestle. Filamentous bacteria attached to each pyramidal structure were detached in sea water and filtered on pre-combusted GF/F filters and oven-dried. Between 0.7 and 1 mg of organic powder from animal tissues and material scrubbed from filters were then placed in tin capsules for isotope analyses. Carbon and nitrogen isotope ratios were determined using a Thermo Scientific FLASH 2000 Organic Elemental Analyser coupled with a Delta V Plus isotope ratio mass spectrometer. Isotopic ratios are expressed in δ (‰) and calculated from international standards (Vienna Pee Dee Belemnite for $\delta^{13}C$ and atmospheric dinitrogen for $\delta^{15}N$) using the formula:

$$\delta X = \left[\left(\frac{R_{sample}}{R_{standard}}\right) - 1\right] \times 1000 \text{ (in ‰)},$$

with δX representing $\delta^{13}C$ or $\delta^{13}N$, and R corresponding to $^{13}C/^{12}C$ or $^{15}N/^{14}N$ ratio.

Species analysed for stable isotopes represented more than 97% of the total taxa identified on the different assemblages and more than 99% of total biomass. Hence, we can consider that our isotopic analysis provides a fair representation of the food web in the communities investigated.

IV.2.3. Data analyses

Biomass characterization

The biomass for each species was measured as grams of Ash-Free Dry Weight (AFDM) per square meter. To assess the biomass of most macrofaunal species in the different samples, we estimated individual AFDW (g) from the measurements of 10 random specimens for each taxa, multiplied by their density in each assemblage. For the engineer species *Bathymodiolus azoricus* and its associated scale-worm *Branchipolynoe seepensis,* we used a length-weight relationship to estimate the total biomass. A positive non-linear regression was identified between the length (L in mm) and the organic matter biomass (AFDW in g) of *Bathymodiolus azoricus* (AFDW = $10^{-4.263}$ x $L^{2.389}$, R^2 = 0.98) and *Branchipolynoe seepensis* (AFDW = $10^{-6.310}$ x $L^{2.645}$, R^2 = 0.83). These equations have been used to infer the total biomass for these two species from the population size structure.

Isotopic niche characteristics

Each species can be classified into different trophic guilds: symbiont host (e.g. hosts chemosynthetic symbiont in specific organs), grazer (e.g. mainly bacterivores, feeding by scrapping the substratum), deposit feeder (e.g. feed on microorganisms and detritus attached to hard substratum or buried) and predator/scavenger (e.g. carnivorous capturing preys or feeding on dead animals). We compiled the trophic guild of each species sampled in this study based on the literature, description of feeding organs and isotopic results (Table 1). For species with unknown diets, we used the trophic guilds of closely related species.

The food web structure was studied using community-wide isotopic metrics along the recovery process (Layman et al., 2007). These metrics are based on the mean position of each species in the bi-dimensional isotopic space of $\delta^{13}C$ and $\delta^{15}N$ for each assemblage and allow the comparison of different aspects of the food-web structure. For example, the total area of

the convex hull (TA) (Layman et al., 2007) and the standard ellipse area (SEA) (Jackson et al., 2011) are two descriptors of the isotopic richness of the community. As some quadrat contained less than 30 measurements, standard ellipse areas corrected for small samples (SEAc) were computed (Jackson et al., 2011). Additionally, other descriptors of various facets of isotopic diversity (Layman et al., 2007) were calculated on each assemblage. Diversity of basal resources was estimated using the range of $\delta^{13}C$ (CR) while the food chain length was inferred by measurement of the $\delta^{15}N$ (NR); the mean distance to the $\delta^{13}C$ – $\delta^{15}N$ centroid (CD) provides an estimation of the degree of dietary separation of the species; mean nearest neighbour distance (MNND) is a measure of density and clustering of species within a community; the standard deviation of the nearest neighbour distance (SDNND) corresponds to a measure of evenness of partial density and packing of the species. All metrics were calculated using the SIBER package (Jackson et al., 2011) in R. One and two year post-disturbance trophic networks were compared with pre-disturbance states to follow the evolution of the food-web structure along the recovery process. Cage and uncaged quadrats were also dissociated in this comparison to identify the role of large predators on the different facets of the trophic structure and in the transfer of biomass along the food chain.

Trophic relationship between *Bathymodiolus azoricus* and *Branchipolynoe seepensis*

Among the individuals sampled in pre-disturbed assemblages, 30 specimens of *Bathymodiolus azoricus* were selected and dissected to extract the polynoid worms *Branchipolynoe seepensis*, potentially living in their palleal cavity. Each of these mussels – ranging from 16 to 73 mm – was colonised by at least one individual of *Branchipolynoe seepensis.* The $\delta^{13}C$ and $\delta^{15}N$ composition was measured in the associated individuals. The relationship between these two species was assessed through a linear regression to identify a potential trophic link.

Table IV.1. Trophic guild and nutritional modes of macrofaunal species associated with the *Bathymodiolus azoricus* assemblages of the Montségur edifice (Lucky Strike vent field, MAR)

Phylum	Class	Family/Order	Espece	Trophic guild	Reference
Annelida	Polychaeta	Ampharetidae	*Amphisamytha lutzi*	Deposit feeder	(Colaço et al. 2002)
		Amphinomidae	*Archinome sp.*	Predator/Scavenger	(Ward et al. 2003) ; (Desbruyères et al. 2006)
		Dorvilleidae	*Ophryotrocha fabriae*	Grazer	(Blake and Hilbig 1990; Bergquist et al. 2007)
		Glyceridae	*Glycera tesselata*	Predator/Scavenger	(Blake 1985; Desbruyères et al. 2006)
		Hesionidae	*Hesiolyra cf. bergi*	Deposit feeder	(Van Dover and Fry 1989)
		Polynoidae	*Branchipolynoe seepensis*	Deposit feeder	(Van Dover et al. 1999; Colaço et al. 2002; Desbruyères et al. 2006; Britayev et al. 2007)
			Branchinotogluma sp.	Predator/Scavenger	(Pettibone, 1988; Bergquist et al., 2007; Lelièvre et al., 2018; Portail et al. 2018)
			Lepidonotopodium jouinae	Predator/Scavenger	(Desbruyères et al., 2000; Jumars 2015, Portail et al., 2018)
			Eulagiscinae sp.	Predator/Scavenger	(Pettibone, 1997; Jumars 2015)
			cf. Thermiphione risensis	Predator/Scavenger	(Jumars et al. 2015)
			Levensteiniella iris	Predator/Scavenger	(Hourdez and Desbruyeres 2003; Bergquist et al. 2007; Lelièvre et al. 2018)
		Ciratulidae	*Cirratulidae sp.*	Deposit feeder	(Jumars et al. 2015)
		Spionidae	*Prionospio unilamellata*	Deposit feeder	(Jumars et al., 2015; Portail et al. 2018)
Mollusca	Gastropoda	Elachisinidae	*Laeviphitus desbruyeresi*	Grazer	(Desbruyères et al. 2006)
		Lepetodrilidae	*Pseudorimula midatlantica*	Grazer	(Desbruyères et al. 2006; De Busserolles et al. 2009)
			Lepetodrilus atlanticus	Grazer	(Colaço et al., 2002; Portail et al. 2018)
		Neolepetospidae	*Paralepetopsis ferrugivora*	Grazer	(Waren et Bouchet, 2001)
		Orbitestellidae	*Lurifax vitreus*	Grazer	(Desbruyères et al. 2006)
		Peltospiridae	*Peltospira smaragdin*	Grazer/ Symbiotic ?	(Goffredi et al. 2004; Desbruyères et al. 2006)
			Lirapex costellatus	Grazer	(Desbruyères et al. 2006; De Busserolles et al. 2009)
		Phenacolepadidae	*Divia briandi*	Grazer	(Desbruyères et al. 2006)
		Raphitomidae	*Phymorhynchus sp.*	Predator/Scavenger	(Desbruyères et al. 2006)
		Xylodisculidae	*Xylodiscula analoga*	Grazer	(Warèn and Bouchet 1993; Desbruyères et al. 2006)
		Skeneidae	*Protolira valvatoides*	Grazer	(Desbruyères et al. 2006; Colaço et al. 2007; Portail et al. 2018)
	Bivalva	Mytilidae	*Bathymodiolus azoricus*	Symbiont host	(Fisher 1990)
Arthropoda	Malacostraca	Alvinocarididae	*Mirocaris fortunata*	Predator/Scavenger	(Colaço et al. 2002; Portail et al. 2018)
		Amphipoda	*Luckia striki*	Deposit feeder	(Desbruyères et al. 2006)
		Bythograeidae	*Segonzacia mesatlantica*	Predator/Scavenger	(Colaço et al. 2002; De Busserolles et al. 2009)
		Copepoda	*Aphotopontius sp.*	Grazer	(Bergquist et al. 2007)
			Harpacticoida sp.	Grazer	(Desbruyères et al. 2006)
		Cumacea	*Thalycrocuma cf. sarradini*	Deposit feeder	(Desbruyères et al. 2006)
			Cumacea sp	Deposit feeder	(Desbruyères et al. 2006)
		Tanaidacea	*Pseudotanais sp.*	Deposit feeder	(Desbruyères et al. 2006)
	Pycnogonida	Ammotheidae	*Sericosura heteroscela*	Predator/Scavenger	(Brescia and Tunnicliffe 1998)
	Ostracoda	Cytheruridae	*Cytheruridae sp.*	Grazer	(Desbruyères et al. 2006)
	Arachnida	Halacaroidea	*Halacaridae sp.*	Predator/Scavenger	(Bergquist et al. 2007)
Sipuncula	Undetermined	Undetermined	*Sipuncula sp.*	Deposit feeder	(Desbruyères et al. 2006)
Cnidaria	Anthozoa	Hexacorallia	*Hexacorallia sp.*	Predator/Scavenger	(Desbruyères et al. 2006)
Echinodermata	Ophiuroidea	Undetermined	*Ophiuroidea sp.*	Predator/Scavenger	(Desbruyères et al. 2006)
Nematoda	Enoplea	Oncholaimidae	*Oncholaimus dyvae*	Predator/Scavenger	(Zeppilli et al. 2019)
Nemerta	Undetermined	Undetermined	*Nemerta sp.*	Predator/Scavenger	(Desbruyères et al. 2006)
Porifera	Undetermined	Undetermined	*Porifera sp.*	Predator/Scavenger	(Desbruyères et al. 2006)

IV.3. Results

IV.3.1. Diversity among trophic guild

Overall, 43 macrofaunal species associated to *Bathymodiolus azoricus* mussel assemblages have been identified within the Montségur active edifice. The engineer species *Bathymodiolus azoricus* is the only confirmed symbiotic species of this edifice. In total, 10 species of the mussel assemblages are described as deposit feeders, including mainly polychaetes but also arthropods and sipunculids. The grazing feeding mode is shared by 14 species, including mostly gastropods as well as copepods and some polychaete species that feed on microbial mats by scrapping the substratum. Finally, 18 species representing a wide taxonomic diversity have been described as predators and/or scavengers (Table IV.1).

The taxonomic richness 1 and 2 years after the disturbance did not reach the pre-disturbed values within the different assemblages except for two samples (C2a and C2acg) where higher species richness were observed after 2 years of recovery (Table IV.2, Marticorena et al. 2021). In pre-disturbed samples, a total of 38 species were found while only 32 and 31 species were sampled one (Post 1) and two year (Post 2) after the disturbance (Table IV.2). This difference is mainly due to a lower taxonomic richness of predators/scavengers, with 10 and 9 species identified in Post 1 and Post 2 assemblages respectively compared to 16 species in the pre-disturbed samples (Table IV.2). The species that did not recover in Post 1 and Post 2 samples were mainly polychaetes (*Archinome sp., Hesiolyra sp., Eulagiscinae sp. Levensteinella sp., Dorvilleidae sp.*), crabs (*Segonzacia mesatlantica*), sponges and the gastropod *Phymorynchus sp.* (Table IV.S1). Most of these species are considered as “rare” due to their low abundance within the eight pre-disturbance samples (Marticorena et al. 2021).

IV.3.2. Biomass recovery

Macrofaunal biomass was dominated by the engineer species *B. azoricus*, representing 98.6% ± 0.3% of the total AFDW within the different assemblages (Figure IV.S1). *B. azoricus* biomass showed a high variability among pre-disturbance samples, ranging from 53 $g.m^{-2}$ to 1147 $g.m^{-2}$ (Figure IV.S1). Furthermore, its mean total biomass decreased from 517.5 ± 351.2 $g.m^{-2}$ in pre-disturbed assemblages to 126.5 ± 129.8 $g.m^{-2}$, one year after the disturbance and 25.25 ± 19.5 $g.m^{-2}$, two years after the disturbance. As *B. azoricus* is considered as a structuring species of the ecosystem, it was not included in the following biomass analysis.

Table IV.2. Taxonomic richness among the different trophic guilds in each assemblage before and after disturbance.

		Trophic guilde			
Assemblage	Pre/post disturbance	Deposit feeder	Grazer	Predator/Scanvanger	Total
C1a	Pre	7	10	14	32
	Post	8	12	6	27
C1b	Pre	6	10	7	24
	Post	6	7	4	18
C1acg	Pre	8	9	9	27
	Post	6	8	7	22
C1bcg	Pre	7	10	7	25
	Post	6	12	5	24
C2a	Pre	6	13	7	27
	Post	8	13	6	28
C2b	Pre	6	9	6	22
	Post	6	7	3	17
C2acg	Pre	4	8	6	19
	Post	7	10	4	22
C2bcg	Pre	8	11	8	28
	Post	8	11	6	26
Total	**Pre**	**9**	**13**	**16**	**38**
	1 year post	**9**	**13**	**10**	**32**
	2 years post	**9**	**13**	**9**	**31**

The total biomass of other species in pre-disturbed samples was also highly variable and ranged from 0.43 to 3.1 g.m^{-2} among the different samples (Figure IV.3A). Total biomass were lower in assemblages sampled 1 year (0.31 ± 0.32 g.m^{-2}) and 2 years (0.08 ± 0.05 g.m^{-2}) after the disturbance compared to pre-disturbed values (0.51 ± 0.66 g.m^{-2}) (Figure IV.3A). With a relative biomass reaching 78%, deposit feeding was the dominant feeding mode in pre-disturbed assemblages, followed by grazing and predation/scavenging, each one accounting for 11% of total biomass (Figure IV.3B). One year after the disturbance, predators/scavengers, mostly represented by the shrimp *Mirocaris fortunata* (Figure IV.4C, species 22) were dominant in uncaged assemblages, representing 80% of the biomass (Figure IV.3B) while deposit feeders dominated caged assemblages (53%) followed by predators/scavenger (24%) and grazer species (23%) (Figure. IV.3B). After two years of recovery, grazers dominated the biomass, respectively representing 51 % and 41 % of the total biomass in caged and uncaged assemblages (Figure IV.3B). Gastropod species, including *Protolira valvatoides* (species 29), *Lurifax vitreus* (species 21), *Pseudorimula midatlantica* (species 30), and *Lepetodrilus atlanticus* (species 16) mainly contributed to the biomass of grazers in these samples (Figs. IV.4D&E).

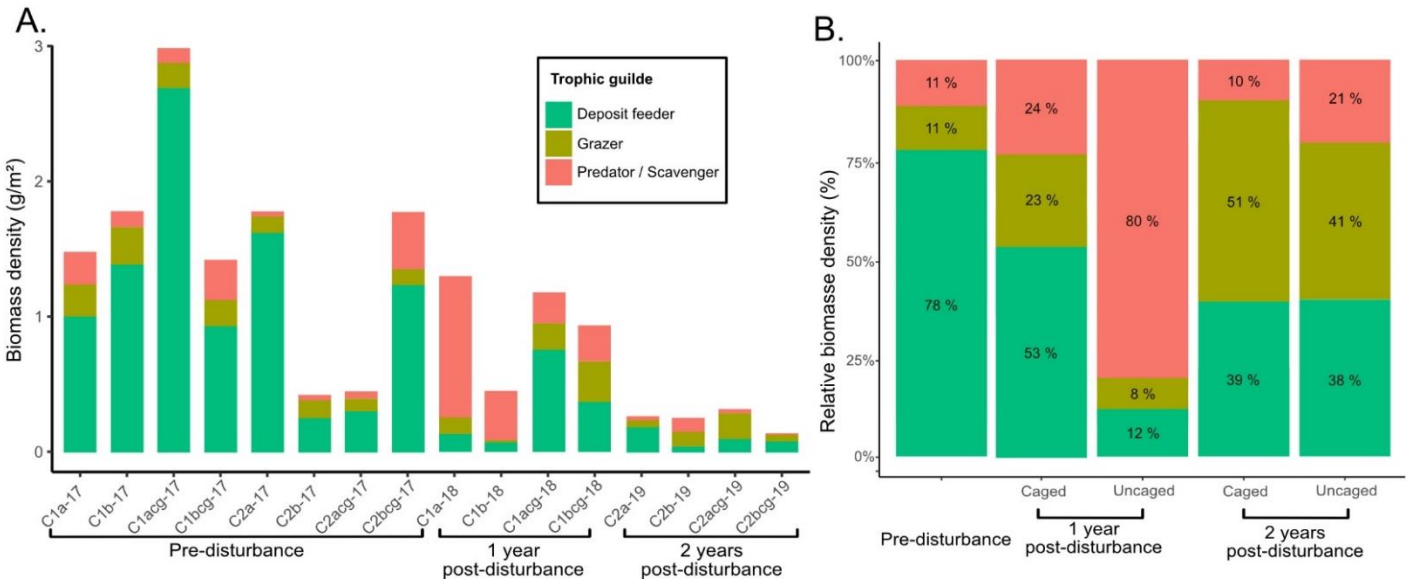

Figure IV.3. A) Biomass of the macrofauna per trophic guild in each experimental quadrat, before and 1 year and 2 years after disturbance. **B**) Relative biomass of the different trophic guilds before the disturbance as well as 1 year and 2 years after the disturbance for caged and uncaged quadrats. The biomass of *Bathymodiolus azoricus* is not represented in this figure as it represents over 90% of the total biomass (see Figure VI.S1 for mussel biomass).

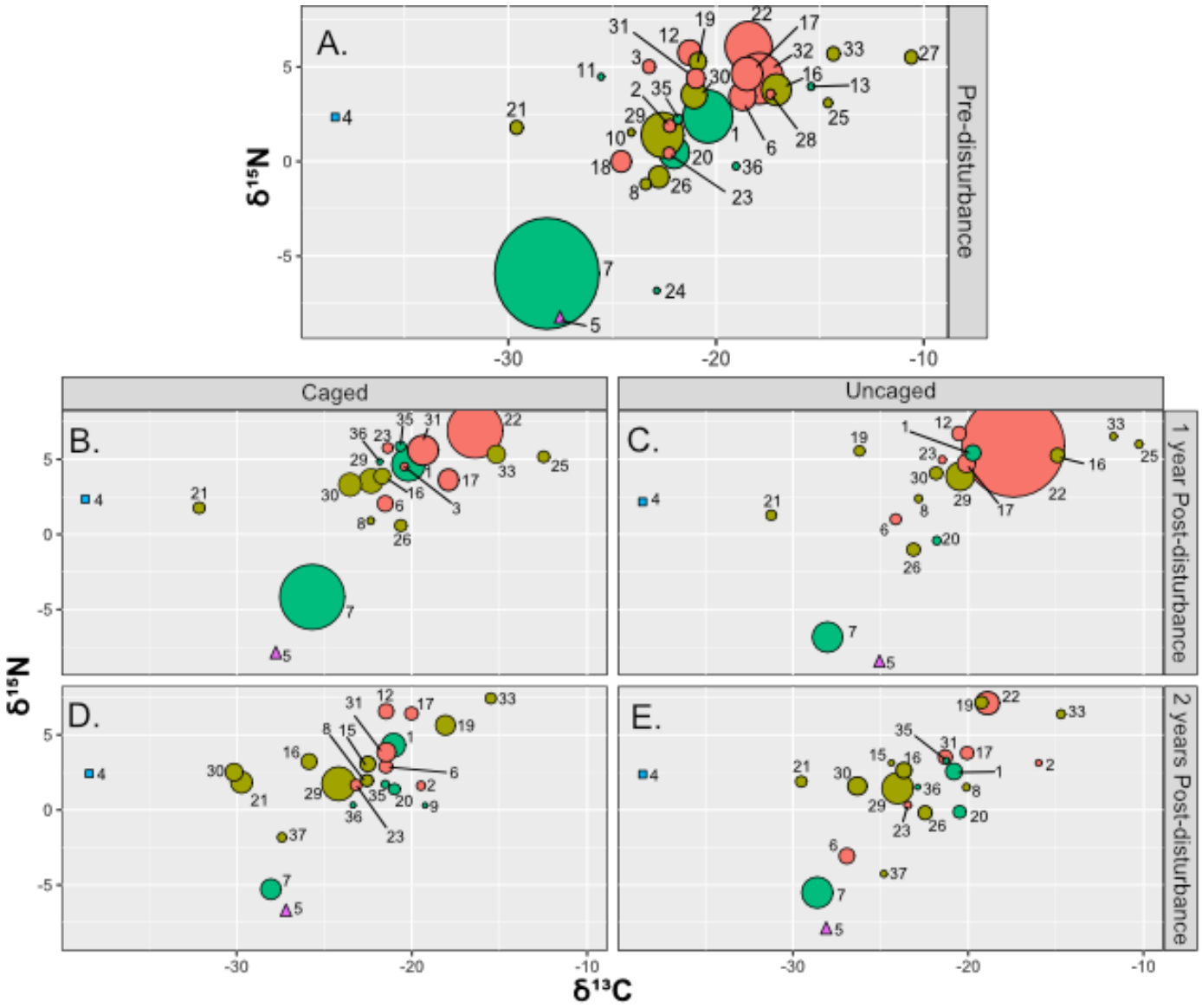

Figure IV.4. Stable isotope bi-plots showing vent consumers' isotope composition weighted by biomass per square metre (filled circles) in the pre-disturbed assemblage (**A)**, after one year (**B** & **C**) and2 years (**D** & **E**) of recolonisation. Results of the predator exclusion experiment are also represented by the caged (**B** & **D**) and uncaged (**C** & **E**) quadrats. Numbers correspond to species: 1 – *Amphisamytha lutzi* 2 – *Hexacorallia* sp.; 3 – *Archinome sp.*; 4 – Bacterial mat; 5 – *Bathymodiolus azoricus*; 6 – *Branchinotogluma* sp.; 7 – *Branchipolynoe seepensis*; 8 – *Aphotopontius* sp.; 9 – *Cumacae* sp.; 10 – *Ophryotrocha fabriae*; 11 – *Porifera* sp.; 12 – *Glycera tesselata*; 13 – *Hesiolyra cf. bergi*; 14 – *cf. Thermiphione risensis*; 15 – *Laeviphitus desbruyeresi*; 16 – *Lepetodrilus atlanticus*; 17 – *Lepidonotopodium jouinae*; 18 – *Levensteiniella iris*; 19 – *Lirapex costellatus*; 20 – *Luckia striki*; 21 – *Lurifax vitreus*; 22 – *Mirocaris fortunata*; 23 – *Oncholaimus dyvae*; 24 – *Nemerta* sp.; 25 – *Ostracod* sp.; 26 – *Paralepetopsis ferrugivora*; 27 – *Peltospira smaragdina*; 28 – *Phymorhynchus* sp.; 29 – *Protolira valvatoides* ; 30 – *Pseudorimula midatlantica*; 31 – *Sericosura heteroscela*; 32 – *Segonzacia mesatlantica*; 33 – *Divia briandi*; 34 – *Sipuncula* sp.; 35 – *Prionospio unilamellata*; 36 – *Pseudotanais* sp.; 37 – *Xylodiscula analoga.* Colors refere to the trophic guild of each species: Symbiotic (pink); chemoautothrophic microorganisms (blue); grazer (khaki green); deposit-feeder (green) and predator (orange)

IV.3.3. $\delta^{13}C$ – $\delta^{15}N$ isotopic composition

The isotopic composition of filamentous bacterial mats ("species"4) sampled on each quadrat showed a high homogeneity within the different assemblages, with a mean $\delta^{13}C$ of -38.4 ± 0.3 ‰ and a mean $\delta^{15}N$ of 2.45 ± 0.1‰ (Figure IV.4). The endosymbiotic species *B. azoricus* showed the lowest $\delta^{15}N$ value on all assemblages and displayed stable isotopic composition along the recovery process with $\delta^{13}C$ ranging from -25.08 to -28.03‰ and $\delta^{15}N$ from -6.4 to -8.3‰ (Figure IV.4). However, when considering a large size range of *B. azoricus* (from 16 to 73 mm), we observed a shift in isotopic composition characterized by an enrichment in $\delta^{13}C$ and $\delta^{15}N$ ratios in larger individuals (Figure IV.S2).

The deposit feeder species displayed a large range of isotopic composition ranging from -28.6 to -15.4‰ in $\delta^{13}C$ and from -6.9 to 5.9‰ in $\delta^{15}N$. Among deposit feeders, the most ^{13}C and ^{15}N depleted composition were observed for the scale-worm *B. seepensis* with an isotopic composition close to that of *B. azoricus*. We identified a linear regression between the isotopic ratios *of B. azoricus* and the correspondent scale-worm (Figure IV.S2). These two species appeared to be isolated from most of the rest of the community in the isotopic bi-plot, except from *Nemerta sp.* (species 24), *Branchinotogluma sp.* (species 6) and *Xylodiscula analoga* (species 37, Figure IV.4). The grazers displayed a very large range of $\delta^{13}C$, varying from -32.1‰ for the gastropod *Lurifax vitreus* (species 21) to -10.25‰ for the gastropod *Peltospira smaragdina* (species 27) and an undetermined ostracod (species 25) (Figure IV.4). Furthermore, the gastropod *Xylodiscula analoga* (species 37) had the lowest $\delta^{15}N$ values with -4.26‰, while *Divia briandi* (species 33) displayed the highest ratio with 7.46‰. Finally, the predator/scavenger species also displayed an important variability of isotopic ratios (Figure IV.4). The polynoid *Branchinotogluma sp.* ($\delta^{13}C$ = -26.9‰, $\delta^{15}N$ = -3.4‰; species 6) showed the most depleted isotopic composition, while the shrimp *Mirocaris fortunata (*$\delta^{13}C$=-16.4‰, $\delta^{15}N$ = 6.9‰; species 22) had higher $\delta^{13}C$ and $\delta^{15}N$ ratios.

Some significant differences in isotopic composition have been identified along the recovery process for the grazer species *Lirapex costellata*, *Ostracoda sp.* and *Protolira valvatoides* as well as for the predators/scavengers *Zoanthidae sp. and Branchinotogluma sp.* (Table IV.S1).

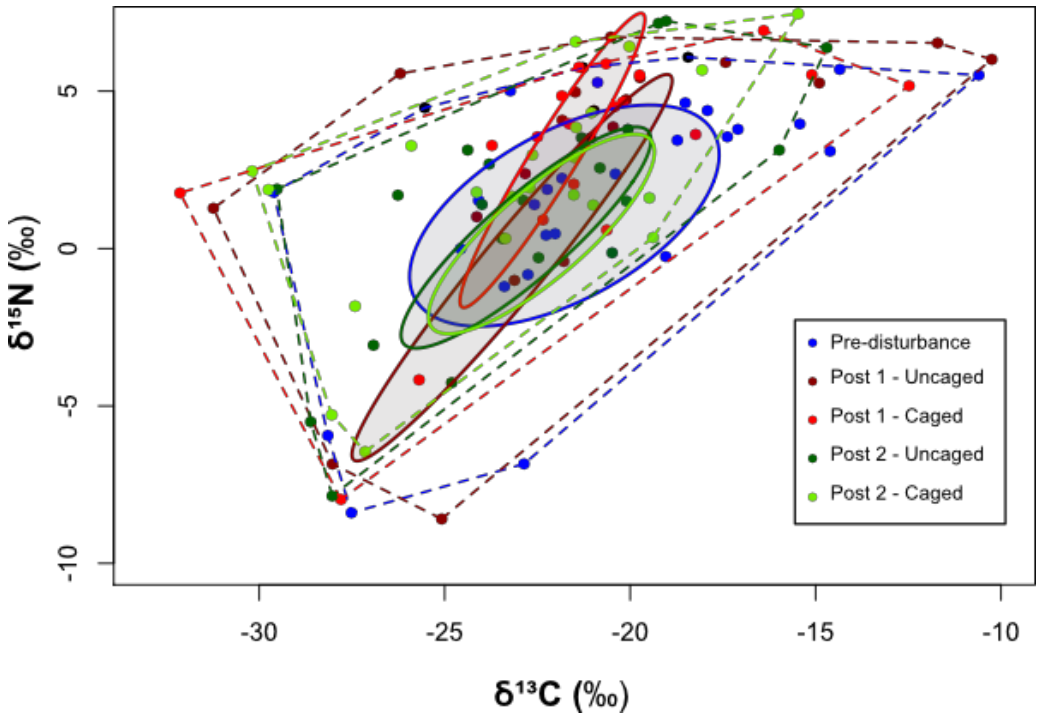

Figure IV.5. Isotopic space of the different assemblages along the recolonisation process. Solid lines enclose the standard ellipse area (SEAc) containing 40% of the data and dashed lines represent the total convex hull area. Colors refer to the year of sampling (Pre/post-disturbance) and shades refer to the predator exclusion treatments, whether or not caged.

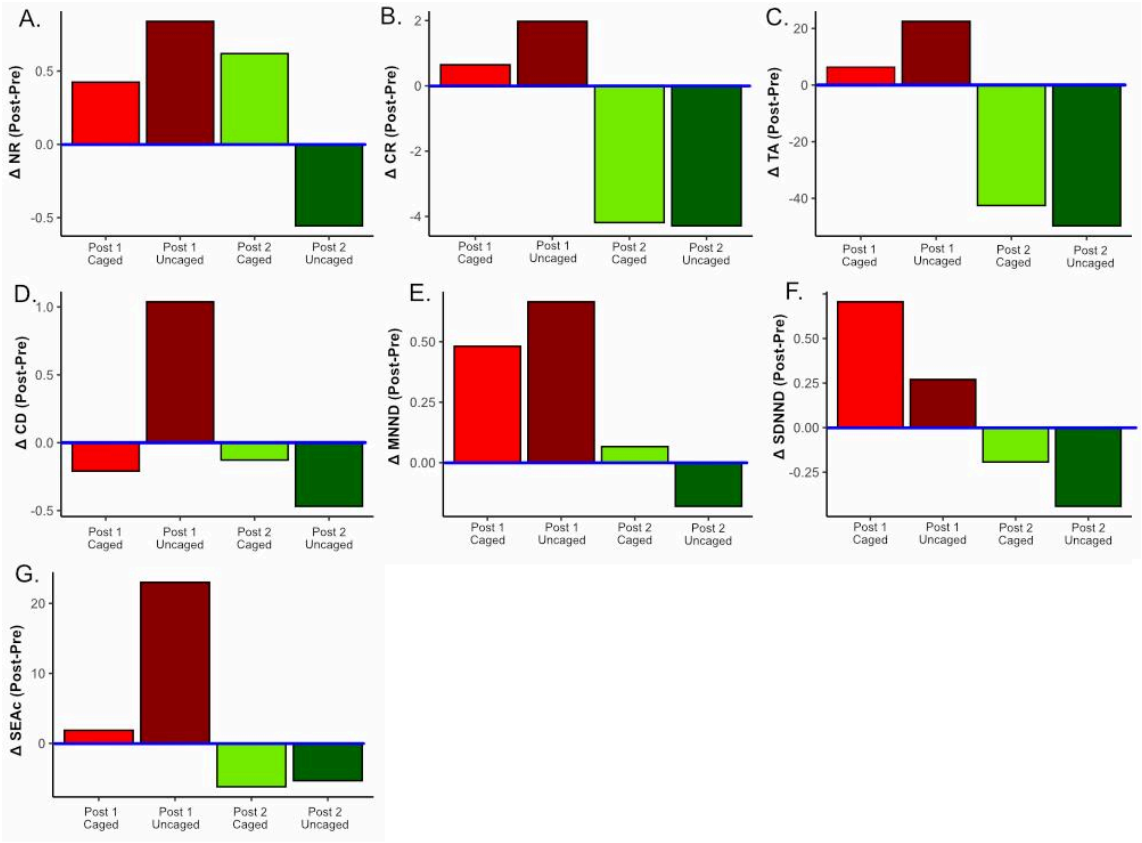

Figure IV.6. Layman metrics associated with the small-scale disturbance experiment on the active edifice Montségur at the Lucky Strike vent field (Mid-Atlantic Ridge). Barplot of anomaly values (Post-disturbance — Pre-disturbance) of the different isotopic metrics are presented along the recolonisation process and considering the predator exclusion experiment.

IV.3.4. Community-wide food web structure

The convex hulls plotted for the samples along the recovery process in caged or uncaged samples showed similar shapes. However, some differences in its width can be observed, especially between pre-disturbance and 2 years after disturbance (Figure IV.5). The standard ellipse drawn for the pre-disturbed assemblages appears wider in comparison to post-disturbance assemblages, which displayed more elliptic shapes (Figure IV.5). Isotopic metrics displayed contrasting results along the recovery process, with higher values of all metrics for Post1 and lower for Post2 samples compared to pre-disturbance (Figure IV.6). Regarding the predator exclusion experiment, one year after the disturbance, caged samples displayed lower metrics values than uncaged ones, except for the standard deviation of nearest neighbour distance (i.e. SDNND). In contrast, two years after the disturbance, caged samples showed higher values of $\delta^{15}N$ range (NR), centroid distance (CD), mean nearest neighbour distance (i.e. MNND) and SDNND while no difference was observed regarding the $\delta^{15}N$ range (CR), the total area of convex hull (TA) and the standard ellipse area (SEA).

IV.4. Discussion

Over the last few decades, studies on vent ecosystems have focused on the recovery rate of hydrothermal communities in response to natural disturbances and described the colonisation dynamics of faunal assemblages using population and community metrics such as diversity, abundance and biomass (Tunnicliffe et al. 1997; Shank et al. 1998; Marcus et al. 2009; Gollner et al. 2015). Many factors may be involved in this process, including larval dispersion and settlement (Van Dover et al. 1988; Mullineaux et al. 2010), environmental conditions (Tunnicliffe et al. 1997; Marcus et al. 2009; Gollner et al. 2015, 2017) and biotic interactions (Shank et al. 1998; Micheli et al. 2002; Mullineaux et al. 2003, 2012; Govenar and Fisher 2007). However, the recovery of the trophic structure following a disturbance has, to our knowledge, not been previously documented for vent communities. Interestingly, the implementation of disturbance experiments can contribute to assess this specific aspect of community recovery.

However, in this work, the induced disturbance was limited to a small spatial scale and the experimental design did not prevent migration of individuals from surrounding faunal

assemblages. Moreover, the impact on faunal communities is not comparable with those expected from large scale natural disturbances or deep-sea mining activities. Indeed, these large-scale disturbances would result in the complete destruction of habitats and eradication of all faunal and microbial communities. Despite these limitations, we identified a clear structural rearrangement of the vent food-web within the first steps of the recovery which will be used to provide additional information to the proposed succession model on the Lucky Strike vent field (Marticorena et al. 2021).

IV.4.1. Taxonomic diversity and biomass along recovery

Hydrothermal ecosystems of the northern part of the Mid-Atlantic Ridge are dominated by dense populations of *Bathymodiolus azoricus,* accounting for more than 90% of the total dry weight and over 99% of the total biomass (Husson et al. 2017). *B. azoricus*, as other vent engineer species, promotes local biodiversity by providing biogenic structures that contribute to increase the colonisation surface and heterogeneity of the habitat, but also to modulate the fluid flux, making the habitat more suitable for other species (Johnson et al. 1986; Jones et al. 1997; Sarrazin et al. 1999, 2015; Van Dover and Trask 2000; Tsurumi and Tunnicliffe 2003). A total of 43 macrofaunal and large meiofaunal taxa were identified among *B. azoricus* assemblages on the Montségur edifice (Marticorena et al. 2021). The dominant taxa were the same as those previously described from communities on the neighbouring edifice Eiffel Tower (Sarrazin et al. 2015). The slow recovery of *B. azoricus* biomass after disturbance, associated with the recolonisation of much smaller mussel individuals (Marticorena et al. 2021) certainly resulted in a reduction of habitat complexity that could explain the slow recovery of biomass for other taxa. Nonetheless, most of the taxonomic richness recovered within two years after the disturbance with the exception of some predator/scavenger taxa (*Archinome sp., Hesiolyra sp., Eulagiscinae sp. Levensteinella sp., Dorvilleidae sp., Segonzacia mesatlantica and Phymorynchus sp.*), present in low abundance in pre-disturbed communities that remained absent two years after the disturbance. Indeed, Marticorena et al. (2021) suggested that the recovery of “rare” predator taxa would probably represent the last step of the ecological succession following a small-scale disturbance at Lucky Strike and their recovery would depend on the establishment and growth of *B. azoricus*. Previous studies conducted at the Juan de Fuca Ridge following a volcanic eruption support the hypothesis that the establishment of engineer species would facilitate the development of associated

assemblages (Marcus et al., 2009). Throughout the 2 years of the experiment, we observed clear successional shifts in the dominant trophic guild within pre- and post-disturbed assemblages.

In the pre-disturbance assemblages, deposit feeders, including non-selective detritivores and bacterivores, were dominant whereas predators/scavengers showed low relative biomass. A similar pattern has already been described for *B. azoricus* assemblages with deposit feeder mainly relying on detrital organic matter such as mussel pseudo-faeces and microbial mats (Portail et al. 2018). One year after the disturbance, the predators/scavengers, mainly represented by the shrimp *Mirocaris fortunata,* dominated the relative biomass, especially in uncaged assemblages. *M. fortunata* is described as an opportunist omnivore, scavenging on dead mussels or exuvia of other shrimps, but also directly grazing on microorganisms attached to mussel shells (Gebruk et al. 2000; Colaço et al. 2002; De Busserolles et al. 2009, Matabos et al. 2015). *M. fortunata* has also been identified as an indicator species of warmer diffused flow habitats (Sarrazin et al. 2015). The environmental characterization performed on the different samples at each step of the recovery process did not show significant differences which could have explained the high biomass of shrimp one year after the disturbance (Marticorena et al. 2021). However, several hypotheses can be formulated to explain this observation. First, the disturbance experiment conducted on the mussel assemblages may have resulted locally in an accumulation of uncollected dead individuals and/or organic material resulting from the mechanical sampling of the area, thus contributing to increase the abundance of scavengers one year after the disturbance. The same process is observed after fishing disturbance by towed gears where mobile scavenger abundances increase and remain important several months after the event (Ramsay et al. 1998; Groenewold and Fonds 2000; Juan et al. 2007). However, considering the high mobility of shrimp in comparison to other identified taxa, it remains difficult to interpret their abundance within the different assemblages so long after the perturbation. On the other hand, the removal of *B. azoricus* may have contributed to increased fluid flux and led to the formation of anhydrite deposit substratum. *M. fortunata* shrimps, accounting for most of predator/scavenger biomass have been described to occupy this specific habitat feeding on organic debris that accumulate on the substratum (Matabos et al., 2015). Finally, some predator species may specifically feed on new settled individuals of *B. azoricus* after the disturbance, which would explain the observed decrease of mussel biomass

the second year. In contrast, the assemblages sampled two years after the disturbance were dominated by grazer species, mainly represented by the gastropods *Protolira valvatoides*, *Lurifax vitreus* and *Pseudorimula midatlantica*. On the East Pacific Rise, gastropods have also been described as the main colonists following the 2006 volcanic eruption (Mullineaux et al., 2010, 2012). Indeed, as most of them are described as bacterivores, they may benefit from the development of free-living microorganisms on bare substrata and primarily occupy the "released'' ecological niche. The low relative biomass of deposit feeders two years after the disturbance in comparison to pre-disturbed communities may be a result of a significant decrease of detrital organic matter accumulation in these assemblages. Moreover, the feeding activity of *B. azoricus* through the production of pseudofeces and the three dimensional structure provided by their shells and byssus filaments must play an important role in detrital matter accumulation as suggested by many authors regarding other engineer species (Sarrazin et al. 2002, Levesque et al. 2003). Yet, the decrease of the relative biomass of deposit feeders may be linked to the poor recovery of *B. azoricus* in the assemblages sampled two years after the disturbance. Finally, the absence of noticeable difference in relative biomass between caged and uncaged assemblages sampled two years after the disturbance suggests that the role of large predators/scavengers in the overall recovery process is limited to the very first months. Micheli et al. (2002) also reported changes in prey's abundances in caged samples on the East Pacific Rise (EPR) and suggest that predation occurred early in the colonisation sequence (8 months) but unlike observed in our study, they also noticed that predation kept playing a major role in community structure through time (Micheli et al. 2002). This divergence may be due to the high temporal variability of faunal communities in EPR vents contrasting with the relative stability of the MAR faunal assemblages (Cuvelier et al. 2011).

The use of biomass to characterise community structure, instead of abundances, allows energy transfer through the food web to be taken into account but some limitations must be considered. First, the important difference in individual biomass between the different species - of several orders of magnitude - may conceal some biodiversity patterns. On the other hand, among hydrothermal vent ecosystems, most symbiotic engineer species primarily play a structuring role but barely contribute to biomass exportation within the food web through predation (Bergquist et al. 2007; De Busserolles et al. 2009). However, scavengers may

significantly contribute to export this high quantity of biomass as suggested by several authors (Bergquist et al. 2007, De Busserolles et al. 2009).

IV.4.2. Trophic structure

Basal food source- The food web of deep-sea chemosynthetic ecosystems mainly relies on autotrophic organic matter provided by microorganisms (Karl 1995). Nonetheless, stable isotope data of these food sources remain scarce due to the difficulty to sample free-living microbial communities (De Busserolles et al. 2009). Moreover, a high diversity of microorganisms using different metabolic pathways, contribute to fuel the vent food web (Childress and Fisher 1992; Nakagawa and Takai 2008; Takai et al. 2013). Sulfide oxidation (thiotrophy), using either the Calvin-Benson-Bassham (CBB) or the reductive tricarboxylic acid (rTCA) cycle, and methanotrophy are considered the most important carbon fixation processes for vent autotrophic taxa (Desbruyères et al. 1994; Tunnicliffe et al. 2003; Campbell and Cary 2004; De Busserolles et al. 2009; Hügler and Sievert 2011). These different basal sources are related to distinct $\delta^{13}C$ (Table 3). At certain vent sites, the contribution of photosynthetic-derived material as energy food source appears to be a component of vent detrital matter together with microbial cell debris, invertebrate body parts and faunal secretion (Levesque and Juniper 2002; Levesque et al. 2005; Limén et al. 2007). On the MAR, photosynthetic-based organic matter display $\delta^{15}N$ values ranging from 4 and 6‰ (Gebruk et al. 2000; Khripounoff et al. 2001) and the most recent studies showed that very few species directly depended on this food source (De Busserolles et al. 2009, Portail et al. 2018). The filamentous bacterial mats, that rapidly developed on the different quadrats of the present study, also sampled at other Lucky Strike vent sites, displayed $\delta^{13}C$ values within the range of thiotrophic primary production using the CBB cycle (Colaço et al. 2002, Portail et al. 2018). These mats are formed by large *Beggiatoa* spp. bacteria but also harbour a variety of other microorganisms (Crépeau et al. 2011).

Table IV.3. Range of $\delta^{13}C$ ratio of the dominant basal sources of hydrothermal vent food web

Metabolic pathway	$\delta^{13}C$ range	Reference
Photosynthetic-derived organic matter	−24 to −22‰	Gebruk et al., 2000; Khripounoff et al., 2001
Chemosynthetic		
Thiotrophy		
Calvin-Benson-Bassham (CBB) cycle	-36 to -30‰	Hügler and Sievert, 2011; Trask and Van Dover, 1999
Reductive tricarboxylic acid (rTCA) cycle	-15 to -10‰	Hügler and Sievert, 2011; Sievert et al., 2008
Methanotrophy	-15 to -11‰	Pond et al. 1998 ; Charlou et al. 2000,2002 ; Portail et al. 2018

The endosymbiotic species *Bathymodiolus azoricus* hosts both thiotrophic and methanotrophic symbionts. A shift in the relative contribution of each pathway, that varies with variations of fluid inputs, a result in a wide range of $\delta^{13}C$ between individuals (Trask and Van Dover 1999; Colaço et al. 2002; De Busserolles et al. 2009; Portail et al. 2018). As already reported, the progressive enrichment in ^{13}C (from -31 ‰ to -18 ‰) correlates well with the size of *B. azoricus*, suggesting that small mussels mainly rely on thiotrophy while larger individuals appeared to shift towards methanotrophy (Figure IV.S1; Trask and Van Dover 1999; De Busserolles et al. 2009). Some studies also identified a spatial variability of endosymbiont proportion that may reflect a high trophic flexibility of the mussels as holobionts, in link with the relative concentrations of reduced compound in their habitats (Colaço et al. 2002; De Busserolles et al. 2009; Portail et al. 2018). This flexibility may represent an advantage to colonise a wide range of habitats with diverse environmental conditions (Colaço et al. 2002).

Consumers- The association of *Bathymodiolus* mussels and the polynoid worm *Branchipolynoe* has been described in many chemosynthetic ecosystems (Desbruyères et al. 1985; Fisher et al. 1994; Van Dover 2002; Britaev et al. 2003; Lindgren et al. 2019) but the nature of their interactions has been extensively debated. While some authors suggested predation (Colaço et al. 2002; De Busserolles et al. 2009; Portail et al. 2018), others hypothesized a kleptoparasitic association, assuming that the polychaete feed on bacteria-laden mucus and pseudofaeces from the host (Fisher et al. 1994; Britayev et al. 2007). Others even suggested a role of the worm on detoxification processes (Bebianno et al. 2018). Our results point towards a trophic relationship with an isotopic shift of 1.16‰ in $\delta^{13}C$ and 3.28‰ in $\delta^{15}N$ between the two species, corresponding to classically accept trophic fractionation (McCutchan et al., 2003). As previously proposed, this result suggests that *B. seepensis* mainly feeds on *B. azoricus* tissues (De Busserolles et al., 2009). Although the isotopic composition of other consumer species did not exclude direct predation on *B. azoricus*, only a few specialized species, such as the crab *Segonzacia mesatlantica* or some polynoids, equipped with strong jaws and proboscis that spread inside-out to bite mussel tissues, would be able to feed on live mussels. Finally, the high variability of isotopic composition between primary consumers suggest the presence of food-source partitioning within the community, possibly supported by the exploitation of different microhabitats, as previously observed in other vent systems (Levesque et al. 2003, Lelièvre et al. 2018). At the LS vent field scale, the overall food-web

structure of macrofaunal assemblages associated with *B. azoricus* on the Montségur edifice showed a high similarity with what has been described for those of the Eiffel Tower edifice (Trask and Van Dover 1999; Colaço et al. 2002; De Busserolles et al. 2009; Portail et al. 2018). Similar patterns have already been noticed regarding species composition (Sarrazin et al. 2020) suggesting a strong relationship between taxonomic and functional diversity in these communities.

Community-wide food web structure along recovery

Community-wide isotopic metrics can be used to describe different aspects of the trophic structure, including trophic diversity (estimation of the extent of $\delta^{13}C$–$\delta^{15}N$ space using the CR, NR, TA and SEA metrics) and trophic redundancy (relative position of each species within the niche space, with CD, MNND and SDNND; Layman et al. 2007). However, the low number of replicate measurements for some species did not allow the use of the Bayesian approach to estimate the propagation error in the calculation of metrics and quantitative comparisons of assemblages (Jackson et al. 2011). The isotopic composition of faunal communities during the recovery process were similar, suggesting that the diversity of basal resources did not change much, even one year after the disturbance. Two hypotheses can be formulated from this result. On one hand, the induced perturbation was not sufficient to remove microbial communities and thereby did not impact the diversity of the basal food sources. On the other hand, if the clearing operation significantly altered microbial communities, this result may indicate a rapid re-colonisation of the cleared surface, which is consistent with the dynamics of substratum colonisation by microbial mats observed within a few months in vent ecosystems. The deployment of microbial colonisation substrata would help to identify patterns in microbial community structure along the recovery process. Such experimental substrates were deployed in 2018 and are still being processed.

One year after the disturbance (Post1), the standard ellipse and the total convex hull area were higher than in pre-disturbed samples, suggesting that the trophic diversity of the community almost fully recovered. Regarding trophic redundancy, the high values of CD, MNND and SDNND and the elongated shape of the ellipses suggest that species are not distributed along a continuous gradient, but rather oddly distributed within the isotopic space, with maxima near the two extremities of the ellipse. This result highlights the fact that all trophic niches were not yet occupied one year after the disturbance and suggests that all

trophic interactions did not recover. Moreover, we noticed higher values of almost all metrics in uncaged samples compared to caged samples, one year after the disturbance. At first glance, this results seems logical considering that as soon as top predators have been removed, the trophic diversity must be reduced. But ellipse shapes and $\delta^{13}C$–$\delta^{15}N$ bi-plot mainly show that large predators mainly affect the taxonomic richness and biomass of species from lower trophic levels. However, predation on small mussels led to a reduction of habitat availability and trophic complexity within the associated food web. Similar hypotheses have been formulated to explain the difference in tubeworm recruitment following a volcanic eruption on the Juan de Fuca Ridge (Marcus et al., 2009). Conversely to what is observed in mature assemblages, mainly structured by food web partitioning and spatial segregation and characterized by a low predation pressure (Levesque et al. 2003; Levin et al. 2013; Portail et al. 2016; Lelièvre et al. 2018), predation appears to be one of the predominant ecological process involved among the first steps of recovery after a disturbance at Montségur.

The low values of the convex hull area (TA) observed in assemblages sampled two years after disturbance (Post 2) is related to a clear reduction of the carbon range (CR). Rather than a decrease of trophic diversity, this can be explained by the absence of the two most ^{13}C-enriched species (*Peltospira smaragdina* and the undetermined ostracod species) as well as by the shift in $\delta^{13}C$ composition of *Lurifax vitreus* in these assemblages, which may be a result of changes in the microbial communities targeted by this species. Besides, these differences are less evident while considering the SEA, less sensitive to extreme values (Jackson et al. 2011). Contrary to those of Post 1, the species of Post 2 were more homogeneously distributed within the isotopic space, resulting in a decrease of isotopic redundancy metrics. The overall trophic structure, two years after the disturbance resembles that of the pre-disturbed assemblages, the main difference lying in the absence of some predators/scavenger species in the former. This first implies that most free-living microbial communities that represent the main basal source of the ecosystem, recovered within the two years of the experiment. This was enabled by the low impact of the induced disturbance regarding the environment, maintaining habitat suitability for faunal installation. Moreover, despite differences observed in taxonomic diversity and community structure after two years of recovery (Marticorena et al. 2021), these results tend to highlight a fair recovery of trophic complexity in response to the induced disturbance.

IV.5. Conclusion

This study provides the first characterisation of trophic structure recovery following a small scale disturbance at an active hydrothermal vent. It significantly increases our knowledge on ecological processes involved in structuring the vent food web along the ecological succession and brings insights on the links between vent species and functional diversity. The biomass and isotopic composition of the reference macrofaunal communities of the Montségur edifice were similar to the previous description of trophic structures at Lucky Strike (Colaço et al. 2002; De Busserolles et al. 2009; Portail et al. 2018). As in most chemosynthetic ecosystems, food-source partitioning and spatial segregation of species seem to be the main structuring processes at community scale (Levesque et al. 2003; Levin et al. 2013; Portail et al. 2016; Lelièvre et al. 2018). Within two years, the colonisation of the engineer species *Bathymodiolus azoricus* was limited to small individuals that did not allow a complete recovery of the tridimensional structure and habitat complexity. However, our results suggest a good recovery of the local food web structure and complexity two years after the small-scale disturbance. Indeed, a return of the basal-source diversity and trophic complexity comparable to pre-disturbed values were observed in this time period. Hence, the role of the engineer species in the diversification of trophic niches along the recovery process was not clearly identified. The predator exclusion experiment suggested that predators and scavengers may play an important role in many ways. They may slow down the establishment of the engineer species *B. azoricus* by feeding on new settled individuals and thus limit habitat complexity and the installation of associated species. They may also benefit from the accumulation of uncollected dead individuals and organic material resulting from the mechanical sampling of the area to feed. This suggests a top-down control of the food web in the first step after a disturbance.

This case study is the first to use biomass and community-wide isotopic metrics to assess functional recovery of vent communities after a small-scale disturbance. It should be kept in mind, however, that the nature and the spatial extent of the induced disturbance is not comparable to natural catastrophic events or mining activities and that it remains hazardous to infer faunal response to larger scale disturbances. Future studies applying functional tools to the whole community would be necessary to improve our knowledge of vent community resilience. One of the main challenges of ecologists so far has been to characterize the link between taxonomic richness and functional diversity. In the context of increasing ecosystem

degradation, maintaining ecosystem functions appears as a priority to avoid the loss of valuable ecosystem services (Gladstone-Gallagher et al., 2019). Moreover, at various ecological scales, some biological traits may confer resilience to disturbances. For example, at the population level, functional traits related to reproduction and dispersion, are crucial to insure connectivity and recolonise damaged ecosystems. Coupling taxonomic and functional trait-based approaches, including isotopic composition, would provide crucial insights into recovery processes of vent communities in response to natural or anthropogenic disturbances.

IV.6. References

Bebianno, M.J., Cardoso, C., Gomes, T., Blasco, J., Santos, R.S., Colaço, A., 2018. Metal interactions between the polychaete Branchipolynoe seepensis and the mussel Bathymodiolus azoricus from Mid-Atlantic-Ridge hydrothermal vent fields. *Mar. Environ. Res*. 135, 70–81.

Beinart, R.A., Sanders, J.G., Faure, B., Sylva, S.P., Lee, R.W., Becker, E.L., Gartman, A., Luther, G.W., Seewald, J.S., Fisher, C.R., Girguis, P.R., 2012. Evidence for the role of endosymbionts in regional-scale habitat partitioning by hydrothermal vent symbioses. *Proc. Natl. Acad. Sci*. 109

Bell, J.B., Reid, W.D.K., Pearce, D.A., Glover, A.G., Sweeting, C.J., Newton, J., Woulds, C., 2016. Hydrothermal activity lowers trophic diversity in Antarctic sedimented hydrothermal vents. *Biogeosciences Discuss* 1–48.

Bergquist, D.C., Eckner, J.T., Urcuyo, I.A., Cordes, E.E., Hourdez, S., Macko, S.A., Fisher, C.R., 2007. Using stable isotopes and quantitative community characteristics to determine a local hydrothermal vent food web. *Mar. Ecol. Prog. Ser*. 330, 49–65.

Blake, J.A., 1985. Polychaeta from the vicinity of deep-sea geothermal vents in the eastern Pacific. I. Euphrosinidae, Phyllodocidae, Hesionidae, Nereididae, Glyceridae, Dorvilleidae, Orbiniidae, and Maldanidae. *Bull Biol Soc Wash* 6, 67–101.

Blake J.A., Hilbig, B., 1990. Polychaeta from the vicinity of deep-sea hydrothermal vents in the eastern Pacific. II. New species and records from the Juan de Fuca and Explorer Ridge systems. *Pacific Science* 44 (3).

Boschen, R.E., Rowden, A.A., Clark, M.R., Gardner, J.P.A., 2013. Mining of deep-sea seafloor massive sulfides: A review of the deposits, their benthic communities, impacts from mining, regulatory frameworks and management strategies. *Ocean Coast. Manag*. 84, 54–67.

Brescia, L.A., Tunnicliffe, V., 1998. Population biology of two pycnogonid species (Ammotheidae) at hydrothermal vents in the northeast Pacific. *Cah Biol Mar.* 39, 233–236.

Britayev, T.A., Martin, D., Krylova, E.M., Von Cosel, R., Aksiuk, T.S., 2007. Life-history traits of the symbiotic scale-worm *Branchipolynoe seepensis* and its relationships with host mussels of the genus Bathymodiolus from hydrothermal vents. *Mar. Ecol.* 28, 36–48.

Campbell, B.J., Cary, S.C., 2004. Abundance of reverse tricarboxylic acid cycle genes in free-living microorganisms at deep-sea hydrothermal vents. *Appl. Environ. Microbiol*. 70, 6282–6289.

Cardinale, B.J., Duffy, J.E., Gonzalez, A., Hooper, D.U., Perrings, C., Venail, P., Narwani, A., Mace, G.M., Tilman, D., Wardle, D.A., Kinzig, A.P., Daily, G.C., Loreau, M., Grace, J.B., Larigauderie, A., Srivastava, D.S., Naeem, S., 2012. Biodiversity loss and its impact on humanity. *Nature* 486, 59–67.

Ceballos, G., Ehrlich, P.R., Barnosky, A.D., García, A., Pringle, R.M., Palmer, T.M., 2015. Accelerated modern human–induced species losses: Entering the sixth mass extinction. *Sci. Adv*. 1

Charlou JL, Donval JP, Douville E, Jean-Baptiste P, Radford-Knoery J, Fouquet Y, Dapoigny A, Stievenard M (2000) Compared geochemical signatures and the evolution of Menez Gwen (37°50′N) and Lucky Strike (37°17′N) hydrothermal fluids, south of the Azores Triple Junction on the Mid-Atlantic Ridge. *Chem Geol* 171:49–75.

Charlou JL, Donval JP, Fouquet Y, Jean-Baptiste P, Holm N (2002) Geochemistry of high H2 and CH4 vent fluids issuing from ultramafic rocks at the Rainbow hydrothermal field (36°14'N, MAR). *Chem Geol* 191:345–359.

Childress, J.J., Fisher, C.R., 1992. The biology of hydrothermal vent animals: physiology, biochemistry, and autotrophic symbioses. Oceanography and Marine Biology. 337–441.

Colaço, A., Dehairs, F., Desbruyères, D., 2002. Nutritional relations of deep-sea hydrothermal fields at the Mid-Atlantic Ridge: a stable isotope approach. *Deep Sea Res. Part Oceanogr. Res*. 49, 395–412.

Crépeau, V., Cambon Bonavita, M.-A., Lesongeur, F., Randrianalivelo, H., Sarradin, P.-M., Sarrazin, J., Godfroy, A., 2011. Diversity and function in microbial mats from the Lucky Strike hydrothermal vent field. *FEMS Microbiol*. Ecol. 76, 524–540.

Cuvelier, D., Sarradin, P.-M., Sarrazin, J., Colaço, A., Copley, J.T., Desbruyères, D., Glover, A.G., Santos, R.S., Tyler, P.A., 2011. Hydrothermal faunal assemblages and habitat characterisation at the Eiffel Tower edifice (Lucky Strike, Mid-Atlantic Ridge). *Mar. Ecol.* 32, 243–255.

Danovaro, R., Fanelli, E., Aguzzi, J., Billett, D., Carugati, L., Corinaldesi, C., Dell'Anno, A., Gjerde, K., Jamieson, A.J., Kark, S., McClain, C., Levin, L., Levin, N., Ramirez-Llodra, E., Ruhl, H., Smith, C.R., Snelgrove, P.V.R., Thomsen, L., Van Dover, C.L., Yasuhara, M., 2020. Ecological variables for developing a global deep-ocean monitoring and conservation strategy. *Nat. Ecol. Evol.* 4, 181–192.

De Busserolles, F., Sarrazin, J., Gauthier, O., Gélinas, Y., Fabri, M.C., Sarradin, P.M., Desbruyères, D., 2009. Are spatial variations in the diets of hydrothermal fauna linked to local environmental conditions? *Deep Sea Res. Part II Top. Stud. Oceanogr.,* 56, 1649

Desbruyères, D., Alayse-Danet, A.-M., Ohta, S., 1994. Deep-sea hydrothermal communities in Southwestern Pacific back-arc basins (the North Fiji and Lau Basins): Composition, microdistribution and food web*. Mar. Geol.* 116, 227–242.

Desbruyères D, Almeida A, Biscoito M, Comtet T, Khripounoff A, Bris NL, Sarradin PM, Segonzac M (2000) A review of the distribution of hydrothermal vent communities along the northern Mid-Atlantic Ridge: Dispersal vs. environmental controls. *Hydrobiologia* 440:201–216.

Desbruyères D, Segonzac M, Bright M, Biologiezentrum OL, Desbruyeres D, Segonzac M, Bright M (2006) Handbook of deep-sea hydrothermal vent fauna, 2nd completely rev. ed. / editors, Daniel Desbruyères, Michel Segonzac&Monika Bright. Linz, Austria : *Land Oberösterreich, Biologiezentrum der Oberösterreichische Landesmuseen*

Dreyer, J.C., Knick, K.E., Flickinger, W.B., Dover, C.L.V., 2005. Development of macrofaunal community structure in mussel beds on the northern East Pacific Rise. *Mar. Ecol. Prog. Ser.* 302, 121–134.

Fisher CR (1990) Chemoautotrophic and methanotrophic symbioses in marine invertebrates*. Rev Aquat Sci* 2:399–436.

Fisher, C.R., Childress, J.J., Macko, S.A., Brooks, J.M., 1994. Nutritional interactions in Galapagos Rift hydrothermal vent communities: inferences from stable carbon and nitrogen isotope analyses. *Mar. Ecol. Prog. Ser.* 45–55.

Gebruk, A.V., Southward, E.C., Kennedy, H., Southward, A.J., 2000. Food sources, behaviour, and distribution of hydrothermal vent shrimps at the Mid-Atlantic Ridge. *J. Mar. Biol. Assoc. U. K.* 80, 485–499.

Gladstone-Gallagher, R.V., Pilditch, C.A., Stephenson, F., Thrush, S.F., 2019. Linking Traits across Ecological Scales Determines Functional Resilience. *Trends Ecol. Evol.* 34, 1080–1091.

Goffredi SK, Warén A, Orphan VJ, Van Dover CL, Vrijenhoek RC (2004) Novel forms of structural integration between microbes and a hydrothermal vent gastropod from the Indian Ocean. *Appl Environ Microbiol* 70:3082–3090.

Gollner, S., Govenar, B., Arbizu, P.M., Mills, S., Le Bris, N., Weinbauer, M., Shank, T.M., Bright, M., 2015. Differences in recovery between deep-sea hydrothermal vent and vent-proximate communities after a volcanic eruption. *Deep Sea Res. Part Oceanogr. Res. Pap.* 106, 167–182.

Gollner, S., Kaiser, S., Menzel, L., Jones, D.O.B., Brown, A., Mestre, N.C., van Oevelen, D., Menot, L., Colaço, A., Canals, M., Cuvelier, D., Durden, J.M., Gebruk, A., Egho, G.A., Haeckel, M., Marcon, Y., Mevenkamp, L., Morato, T., Pham, C.K., Purser, A., Sanchez-Vidal, A., Vanreusel, A., Vink, A., Martinez Arbizu, P., 2017. Resilience of benthic deep-sea fauna to mining activities. *Mar. Environ. Res.* 129, 76–101.

Govenar, B., 2012. Energy transfer through food webs at hydrothermal vents: Linking the lithosphere to the biosphere. *Oceanography* 25, 246–255.

Govenar, B., Fisher, C.R., 2007. Experimental evidence of habitat provision by aggregations of Riftia pachyptila at hydrothermal vents on the East Pacific Rise. *Mar. Ecol.* 28, 3–14.

Govenar, B., Fisher, C.R., Shank, T.M., 2015. Variation in the diets of hydrothermal vent gastropods. *Deep Sea Res. Part II Top. Stud. Oceanogr*., 121: 193–201.

Groenewold, S., Fonds, M., 2000. Effects on benthic scavengers of discards and damaged benthos produced by the beam-trawl fishery in the southern North Sea. ICES *J. Mar. Sci.* 57: 1395–1406.

Hoekstra, J.M., Boucher, T.M., Ricketts, T.H., Roberts, C., 2005. Confronting a biome crisis: global disparities of habitat loss and protection. *Ecol. Lett.* 8:23–29.

Holling, C.S., 1973. Resilience and Stability of Ecological Systems. *Annu. Rev. Ecol. Syst.* 4:1–23.

Hooper, D.U., Chapin, F.S., Ewel, J.J., Hector, A., Inchausti, P., Lavorel, S., Lawton, J.H., Lodge, D.M., Loreau, M., Naeem, S., Schmid, B., Setälä, H., Symstad, A.J., Vandermeer, J., Wardle, D.A., 2005. Effects of Biodiversity on Ecosystem Functioning: A Consensus of Current Knowledge. *Ecol. Monogr.* 75:3–35.

Hourdez S, Desbruyeres D (2003) A new species of scale-worm (Polychaeta: Polynoidae), Levensteiniella iris sp nov., from the Rainbow and Lucky Strike vent fields (Mid-Atlantic Ridge). *Cah Biol Mar* 44:13–21.

Hügler, M., Sievert, S.M., 2011. Beyond the Calvin Cycle: Autotrophic Carbon Fixation in the Ocean. *Annu. Rev. Mar. Sci.* 3:261–289.

Husson, B., Sarradin, P.-M., Zeppilli, D., Sarrazin, J., 2017. Picturing thermal niches and biomass of hydrothermal vent species. *Deep Sea Res. Part II Top. Stud. Oceanogr.,* 137:6–25.

Jackson, A.L., Inger, R., Parnell, A.C., Bearhop, S., 2011. Comparing isotopic niche widths among and within communities: SIBER – Stable Isotope Bayesian Ellipses in R. *J. Anim. Ecol.* 80:595–602.

Jannasch, H.W., 1985. Review Lecture - The chemosynthetic support of life and the microbial diversity at deep-sea hydrothermal vents. *Proc. R. Soc. Lond. B Biol. Sci*. 225:277–297.

Johnson, K.S., Beehler, C.L., Sakamoto-Arnold, C.M., Childress, J.J., 1986. In situ measurements of chemical distributions in a deep-sea hydrothermal vent field. *Science* 231:1139–1141.

Jollivet D, Empis A, Baker MC, Hourdez S, Comtet T, Jouin-Toulmond C, Desbruyères D, Tyler PA (2000) Reproductive biology, sexual dimorphism, and population structure of the deep sea hydrothermal vent scale-worm, Branchipolynoe seepensis (Polychaeta: Polynoidae). *J Mar Biol Assoc U K* 80:55–68.

Jones, C.G., Lawton, J.H., Shachak, M., 1997. Positive and negative effects of organisms as physical ecosystem engineers. *Ecology* 78:1946–1957.

Juan, S. de, Thrush, S.F., Demestre, M., 2007. Functional changes as indicators of trawling disturbance on a benthic community located in a fishing ground (NW Mediterranean Sea). *Mar. Ecol. Prog*. 334:117–129

Jumars PA, Dorgan KM, Lindsay SM (2015) Diet of worms emended: an update of polychaete feeding guilds. *Ann Rev Mar Sci*. 7:497-520.

Karl, D.M., 1995. Ecology of free-living, hydrothermal vent microbial community. *Microbiol*. Deep-Sea Hydrothermal Vents.

Khripounoff, A., Vangriesheim, A., Crassous, P., Segonzac, M., Colaco, A., Desbruyeres, D., Barthelemy, R., 2001. Particle flux in the Rainbow hydrothermal vent field (Mid-Atlantic Ridge): Dynamics, mineral and biological composition. *J. Mar. Res.* 59:633–656.

Layman, C.A., Arrington, D.A., Montaña, C.G., Post, D.M., 2007. Can Stable Isotope Ratios Provide for Community-Wide Measures of Trophic Structure? *Ecology* 88:42–48.

Le Bris, N., Yücel, M., Das, A., Sievert, S.M., LokaBharathi, P., Girguis, P.R., 2019. Hydrothermal Energy Transfer and Organic Carbon Production at the Deep Seafloor. *Front. Mar. Sci.* 5.

Lelièvre, Y., Sarrazin, J., Marticorena, J., Schaal, G., Day, T., Legendre, P., Hourdez, S., Matabos, M., 2018. Biodiversity and trophic ecology of hydrothermal vent fauna associated with tubeworm assemblages on the Juan de Fuca Ridge. *Biogeosciences* 15:2629–2647.

Levesque, C., Juniper, S.K., 2002. Particulate matter as a food source at a nascent hydrothermal vent on the Juan de Fuca Ridge. *Cah. Biol. Mar.* 43:289–292.

Levesque, C., Juniper, S.K., Marcus, J., 2003. Food resource partitioning and competition among alvinellid polychaetes of Juan de Fuca Ridge hydrothermal vents. *Mar. Ecol. Prog. Ser.* 246:173–182.

Levesque, C., Limén, H., Juniper, S.K., 2005. Origin, composition and nutritional quality of particulate matter at deep-sea hydrothermal vents on Axial Volcano, NE Pacific. *Mar. Ecol. Prog. Ser.* 289:43–52.

Levin, L.A., Baco, A.R., Bowden, D.A., Colaco, A., Cordes, E.E., Cunha, M.R., Demopoulos, A.W.J., Gobin, J., Grupe, B.M., Le, J., Metaxas, A., Netburn, A.N., Rouse, G.W., Thurber, A.R., Tunnicliffe, V., Van Dover, C.L., Vanreusel, A., Watling, L., 2016. Hydrothermal Vents and Methane Seeps: Rethinking the Sphere of Influence. *Front. Mar. Sci*. 3.

Levin, L.A., Mendoza, G.F., Konotchick, T., Lee, R., 2009. Macrobenthos community structure and trophic relationships within active and inactive Pacific hydrothermal sediments. *Deep Sea Res. Part II Top. Stud. Oceanogr.* 56:1632–1648.

Levin, L.A., Ziebis, W., F. Mendoza, G., Bertics, V.J., Washington, T., Gonzalez, J., Thurber, A.R., Ebbe, B., Lee, R.W., 2013. Ecological release and niche partitioning under stress: Lessons from dorvilleid polychaetes in sulfidic sediments at methane seeps. *Deep Sea Res. Part II Top. Stud. Oceanogr.* 92:214–233.

Limen, H., Juniper, S.K., 2006. Habitat controls on vent food webs at Eifuku Volcano, Mariana Arc. *Cah. Biol. Mar.* 47:449.

Limén, H., Levesque, C., Kim Juniper, S., 2007. POM in macro-/meiofaunal food webs associated with three flow regimes at deep-sea hydrothermal vents on Axial Volcano, Juan de Fuca Ridge. *Mar. Biol.* 153:129–139.

Marcus, J., Tunnicliffe, V., Butterfield, D.A., 2009. Post-eruption succession of macrofaunal communities at diffuse flow hydrothermal vents on Axial Volcano, Juan de Fuca Ridge, Northeast Pacific. *Deep Sea Res. Part II Top. Stud. Oceanogr.,* 56:1586–1598.

Matabos, M., Cuvelier, D., Brouard, J., Shillito, B., Ravaux, J., Zbinden, M., Barthelemy, D., Sarradin, P.M., Sarrazin, J., 2015. Behavioural study of two hydrothermal crustacean decapods: Mirocaris fortunata and Segonzacia mesatlantica, from the Lucky Strike vent field (Mid-Atlantic Ridge). *Deep Sea Res. Part II Top. Stud. Oceanogr.,* 121:146–158.

McCutchan Jr, J.H., Lewis Jr, W.M., Kendall, C., McGrath, C.C., 2003. Variation in trophic shift for stable isotope ratios of carbon, nitrogen, and sulfur. *Oikos* 102, 378–390.

Mengerink, K.J., Dover, C.L.V., Ardron, J., Baker, M., Escobar-Briones, E., Gjerde, K., Koslow, J.A., Ramirez-Llodra, E., Lara-Lopez, A., Squires, D., Sutton, T., Sweetman, A.K., Levin, L.A., 2014. A Call for Deep-Ocean Stewardship. *Science* 344:696–698.

Micheli, F., Peterson, C.H., Mullineaux, L.S., Fisher, C.R., Mills, S.W., Sancho, G., Johnson, G.A., Lenihan, H.S., 2002. Predation Structures Communities at Deep-Sea Hydrothermal Vents. *Ecol. Monogr.* 72:365–382.

Mullineaux, L.S., Adams, D.K., Mills, S.W., Beaulieu, S.E., 2010. Larvae from afar colonise deep-sea hydrothermal vents after a catastrophic eruption. *Proc. Natl. Acad. Sci.* 107:7829–7834.

Mullineaux, L.S., Bris, N.L., Mills, S.W., Henri, P., Bayer, S.R., Secrist, R.G., Siu, N., 2012. Detecting the Influence of Initial Pioneers on Succession at Deep-Sea Vents. *PLOS ONE* 7, e50015.

Mullineaux, L.S., Metaxas, A., Beaulieu, S.E., Bright, M., Gollner, S., Grupe, B.M., Herrera, S., Kellner, J.B., Levin, L.A., Mitarai, S., Neubert, M.G., Thurnherr, A.M., Tunnicliffe, V., Watanabe, H.K., Won, Y.-J., 2018. Exploring the Ecology of Deep-Sea Hydrothermal Vents in a Metacommunity Framework. *Front. Mar. Sci.* 5.

Mullineaux, L.S., Peterson, C.H., Micheli, F., Mills, S.W., 2003. Successional Mechanism Varies Along a Gradient in Hydrothermal Fluid Flux at Deep-Sea Vents. *Ecol. Monogr.* 73: 523–542.

Nakagawa, S., Takai, K., 2008. Deep-sea vent chemoautotrophs: diversity, biochemistry and ecological significance. *FEMS Microbiol. Ecol.* 65:1–14.

Peterson, B.J., Fry, B., 1987. Stable isotopes in ecosystem studies. *Annu. Rev. Ecol. Syst.* 18:293–320.

Pettibone MH (1988) New species and new records of scaled polychaetes (Polychaeta: Polynoidae) from hydrothermal vents of the Northeast Pacific Explorer and Juan de Fuca Ridges. *Proceedings of the Biological Society of Washington.*

Pond DW, Bell MV, Dixon DR, Fallick AE, Segonzac M, Sargent JR (1998) Stable-carbon-isotope composition of fatty acids in hydrothermal vent mussels containing methanotrophic and thiotrophic bacterial endosymbionts. *Appl Environ Microbiol* 64:370–375.

Portail, M., Brandily, C., Cathalot, C., Colaço, A., Gélinas, Y., Husson, B., Sarradin, P.-M., Sarrazin, J., 2018. Food-web complexity across hydrothermal vents on the Azores triple junction. *Deep Sea Res. Part Oceanogr. Res. Pap.* 131:101–120.

Portail, M., Olu, K., Dubois, S.F., Escobar-Briones, E., Gelinas, Y., Menot, L., Sarrazin, J., 2016. Food-Web Complexity in Guaymas Basin Hydrothermal Vents and Cold Seeps. *PLOS ONE* 11, e0162263.

Post, D.M., 2002. Using Stable Isotopes to Estimate Trophic Position: Models, Methods, and Assumptions. *Ecology* 83, 703–718

Ramirez-Llodra, E., Tyler, P.A., Baker, M.C., Bergstad, O.A., Clark, M.R., Escobar, E., Levin, L.A., Menot, L., Rowden, A.A., Smith, C.R., Dover, C.L.V., 2011. Man and the Last Great Wilderness: Human Impact on the Deep Sea. *PLOS ONE* 6, e22588.

Ramsay, K., Kaiser, M.J., Hughes, R.N., 1998. Responses of benthic scavengers to fishing disturbance by towed gears in different habitats. *J. Exp. Mar. Biol. Ecol.* 224:73–89.

Rigolet, C., Thiébaut, E., Brind'Amour, A., Dubois, S.F., 2015. Investigating isotopic functional indices to reveal changes in the structure and functioning of benthic communities. *Funct. Ecol.* 29 :1350–1360.

Sarrazin, J., Legendre, P., de Busserolles, F., Fabri, M.-C., Guilini, K., Ivanenko, V.N., Morineaux, M., Vanreusel, A., Sarradin, P.-M., 2015. Biodiversity patterns, environmental drivers and indicator species on a high-temperature hydrothermal edifice, Mid-Atlantic Ridge. *Deep Sea Res. Part II Top. Stud. Oceanogr.* 121:177–192.

Sarrazin, J., Levesque, C., Juniper, S., Tivey, M., 2002. Mosaic community dynamics on Juan de Fuca Ridge sulphide edifices: substratum, temperature and implications for trophic structure. *CBM - Cah. Biol. Mar.* 43:275–279.

Sarrazin, J., V, R., Sk, J., Jr, D., 1997. Biological and geological dynamics over four years on a high-temperature sulfide structure at the Juan de Fuca Ridge hydrothermal observatory. *Mar. Ecol. Prog. Ser.* 153:5–24.

Sievert SM, Hügler M, Taylor CD, Wirsen CO (2008) Sulfur oxidation at deep-sea hydrothermal vents. In: Microbial sulfur metabolism. *Springer*, 238–258

Shank, T.M., Fornari, D.J., Von Damm, K.L., Lilley, M.D., Haymon, R.M., Lutz, R.A., 1998. Temporal and spatial patterns of biological community development at nascent deep-sea hydrothermal vents (9°50'N, East Pacific Rise). *Deep Sea Res. Part II Top. Stud. Oceanogr.* 45:465–515.

Takai, K., Nakagawa, S., Reysenbach, A.-L., Hoek, J., 2013. Microbial Ecology of Mid-Ocean Ridges and Back-Arc Basins, in: Back-Arc Spreading Systems: Geological, Biological, Chemical, and Physical Interactions. *American Geophysical Union (AGU),* 185–213.

Trask, J.L., Van Dover, C.L., 1999. Site-specific and ontogenetic variations in nutrition of mussels (Bathymodiolus sp.) from the Lucky Strike hydrothermal vent field, Mid-Atlantic Ridge. *Limnol. Oceanogr.* 44:334–343.

Tsurumi, M., Tunnicliffe, V., 2003. Tubeworm-associated communities at hydrothermal vents on the Juan de Fuca Ridge, northeast Pacific. *Deep Sea Res. Part Oceanogr. Res. Pap.* 50:611–629.

Tunnicliffe, V., 1991. The biology of hydrothermal vents : ecology and evolution. *Biol. Hydrothermal Vents Ecol. Evol.* 29:319–407.

Tunnicliffe, V., Embley, R.W., Holden, J.F., Butterfield, D.A., Massoth, G.J., Juniper, S.K., 1997. Biological colonisation of new hydrothermal vents following an eruption on Juan de Fuca Ridge. *Deep Sea Res. Part Oceanogr. Res. Pap.* 44:1627–1644.

Van Dover CL, Fry B (1989) Stable isotopic compositions of hydrothermal vent organisms. *Mar Biol* 102:257–263.

Van Dover CL, Trask J, Gross J, Knowlton A (1999) Reproductive biology of free-living and commensal polynoid polychaetes at the Lucky Strike hydrothermal vent field (Mid-Atlantic Ridge*). Mar Ecol Prog Ser* 181:201–214.

Van Dover, C.L., Trask, J.L., 2000. Diversity at deep-sea hydrothermal vent and intertidal mussel beds. *Mar. Ecol. Prog. Ser.* 195:169–178.

Van Dover, L. C., 2011. Mining seafloor massive sulphides and biodiversity: what is at risk*? ICES J. Mar. Sci.* 68:341–348.

Walker, B., Holling, C.S., Carpenter, S., Kinzig, A., 2004. Resilience, Adaptability and Transformability in Social–ecological Systems. *Ecol. Soc.* 9.

Ward ME, Jenkins CD, Dover CLM (2003) Functional morphology and feeding strategy of the hydrothermal-vent polychaete Archinome rosacea (family Archinomidae). *Can J Zool* 81:582–590.

Warèn A (2001) Gastropoda and Monoplacophora from hydrothermal vents and seeps ; new taxa and records. *The Veliger* 44:116–231.

Warèn A, Bouchet P (1993) New records, species, genera, and a new family of gastropods from hydrothermal vents and hydrocarbon seeps. *Zool Scr* 22:1–90.

Zeppilli D, Bellec L, Cambon-Bonavita M-A, Decraemer W, Fontaneto D, Fuchs S, Gayet N, Mandon P, Michel LN, Portail M, Smol N, Sørensen MV, Vanreusel A, Sarrazin J (2019) Ecology and trophic role of Oncholaimus dyvae sp. nov. (Nematoda: Oncholaimidae) from the lucky strike hydrothermal vent field (Mid-Atlantic Ridge). BMC Zool 4:6.

IV.7. Supplementary files

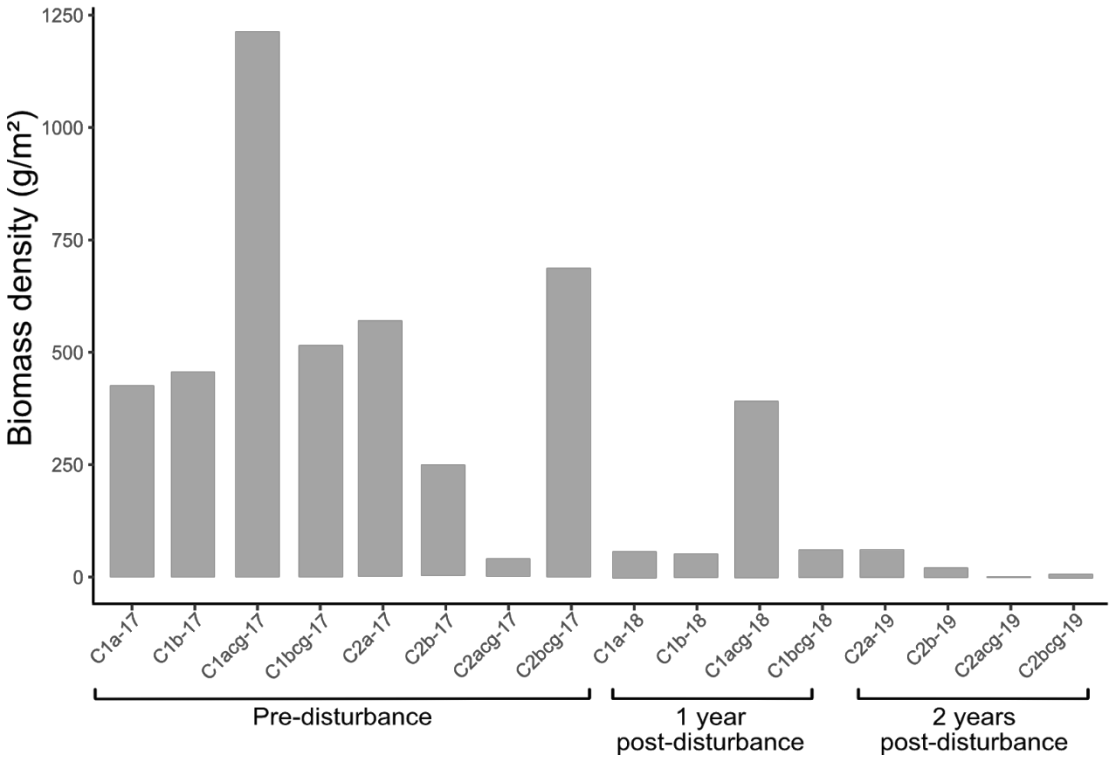

Figure IV.S1. Biomass of *Bathymodiolus azoricus* among all the different assemblages of the experiment.

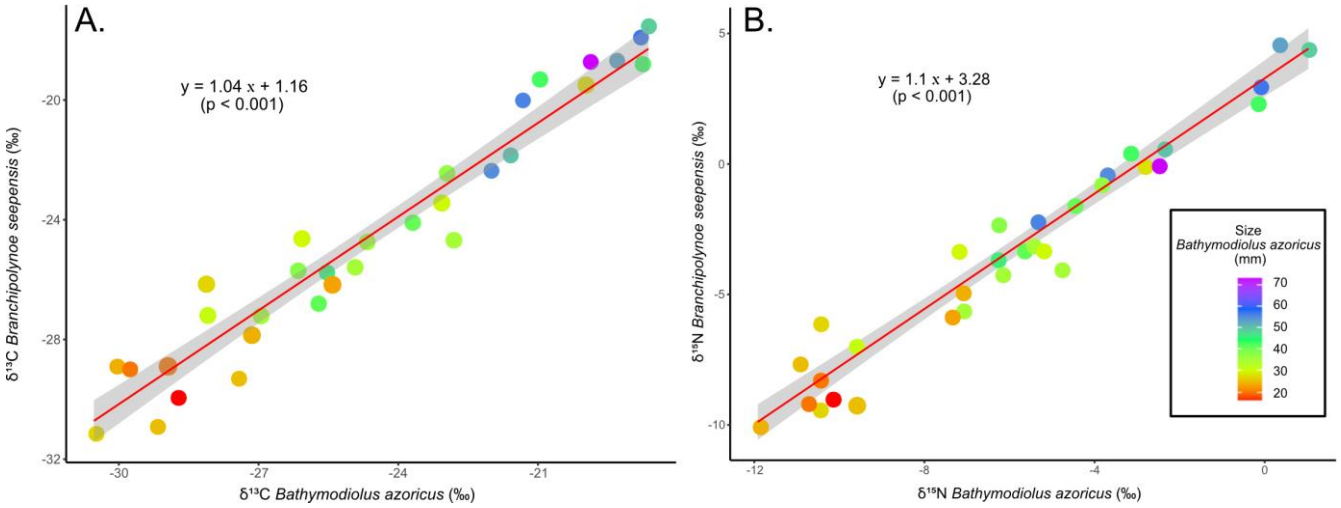

Figure IV.S2. Stable isotope relationship between the engineer species *Bathymodiolus azoricus* and its commensal worm *Branchipolynoe seepensis*. A positive linear regression has been fitted between the $\delta^{13}C$ (A) and the δ15N (B) of the two species. The color and size of the dots refer to the size of *Bathymodiolus azoricus,* which is also correlated with the size of the worm inhabiting its palleal cavity.

Table IV.S1. Stable isotope composition of the different species found among the assemblages of the experiment before and after disturbance. Bold values indicate a significant difference identified along the recolonisation process (Wilcoxon test, p-value < 0.05)

Trophic guilde	Species	$\delta^{13}C$ (mean ± sd)			$\delta^{15}N$ (mean ± sd)		
		Pre-disturbance	Post 1	Post 2	Pre-disturbance	Post 1	Post 2
Deposit feeder	*Amphisamytha lutzi*	-20,04 ± 3,14	-19,96 ± 0,92	-20,93 ± 1,09	2,62 ± 2,68	4,04 ± 1,19	3,43 ± 1,21
	Branchipolynoe seepensis	-28,15 ± 2,8	-26,85 ± 1,92	-28,32 ± 0,82	-5,96 ± 2,93	-5,5 ± 2,2	-5,39 ± 1,93
	Cumacae sp.			-19,38			0,35
	Porifera sp.	-25,42 ± 0,63			3,85 ± 1,75		
	Hesionidae sp.	-15,42 ± 4,51			3,96 ± 3,57		
	Luckia stricki	-21,6 ± 2,23	-21,79	-20,74 ± 0,65	0,46 ± 3,07	-0,41	0,62 ± 1,69
	Sipuncula sp.	-17,99	-18,92 ± 1,1	-19,79 ± 0,65	5,05	4,72 ± 0,53	3,92 ± 0,69
	Spionidae sp.	-21,02 ± 1,63	-20,65	-21,38 ± 1,24	1,99 ± 1,54	2,87	2,5 ± 1,95
	Tanaidacae sp.	-19,04 ± 6,56	-21,84	-21,12 ± 0,33	-0,25 ± 1,53	0,85	0,92 ± 0,85
Grazer	*Aphotopontius sp.*	-23,18 ± 1,27	-22,59 ± 0,33	-21,84 ± 2,53	-1,1 ± 1,65	1,64 ± 1,03	1,79 ± 1,48
	Dorvillidae sp.	-24,08 ± 0,64			1,53 ± 2,44		
	Laeviphitus debruyeris			-23,21 ± 1,65			3,02 ± 0,15
	Lepetodrilus atlanticus	-17,07 ± 2,99	-18,27 ± 4,84	-19,85 ± 3,21	3,78 ± 1,44	4,61 ± 1,03	2,97 ± 0,53
	Lirapex costellata	**-21,13 ± 4,35**	**-26,2**	**-18,84 ± 3,02**	5,13 ± 1,32	5,56 ±	6,66 ± 1,25
	Lurifax vitreus	-29,27 ± 3,66	-31,68 ± 1,59	-29,63 ± 1,37	1,74 ± 1,32	1,52 ± 0,46	1,88 ± 0,39
	Ostracoda sp.	**-14,61 ± 0,28**	**-11,92± 1,57**		3,09 ± 0,31	5,59 ± 0,59	
	Paralepetopsis ferrugivora	-22,4 ± 1,56	-21,87 ± 1,76	-22,47	-0,85 ± 1,24	-0,21 ± 1,13	-0,29
	Peltospira smaragdina	-10,6 ± 0,59		-11,03	5,51 ± 0,29		6,43
	Protolira valvatoides	**-22,58 ± 1,65**	**-21,48 ± 3,31**	**-24,06 ± 0,38**	**1,39 ± 1,01**	**3,7 ± 1,04**	**1,59 ± 0,58**
	Pseudorimula midatlantica	-21,83 ± 2,76	-22,77 ± 2,32	-28,22 ± 3,41	3,28 ± 1,27	3,67 ± 0,97	2,07 ± 1,83
	Divia briandi	-14,4 ± 2,55	-13,4 ± 2,39	-15,08 ± 0,54	5,57 ± 1,41	6,02 ± 0,71	6,92 ± 0,76
	Xylodiscula analoga			-26,54 ± 4,25		-2,64 ± 3,18	
Predator / Scavanger	*Zoanthidae sp.*	**-22,24 ± 0,86**	**-19,22**	**-17,73 ± 2,47**	**1,72 ± 1,77**	**4,61**	**2,37 ± 1,07**
	Archinome sp.	-23,23 ± 3,25	-23,29 ± 4,05		5 ± 1,42	4,46 ± 0,07	
	Branchinotogluma sp.	**-19,18 ± 6,21**	**-23,26 ± 1,54**	**-24,2 ± 4,96**	3,01 ± 5,8	1,35 ± 2,04	-0,09 ± 5,98
	Glycera sp.	-22,22 ± 1,68	-20,52	-21,47	4,45 ± 1,87	6,72	6,57
	Iphionella sp.			-23,02			1,32
	Lepidonotopodium sp.	-16,7 ± 4,22	-19,17 ± 4,19	-20,04 ± 0,02	6,3 ± 3,52	4,17 ± 4,63	5,1 ± 1,85
	Levensteinella sp.	-23,66 ± 2,42			-0,04 ± 3,2		
	Mirocaris fortunata	-18,11 ± 1,8	-16,91 ± 1,57	-18,71 ± 0,45	6,03 ± 1,39	6,42 ± 0,66	6,29 ± 1,32
	Oncholaimus dyvae	-22,04 ± 1,99	-21,44 ± 0,52	-23,27 ± 0,24	0,55 ± 3	5,23 ± 0,6	1,21 ± 0,87
	Nemerta sp.	-22,86			-6,84		
	Phymorhynchus sp.	-17,38			3,55		
	Sericosura sp.	-20,95 ± 1,9	-20,05 ± 1,55	-21,4 ± 0,15	4,25 ± 1,96	5,7 ± 1,17	3,73 ± 1,38
	Segonzacia mesatlantica	-19,09 ± 3,07			3,32 ± 2,86		
Primary producer	*Filamentous bacteria*	-38,39 ± 0,21	-38,48 ± 0,05	-38,46 ± 0,12	2,44 ± 0,06	2,45 ± 0,03	2,46 ± 0,04
Symbiotic	*Bathymodiolus azoricus*	-27,64 ± 4,34	-26,43 ± 2,07	-27,58 ± 1,44	-8,51 ± 2,54	-8,28 ± 1,19	-7,15 ± 1,94

IV.8. Synthèse des résultats

L'expérience de perturbation mise en place sur l'édifice actif Montségur nous a permis de décrire la dynamique de recolonisation des assemblages de macrofaune à la suite d'une perturbation à petite échelle. Aussi bien le suivi de la structure des communautés que l'étude du réseau trophique nous ont permis d'identifier plusieurs espèces de gastéropodes brouteurs *(Protolira valvatoides*, *Lepetodrilus atlanticus* ou *Pseudorimula midatlantica)* comme premiers colonisateurs des habitats perturbés sur l'édifice Montségur. Ces espèces, figurant en outre parmi les plus abondantes des assemblages matures à l'échelle du champ hydrothermal Lucky Strike (Sarrazin et al. 2015, 2020, Chapitre III de cette thèse), semblent jouer un rôle clé dans les premières étapes de ce rétablissement. Un tel succès au sein de l'écosystème peut être en partie justifié par leur comportement trophique. En effet, ces gastéropodes se nourrissent des mattes microbiennes qui se développent à la surface des substrats durs ou sur la coquille des *B. azoricus*. Il est fort probable que les communautés microbiennes n'aient été que peu impactées par l'expérience de défaunation et/ou qu'elles se soient rapidement développées à la suite de la perturbation, permettant ainsi de soutenir une forte biomasse de consommateurs primaires. D'autre part, l'arrivée de ces espèces clés va fortement dépendre de la disponibilité des larves et donc des aptitudes de dispersion de l'espèce, elles-mêmes conditionnées par les traits reproducteurs qui esa caractérisent. En effet, la fréquence de la reproduction, la fécondité, l'âge de maturité ou encore le mode de développement des larves sont des processus clés dans la dispersion des espèces. Au sein du champ hydrothermal Lucky Strike, peu d'informations étaient disponibles sur la reproduction de certaines espèces de gastéropodes dominants.

Ainsi afin de d'évaluer la capacité de ces organismes à se maintenir au sein de leur habitat et de mieux appréhender leurs aptitudes de dispersion à plus grande échelle, des analyses histologiques ont été menées sur deux espèces de gastéropodes dominants *Protolira valvatoides et Pseudorimula midatlantica.* Dans ce dernier chapitre, nous avons caractérisé la gamétogenèse et décrit la structure des populations de ces deux espèces. Un deuxième objectif était de rendre compte de la variabilité de ces traits reproducteurs à l'échelle de l'édifice en relation avec les paramètres environnementaux à travers l'analyse d'individus récoltés au sein de différents assemblages. Enfin, l'un des objectifs initiaux de ce chapitre était également de comparer le statut reproducteur des individus au sein des assemblages au cours

du processus de rétablissement en estimant notamment la proportion d'individus matures par exemple. Il s'est avéré que, malgré la grande étendue de taille des individus sélectionnés pour les analyses histologiques, tous les individus étaient matures, et ce, même pour les individus issus de la recolonisation, un an après la perturbation. En effet, en replaçant la taille des individus analysés histologiquement (i.e. 1,8-3,5 mm pour *P. valvatoides* et 3,6-6,5 mm pour *P. midatlantica*) au sein de la structure démographique des populations, nous avons constaté que les individus sélectionnés n'étaient pas représentatifs de l'ensemble de la population, mais majoritairement des spécimens de grande taille. Nous avons donc considéré dans la rédaction de ce chapitre tous les assemblages échantillonnés comme des réplicats, ce qui nous a permis de vérifier la variabilité spatiale (à l'échelle de l'édifice) et temporelle (entre différentes périodes de l'année) des traits reproductifs pour ces deux espèces.

V. Biologie de la reproduction des gastéropodes

Contrasting reproductive biology of two hydrothermal gastropods from the Mid-Atlantic Ridge: implications for resilience of vent communities

J Marticorena[1], M Matabos[1], J Sarrazin[1], E Ramirez-Llodra[2,3]

[1] Ifremer, REM/EEP, F - 29280 Plouzané, France

[2] Norwegian Institute for Water Research, Gaustadalleen 21, 0349 Oslo, Norway

[3] REV Ocean, Oksenøyveien 10, 1366 Lysaker, Norway

Corresponding author: Julien Marticorena (julienmarticorena@gmail.fr)

ORCID : Julien Marticorena (0000-0003-3295-2615)

Marjolaine Matabos (0000-0003-1983-9896)

Jozée Sarrazin (0000-0002-5435-8011)

Eva Ramirez-Llodra (0000-0003-0137-1906)

Marine Biology (2020) 167:109
https://doi.org/10.1007/s00227-020-03721-x

ORIGINAL PAPER

Contrasting reproductive biology of two hydrothermal gastropods from the Mid-Atlantic Ridge: implications for resilience of vent communities

J. Marticorena[1] · M. Matabos[1] · J. Sarrazin[1] · E. Ramirez-Llodra[2,3]

Received: 29 January 2020 / Accepted: 27 May 2020

Abstract

The recovery of populations and their ability to re colonise a disturbed habitat is mainly dependent on their reproductive biology (e.g. fecundity, frequency of reproduction, time to maturity) and recruitment success. To assess recolonisation processes and connectivity of vent communities, and infer their resilience to natural and anthropogenic disturbances, we studied the life-history traits of two dominant species of vent gastropods from the northern Mid-Atlantic Ridge: *Protolira valvatoides* and *Pseudorimula midatlantica*. Gonad morphology, gametogenesis and reproductive outputs related to shell length were described using histological analyses, and population structure was assessed from individual's size frequency distributions. Samples were collected at different locations of the Montségur and Eiffel Tower edifices (Lucky Strike vent field) in April 2015, July 2017 and August 2018 to inform on spatial and temporal variations of their reproductive outputs and demography. All stages of oocyte development were found in the gonads of both species, suggesting a continuous gametogenesis and asynchronous reproduction. However, the two species showed contrasting reproductive strategies. Indeed, while *P. midatlantica* is gonochoric with a fecundity of up to 327 mature oocytes, *P. valvatoides* is hermaphrodite with an extremely low fecundity including a maximum of 8 vitellogenic oocytes. Maximum oocyte size was 176 µm for *P. midatlantica* and 272 µm for *P. valvatoides.* We inferred from previous knowledge and our results that both species exhibit a lecithotrophic development of larvae. There was no evidence of temporal variability of reproductive traits, but environmental conditions seem to affect gametogenetic maturity and oocyte size of *P. midatlantica* limpets. Variations in population structure at the edifice scale suggest habitat selection of individuals related to biotic and abiotic factors.

V.1. Introduction

Current worldwide demand in minerals and metals is rising while land-based resources are severely decreasing (Hein et al. 2013). In this context, the interest of companies and countries in deep-sea mining is escalating, targeting various high metal-based environments such as Seafloor Massive Sulphide (SMS) deposits at hydrothermal vents, polymetallic nodules on abyssal plains and cobalt-rich ferromanganese crusts at seamounts (Gollner et al. 2017). Although commercial exploitation of seabed minerals has not yet begun, expected consequences of deep-sea mining on ecosystems comprise direct and indirect impacts that will vary with mining strategies (Ramirez-Llodra et al. 2011; Clark and Smith, 2013; Van Dover, 2014; Levin 2016) as well as with the biological and environmental characteristics of the targeted ecosystems (Gollner 2017). In this context, it is urgent to evaluate the resilience of deep-sea communities to inform the development of environmental management plans.

Resilience can be defined as the ability of an ecosystem to maintain its structure and function in response to a perturbation (Carpenter et al. 2001; Cumming et al. 2012). This definition involves two distinct processes: (1) resistance, related to the ability of a system to absorb the effects of disturbance without changing (Connell and Ghedini 2015) and (2) recovery, which is the capacity of an ecosystem to return to its undisturbed state (Ingrisch and Bahn 2018). Functional resilience occurs at multiple scales of ecological organisation, ranging from individual to community levels (Oliver et al. 2015). At the population-level, resilience refers to the ability of a species to occupy new space and recolonise a disturbed area. It is partly related to reproductive traits such as reproductive frequency, fecundity, time to maturity and recruitment success (see Gladstone-Gallagher et al. 2019). Thus, the recovery of impacted habitats is highly dependent on the dispersal and recolonisation potential of the different species.

Hydrothermal vents represent extremely fragmented and transient habitats that can be separated by tens to hundreds of kilometres along mid-ocean ridges and back-arc basins. Consequently, the recovery of impacted vent communities will strongly depend on larval supply reaching from preserved areas and on the success of recruitment events. Connectivity patterns are major drivers of the demographic stability of local populations. Two complementary methods can help to assess the connectivity between populations: i)

population genetic based models (Tyler and Young 1999; Vrijenhoek 2010; Baco et al. 2016) and ii) coupled biophysical models that include ocean circulation and early life-history traits such as timing of spawning, fecundity, larval mortality and planktonic larval duration (Pradillon et al. 2001; Metaxas and Saunders 2009; Hilario et al. 2015; Suzuki et al. 2018; Vic et al. 2018). However, despite their relevance, discrepancies in the results of these modelling approaches highlight a lack of knowledge of both physical and biological variables in deep-sea ecosystems (Breusing et al. 2016). Indeed, for most deep-sea species, empirical data on early life-history traits is, at best, fragmentary but often completely lacking (Tyler and Young 1999). It is therefore urgent to increase our knowledge about the natural processes driving population connectivity, colonisation patterns and ecosystem recovery, to better understand the resilience of vent communities following a disturbance (Mullineaux et al. 2010; Gollner et al. 2015; Boschen et al. 2016; Gollner et al. 2017).

Hydrothermal vent communities in the northern part of the mid-Atlantic ridge and specifically at the Lucky Strike vent field (LS) are characterised by dense assemblages of macrofauna, structured by the engineer species *Bathymodiolus azoricus*. *B. azoricus* mussel beds provide a three-dimensional habitat promoting high-density populations of gastropods (*Protolira valvatoides, Pseudorimula midatlantica, Lepetodrilus atlanticus*) and polychaetes (*Branchipolynoe seepensis, Amphisamytha lutzi* (Cuvelier et al. 2014; Sarrazin et al. 2015). While basic reproductive traits are known for most species in the area, only the reproductive biology of *B. azoricus*, *L. atlanticus*, *B. seepensis* and *A. lutzi* has been described in details (Van Dover et al. 1999; Jollivet et al. 2000; Blake and Van Dover 2005; Colaco et al. 2006; Dixon et al. 2006; Tyler et al. 2008), and our knowledge of gastropods remains limited. Gathering this information is key in understanding the establishment of vent faunal communities and ecosystem functioning.

Gametogenesis, and especially vitellogenetic mechanisms, defined as the synthesis and storage of energetic reserves in the growing oocytes, appears to be phylogenetically constrained (Eckelbarger 1995; Tyler and Young 1999). In contrast, the number and quality of the eggs, and also the time of spawning, can be affected by environmental conditions (Ramirez-Llodra 2002; Kelly and Metaxas 2007; Matabos and Thiebaut 2010). The continuous supply of energy introduced in the food web by chemoautotrophic bacteria at hydrothermal vents can support an asynchronous and quasi-continuous production of eggs by benthic

species, but seasonal reproduction has also been observed in bathymodiolin mussels (reviewed by Laming et al. 2018). Energy availability can also shape the trade-off between egg size and fecundity (Ramirez-Llodra 2002), and the size of mature oocytes can provide information about larval development mode and help determining the type of larvae. Planktotrophic larvae are those feeding in the water-column, while lecithotrophic larvae feed on the egg's yolk until settlement. As a general pattern, species producing a large number of small eggs (< 200 µm) have planktotrophic larval feeding modes, while lecithotrophic species produce a small number of larger eggs (> 200 µm) (Jaekle 1995; Levin and Bridges 1995). For molluscs, larval shell morphology has also been used to infer larval development and dispersal, based on observations of shallow-water species (Gustafson and Lutz 1994). *Protolira* species are hermaphroditic and have a spirally coiled propodial appendage interpreted as a penis and thus with assumed pseudo-internal fertilization occurring in the pallial cavity (Warén and Bouchet 1993. *P. midatlantica* (Mclean 1992) is described as gonochoristic and characterized by a hypertrophied gonad that displaces the foot on the left side of the animal, probably in response to the need of a greater reproductive output (Mclean 1992).

In this study, we describe for the first time the gametogenesis, population structure and infer the reproductive output at the time of sampling of two abundant MAR gastropods (*Protolira valvatoides* and *Pseudorimula midatlantica*), providing novel data to better assess the recovery potential of vent ecosystems in face of natural and anthropogenic disturbances. This work is part of a larger study that aims at evaluating the rate and success of recovery of active hydrothermal vent communities after an induced disturbance using a 2 year *in situ* experiment. Community recolonisation one year and two years after disturbance (faunal removal) was monitored and the role of biological and chemical factors on recolonisation dynamics evaluated.

V.2. Material and Methods

V.2.1. Field sampling

All specimens of *Protolira valvatoides* and *Pseudorimula midatlantica* were sampled using the hydraulic arm and suction sampling device of the Remotely Operated Vehicle *Victor6000*. They were collected in *Bathymodiolus azoricus* assemblages on diffused flow habitats on the Montségur and Eiffel Tower edifices (Lucky Strike vent field, MAR) at 1700 m depth (Figure

V.1). To investigate spatial variation of reproductive and population structure features, samples were collected at different sampling locations with varying environmental conditions (Figure V.1, Table V.1). Sample names refer to a disturbance experiment that was held on the Montségur edifice from 2017 to 2019. Individuals from three cruises, occurring in May 2015 (MOMARSAT2015), July 2017 (MOMARSAT2017) and August 2018 (MOMARSAT2018), were compared to test for temporal variations across the two species.

To complete the dataset, *in situ* temperature measurements were conducted year-round with autonomous MISO (2015, WHOI-MISO low temp-ONSET®) and iButtons™ (2017 and 2018) probes deployed directly on the mussel assemblages.

On board, all faunal samples were washed on a 300 µm sieve and gastropods were identified to species level. Five to twenty individuals of *P. valvatoides* and *P. midatlantica* from each sample were stored in buffered 4% formaldehyde for reproduction studies, whereas all other specimens were preserved in 96% ethanol for population structure analyses.

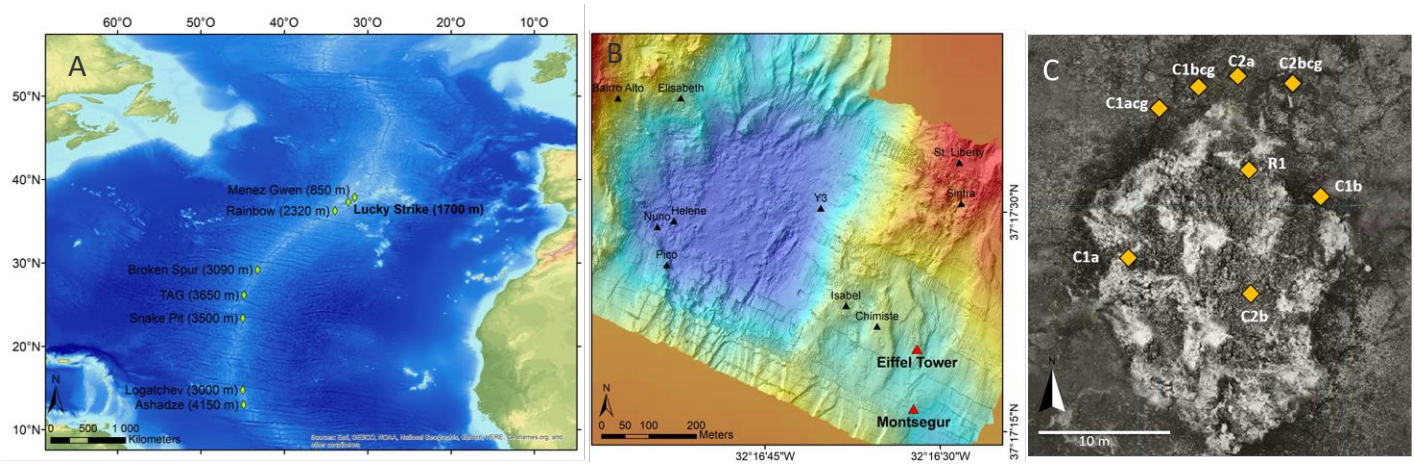

Figure V.1 A) Location of the Lucky Strike vent field on the Mid-Atlantic ridge, south of the Azores. **B)** The 1 km² LS vent field with the Montségur and Eiffel Tower edifices on the south-east. **C)** Location of the different sampling locations on and around the Montségur edifice

Table V.1. Summary of vent sites and stations, time of sampling, number of individuals and shell size range of all individuals of the two species used for histological analyses in this study. Mean and standard deviation of temperature measured on each quadrat during a year are also presented.

Species	Edifice	Station	Date	Number of individuals	Shell length range (mm)	Temperature (°C) (mean ± sd)
Prototolira valvatoides	Montségur	C1a	July 2017	5	1.7–2.6	5.7 ± 0.26
			August 2018	5	1.9–2.7	
		C1acg	July 2017	4	1.9–2.8	5.1 ± 0.08
			August 2018	12	1.8–3.1	
		C1bcg	August 2018	7	1.9–2.6	5.3 ± 0.38
		C2a	July 2017	3	1.7–2.7	6.6 ± 0.92
		R1	August 2018	4	1.8–2.9	8.3 ± 1.13
	Eiffel Tower	ET	April 2015	18	1.8–3.5	5.3 ± 0.36
Pseudorimula midatlantica	Montségur	C1a	July 2017	1	4.7	5.7 ± 0.26
		C1acg	August 2018	10	4–6.5	5.1 ± 0.08
		C1b	August 2018	3	3.6–5	5.1 ± 0.3
		C1bcg	August 2018	5	3.3–5.7	5.3 ± 0.38
		C2a	July 2017	5	4.2–5.9	6.6 ± 0.92
		C2bcg	July 2017	2	4.6–5.3	5.3 ± 0.42
		R1	July 2018	3	3.9–6.7	8.3 ± 1.13
	Eiffel Tower	ET	April 2015	5	4.1–5.8	5.3 ± 0.36

V.2.2. Population structure

Size-frequency distributions of both species were only analysed for the samples from the Montségur edifice, as most of the Eiffel Tower specimens were used for other analyses and therefore not measured. To characterize demographic population structure, photos of *P. midatlantica* and *P. valvatoides* were captured with a Leica MC 170 HD camera mounted on a Leica M125 dissecting microscope. The curvilinear distance (i.e. longest length from the apex to the anterior edge of the shell along the dorsal side) of *P. midatlantica* and the longest shell dimension of *P. valvatoides* (see Bates et al. 2006 for protocol) were measured to the nearest 0.001 mm using the Leica Application Suite software. Measurement error was calculated as the maximum difference among 10 measures of the same individual on 10 specimens comprising a range of all sizes for each species. It was fixed at 0.052 mm for *P. midatlantica* and 0.029 mm for *P. valvatoides*.

For each assemblage sampled, length-frequency distribution was plotted for the two species using a size-class interval of 0.3 mm for *P. midatlantica* and 0.2 mm for *P. valvatoides*. The intervals were chosen according to three criteria: i) most size-classes must have at least five individuals; ii) the number of adjacent empty classes must be minimized; and iii) the interval has to be much greater than the measurement error (see Jollivet et al. 2000). Size-frequency distributions were compared to a normal distribution using a one-sample Kolmogorov-Smirnov test and non-parametric Kruskal-Wallis multisample tests were performed to identify differences in size-frequency distribution between samples. To determine which individuals contributed to the observed differences, multiple comparison Nemenyi and Dunn tests were computed (Zar, 2007).

When distributions differed significantly from a normal distribution, and assuming that gastropod sizes followed a Gaussian distribution within each cohort, a modal decomposition was ran for all sampled assemblages of *P. valvatoides*. Modal decomposition analyses were not performed for *P. midatlantica* because at least 100 to 300 specimens are required to have a fairly good representation of the population, which was not the case in some of our samples for this species. The modal decomposition analyses of *P. valvatoides* was conducted with the Mixdist package (Macdonald and Du, 2018) in R (RStudio Team, 2016), which identifies the total number of cohorts within the natural distribution and calculates the mean size, standard deviation and proportion of the overall population in each cohort. The goodness of fit of

identified size cohorts was verified using a chi-squared test. Seven individuals of *P. valvatoides* were removed from the distribution of C1a, C1acg and R1 before the MIX analysis to avoid null classes separating the modes.

V.2.3. Reproductive biology

The shells of *P. midatlantica* were gently removed using forceps, while *P. valvatoides* individuals were rapidly decalcified using a HCL 10% solution before removing the periostracum under a dissecting microscope. The entire soft body was then processed through graded ethanol and dehydrated in absolute isopropanol before being embedded in paraffin wax. For histological analyses, serial horizontal 7 µm thick sections of gonads were prepared using a microtome. Sections were stained with the routine staining haematoxylin and eosin protocol (Gabe, 1968). Observations were performed using the AxioZoom stereomicroscope (Zeiss, Oberkochen, Germany) equipped with an ApoTome.2 slider module (Zeiss) and a HXP 200C light technology (Zeiss) and using an AxioCam MRm (Zeiss) camera. Micrographs were analyzed using the Zen (Zeiss) software.

For gametogenesis studies, at least 100 oocytes per specimen were measured using the image J © software (Schneider et al. 2012) from 2 to 3 serial sections for *P. midatlantica.* For *P. valvatoides,* the very low number of oocytes was insufficient to reach 100 oocytes even when using serial sections of the entire gonad. Only oocytes that had been sectioned through the nucleus were measured using the feret diameter, which estimates the diameter of a hypothetical disc with the same area as the measured object. Oocyte sizes were grouped into 10 µm classes for frequency diagrams constructed for each sampling location. To assess synchrony of gametogenesis among and between samples, non-parametric Kruskal-Wallis multi-sample and Nemenyi and Dunn tests were performed on oocyte size. Gametogenetic maturity was estimated from the percentage of vitellogenic oocytes on the total of oocytes measured for each animal and comparisons among samples were made using the same methods as previously described.

Instantaneous fecundity was quantified as the number of vitellogenic oocytes in the entire ovary of an individual at the time of sampling (Tyler and Billett 1988; Ramirez-Llodra 2002).

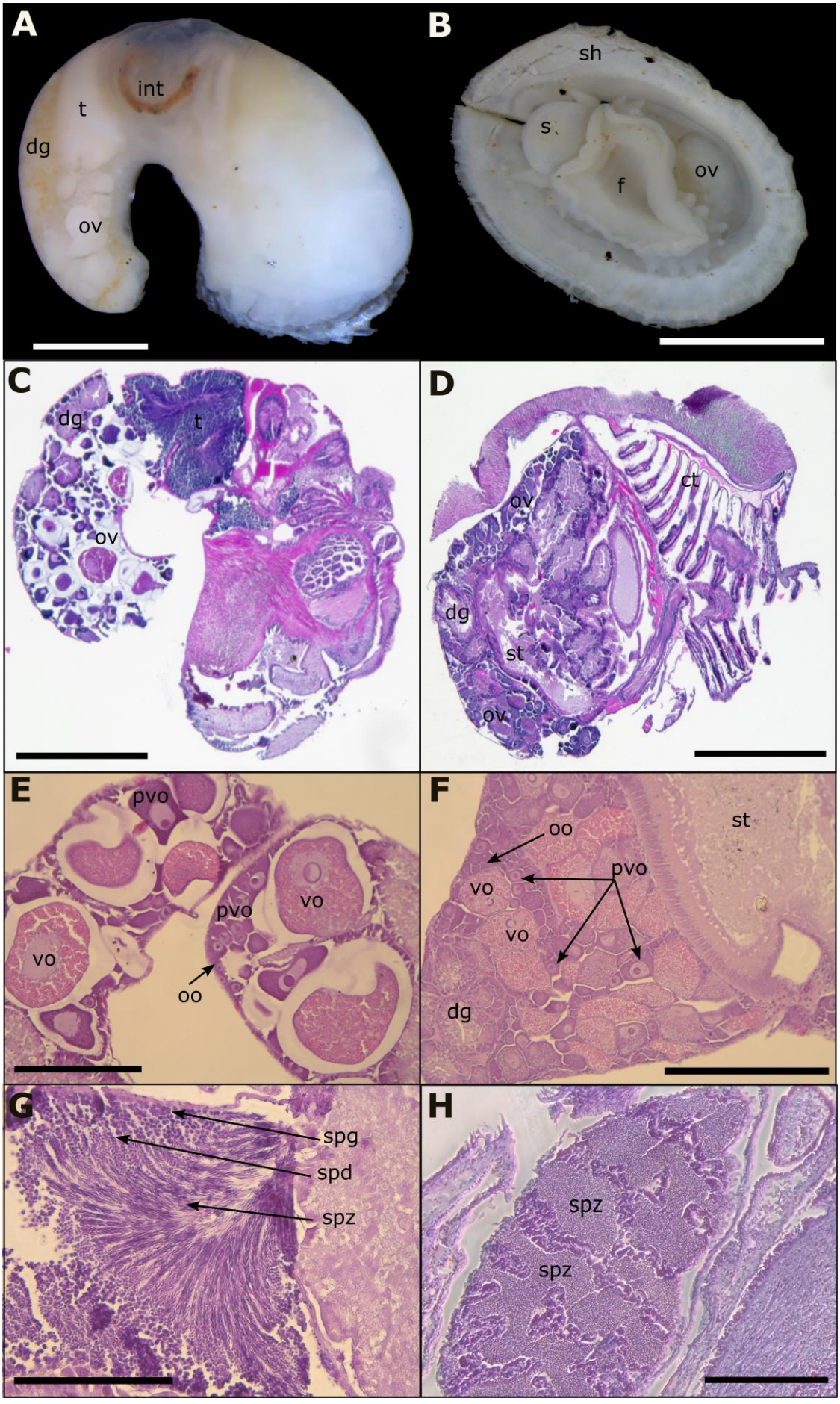
A
int
t
dg
ov
B
sh
s
f
ov
C
dg
t
ov
D
ov
ct
dg
st
ov
E
pvo
pvo
vo
vo
oo
F
oo
st
pvo
vo
vo
dg
G
spg
spd
spz
H
spz
spz

◀ **Figure V.2** Morphology of reproductive structures of *Protolira valvatoides* (left) and *Pseudorimula midatlantica* (right). **A** Dorsal view of *P. valvatoides* soft body. **B** Ventral view of *P. midatlantica* soft body. **C** General view of a transversal section of *P. valvatoides.* **D** General view of a transversal section of a *P. midatlantica* female. **E** Detailed view of *P. valvatoides* ovary. **F** Detailed view of *P. midatlantica* ovary. **G** Detailed of *P. valvatoides* testis. **H** Detailed view of *P. midatlantica* testis. *ct* ctenidium; *dg* digestive gland; *f* foot, *ov* ovary; *oo* oogonia; *pvo* previtellogenic oocyte; *s* snout; *st* stomach; *spd* spermatid; *spg* spermatogonia; *spz* spermatozoa; *t* testis; *vo* vitellogenic oocytes. Scale bars: a and c = 1 mm; b and d = 2 mm; e, f and h = 200 µm; g = 50 µm

Fecundity was quantified in 10 individuals for *P. midatlantica* and 9 individuals for *P. valvatoides*. To ensure that a vitellogenic oocyte was not counted more than once, the overlying sections were compared.

V.3. Results

V.3.1. Environmental conditions

The mean temperatures measured over the year within the different quadrats varied between 5.1 and 8.3°C and were typical of a diffuse flow venting area (Figure V.1). Significant spatial variations of mean temperature have been identified with the presence of warmer habitats in R1, C2a and C1a quadrats (ANOVA, F = 6591, p-value < 0.001).

V.3.2. Gonad morphology and gametogenesis

In total, 58 individuals of *Protolira valvatoides* and 34 females of *Pseudorimula midatlantica*, collected at different sampling locations, over three years, were analyzed (Table V.1).

The hermaphroditic genital system of *Protolira valvatoides* consists of separate ovary with oviduct and a testis with a *vas deferens* (Figure V.2a and c). The large ovary is situated dorsally and occupies, together with the digestive gland, the uppermost whorl of the shell (Figure V.2a and c). The testis is located anterio-ventrally of the ovary, extending on the right side of the animal. Spermatogenesis begins with the development of germinal spermatogonia with a mean diameter of 4 µm from the wall of testis tubules. Spermatogonia differentiate in spermatocytes and spermatids *via* mitotic divisions, before developing into flagellated spermatozoa in the lumen of the testis (Figure V.2g). During oogenesis, the oogonia proliferate in the germinal epithelium, which extends throughout the entire ovary. Oogonia grow to approximatively 20 µm before developing in previtellogenic oocytes. Oogonia appear in histological sections as small cells with a large and dark stained nucleus occupying the entire cell, while previtellogenic oocytes are larger (20–100 µm) with a basophilic and more

voluminous cytoplasm that stain in light purple (Figure V.2e). Previtellogenic oocytes grow until reaching 80–100 µm, when they undergo vitellogenesis. At the beginning of vitellogenesis, yolk granules are visible at the periphery of the oocytes and spread to the entire oocyte. Vitellogenic oocytes show an eccentric germinal vesicle and acidophilic cytoplasm stained in pale pink with eosin (Figure V.2e). For *Protolira valvatoides*, the mean size of vitellogenic oocytes was 185 µm (ferret diameter) and the maximum size measured was 272 µm.

Pseudorimula midatlantica is a gonochoric species with separated male and female individuals. In females, the ovary occupies a large volume of the animal, extending from the very posterior end to the pallial roof on the right side (Figure V. 2b). It is ventrally replaced by the stomach and digestive glands and surrounded on both sides by the shell muscle (Figure V.2d). The development and maturation of oocytes and spermatozoa are similar to *P. valvatoides* (Figure V.2H). In the ovary, the previtellogenic oocytes grow to a size of 40–50 µm before starting vitellogenesis (Figure V.2f). The mean size of vitellogenic oocyte for *P. midatlantica* was 81 µm, with a maximum size of 176 µm, and yolk was distributed all over the oocyte (Figure V.2f). All developmental stages of oocytes (i.e. oogonia, previtellogenic oocytes and vitellogenic oocytes) were observed in all individuals analysed for both species.

V.3.3. Oocyte size-frequency distribution

For both species, oogonia were much more abundant in ovaries than previtellogenic and vitellogenic oocytes. Hence, oogonia were not considered for oocyte-size distribution analyses. For both species, the Kruskal-Wallis multisample test showed intra-sample differences in mean oocytes size and the post-hoc Dunn's multi-sample test indicated that only one to three individuals of each sample contributed to these differences (Table V.S1). To ensure that there was no individual size effect among samples in testing the spatial and temporal variation of oocyte distribution, we compared shell length of the examined individuals. No significant differences were identified (Test Kruskal-Wallis, $H = 0.44$, $df = 7$, p-value > 0.05 for *P. valvatoides* and $H = 11.07$, $df = 7$, p-value > 0.05 for *P. midatlantica*). Oocyte size-frequency distributions were highly variable between individuals and there was no evidence of synchronous oogenesis. However, the two species displayed the same polymodal pattern in oocyte-frequency distribution skewed towards smaller oocytes with a tail in larger sizes that may contain several modes (Figure V.3 and V.4).

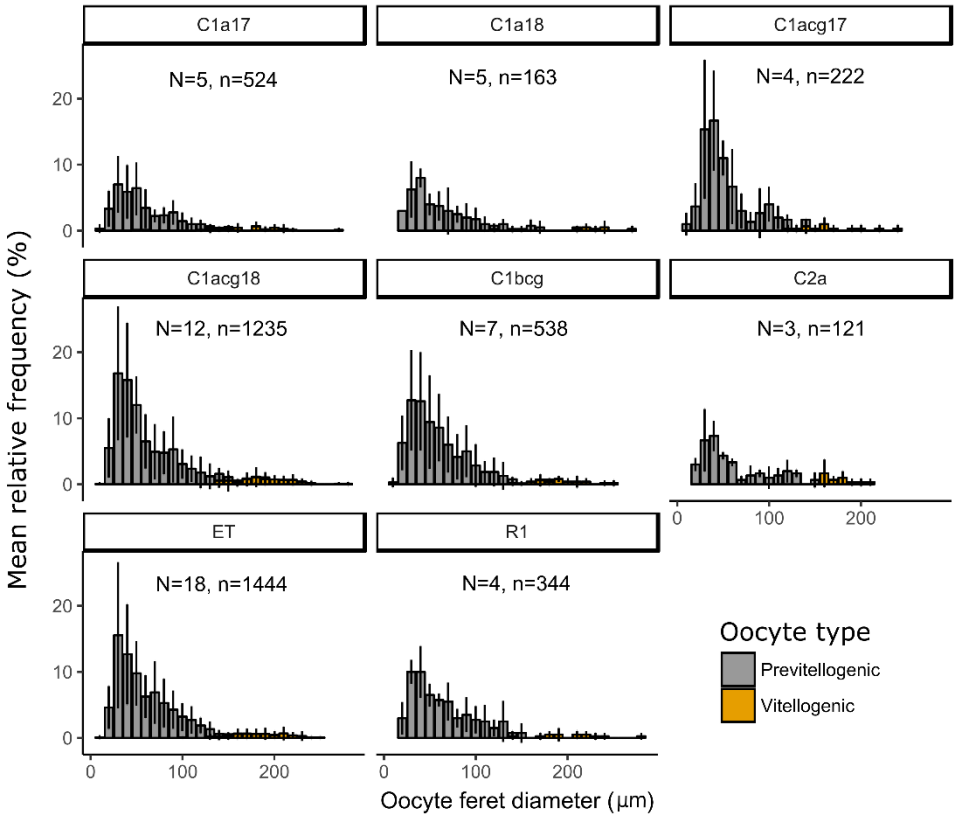

Figure V.3 Mean oocyte size–frequency histograms (mean ± SD) of pooled individuals of *Protolira valvatoides* for each quadrat. Colors: Grey bars represent previtellogenic oocytes and yellow bars represent vitellogenic oocytes. *N* number of individuals; *n* number of oocytes measured

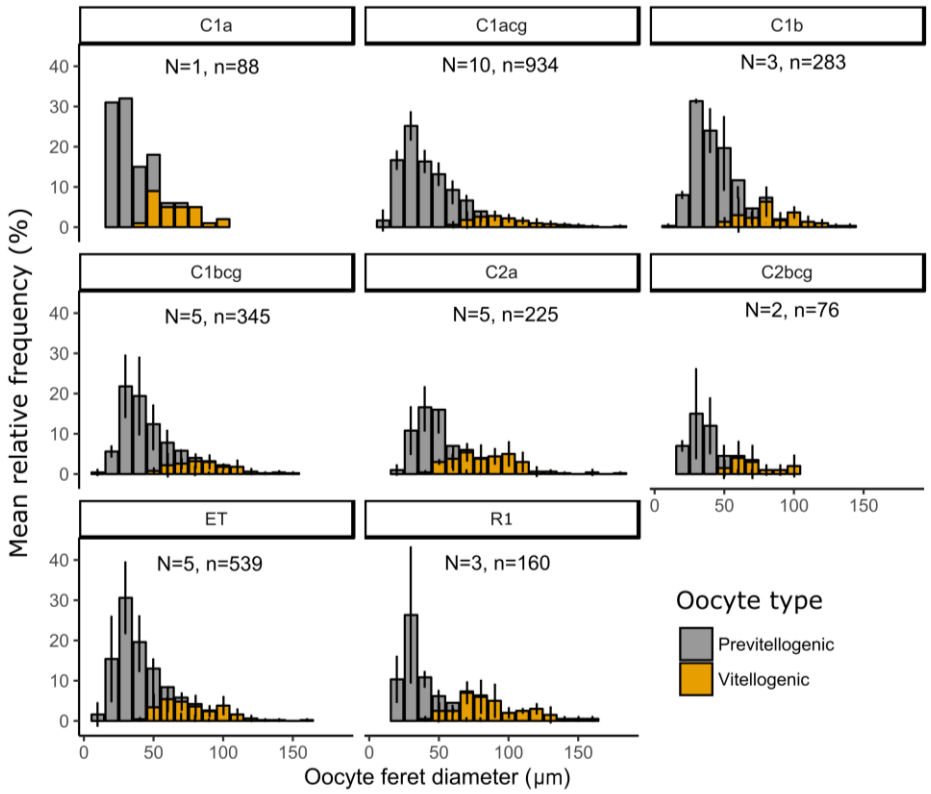

Figure V.4 Mean oocyte size–frequency histograms (mean ± SD) of pooled individuals of *Pseudorimula midatlantica* for each quadrat. Colors: grey bars represent previtellogenic oocytes and yellow bars represent vitellogenic oocytes. *N* number of individuals; *n* number of oocytes measured

For *P. valvatoides*, oocyte size ranged from 9 to 272 µm (Figure V.3) and the size-frequency distribution showed a first peak containing between 91 and 96 % of the total number of oocytes, corresponding to previtellogenic oocytes (< 100 µm). The rest of the distribution contained one or more peaks of larger oocytes (> 100 µm), corresponding to previtellogenic oocytes at the onset of vitellogenesis and truly vitellogenic oocytes. Kruskal-Wallis multi-sample tests showed that oocytes size distributions between locations and sampling period did not differ significantly (Figure V.5a and c, Figure V.S1). The percentage of mature oocytes ranged from 3% to 18% of all oocytes and was not correlated with the animal body length (R^2 = -0.014, p-value = 0.91) (Figure V.6a). Finally, no difference was observed regarding the proportion of vitellogenic oocytes among localities (Kruskal-Wallis test, H = 7.23, df = 5, p-value > 0.05; Figure V.5c)

For *P. midatlantica,* oocyte size ranged from 4 to 176 µm (Figure V.4) and size frequency distribution showed a first peak, containing between 31 and 82 % of the total population, which corresponded to previtellogenic oocytes (< 50 µm). A second and minor peak was mostly constituted by larger vitellogenic oocytes (> 50 µm). An intermediate peak including oocytes at the beginning of vitellogenesis (between 40 and 50 µm) was also present for most of the localities (Figure V.4). *P. midatlantica* showed a significant spatial variation in oocyte size distribution among the different sites with smaller oocytes in the C1a sample and larger oocytes in the C2a sample (Figure V.5b and d). Nevertheless, there was no evidence of temporal variation in mean oocyte size of *P. midatlantica* (Figure V.S2). For this species, the percentage of mature oocytes was independent of body size and ranged from 6% to 51% of all oocytes (Figure V.6B). The percentage of mature oocytes varied significantly among localities, with a larger proportion of vitellogenic oocytes in the C2a and R1 samples (Kruskal-Wallis test, H = 19.43, df = 6, p-value < 0.005).

V.3.4. Fecundity

An estimation of instantaneous fecundity was measured from individuals randomly selected among the C1a sample. In total, 9 individuals of *P. valvatoides* with sizes ranging from 2.2 to 3.4 mm, and 10 females of *P. midatlantica,* with shell lengths comprised between 4.1 and 8 mm, were analysed. In this study, even the smallest individuals examined possessed vitellogenic oocytes, so it was not possible to assess the minimal size at first maturity. Furthermore, for both species, mature individuals with shell length about half of their

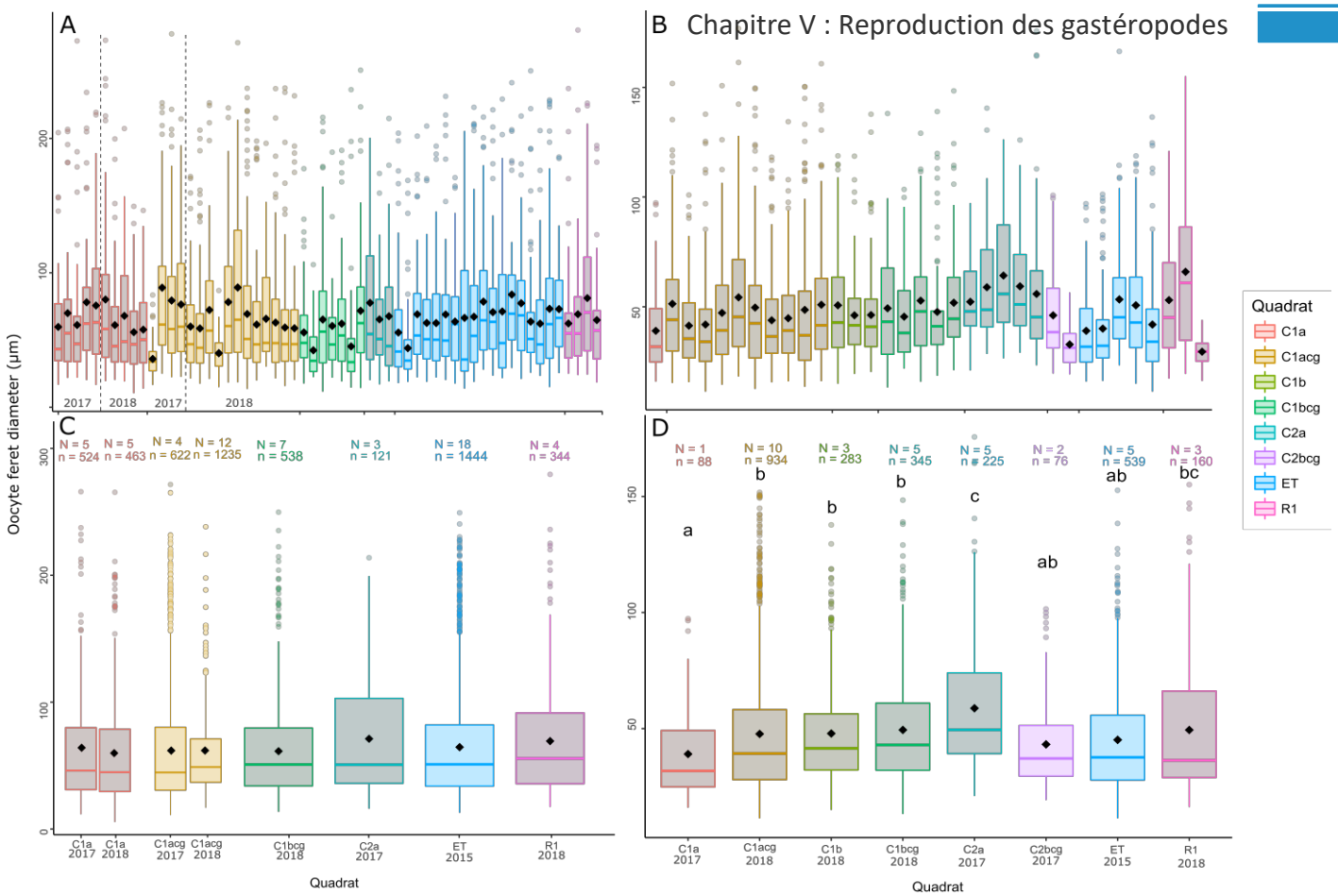

Figure V.5 Box plot of the oocyte size distribution of the two studied gastropods *Protolira valvatoides* (left) and *Pseudorimula midatlantica* (right) among the different samples. The mean oocyte size is represented by a black diamond **A)** Boxplot showing the oocytesize distribution of each individual of *P. valvatoides* among the different samples. **B)** Boxplot showing the oocyte-size distribution of each individual of *P. midatlantica* among the different samples. **C)** Boxplot showing the oocyte-size distribution of pooled individuals of *P. valvatoides* among the different samples. **D)** Boxplot showing the oocyte-size distribution of pooled individuals of *P. midatlantica* among the different samples. *N* number of individuals; *n* number of oocytes measured. Multisample comparisons were performed using the Nemenyi and Dunn test; homogeneous groups share the same letter

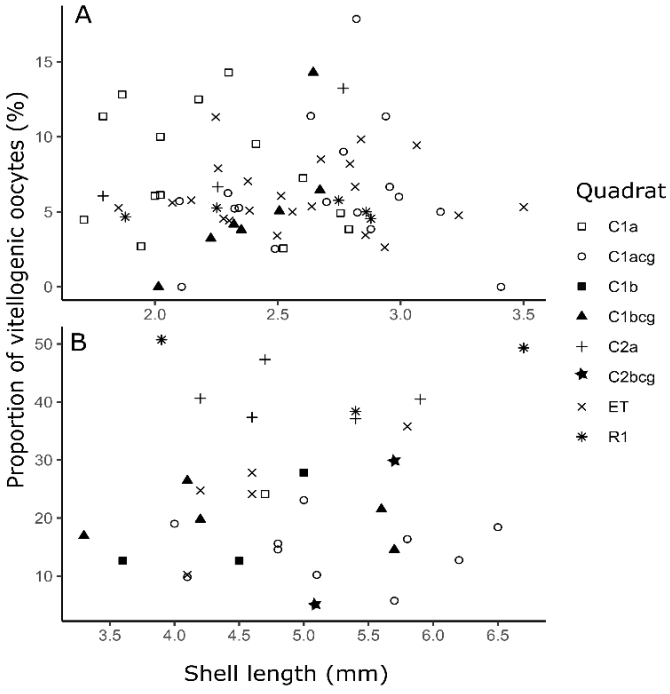

Figure V.6 Relationship between animal shell length and proportion of vitellogenic oocytes for each specimen of **A)** *Protolira valvatoides* and **B)** *Pseudorimula midatlantica* among the different samples

maximum size have been found. In *P. valvatoides*, the maximum instantaneous fecundity was very low, with only 8 vitellogenic oocytes through the entire ovary. Fecundity appears to be independent of animal size for the 9 individuals analysed (R^2=0.007, p-value = 0.34). Mean instantaneous fecundity of *P. midatlantica* was 187 ± 44 oocytes per female, with a maximum of 327 oocytes found in an individual with a length of 8 mm. Fecundity and shell length showed a positive linear relationship for the 10 examined specimens of *P. midatlantica* (R^2 = 0.84, p-value < 0.001).

V.3.5. Population structure

The demographic structures of the two species for each sample collected on Montségur in 2017 are presented in Figures V.7A and B. All frequency distributions significantly differed from the normal distribution (Kolmogorov-Smirnov test, p-value <0.001) and were thus assumed to be polymodal. For *P. valvatoides*, specimens ranged in shell length from 0.51 to 3.84 mm. Distributions were dominated by large individuals with a major peak between 2 and 2.5 mm (Figure V.7). However, while the chi² tests associated with the MIX modal decomposition highlighted no significant differences between the observed and obtained theoretical distributions, the low level of acceptance did not allow to determine reliable cohorts within the studied population. This might be due to the limited number of individuals analysed, or related to processes other than discontinuous recruitment. The Kruskal-Wallis multi-sample test identified significant differences in size-frequency distribution between the different samples (H = 49.424, df = 3, p-value < 0.001) and the post-hoc Dunn's multi-sample test showed that every sample was different from each other, except for C1acg which is not significantly different from C2a and R1 (Table V.2).

The low abundance of *P. midatlantica* did not allow to perform modal decomposition analysis, but the size distribution is highly variable across the different samples with, for example, a mean size of 2.4 ± 0.7 mm in the C1a sample against 3.7 ± 1.1 mm in C2a. The Kruskal-Wallis multi-sample test confirmed the observed difference among the localities (H = 112.04, df = 6, p-value < 0.001) and the post-hoc multiple Dunn's test highlighted significant differences between most of the samples, except for the C1b which contained only 16 individuals (Table V.2).

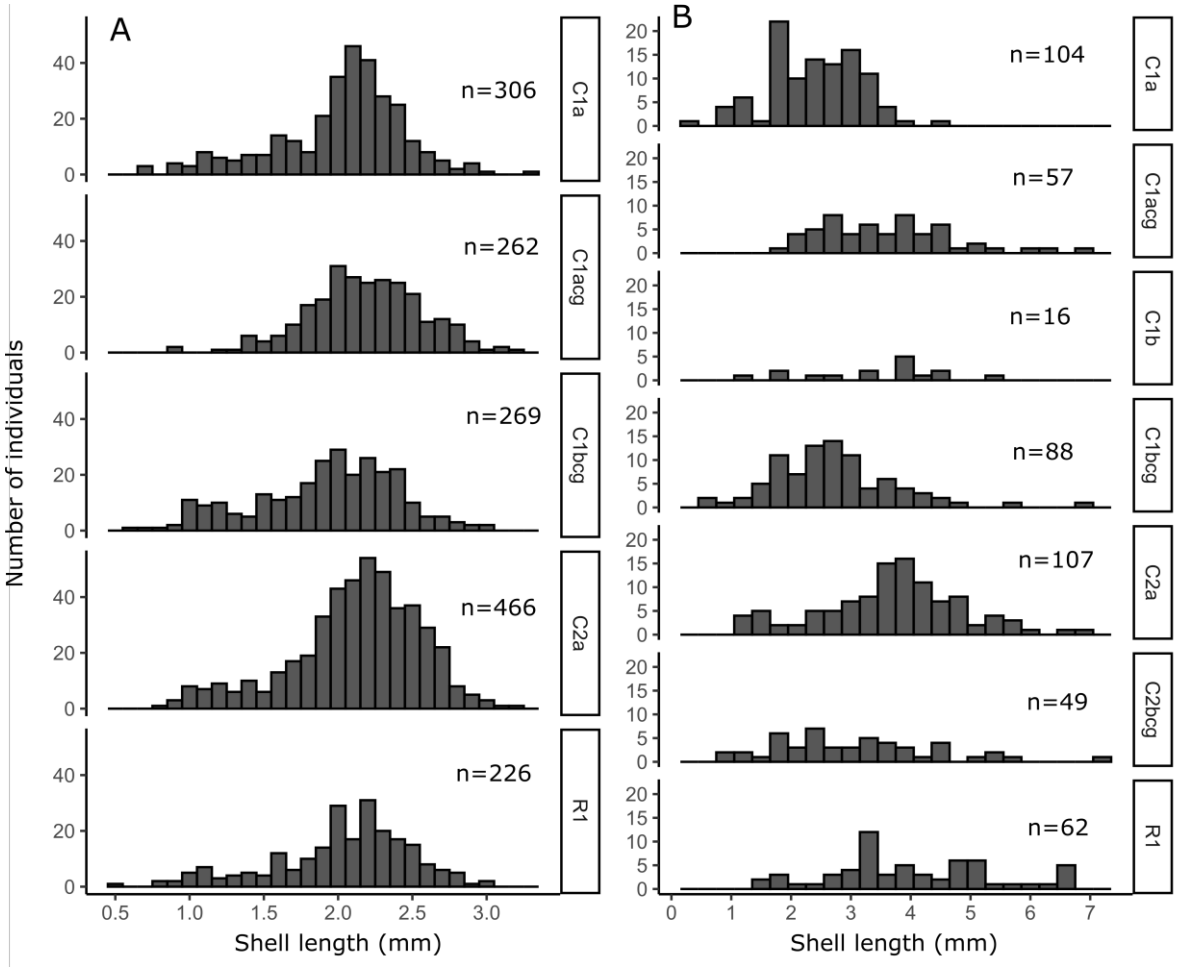

Figure V.7 Size–frequency distribution of shell length of **A)** *Protolira valvatoides* and **B)** *Pseudorimula midatlantica* among the different samples. *N* number of individuals measured.

Table V.2. Matrix of p-value of the Nemenyi and Dunn multiple range test used to compare the shell length distribution of *Protolira valvatoides* (up-right) and *Pseudorimula midatlantica* (down-left) among the different locations. ns = not significant ; *p<0.05; **p<0.01; ***p<0.001.

Quadrat	C1a	C1acg	C1b	C1bcg	C2a	C2bcg	R1
C1a		***	.	*	**	.	*
C1acg	***		.	***	ns	.	ns
C1b	***	ns		.	.	.	.
C1bcg	*	***	*		***	.	**
C2a	***	**	ns	***		.	*
C2bcg	**	*	ns	ns	***		.
R1	***	ns	ns	***	***	***	

V.4. Discussion

V.4.1. Reproductive anatomy

The reproductive anatomy of *Protolira valvatoides* and *Pseudorimula midatlantica* showed some differences leading to distinct reproductive attributes. *Protolira valvatoides* is a simultaneous hermaphroditic gastropod with separated ovary and testis, characterized by the presence of a propodial penis (Warén and Bouchet 1993) and internal fertilization as most of the Skeneidae species (Haszprunar et al. 2016). Internal or pseudo-internal (i.e. entaquatic) fertilization is an advantageous strategy adopted by many vent species that could ensure a high level of fertilization by preventing the rapid dilution of gametes in the turbulent flow regime of vents (Fretter 1989; Tyler and Young 1994; Hilario et al. 2005). Conversely, *Pseudorimula midatlantica* is a gonochoric species with a large ovary occupying almost a third of the body size. Unlike other genera of the Lepetodrilidae family (e.g. *Clypeosectus*, *Gorgoleptis* and *Lepetodrilus*), *Pseudorimula* lack secondary reproductive organs such as a penis or seminal groove (Haszprunar 1989; Warèn and Bouchet 2001) and no vesicle containing sperm or fertilized oocytes have been found in females of this study. However, Haszprunar (1989) identified the presence of ripe spermatozoa in contact with mucous droplets of the prostate gland in *Pseudorimula marianae* males, suggesting an entaquatic fertilization occurring after copulation in the female mantle cavities when oocytes are released in the sea water. While the two species analysed in this study are known to be associated with *Bathymodiolus azoricus* in cold habitats (Sarrazin et al. 2015), warmer fluid zones can be as close as few to tens of centimetres (Sarrazin et al. 2014; Matabos et al. 2015). Gametes released in seawater could thus easily be exposed to temperature above 100°C. Some deep-sea gastropods are known to enclose embryos within egg capsules or gelatinous mucus to protect them from harsh conditions (Berg 1985; Gustafson et al. 1991; Bouchet and Warén 1991; Warén and Bouchet 2001; Martell et al. 2002; Watanabe et al. 2009), but to our knowledge, none of the species belonging to the two investigated families display this type of development.

V.4.2. Gametogenesis

The two species investigated displayed a similar gametogenic pattern with the presence of all stages of oocyte development. The small oogonia of around 20 µm develop from the germinal epithelium and evolve to previtellogenic oocytes. These previtellogenic oocytes reach 80-100

µm for *P. valvatoides* and 40-50 µm for *P. midatlantica,* after which they undergo vitellogenesis, with a mean size of 185 µm for *P. valvatoides* and 81 µm for *P. midatlantica*. The polymodal distribution and the absence of temporal variation of oocyte-size frequency identified in this study for both species suggest iteroparity with a quasi-continuous and asynchronous gametogenesis among individuals. These reproductive patterns have been observed in many vent gastropod families such as Lepetodrilidae (Kelly and Metaxas 2007; Tyler et al. 2008, Bayer et al. 2011; Nakamura et al. 2014), Peltospiridae (Fretter 1988; Matabos and Thiebaut 2010) and Sutilizonidae (Hazsprunar 1989; Gustafson and Lutz, 1994). Continuous or quasi-continuous gametogenesis is also found in other vent taxa, including polychaetes (e.g. Alvinellidae, Ampharetidae, Polynoidae, and Siboglinidae families; McHugh and Tunnicliffe 1994; McHugh 1995; Zal et al. 1995; Van Dover et al. 1999; Jollivet et al. 2000; Blake and Van Dover 2005), shrimps (e.g. *Rimicaris chacei*, *Mirocaris fortunata*; Ramirez-Llodra et al. 2000) and amphipods (*Halice hesmonectes, Bouvierella curtirama*; Sheader et al. 2000; 2004). This continuity in gametogenesis may be linked to the continuous supply of energy in the vent environment, introduced in the food web by chemoautotrophic microorganisms (Tyler et al. 1994). Thus, invertebrate species can allocate a constant supply of energy for egg production and enhance the number of offspring throughout the year. However, despite the absence of energy limitation, some vent species such as *Bathymodiolus azoricus* display a seasonal reproduction with an annual emission of gametes around January (Colaço et al. 2006; Dixon et al. 2006). Their periodic spawning and fertilisation events and development of embryos into planktotrophic larvae seem to be linked to the seasonal input of phytoplankton detritus from the surface sinking through the water column to the seafloor (Gage and Tyler, 1991; Eckelbarger and Watling, 1995).

Table V.3. Summary of known reproductive traits of hydrothermal vent limpets from the *Lepetodrilidae* family. *JDFR* Juan de Fuca Ridge, *EPR* East Pacific Rise, *MAR* Mid-Atlantic Ridge

Species	Date	Location	Maximum size of vitellogenic oocytes (µm)	Onset of vitellogenesis (µm)	Instantaneous fecundity (Mean ± SD) [Max]	References
Lepetodrilus fucensis	Jul. 2001	JFDR	110	35–45	125.7 ± 121.4 [5149]	Kelly and Metaxas (2007)
	Jul–Sept. 1984		140			Fretter (1988)
Lepetodrilus pustulosus	Mar. 1984	EPR	120			Fretter (1988)
	Dec. 2001		84	30–35	53.9 ± 42.3 [850]	Pendlebury (2005); Tyler et al. (2008)
	Apr–May 1979		104			Berg (1985)
Lepetodrilus elevatus	Dec. 2001	EPR	84	30–35	[1800]	Pendlebury (2005); Tyler et al. (2008)
	Apr–May 1979		95			Berg (1985)
Lepetodrilus ovalis	Dec. 2001	EPR	87	30–35	27.9 ± 32.6 [400]	Pendlebury (2005); Tyler et al. (2008)
Lepetodrilus cristatus	Mar. 1984	EPR	150	30–35		Fretter (1988)
Lepetodrilus tevnianus	Dec. 2006	EPR	210	35–40		Bayer et al. (2011)
Lepetodrilus atlanticus	Mar–Apr. 2001	MAR	92	35–40	37.2 ± 24.1 [300]	Pendlebury (2005); Tyler et al. (2008)
Pseudorimula midatlantica	Apr. 2015	MAR	155	40–50	187 ± 44 [327]	This study
	Jul. 2017		175			This study
	Aug. 2018		176			This study

Table V.4. Summary of known reproductive traits of dominant species of the Lucky Strike vent field. *Fecundity refers to the total number of oocytes within a female regardless of the development stage while it refers to the number of vitellogenic oocytes for the other studies

Species	Reproductive strategy	Size of vitellogenic oocytes (µm)	Fecundity	Larval development	Seasonality	References
Bathymodiolus azoricus	Gonochoric	70–80	No data	Planktotrophic	Seasonal	Colaço et al. (2006) Dixon et al. (2006)
Branchipolynoe seepensis	Gonochoric	250–500	100–300	Lecithotrophic	Quasi-continuous	Jollivet et al. (2006)
Amphisamytha lutzi	Gonochoric	150–190	> 2500*	Lecithotrophic	Quasi-continuous	Blake and Dover (2005)
Lepetodrilus atlanticus	Gonochoric	50–92	95–300	Lecithotrophic	Quasi-continuous	Tyler et al. (2008)
Pseudorimula midatlantica	Gonochoric	80–176	107–327	Lecithotrophic	Quasi-continuous	This study
Protolira valvatoides	Hermaphrodite	120–272	4–8	Lecithotrophic	Quasi-continuous	This study

V.4.3. Reproductive output

The maximum oocyte-size found in *P. midatlantica* (176 µm) fell in the range of sizes previously observed in the Lepetodrilidae family. Oocytes are larger than those of *Lepetodrilus atlanticus, L. elevatus* and *L. ovalis*, but in the same order of magnitude as those of *L. fucensis*, *L. cristatus*, *L. pustulosus* and *L. tevnianus* (Fretter 1988, Kelly and Metaxas 2007; Tyler et al. 2008; Matabos and Thiebaut 2010; Bayer et al. 2011). Oocyte size is commonly used as an indicator of larval development mode. This assumes that large oocytes accumulate more yolk and can provide enough energetic resources for a lecithotrophic nutrition when the larvae disperse in the water column feeding only on the reserves accumulated in the eggs. On the contrary, smaller eggs do not contain enough food reserves to support dispersing larvae, and thus these larvae are mostly planktotrophic, feeding on bacteria, phytoplankton or detritus in the water-column (Tyler 1988). The maximum egg size of 176 µm for *Pseudorimula midatlantica* suggests a planktotrophic development for this species (Jaekle 1995; Levin and Bridges 1995). However, for lepetodrilid species egg size appears to be a poor indicator of larval development (Tyler et al. 2008). For instance, even if all lepetodrilid species studied to date display quite small maximum oocytes size (<200 µm, Table V.3), the morphology of their larval shell is consistent with a lecitothrophic development (Tyler et al. 2008, Lutz et al. 1986). This trait was proposed to reflect a phylogenetic constraint on vent taxa (Lutz et al. 1984). In general, larvae that are dependent on the energy from the yolk have a limited dispersion ability compared to planktotrophic larvae (Levin 2006). However, it has been demonstrated that for deep-sea species, cold temperatures can lead to a reduction of the metabolism and a delay of metamorphosis. This would enhance planktonic larval duration (PLD), suggesting the potential for a wider dispersal range (Pradillon et al. 2001; Young 2003, Watanabe et al. 2006; Adams et al. 2012).

When analysing the spatial variation of mean oocyte size and individual maturity for *P. midatlantica* within LS vent field, we observed differences at the edifice scale, with larger oocytes and higher proportion of mature oocytes in individuals of the C2a and R1 sites and lower values in the C1a sample. In C1a, there was only one female among the 10 examined individuals that could account for the observed difference in mean oocyte size compared to other samples. Interestingly, the C2a and R1 locations displayed the warmer and more variable temperatures, with mean temperature of 6.6 $\pm$ 0.9 °C for C2a and 8.3 $\pm$ 1.1 °C for

R1 compared to 5.7 ± 0.26 in C1a. The same observation was reported by Kelly and Metaxas (2007) between active and senescent habitats for *L. fucensis* in the Juan de Fuca Ridge. These authors showed poorly developed oocytes and lower fecundity in species inhabiting senescent environments, suggesting an influence of habitat characteristics on reproductive outputs (i.e. fecundity and oocyte size). Indeed, the proximity of vent emissions of warmer habitats might enhance chemoautotrophic production (Guezennec et al. 1998, Sievert et al., 2000) and provide a greater food supply for gastropods, allowing individuals to allocate more energy in vitellogenesis.

Female fecundity and shell size showed a strong linear relationship in *P. midatlantica.* The size-dependence of fecundity is a characteristic among many invertebrates, since larger females are able to enhance their resource acquisition and allocate them to reproductive processes (Bridges et al. 1994; Ramirez-Llodra 2002). This can also be supported by a positive correlation between body size and the volume of the ovary that may contain more oocytes (Honkoop and Van der Meer 1997). The maximum instantaneous fecundity of *P. midatlantica* was 327 oocytes, measured in an individual of 8 mm. The lower fecundity of *P. midatlantica* compared to other species of Lepetodrilid (Table V.3) can be a result of the difference observed in oocyte size: as this species has larger oocytes, less of them can be stored in the ovary.

P. valvatoides displayed an extremely low fecundity, with a maximum of 8 oocytes and no relationship between fecundity and body size was observed. The specific trade-off between size and number of mature oocytes due to individual body-size constraints can explain the low fecundity observed in this species. The very small body size of *P. valvatoides* (below 4 mm) is a common characteristic of Skeneidae species. However, *P. valvatoides* have large and yolky vitellogenic oocytes with a maximum size of 272 µm, suggesting a lecithotrophic development of the larvae (Haszprunar et al. 2016), similar to most vent gastropods (Lutz et al. 1984; Berg 1985; Gustafson and Lutz 1994). While the low fecundity observed in *P. valvatoides* may result in a very weak probability to disperse at large scale and reach a new habitat, this species remains very abundant within vent communities. The simultaneous hermaphroditism observed in this species might contribute to maximizing the number of fertilized individuals, resulting in a larger effective population size (i.e. number of individuals contributing to the next generation). Hence, a large number of reproducing individuals could counteract the low fecundity observed in *P. valvatoides* by ensuring a high retention rate and increasing the

number of larvae available for dispersal. This hypothesis requires further investigation and population genetics approaches would bring additional insights in the dispersal of this species.

V.4.4. Recruitment and population structure

The polymodal size-frequency distribution observed within the different samples for both species suggest episodic recruitment events. The discrepancy between continuous gametogenesis and discontinuous recruitment has been previously observed in vent gastropods (Matabos and Thiebaut 2010) and can be related to the occurrence of discrete spawning events and/or post-settlement processes, including mortality and differential growth. In addition, the number of juveniles found in this study is low and many factors can explain this observation. First, the observed fecundity of the two species studied is low, thus each spawning event would supply a small number of larvae, resulting in the settlement of only a few specimens. Secondly, biotic and abiotic factors like competition for space or physical stress on post-settled individuals may play a major role on mortality rates (Kelly and Metaxas 2007). The observed differences in population structure among sampling locations suggest variations in recruitment between different microhabitats, or could be linked to differential mortality and growth rates specific to the habitat. This may be driven by spatial variations in hydrothermal fluid flux, habitat heterogeneity or linked to differences in local diversity that can, in turn, influence biotic interactions. Despite the extremely low fecundity of P. valvatoides, the adult population present a high abundance of individuals that can reach up to 4000 individuals.m^{-2} (Husson et al. 2017) in the different locations. Many hypotheses can support this observation. On one hand, the combination of high density of organisms and hermaphroditism might ensure the release of enough fertilized eggs to sustain the local population. On the other hand, it could be possible that the emitted eggs are non-buoyant or directly lay on hard substratum, as observed in other vent gastropods (Gustafson et al. 1991; Fretter and Graham 1994; Yahagi et al. 2017). The direct development of this species within the parental community would result in a high rate of retention within the community. In fact, we noticed the presence of eggs laying on the sulphide substratum among faunal assemblages, which could belong to *P. valvatoides*. Population genetic studies are necessary to better understand the dispersal abilities for this species and determine the level of population retention at the site scale.

V.4.5. Implications for the resilience of vent communities

A major disturbance at active hydrothermal vents, for example during deep-sea mining operations, would lead to the collapse of the established faunal community. The first step in the colonisation of newly formed low-temperature habitats is marked by the development of free-living microbial communities (Shank et al. 1998). This large microbial production allows the establishment of numerous metazoan species, among which, grazers and scavengers represent the pioneer colonisers (Shank et al. 1998; Mullineaux et al. 2010; Mullineaux et al. 2012; Cuvelier et al. 2018). Then, the main pathway of macrofaunal recolonisation after a large-scale disturbance is the settlement of larvae coming from adjacent areas (regional pool), which results from the coincidence between the timing of disturbance and that of colonist availabilities (Lutz et al. 1984; Pradillon et al. 2005, Mullineaux et al. 2010, 2012). Although our knowledge regarding reproductive biology and dispersal capacity of vent species remains scarce, some reproductive features of four dominant macrofaunal species of the Lucky Strike vent field in the Mid-Atlantic Ridge have been investigated (Table V.4). These species, which include three gastropods (*L. atlanticus*, *P. midatlantica* and *P. valvatoides*) and the polychaete *Amphisamytha lutzi,* are characterized by early maturity, quasi-continuous gametogenesis and lecithotrophic larval development, which appears to be a common and widespread successful reproductive strategy at vents. Continuous gametogenesis and lecithotrophic development might ensure the continual presence of larvae in the environment and their retention in the surrounding area.

Previous studies have hypothesized the implication of organic falls (e.g. whale falls) as “stepping stones” that represent islands of food resources and suitable habitats for chemosynthetically-fuelled species, and can thus play a connectivity role between vent and seep habitats (Hecker 1985, Smith et al. 1989). *Protolira* species appear to be able to develop on organic falls and feed on the local microbial production. Indeed, *Protolira thorvaldssoni* has been found both at vent and seep environments, but also on whale bones, from which the species was originally described (Waren 1996). *P. valvatoides* has also been recorded on wood substrata deployed in inactive areas on the LS vent field (Alfaro-Lucas et al. in revision). Despite their extremely low fecundity, *P. valvatoides* seems to be able to disperse as larvae, and reach organic substrata, few hundred meters from active vents. This observation is not consistent with our hypotheses of direct development of larvae and high retention rate for

this species, and many uncertainties remain regarding their dispersion. It is more likely that the simultaneous hermaphroditism observed in this species represents an advantage over gonochorism in situations in which finding a mate is difficult (Heller et al. 2008). Thus, even in the case of low density of organisms on organic falls, *P. valvatoides* might ensure a relatively good reproductive success and enhance their establishment by maximising the number of offsprings.

To conclude, the two gastropod species considered in the present study exhibit some common phylogenetically constrained reproductive traits, such as early maturity, quasi-continuous gametogenesis and lecithotrophic larval development. This combination of reproductive traits appears to be a widespread attribute among vent invertebrates to ensure the continuity of larval supply and improve the sustainability of populations in the surrounding environment. However, the two species showed contrasting reproductive features in terms of fecundity, oocyte size and reproductive mode. Indeed, there is an important trade-off between the size and the number of eggs produced by adults that is constrained by morphological and physiological features and is highly dependent on energy availability. In this context, *P. midatlantica* is characterized by the production of smaller mature oocytes counterbalanced by a higher fecundity compared to *P. valvatoides*. This specific strategy may enhance recruitment success by maximizing the number of offsprings but reduce the ability to disperse further because less energy is allocated to a single oocyte. Conversely, *P. valvatoides* produces a very low number of bigger oocytes. For this species, small adult size associated with reduced ovary volume constrain the reproductive output. Despite its low fecundity, *P. valvatoides* hermaphroditism may be an advantage to enhance the number of fertilized eggs and maintain an important effective population size at the local scale. Therefore, in the context of major disturbance, habitat destruction could lead to a collapse of local populations for both species. Furthermore, despite differences in the reproductive characteristics of the two investigated species, their ability to disperse widely from a preserved area and reach impacted sites seems highly limited by their low fecundity and their dispersal mode (lecithotrophy). However, previous results suggest that *P. valvatoides* might be able to use organic falls as stepping stones to disperse and recolonise an impacted area.

Finally, this study provides new data on key biological features that can feed bio-physical models of connectivity. In addition, it highlighted that the description of reproductive biology is not sufficient to comprehend all the mechanisms involved in the dispersion and establishment of vent species. Indeed, the role of environmental factors, particularly ocean currents and water column food supply, are essential factors to ensure the settlement of dispersing larvae in newly formed habitats. Therefore, knowledge of biological features and environmental factors associated with population genetics/genomics approaches are needed to better understand the dispersal potential of species inhabiting chemosynthetic-based ecosystems, and the resilience of vent communities (Hilario et al., 2015; Baco et al., 2016). This knowledge is fundamental to define restoration actions that might be implemented to ensure ecosystem sustainability in case of large-scale disturbances induced by mining activities. Thus, the establishment of efficient protected areas with buffer zones and the deployment of artificial substrata that can act as stepping stones for vent species to recolonise impacted areas, represent important measures to take into consideration.

Acknowledgements
We would like to thank the captains and crews of the oceanographic cruises Momarsat 2015, 2017 and 2018 aboard the vessels N/O Pourquoi pas? and L'Atalante, as well as the ROV Victor6000 team. We are particularly grateful to Pierre-Marie Sarradin and Mathilde Cannat, chief scientists of the cruises who greatly supported our sampling program. We are also sincerely thankful to Sandra Fuchs for sample collection and Julie Tourolle for providing the map as well as all the technicians of the deep sea Ifremer lab. Many thanks to all members of the histological lab of the Norwegian Veterinary Institute and especially to Randi Terland who provided valuable help and assistance with histological processes. We are also grateful to Lucile Durand for the help on imagery acquisition and Florence Pradillon for proofreading the last version of this manuscript. This research was supported by the European H2020 MERCES (Project ID 689518) and by the eCOREF project funded by Equinor (Norway). Julien Marticorena PhD project was funded by Ifremer and Equinor. This project is part of the EMSO-Azores (http://www.emso-fr.org) regional node and EMSO ERIC Research Infrastructure (http://emso.eu/). ERLL was supported by the European H2020 MERCES (Project ID 689518).

Compliance with Ethical Standards

Fundings This research was supported by the European H2020 MERCES (Project ID 689518) and by the eCOREF project funded by Equinor (Norway). Julien Marticorena PhD project was funded by Ifremer and Equinor. This project is part of the EMSO-Azores (http://www.emso-fr.org) regional node and EMSO ERIC Research Infrastructure (http://emso.eu/). ERLL was supported by the European H2020 MERCES (Project ID 689518).

Conflicts of interest The authors declare that they have no conflict of interest.

Ethics approval All applicable international, national, and/or institutional guidelines for sampling were followed in the current study.

Consent to participate Not applicable

Consent for publication The Author hereby consents to publication of the work in any and all Springer publications. The Author warrants that the work has not been published in any form except as a preprint that the work is not being concurrently submitted to and is not under consideration by another publisher.

Availability of data and material Not applicable

Code availability Not applicable

Authors' contributions JM, MM, JS and ERLL conceived the ideas and designed the methodology. JM, MM and JS collected the data and JM processed and analysed the data. JM wrote the first draft of the manuscript and all authors commented on previous versions of the manuscript. All authors read and approved the final manuscript.

DOI of the cruises involved

SARRADIN Pierre-Marie, CANNAT Mathilde (2015) MOMARSAT2015 cruise, RV Pourquoi pas ?, https://doi.org/10.17600/15000200

SARRADIN Pierre-Marie, CANNAT Mathilde (2017) MOMARSAT2017 cruise, RV Pourquoi pas ?, https://doi.org/10.17600/17000500

CANNAT Mathilde (2018) MOMARSAT2018 cruise, RV L'Atalante, https://doi.org/10.17600/18000514

V.5. References

Adams, D.K., S.M. Arellano, and B. Govenar. (2012). Larval dispersal: Vent life in the water column. *Oceanography* 25: 256–268.

Baco AR, Etter RJ, Ribeiro PA, Heyden S von der, Beerli P, Kinlan BP (2016) A synthesis of genetic connectivity in deep-sea fauna and implications for marine reserve design. *Mol Ecol* 25: 3276–3298.

Bates AE (2006) Population and feeding characteristics of hydrothermal vent gastropods along environmental gradients with a focus on bacterial symbiosis hosted by *Lepetodrilus fucensis* (Vetigastropoda). PhD Thesis

Bayer SR, Mullineaux LS, Waller RG, Solow AR (2011) Reproductive traits of pioneer gastropod species colonising deep-sea hydrothermal vents after an eruption. *Mar Biol* 158: 181–192.

Blake EA, Dover CLV (2005) The reproductive biology of Amathys lutzi, an ampharetid polychaete from hydrothermal vents on the Mid-Atlantic Ridge. *Invertebr Biol* 124: 254–264.

Berg, C. J. (1985) Reproductive strategies of mollusks from abyssal hydrothermal vent communities. *Bull Biol Soc Wash* 6:185-197

Boschen RE, Rowden AA, Clark MR, Pallentin A, Gardner JPA (2016) Seafloor massive sulfide deposits support unique megafaunal assemblages: Implications for seabed mining and conservation. *Mar Environ Res* 115:78–88.

Bouchet, P. and Warén, A. (1991) *Ifremeria nautilei,* a new gastropod from hydrothermal vents, probably associated with symbiotic bacteria. *Comptes Rendus Academie des Sciences (Paris)*, 612: 495-501.

Breusing C, Biastoch A, Drews A, Metaxas A, Jollivet D, Vrijenhoek RC, Bayer T, Melzner F, Sayavedra L, Petersen JM, Dubilier N, Schilhabel MB, Rosenstiel P, Reusch TBH (2016) Biophysical and Population Genetic Models Predict the Presence of "Phantom" Stepping Stones Connecting Mid-Atlantic Ridge Vent Ecosystems. *Curr Biol* 26:2257–2267.

Bridges TS, Levin LA, Cabrera D, Plaia G (1994) Effects of sediment amended with sewage, algae, or hydrocarbons on growth and reproduction in two opportunistic polychaetes. *J Exp Mar Biol Ecol* 177:99–119.

Carpenter S, Walker B, Anderies JM, Abel N (2001) From Metaphor to Measurement: Resilience of What to What? *Ecosystems* 4:765–781.

Clark, M.R., Smith, S., (2013) Environ Manag Consid. In: Deep Sea Minerals: Manganese Nodules, A Physical, Biological, Environmental and Technical Review, SPC1B, 27-41

Colaço A, Martins I, Laranjo M, Pires L, Leal C, Prieto C, Costa V, Lopes H, Rosa D, Dando PR, Serrão-Santos R (2006) Annual spawning of the hydrothermal vent mussel, *Bathymodiolus azoricus*, under controlled aquarium, conditions at atmospheric pressure. *J Exp Mar Biol Ecol* 333:166–171.

Colaço A, Desbruyères D, Guezennec J (2007) Polar lipid fatty acids as indicators of trophic associations in a deep-sea vent system community. *Mar Ecol* 28:15–24.

Connell SD, Ghedini G (2015) Resisting regime-shifts: the stabilising effect of compensatory processes. *Trends Ecol Evol* 30:513–515.

Cumming GS, Olsson P, Chapin FS, Holling CS (2013) Resilience, experimentation, and scale mismatches in social-ecological landscapes. *Landscape Ecol* 28:1139–1150.

Cuvelier D, Beesau J, Ivanenko VN, Zeppilli D, Sarradin P-M, Sarrazin J (2014) First insights into macro- and meiofaunal colonisation patterns on paired wood/slate substrata at Atlantic deep-sea hydrothermal vents. *Deep-Sea Res Pt I.* 87:70–81.

Cuvelier D, Gollner S, Jones DOB, Kaiser S, Arbizu PM, Menzel L, Mestre NC, Morato T, Pham C, Pradillon F, Purser A, Raschka U, Sarrazin J, Simon-Lledó E, Stewart IM, Stuckas H, Sweetman AK, Colaço A (2018) Potential Mitigation and Restoration Actions in Ecosystems Impacted by Seabed Mining. *Front Mar Sci*. 5 :467

De Busserolles F, Sarrazin J, Gauthier O, Gélinas Y, Fabri MC, Sarradin PM, Desbruyères D (2009) Are spatial variations in the diets of hydrothermal fauna linked to local environmental conditions? *Deep-Sea Res Pt II* 56:1649–1664.

DeFreese DE, Clark KB (1983) Analysis of reproductive energetics of Florida Opisthobranchia (Mollusca: Gastropoda). *Int J Inver Rep* 6: 1–10.

Desbruyères D, Biscoito M, Caprais J-C, Colaço A, Comtet T, Crassous P, Fouquet Y, Khripounoff A, Le Bris N, Olu K, Riso R, Sarradin P-M, Segonzac M, Vangriesheim A (2001) Variations in deep-sea hydrothermal vent communities on the Mid-Atlantic Ridge near the Azores plateau. *Deep-Sea Res Pt I* 48:1325–1346.

Desbruyères D, Segonzac M, Bright M, Biologiezentrum OL, Desbruyeres D, Segonzac M, Bright M (2006) Handbook of deep-sea hydrothermal vent fauna, 2nd completely rev. ed. / editors, Daniel Desbruyères, Michel Segonzac and Monika Bright. Linz, Austria : *Land Oberösterreich, Biologiezentrum der Oberösterreichische Landesmuseen*

Dixon DR, Lowe DM, Miller PI, Villemin GR, Colaço A, Serrão-Santos R, Dixon LRJ (2006) Evidence of seasonal reproduction in the Atlantic vent mussel *Bathymodiolus azoricus*, and an apparent link with the timing of photosynthetic primary production. *J of the J Mar Biol Assoc UK* 86:1363–1371.

Eckelbarger KJ, Eckelbarger KJ (1994) Diversity Of Metazoan Ovaries And Vitellogenic Mechanisms - Implications For Life history Theory. *P Biol Soc Wash* 107:193–218.

Eckelbarger KJ, Watling L (1995) Role of Phylogenetic Constraints in Determining Reproductive Patterns in Deep-Sea Invertebrates. *Inver Biol* 114:256–269.

Fretter V (1988) New archaeogastropod limpets from hydrothermal vents; Superfamily Lepetodrilacea. II. Anatomy. *Philos T Roy Soc B* 319:33–82.

Fretter V (1989) The anatomy of some new archaeogastropod limpets (Superfamily Peltospiracea) from hydrothermal vents. *J Zool* 218:123–169.

Fretter V, Graham A (1994) British prosobranch molluscs. Their functional anatomy and ecology. *Publ Brit Ray Soc*, 144

Gabe M (1968) Techniques histologiques. *Masson*

Gage JD, Tyler PA (1991) Deep-Sea Biology: A Natural History of Organisms at the Deep-Sea *Floor. Camb U Pr*

Galkin SV, Goroslavskaya EI (2010) Bottom fauna associated with *Bathymodiolus azoricus* (Mytilidae) mussel beds in the hydrothermal fields of the Mid-Atlantic Ridge. *Oceanology* 50:51–60.

Gladstone-Gallagher RV, Pilditch CA, Stephenson F, Thrush SF (2019) Linking Traits across Ecological Scales Determines Functional Resilience. *Trends Ecol Evol* 34:1080–1091.

Gollner S, Govenar B, Arbizu PM, Mills S, Le Bris N, Weinbauer M, Shank TM, Bright M (2015) Differences in recovery between deep-sea hydrothermal vent and vent-proximate communities after a volcanic eruption. *Deep-Sea Res Pt I* 106:167–182.

Gollner S, Kaiser S, Menzel L, Jones DOB, Brown A, Mestre NC, van Oevelen D, Menot L, Colaço A, Canals M, Cuvelier D, Durden JM, Gebruk A, Egho GA, Haeckel M, Marcon Y, Mevenkamp L, Morato T, Pham CK, Purser A, Sanchez-Vidal A, Vanreusel A, Vink A, Martinez Arbizu P (2017) Resilience of benthic deep-sea fauna to mining activities. *Mar Environ Res* 129:76–101.

Guezennec J, Ortega-Morales O, Raguenes G, Geesey G (1998) Bacterial colonisation of artificial substrate in the vicinity of deep-sea hydrothermal vents. *FEMS Microbiol Ecol* 26:89–99.

Gustafson RG, Littlewood DTJ, Lutz RA (1991) Gastropod Egg Capsules and Their Contents From Deep-Sea Hydrothermal Vent Environments. *Biol Bull* 180:34–55.

Gustafson RG and Lutz RA (1994). Molluscan life history traits at deep sea hydrothermal vents and cold methane/ sulfide seeps. In Reproduction, larval biology, and recruitment in deep-sea benthos (ed. C.M. Young and K. Eckelbarger), 76-97

Haszprunar G (1989) New slit-limpets (Scissurellacea and Fissurellacea) from hydrothermal vents. Part 2. Anatomy and relationships. *Contrib. sci.* 408:1-17.

Haszprunar G, Kunze T, Brückner M, Heß M (2016) Towards a sound definition of Skeneidae (Mollusca, Vetigastropoda): 3D interactive anatomy of the type species, Skenea serpuloides (Montagu, 1808) and comments on related taxa. *Org Divers Evol* 16:577–595.

Hecker B (1985) Fauna from a cold sulfur-seep in the Gulf of Mexico: comparison with hydrothermal vent communities and evolutionary implications. *Bull Biol Soc Wash* 6:465-473.

Hein JR, Mizell K, Koschinsky A, Conrad TA (2013) Deep-ocean mineral deposits as a source of critical metals for high- and green-technology applications: Comparison with land-based resources. *Ore Geol Rev* 51:1–14.

Heller J (1993) Hermaphroditism in molluscs. *Biol J Linn Soc* 48:19–42.

Hilário A, Young CM, Tyler PA (2005) Sperm Storage, Internal Fertilization, and Embryonic Dispersal in Vent and Seep Tubeworms (Polychaeta: Siboglinidae: Vestimentifera). *Biol Bull 208:*20–28.

Hilário A, Metaxas A, Gaudron SM, Howell KL, Mercier A, Mestre NC, Ross RE, Thurnherr AM, Young C (2015) Estimating dispersal distance in the deep sea: challenges and applications to marine reserves. *Front Mar Sci.* 2:6

Honkoop PJC and Van der Meer J (1997). Reproductive output of Macoma balthica populations in relation to winter-temperature and intertidalheight mediated changes of body mass. *Mar Ecol Prog. Ser.* 149:155-162.

Husson B, Sarradin P-M, Zeppilli D, Sarrazin J (2017) Picturing thermal niches and biomass of hydrothermal vent species. *Deep-Sea Res Pt II* 137:6–25.

Ingrisch J, Bahn M (2018) Towards a Comparable Quantification of Resilience. *Trends Ecol Evol* 33:251–259.

Jaeckle W (1995) Variation in the Size, Energy Content, and Biochemical Composition of Invertebrate Eggs: Correlates to the Mode of Larval Development. *Ecol of Mar Inver Larv*. 49 –77

Jollivet D, Empis A, Baker MC, Hourdez S, Comtet T, Jouin-Toulmond C, Desbruyères D, Tyler PA (2000) Reproductive biology, sexual dimorphism, and population structure of the deep sea hydrothermal vent scale-worm, *Branchipolynoe seepensis* (Polychaeta: Polynoidae). *J Mar Biol Ass UK* 80: 55–68.

Kelly NE, Metaxas A (2007) Influence of habitat on the reproductive biology of the deep-sea hydrothermal vent limpet *Lepetodrilus fucensis* (Vetigastropoda: Mollusca) from the Northeast Pacific. *Mar Biol* 151:649–662.

Laming SR, Gaudron SM, Duperron S (2018) Lifecycle Ecology of Deep-Sea Chemosymbiotic Mussels: A Review. *Front Mar Sci. 5:282*

Levin LA., Bridges TS. (1995) Pattern and diversity in reproduction and development. *Ecol Mar Inver Larv.* 1-48.

Levin LA (2006) Recent progress in understanding larval dispersal: new directions and digressions. *Integr Comp Biol* 46:282–297.

Levin LA, Mengerink K, Gjerde KM, Rowden AA, Van Dover CL, Clark MR, Ramirez-Llodra E, Currie B, Smith CR, Sato KN, Gallo N, Sweetman AK, Lily H, Armstrong CW, Brider J (2016) Defining “serious harm” to the marine environment in the context of deep-seabed mining. *Mar Pol* 74:245–259.

Lutz RA, Jablonski D, Turner RD (1984) Larval Development and Dispersal at Deep-Sea Hydrothermal Vents. *Science* 226:1451–1454.

Lutz RA, Bouchet P, Jablonski D, Turner RD, and Warén A (1986), Larval ecology of mollusks at deep-sea hydrothermal vents, *Malacol Bull* 4:49-54,

Mac Donald P, Du with contributions from J (2018) mixdist: Finite Mixture Distribution Models.

Martell KA, Tunnicliffe V, Macdonald IR (2002) Biological features of a buccinid whelk (Gastropoda, Neogastropoda) at the Endeavour Vent-field of Juand de Fuca Ridge, Northest Pacific. *J Molluscan Stud* 68:45–53.

Matabos M, Thiebaut E (2010) Reproductive biology of three hydrothermal vent peltospirid gastropods (*Nodopelta heminoda, N. subnoda* and *Peltospira operculata*) associated with Pompeii worms on the East Pacific Rise. *J Molluscan Stud* 76:257–266.

Matabos M, Cuvelier D, Brouard J, Shillito B, Ravaux J, Zbinden M, Barthelemy D, Sarradin PM, Sarrazin J (2015) Behavioural study of two hydrothermal crustacean decapods: *Mirocaris fortunata* and *Segonzacia mesatlantica*, from the Lucky Strike vent field (Mid-Atlantic Ridge). *Deep-Sea Res Pt II* 121:146–158.

McHugh D (1995) Unusual Sperm Morphology in a Deep-Sea Hydrothermal-Vent Polychaete, *Paralvinella pandorae* (Alvinellidae). *Inver Biol* 114:161–168.

McHugh D, Tunnicliffe V (1994) Ecology and reproductive biology of the hydrothermal vent polychaete *Amphisamytha galapagensis* (Ampharetidae). *Mar Ecol Progr Ser* 106:111–120.

McLean JH, Haszprunar G (1987) Pyropeltidae, a new family of cocculiniform limpets from hydrothermal vents. *Veliger.* 30:196–205

McLean JH (1992) A new species of Pseudorimula (Fissurellacea: Clypeosectidae) from hydrothermal vents of the Mid-Atlantic Ridge. *Nautilus* 106:115-118

Metaxas A, Saunders M (2009) Quantifying the "Bio-" Components in Biophysical Models of Larval Transport in Marine Benthic Invertebrates: Advances and Pitfalls. *Biol Bull* 216: 257–272.

Mullineaux LS, Adams DK, Mills SW, Beaulieu SE (2010) Larvae from afar colonise deep-sea hydrothermal vents after a catastrophic eruption. *PNAS* 107:7829–7834.

Mullineaux LS, Bris NL, Mills SW, Henri P, Bayer SR, Secrist RG, Siu N (2012) Detecting the Influence of Initial Pioneers on Succession at Deep-Sea Vents. *PLOS ONE* 7:e50015.

Nakamura M, Watanabe H, Sasaki T, Ishibashi J, Fujikura K, Mitarai S (2014) Life history traits of *Lepetodrilus nux* in the Okinawa Trough, based upon gametogenesis, shell size, and genetic variability. *Mar Ecol Progr Ser* 505:119–130.

Oliver TH, Heard MS, Isaac NJB, Roy DB, Procter D, Eigenbrod F, Freckleton R, Hector A, Orme CDL, Petchey OL, Proença V, Raffaelli D, Suttle KB, Mace GM, Martín-López B, Woodcock BA, Bullock JM (2015) Biodiversity and Resilience of Ecosystem Functions. *Trends Ecol Evol* 30:673–684.

Portail M, Brandily C, Cathalot C, Colaço A, Gélinas Y, Husson B, Sarradin P-M, Sarrazin J (2018) Food-web complexity across hydrothermal vents on the Azores triple junction. *Deep-Sea Res Pt I* 131:101–120.

Pradillon F, Shillito B, Young CM, Gaill F (2001) Developmental arrest in vent worm embryos. *Nature* 413:698–699.

Pradillon F, Bris NL, Shillito B, Young CM, Gaill F (2005) Influence of environmental conditions on early development of the hydrothermal vent polychaete *Alvinella pompejana. J Exp Biol* 208:1551–1561.

Pendlebury S (2005) Ecology of hydrothermal vent gastropods. PhD thesis. School of Ocean and Eart Sciences, Southampton, 148

Ramirez-Llodra E (2002) Fecundity and life-history strategies in marine invertebrates. In: Adv *Mar Biol*. 87–170

Ramirez-Llodra E, Tyler PA, Baker MC, Bergstad OA, Clark MR, Escobar E, Levin LA, Menot L, Rowden AA, Smith CR, Dover CLV (2011) Man and the Last Great Wilderness: Human Impact on the Deep Sea. *PLOS ONE* 6:e22588.

Ramirez-Llodra R, Tyler PA, Copley JTP (2000) Reproductive biology of three caridean shrimp, *Rimicaris exoculata, Chorocaris chacei* and *Mirocaris fortunata* (Caridea: Decapoda), from hydrothermal vents. *J Mar Biol Ass U K* 80:473–484.

R Studio Team (2016). RStudio: Integrated Development Environment for R. Boston, MA: RStudio, Inc. Available at: http://www.rstudio.com

Sarrazin J, Cuvelier D, Peton L, Legendre P, Sarradin PM (2014) High-resolution dynamics of a deep-sea hydrothermal mussel assemblage monitored by the EMSO-Açores MoMAR observatory. *Deep-Sea Res Pt I* 90:62–75.

Sarrazin J, Legendre P, de Busserolles F, Fabri M-C, Guilini K, Ivanenko VN, Morineaux M, Vanreusel A, Sarradin P-M (2015) Biodiversity patterns, environmental drivers and indicator species on a high-temperature hydrothermal edifice, Mid-Atlantic Ridge. *Deep-Sea Res Pt II* 121:177–192.

Sasaki T, Warén A, Kano Y, Okutani T, Fujikura K (2010) Gastropods from Recent Hot Vents and Cold Seeps: Systematics, Diversity and Life Strategies. In: Kiel S (ed) The Vent and Seep Biota: Aspects from Microbes to Ecosystems. *Springer Netherlands, Dordrecht*, 169–254

Schneider CA, Rasband WS, Eliceiri KW (2012) NIH Image to ImageJ: 25 years of image analysis. *Nat Methods* 9:671–675.

Shank TM, Fornari DJ, Von Damm KL, Lilley MD, Haymon RM, Lutz RA (1998) Temporal and spatial patterns of biological community development at nascent deep-sea hydrothermal vents (9°50'N, East Pacific Rise). *Deep-Sea Res Pt II* 45:465–515.

Sheader M, Van Dover CL, Shank TM (2000) Structure and function of *Halice hesmonectes* (Amphipoda: Pardaliscidae) swarms from hydrothermal vents in the eastern Pacific. *Mar Biol* 136:901–911.

Sheader M, Van Dover CL, Thurston MH (2004) Reproductive ecology of *Bouvierella curtirama* (Amphipoda: Eusiridae) from chemically distinct vents in the Lucky Strike vent field, Mid-Atlantic Ridge. *Mar Biol* 144:503–514.

Sievert SM, Ziebis W, Kuever J, Sahm K (2000) Relative abundance of Archaea and Bacteria along a thermal gradient of a shallow-water hydrothermal vent quantified by rRNA slot-blot hybridization. *Microbiol* 146:1287–1293.

Smith CR, Kukert H, Wheatcroft RA, Jumars PA, Deming JW (1989) Vent fauna on whale remains. *Nature* 341:27–28.

Suzuki K, Yoshida K, Watanabe H, Yamamoto H (2018) Mapping the resilience of chemosynthetic communities in hydrothermal vent fields. *Sci Rep* 8:9364.

Turnipseed M, Jenkins CD, Van Dover CL (2004) Community structure in Florida Escarpment seep and Snake Pit (Mid-Atlantic Ridge) vent mussel beds. *Mar Biol* 145:121–132.

Tyler PA, Billett DSM (1988) The Reproductive Ecology of Elasipodid Holothurians from the N. E. Atlantic. *Biological Oceanography* 5:273–296.

Tyler PA, 1988. Seasonality in the deep-sea. *Oceanogr Mar Biol. Annual Review* 26:227-258.

Tyler PA, Campos-Creasey, L.S. and Giles, L.A., 1994. Environmental control of quasi-continuous and seasonal reproduction in deep-sea benthic invertebrates. In Reproduction, Larval Biology and Recruitment of the Deep-Sea Benthos, edited by C. M. Young and K. J. Eckelbarger. New York: Columb U Pr, pp. 158-178.

Tyler PA, Young CM (1999) Reproduction and dispersal at vents and cold seeps. *J Mar Biol Assoc UK* 79:193–208.

Tyler PA, Pendlebury S, Mills SW, Mullineaux L, Eckelbarger KJ, Baker M, Young CM (2008) Reproduction of Gastropods from Vents on the East Pacific Rise and the Mid-Atlantic Ridge. *J Shellfish Res.* 27:107–118.

Van Dover CL (2014) Impacts of anthropogenic disturbances at deep-sea hydrothermal vent ecosystems: A review. *Mar Environ Res* 102:59–72.

Van Dover CL, Trask J, Gross J, Knowlton A (1999) Reproductive biology of free-living and commensal polynoid polychaetes at the Lucky Strike hydrothermal vent field (Mid-Atlantic Ridge*). Mar Ecol Progr Ser* 181:201–214.

Vic C, Gula J, Roullet G, Pradillon F (2018) Dispersion of deep-sea hydrothermal vent effluents and larvae by submesoscale and tidal currents. *Deep-Sea Res Pt I* 133:1–18.

Vrijenhoek RC (2010) Genetic diversity and connectivity of deep-sea hydrothermal vent metapopulations*. Mol Ecol* 19:4391–4411.

Warèn A, Bouchet P (2001) Gastropoda and Monoplacophora from hydrothermal vents and seeps ; new taxa and records. *The Veliger* 44:116–231.

Warèn A, Bouchet P (1993) New records, species, genera, and a new family of gastropods from hydrothermal vents and hydrocarbon seeps. *Zool Scr* 22:1–90.

Warén A (1996) New and little known mollusca from Iceland and Scandinavia. Part 3. *Sarsia* 81:197–245.

Watanabe H, Kado R, Kaida M, Tsuchida S, Kojima S (2006) Dispersal of vent-barnacle (genus Neoverruca) in the Western Pacific. *Cah Biol Mar* 47: 353−357

Watanabe H, Fujikura K, Kinoshita G et al (2009) Egg capsule of *Phymorhynchus buccinoides* (Gastropoda: Turridae) in a deep-sea methane seep site in Sagami Bay, Japan. *Venus* 67:181–188

Yahagi T, Watanabe HK, Kojima S, Kano Y (2017) Do larvae from deep-sea hydrothermal vents disperse in surface waters? *Ecology* 98:1524–1534.

Young CM, Eckelbarger KJ, Eckelbarger K (1994) Reproduction, Larval Biology, and Recruitment of the Deep-sea Benthos. Columb U Pr

Young CM. (2003) Reproduction, Development and Life History Traits, in: Ecosystems of the World, Vol. 28, Ecosystems of the Deep Oceans, edited by: Tyler, P. A*., Elsevier, London*, 381–426

Zal F, Jollivet D, Chevaldonné P, Desbruyères D (1995) Reproductive biology and population structure of the deep-sea hydrothermal vent worm *Paralvinella grasslei* (Polychaeta: Alvinellidae) at 13°N on the East Pacific Rise. *Mar Biol*. 122:637–648.

Zar JH (2007) Biostatistical Analysis (5th Edition). Prentice-Hall, Inc., Upper Saddle River, NJ, USA

V.6. Supplementary files

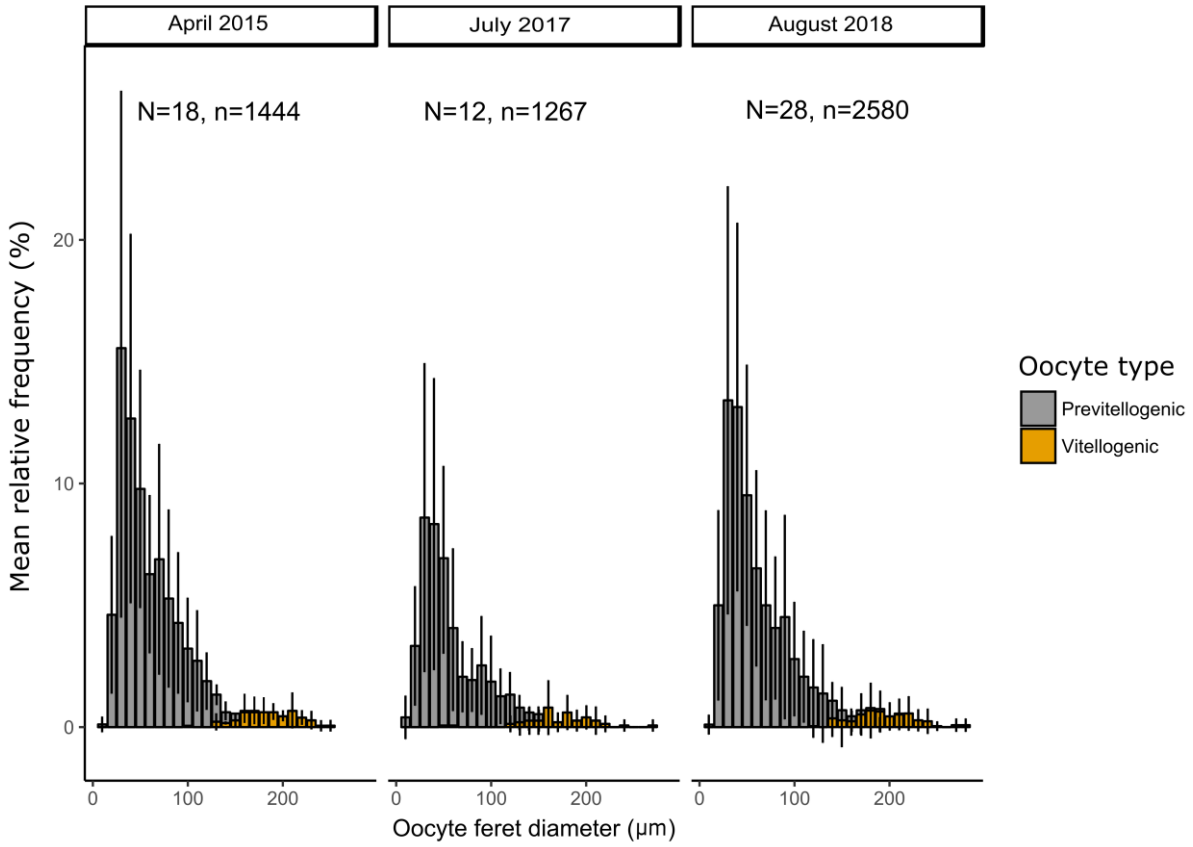

Figure V.S1 Mean oocyte size-frequency histograms (mean ± SD) of pooled individuals of *Protolira valvatoides* for each sampling period. Colors: Grey bars represent previtellogenic oocytes and yellow bars represent vitellogenic oocytes. Abbreviations: N, number of individuals; n, number of oocytes measured.

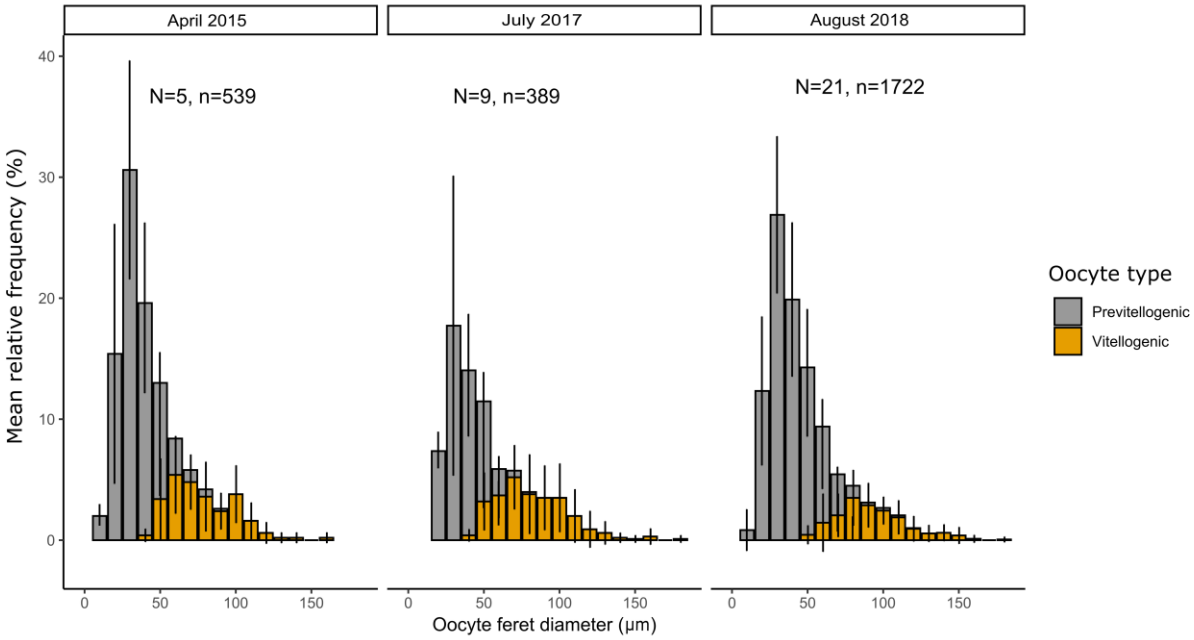

Figure V.S2 Mean oocyte size-frequency histograms (mean ± SD) of pooled individuals of *Pseudorimula midatlantica* for each sampling period. Colors: Grey bars represent previtellogenic oocytes and yellow bars represent vitellogenic oocytes. Abbreviations: N, number of individuals; n, number of oocytes measured.

Table S1. Results of Kruskal–Wallis multisample tests and the Nemenyi and Dunn multiple range tests comparing oocyte size distributions between individuals of the two gastropod species within each sample.

Species	Edifice	Station	Date	Number of individuals	Kruskal-Wallis multisample test	Nemenyi and Dunn multiple range test
Prototolira valvatoides	Montségur	C1a	July 2017	5	H = 29.69, df = 4, P < 0.001	1/5 different
			August 2018	5	H = 7.87, df = 4, P < 0.05	2/5 different
		C1acg	July 2017	4	H = 6.25, df = 3, P < 0.05	1/4 different
			August 2018	12	H = 153.72, df = 11, P < 0.001	3/12 different
		C1bcg	August 2018	7	H = 70.49, df = 6, P < 0.001	2/7 different
		C2a	July 2017	3	H = 1.23, df = 2, P > 0.05	-
		R1	August 2018	4	H = 13.12, df = 4, P < 0.05	1/4 different
	Eiffel Tower	ET	April 2015	18	H = 107.51, df = 17, P < 0.001	2/18 different
Pseudorimula midatlantica	Montséegur	C1a	July 2017	1	-	-
		C1acg	August 2018	10	H = 23.54, df = 9, P < 0.05	2/10 different
		C1b	August 2018	3	H = 1.89, df = 2, P > 0.05	-
		C1bcg	August 2018	5	H = 8.66, df = 4, P > 0.05	-
		C2a	July 2017	5	H = 10.47, df = 4, P < 0.01	1/5 different
		C2bcg	July 2017	2	H = 8.22, df = 1, P < 0.05	1/2 different
		R1	July 2017	3	H = 63.06, df = 2, P < 0.001	1/3 different
	Eiffel Tower	ET	April 2015	5	H = 40.10, df = 4, P < 0.001	2/5 different

VI. Discussion générale

Cette étude avait pour principal objectif de fournir de nouvelles données sur les processus impliqués dans la recolonisation des communautés de macrofaune en réponse à une perturbation au sein du champ hydrothermal Lucky Strike (dorsale médio-Atlantique) afin de mieux appréhender leur capacité de résilience.

En raison de la forte stabilité des conditions environnementales et de la faible fréquence d'occurrence de perturbations naturelles au sein des systèmes de dorsales lentes (Cuvelier et al. 2011 ; Du Preez et Fisher 2018), nous avons privilégié une approche expérimentale pour décrire la dynamique de recolonisation des assemblages faunistiques à la suite d'une perturbation induite. Il s'agissait, dans un premier temps, de caractériser l'état de référence de la structure des communautés et de la diversité fonctionnelle au sein des assemblages de *Bathymodiolus azoricus* puis d'induire une perturbation de défaunation à petite échelle. Un suivi de deux ans, consécutifs à la perturbation, nous a permis de décrire les premières étapes de la recolonisation et d'évaluer la capacité de rétablissement des assemblages sur l'édifice actif Montségur. La mise en place d'un suivi rigoureux des paramètres physico-chimiques et le déploiement d'une expérience d'exclusion des prédateurs ont confirmé le rôle combiné des facteurs environnementaux et des interactions biotiques sur les processus de colonisation et de succession écologique des écosystèmes hydrothermaux associés à la dorsale médio-Atlantique (Sarrazin et al. 1997 ; Tunnicliffe et al. 1997 ; Shank et al. 1998 ; Mullineaux et al. 2000 ; Micheli et al. 2002 ; Lenihan et al. 2008). En parallèle, nous avons cherché à réaliser une caractérisation quantitative de la composition faunistique au sein de deux habitats inactifs (en périphérie proche de l'édifice actif Montségur et sur la structure d'une cheminée inactive). Il s'est avéré que la méthodologie employée et le manque de réplication étaient insuffisants pour avoir une vision représentative de la diversité de ces habitats qui serait a priori très élevée (Levin et al. 2009 ; Cowart et al. 2020).

Au niveau du site hydrothermal actif, l'étude de la diversité taxonomique et le suivi de la diversité fonctionnelle nous ont permis d'identifier plusieurs espèces de gastéropodes brouteurs comme premiers colonisateurs des habitats perturbés sur Montségur et de mettre en évidence leur rôle clé dans le rétablissement des assemblages. Étant donné l'importance des gastéropodes sur la structuration des communautés et le manque de connaissance sur leurs cycles de vie, nous avons également cherché à analyser les traits reproductifs de deux espèces dominantes (*Protolira valvatoides* et *Pseudorimula midatlantica*). Ces analyses

permettent d'évaluer la capacité de ces espèces à se maintenir et perdurer au sein de leur habitat et également à appréhender leur aptitude à se disperser à plus large échelle pour atteindre des zones potentiellement impactées. Les principaux résultats des différentes parties de ce travail sont synthétisés dans l'encart 5.

VI.1. Limites de l'expérience

Au cours de ce travail, notre choix d'induire une perturbation directement au sein des habitats hydrothermaux, plutôt que d'avoir recours à des substrats de colonisation, a été motivé par la volonté de conserver les caractéristiques physiques et chimiques du milieu.

En effet, cette approche permet de s'affranchir de l'impact potentiel du matériau d'un substrat de colonisation, de sa taille ou de sa complexité et d'éviter d'éventuelles modifications des conditions environnementales subies par les organismes. Une telle approche permet également de tenir compte de l'importante hétérogénéité spatiale des conditions abiotiques au sein de l'habitat naturel. Cette expérimentation présente néanmoins certaines limites qu'il est important de prendre en compte dans l'interprétation des résultats. Dans un premier temps, bien que de gros progrès aient été accomplis en ce qui concerne l'échantillonnage des substrats durs, il demeure relativement compliqué de réaliser un échantillonnage quantitatif et de s'assurer de la collecte de la totalité des petits organismes attachés au substrat ou nichés dans les anfractuosités de la roche (Gauthier et al. 2010). De la même façon, il était difficile de constater si la perturbation induite pouvait avoir modifié les paramètres physiques de la roche et/ou impacté les communautés microbiennes qui s'y établissent. Or, il a été mis en évidence que la stabilisation des conditions environnementales et le développement des mattes microbiennes constituaient les toutes premières étapes du processus de succession écologique au niveau des écosystèmes hydrothermaux de la dorsale Pacifique (Shank et al. 1998 ; Marcus et al. 2009). D'autre part, pour préserver la diversité et limiter l'impact de l'échantillonnage à l'échelle de l'édifice, la perturbation induite sur l'ensemble des échantillons de cette étude n'excède pas 1 m^2, ce qui rend certains résultats difficiles à extrapoler à grande échelle. Il est à noter également que le nombre de réplicats, quoiqu'assez nombreux pour une telle étude en milieu profond, est encore insuffisant pour tirer de solides conclusions. Par ailleurs, la nature de la perturbation induite diffère grandement de ce qui est observé au cours d'éruptions volcaniques ou de ce qui sera provoqué dans le cadre une d'une activité d'exploitation minière, qui entraînent tous deux

une destruction complète de l'habitat et l'éradication totale des communautés à plus ou moins grande échelle (Ramirez-Llodra et al. 2011 ; Van Dover 2014 ; Gollner et al. 2017). Enfin, les quadrats expérimentaux utilisés pour estimer le rétablissement des assemblages hydrothermaux ont été déployés directement sur l'édifice actif ou à sa base et les zones défaunées étaient entourées par des assemblages matures de *Bathymodiolus azoricus*. Cette proximité a notamment permis à certains individus adultes de migrer afin d'occuper l'habitat libéré par l'expérience de perturbation. En effet, nous avons identifié dans certains quadrats échantillonnés récoltés 1 an après la perturbation, à la fois un grand nombre de post-larves de *Bathymodiolus azoricus* n'excédant pas 600 µm de longueur mais également quelques individus de plusieurs centimètres. Étant donné le peu d'informations disponibles sur la croissance des espèces hydrothermales, il est difficile de fixer une limite de taille qui permettrait de discriminer les individus issus du recrutement ou de la migration. Cependant, des observations de juvéniles de *B. azoricus* sur l'édifice actif voisin Tour Eiffel ont montré une croissance de moins de 2 $mm.an^{-1}$ (V. Courant, rapport M2), suggérant que toute modiole de plus de 2 mm sur un quadrat dénudé pourrait provenir des assemblages limitrophes. Il est donc important de garder à l'esprit que la recolonisation étudiée à la suite de la perturbation comprend à la fois des organismes issus du recrutement de post-larves ayant atteint la surface libre par le biais de la dispersion larvaire, mais également des individus sessiles qui ont migré depuis les assemblages alentours.

Encart 5 | Synthèse des principaux résultats

I- Rétablissement de la structure des communautés en réponse à une perturbation

>> Dans les deux années qui ont suivi la perturbation de défaunation, une **recolonisation partielle** de l'espèce ingénieure *Bathymodiolus azoricus* a été observée, colonisation qui semble être limitée par la présence de prédateurs de plus grande taille (ex. crevettes, crabes).

>> Un **rétablissement de la richesse taxonomique** de l'ordre de 80 % des assemblages de macrofaune a été observé. Seules quelques espèces de prédateurs, considérées comme « rares » dans les assemblages de référence, demeurent absentes à l'issue de l'expérimentation.

>> Nos résultats suggèrent **un faible rétablissement en termes de densité** d'organismes. Des **divergences dans la structure des communautés** ont également été identifiées au cours du processus de recolonisation.

>> L'élaboration d'un premier **modèle de succession** post-perturbation suggère que les **gastéropodes** font partie des **espèces pionnières,** précédant l'installation de *B. azoricus* qui, en grandissant, contribue à la complexification de l'habitat et facilite l'établissement des espèces **«** rares **».**

II- Description de la reproduction et évaluation de la dispersion des gastéropodes

>> Les deux espèces étudiées, *Protolira valvatoides* et *Pseudorimula midatlantica,* affichent une **gamétogénèse quasi-continue** alors que leur structure démographique plaide en faveur d'un **recrutement discontinu**.

>> En revanche, elles présentent certaines divergences relatives à leur **mode de reproduction**, leur **fécondité** ainsi qu'à la **taille des ovocytes** matures, ce qui peut se traduire par des différences dans leur capacité de maintenir une population effective ou de coloniser d'autres habitats.

>> Nos résultats suggèrent également que les deux espèces présentent un mode de développement **larvaire lécithotrotrophe** associé à une **faible fécondité.**

>> Les traits reproductifs identifiés suggèrent une faible **capacité de dispersion à grande échelle limitée**, favorisant plutôt une forte rétention des larves au sein des populations adultes qui permettrait de maximiser la population effective locale.

III- Rétablissement de la structure du réseau trophique en réponse à une perturbation

>> À l'état de référence, le **partitionnement des ressources** et la **sélection de l'habitat** sont les principaux facteurs de structuration des communautés. Les mattes microbiennes sont une source importante de nourriture du réseau trophique de l'édifice Montségur et peu d'espèces semblent se nourrir directement de l'espèce ingénieure *B. azoricus.*

>> Un an après la perturbation, on assiste à un bon rétablissement de la diversité trophique mais la **dominance des prédateurs/nécrophages** semble impacter la biomasse des échelons trophiques inférieurs et réduire la complexité du réseau trophique.

>> En deux ans, le réseau trophique semble avoir retrouvé une **structure et une complexité** proches de celles des assemblages de référence sur Montségur. Les **gastéropodes brouteurs,** tirant bénéfice du nouvel espace libéré et du développement des communautés microbiennes, prédominent ces assemblages.

VI.2. Processus de colonisation des communautés actives

Les écosystèmes hydrothermaux constituent un habitat très fragmenté, avec des sites parfois séparés de plusieurs dizaines à plusieurs centaines de kilomètres, qui peuvent être apparentés à des « patches » interconnectés et étudiés dans un cadre général de métacommunautés (Breusing et al. 2016 ; Mullineaux et al. 2018). Cette approche implique l'imbrication de multiples échelles qui doivent être prises en considération pour l'étude de la dynamique des communautés hydrothermales. En effet, celle-ci peut être appréhendée à grande échelle, dans le cadre de la connectivité des populations et de la dispersion larvaire (Lowe et Allendorf 2010 ; Baco et al. 2016 ; Laurent et al. 2016 ; Boschen et al. 2016), mais elle dépend également de processus locaux qui régissent le recrutement et la survie des individus, tels que la soutenabilité de l'habitat, les interactions biotiques et la disponibilité en ressources nutritionnelles (Micheli et al. 2002 ; Mullineaux et al. 2003 ; Hunt et al. 2004 ; Kelly et al. 2007 ; Cuvelier et al. 2014).

La dispersion larvaire joue un rôle primordial dans la dynamique des populations des écosystèmes hydrothermaux, car elle assure à la fois la persistance des assemblages établis à l'échelle locale et contribue à la colonisation de nouveaux habitats et au maintien de la connectivité à l'échelle régionale (Adams et al. 2012). En raison d'importantes difficultés méthodologiques pour échantillonner les larves, deux méthodes indirectes sont utilisées pour caractériser et quantifier la dispersion larvaire : 1) les analyses génétiques de flux génique (Vrijenhoek 2010 ; Baco et al. 2016) et 2) l'utilisation de modèles bio-physiques combinant des simulations hydrodynamiques et des paramètres biologiques (par ex. fécondité, durée de vie larvaire) et qui permettent de traquer des particules dans la colonne d'eau (Metaxas 2004 ; Cowen et Sponaugle 2009 ; Breusing et al. 2016 ; Vic et al. 2018). La mise en place de ces modèles nécessite cependant une connaissance préalable de certains paramètres biologiques des espèces, tels que la fécondité, la durée de vie larvaire pélagique et/ou la période de reproduction. Or, les organismes benthiques qui dominent les assemblages hydrothermaux présentent une grande diversité de stratégies reproductives qui entraînent des divergences de leur capacité de dispersion et celle à coloniser de nouveaux habitats (Llodra et al. 2000 ; Marsh et al. 2001 ; Pradillon et al. 2005 ; Tyler et al. 2008 ; Bayer et al. 2011 ; Laming et al. 2018). Dans un premier temps, la fécondité et la fréquence des événements de ponte au cours

de l'année jouent un rôle clé sur le nombre de larves émises dans la colonne d'eau et ainsi sur le succès de recrutement. D'autre part, le mode de développement et de nutrition des larves influence leur flottabilité et leur durée de vie planctonique (Marsh et al. 2001 ; Pradillon et al. 2001 ; Hilário et al. 2015). Ces données biologiques, essentielles à la paramétrisation des modèles bio-physiques, sont manquantes et/ou insuffisantes, et constituent l'une des limites principales à la compréhension des mécanismes de dispersion larvaire au niveau des écosystèmes hydrothermaux. Cette thèse a ainsi contribué à une meilleure connaissance de la biologie des espèces hydrothermales avec la description de la gamétogenèse et de la structure des populations de deux espèces de gastéropodes abondantes sur Lucky Strike (*Protolira valvatoides et Pseudorimula midatlantica* ; Marticorena et al. 2020). Ces informations viennent compléter les données déjà acquises sur la reproduction des autres espèces dominantes *Bathymodiolus azoricus* (Colaço et al. 2006 ; Dixon et al. 2006), *Branchipolynoe seepensis* (Van Dover et al. 1999), *Amphisamytha lutzi* (Blake et Dover 2005) *et Lepetodrilus atlanticus* (Tyler et al. 2008). Malgré des différences identifiées entre les deux espèces de gastéropodes pour certains traits reproducteurs, leur faible fécondité, en particulier pour *Protolira valvatoides,* et la production de larves lécitotrophes suggèrent des capacités de dispersion à grande échelle limitées et une importante rétention des larves au sein de la population locale. D'autre part, des pontes de gastéropodes attachées au substrat ont été retrouvées dans certains échantillons et des analyses moléculaires sont en cours pour tenter de déterminer à quelle espèce elles appartiennent. Plusieurs espèces de gastéropodes hydrothermaux, tels que certains Phenacolepadidae (ex. *Divia briandi)*, Peltospiridae (ex. *Lirapex costellata*) ou Raphitomidae (ex. *Phymorhyncus sp*.), enferment les embryons dans des capsules ou des boules de mucus afin de les protéger des rudes conditions du milieu et maximiser leur succès de recrutement (Berg 1985 ; Gustafson et al. 1991 ; Warèn et Bouchet 1993 ; Gustafson 1994 ; Waren et Bouchet 2001 ; Martell et al. 2002, Watanabe et al. 2009, Yahagi et al. 2019). Ainsi, quoiqu'ayant des stratégies de reproduction distinctes, les espèces hydrothermales semblent caractérisées par une faible capacité de dispersion sur de grandes distances, ce qui explique mal leurs gradients de distribution étendus. De nombreuses hypothèses ont été proposées afin d'expliquer cette incohérence telle qu'une prolongation de la phase larvaire pélagique chez les mollusques (Arellano et al. 2009) ou l'arrêt du développement embryonnaire chez le polychète *Alvinella pompejana* (Pradillon et al. 2001). Plus récemment, une étude à grande échelle réalisée le long de la dorsale médio-Atlantique,

couplant les résultats d'un modèle de dispersion de *Bathymodiolus spp*. avec des informations de génétique des populations, a suggéré l'existence de « sites fantômes » non identifiés qui pourraient favoriser la dispersion entre les différents champs hydrothermaux (Breusing et al. 2016).

À l'échelle locale, la recolonisation peut s'effectuer par l'intermédiaire de la migration d'individus adultes depuis les assemblages faunistiques adjacents pour occuper un habitat vacant. *Bathymodiolus azoricus* est capable de se déplacer grâce au byssus qu'elle produit et peut fréquemment parcourir des distances de plusieurs décimètres voire mètres (Matabos & Sarrazin, pers. obs., C. Raffault, stage M1). D'autre part, Zal et al. (1995) ont suggéré que certaines espèces mobiles comme les crabes sont susceptibles d'entraîner la dissémination d'autres espèces en se déplaçant d'un site à un autre. Au cours de notre expérimentation, le suivi de la structure démographique des populations révèle la présence d'individus de grande taille au cours des deux années consécutives à la perturbation, confirmant la migration d'individus adultes. En revanche, la proportion de nouvelles recrues de très petites tailles (< 2 mm) était plus élevée au sein des échantillons prélevés après la défaunation que dans les assemblages de référence. Ces résultats tendent à montrer que le recrutement de larves prédomine la recolonisation par rapport à la migration d'individus adultes.

VI.3. Rétablissement des communautés à petite échelle

La mesure du rétablissement d'une communauté à la suite d'une perturbation consiste principalement à étudier l'évolution de variables réponses à différentes échelles pour les comparer aux conditions de référence lorsque celles-ci sont disponibles (Lotze et al. 2011). Par exemple, à l'échelle des populations, il peut s'agir de suivre l'abondance, la distribution démographique ou le rôle fonctionnel alors qu'à l'échelle de l'écosystème, on peut s'intéresser à la diversité taxonomique, aux conditions environnementales ou à la structure du réseau trophique (Lotze et al. 2011).

Dans le cadre de cette expérimentation, le premier travail consistait donc à caractériser l'état de référence de la communauté faunistique de Montségur, jusqu'alors très peu étudiée en comparaison à l'édifice voisin Tour Eiffel (~ 100 mètres). L'ensemble des résultats obtenus nous ont permis de schématiser l'avancement du rétablissement des assemblages, deux ans

après la perturbation (Figure VI.1), au regard des différents attributs identifiés au début de la thèse (voir Encart 2 et Annexe 1 pour interprétation). La caractérisation de la biodiversité, la structure des communautés ainsi que la structure du réseau trophique des assemblages à partir de nombreux descripteurs ont permis de mettre en évidence le rôle des conditions environnementales sur la distribution et la dynamique naturelle des communautés de macrofaune de cet édifice. Cette étude confirme également une forte similitude de la composition des assemblages associés à l'espèce *Bathymodiolus azoricus* entre les différents édifices du champ hydrothermal Lucky Strike (Sarrazin et al. 2020). Cette étude, tout comme celle de Cuvelier et al. (2011), a permis de mettre en évidence une importante stabilité temporelle des communautés de référence à l'échelle de l'édifice au cours des trois années de suivi.

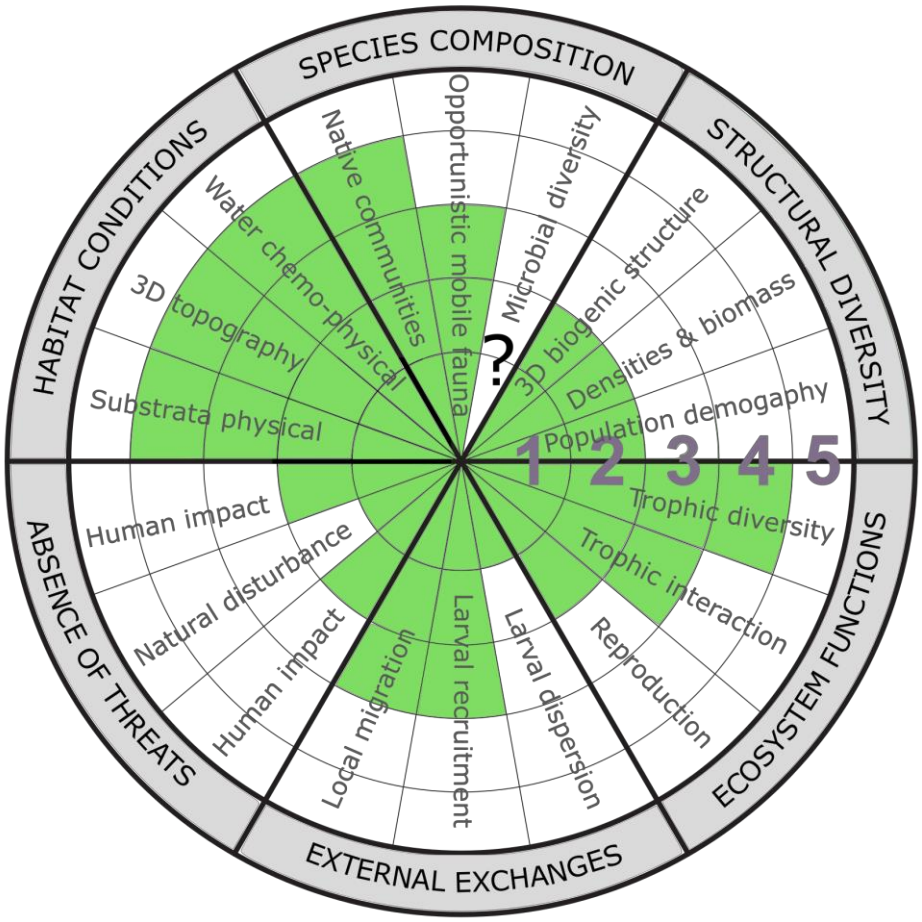

Figure VI.1. Schéma illustrant la progression du rétablissement des assemblages de macrofaune, deux ans après l'induction d'une perturbation sur l'édifice actif Montségur, pour les six attributs et 18 sous-attributs définis initialement comme représentatifs des écosystèmes hydrothermaux (voir Encart 2). Les conditions nécessaires à l'attribution de 1 à 5 étoiles pour les différents attributs sont détaillées dans l'annexe 1.

La perturbation induite dans le cadre de l'expérimentation ne semble pas avoir significativement modifié les caractéristiques environnementales au sein des différents quadrats étudiés et aucune variation significative de ces facteurs n'a été observée au cours du processus de recolonisation. Cependant, il est important de noter ici qu'en raison de la forte variabilité environnementale à l'échelle d'un quadrat, la caractérisation a été réalisée à partir de trois mesures répétées en trois points distincts afin de prendre en compte cette variabilité spatiale. En l'absence de *B. azoricus*, nous nous attendions à une augmentation locale du débit des émissions comme en témoigne la formation d'anhydrite après défaunation au niveau des fissures observées sur certains quadrats.

Un an après la défaunation, à l'exception de quelques espèces rares, la quasi-totalité des espèces présentes initialement avait recolonisé l'espace libéré. Très peu de variations de la composition isotopique des différentes espèces ont été identifiées au cours de la recolonisation et les métriques calculées à l'échelle de la communauté indiquent un bon rétablissement de la diversité des sources trophiques après 1 an. En revanche, la faible recolonisation de l'espèce ingénieure *Bathymodiolus azoricus* pourrait expliquer le faible rétablissement des densités d'organismes en comparaison à l'état de référence. En effet, certaines études ont évoqué un rôle de facilitation des espèces ingénieures pour l'établissement d'espèces associées, par l'intermédiaire de la création d'une structure tridimensionnelle permettant une diversification des niches écologiques (Bergquist et al. 2007 ; Lelièvre et al. 2018). D'autre part, nos résultats ont mis en évidence d'importantes différences en termes de structure des communautés, marquées par une répartition plus uniforme des espèces un an après la perturbation. Cela suggère que l'espace et les ressources disponibles au sein de l'habitat permettent l'établissement d'une grande diversité d'espèces mais que les interactions biotiques (ex. compétition, prédation), qui aboutissent généralement à la dominance de certains taxa, n'ont pas encore pris place. Toutefois, à ce stade de la succession écologique, les prédateurs/charognards semblent jouer un rôle clé sur la complexité du réseau trophique. En effet, nos résultats supposent que certaines espèces de prédateurs, comme les crevettes *Mirocaris fortunata* se nourrissent des recrues de *Bathymodiolus azoricus,* retardant ainsi leur rétablissement et la complexification du réseau trophique (Sancho et al. 2005). Deux ans après la perturbation, on assiste à une augmentation des densités relatives et de la biomasse de plusieurs espèces de gastéropodes brouteurs.

Malgré des densités d'organismes nettement inférieures à l'état de référence, un bon rétablissement de la diversité (> 80 % de la richesse spécifique initiale) et de la complexité du réseau trophique est observé. Notre modèle de succession écologique (Figure III.9) suggère que ces différentes espèces de gastéropodes, sont les pionnières des assemblages benthiques de l'édifice Montségur et qu'ils profitent du développement *de novo* des mattes microbiennes sur le substrat nu pour se nourrir, comme cela a déjà été observé au niveau d'autres écosystèmes hydrothermaux (Mullineaux et al. 2012, 2010).

À l'issue de l'expérience de recolonisation, on constate donc un bon rétablissement de la diversité taxonomique et de la structure du réseau trophique. Dans ce travail, les indicateurs de structure du réseau trophique utilisés sont très dépendants de la richesse taxonomique et ne tiennent pas compte de la distribution des biomasses ou de l'abondance dans les assemblages. Le choix de ne pas utiliser des métriques pondérées par la biomasse des différentes espèces, a été motivé par le constat qu'au sein des écosystèmes hydrothermaux, toute la biomasse n'est pas disponible de la même manière. Par exemple, certaines espèces représentant la grande majorité de la biomasse totale jouent principalement un rôle structurant de la communauté et très peu d'autres espèces semblent en mesure de les prédater. C'est principalement le cas de *Bathymodiolus azoricus* qui compte pour 98 % de la biomasse totale (Husson et al. 2017 ; cette étude) mais qui n'est pas disponible pour la communauté en raison de la présence d'une coquille. Enfin, malgré la proximité entre les quadrats expérimentaux et les assemblages matures de l'édifice Montségur, on constate un très faible rétablissement des densités d'organismes ainsi que des changements importants dans la structure des communautés en comparaison aux assemblages de référence. Ces résultats contrastent avec les taux de rétablissement observés dans le Pacifique, où les densités peuvent être récupérées après quelques années (Shank et al. 1998 ; Tunnicliffe et al. 1997 ; Marcus et al. 2009 ; Gollner et al. 2015), et soutiennent l'existence d'une dynamique contrastée, plus lente au niveau des systèmes de dorsales lentes caractérisées par une plus forte stabilité temporelle (Du Preez et Fisher 2018 ; Cuvelier et al. 2011). À la fin de ces 2 années d'expérimentation, le temps nécessaire à ces assemblages pour retrouver la structure de l'état de référence demeure inconnu. Un suivi prolongé nous permettra d'obtenir plus d'informations sur les processus impliqués dans la recolonisation et de vérifier la validité du modèle de succession écologique présenté. D'autre part, la mise en place d'analyses de

diversité fonctionnelle avec l'utilisation de traits relatifs à la reproduction, à la structuration de l'habitat et à la productivité pourrait nous permettre de mieux appréhender la résilience de ces communautés.

VI.4. Résilience des écosystèmes hydrothermaux : de nouvelles connaissances essentielles à la mise en place de plans de gestion

Les écosystèmes hydrothermaux sont naturellement sujets à des perturbations de grande envergure liées à l'activité tectonique et volcanique. En effet, depuis la découverte des sources hydrothermales, plusieurs éruptions volcaniques ont été enregistrées, principalement sur des dorsales à expansion rapide (Tunnicliffe et al. 1997 ; Shank et al. 1988 ; Marcus et al. 2009, Gollner et al. 2015). Ces événements extrêmes entraînent une éradication complète des communautés et une modification significative des conditions environnementales à l'échelle locale et offrent des opportunités uniques d'étudier le taux de rétablissement des assemblages de faune (Butterfield et al. 1997 ; Tunnicliffe et al. 1997 ; Shank et al. 1998 ; Nees et al. 2008 ; Gollner et al. 2017). Ces trente dernières années, de nombreuses études ont d'ailleurs contribué à caractériser la dynamique de recolonisation des communautés hydrothermales à la suite d'éruptions volcaniques sur les dorsales est-Pacifique et Juan de Fuca (Tunnicliffe et al. 1997 ; Shank et al. 1998 ; Marcus et al. 2009 ; Mullineaux et al. 2010 ; Gollner et al. 2013, 2015 ; O'Brien et al. 2015). Néanmoins, les divergences méthodologiques et le manque de données relatives aux assemblages de référence sur les différents sites étudiés conduisent à une grande variabilité des taux de rétablissement et rendent délicate toute comparaison (Gollner et al. 2017). Les principaux résultats suggèrent cependant une recolonisation rapide des espèces ingénieures et un bon rétablissement de la diversité et des densités des assemblages au cours des cinq années qui ont suivi les éruptions volcaniques (Tunnicliffe et al. 1997 ; Marcus et al. 2009 ; Gollner et al. 2015). Or, la totalité de ces études ont été réalisées sur des systèmes de dorsales caractérisées par des vitesses d'expansion intermédiaires et rapides (60 - 80 $mm.an^{-1}$) où la nature et la fréquence des perturbations naturelles sont radicalement différentes de celles des dorsales lentes comme la MAR (Baker et German, 2004). De plus, les caractéristiques géologiques et la distance entre les sites hydrothermaux varient fortement en fonction de la vitesse d'expansion du système, conduisant ainsi à d'importantes différences en termes de dispersion larvaire et de

connectivité. Ainsi, les champs hydrothermaux sont beaucoup plus rapprochés au niveau des dorsales rapides (centaine de mètres ; Tolstoy et al. 2006) qu'au niveau des dorsales lentes (plusieurs centaines de kilomètres ; Beaulieu et al. 2015). Plusieurs auteurs ont d'ailleurs émis l'hypothèse que les aptitudes de rétablissement des assemblages de dorsales rapides seraient plus élevées en raison de la forte variabilité naturelle et de l'instabilité des conditions environnementales qu'ils subissent en comparaison aux dorsales lentes (< 50 $mm.an^{-1}$) (Tunnicliffe et al. 1991 ; Boschen et al. 2013 ; Gollner et al. 2015b, 2017 ; Suzuki et al. 2018 ; Smith et al. 2020). À ce jour, la seule étude qui offre des données sur la capacité de recolonisation des assemblages hydrothermaux de systèmes d'expansion lente est basée sur un modèle de dispersion larvaire et montre que le rétablissement nécessiterait plusieurs dizaines d'années avant d'atteindre l'état de référence (Suzuki et al. 2018). Cette étude revêt une importance capitale, car les systèmes d'expansion lente sont caractérisés par de fortes concentrations en dépôts de sulfures polymétalliques (Seafloor Massive Sulfides : SMS) et sont particulièrement ciblés par des activités d'extraction minière à grande échelle (Corliss et al. 1979 ; Spiess et al. 1980 ; Van Dover, 2011 ; Hoagland et al. 2010 ; Hannington et al. 2011). En revanche, cette étude ne permet pas de caractériser la dynamique de recolonisation à l'échelle des assemblages en réponse à une perturbation à grande échelle. Ainsi, c'est dans l'optique de décrire les processus environnementaux et biologiques impliqués dans le rétablissement des assemblages que ce projet de thèse a été construit. Nous sommes conscients que la nature, l'étendue et la persistance de la perturbation induite au cours de notre expérimentation sont incomparables avec les potentiels impacts de l'activité minière à grande échelle. En effet, nous avons pu constater que la recolonisation a été fortement facilitée par la présence d'assemblages matures tout autour des quadrats expérimentaux. Malgré de grandes incertitudes concernant l'étendue des impacts potentiels dans le cadre d'opérations d'extraction minière profonde (Washburn et al. 2019), de nombreux experts s'accordent à dire que la principale menace est la destruction de l'habitat et l'éradication des communautés associées (Van Dover et al. 2007 ; Ramirez-Llodra et al. 2011 ; Levin et al. 2016 ; Van Dover et al. 2017 ; Orcutt et al. 2020). De nombreux impacts indirects sont anticipés incluant la création d'un panache de sédiment qui s'étend au-delà de la zone d'exploitation, une modification de la composition chimique de l'eau, des sédiments et de la circulation océanique ou encore une production sonore et électromagnétique des engins d'extraction (Thiel 2003 ; Halfar et Fujita 2007 ; Coffey Natural Systems 2008 ; Baker et al. 2010 ; Van Dover

2011 ; Ramirez-Llodra et al. 2011 ; Van Dover 2014, Gollner et al 2017). Bien que les sites hydrothermaux inactifs soient préférentiellement ciblés par les compagnies minières (Van Dover et al. 2020), il est impossible d'exclure que certains impacts atteignent les sites actifs (Van Dover et al. 2018). La communauté internationale se mobilise d'ailleurs pour que les sites actifs soient classés comme « sites à protéger » (Van Dover et al. 2018 ; Gollner et al. 2021). Dans ces circonstances, les communautés pourraient être impactées sur plusieurs kilomètres carrés et leur rétablissement nécessiterait le passage par un grand nombre d'étapes. En premier lieu, la création d'un nouvel habitat et la stabilisation des conditions environnementales permettraient d'offrir un substrat et une source d'énergie pour le développement des communautés microbiennes (Marcus et al. 2009). Par la suite, la recolonisation dépendrait du recrutement d'organismes pionniers en provenance de sites éloignés par l'intermédiaire de la dispersion larvaire (Shank et al. 1998 ; Mullineaux et al. 2003, 2012 ; Marcus et al. 2009 ; Gollner et al. 2015, 2017). Enfin, les différentes étapes de la succession écologique impliquant les paramètres abiotiques et les interactions biotiques permettraient d'aboutir à un rétablissement complet des communautés. En définitive, de nombreuses incertitudes demeurent concernant l'étendue des impacts et le temps de rétablissement des communautés perturbées dans le cadre d'opération d'extraction minière à grande échelle, et l'acquisition de données fondamentales sur la dispersion, la dynamique de colonisation et la succession écologique des communautés semble nécessaire pour lever ces zones d'ombre et fournir des données essentielles à l'établissement de mesures de gestion environnementale.

En résumé, en dépit des divergences précédemment évoquées entre l'expérimentation à petite échelle mise en place dans cette thèse et les perturbations naturelles ou anthropiques de grande envergure, ce travail nous a permis de contribuer à l'évaluation de la résilience des écosystèmes hydrothermaux. Concrètement, le suivi de la structure des communautés à la suite d'une perturbation nous a permis d'identifier plusieures espèces de gastéropodes (*P. valvatoides*, *P. mesatlantica*, *L. vitreus* et *X. analoga*) en tant que premiers colonisateurs des assemblages du champ hydrothermal Lucky Strike (Chapitre III). En revanche, la forte proportion d'individus adultes suggère que la recolonisation observée est principalement issue de la migration d'individus depuis les assemblages limitrophes. De plus, l'analyse des traits reproducteurs de certaines de ces espèces, ubiquistes de la partie nord de la dorsale

médio-Atlantique, évoque une forte rétention des larves à l'échelle locale et de faibles aptitudes à la dispersion à grande échelle (Chapitre V). Seule l'espèce ingénieure *Bathymodiolus azoricus* semble présenter des caractéristiques nécessaires à une dispersion à grande échelle (larve planctotrophique et forte fécondité ; Colaço et al. 2006 ; Dixon et al. 2006 ; Vic et al. 2018), mais à ce jour trop peu d'informations sont disponibles pour appréhender le rôle qu'elle pourrait jouer sur le rétablissement des communautés. Cette étude nous a permis de mettre en évidence des lacunes fondamentales sur la temporalité de la colonisation et de la succession écologique des écosystèmes hydrothermaux associés aux dorsales lentes. En l'état des connaissances actuelles, il est donc impossible d'appliquer les principes et les standards préconisés par la Société de Restauration Écologique (SER, 2016) sur ces écosystèmes.

En outre, la résilience des écosystèmes a été définie dans ce travail comme la capacité d'un écosystème à conserver sa structure principale et à assurer les mêmes fonctions en réponse à des changements induits par une perturbation. Ce concept implique deux mécanismes majeurs : la résistance et le rétablissement. L'expérience réalisée durant cette thèse nous a permis d'obtenir des informations sur le rétablissement des communautés, mais ne nous a pas permis d'étudier leur résistance face à une perturbation. À ce jour, peu de données sont disponibles sur la résistance des espèces en réponse à des perturbations en lien avec les activités minières profondes (Nautilus Minerals, 2008 ; Gollner et al. 2017). Il paraît donc primordial de se focaliser sur cet aspect en testant la résistance des communautés à des impacts de natures (bruit, lumière, vibration, ensevelissement, etc.), d'intensité et d'étendue spatio-temporelles différentes afin de mieux appréhender la résilience de ces écosystèmes.

VI.5. Perspectives

Au début de l'expérimentation, des caméras autonomes ont été déployées sur l'ensemble des quadrats afin d'obtenir des séquences vidéo quotidiennes qui nous auraient permis d'acquérir des données sur les interactions biotiques et de suivre la recolonisation des communautés avec une forte résolution temporelle. Malheureusement, en raison de problèmes électroniques inhérents aux conditions extrêmes du milieu, les enregistrements ont cessé rapidement après le déploiement. Les hypothèses mises en avant dans cette thèse sur les premières étapes de la recolonisation pourraient donc être vérifiées avec l'utilisation future

de ce type d'approche. D'autre part, seuls les compartiments de la méga- et macrofaune ont été investigués au cours de ce travail mais l'échantillonnage de la méiofaune a également été réalisé. L'étude de ce compartiment sera complétée et les résultats comparés avec ceux de la faune de plus grande taille. Le déploiement de substrats de colonisation pour les microorganismes (petits blocs de sulfures) a aussi été mené sur chaque quadrat. Les cailloux recueillis après un an de recolonisation ont été broyés et l'ADN microbienne extraite et séquencée, mais les résultats n'ont pas encore été analysés. L'intégration de tous ces compartiments de la diversité (microorganismes + faune de toutes tailles) nous permettra d'obtenir une vision plus holistique des processus de recolonisation et d'ainsi répondre plus précisément aux questions soulevées dans cette thèse.

Les premiers résultats sur la diversité des assemblages en périphérie de Montségur ainsi qu'au sein de l'édifice inactif obtenus par le biais de l'utilisation conjointe des approches morphologiques et moléculaires (collaboration avec Dr Dominique Cowart), ouvrent de nouvelles perspectives quant à la richesse taxonomique qu'ils abritent (Cowart et al. 2020). À ce jour, très peu d'informations sont disponibles sur les communautés qui s'établissent au sein de ces habitats inactifs et leur caractérisation se résume généralement à une description visuelle grâce à des séquences vidéo réalisées par les engins submersibles (Van Dover 2019). Pour pallier la difficulté d'échantillonnage de ces assemblages, le recours à l'utilisation de méthodes moléculaires a permis de mettre en évidence une très forte richesse taxonomique au sein de ces habitats (Cowart et al. 2020). Un important effort dans la caractérisation de l'état de référence des communautés des dépôts massifs de sulfure est nécessaire pour évaluer leur vulnérabilité et mettre en place des actions qui permettront de limiter les impacts et favoriser leur rétablissement (Cuvelier et al. 2018 ; Van Dover 2019 ; Van Dover et al. 2020).

Au-delà de l'évaluation de la dynamique de colonisation à l'échelle locale, l'analyse des traits reproducteurs des espèces dominantes nous a permis d'obtenir des informations fondamentales sur leur capacité de dispersion. À l'échelle de la dorsale médio-Atlantique, deux principales études basées sur l'utilisation de modèles bio-physiques ont permis d'étudier la dispersion larvaire des individus (Breusing et al. 2016 ; Vic et al. 2018). Cependant, ces études se sont limitées à *Bathymodiolus spp.* et n'ont pas permis de résoudre complètement la connectivité entre les différents sites hydrothermaux en raison d'incertitudes sur la durée de vie planctonique et la flottabilité des larves. Il serait intéressant d'approfondir nos

connaissances de la reproduction de l'ensemble des espèces afin de les intégrer aux modèles physiques déjà existants et estimer leur capacité de dispersion et leur aptitude à recoloniser des sites potentiellement impactés.

Enfin, de manière à mieux appréhender le rétablissement des communautés en réponse à des perturbations majeures, qui se rapprochent plus des impacts occasionnés par l'extraction minière, il pourrait être envisageable de conduire une expérience de perturbation à l'échelle d'un édifice entier. Cette approche permettrait de suivre les premières étapes de la reconstruction physique de l'habitat et de stabilisation des facteurs environnementaux. Une fois l'habitat soutenable, l'ensemble du processus de recolonisation des assemblages pourrait être suivi grâce au déploiement d'un module d'observation écologique (module d'observation et de mesures des paramètres abiotiques), comparable à TEMPO (Sarrazin et al. 2007), déjà déployé sur l'édifice Tour Eiffel. Ces observations pourraient être complétées par des échantillonnages réguliers pour obtenir des informations sur l'évolution de la structure des communautés et leur écologie fonctionnelle tout au long du processus de rétablissement.

Bibliographie

A

Adams DK, Arellano SM, Govenar B (2012) Larval dispersal : vent life in the water column. *Oceanography*, *25*:256-268.

Alfaro-Lucas JM, Pradillon F, Zeppilli D, Michel LN, Martinez-Arbizu P, Tanaka H, Foviaux M, Sarrazin J (2020) High environmental stress and productivity increase functional diversity along a deep-sea hydrothermal vent gradient. *Ecology* 101:11

Angeler DG, Allen CR (2016) Quantifying resilience. *J Appl Ecol* 53:617–624.

Arellano SM, Van Gaest AL, Johnson SB, Vrijenhoek RC, Young CM (2014) Larvae from deep-sea methane seeps disperse in surface waters. *Proc R Soc B Biol Sci* 281:2013

B

Bachraty C, Legendre P, Desbruyères D (2009) Biogeographic relationships among deep-sea hydrothermal vent faunas at global scale. *Deep Sea Res Part Oceanogr Res Pap* 56:1371–1378.

Baho D, Allen C, Garmestani A, Fried-Petersen H, Renes S, Gunderson L, Angeler D (2017) A quantitative framework for assessing ecological resilience. *Ecol Soc* 22 (3):1

Baker MC, Ramirez-Llodra EZ, Tyler PA, German CR, Boetius A, Cordes EE, Dubilier N, Fisher CR, Levin LA, Metaxas A, Rowden AA, Santos RS, Shank TM, Dover CLV, Young CM, Warén A (2010) Biogeography, Ecology, and Vulnerability of Chemosynthetic Ecosystems in the Deep Sea. In: *Life in the World's Oceans.* John Wiley & Sons, 161–182

Baldrighi E, Zeppilli D, Crespin R, Chauvaud P, Pradillon F, Sarrazin J (2018) Colonisation of synthetic sponges at the deep-sea Lucky Strike hydrothermal vent field (Mid-Atlantic Ridge): a first insight. *Mar Biodivers* 48:89–103.

Balvanera P, Pfisterer AB, Buchmann N, He J-S, Nakashizuka T, Raffaelli D, Schmid B (2006) Quantifying the evidence for biodiversity effects on ecosystem functioning and services. *Ecol Lett* 9:1146–1156.

Barreyre T, Escartín J, Sohn RA, Cannat M, Ballu V, Crawford WC (2014) Temporal variability and tidal modulation of hydrothermal exit-fluid temperatures at the Lucky Strike deep-sea vent field, Mid-Atlantic Ridge. *J Geophys Res Solid Earth* 119:2543–2566.

Bates AE, Lee RW, Tunnicliffe V, Lamare MD (2010) Deep-sea hydrothermal vent animals seek cool fluids in a highly variable thermal environment. *Nat Commun* 1:14.

Bayer SR, Mullineaux LS, Waller RG, Solow AR (2011) Reproductive traits of pioneer gastropod species colonising deep-sea hydrothermal vents after an eruption. *Mar Biol* 158:181–192.

Bearhop S, Adams CE, Waldron S, Fuller RA, MacLeod H (2004) Determining trophic niche width: a novel approach using stable isotope analysis. *J Anim Ecol* 73:1007–1012.

Beaulieu SE, Szafrański KM (2020) InterRidge Global Database of Active Submarine Hydrothermal Vent Fields Version 3.4. http://vents-data.interridge.org.

Beaulieu SE, Mullineaux LS, Adams DK, Mills SW (2009) Comparison of a sediment trap and plankton pump for time-series sampling of larvae near deep-sea hydrothermal vents. *Limnol Oceanogr Methods* 7:235–248.

Beedessee G, Watanabe H, Ogura T, Nemoto S, Yahagi T, Nakagawa S, Nakamura K, Takai K, Koonjul M, Marie DEP (2013) High Connectivity of Animal Populations in Deep-Sea Hydrothermal Vent Fields in the Central Indian Ridge Relevant to Its Geological Setting. *PLOS ONE* 8:22–37.

Bellec L, Cambon-Bonavita M-A, Cueff-Gauchard V, Durand L, Gayet N, Zeppilli D (2018) A Nematode of the Mid-Atlantic Ridge Hydrothermal Vents Harbors a Possible Symbiotic Relationship. *Front Microbiol* 9:2246.

Bemis K, Lowell RP, Farough A (2012) Diffuse Flow: On and Around Hydrothermal Vents at Mid-Ocean Ridges. *Oceanography* 25:182–191.

Berg CJ, (1985) Reproductive strategies of mollusks from abyssal hydrothermal vent communities. *Bulletin of the biological society of Washington*. 6:185-197.

Bergquist DC, Eckner JT, Urcuyo IA, Cordes EE, Hourdez S, Macko SA, Fisher CR (2007) Using stable isotopes and quantitative community characteristics to determine a local hydrothermal vent food web. *Mar Ecol Prog Ser* 330:49–65.

Blake JA, Maciolek NJ, Ota AY, Williams IP (2009) Long-term benthic infaunal monitoring at a deep-ocean dredged material disposal site off Northern California. *Deep Sea Res Part II.* 56:1775–1803.

Boschen RE, Rowden AA, Clark MR, Gardner JPA (2013) Mining of deep-sea seafloor massive sulfides: A review of the deposits, their benthic communities, impacts from mining, regulatory frameworks and management strategies. *Ocean Coast Manag* 84:54–67.

Boschen RE, Rowden AA, Clark MR, Pallentin A, Gardner JPA (2016) Seafloor massive sulfide deposits support unique megafaunal assemblages: Implications for seabed mining and conservation. *Mar Environ Res* 115:78–88.

Breusing C, Biastoch A, Drews A, Metaxas A, Jollivet D, Vrijenhoek RC, Bayer T, Melzner F, Sayavedra L, Petersen JM, Dubilier N, Schilhabel MB, Rosenstiel P, Reusch TBH (2016) Biophysical and Population Genetic Models Predict the Presence of “Phantom” Stepping Stones Connecting Mid-Atlantic Ridge Vent Ecosystems. *Curr Biol* 26:2257–2267.

Butterfield DA, Jonasson IR, Massoth GJ, Feely RA, Roe KK, Embley RE, Holden JF, McDuff RE, Lilley MD, Delaney JR (1997) Seafloor eruptions and evolution of hydrothermal fluid chemistry. *Philos Trans R Soc Lond Ser Math Phys Eng Sci* 355:369–386.

C

Cannat M, Lagabrielle Y, Bougault H, Casey J, de Coutures N, Dmitriev L, Fouquet Y (1997) Ultramafic and gabbroic exposures at the Mid-Atlantic Ridge: geological mapping in the 15°N region. *Tectonophysics* 279:193–213.

Cardinale BJ, Duffy JE, Gonzalez A, Hooper DU, Perrings C, Venail P, Narwani A, Mace GM, Tilman D, Wardle DA, Kinzig AP, Daily GC, Loreau M, Grace JB, Larigauderie A, Srivastava DS, Naeem S (2012) Biodiversity

loss and its impact on humanity. *Nature* 486:59–67.

Carpenter S, Cottingham K (1997) Resilience and Restoration of Lakes. *Conserv Ecol*. 1

Carpenter S, Walker B, Anderies JM, Abel N (2001) From Metaphor to Measurement: Resilience of What to What? *Ecosystems* 4:765–781.

Chambers JC, Allen CR, Cushman SA (2019) Operationalizing Ecological Resilience Concepts for Managing Species and Ecosystems at Risk. *Front Ecol Evol* 7:241

Childress JJ, Fisher CR (1992) The biology of hydrothermal vent animals: physiology, biochemistry, and autotrophic symbioses. *Oceanography and Marine Biology 30:*337–441.

Childress JJ, Fisher CR, Brooks JM, Kennicutt MC, Bidigare R, Anderson AE (1986) A methanotrophic marine molluscan (bivalvia, mytilidae) symbiosis: mussels fueled by gas. *Science* 233:1306–1308.

Colaço A, Martins I, Laranjo M, Pires L, Leal C, Prieto C, Costa V, Lopes H, Rosa D, Dando PR, Serrão-Santos R (2006) Annual spawning of the hydrothermal vent mussel, Bathymodiolus azoricus, under controlled aquarium, conditions at atmospheric pressure. *J Exp Mar Biol Ecol* 333:166–171.

Comtet T, Desbruyères D (1998) Population structure and recruitment in mytilid bivalves from the Lucky Strike and Menez Gwen hydrothermal vent fields (37°17\'N and 37°50\'N on the Mid-Atlantic Ridge). *Mar Ecol Prog Ser* 163:165–177.

Connell SD, Ghedini G (2015) Resisting regime-shifts: the stabilising effect of compensatory processes. *Trends Ecol Evol* 30:513–515.

Connell SD, Nimmo DG, Ghedini G, Mac Nally R, Bennett AF (2016) Ecological Resistance – Why Mechanisms Matter: A Reply to Sundstrom et al. *Trends Ecol Evol* 31:413–414.

Corliss JB, Dymond J, Gordon LI, Edmond JM, Herzen RP von, Ballard RD, Green K, Williams D, Bainbridge A, Crane K, Andel TH van (1979) Submarine Thermal Springs on the Galápagos Rift. *Science* 203:1073–1083.

Côté IM, Darling ES (2010) Rethinking Ecosystem Resilience in the Face of Climate Change. *PLOS Biol* 8:121.

Courant V. M2 Université de Bordeaux, dérigé par Marjolaine matabos et Jozée Sarrazin. Dynamique temporelle et comportements des assemblages associés à Bathymodiolus azoricus au sein de l'édifice Tour Eiffel, Lucky Strike, MAR

Cowart DA, Matabos M, Brandt MI, Marticorena J, Sarrazin J (2020) Exploring Environmental DNA (eDNA) to Assess Biodiversity of Hard Substratum Faunal Communities on the Lucky Strike Vent Field (Mid-Atlantic Ridge) and Investigate Recolonisation Dynamics After an Induced Disturbance. *Front Mar Sci* 6:783.

Cowen RK, Sponaugle S (2009) Larval Dispersal and Marine Population Connectivity. *Annu Rev Mar Sci* 1:443–466.

Cucherousset J, Villéger S (2015) Quantifying the multiple facets of isotopic diversity: New metrics for stable isotope ecology. *Ecol Indic* 56:152–160.

Cuvelier D, Sarrazin J, Colaço A, Copley J, Desbruyères D, Glover AG, Tyler P, Serrão Santos R (2009) Distribution and spatial variation of hydrothermal faunal assemblages at Lucky Strike (Mid-Atlantic Ridge) revealed by high-resolution video image analysis. *Deep Sea Res Part Oceanogr Res Pap* 56:2026–2040.

Cuvelier D, Sarradin P-M, Sarrazin J, Colaço A, Copley JT, Desbruyères D, Glover AG, Santos RS, Tyler PA (2011) Hydrothermal faunal assemblages and habitat characterisation at the Eiffel Tower edifice (Lucky Strike, Mid-Atlantic Ridge). *Mar Ecol* 32:243–255.

Cuvelier D, Beesau J, Ivanenko VN, Zeppilli D, Sarradin P-M, Sarrazin J (2014) First insights into macro- and meiofaunal colonisation patterns on paired wood/slate substrata at Atlantic deep-sea hydrothermal vents. *Deep Sea Res Part Oceanogr Res Pap* 87:70–81.

D

Dattagupta S, Martin J, Liao S, Carney RS, Fisher CR (2007) Deep-sea hydrocarbon seep gastropod Bathynerita naticoidea responds to cues from the habitat-providing mussel Bathymodiolus childressi. *Mar Ecol* 28:193–198.

De Busserolles F, Sarrazin J, Gauthier O, Gélinas Y, Fabri MC, Sarradin PM, Desbruyères D (2009) Are spatial variations in the diets of hydrothermal fauna linked to local environmental conditions? *Deep Sea Res Part II Top Stud Oceanogr* 56:1649–1664.

Desbruyères D, Biscoito M, Caprais J-C, Colaço A, Comtet T, Crassous P, Fouquet Y, Khripounoff A, Le Bris N, Olu K, Riso R, Sarradin P-M, Segonzac M, Vangriesheim A (2001) Variations in deep-sea hydrothermal vent communities on the Mid-Atlantic Ridge near the Azores plateau. *Deep Sea Res Part Oceanogr Res Pap* 48:1325–1346.

Desjardins E, Barker G, Lindo Z, Dieleman C, Dussault AC (2015) Promoting resilience. Q *Rev Biol* 90:147–165.

Dick GJ (2019) The microbiomes of deep-sea hydrothermal vents: distributed globally, shaped locally. *Nat Rev Microbiol* 17:271–283.

Dixon DR, Lowe DM, Miller PI, Villemin GR, Colaço A, Serrão-Santos R, Dixon LRJ (2006) Evidence of seasonal reproduction in the Atlantic vent mussel Bathymodiolus azoricus, and an apparent link with the timing of photosynthetic primary production. *J Mar Biol Assoc U K* 86:1363–1371.

Druffel ER, Lalou C, Thompson G, Arnold M, Brichet E, Druffel E, Rona PA (1990) Geochronology of TAG and Snakepit hydrothermal fields, Mid-Atlantic Ridge: witness to a long, complex hydrothermal history. *Earth Planet Sci Lett* 97:113–128.

Du Preez C, Fisher CR (2018) Long-Term Stability of Back-Arc Basin Hydrothermal Vents. *Front Mar Sci* 5:54

Dubilier N, Bergin C, Lott C (2008) Symbiotic diversity in marine animals: the art of harnessing chemosynthesis. *Nat Rev Microbiol* 6:725–740.

E

Eckelbarger KJ, Eckelbarger KJ (1994) Diversity Of Metazoan Ovaries And Vitellogenic Mechanisms - Implications For Life history Theory. *Proc Biol Soc Wash* 107:193–218.

Eckelbarger KJ, Watling L (1995) Role of Phylogenetic Constraints in Determining Reproductive Patterns in Deep-Sea Invertebrates. *Invertebr Biol* 114:256–269.

Edwards KJ, Bach W, McCollom TM, Rogers DR (2004) Neutrophilic Iron-Oxidizing Bacteria in the Ocean: Their Habitats, Diversity, and Roles in Mineral Deposition, Rock Alteration, and Biomass Production in the Deep-Sea. *Geomicrobiol J* 21:393–404.

Elmqvist T, Folke C, Nyström M, Peterson G, Bengtsson J, Walker B, Norberg J (2003) Response diversity, ecosystem change, and resilience. *Front Ecol Environ* 1:488–494

F

Fisher C, Takai K, Le Bris N (2007) Hydrothermal Vent Ecosystems. *Oceanography* 20:14–23.

Flynn DFB, Gogol-Prokurat M, Nogeire T, Molinari N, Richers BT, Lin BB, Simpson N, Mayfield MM, DeClerck F (2009) Loss of functional diversity under land use intensification across multiple taxa. *Ecol Lett* 12:22–33.

Folke C, Carpenter S, Walker B, Scheffer M, Elmqvist T, Gunderson L, Holling CS (2004) Regime Shifts, Resilience, and Biodiversity in Ecosystem Management. *Annu Rev Ecol Evol Syst* 35:557–581.

Folke C, Carpenter S, Walker B, Scheffer M, Chapin T, Rockström J (2010) Resilience Thinking: Integrating Resilience, Adaptability and Transformability. *Ecol Soc* 15:4

G

Gagic V, Bartomeus I, Jonsson T, Taylor A, Winqvist C, Fischer C, Slade EM, Steffan-Dewenter I, Emmerson M, Potts SG, Tscharntke T, Weisser W, Bommarco R (2015) Functional identity and diversity of animals predict ecosystem functioning better than species-based indices. *Proc R Soc B Biol Sci* 282:2014

Gauthier O, Sarrazin J, Desbruyères D (2010) Measure and mis-measure of species diversity in deep-sea chemosynthetic communities. *Mar Ecol Prog Ser* 402:285–302.

German CR, Parson LM (1998) Distributions of hydrothermal activity along the Mid-Atlantic Ridge: interplay of magmatic and tectonic controls. *Earth Planet Sci Lett* 160:327–341.

Giere O (2008) Meiobenthology: the microscopic motile fauna of aquatic sediments. *Springer Science & Business Media*

Gladstone-Gallagher RV, Pilditch CA, Stephenson F, Thrush SF (2019) Linking Traits across Ecological Scales Determines Functional Resilience. *Trends Ecol Evol* 34:1080–1091.

Glasby GP (2000) Lessons Learned from Deep-Sea Mining. *Science* 289:551–553.

Glover AG, Smith CR (2003) The deep-sea floor ecosystem: current status and prospects of anthropogenic change by the year 2025. *Environ Conserv* 30:219–241.

Gollner S, Miljutina M, Bright M (2013) Nematode succession at deep-sea hydrothermal vents after a recent volcanic eruption with the description of two dominant species. *Org Divers Evol* 13:349–371.

Gollner S, Govenar B, Arbizu PM, Mills S, Le Bris N, Weinbauer M, Shank TM, Bright M (2015a) Differences in recovery between deep-sea hydrothermal vent and vent-proximate communities after a volcanic eruption. *Deep Sea Res Part Oceanogr Res Pap* 106:167–182.

Gollner S, Govenar B, Arbizu PM, Mills S, Le Bris N, Weinbauer M, Shank TM, Bright M (2015b) Differences in recovery between deep-sea hydrothermal vent and vent-proximate communities after a volcanic

eruption. *Deep Sea Res Part Oceanogr Res Pap* 106:167–182.

Gollner S, Govenar B, Fisher CR, Bright M (2015c) Size matters at deep-sea hydrothermal vents: different diversity and habitat fidelity patterns of meio- and macrofauna. *Mar Ecol Prog Ser* 520:57–66.

Gollner S, Kaiser S, Menzel L, Jones DOB, Brown A, Mestre NC, van Oevelen D, Menot L, Colaço A, Canals M, Cuvelier D, Durden JM, Gebruk A, Egho GA, Haeckel M, Marcon Y, Mevenkamp L, Morato T, Pham CK, Purser A, Sanchez-Vidal A, Vanreusel A, Vink A, Martinez Arbizu P (2017) Resilience of benthic deep-sea fauna to mining activities. *Mar Environ Res* 129:76–101.

Govenar B (2010) Shaping Vent and Seep Communities: Habitat Provision and Modification by Foundation Species. In: Kiel S (ed) The Vent and Seep Biota: Aspects from Microbes to Ecosystems. *Springer Netherlands, Dordrecht,* 403–432

Govenar B, Fisher CR (2007) Experimental evidence of habitat provision by aggregations of Riftia pachyptila at hydrothermal vents on the East Pacific Rise. *Mar Ecol* 28:3–14.

Govenar B, Le Bris N, Gollner S, Glanville J, Aperghis AB, Hourdez S, Fisher CR (2005) Epifaunal community structure associated with Riftia pachyptila aggregations in chemically different hydrothermal vent habitats. *Mar Ecol Prog Ser* 305:67–77.

Gunderson LH (2000) Ecological Resilience--In Theory and Application. *Annu Rev Ecol Syst* 31:425–439.

Gustafson RG, Littlewood DTJ, Lutz RA (1991) Gastropod Egg Capsules and Their Contents From Deep-Sea Hydrothermal Vent Environments. *Biol Bull* 180:34–55.

H

Halfar J, Fujita RM (2007) Danger of Deep-Sea Mining. *Science* 316:987–987.

Hannington MD, Jonasson IR, Herzig PM, Petersen S (1995) Physical and Chemical Processes of Seafloor Mineralization at Mid-Ocean Ridges. In: Seafloor Hydrothermal Systems: Physical, Chemical, Biological, and Geological Interactions. *American Geophysical Union (AGU)* 115–157

Hein JR, Mizell K, Koschinsky A, Conrad TA (2013) Deep-ocean mineral deposits as a source of critical metals for high- and green-technology applications: Comparison with land-based resources. *Ore Geol Rev* 51:1–14.

Hilario A (2005) Reproductive ecology of Vestimentifera (Polychaeta: Siboglinidae) from hydrothermal vents and cold seeps. Phd, *University of Southampton*

Hodgson D, McDonald JL, Hosken DJ (2015) What do you mean, 'resilient'? *Trends Ecol Evol* 30:503–506.

Hodgson D, McDonald JL, Hosken DJ (2016) Resilience Is Complicated, but Comparable: A Reply to Yeung and Richardson. *Trends Ecol Evol* 31:3–4.

Holling CS (1973) Resilience and Stability of Ecological Systems. *Annu Rev Ecol* Syst 4:1–23.

Holling CS (1996) Engineering resilience versus ecological resilience. *Eng Ecol Constraints* 31:32.

Hooper DU, Chapin FS, Ewel JJ, Hector A, Inchausti P, Lavorel S, Lawton JH, Lodge DM, Loreau M, Naeem S, Schmid B, Setälä H, Symstad AJ, Vandermeer J, Wardle DA (2005) Effects of Biodiversity on Ecosystem Functioning: A Consensus of Current Knowledge. *Ecol Monogr* 75:3–35.

Hourdez S, Lallier FH (2006) Adaptations to hypoxia in hydrothermal-vent and cold-seep invertebrates. *Rev Environ Sci Biotechnol* 6:143–159.

Hunt HL, Metaxas A, Jennings RM, Halanych KM, Mullineaux LS (2004) Testing biological control of colonisation by vestimentiferan tubeworms at deep-sea hydrothermal vents (East Pacific Rise, 9°50'N). Deep Sea Res Part Oceanogr Res Pap 51:225–234.

Hurtado LA, Lutz RA, Vrijenhoek RC (2004) Distinct patterns of genetic differentiation among annelids of eastern Pacific hydrothermal vents. Mol Ecol 13:2603–2615.

Husson B, Sarradin P-M, Zeppilli D, Sarrazin J (2017) Picturing thermal niches and biomass of hydrothermal vent species. Deep Sea Res Part II Top Stud Oceanogr 137:6–25.

I

Ingrisch J, Bahn M (2018) Towards a Comparable Quantification of Resilience. Trends Ecol Evol 33:251–259.

J

Jackson AL, Inger R, Parnell AC, Bearhop S (2011) Comparing isotopic niche widths among and within communities: SIBER – Stable Isotope Bayesian Ellipses in R. J Anim Ecol 80:595–602.

Jannasch HW (1985) Review Lecture - The chemosynthetic support of life and the microbial diversity at deep-sea hydrothermal vents. *Proc R Soc Lond B Biol Sci* 225:277–297.

Johnson KS, Childress JJ, Beehler CL (1988) Short-term temperature variability in the Rose Garden hydrothermal vent field: an unstable deep-sea environment. *Deep Sea Res Part Oceanogr Res Pap* 35:1711–1721.

Jollivet D, Chevaldonne P, Planque B (1999) Hydrothermal-Vent Alvinellid Polychaete Dispersal in the Eastern Pacific. 2. a Metapopulation Model Based on Habitat Shifts. *Evolution* 53:1128–1142.

K

Karson JA, Thompson G, Humphris SE, Edmond JM, Bryan WB, Brown JR, Winters AT, Pockalny RA, Casey JF, Campbell AC, Klinkhammer G, Palmer MR, Kinzler RJ, Sulanowska MM (1987) Along-axis variations in seafloor spreading in the MARK area. *Nature* 328:681–685.

Karson JA, Kelley DS, Fornari DJ, Perfit MR, Shank TM (2015) Discovering the Deep: A Photographic Atlas of the Seafloor and Ocean Crust. *Cambridge University Press*

Kelley DS, Baross JA, Delaney JR (2002) Volcanoes, Fluids, and Life at Mid-Ocean Ridge Spreading Centers. *Annu Rev Earth Planet Sci* 30:385–491.

Kelly N, Metaxas A, Butterfield D (2007) Spatial and temporal patterns of colonisation by deep-sea hydrothermal vent invertebrates on the Juan de Fuca Ridge, NE Pacific. *Aquat Biol* 1:1–16.

Kelly NE, Metaxas A (2007) Influence of habitat on the reproductive biology of the deep-sea hydrothermal vent limpet Lepetodrilus fucensis (Vetigastropoda: Mollusca) from the Northeast Pacific. *Mar Biol* 151:649–662.

Khripounoff A, Vangriesheim A, Crassous P, Segonzac M, Lafon V, Warén A (2008) Temporal variation of currents, particulate

flux and organism supply at two deep-sea hydrothermal fields of the Azores Triple Junction. *Deep Sea Res Part Oceanogr Res Pap* 55:532–551.

L

Laliberté E, Wells JA, DeClerck F, Metcalfe DJ, Catterall CP, Queiroz C, Aubin I, Bonser SP, Ding Y, Fraterrigo JM, McNamara S, Morgan JW, Merlos DS, Vesk PA, Mayfield MM (2010) Land-use intensification reduces functional redundancy and response diversity in plant communities. *Ecol Lett* 13:76–86

Lalou C, Reyss J-L, Brichet E, Arnold M, Thompson G, Fouquet Y, Rona PA (1993) New age data for Mid-Atlantic Ridge hydrothermal sites: TAG and Snakepit chronology revisited. *J Geophys Res Solid Earth* 98:9705–9713.

Laming SR, Gaudron SM, Duperron S (2018) Lifecycle Ecology of Deep-Sea Chemosymbiotic Mussels: A Review. *Front Mar Sci* 5:282

Langmuir C, Humphris S, Fornari D, Van Dover C, Von Damm K, Tivey MK, Colodner D, Charlou J-L, Desonie D, Wilson C, Fouquet Y, Klinkhammer G, Bougault H (1997) Hydrothermal vents near a mantle hot spot: the Lucky Strike vent field at 37°N on the Mid-Atlantic Ridge. *Earth Planet Sci Lett* 148:69–91.

Laurent S, Pfeifer SP, Settles ML, Hunter SS, Hardwick KM, Ormond L, Sousa VC, Jensen JD, Rosenblum EB (2016) The population genomics of rapid adaptation: disentangling signatures of selection and demography in white sands lizards. *Mol Ecol* 25:306–323.

Layman CA, Arrington DA, Montaña CG, Post DM (2007) Can Stable Isotope Ratios Provide for Community-Wide Measures of Trophic Structure? *Ecology* 88:42–48.

Le Bris N, Gaill F (2006) How does the annelid Alvinella pompejana deal with an extreme hydrothermal environment? *Rev Environ Sci Biotechnol* 6:197.

Lelièvre Y, Sarrazin J, Marticorena J, Schaal G, Day T, Legendre P, Hourdez S, Matabos M (2018) Biodiversity and trophic ecology of hydrothermal vent fauna associated with tubeworm assemblages on the Juan de Fuca Ridge. *Biogeosciences* 15:2629–2647.

Lenihan HS, Mills SW, Mullineaux LS, Peterson CH, Fisher CR, Micheli F (2008) Biotic interactions at hydrothermal vents: Recruitment inhibition by the mussel Bathymodiolus thermophilus. *Deep Sea Res Part Oceanogr Res Pap* 55:1707–1717.

Levesque C, Juniper SK, Marcus J (2003) Food resource partitioning and competition among alvinellid polychaetes of Juan de Fuca Ridge hydrothermal vents. *Mar Ecol Prog Ser* 246:173–182.

Levesque C, Kim Juniper S, Limén H (2006) Spatial organization of food webs along habitat gradients at deep-sea hydrothermal vents on Axial Volcano, Northeast Pacific. *Deep Sea Res Part Oceanogr Res Pap* 53:726–739.

Levin LA, Mendoza GF, Konotchick T, Lee R (2009) Macrobenthos community structure and trophic relationships within active and inactive Pacific hydrothermal sediments. *Deep Sea Res Part II Top Stud Oceanogr* 56:1632–1648.

Levin LA, Mengerink K, Gjerde KM, Rowden AA, Van Dover CL, Clark MR, Ramirez-Llodra E, Currie B, Smith CR, Sato KN, Gallo N, Sweetman AK, Lily H, Armstrong CW, Brider J (2016a) Defining “serious harm” to the

marine environment in the context of deep-seabed mining. *Mar Policy* 74:245–259.

Levin LA, Baco AR, Bowden DA, Colaco A, Cordes EE, Cunha MR, Demopoulos AWJ, Gobin J, Grupe BM, Le J, Metaxas A, Netburn AN, Rouse GW, Thurber AR, Tunnicliffe V, Van Dover CL, Vanreusel A, Watling L (2016b) Hydrothermal Vents and Methane Seeps: Rethinking the Sphere of Influence. *Front Mar Sci 3:72*

Lilley MD, Feely RA, Trefry JH (1995) Chemical and Biochemical Transformations in Hydrothermal Plumes. In: Seafloor Hydrothermal Systems: Physical, Chemical, Biological, and Geological Interactions. *American Geophysical Union (AGU)* 369–391

Llodra ER, Tyler PA, Copley JTP (2000) Reproductive biology of three caridean shrimp, Rimicaris exoculata, Chorocaris chacei and Mirocaris fortunata (Caridea: Decapoda), from hydrothermal vents. *J Mar Biol Assoc U K* 80:473–484.

Lonsdale P (1977) Clustering of suspension-feeding macrobenthos near abyssal hydrothermal vents at oceanic spreading centers. *Deep Sea Res* 24:857–863.

Lotze HK, Coll M, Magera AM, Ward-Paige C, Airoldi L (2011) Recovery of marine animal populations and ecosystems. *Trends Ecol Evol* 26:595–605.

Lowe WH, Allendorf FW (2010) What can genetics tell us about population connectivity? *Mol Ecol* 19:3038–3051.

Luther GW, Rozan TF, Taillefert M, Nuzzio DB, Di Meo C, Shank TM, Lutz RA, Cary SC (2001) Chemical speciation drives hydrothermal vent ecology. *Nature* 410:813–816.

M

Marcus J, Tunnicliffe V (2002) Living on the edges of diffuse vents on the Juan de Fuca Ridge. *Cah Biol Mar* 43:263–266.

Marcus J, Tunnicliffe V, Butterfield DA (2009) Post-eruption succession of macrofaunal communities at diffuse flow hydrothermal vents on Axial Volcano, Juan de Fuca Ridge, Northeast Pacific. *Deep Sea Res Part II Top Stud Oceanogr* 56:1586–1598.

Margolis SV, Burns RG (1976) Pacific Deep-Sea Manganese Nodules: Their Distribution, Composition, and Origin. *Annu Rev Earth Planet Sci* 4:229–263.

Marsh AG, Mullineaux LS, Young CM, Manahan DT (2001) Larval dispersal potential of the tubeworm Riftia pachyptila at deep-sea hydrothermal vents. *Nature* 411:77–80.

Martell KA, Tunnicliffe V, Macdonald IR (2002) Biological features of a buccinid whelk (Gastropoda, Neogastropoda) at the endeavour ventfields of juan de fuca ridge, northeast pacific. *J Molluscan Stud* 68:45–53.

Marticorena J, Matabos M, Sarrazin J, Ramirez-Llodra E (2020) Contrasting reproductive biology of two hydrothermal gastropods from the Mid-Atlantic Ridge: implications for resilience of vent communities. *Mar Biol* 167:109.

Mat AM, Sarrazin J, Markov GV, Apremont V, Dubreuil C, Eché C, Fabioux C, Klopp C, Sarradin P-M, Tanguy A, Huvet A, Matabos M (2020) Biological rhythms in the deep-sea hydrothermal mussel Bathymodiolus azoricus. *Nat Commun* 11:3454.

Matabos M, Bris NL, Pendlebury S, Thiébaut E (2008) Role of physico-chemical environment on gastropod assemblages at

hydrothermal vents on the East Pacific Rise (13°N/EPR). *J Mar Biol Assoc U K* 88:995–1008.

McClanahan TR, Donner SD, Maynard JA, MacNeil MA, Graham NAJ, Maina J, Baker AC, I JBA, Beger M, Campbell SJ, Darling ES, Eakin CM, Heron SF, Jupiter SD, Lundquist CJ, McLeod E, Mumby PJ, Paddack MJ, Selig ER, Woesik R van (2012) Prioritizing Key Resilience Indicators to Support Coral Reef Management in a Changing Climate. *PLOS ONE* 7:e42884.

McMullin ER, Bergquist DC, Fisher CR (2000) Metazoans in extreme environments: adaptations of hydrothermal vent and hydrocarbon seep fauna. Gravitational Space *Biol Bull Publ Am Soc Gravitational Space Biol* 13:13–23.

Metaxas A (2004) Spatial and temporal patterns in larval supply at hydrothermal vents in the northeast Pacific Ocean. *Limnol Oceanogr* 49:1949–1956.

Metaxas A (2011) Spatial patterns of larval abundance at hydrothermal vents on seamounts: evidence for recruitment limitation. *Mar Ecol Prog Ser* 437:103–117.

Metaxas A, Saunders M (2009) Quantifying the “Bio-” Components in Biophysical Models of Larval Transport in Marine Benthic Invertebrates: Advances and Pitfalls. *Biol Bull* 216:257–272.

Micheli F, Halpern BS (2005) Low functional redundancy in coastal marine assemblages. *Ecol Lett* 8:391–400.

Micheli F, Peterson CH, Mullineaux LS, Fisher CR, Mills SW, Sancho G, Johnson GA, Lenihan HS (2002) Predation Structures Communities at Deep-Sea Hydrothermal Vents. *Ecol Monogr* 72:365–382.

Mittelstaedt E, Escartín J, Gracias N, Olive J-A, Barreyre T, Davaille A, Cannat M, Garcia R (2012) Quantifying diffuse and discrete venting at the Tour Eiffel vent site, Lucky Strike hydrothermal field. *Geochem Geophys Geosystems* 13:4

Moalic Y, Desbruyères D, Duarte CM, Rozenfeld AF, Bachraty C, Arnaud-Haond S (2012) Biogeography revisited with network theory: retracing the history of hydrothermal vent communities. *Syst Biol* 61:127–137.

Montagna PA, Baguley JG, Hsiang C-Y, Reuscher MG (2017) Comparison of sampling methods for deep-sea infauna. *Limnol Oceanogr Methods* 15:166–183.

Mori AS, Furukawa T, Sasaki T (2013) Response diversity determines the resilience of ecosystems to environmental change. *Biol Rev* 88:349–364.

Mouillot D, Graham NAJ, Villéger S, Mason NWH, Bellwood DR (2013) A functional approach reveals community responses to disturbances. *Trends Ecol Evol* 28:167–177.

Mullineaux LS, Fisher CR, Peterson CH, Schaeffer SW (2000) Tubeworm succession at hydrothermal vents: use of biogenic cues to reduce habitat selection error? *Oecologia* 123:275–284.

Mullineaux LS, Peterson CH, Micheli F, Mills SW (2003) Successional Mechanism Varies Along a Gradient in Hydrothermal Fluid Flux at Deep-Sea Vents. *Ecol Monogr* 73:523–542.

Mullineaux LS, Mills SW, Sweetman AK, Beaudreau AH, Metaxas A, Hunt HL (2005) Vertical, lateral and temporal structure in larval distributions at hydrothermal vents. *Mar Ecol Prog Ser* 293:1–16.

Mullineaux LS, Metaxas A, Beaulieu SE, Bright M, Gollner S, Grupe BM, Herrera S, Kellner JB, Levin LA, Mitarai S, Neubert MG, Thurnherr AM, Tunnicliffe V, Watanabe HK,

Won Y-J (2018) Exploring the Ecology of Deep-Sea Hydrothermal Vents in a Metacommunity Framework. *Front Mar Sci* 5:49

N

Nakagawa S, Takai K (2008) Deep-sea vent chemoautotrophs: diversity, biochemistry and ecological significance. *FEMS Microbiol Ecol* 65:1–14.

Nautilus Minerals, N.L., 2008. Main Report. Environmental Impact Statement: Solwara 1 Project, 1:226

Nedoncelle K, Lartaud F, de Rafelis M, Boulila S, Le Bris N (2013) A new method for high-resolution bivalve growth rate studies in hydrothermal environments. *Mar Biol* 160:1427–1439.

Nees HA, Moore TS, Mullaugh KM, Holyoke RR, Janzen CP, Ma S, Metzger E, Waite TJ, Yucel M, Lutz RA, Shank TM, Vetriani C, Nuzzio DB, Luther GW (2008) Hydrothermal vent mussel habitat chemistry, pre- and post-eruption at 9°50'North on the East Pacific Rise. *Journal of Shellfish Research* 27: 169-175.

Neubert MG, Mullineaux LS, Hill MF (2006) CHAPTER 9 - A Metapopulation Approach to Interpreting Diversity at Deep-Sea Hydrothermal Vents. In: Kritzer JP, Sale PF (eds) Marine Metapopulations. *Academic Press, Burlington.* 321–350

O

O'Brien KR, Waycott M, Maxwell P, Kendrick GA, Udy JW, Ferguson AJP, Kilminster K, Scanes P, McKenzie LJ, McMahon K, Adams MP, Samper-Villarreal J, Collier C, Lyons M, Mumby PJ, Radke L, Christianen MJA, Dennison WC (2018) Seagrass ecosystem trajectory depends on the relative timescales of resistance, recovery and disturbance. *Mar Pollut Bull* 134:166–176.

Oksanen J, Blanchet FG, Friendly M, Kindt R, Legendre P, McGlinn D, Minchin PR, O'Hara RB, Simpson GL, Solymos P, Stevens MHH, Szoecs E, Wagner H (2019) vegan: Community Ecology Package.

Oliver TH, Heard MS, Isaac NJB, Roy DB, Procter D, Eigenbrod F, Freckleton R, Hector A, Orme CDL, Petchey OL, Proença V, Raffaelli D, Blake Suttle K, Mace GM, Martín-López B, Woodcock BA, Bullock JM (2016) A Synthesis is Emerging between Biodiversity–Ecosystem Function and Ecological Resilience Research: Reply to Mori. *Trends Ecol Evol* 31:89–92.

Ondreas H, Cannat M, Fouquet Y, Normand A, Sarradin P, Sarrazin J (2009) Recent volcanic events and the distribution of hydrothermal venting at the Lucky Strike hydrothermal field, Mid-Atlantic Ridge. *Geochem Geophys Geosystems* 10

O'Neill RV, Deangelis DL, Waide JB, Allen TFH, Allen GE (1986) A Hierarchical Concept of Ecosystems. *Princeton University Press* 23

Orcutt BN, Bradley JA, Brazelton WJ, Estes ER, Goordial JM, Huber JA, Jones RM, Mahmoudi N, Marlow JJ, Murdock S, Pachiadaki M (2020) Impacts of deep-sea mining on microbial ecosystem services. *Limnol Oceanogr* 65:1489-1510.

P

Perfit MR, Chadwick WW (1998) Magmatism at Mid-Ocean Ridges: Constraints from Volcanological and Geochemical Investigations. In: Faulting and Magmatism at Mid-Ocean Ridges. *American Geophysical Union (AGU)*, 59–115

Petersen JM, Zielinski FU, Pape T, Seifert R, Moraru C, Amann R, Hourdez S, Girguis PR,

Wankel SD, Barbe V, Pelletier E, Fink D, Borowski C, Bach W, Dubilier N (2011) Hydrogen is an energy source for hydrothermal vent symbioses. *Nature* 476:176–180.

Pimm SL (1984) The complexity and stability of ecosystems. *Nature* 307:321–326.

Plouviez S, Faure B, Le Guen D, Lallier FH, Bierne N, Jollivet D (2013) A new barrier to dispersal trapped old genetic clines that escaped the Easter Microplate tension zone of the Pacific vent mussels. *PLoS One* 8:e81555.

Plum C, Pradillon F, Fujiwara Y, Sarrazin J (2017) Copepod colonisation of organic and inorganic substrata at a deep-sea hydrothermal vent site on the Mid-Atlantic Ridge. *Deep Sea Res Part II Top Stud Oceanogr* 137:335–348.

Powell MA, Somero GN (1986) Adaptations to sulfide by hydrothermal vent animals: sites and mechanisms of detoxification and metabolism. *Biol Bull* 171:274–290.

Pradillon F, Shillito B, Young CM, Gaill F (2001) Developmental arrest in vent worm embryos. *Nature* 413:698–699.

Pradillon F, Bris NL, Shillito B, Young CM, Gaill F (2005) Influence of environmental conditions on early development of the hydrothermal vent polychaete Alvinella pompejana. *J Exp Biol* 208:1551–1561.

Q

Qiu J (2010) Oceanography: Death and rebirth in the deep. *Nature* 465:284–286.

R

Ramirez Llodra E (2002) Fecundity and life-history strategies in marine invertebrates. In: *Advances in Marine Biology. Academic Press,* 87–170

Ramirez-Llodra E, Shank T himothy M, German CR (2007) Biodiversity and biogeography of hydrothermal vent species: Thirty years of discovery and investigations. *Oceanography 20:30* – 41

Ramirez-Llodra E, Tyler PA, Baker MC, Bergstad OA, Clark MR, Escobar E, Levin LA, Menot L, Rowden AA, Smith CR, Dover CLV (2011) Man and the Last Great Wilderness: Human Impact on the Deep Sea. *Plose One* 6:e22588.

Rittschof D, Jr RBF, Cannon G, Welch JM, Jr MM, Holm ER, Clare AS, Conova S, McKelvey LM, Bryan P, Dover CL van (1998) Cues and context: Larval responses to physical and chemical cues. *Biofouling* 12:31–44.

Roberts CP, Twidwell D, Burnett JL, Donovan VM, Wonkka CL, Bielski CL, Garmestani AS, Angeler DG, Eason T, Allred BW, Jones MO, Naugle DE, Sundstrom SM, Allen CR (2018) Early Warnings for State Transitions. *Rangel Ecol Manag* 71:659–670.

Rogers AD, Tyler PA, Connelly DP, Copley JT, James R, Larter RD, Linse K, Mills RA, Garabato AN, Pancost RD, Pearce DA, Polunin NVC, German CR, Shank T, Boersch-Supan PH, Alker BJ, Aquilina A, Bennett SA, Clarke A, Dinley RJJ, Graham AGC, Green DRH, Hawkes JA, Hepburn L, Hilario A, Huvenne VAI, Marsh L, Ramirez-Llodra E, Reid WDK, Roterman CN, Sweeting CJ, Thatje S, Zwirglmaier K (2012) The Discovery of New Deep-Sea Hydrothermal Vent Communities in the Southern Ocean and Implications for Biogeography. *PLOS Biol* 10:e1001234.

Roterman CN, Copley JT, Linse KT, Tyler PA, Rogers AD (2016) Connectivity in the cold: the comparative population genetics of

vent-endemic fauna in the Scotia Sea, Southern Ocean. *Mol Ecol* 25:1073–1088.

Rubin, K. H., Soule, S. A., Chadwick Jr, W. W., Fornari, D. J., Clague, D. A., Embley, R. W., Dziak, R. P. (2012). Volcanic eruptions in the deep sea. *Oceanography*, 25(1), 142-157.

S

Sarrazin J, Juniper SK (1999) Biological characteristics of a hydrothermal edifice mosaic community. *Mar Ecol Prog Ser* 185:1–19.

Sarrazin J, V R, Sk J, Jr D (1997) Biological and geological dynamics over four years on a high-temperature sulfide structure at the Juan de Fuca Ridge hydrothermal observatory. *Mar Ecol Prog Ser* 153:5–24.

Sarrazin J, Cuvelier D, Peton L, Legendre P, Sarradin PM (2014) High-resolution dynamics of a deep-sea hydrothermal mussel assemblage monitored by the EMSO-Açores MoMAR observatory. *Deep Sea Res Part Oceanogr Res Pap* 90:62–75.

Sarrazin J, Legendre P, de Busserolles F, Fabri M-C, Guilini K, Ivanenko VN, Morineaux M, Vanreusel A, Sarradin P-M (2015) Biodiversity patterns, environmental drivers and indicator species on a high-temperature hydrothermal edifice, Mid-Atlantic Ridge. *Deep Sea Res Part II Top Stud Oceanogr 121:177–192*.

Sarrazin J, Portail M, Legrand E, Cathalot C, Laes A, Lahaye N, Sarradin PM, Husson B (2020) Endogenous versus exogenous factors: What matters for vent mussel communities? *Deep Sea Res Part Oceanogr* 160:103260.

Scheirer DS, Shank TM, Fornari DJ (2006) Temperature variations at diffuse and focused flow hydrothermal vent sites along the northern East Pacific Rise. *Geochem Geophys Geosystems* 7:3

Schneider CA, Rasband WS, Eliceiri KW (2012) NIH Image to ImageJ: 25 years of image analysis. *Nat Methods* 9:671–675.

Schöne BR, Giere O (2005) Growth increments and stable isotope variation in shells of the deep-sea hydrothermal vent bivalve mollusk Bathymodiolus brevior from the North Fiji Basin, Pacific Ocean. *Deep Sea Res Part Oceanogr Res Pap* 52:1896–1910.

Sen A, Kim S, Miller AJ, Hovey KJ, Hourdez S, Luther GW, Fisher CR (2016) Peripheral communities of the Eastern Lau Spreading Center and Valu Fa Ridge: community composition, temporal change and comparison to near-vent communities. *Mar Ecol* 37:599–617.

Shank TM, Fornari DJ, Von Damm KL, Lilley MD, Haymon RM, Lutz RA (1998) Temporal and spatial patterns of biological community development at nascent deep-sea hydrothermal vents (9°50'N, East Pacific Rise). *Deep Sea Res Part II Top Stud Oceanogr* 45:465–515.

Sheader M, Dover CLV (2007) Temporal and spatial variation in the reproductive ecology of the vent-endemic amphipod Ventiella sulfuris in the eastern Pacific. *Mar Ecol Prog Ser* 331:181–194.

Smith CR, Tunnicliffe V, Colaço A, Drazen JC, Gollner S, Levin LA, Mestre NC, Metaxas A, Molodtsova TN, Morato T, Sweetman AK, Washburn T, Amon DJ (2020) Deep-Sea Misconceptions Cause Underestimation of Seabed-Mining Impacts. *Trends Ecol Evol*. 35:853-857

Spiess FN, Macdonald KC, Atwater T, Ballard R, Carranza A, Cordoba D, Cox C, Garcia VM, Francheteau J, Guerrero J, Hawkins J, Haymon R, Hessler R, Juteau T, Kastner M,

Larson R, Luyendyk B, Macdougall JD, Miller S, Normark W, Orcutt J, Rangin C (1980) East pacific rise: hot springs and geophysical experiments. *Science* 207:1421–1433.

Standish RJ, Hobbs RJ, Mayfield MM, Bestelmeyer BT, Suding KN, Battaglia LL, Eviner V, Hawkes CV, Temperton VM, Cramer VA, Harris JA, Funk JL, Thomas PA (2014) Resilience in ecology: Abstraction, distraction, or where the action is? *Biol Conserv* 177:43–51.

Stearns SC (1992) The Evolution of Life Histories. OUP Oxford, Oxford ; New York

Suding KN, Hobbs RJ (2009) Threshold models in restoration and conservation: a developing framework. *Trends Ecol Evol* 24:271–279.

Sundstrom SM, Allen CR, Gunderson L (2016) Resisting Resilience Theory: A Response to Connell and Ghedini. *Trends Ecol Evol* 31:412–413.

Suzuki K, Yoshida K, Watanabe H, Yamamoto H (2018) Mapping the resilience of chemosynthetic communities in hydrothermal vent fields. *Sci Rep* 8:9364.

T

Takai K, Gamo T, Tsunogai U, Nakayama N, Hirayama H, Nealson KH, Horikoshi K (2004) Geochemical and microbiological evidence for a hydrogen-based, hyperthermophilic subsurface lithoautotrophic microbial ecosystem (HyperSLiME) beneath an active deep-sea hydrothermal field. *Extrem Life Extreme Cond* 8:269–282.

Teixeira S, Olu K, Decker C, Cunha RL, Fuchs S, Hourdez S, Serrão EA, Arnaud-Haond S (2013) High connectivity across the fragmented chemosynthetic ecosystems of the deep Atlantic Equatorial Belt: efficient dispersal mechanisms or questionable endemism? *Mol Ecol* 22:4663–4680.

Thaler AD, Amon D (2019) 262 Voyages Beneath the Sea: a global assessment of macro- and megafaunal biodiversity and research effort at deep-sea hydrothermal vents. *PeerJ* 7:e7397.

Thiel H (2003) Anthropogenic impacts on the deep sea. *Ecosyst World* 427–472.

Thomson RE, Mihály SF, Rabinovich AB, McDuff RE, Veirs SR, Stahr FR (2003) Constrained circulation at Endeavour ridge facilitates colonisation by vent larvae. *Nature* 424:545–549.

Tilman D (2001) Functional Diversity. In: Levin SA (ed) Encyclopedia of Biodiversity. Elsevier, New York, 109–120

Tivey MK (2007) Generation of seafloor hydrothermal vent fluids and associated mineral deposits. *Oceanography* 20:50-65.

Tivey MK, Bradley AM, Joyce TM, Kadko D (2002) Insights into tide-related variability at seafloor hydrothermal vents from time-series temperature measurements. *Earth Planet Sci Lett* 202:693–707.

Tolstoy M, Cowen JP, Baker ET, Fornari DJ, Rubin KH, Shank TM, Waldhauser F, Bohnenstiehl DR, Forsyth DW, Holmes RC, Love B, Perfit MR, Weekly RT, Soule SA, Glazer B (2006) A Sea-Floor Spreading Event Captured by Seismometers. *Science* 314:1920–1922.

Tredgold MT (1818) XXXVII. On the transverse strength and resilience of timber. *Philos Mag* 51:214–216.

Tugade MM, Fredrickson BL (2004) Resilient Individuals Use Positive Emotions to Bounce Back From Negative Emotional Experiences. *J Pers Soc Psychol* 86:320–333.

Tunnicliffe V (1991) The biology of hydrothermal vents : ecology and evolution. *Biol Hydrothermal Vents Ecol Evol* 29:319–407.

Tunnicliffe V, Bone Q (1988) Biogeography and evolution of hydrothermal-vent fauna in the eastern Pacific Ocean. *Proc R Soc Lond B Biol Sci* 233:347–366.

Tunnicliffe V, Fowler MR (1996) Influence of sea-floor spreading on the global hydrothermal vent fauna. *Nature* 379:531–533.

Tunnicliffe V, Kim Juniper S (1990) Dynamic character of the hydrothermal vent habitat and the nature of sulphide chimney fauna. *Prog Oceanogr* 24:1–13.

Tunnicliffe V, Embley RW, Holden JF, Butterfield DA, Massoth GJ, Juniper SK (1997) Biological colonisation of new hydrothermal vents following an eruption on Juan de Fuca Ridge. *Deep Sea Res Part Oceanogr Res Pap* 44:1627–1644.

Tyler PA, Young CM (1999) Reproduction and dispersal at vents and cold seeps. *J Mar Biol Assoc U K* 79:193–208.

Tyler PA, German CR, Ramirez-Llodra E, Van Dover CL (2002) Understanding the biogeography of chemosynthetic ecosystems. *Oceanol Acta* 25:227–241.

V

Van den Hove S, Moreau V (2007) Deep-sea Biodiversity and Ecosystems: A Scoping Report on Their Socio-economy, *Management and Governanace. UNEP/Earthprint* 184

Van Dover C (2002) Trophic relationships among invertebrates at the Kairei hydrothermal vent field (Central Indian Ridge). *Mar Biol* 141:761–772.

Van Dover CL, Fry B, Grassle JF, Humphris S, Rona PA (1988) Feeding biology of the shrimp Rimicaris exoculata at hydrothermal vents on the Mid-Atlantic Ridge. *Mar Biol* 98:209–216.

Van Dover CL, Desbruyères D, Segonzac M, Comtet T, Saldanha L, Fiala-Medioni A, Langmuir C (1996) Biology of the Lucky Strike hydrothermal field. *Deep Sea Res Part Oceanogr Res Pap* 43:1509–1529.

Van Dover CL, German CR, Speer KG, Parson LM, Vrijenhoek RC (2002) Evolution and biogeography of deep-sea vent and seep invertebrates. *Science* 295:1253–1257.

Van Dover CL, Aronson J, Pendleton L, Smith S, Arnaud-Haond S, Moreno-Mateos D, Barbier E, Billett D, Bowers K, Danovaro R, Edwards A, Kellert S, Morato T, Pollard E, Rogers A, Warner R (2014) Ecological restoration in the deep sea: Desiderata. *Mar Policy* 44:98–106.

Van Dover CL, Arnaud-Haond S, Gianni M, Helmreich S, Huber JA, Jaeckel AL, Metaxas A, Pendleton LH, Petersen S, Ramirez-Llodra E, Steinberg PE, Tunnicliffe V, Yamamoto H (2018) Scientific rationale and international obligations for protection of active hydrothermal vent ecosystems from deep-sea mining. *Mar Policy* 90:20–28.

Vic C, Gula J, Roullet G, Pradillon F (2018) Dispersion of deep-sea hydrothermal vent effluents and larvae by submesoscale and tidal currents. *Deep Sea Res Part Oceanogr Res Pap* 133:1–18.

Vitousek PM, Mooney HA, Lubchenco J, Melillo JM (1997) Human Domination of Earth's Ecosystems. *Science* 277:494–499.

Vrijenhoek R (1998) Gene Flow and Genetic Diversity in Naturally Fragmented Metapopulations of Deep-Sea Hydrothermal Vent Animals. *J Hered* 88:285–93.

Vrijenhoek RC (2009) Cryptic species, phenotypic plasticity, and complex life histories: Assessing deep-sea faunal diversity with molecular markers. *Deep Sea Res Part II Top Stud Oceanogr* 56:1713–1723.

Vrijenhoek RC, Schutz SJ, Gustafson RG, Lutz RA (1994) Cryptic species of deep-sea clams (Mollusca: Bivalvia: Vesicomyidae) from hydrothermal vent and cold-water seep environments. *Deep Sea Res Part Oceanogr Res Pap* 41:1171–1189.

W

Walker BH (1992) Biodiversity and Ecological Redundancy. *Conserv Biol* 6:18–23.

Washburn TW, Turner PJ, Durden JM, Jones DOB, Weaver P, Van Dover CL (2019) Ecological risk assessment for deep-sea mining. *Ocean Coast Manag* 176:24–39.

Watanabe H, Fujikura K, Kinoshita G, Yamamoto H, Okutani T (2009) Egg capsule of Phymorhynchus buccinoides (Gastropoda: Turridae) in a deep-sea methane seep site in Sagami Bay, Japan. *Venus*

Wedding LM, Reiter SM, Smith CR, Gjerde KM, Kittinger JN, Friedlander AM, Gaines SD, Clark MR, Thurnherr AM, Hardy SM, Crowder LB (2015) Managing mining of the deep seabed. *Science* 349:144–145.

Won Y, Young CR, Lutz RA, Vrijenhoek RC (2003) Dispersal barriers and isolation among deep-sea mussel populations (Mytilidae: Bathymodiolus) from eastern Pacific hydrothermal vents. *Mol Ecol* 12:169–184.

Y

Yahagi T, Watanabe H, Ishibashi J, Kojima S (2015) Genetic population structure of four hydrothermal vent shrimp species (Alvinocarididae) in the Okinawa Trough, Northwest Pacific. *Mar Ecol Prog Ser* 529:159–169.

Yeung ACY, Richardson JS (2016) Some Conceptual and Operational Considerations when Measuring 'Resilience': A Response to Hodgson et al. *Trends Ecol Evol* 31:2–3.

Yeung ACY, Richardson JS (2018) Expanding Resilience Comparisons to Address Management Needs: A Response to Ingrisch and Bahn. *Trends Ecol Evol* 33:647–649.

Z

Zal F, Jollivet D, Chevaldonné P, Desbruyères D (1995) Reproductive biology and population structure of the deep-sea hydrothermal vent worm Paralvinella grasslei (Polychaeta: Alvinellidae) at 13°N on the East Pacific Rise. *Mar Biol* 122:637–648.

Annexes

Annexe 1. Tableau d'interprétation de la roue de rétablissement

Échelle d'évaluation du rétablissement des écosystèmes hydrothermaux (entre 1 et 5) pour les différents attributs identifiés et présentés dans la roue de rétablissement. Cette échelle à 5 étoiles représente un gradient cumulatif allant d'un très faible rétablissement (1 étoile) à des conditions comparables à l'écosystème de référence (5 étoiles). Elle ne fournit qu'un cadre générique et nécessite l'utilisation d'indicateurs et de métriques adaptées pour assurer la surveillance des différents attributs au cours du rétablissement.

ATTRIBUTE	*	**	***	****	*****
Habitat conditions	Gross physical and chemical problems remediated (e.g., hight temperature, modification of substrate porosity etc.)	Substrate chemical and physical properties on track to stabilize within natural range	Substrate stabilized within natural range and supporting growth of characteristic species	Substrate maintaining conditions suitable for ongoing growth and recruitment of characteristic species	Substrate exhibiting physical and chemical characteristics highly similar to the reference with evidence they can sustain species and processes
Species composition	Poor recovery of species richness (<5% of reference assemblages)	Colonisation of few characteristic sprecies (5%-30% of reference) allowing onset of interactions	Recovery of key species promoting diversity (30%-60% of reference)	Recovery to high diversity levels (60%-90% reference) and complex interactions	Diversity similar to reference ecosystems (>90% of reference), improving potential for colonisation of more species over time to reach climax communities
Structural diversity	Very low biogenic structure asseociated with poor density recovery relative to reference	Start of habitat diversificatioin thanks to biogenic structure increasing but low relative diversity and less cohorts in populations	Intermediate recovery of engineer species, providing habitat heterogeneity and allowing more complex diversity structure	Good recovery of engineer species enhancing other species densities and biomass and many cohorts are identified	Complete recovery of diversity structure, spatial patterning and population demographic. Further complexity and spatial pattering able to self-organize to highly resemble reference ecosystem.
Ecosystem functioning	Almost no recovery of ecosystem functions (trophic diversity and reproduction)	Ecosystem functions remain low compared to reference (few mature individuals and limited trophic diversity)	Evidence of functions commencing (increasing in food-web ressources diversity and onset of trophic interactions)	Substantial evidence of key functions and processes commencing including reproduction, and trophique diversity and complexity	Considerable evidence of functions and processes on a secure trajectory towards reference and evidence of ecosystem resilience likely after reinstatement of appropriate disturbance regimes.
External exchanges	Very few exchanges throught immigration or dispersion with surounding habitats	Some exchanges identified with surrounding habitats but low connectivity	Connectivity increasing and exchanges between site and external environment starting to be evident (e.g., more species, recruitment etc.).	High level of connectivity with other natural areas established, rapid colonisation of diverse species	Evidence that potential for external exchanges is highly similar to reference and enhancing résilience to future disturbance
Absence of threats	Total interruption of further deterioration	Low intensity threats are very limited in spatial and temporal scale	Some threats remains temporarily with medium intensity	Most of threats are not managed and still remain	Persistance of all threats impacting recovery

Annexe 2 Article ADN environnemental

Exploration de l'ADN environnemental (eDNA) pour évaluer la biodiversité des communautés fauniques du substrat dur sur le Lucky Strike Vent Field (dorsale médio-atlantique) et étudier les dynamiques de recolonisation après une perturbation induite

frontiers in Marine Science

ORIGINAL RESEARCH
published: 09 January 2020
doi: 10.3389/fmars.2019.00783

Exploring Environmental DNA (eDNA) to Assess Biodiversity of Hard Substratum Faunal Communities on the Lucky Strike Vent Field (Mid-Atlantic Ridge) and Investigate Recolonization Dynamics After an Induced Disturbance

Dominique A. Cowart[1], Marjolaine Matabos[1]*, Miriam I. Brandt[2], Julien Marticorena[1] and Jozée Sarrazin[1]**

[1] Ifremer Centre de Bretagne, REM/EEP, Laboratoire Environnement Profond, Plouzané, France, [2] IRD, CNRS, MARBEC, Ifremer, Université de Montpellier, Sète, France

OPEN ACCESS

Edited by:
Cinzia Corinaldesi,
Marche Polytechnic University, Italy

Reviewed by:
James Davis Reimer,
University of the Ryukyus, Japan
Olivier Laroche,
University of Hawai'i at Mānoa, United States

***Correspondence:**
Dominique A. Cowart
dominique.cowart@gmail.com
Marjolaine Matabos
marjolaine.matabos@ifremer.fr
Jozée Sarrazin
jozee.sarrazin@ifremer.fr

Specialty section:
This article was submitted to Deep-Sea Environments and Ecology, a section of the journal Frontiers in Marine Science

Received: 30 July 2019
Accepted: 04 December 2019
Published: 09 January 2020

Citation:
Cowart DA, Matabos M, Brandt MI, Marticorena J and Sarrazin J (2020) Exploring Environmental DNA (eDNA) to Assess Biodiversity of Hard Substratum Faunal Communities on the Lucky Strike Vent Field (Mid-Atlantic Ridge) and Investigate Recolonization Dynamics After an Induced Disturbance. Front. Mar. Sci. 6:783. doi: 10.3389/fmars.2019.00783

Deep ocean hydrothermal vent ecosystems face physical disturbances from naturally occurring volcanic and tectonic activities and are at increasing risk of mineral resource exploitation, raising concerns about the resilience of endemic biological communities. Following destructive events, efficient and rapidly applicable surveys of organisms are required to monitor the state, evolution and a possible return of these ecosystems to their original baseline status. In this study, we explored the environmental DNA (eDNA) approach as a tool (1) to assess biodiversity of benthic communities associated with deep-sea hard substrata and (2) tracked the recolonization dynamics of benthic invertebrate communities living on the Montségur edifice within the Lucky Strike vent field (Mid-Atlantic Ridge), after an induced disturbance that consisted of faunal clearance within experimental quadrats. Hard substratum samples were collected prior to and one year after the disturbance, for eDNA metabarcoding using one marker of the mitochondrial Cytochrome Oxidase I (COI) gene and three markers of the nuclear 18S ribosomal RNA (18S) gene. We also generated a DNA barcoding inventory that consisted of taxa physically collected from Montségur and morphologically identified. This inventory contained amplified barcodes from COI, 18S and the nuclear large subunit ribosomal RNA (28S) gene. The resulting sequence information from the COI and 18S were used for eDNA taxonomic assignment. The eDNA datasets uncovered a high diversity of metazoan OTUs, which included macro- and meiofauna common to Lucky Strike. Baseline data collected at the start of the experiment identified higher OTU richness at sites peripheral to the active edifice, as well as at inactive sites. One year following the initial disturbance, analysis of recolonization data found no statistical difference in presence/absence from baseline communities. The eDNA protocols provide a reproducible strategy to quickly assess biodiversity associated with

deep sea hard substratum, enabling comparisons across various habitats. To follow recolonization dynamics at small spatial scales, however, we recommend an approach that uses both molecular and morphological-based traditional methods. Finally, we present original data on the "unseen" diversity of the fauna inhabiting the poorly studied inactive sites, locations that are targeted by commercial mining. Continued monitoring of these sites is currently ongoing and will bring new insight on recovery potential over time, with the ultimate goal of informing conservation and management decisions in relation to the protection of hydrothermal vent ecosystems.

Keywords: natural regeneration, clearance, *Bathymodiolus azoricus*, monitoring, hard substratum, active and inactive vent sites

INTRODUCTION

Deep ocean hydrothermal vent ecosystems are dynamic and irregular habitats that experience severe environmental conditions, including a complete absence of sunlight, high hydrostatic pressures, wide variations in local temperatures, as well as toxic levels of sulfides and heavy metals (Johnson et al., 1988; Childress and Fisher, 1992; Tunnicliffe, 1992). Despite these harsh conditions, several species of benthic invertebrates exhibit physiological tolerances that allow them to successfully colonize vent habitats (Desbruyères et al., 2000). Vent communities are sustained by a complex trophic network, in which microorganisms serve as primary producers/consumers that harvest energy from the chemical compounds present within the hot fluids (up to 400°C) emitted from the seafloor (Karl et al., 1980; Baross and Hoffman, 1985; Tunnicliffe et al., 1997). This chemosynthetic activity drives thriving faunal communities that often consist of assemblages dominated by large symbiotic taxa such as mytilid mussels, siboglinid polychaetes and alvinocaridid shrimp (Tunnicliffe, 1991; Cuvelier et al., 2011a).

Communities living at active vents are often characterized as transitory, due to variations in environmental conditions caused by tectonic activity and sporadic volcanic eruptions (Lutz and Kennish, 1993; Butterfield et al., 1997). These naturally occurring disturbances can lead to the alteration of vent fluid chemistry, the reduction or sealing off of fluid emission and changes in the physical environment such as the collapse of sulfide edifices, thus greatly influencing community presence, composition and trophic dynamics (Tunnicliffe and Juniper, 1990; Sarrazin et al., 1997; Sarrazin and Juniper, 1999; Tsurumi, 2003; Kelly et al., 2007). Active vent ecosystems host high biomass of endemic organisms capable of coping with this unique environment as well as intermittent changes in fluid flow and oxygen access. Less active areas, such as sites peripheric to active vent edifices, as well as inactive sulfide mounds, are known to host lower densities and biomass as a result of less energy flow provided by hydrothermal output (Levin et al., 2016). Furthermore, active hydrothermal sediments are characterized by greater dominance and lower diversity relative to inactive background sediments (Vanreusel et al., 1997; Levin et al., 2009). Recovery of communities living at active vent sites after a disturbance is influenced by several factors. Among these are reproductive strategies, larval life histories and dispersal distances from nearby established assemblages, the presence of ideal substratum for settlement, biotic and abiotic chemical cues, as well as competition and predation levels (Mullineaux, 2000; Micheli et al., 2002; Mullineaux et al., 2003; Hunt et al., 2004; Kelly et al., 2007; Cuvelier et al., 2014).

While the most common disturbance experienced at vents originates from tectonic and volcanic events, human activities have increasingly emerged as additional sources of perturbation (Ramirez-Llodra et al., 2011). These activities range from having no measurable impact, such as photo surveys, to those having substantial impacts, such as drilling, trawling and mineral extraction (Van Dover, 2014). Mineral mining of deep-sea resources, notably seafloor massive sulfides (SMS), is one such activity with the potential for substantial destruction of vent habitats. SMS form by rapid mineral precipitation from overheated vent fluids as they are ejected from the seafloor and interact with cooler ambient seawater (Fisher et al., 2007; Rona, 2008; Boschen et al., 2013). The resulting deposits exist in active or inactive zones and can take hundreds of years to form high concentrations of lead, zinc, copper, cobalt, gold and silver; this consistency of some deposits make them economically valuable and of possible interest to prospecting companies (Krasnov et al., 1995; Hoagland et al., 2010; ISA, 2010; Boschen et al., 2013). While little is known regarding how commercial mineral extraction efforts would proceed at vents, collections of deposits will be similar to open-cut mining seen at land-based sites, with the extraction phase causing the removal of organisms, the loss of habitat, decreases in primary productivity and biodiversity, as well as extinctions of rare taxa, particularly at inactive locations where faunal communities are poorly known (Van Dover, 2011, 2014; Boschen et al., 2013; Gollner et al., 2017). The potential for mining deposits has therefore raised concerns about the future of benthic communities present at sites where SMS are found, as well as encouragement for continued investigations into the resilience of possibly impacted communities (Ramirez-Llodra et al., 2011; Mengerink et al., 2014; Gollner et al., 2017).

The Mid-Atlantic Ridge (MAR) vent system is one such region where unique geological features and geochemical attributes allow SMS formation (Hannington et al., 2011; Monecke et al., 2015). While slower-spreading and more stable compared to vents at Juan de Fuca ridge and East Pacific Rise, MAR systems may also experience occasional volcanic events (Humphris et al., 2002; Van Dover et al., 2002). So far, however, the scarcity of

these events prevented the study of faunal recovery after natural disturbance, as was done along the East Pacific ridge systems (Shank et al., 1998; Mullineaux et al., 2010). One alternative approach to gain insights into colonization and recovery processes is the deployment of artificial substrata on the seafloor. At the Lucky Strike (LS) hydrothermal vent field along the MAR, such an experiment showed that after 2 years, vent activity and biological interactions were the most important structuring factors explaining meio- and macrofaunal colonization of newly available substrata (Cuvelier et al., 2014). The deployment of a separate set of experiments in the same area found that after only 9 months, different meiofaunal taxa had preferentially colonized one substratum or the other, but the 9 months time scale still supported hydrothermal activity as the prominent factor influencing community structure (Zeppilli et al., 2015). These studies suggest that colonization at LS can occur fairly rapidly, however, how quickly communities can return to their baseline status (recolonize) after a disturbance requires additional investigation (Mengerink et al., 2014; Van Dover, 2014).

The assessments of vent faunal colonization patterns based on the deployment of artificial substratum involves identification of settled fauna through video stream (only larger species) and/or physical taxa sorting (Hunt et al., 2004; Kelly et al., 2007; Gaudron et al., 2010; Cuvelier et al., 2014; Zeppilli et al., 2015). These strategies request extensive handling of collections and taxonomic expertise for identification, which can be difficult when working with early life stages or faunal remains. Furthermore, these methods may miss microscopic, rare or cryptic fauna possibly critical for interpreting community dynamics. In contrast, High-Throughput Sequencing technologies (HTS) have enabled the development of sensitive biodiversity surveys to allow the screening of bulk environmental samples (water, sediment, and other mass collections) containing a mix of genetic information from many organisms ("biodiversity soup," Yu et al., 2012). DNA metabarcoding – the use of one or more genes to simultaneously identify taxa present within bulk samples (Coissac et al., 2012) – has already provided rapid and thorough assessments of entire communities, while revealing higher levels of diversity than physical sampling methods (Ji et al., 2013; Lindeque et al., 2013; Cowart et al., 2015; Leray and Knowlton, 2015). In particular, environmental samples containing free cells and nucleic acids released by organisms into their habitat (environmental DNA/RNA – eDNA/eRNA, Taberlet et al., 2012a; Barnes and Turner, 2016) have provided a comprehensive characterization of organisms from both past and contemporary assemblages and helped inform on the ecological trajectory of impacted communities (Hänfling et al., 2016; Valentini et al., 2016; Laroche et al., 2017, 2018). The relative inaccessibility of hydrothermal vents due to technological and logistical constraints and sampling difficulties makes eDNA metabarcoding monitoring particularly attractive for evaluating biodiversity and the recolonization of faunal communities. First, eDNA is often less destructive when compared to surveys that require animal collection (Thomsen and Willerslev, 2015); this is especially important when attempting to obtain data from newly established communities hosting early life stages. Secondly, eDNA is effective for recovering genetic signals of small, rare or transient taxa missed by physical collection or observational surveys (Thomsen et al., 2016; Valentini et al., 2016). This characteristic is useful within the deep-sea framework, where collections are done by remote mechanical manipulation that may overlook these "hidden" organisms.

In the present investigation, we explore eDNA as a method for assessing the diversity of deep-sea benthic communities living on hard substrata, as well as provide an early evaluation of the resilience of hydrothermal vent biological communities to a disturbance experiment by following the recolonization dynamics of benthic invertebrate communities at the LS vent field on the MAR. The experiment was carried out at 1,700 m depth along an environmental gradient that includes the Montségur active sulfide structure, a sedimentary site at its periphery (∼30 m) and an inactive site, approximately 400 m away from it. This experimental setting allowed us to monitor community recolonization on active sites, approximately 1 year after the induced disturbance. As there were no significant changes to fluid flow during the induced disturbance event, we primarily address the role of biotic processes on recolonization dynamics, which have been shown to be critical in structuring vent communities. We chose to perform eDNA metabarcoding of retrieved substratum to (1) provide a comprehensive overview of taxa (Operational Taxonomic Units – OTUs) present at experimental sites prior to and 1 year after the disturbance, (2) examine the possible impact of mobile predators on community re-establishment during this time period and (3) investigate how vent activity along an environmental gradient influences the structure of communities. We additionally provide protocols for eDNA collection and processing of hydrothermal sulfide remains, an inventory of taxa physically collected, morphologically identified and DNA barcoded for comparison against eDNA sequence data, as well as suggested improvements for future studies.

MATERIALS AND METHODS

Location of the Experiment

The LS hydrothermal vent field is located within a marine protected area along the MAR, southwest of the Azores Archipelago (**Figure 1**, top left, center). LS has a mean depth of 1,700 m and consists of three seamounts that surround a lava filled depression ("lava lake," Barreyre et al., 2014). The vent field hosts over twenty active vent edifices, including Montségur situated in the southeastern sector of LS and encompassing an area of ∼384 m^2 (**Figure 1** top right, Langmuir et al., 1997; Ondréas et al., 2009; Barreyre et al., 2014). Montségur is a large active sulfide edifice surrounded by a large fissured slab through which diffused fluids expel. Samples were taken both on the structure itself and at its base on the seafloor. The site at the periphery is likely composed of a mixture of hydrothermal particles and surface material sediments. Finally, the inactive site, located approximately 400 m away from Montségur, is composed of indurated sulfides.

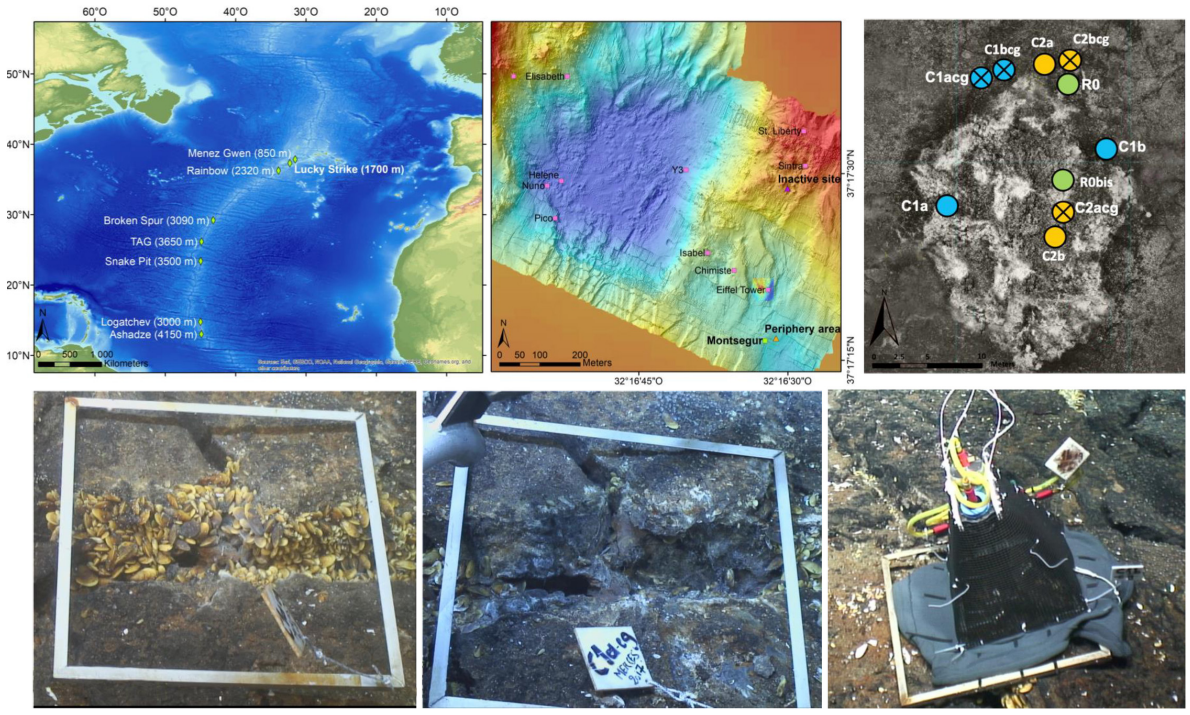

FIGURE 1 | (Top left) Location of the Lucky Strike vent field on the Mid-Atlantic Ridge, south of the Azores. **(Top center)** The 1 km^2 Lucky Strike vent field with the Montségur edifice on the south-east. **(Top right)** View of the full *in situ* experiment on the Montségur hydrothermal edifice. **(Bottom left)** Experimental quadrat C1a_cg at the base of Montségur and *Bathymodiolus* assemblage, prior to clearance. **(Bottom center)** Experimental quadrat C1a_cg after clearance; the suction device (metal pipe) is shown at the top left corner of this panel. **(Bottom right)** Experimental quadrat that has been covered by pyramidal cage and a skirt in 2018. All quadrats measure 50 × 50 cm in size.

The Montségur edifice harbors a similar faunal composition to Eiffel Tower, another active but better studied vent edifice within LS (**Figure 1**, top center Cuvelier et al., 2011a,b). From this particular edifice, approximately 70 taxa are known, and conspicuous species include *Bathymodiolus azoricus* mussels, *Mirocaris fortunata* shrimp, *Branchipolynoe seepensis* and *Amphisamytha lutzi* polychaetes, as well as *Lepetodrilus atlanticus* and *Protolira valvatoides* gastropods (Sarrazin et al., 2015). These dominant macrofaunal species live in association with a variety of other organisms including those belonging to the meiofaunal compartment primarily composed of nematodes and copepods (Zeppilli et al., 2015; Plum et al., 2017). Two faunal assemblages were described in this area: the first is dominated by *Bathymodiolus azoricus* mussels that live in lower temperatures and chemical outputs, while exhibiting higher taxonomic diversity and densities. The second is dominated by *Mirocaris fortunata* shrimp that live in higher temperatures and chemical outputs, while exhibiting lower taxonomic diversity and densities (Desbruyères et al., 2000; Cuvelier et al., 2009, 2011a; Sarrazin et al., 2015).

Experiment Deployment and Sample Acquisition

The *in situ* experiment was deployed at LS during the Momarsat 2017 cruise that occurred in July 2017 on the R/V *Pourquoi pas?* using the ROV *Victor6000*, as part of the EMSO-Azores observatory annual maintenance. It consisted of ten quadrats sized 50 x 50 cm each, deployed on and at the base of Montségur in *Bathymodiolus azoricus* assemblages described previously (**Figure 1**, bottom left). Eight of these quadrats were positioned to study recolonization processes following faunal clearance after 1 year (C1) and 2 years (C2). Replicate samples for each year were denoted as "a" or "b" (**Table 1**). In addition, two quadrats were sampled the first year as reference (R) for comparison with experimental (C) quadrats. All 10 quadrats were placed at approximately 1,700 m depth and used to either observe natural succession patterns (reference) or passive recolonization of communities after disturbance (experimental).

Prior to clearance, initial physical and chemical characterizations were done. Fauna was then removed/cleared from the experimental quadrats using the robotic arm and claw of *Victor6000* to physically grab and scrub the animals from the hard substrata; animals were then placed in bioboxes (**Figure 1**, bottom center). This operation was followed by the use of a suction device to vacuum the remaining organisms within the quadrat. There were, however, animals remaining underneath some quadrats in small fractures, as access for removal was difficult (**Figure 1**). After clearance, quadrats underwent a final physico-chemical characterization of the bare substratum. To better evaluate the role of mobile predators on local recolonization, pyramidal structures encased in 1 cm plastic

TABLE 1 | Details of each substratum sample obtained from the *in situ* experiment that was deployed on and at the base of the Montségur edifice, as well as at the peripheric and inactive habitats.

Quadrat	Presence of Cage	Sampling year		Location	Sampling Depth (m)	Substratum	Sample Weight (g)
		2017	2018				
Reference							
R0	No	X		Structure	1700	Sulfide	10.61
R0-bis	No	X		Base	1700	Slab	9.62
Experimental (Active)							
C1a	No	X	X	Structure	1700	Sulfide	$10.67_{(2017)}$ $9.91_{(2018)}$
C1a-cg	Yes	X	X	Base	1700	Slab	$10.03_{(2017)}$ $10.15_{(2018)}$
C1b	No	X	X	Base	1700	Slab	$6.93_{(2017)}$ $9.57_{(2018)}$
C1b-cg	Yes	X	X	Base	1700	Slab	$10.16_{(2017)}$ $9.95_{(2018)}$
C2a	No	X		Base	1700	Slab	10.04
C2a-cg	Yes	X		Structure	1700	Sulfide	10.20
C2b	No	X		Structure	1700	Sulfide	10.00
C2b-cg	Yes	X		Base	1700	Slab	9.64
Other habitats							
P1	No		X	Periphery	1703	Muddy	2.31
P2	No		X	Periphery	1703	Muddy	2.52
I1	No		X	Inactive	1651	Rocky	10.3
I2	No		X	Inactive	1651	Rocky	9.67

mesh were placed over specific quadrats denoted as "cg" for caged (**Figure 1**, bottom right). When possible, paired quadrats (caged and uncaged) were placed next to each other (**Figure 1**, top right). Upon arrival of the bioboxes onboard the ship and prior to faunal sorting, 9 – 10 g of substratum, debris and pebbles from each quadrat collection was immediately removed directly from the bioboxes using tweezers and spoons previously sterilized with 10% bleach solution. Each sample was then placed in sterile 50-ml centrifuge tubes and stored at −80°C until eDNA extraction could be carried out at the shore-based laboratory. Fauna remaining after substratum collection were preserved in 96° ethanol for further identification.

The Montségur experiment was re-visited 13 months later during the Momarsat 2018 cruise on the R/V *L'Atalante*, using the ROV *Victor6000* to retrieve additional faunal and substratum samples. At this time, quadrats dedicated to the study of 1-year recolonization processes following disturbance (C1 experimental quadrats) were sampled (**Table 1**). To complement our experiment with baseline data from additional habitats, four new quadrats were deployed: two replicate samples were collected at 1,703 m depth in a sedimented peripheral area (denoted as "P"), located about 30 m away from Montségur, and two replicate samples were collected at 1,651 m depth on an inactive edifice (denoted as "I") situated 400 m north of Montségur (**Figure 1** top center and **Table 1**). In these areas, only the suction device was used to vacuum the substrata along with its fauna, collecting approximately 2.50 g of substratum for the peripheral sites and 9 – 10 g of substratum for inactive sites (**Table 1**). Onboard processing was conducted as stated above. For every quadrat visited in 2018, characterization of abiotic conditions and substratum sampling were performed following the same strategy and protocols as in 2017, yielding a total of 18 substratum samples across both years (**Table 1**).

DNA Extraction and Barcoding of Taxa

Individuals from each faunal group were identified on the basis of morphology to the lowest taxonomic group possible prior to DNA extraction, which was most frequently the species level. DNA from every individual was extracted separately for genetic confirmation of their putative morphological identities. Genomic DNA was extracted from the tissues of 1–12 individuals of each morphologically identified taxon, depending on the number of individuals available for processing. Extracted DNA was obtained from multiple individuals per taxonomic group, in an attempt to account for intraspecific diversity. DNA extractions occurred using either the CTAB method (Doyle, 1991) or the DNeasy Blood and Tissue kit (Qiagen, Hildren, Germany) following the manufacturer's instructions. Negative control samples, containing only reagents, were included for each extraction series. Following extraction, an aliquot of each sample was electrophoresed on a 1 % agarose gel stained with ethidium bromide to visualize extract quality. Newly extracted DNA samples were stored at −20°C until end-point PCR amplification assays.

PCR assays were performed to amplify fragments of the mitochondrial gene Cytochrome Oxidase I (COI) and nuclear genes 28S large subunit ribosomal RNA (28S) and 18S small subunit ribosomal RNA (18S); each assay round included a

negative control with molecular grade H_2O instead of DNA extract and extraction negative controls to assess for potential contamination. Fragments of the COI gene were amplified using degenerate versions of Folmer's primers (Folmer et al., 1994; Leray et al., 2013), while 28S gene regions D2D3 and D9D10 were amplified using primers from De Ley et al. (1999) and Machida and Knowlton (2012). For 18S, the V1V2, V7V8 and V9 regions were amplified using primers developed by Amaral-Zettler et al. (2009), Stoeck et al. (2010), Machida and Knowlton (2012), and Sinniger et al. (2016). All protocols, including PCR master mixes and cycling conditions for each gene region, are detailed in **Supplementary Material S1**. Prior to Sanger sequencing, all PCR products were electrophoresed as described above; none of the negative controls or extraction blanks showed evidence of contamination. PCR products showing evidence of amplification were sent to Eurofins/GATC Biotech or Macrogen where purification and sequencing reactions were performed using the ABI BigDye® Terminator v3.1 Cycle Sequencing Kit (Applied Biosystems, Waltham, MA, United States) and read on an ABI 3730xl sequencer following the protocols supplied by the manufacturer. Resulting sequence chromatograms were visualized, assembled and edited using Geneious v.10.0.5 (Kearse et al., 2012). Finally, the NCBI blastn algorithm (Johnson et al., 2008) was used to match sequences to publicly available databases and determine their nearest identities at <98 – 100%; confirmed sequences were integrated into larger reference databases for the eventual matching to eDNA sequence data.

eDNA Extraction, Library Construction and Metabarcoding

Genomic DNA was extracted from up to 10 g of substrate from each of the 18 samples using the Qiagen PowerMax® Soil DNA Isolation kit following the manufacturer's instructions. To reduce the risk of contamination, eDNA extractions were carried out under a Captair® bio BioCap DNA/RNA workstation (rlab, Rowley, MA, United States) with UV sterilization and filtered airflow. Tools and equipment were UV sterilized and washed with 50% bleach solution as per sterilization protocols suggested by Goldberg et al. (2016). Samples were manipulated using a newly purchased and dedicated set of pipettes fitted with filter tips to avoid cross-contamination. Negative extraction controls (no substratum, only reagents) and positive extraction controls (local shallow water sand collected at 0 m depth from Plage du Dellec, Plouzané, France) were included during each set of extractions to assess potential contamination (−) or confirm that the protocol was successful (+). Aliquots of extract were used to determine the concentration of each sample via the Qubit® dsDNA HS Assay Kit (Thermo Fisher Scientific, Waltham, MA, United States) prior to submission to MR DNA (Shallowater, TX, United States) for amplicon generation, library preparation and subsequent metabarcode sequencing. Positive controls contained measurable quantities of DNA; none of the seven negative controls showed evidence of contamination and were sent, along with the true eDNA samples, to MR DNA for amplicon sequencing.

Given the (1) extensiveness of the publicly available sequence databases for COI and 18S genes, (2) the ability of the COI and 18S primer sets to amplify across several taxa ("universality") and (3) the short length of amplicons necessary for working with fragmented eDNA, primers amplifying 18S-V1V2 (350-bp), 18S-V4 (270-bp), 18S-V9 (130-bp), and COI (313-bp) were used for eDNA metabarcoding. PCR amplification was completed using the Qiagen HotStarTaq Plus Master Mix Kit, in a final volume of 25 μl. The final concentration for each reagent of the master mix was: 1.44 mM $MgCl_2$, 192 μM of each dNTP, 0.25 μM for each primer, 0.8 units of HotStarTaq Plus DNA polymerase and 1 μl of each sample was added to the reaction. Additionally, assays were optimized by increasing the final concentration of $MgCl_2$ to 1.64 mM, as well as adding a final concentration of 1.6 mg/ml bovine serum albumin (BSA). Each sample underwent cycling conditions as follows: 94°C for 3 min, followed by 28 cycles of 94°C for 30 s, 53°C for 40 s and 72°C for 1 min, finalizing an elongation step at 72°C for 5 min. Generated amplicons were used for the preparation of sequencing libraries by mixing all amplicon products from different samples in equal concentrations and purifying using Agencourt Ampure beads (Agencourt Bioscience Corporation, Beverly, MA, United States). The manufacturer's recommendation of 100 ng (350-bp insert size) of the purified amplicon pool was used as input for the Illumina TruSeq DNA protocol. After library purification, the final concentration of the pooled library was calculated using the Qubit® dsDNA HS assay and diluted to 10 nM in preparation for sequencing. Libraries were sequenced paired end for 600 cycles (300 cycles in one direction and 300 cycles in the opposite direction) on the Illumina MiSeq, ensuring the complete insert was sequenced.

Bioinformatic Workflow and Statistical Strategy for Analyzing eDNA Datasets

Resulting raw sequence reads were processed with the FROGS v.2.0 pipeline (Escudié et al., 2017), using both Galaxy web and command-line interfaces. Reads were first demultiplexed then merged at a mismatch rate of 0.1 for each gene. Given the short length of the 18S-V9 fragment and the 2 × 300-bp read length achieved by Illumina sequencing, Trimmomatic v.0.39 (Bolger et al., 2014) was used to trim the length of each direction for this dataset to 140-bp, prior to merging the reads in FROGS. After merging, the minimum and maximum amplicon lengths for each gene were as follows: 250 and 450-bp for COI; 300 and 500-bp for 18S-V1V2; 280 and 500-bp for 18S-V4; 50 and 250-bp for 18S-V9. Next, datasets underwent swarm clustering (Mahé et al., 2014) at small local linking threshold of $d = 2$. Chimera and singleton filtering followed, with FROGS implementing VSEARCH (Rognes et al., 2016) to detect chimeras *de novo* in each sample. Next, filtering was done to keep OTUs that had a minimum number of 2 sequences assigned. Afterward, blastn+ was implemented to assign taxonomy by finding alignments between the resulting OTUs and specifically compiled reference databases. FROGS recommended the use of taxonomic filters in situations of well-known communities, when poorly characterized taxa are of no interest, or if researchers are interested only in some chosen and known taxa. An initial test implementing Blastn+

to assign taxonomy only to the COI dataset using a 96% percent identity threshold (Hebert et al., 2003; Bellec et al., 2018) ejected the majority of the OTUs and reduced the power of statistical analyses. Given this result, as well as our interest in the identities of multiple species in largely unknown and poorly characterized communities, taxonomic thresholds were not implemented at this stage. Additional filters, however, were performed during downstream bioinformatic processing describe below. Further, all resulting assignments produced e-values below 8e-7, while percentage identities were between 72.5 and 100%, with metazoans matches from 85% and above. Reference databases for taxonomic assignment were compiled by retrieving publicly available sequences from the Silva release 132 (Quast et al., 2012) for the 18S fragments and the NCBI GenBank Core Nucleotide, October 2017 release for COI. DNA barcoded taxa from this study were concatenated onto the relevant public reference databases prior to taxonomic assignment.

Additional processing, including filtering, data normalization, total taxa and metazoan specific community composition visualization and statistical analyses of curated data was conducted using the Phyloseq R package (McMurdie and Holmes, 2013) in R Studio v.3.5.1. Briefly, Phyloseq was implemented to examine the overall sequencing depth across samples before and after the removal of non-metazoan taxa to determine if sequencing was sufficient to characterize communities at the time of sampling, as well as normalization via rarefaction without replacement and the filtering of OTUs with fewer than 3 reads per sample. The generation of rarefaction curves and biodiversity analyses were performed within the R vegan package (v2.5-2) (Oksanen, 2015), including the estimation of metazoan species richness for incidence data (Chao 2, Chao and Chiu, 2016).

We sought to explore potential dissimilarities in faunal compositions and diversity between differing treatment factors. Our strategy for comparing communities is based on the experimental design that takes into account (1) habitat type for reference (or "baseline") data (active, periphery and inactive) to test for the influence of vent activity; (2) location in the active area (edifice vs. base) to test for substratum type (sulfide versus slab); (3) collection year (2017 "baseline data" vs. 2018 "recolonization data") to test for the disturbance impact; (4) the presence of cages (2018 cage data vs. 2018 non-caged data) to test for the effect of predators on recolonization patterns. Aided by the vegan package, the role of each factor (habitat, location, year and cages) was tested using Analysis of Similarity (ANOSIM, Clark, 1993), or the *anosim* function, to examine potential differences among communities. In addition, we tested for differences between samples based on a given factor using Permutational multivariate analysis of variance (PERMANOVA, Anderson, 2001), or the *adonis* function, implemented with 999 permutations and the Jaccard distance for pairwise distance between groups to minimize the weight given to absence values. When testing of factors was significant, pairwise comparisons under Bonferroni corrections were done with PAST3 (Hammer et al., 2001). Furthermore, Canonical correspondence analysis (Goldberg et al., 2016) ordination plots were generated using Jaccard distance matrices in Phyloseq to visualize relationships between treatments and identify which environmental factors are most important (Ter Braak and Verdonschot, 1995).

RESULTS

DNA Barcode Database

Morphological inventories identified several taxonomic groups collected from the Montségur edifice; from these, 22 were available in sufficient numbers for DNA barcoding for the present project, which encompassed a total of 144 individuals (**Table 2**). The barcoding effort produced a total of 580 sequences; 318 (55%) of these sequences were amplified from the 18S regions V1V2 and V9, as well as the short COI fragment (313-bp), and were added to their respective taxonomic reference databases, against which the eDNA metabarcoding datasets were assigned. The remaining 262 sequences (45%) were amplified from 28S regions D2D3 and D9D10, 18S region V7V8 and the long COI fragment (500 – 660-bp, **Supplementary Material S1**) and were not added to any reference databases for the present study, as we did not survey eDNA samples using these amplicons. Every sequence, however, has been made publicly available at NCBI GenBank under accession numbers MK591147–MK591726. **Table 2** provides general information for each successfully barcoded taxon using one or more of the gene fragments described in this study, and whether or not the taxon was recovered in the respective eDNA dataset.

eDNA Metabarcoding Datasets

A total of 18 eDNA samples and seven negative extraction controls were sent for metabarcoding using four gene fragments: COI; 18S-V1V2, 18S-V4 and 18S-V9, which will be referred to as V1V2, V4 and V9. None of the negative controls produced amplicons for library preparation, and thus were considered clear of contamination. After bioinformatic filtering, the metabarcoding effort yielded a total of 701,880 sequences for V1V2, 618,384 sequences for V4, 920,241 sequences for V9 and 1,098,025 sequences for the COI datasets. Additional information on sequencing depths for each dataset, mean number of reads per sample and OTU, as well as mean number of OTUs per sample can be found in **Supplementary Figures S1, S2** and **Supplementary Table S1**.

Non-metazoan taxa included archaea, bacteria, fungi, plants (photosynthetic eukaryotes), protists or organisms unknown/unassigned at the phylum level; these non-metazoans comprised between 65.86% (COI) to 93.43% (V9) of all OTUs. **Figure 2** illustrates the top 10 most common taxonomic groups, including non-metazoans, in each dataset, described by percentage of OTUs versus percentage of sequences for each phylum. While taxonomic patterns of OTU percentages were variable among markers, Annelida and Mollusca were clearly represented in each eDNA datasets in terms of high percentage of sequences assigned to few OTUs. Regarding the total number of sequences, Annelida represented 29.8% (V9), 33.1% (V4), 32.7% (COI), and 40.7% (V1V2), while

TABLE 2 | DNA barcode inventory for 22 taxa collected from the Montségur edifice.

Taxon Code	Phylum	Class	Species	Number of individuals	Barcodes amplified	Recovered in eDNA
BS	Annelida	Polychaeta	*Branchipolynoe seepensis*	10	18S (V1V2, V7V8, V9) 28S (D2D3, D9D10) COI	V1V2, V9, COI *V4 (genus)*
AL	Annelida	Polychaeta	*Amphisamytha lutzi*	11	18S (V1V2, V7V8, V9) 28S (D2D3) COI	V1V2, V9, COI
SP	Annelida	Polychaeta	*Prionospio* sp.	5	18S (V1V2, V9) COI	V4, V9, COI
LD	Annelida	Polychaeta	*Lepidonotopodium jouinae*	5	18S (V1V2, V7V8, V9) COI	V1V2, V9, COI
GY	Annelida	Polychaeta	*Glycera* sp.	3	18S (V1V2, V7V8, V9)	V1V2 *V4*, *V9*, *COI (different species)*
BN	Annelida	Polychaeta	*Branchinotogluma* sp.	5	18S (V1V2, V7V8, V9) 28S (D2D3) COI	V1V2, V9, COI, *V4 (different species)*
MF	Arthropoda	Malacostraca	*Mirocaris fortunata*	11	18S (V1V2, V7V8, V9) 28S (D9D10) COI	V1V2, V9, COI
CP	Arthropoda	Hexanauplia	Unidentified copepod taxa	5	18S (V7V8, V9) 28S (D2D3) COI	V9, COI
AP	Arthropoda	Malacostraca	*Luckia striki*	5	18S (V7V8, V9) 28S (D2D3) COI	V9, COI
OST	Arthropoda	Ostracoda	Unidentified ostracod taxa	5	18S (V7V8, V9) 28S (D2D3)	V9
SM	Arthropoda	Malacostraca	*Segonzacia mesatlantica*	1	18S (V1V2, V7V8, V9) 28S (D2D3) COI	V9, COI
AT	Cnidaria	Anthozoa	Unidentified zoanthid taxon	5	18S (V1V2, V7V8, V9) 28S (D2D3)	V1V2
SK	Mollusca	Gastropoda	*Divia briandi*	5	18S (V1V2, V7V8, V9) 28S (D2D3)	V1V2, V9
LX	Mollusca	Gastropoda	*Lirapex* sp.	5	18S (V1V2, V7V8, V9) 28S (D2D3) COI	V1V2, V9, COI
PT	Mollusca	Gastropoda	*Paralepetopsis ferrugivora*	5	18S (V1V2, V7V8, V9) 28S (D2D3) COI	V9, COI
BA	Mollusca	Bivalva	*Bathymodiolus azoricus*	10	18S (V1V2, V7V8, V9) 28S (D2D3, D9D10) COI	V1V2, V4, V9, COI
LA	Mollusca	Gastropoda	*Lepetodrilus atlanticus*	10	18S (V1V2, V7V8, V9) 28S (D2D3) COI	V1V2, V9, COI, *V4 (different species)*
PV	Mollusca	Gastropoda	*Protolira valvatoides*	10	18S (V1V2, V7V8, V9) 28S (D2D3) COI	V1V2, COI *V4, V9 (genus)*
PM	Mollusca	Gastropoda	*Pseudorimula midatlantica*	10	18S (V1V2, V7V8, V9) 28S (D2D3) COI	V1V2, V9, COI
LV	Mollusca	Gastropoda	*Lurifax vitreus*	10	18S (V1V2, V7V8, V9) 28S (D2D3) COI	V1V2, V9, COI
EV	Mollusca	Gastropoda	*Laeviphitus desbruyeresi*	3	COI	COI
NEM	Nematoda	Unknown	Unidentified nematode taxa	5	18S (V7V8, V9) 28S (D2D3)	V9

Taxon code is followed by known taxonomy and the number of individuals barcoded. A list of fragments ("barcodes") successfully amplified for each taxon is provided by gene. Finally, the gene fragment is listed for a taxon if it was recovered within the respective eDNA dataset. Italicized gene fragments indicate that for these eDNA datasets, the taxon uncovered was either only the genus, or a different species. "Unidentified" indicates that our morphological expertise was only able to identify the collected individuals at the time of this study to the following groups: Zoanthid, Copepod, Ostracod, and Nematode. NCBI BLAST results for these unidentified taxa were as follows: colonial anemone (Order: Zoantharia), Ostracod (Family: Pontocyprididae), Copepod (Family: Dirivultidae), Nematode (Genus: Oncholaimus).

Mollusca represented 17.3% (V4), 35% (V9), 37.1% (V1V2) and 37.6% (COI). For V1V2 and V4, the majority of OTUs originated from Protista, although the percentage of sequences comprising these OTUs was much smaller, suggesting the presence of many distinct species (**Figure 2**). Within V4, however, many OTUs were unknown/unidentified, though they were only a small proportion of total sequences. Further, the V9 fragment dataset uncovered a high percentage of OTUs and sequences assigned to Bacteria and other non-metazoans (**Figure 2**). COI identified the most OTUs assigned to Arthropoda, compared to few OTUs originating from Annelida and Mollusca, comprising nearly two-thirds of all sequences in this dataset. As with the V4 dataset, unknown/undefined assignments dominated a large percentage of OTUs within COI.

The 18S fragments uncovered Nematoda and Platyhelminthes within the top 10 most common taxonomic groups, while COI identified Chordata, Cnidaria and Porifera. After non-metazoan taxa were filtered from each dataset, metazoan OTUs numbered 414 for V1V2, 304 for V4, 291 for V9 and 560 for COI. Unless otherwise stated, the proceeding results are primarily concerned with these metazoan datasets.

Common Metazoans Uncovered in eDNA From Montségur

Every metazoan taxon that underwent DNA barcoding was recovered in the global environmental DNA dataset of four markers (**Table 2**). This included taxa not yet identified to the species level, such as zoanthids (colonial anemones), copepods, ostracods and nematodes (**Table 2**). In addition, nearly all taxa identified to the genus or species level were found within the eDNA dataset for which they had been successfully barcoded. Exceptions were *Paralepetopsis ferrugivora* and *Prionospio* sp., which despite being barcoded for V1V2, were not identified within that eDNA dataset, as well as the unidentified zoanthid taxon, found only in V1V2, and not in V9 eDNA (**Table 2**). *Bathymodiolus azoricus* was the only barcoded species present in every eDNA dataset. Furthermore, *Protolira valvatoides* gastropods and *Glycera* sp. polychaetes either matched to the

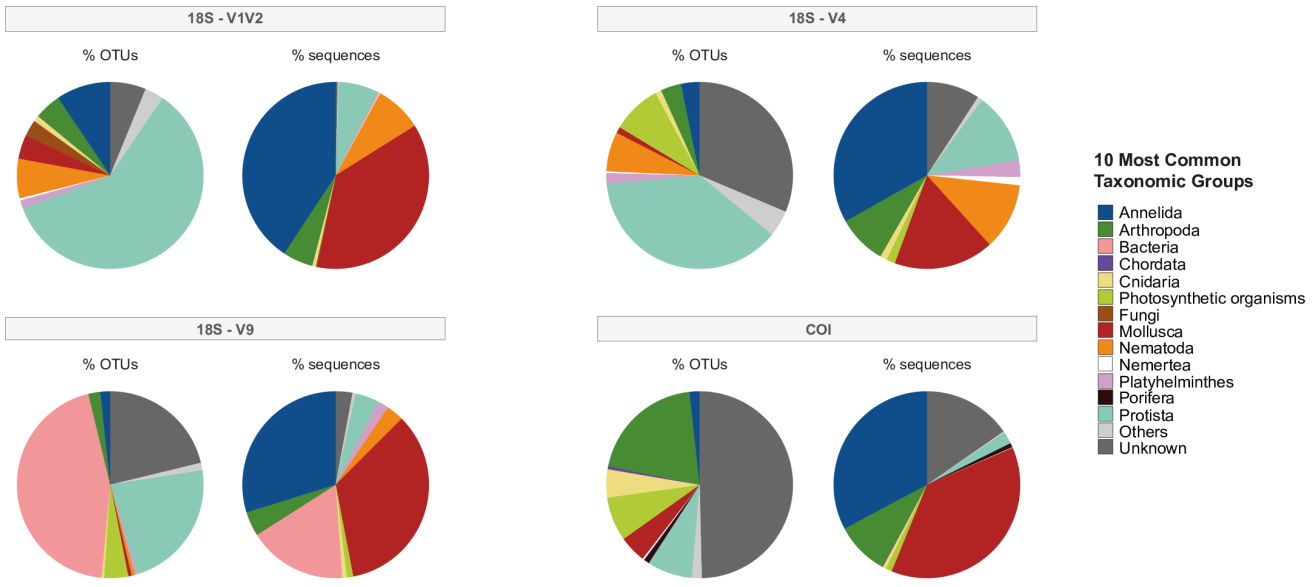

FIGURE 2 | The top 10 most common taxonomic groups, including non-metazoans, from the global eDNA sequencing effort for the four eDNA datasets. Percentage of OTUs refers to the proportion of OTUs ("species") originating from each phylum and percentage of sequences ("abundance") refers to the proportion of reads originating from each phylum.

genus level (*Protolira* sp.) or to a particular species (*Glycera capitata* or *tesselata*), despite being DNA barcoded.

The top 10 most common species, in terms of sequence abundance, for the V1V2 and COI datasets are shown in **Figure 3**. Each graph identifies expected species (those collected from Montségur and DNA barcoded, see **Table 2**) and additional species. "Additional" species are those not barcoded by us, yet present within the Silva or NCBI public databases, some of which are not known from hydrothermal vents (**Figure 3**, non-bold). The top 10 most common species uncovered within the V1V2 dataset are all found at vents; however, the "non-vent species" for V4, V9 and COI datasets represented only 4.5, 7.3, and <2%, of these sequences, respectively (**Figure 3** and **Supplementary Figure S3**). The V1V2 dataset found that expected species *Amphisamytha lutzi, Bathymodiolus azoricus,* and *Branchinotogluma* sp. comprise the majority of metazoan sequences. Oncholaimidae sp., a family of nematodes whose members are found in aquatic sediments world-wide including at LS, is the next most abundant group in this dataset (**Figure 3**), supporting the presence of local vent nematode species matching to this family. The COI dataset identified expected species *A. lutzi*, *Branchinotogluma* sp., *Protolira valvatoides, Mirocaris fortunata,* and *Lepetodrilus atlanticus* dominating metazoan abundance, while sequences assigned to *Hesiolyra* cf. *bergi*, an hesionid polychaete known from hydrothermal vents in the eastern Pacific (Blake, 1985), represents another common species in the dataset. While expected species such as *B. azoricus*, *Branchinotogluma* sp., *Branchipolynoe seepensis* and *P. valvatoides* are some of the most abundant within the V4 dataset, there are few species not expected from Montségur (including non-vent taxa, **Supplementary Figure S3**). Finally, for the V9 dataset, the majority of metazoan sequences were assigned to expected species *B. azoricus*, *A. lutzi* and *B. seepensis* (**Supplementary Figure S3**).

Baseline Data: Effect of Habitat (Venting Influence) and Location

Baseline accumulation curves for V1V2 highlight differences between communities based on habitat/venting influence (**Figure 4**). When considering all taxa, peripheric and inactive sites exhibit much higher OTU counts compared to active sites at Montségur, with no difference seen between structure and base communities (**Figure 4**, top left). A similar pattern is seen with COI (**Figure 5**, top left), as well as within the other markers (**Supplementary Figures S4, S5**). Curves for all "baseline" taxa begin to reach plateau with increasing number of sequences, identifying that the sequencing depth was effective for characterizing most of the diversity present within each sample originating from the differing habitats. Upon considering baseline metazoan taxa only, a contrasting picture emerges: periphery and inactive sites are more similar to active sites in terms of OTUs counts for V1V2 (**Figure 4**, bottom left), V4 and V9 (**Supplementary Figures S4, S5**), although the initial slope of the curves remains steeper for inactive sites. The exception is COI, in which higher metazoan diversity is maintained for inactive, compared to peripheric and active sites (**Figure 5**, bottom left). Noting the differing graphic scales for baseline data between all taxa and metazoans-only, comparisons between the two clarify that much of the diversity recovered from the inactive habitat is non-metazoan taxa, though V1V2 and COI also identify similar or even higher levels of metazoan diversity at inactive sites, comparative to the other habitats (**Figures 4**, **5**). These patterns are supported by estimated OTU

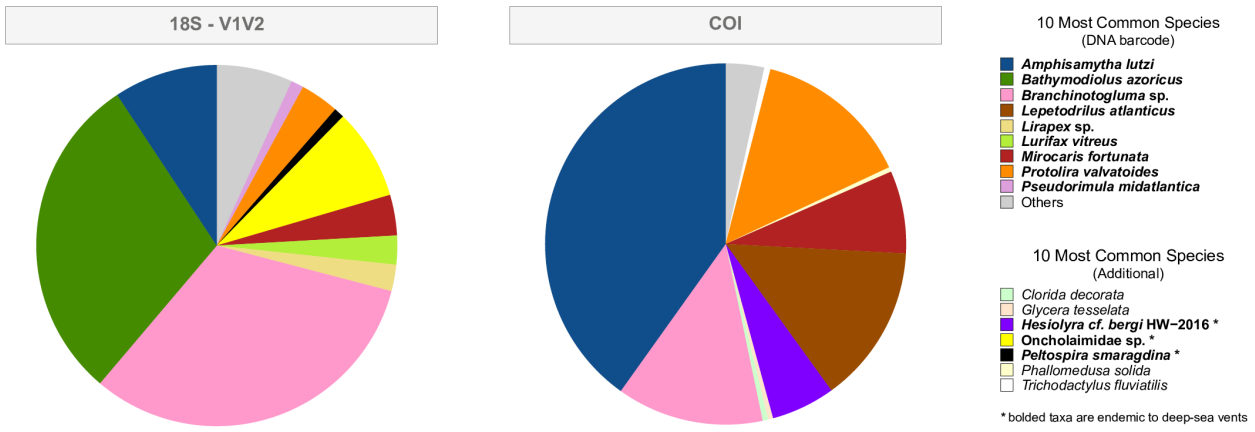

FIGURE 3 | The top 10 most common species, in terms of sequence abundance, for the 18S-V1V2 and COI eDNA datasets. "DNA barcode" are those species that were physically collected from Montségur and DNA barcoded in the current project (**Table 1**). "Additional" are species that were not DNA barcoded by the present project yet were within the NCBI GenBank database prior to the taxonomic assignment of eDNA. Species in bold are those found at hydrothermal vents, while non-bolded species are not found at hydrothermal vents. The presence of these non-vent assignments suggests that these sequences were assigned to the closest taxon within the database, and not that these non-vent species are present in the deep-sea.

richness (**Table 3**), which varied depending on the habitat and location. Notably, the COI dataset identifies the inactive site as having the highest number of OTUs at 321 and an estimated OTU richness of 484.8 $\pm$ 30.5, compared to the other habitats (**Table 3**). The 18S datasets, however, show contrasting values, with active sites, particularly the base of Montségur, as having higher estimated OTU richness than the structure itself, the periphery or inactive sites.

ANOSIM testing revealed that the habitats host significantly different metazoan communities, a pattern seen across all four eDNA datasets (**Table 4**). Habitat differentiation based on community is spatially illustrated by the CCA ordination for V1V2 and COI in **Figure 6**, as well for V4 and V9 in **Supplementary Figure S6**. With 26.3–35.5% of taxonomic variation explained within the two axes, habitat is supported as the most important factor influencing taxonomic composition and distance away from or toward active sites determines composition (**Figure 6**). PERMANOVA testing was also significant for the habitat factor, supporting a lack of homogeneity of communities among the habitat sample groups (**Table 4**). Pairwise comparisons between the differing habitats identified the strongest distinction between active and inactive sites ($p < 0.05$). Following the location factor that compares Montségur structure and base active communities, statistical analyses reveal dissimilarities among these communities from V4 and V9 datasets, though PERMANOVA testing suggest weak effects of this factor, as does the unclear separation of communities shown in **Supplementary Figure S6**. The dissimilarities between structure and base communities, however, are most strongly supported within the V9 dataset (**Table 4**).

Examining taxonomic composition identified specific differences in metazoan composition across habitats, samples and eDNA datasets. Higher numbers of OTUs assigned to Annelida were found at active locations, compared to inactive sites, which was true for all datasets (**Figure 7** and **Supplementary Figure S7**). However, fewer OTUs originating from Arthropoda were observed at active sites, compared to the non-active sites. Higher numbers of OTUs assigned to Cnidaria, Echinodermata and Porifera were observed within the COI dataset, specifically within periphery and inactive samples, compared to 18S (**Figure 7**). Conversely, 18S markers identified higher numbers of OTUs from Nematoda, particularly V1V2 (**Figure 7**, left) and V4 (**Supplementary Figure S7**). Furthermore, the 18S datasets uncovered less well studied meiofaunal taxa, such as Xenacoelomorpha at peripheric and inactive sites within V1V2 and V9, as well as Gastrotricha and Kinorhyncha from V4 and V9 (**Supplementary Figure S7**).

Recolonization Processes: Effect of Time and Cages

Accumulation curves comparing 2017 "baseline" samples with 2018 caged and uncaged samples identified similar trajectories for these communities, across all datasets (**Figures 4**, **5** and **Supplementary Figures S4, S5**). Considering all taxa, the curves for each dataset begin to level into a plateau shape, but still indicating that additional diversity remains undescribed (**Figures 4**, **5**, top right). When focusing on only metazoan taxa, we observed no specific pattern of differentiation between years or cage presence (**Figures 4**, **5**, bottom right). Estimated OTU richness is consistently higher in 2018 active communities compared to 2017 active communities, while non-caged communities have higher richness compared to those that were caged, a finding seen across all eDNA datasets (**Table 3**).

The lack of community differentiation depending on time and predation factors seen in **Figures 4**, **5** was also supported by statistical testing (**Table 4**). In terms of taxonomic composition, no strikingly different patterns based on sample or treatment are observed, though the COI dataset uncovered higher numbers of OTUs originating from Cnidaria and Mollusca across

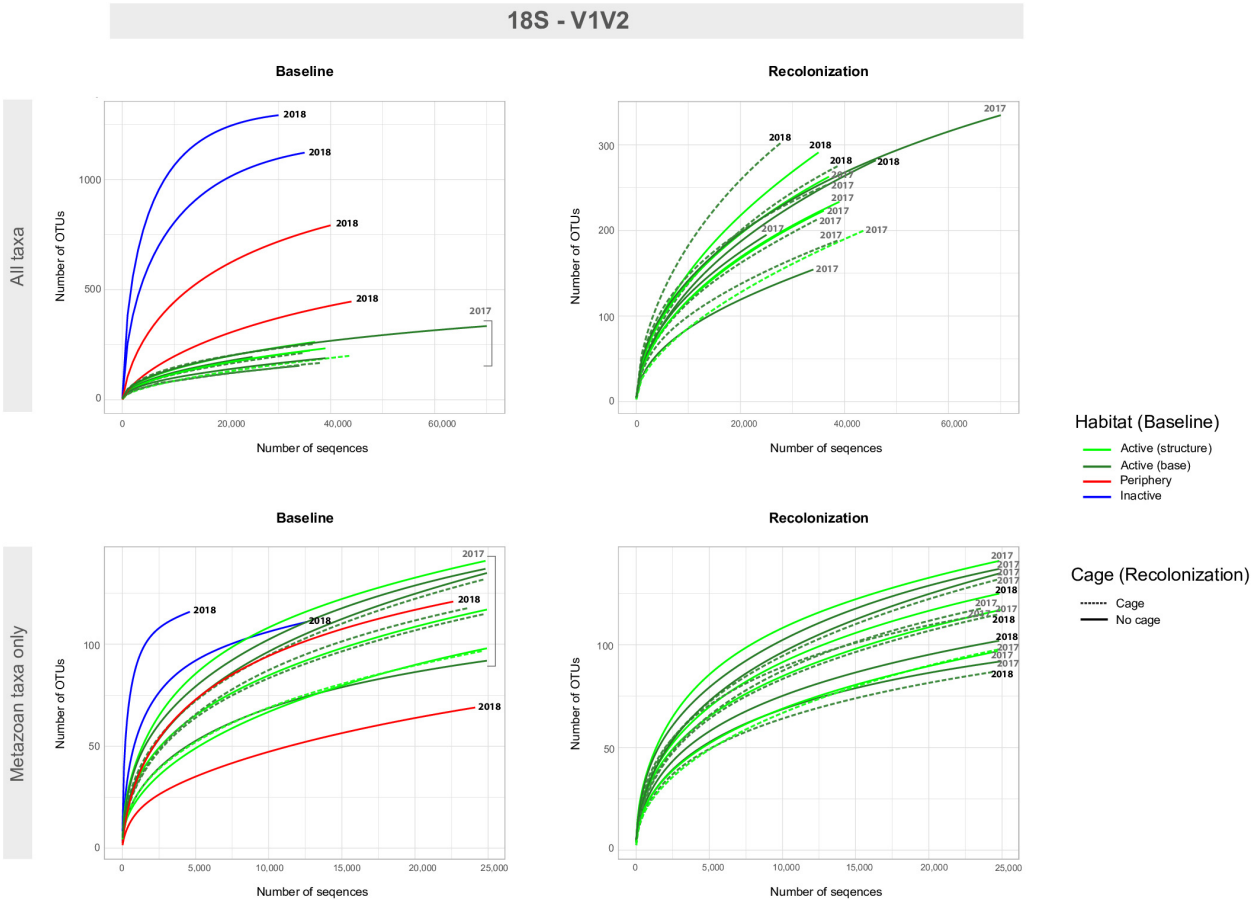

FIGURE 4 | Accumulation curves for the 18S-V1V2 eDNA dataset, for both baseline **(left)** and recolonization **(right)** data across all taxa (non-metazoans and metazoans, **top**) and metazoan taxa only **(bottom)**. Baseline data focuses on sample communities from differing habitats/vent activity, as well as those from differing locations on the active edifice (base and structure). Recolonization data focuses on sample communities from differing years, as well as those that were caged against those non-caged at active sites. Note the difference in scales for number of OTUs and number of sequences between "All taxa" and "Metazoan taxa only." Recolonization data are only available for the active sites.

sample years, while 18S genes were still better at uncovering animal groups known from the meiofaunal compartment (**Supplementary Figure S8**). Overall, the characterization of communities across the time and cage treatments, using several gene fragments originating from mitochondrial and nuclear genes, identified a similar community composition after one year of passive recolonization.

DISCUSSION

The present study offers a broad taxonomic characterization of LS *Bathymodiolus* assemblages and their associated macro- and meiofaunal communities, present along an environmental gradient from an active sulfide edifice, to a more distant, inactive zone. We also provide original findings from an *in-situ* experiment and monitoring effort for tracking faunal recolonization at an active hydrothermal vent edifice located within the LS vent field (MAR). For this, we implemented the normally less intrusive environmental DNA (eDNA) metabarcoding method for comparing community temporal changes following the induced disturbance. Our protocol for processing hydrothermal vent material produced a comprehensive eDNA dataset composed of information from four genetic markers and encourages replication along a longer temporal scheme, as well as for future, unrelated survey efforts.

Seafloor Massive Sulfides (SMS) and Benthic Assemblages Along an Environmental Gradient

The International Seabed Authority reports that commercial interest in seafloor massive sulfides (SMS) is expected to occur in the near future, with calls for the establishment of environmental baseline data (Juniper, 2002; ISA, 2010). Using a new approach that allows for quick assessment of taxonomic biodiversity, our results contribute to fulfilling these recommendations by providing a consistent taxonomic richness comparison along a gradient of venting influence. Our eDNA analyses of substratum samples, retrieved from an inactive location where conspicuous

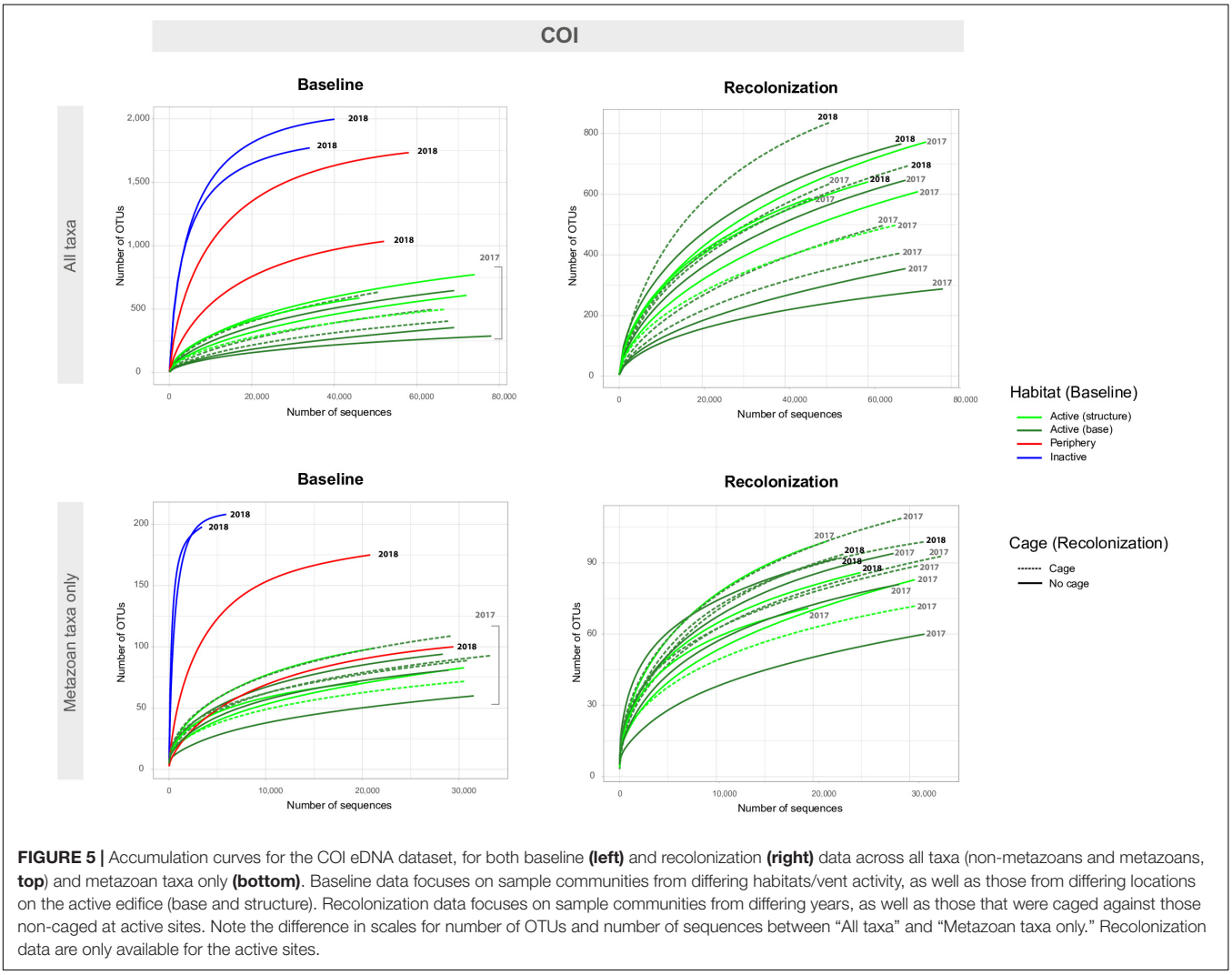

FIGURE 5 | Accumulation curves for the COI eDNA dataset, for both baseline **(left)** and recolonization **(right)** data across all taxa (non-metazoans and metazoans, **top**) and metazoan taxa only **(bottom)**. Baseline data focuses on sample communities from differing habitats/vent activity, as well as those from differing locations on the active edifice (base and structure). Recolonization data focuses on sample communities from differing years, as well as those that were caged against those non-caged at active sites. Note the difference in scales for number of OTUs and number of sequences between "All taxa" and "Metazoan taxa only." Recolonization data are only available for the active sites.

fauna were not observed, revealed genetic signals from Cnidaria, Porifera, Mollusca and Nematoda. Inactive zones are known for low biomass assemblages of long-lived, slow growing suspension feeders and scavengers, including sponges, cnidarians (hydroids, corals and anemones) and echinoderms. These communities are referred to as "background fauna," as they are non-vent specialists that can be found in differing habitats on the seafloor (Levin et al., 2009, 2016; Collins et al., 2012). A third and relatively unknown community consisting of endemic fauna inhabiting inactive zones is also suspected, possibly having nutritional dependencies linked to weathering inactive sulfide deposits (Van Dover, 2011; Boschen et al., 2013). Assemblages in inactive zones are far less studied than their active counterparts (Juniper, 2002), yet the possibility of inactive zones being the primary target of lucrative prospective initiatives makes these slow-growing communities especially vulnerable (Hoagland et al., 2010; Gollner et al., 2017). To date, there is an absence of information on recovery potential or resilience of inactive SMS communities and further investigations are warranted to fill these gaps in our knowledge.

Our analyses uncovered distinct differences between communities inhabiting active and inactive zones at LS, as well as high levels of estimated OTU richness associated with active periphery and inactive sites. These findings are in line with those on macrofaunal communities at some Pacific SMS locations, including those sites proposed for mining off of Papua New Guinea (Manus Basin) and New Zealand (Levin et al., 2009; Collins et al., 2012; Boschen et al., 2016), as well as meiofaunal (nematode) communities off of Fiji (Vanreusel et al., 1997). Results suggest that inactive sites at LS are highly diverse compared to their active counterparts, and that the metazoans and non-metazoans at these locations may have several origins. Those organisms not found at active sites possibly represent a combination of background organisms, pelagic organisms that settled from the surface to the seafloor and unclassified communities suspected to be endemic to inactive SMS habitats. Additionally, more accurate information on levels of diversity in these habitats may come from a more thorough analysis of protists. Deep-sea protists, specifically foraminifera, have been found to be important for structuring metazoan communities

TABLE 3 | Metazoan species richness values of baseline and recolonization data for the four eDNA datasets.

		18S-V1V2		18S-V4		18S-V9		COI	
Baseline									
Habitat	*N*	OTUs	*Chao2 ± SE*	OTUs	*Chao2 ± SE*	OTUs	*Chao2 ± SE*	OTUs	*Chao2 ± SE*
Active: Structure$_{(2017)}$	4	224	310.0 ± 22.7	140	173.1 ± 12.1	177	254.8 ± 23.3	164	195.2 ± 10.3
Active: Base $_{(2017)}$	6	251	313.2 ± 18.4	168	213.2 ± 15.9	181	215.7 ± 12.6	179	202.3 ± 9.0
Periphery $_{(2018)}$	2	149	220.1 ± 19.5	128	187.0 ± 17.5	152	185.9 ± 10.2	227	393.9 ± 37.0
Inactive $_{(2018)}$	2	164	204.5 ± 11.5	111	132.8 ± 7.8	132	147.0 ± 5.7	321	484.8 ± 30.5
Recolonization									
Year	*N*	OTUs	*Chao2 ± SE*	OTUs	*Chao2 ± SE*	OTUs	*Chao2 ± SE*	OTUs	*Chao2 ± SE*
Active $_{(2017\ baseline)}$	4	206	236.3 ± 10.0	155	189.6 ± 11.8	163	192.4 ± 10.6	175	213.6 ± 12.4
Active $_{(2018\ after\ recolonization)}$	4	220	312.6 ± 24.1	158	230.0 ± 21.8	181	249.5 ± 20.9	189	242.1 ± 15.5
Recolonization									
Predation	*N*	OTUs	*Chao2 ± SE*	OTUs	*Chao2 ± SE*	OTUs	*Chao2 ± SE*	OTUs	*Chao2 ± SE*
Cage $_{(2018)}$	2	148	189.0 ± 12.0	105	124.0 ± 7.1	124	151.4 ± 9.1	140	175.7 ± 10.9
No-cage $_{(2018)}$	2	170	226.0 ± 15.0	114	156.2 ± 13.5	148	172.5 ± 7.9	137	193.2 ±16.3

The experimental variables listed under baseline and recolonization are followed by the collection year of the samples, in parentheses. N refers to the number of samples analyzed within the specific variable, and OTU refers to the number of operational taxonomic units recovered within those samples. The value following ± indicates the standard error of Chao2 metric.

and are associated with high eukaryotic richness (Levin, 1991; Lecroq et al., 2009). Within our eDNA survey, protists represent a substantial number of OTUs across all four gene marker datasets (**Figure 2**) but lack investigation in active and inactive vent environments. Integrating protist taxonomic information with that of metazoans would likely reveal previously unknown information about biodiversity patterns in the vicinity of vents.

Recolonization at Montségur

Abiotic and biotic factors are responsible for driving colonization at vents. As this experiment was an artificial clearance of vent fauna, there were no significant changes in abiotic conditions such as fluid flow or chemistry that often accompany natural disturbance events. Thus, for the purposes of this project, the intensity of the induced disturbance could be classified as minor, as it consisted of small localized changes (at scale of centimeters) as opposed to a large-scale activities (at scale of hundreds of meters) projected to occur during mining activities (Van Dover, 2014). We therefore focus primarily on the role of biotic interactions on recolonization processes.

Contrary to what was expected, the exclusion of predators led to a lower taxonomic richness in our samples than for the uncaged experiments; though using the eDNA approach, we saw no significant difference between the two treatments after 13 months (**Table 4**). Several temporal studies have shown that in addition to environmental conditions, facilitation, competition and predation would trigger successional processes at vents (Sarrazin et al., 1997; Shank et al., 1998; Micheli et al., 2002; Mullineaux et al., 2003). Here, the lower values can be due to the influence of the cage that could have blocked the settlement of certain species. Micheli et al. (2002), through the deployment of caged and uncaged recruitment substrata, found that the exclusion of predators enhanced taxonomic richness. Their experiment, however, lasted less than a year (i.e., 5 and 8 months) and the authors used a smaller mesh size for the cages (6 mm). It is thus possible that our larger mesh size (10 mm) did not exclude the full range of possible predators on new recruits. As an example, gastropods are known to graze on new recruits (Mullineaux et al., 2003) and are often smaller than a centimeter. We also suspect that the cages used were not as effective as we thought, as a fish was found in one of them upon returning to the experiment. The addition of a skirt in the 2018 experiment should help better seal the cage to the substratum.

The 2018 recolonization samples proved to have slightly higher species richness than prior to the disturbance, possibly recruiting from adjacent populations, but these differences were not statistically significant. Indeed, recolonization is possible at active sites as a result of migration of mobile adults from nearby

TABLE 4 | ANOSIM and PERMANOVA statistical results for testing baseline and recolonization data.

Dataset	Baseline		Recolonization	
	Factor: Habitat	***Factor: Location***	***Factor: Year***	***Factor: Predation***
ANOSIM				
18S - V1V2	0.001** (0.973)	0.074 (0.266)	0.322 (0.094)	1.000 (−0.750)
18S - V4	0.002** (1.000)	0.215 (0.091)	0.969 (−0.240)	0.667 (0.250)
18S - V9	0.001** (0.906)	0.003* (0.560)	0.189 (0.099)	1.000 (−0.500)
COI	0.001** (0.997)	0.147 (0.191)	0.700 (−0.073)	0.667 (0.000)
PERMANOVA				
18S - V1V2	0.001** (3.047)	0.141 (1.283)	0.299 (1.109)	1.000 (0.841)
18S - V4	0.002** (3.494)	0.037* (1.328)	1.000 (0.674)	0.333 (1.205)
18S - V9	0.002** (2.633)	0.023* (1.712)	0.132 (1.267)	1.000 (0.894)
COI	0.003** (3.643)	0.123 (1.243)	0.460 (1.072)	0.667 (0.943)

*Significance value is followed by R-value (ANOSIM) or F-value (PERMANOVA) in parentheses to denote level of influence of factors. **Significant at 0.005; *significant at 0.05.*

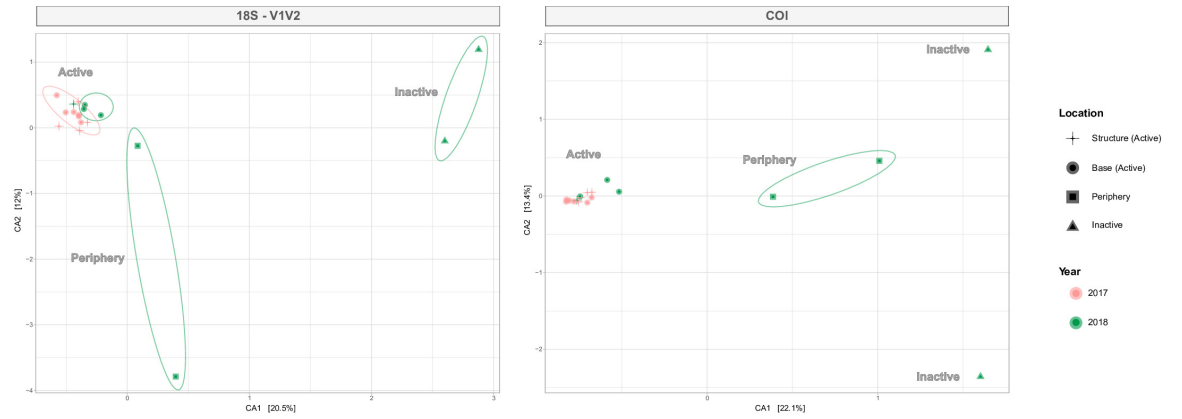

FIGURE 6 | Canonical correspondence analysis (CCA) plots for 18S-V1V2 and COI, illustrating metazoan community distributions by active, periphery or inactive habitats. Shapes denote habitat type and location (active only) and the number of shapes corresponds to the number of eDNA samples retrieved from each habitat. Colors refer to year and ellipses identify the relationships within habitats. The environmental gradient moves from right to left with increasing level of venting influence.

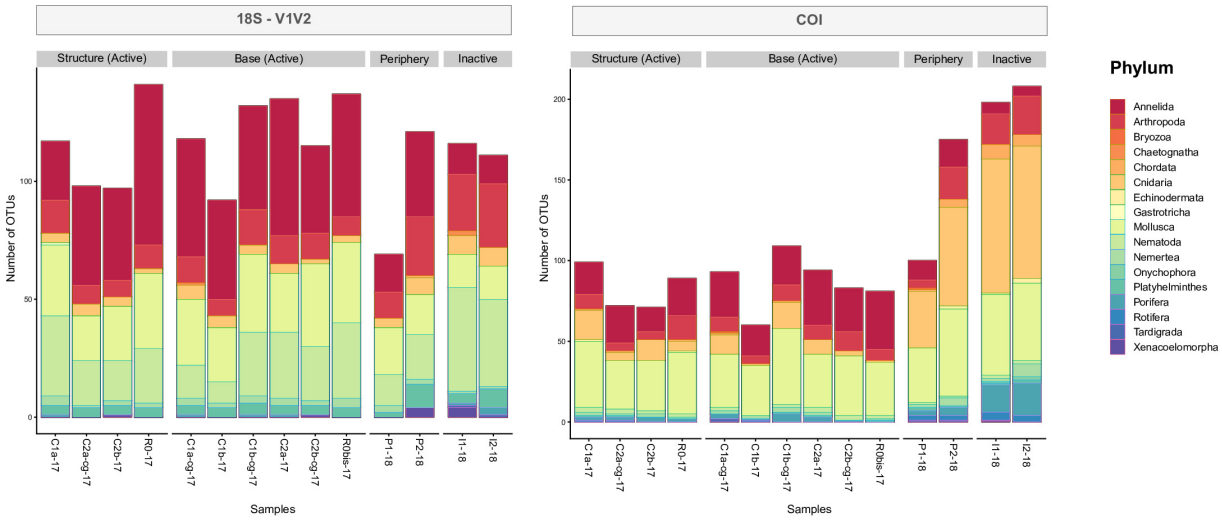

FIGURE 7 | Taxonomic characterizations of 18S-V1V2 and COI eDNA datasets by phylum, based on number of OTUs (incidence) and identified from samples distributed around the active edifice, periphery and inactive sites.

sites, though primarily from the dispersing local larval pool (Mullineaux, 2014). These metapopulations may also be at risk of destruction in case of large-scale mining, limiting recolonization capabilities, especially if the other populations are too far away to replenish impacted sites (Juniper, 2002; Mullineaux et al., 2018). It is possible that the newly recruited community is more diverse upon settlement and that taxa are lost over time in response to competition for space and/or food, and predation (e.g., grazing) (Micheli et al., 2002; Mullineaux et al., 2003; Sancho et al., 2005). Our present eDNA results, however, may not provide the most accurate results in terms of tracking recolonization, as abundance data from physical sampling show a severe decrease in abundance from 2017 to 2018 (Marticorena et al., unpublished). This suggests that eDNA metabarcoding of hard substrata alone is not suitable for monitoring temporal changes in faunal communities after a disturbance at smaller spatial scales.

After the clearance effort, few animals remained within some quadrats, especially in small factures, given the difficulties of removing every single animal in such rough topographies with submersible sampling tools (**Figure 1**). The presence of these individuals may have had an effect on the statistical lack of difference in terms of recolonization. Indeed, at the scale of our study and with the current technology (ROV sampling tools), it is nearly impossible to effectively clean all DNA from a small surface and therefore, remaining animals and persisting extracellular DNA may create false positive detections at sample sites with surveys using presence/absence criteria, such as eDNA (Chambert et al., 2015). More precise diversity assessments of these habitats would require coupling eDNA data with (1) traditional surveys where animals were physically collected, morphologically identified and counted, which is currently ongoing (Marticorena et al., unpublished)

and (2) models that estimate the probability of detecting OTUs present (site occupancy detection models [SODM], Guillera-Arroita et al., 2017) which can account for both false positive and negative detection errors (MacKenzie et al., 2002; Chambert et al., 2015), especially in eDNA studies (Ficetola et al., 2015; Lahoz-Monfort et al., 2016; Guillera-Arroita et al., 2017). At present, we focused on extracting eDNA from substratum, which would be the primary type of media to be removed by mining activities. However, the simultaneous collection and comparison of substrate and water samples as a "double-eDNA" survey would likely improve detection probabilities of taxa. Further, with the exception of the peripheral site, our sample substrata weights were similar across habitats (**Table 1**). Nevertheless, differing sample weights may influence OTUs detection (Wei et al., 2018) and therefore, we suggest improved standardization for future studies. Given these findings, this molecular approach appears to be better suited over longer term investigations and at the larger scales of industrial mining, which would potentially affect hundreds of square meters of seafloor.

At Montségur, no significant difference was observed between the composition and diversity of communities of each active location (i.e., base and edifice). This supports the use of these data as "baseline" information in terms of diversity and community composition, as the presence of historical baseline data is important for assessing the magnitude of future recovery attempts (Lotze et al., 2011). Finally, the baseline data obtained for the periphery and inactive sites in 2018 encourage the analysis of additional samples along longer temporal scales to assess their recovery potential compared to active areas.

Benefits and Limitations of eDNA Metabarcoding at Hydrothermal Vents

The success of environmental DNA over the last several years is in part due to its ubiquity in the environment: animals continuously expel DNA into their surroundings and this genetic material is freely available to be collected and analyzed (Thomsen and Willerslev, 2015). There are many benefits for extending this approach to deep-sea ecosystems. Indeed, this environment is logistically challenging to sample, requiring the use of submersibles – most notably Human Occupied Vehicles (HOVs) and Remotely Operated Vehicles (ROVs). Historically, biological studies at depth have been performed by video streams and physical sampling of animals which require the observation of whole animals for identification (Cuvelier et al., 2009, 2012). In addition, sampling protocols related to the use of vehicles to collect animals, combined with the fastidiousness of animal sorting and identification, still result in the oversight of organisms that are small, rare or transient (Gauthier et al., 2010). Conversely, eDNA does not require whole animals and provides a mix of genetic information from even the smallest organisms that can be collected through bulk sampling and preserved for later sequencing and informatic-based taxonomic assignment. eDNA processing also lends itself more easily to technical standardization compared to methods dependent upon sorting of complex samples and taxonomic expertise, the later becoming a major issue as the number of skilled experts decreases (Hebert et al., 2003; Bohmann et al., 2014). Once baseline studies are established and protocols optimized, eDNA has the potential to be less costly and less-destructive than physical sampling (Rees et al., 2014; Sigsgaard et al., 2015), which is particularly important for conservation studies that seek to track re-establishment of previously impacted populations. eDNA also contributes to increasing the amount of information on habitat diversity while augmenting bio-inventories (Bohmann et al., 2014), useful for poorly studied habitats, such as deep-sea active and inactive hydrothermal vents.

The application of eDNA for characterizing metazoan communities is still relatively new and making rapid advances. There are, however, still several limitations to the method that require resolving that accompanies continued development. First, eDNA is most accurate when focusing on incidence data (presence/absence), given the number of times that a sequence is observed can be influenced by factors other than the abundance of taxa (i.e., number of biological cells present, the physical parameters of the local environment, etc.) (Lacoursière-Roussel et al., 2016). In this context, morphological approaches that require observation and/or physical collection of individuals can provide more precise estimates of abundance, as well as the ability to distinguish between living and dead animals, various life stages and sexes (Rees et al., 2014; Thomsen and Willerslev, 2015). While primarily focusing on a single or few species, some studies have already successfully linked eDNA concentrations with abundance in the form of biomass, organismal density or both (Lacoursière-Roussel et al., 2016; Yamamoto et al., 2016; Doi et al., 2017).

Furthermore, total DNA in the environment (hard and soft substrata) includes intracellular DNA that originates from living cells and extracellular DNA that originates from cell lysis (Pietramellara et al., 2009). Upon being released, extracellular DNA can persist in the environment after an organism is no longer present, possibly impacting the accuracy of eDNA biodiversity surveys (Corinaldesi et al., 2011; Dejean et al., 2011), although more recent research has shown that under certain conditions, extracellular DNA has a surprisingly minimal effect on genetic estimates of taxonomic and phylogenetic diversity (Lennon et al., 2018; Torti et al., 2018). In attempts to improve the efficiency of molecular methods for detecting living communities, as well as provide more accurate assessments of biodiversity over time, studies have used treatments during the DNA extraction phase to separate intra and extracellular DNA within environmental samples (Wagner et al., 2008; Taberlet et al., 2012b; Seidel et al., 2017). Additional strategies have extracted eRNA of microorganisms, as eRNA is less stable and degrades more rapidly than eDNA and can thus improve biodiversity assessment of contemporary communities (Barnes and Turner, 2016; Pochon et al., 2017; Laroche et al., 2018; Brandt et al., 2019). Next, the incompleteness of public databases used for taxonomic assignment during high-throughput sequencing projects, as well as the selection of genetic markers, heavily influence eDNA studies. Gaps in databases will continue to be a limitation for habitats where communities are not well characterized to the species level (Thomsen and Willerslev, 2015), though repositories are rapidly expanding (Porter and Hajibabaei, 2018). In our

case, some taxa denoted as "common" correspond to species not found in the deep sea or at hydrothermal vents. When taxa are poorly represented or absent in the database, sequences may have no match or may match to the nearest relative that has more abundant and available data (Dayrat, 2005; Kvist, 2013). The presence of non-vent assignments in our datasets suggests that sequences were assigned to the closest taxon within the database and not that these "non-vent species" are present in the deep-sea. Alternatively, our bioinformatic assignment protocol may not have been optimal for finding the best matches present. To address these shortcomings, the best strategy includes the continued inclusion of well curated data from hydrothermal vent and deep-sea fauna into public inventories, to which we have contributed in the present study via our barcoding efforts. Furthermore, the use of a standardized bioinformatic pipeline targeting poorly surveyed marine habitats that outlines specific parameters and filters would allow more precise and uniform results and this effort is currently underway (Brandt et al., 2019). These outcomes also emphasize the importance of collaborative efforts of morphological and molecular approaches, at least during the initial stages of community characterization (Cowart et al., 2015).

Finally, challenges for finding optimal metabarcoding markers for the simultaneous characterization of several taxonomic groups are partially linked to differing rates of evolution across animals and the lengths of amplicons (Hebert et al., 2003; Epp et al., 2012; Sinniger et al., 2016). Notably, some fragments of the 18S SSU ribosomal RNA (18S) exhibit uneven phylogenetic resolution across taxonomic groups and have difficulties disentangling taxa at the genus and species levels when compared to lesser conserved mitochondrial markers (Tang et al., 2012; Wu et al., 2015). Additionally, smaller amplicons, termed "mini-barcodes," often provide taxonomic information for samples containing highly degraded DNA (Meusnier et al., 2008; Barnes et al., 2014) but in some cases, may be too short to be phylogenetically informative. The marker 18S-V9 was chosen due to its short amplicon length and availability of primers, yet the 18S-V9 dataset primarily uncovered taxa of non-interest such as Bacteria (**Figure 2**), possibly as a result of both its conservation and size. Thus, for environments where community composition remains largely unknown, such as deep-sea vents, future studies could instead employ less conserved mitochondrial mini barcodes, such as the COI-mini barcode proposed by Günther et al. (2018).

In comparison, the Cytochrome Oxidase I (COI) gene has often been designated the DNA barcode standard for animals, as it is better at resolving taxa at the species level given its faster mutational rate, as well as the presence of robust "universal" primers, all aided by an extensive reference databank for taxonomic matching (Hebert et al., 2003; Hajibabaei et al., 2007; Bucklin et al., 2011; Porter and Hajibabaei, 2018). COI, however, is not without limitations that have been discussed extensively; this includes biases associated with maternal inheritance, overestimations of species divergence and the presence of pseudogenes, which can skew diversity assessments (Frézal and Leblois, 2008; Buhay, 2009; Bucklin et al., 2011; Deagle et al., 2014). Another disadvantage of the COI primers we used is their degeneracy which is useful for providing broad coverage of metazoans, but also allows for the amplification of some non-metazoans (Lear et al., 2018).

The novelty of our project and the goal to sequence across several hydrothermal vent taxa led us to implement four COI and 18S fragments that produced amplicons small enough to amplify degraded DNA material, yet long enough to provide information at various taxonomic levels. Comparing taxonomic results between COI and 18S, some taxa were found within certain datasets, yet not others (**Figure 2**). Previous authors also had similar findings while employing COI and 18S markers on environmental data (Cowart et al., 2015; Günther et al., 2018), linked to the factors described above. As an example, COI is known to have poor species resolution in some taxa and is unreliable for barcoding nematodes (De Ley et al., 2005; Pochon et al., 2013) and as such, 18S is preferred in these instances (Bhadury et al., 2006, 2008). This further supports that several factors, including marker amplicon length, the presence of pseudogenes or introns and differing evolution rates influence taxonomic "preferences" of markers. Despite these differences, the comparison of our eDNA datasets identified congruent statistical findings (**Table 4**), which included differences in community composition across habitats, as well as high diversity in inactive sites, similar to what has been seen using more traditional sampling strategies (Vanreusel et al., 1997; Levin et al., 2009). As there is no currently known perfect marker for properly characterizing all phyla, recommended strategies suggest using either a single marker for investigations of specific groups, or the use of multiple markers simultaneously to enhance biodiversity resolution (Dupuis et al., 2012; De Barba et al., 2014; Cowart et al., 2015). Other genes, such as 12S SSU rRNA and 28S LSU rRNA, should also be considered as viable options for metabarcoding due to their variability, ease of amplification and presence of public sequence data (Machida and Knowlton, 2012; Valentini et al., 2016; Lear et al., 2018).

Future of SMS Disturbances at Vents

The effects of mining activities on animal communities differ from natural disturbances, as mining would include not only the removal of substratum and associated faunal communities by machinery, but also generate a particulate plume that could smother individuals, as well as alter venting activity and fluid flow by clogging fluid channels (Juniper, 2002; Van Dover, 2011, 2014). If the scale of this destruction is widespread, these actions could not only hinder recovery, but may force the affected habitat past its tipping point, causing irreversible damages (Lotze et al., 2011; Veraart et al., 2012; Mullineaux et al., 2018). The current *in situ* experiment simulates a minor disturbance event in which fluid flow or chemistry was not altered. Additionally, our recolonization experiment focused on active areas, rather than inactive areas, where commercial mining is expected to occur. Finally, it was done at a far smaller scale than those expected for mining activities, although in the event of a large-scale mining operation, particulate plumes could likely affect nearby active venting sites. Despite these limitations, we provide foundational data on the diversity present at inactive sites, demonstrating that despite the absence of visible fauna, these sites may harbor an incredible level of diversity, especially in the microbial

realm. To date, information regarding recolonization processes in these habitats are fully missing, and the resampling of these quadrats after one or two more years of recolonization will bring new insight on inactive SMS recovery potential. Extending these types of experiments in space and time might also prove useful for the development of new methodologies for ecosystem monitoring using quick and reproducible approaches, such as environmental DNA.

DATA AVAILABILITY STATEMENT

DNA barcoding and metabarcoding datasets are available online at NCBI under GenBank accessions MK591147–MK591726 and SRA accession PRJNA540908. DOI of the cruises: SARRADIN Pierre-Marie, CANNAT Mathilde (2017) MOMARSAT2017 cruise, RV Pourquoi pas?, https://doi.org/10.17600/17000500; CANNAT Mathilde (2018) MOMARSAT2018 cruise, RV L'Atalante, https://doi.org/10.17600/18000514.

ETHICS STATEMENT

Our project occurred within the Portuguese EEZ and also a Marine Protected Area available for scientific access. Specific permissions were required to work and perform collections at the Lucky Strike hydrothermal vent field. Our work did not involve the collection or handling of endangered nor protected species.

AUTHOR CONTRIBUTIONS

MM and JS conceptualized the study, secured funding, and provided supervision for the work. MM, JM, and JS performed the acquisition and preservation of samples. JM performed analyses and laboratory curation of the morphological data. DC undertook all other laboratory analyses, sequencing preparation, bioinformatic and statistical analyses, as well as wrote the manuscript. MB contributed to the choice of markers and statistical analyses. MM, JM, MB, and JS edited the manuscript.

FUNDING

This research was supported by the European H2020 MERCES (Project ID 689518) and the Ifremer ABYSS projects. It is part of the EMSO-Azores (http://www.emso-fr.org) regional node, and of the EMSO ERIC Research Infrastructure (http://emso.eu/).

ACKNOWLEDGMENTS

We would like to thank the captains and crews of the oceanographic cruise campaigns of Momarsat 2017 and 2018 aboard the vessels N/O *Pourquoi pas?* and *L'Atalante*, as well as the ROV *Victor6000* team. We are also sincerely thankful to the following people for their assistance in various aspects of this project: Sophie Arnaud-Haond, Laure Quintric, Patrick Durand, Johanne Aube, Olivier Soubigou, Colomban de Vargas, Cathy Liautard-Haag, and the technicians and engineers of the deep sea Ifremer lab.

SUPPLEMENTARY MATERIAL

The Supplementary Material for this article can be found online at: https://www.frontiersin.org/articles/10.3389/fmars.2019.00783/full#supplementary-material

FIGURE S1 | Sequencing depth of non-metazoans and metazoans combined ("overall") for the four eDNA datasets. The number of reads in each OTU **(right)** and 18 samples **(left)** are shown for each gene marker.

FIGURE S2 | Sequencing depth of metazoans only for the four eDNA datasets. The number of reads in each OTU **(right)** and 18 samples **(left)** are shown for each gene marker.

FIGURE S3 | The top 10 most common species, in terms of sequence abundance, for the 18S-V4 and 18S-V9 eDNA datasets. "DNA barcode" are those species that were physically collected from Montségur and DNA barcoded in the current project (**Table 1**). "Additional" are species that were not DNA barcoded by the present project yet were apparently within the NCBI GenBank database prior to the taxonomic assignment of eDNA. Species in bold are those found at hydrothermal vents, while non-bolded species are not found at hydrothermal vents. The presence of these non-vent assignments suggests that these sequences were assigned to the closest taxon within the database, and not that these non-vent species are present in the deep-sea.

FIGURE S4 | Accumulation curves for the 18S-V4 eDNA dataset, for both baseline **(left)** and recolonization **(right)** data across all taxa (non-metazoans and metazoans) and metazoan taxa only. Baseline data focuses on sample communities from differing habitats/vent activity, as well as those from differing locations on the active edifice (base and structure). Recolonization data focuses on sample communities from differing years, as well as those that were caged against those non-caged at active sites. Note the difference in scales for number of OTUs and number of sequences between "All taxa" and "Metazoan taxa only." Recolonization data are only available for the active sites.

FIGURE S5 | Accumulation curves for the 18S-V9 eDNA dataset, for both baseline **(left)** and recolonization **(right)** data across all taxa (non-metazoans and metazoans) and metazoan taxa only. Baseline data focuses on sample communities from differing habitats/vent activity, as well as those from differing locations on the active edifice (base and structure). Recolonization data focuses on sample communities from differing years, as well as those that were caged against those non-caged at active sites. Note the difference in scales for number of OTUs and number of sequences between "All taxa" and "Metazoan taxa only." Recolonization data are only available for the active sites.

FIGURE S6 | Canonical correspondence analysis (CCA) plots for 18S-V4 and 18S-V9, illustrating metazoan community distributions by active, periphery or inactive habitats. Shapes denote habitat type and location (active only) and the number of shapes corresponds to the number of eDNA samples retrieved from each habitat. Colors refer to year and ellipses identify the relationships within habitats. The environmental gradient moves from right to left with increasing level of venting influence.

FIGURE S7 | Taxonomic characterizations of 18S-V4 and 18S-V9 eDNA datasets by phylum, based on number of OTUs (incidence) and identified from samples distributed around the active edifice, periphery and inactive sites.

FIGURE S8 | Taxonomic characterizations of the four eDNA datasets by phylum, based on number of OTUs (incidence) and identified from samples collected in 2017 and 2018, for visualization of recolonization across years and presence of cages.

TABLE S1 | Sequencing depth values for all taxa and metazoan taxa only, for the four eDNA datasets and across the 18 collected samples.

MATERIAL S1 | PCR protocols for DNA barcoding of animal tissue.

REFERENCES

Amaral-Zettler, L. A., McCliment, E. A., Ducklow, H. W., and Huse, S. M. (2009). A method for studying protistan diversity using massively parallel sequencing of V9 hypervariable regions of small-subunit ribosomal RNA genes. *PLoS One* 4:e6372. doi: 10.1371/journal.pone.0006372

Anderson, M. (2001). A new method for non-parametric multivariate analysis of variance. *Austral Ecol.* 26, 32–46. doi: 10.1111/j.1442-9993.2001.01070.pp.x

Barnes, M., and Turner, C. (2016). The ecology of environmental DNA and implications for conservation genetics. *Conserv. Genet.* 17, 1–17. doi: 10.1007/s10592-015-0775-4

Barnes, M., Turner, C., Jerde, C., Renshaw, M., Chadderton, W., and Lodge, D. (2014). Environmental conditions influence eDNA persistence in aquatic systems. *Environ. Sci. Technol.* 48, 1819–1827. doi: 10.1021/es404734p

Baross, J., and Hoffman, S. (1985). Submarine hydrothermal vents and associated gradient environments as sites for the origin and evolution of life. *Orig. Life Evol. Biosph.* 15, 327–345. doi: 10.1007/bf01808177

Barreyre, T., Escartin, J., Sohn, R., Cannat, M., Ballu, V., and Crawford, W. (2014). Temporal variability and tidal modulation of hydrothermal exit-fluid temperatures at the Lucky Strike deep-sea vent field, Mid-Atlantic Ridge. *J. Geophys. Res. Solid Earth* 119, 2543–2566. doi: 10.1002/2013jb010478

Bellec, L., Cambon-Bonavita, M.-A., Cueff-Gauchard, V., Durand, L., Gayet, N., and Zeppilli, D. (2018). A nematode of the Mid-Atlantic Ridge hydrothermal vents harbors a possible symbiotic relationship. *Front. Microbiol.* 9:2246. doi: 10.3389/fmicb.2018.02246

Bhadury, P., Austen, M., Bilton, D., Lambshead, P., Rogers, A., and Smerdon, G. (2006). Development and evaluation of a DNA-barcoding approach for the rapid identification of nematodes. *Mar. Ecol. Prog. Ser.* 320, 1–9. doi: 10.3354/meps320001

Bhadury, P., Austen, M., Bilton, D., Lambshead, P., Rogers, A., and Smerdon, G. (2008). Evaluation of combined morphological and molecular techniques for marine nematode (*Terschellingia* spp.) identification. *Mar. Biol.* 154, 509–518. doi: 10.1007/s00227-008-0945-8

Blake, J. (1985). Polycaeta from the vicinity of deep-sea geothermal vents in the eastern Pacific. I: euphrosinidae, phyllodocidae, hesionidae, nereididae, glyceridae, dorvilleidae, orbiniidae and maldanidae. *Bull. Biol. Soc. Washington* 6, 67–101.

Bohmann, K., Evans, A., Gilbert, M., Carvalho, G., Creer, S., Knapp, M., et al. (2014). Environmental DNA for wildlife biology and biodiversity monitoring. *Trends Ecol. Evol.* 29, 358–365.

Bolger, A., Lohse, M., and Usadel, B. (2014). Trimmomatic: a flexible trimmer for Illumina sequence data. *Bioinformatics* 30, 2114–2120. doi: 10.1093/bioinformatics/btu170

Boschen, R., Rowden, A., Clark, M., and Gardner, J. (2013). Mining of deep-sea seafloor massive sulfides: a review of the deposits, their benthic communities, impacts from mining, regulatory frameworks and management strategies. *Ocean Coast. Manag.* 84, 54–67. doi: 10.1016/j.ocecoaman.2013.07.005

Boschen, R., Rowden, A., Clark, M., Pallentin, A., and Gardner, J. (2016). Seafloor massive sulfide deposits support unique megafaunal assemblages: implications for seabed mining and conservation. *Mar. Environ. Res.* 115, 78–88. doi: 10.1016/j.marenvres.2016.02.005

Brandt, M., Trouche, B., Quintric, L., Wincker, P., Poulain, J., and Arnaud-Haond, S. (2019). A flexible pipeline combining bioinformatic correction tools for prokaryotic and eukaryotic metabarcoding. *bioRxiv [Preprint]*. doi: 10.1101/717355

Bucklin, A., Steinke, D., and Blanco-Bercial, L. (2011). DNA barcoding of marine metazoa. *Ann. Rev. Mar. Sci.* 3, 471–508. doi: 10.1146/annurev-marine-120308-080950

Buhay, J. (2009). "COI-like" sequences are becoming problematic in molecular systematic and DNA barcoding studies. *J. Crustacean Biol.* 29, 96–110. doi: 10.1651/08-3020.1

Butterfield, D., Jonasson, I., Massoth, G., Feely, R., Roe, K., Embley, R., et al. (1997). Seafloor eruptions and evolution of hydrothermal fluid chemistry. *Philos. Trans. R. Soc. Lond. Ser. A Math. Phys. Eng. Sci.* 355, 369–386.

Carr, C. M., Hardy, S. M., Brown, T. M., Macdonald, T. A., and Hebert, P. D. (2011). A tri-oceanic perspective: DNA barcoding reveals geographic structure and cryptic diversity in Canadian polychaetes. *PLoS One* 6:e22232. doi: 10.1371/journal.pone.0022232

Chambert, T., Miller, D., and Nichols, J. (2015). Modeling false positive detections in species occurrence data under different study designs. *Ecology* 96, 332–339. doi: 10.1890/14-1507.1

Chao, A., and Chiu, C. H. (2016). *Species Richness: Estimation and Comparison*. Hoboken, NJ: Wiley, 1–26.

Childress, J., and Fisher, C. (1992). The biology of hydrothermal vent animals: physiology, biochemistry and autotrophic symbioses. *Oceanogr. Mar. Biol. Annu. Rev.* 20, 337–441.

Clark, K. (1993). Non-parametric multivariate analyses of changes in community structure. *Aust. J. Ecol.* 18, 117–143. doi: 10.1111/j.1442-9993.1993.tb00438.x

Coissac, E., Riaz, T., and Puillandre, N. (2012). Bioinformatic challenges for DNA metabarcoding of plants and animals. *Mol. Ecol.* 21, 1834–1847. doi: 10.1111/j.1365-294X.2012.05550.x

Collins, P., Kennedy, R., and Van Dover, C. (2012). A biological survey method applied to seafloor massive sulphides (SMS) with contagiously distributed hydrothermal-vent fauna. *Mar. Ecol. Prog. Ser.* 452, 89–107. doi: 10.3354/meps09646

Corinaldesi, C., Barucca, M., Luna, G., and Dell'Anno, A. (2011). Preservation, origin and genetic imprint of extracellular DNA in permanently anoxic deep-sea sediments. *Mol. Ecol.* 20, 642–654. doi: 10.1111/j.1365-294X.2010.04958.x

Cowart, D., Pinheiro, M., Mouchel, O., Maguer, M., Grall, J., Miné, J., et al. (2015). Metabarcoding is powerful yet still blind: a comparative analysis of morphological and molecular surveys of seagrass communities. *PLoS One* 10:e0117562. doi: 10.1371/journal.pone.0117562

Cuvelier, D., Beesau, J., Ivanenko, V., Zeppilli, D., Sarradin, P., and Sarrazin, J. (2014). First insights into macro-and meiofaunal colonisation patterns on paired wood/slate substrata at Atlantic deep-sea hydrothermal vents. *Deep Sea Res Part I Oceanogr. Res. Pap.* 87(Part 1), 70–81. doi: 10.1016/j.dsr.2014.02.008

Cuvelier, D., Busserolles, F. D., Lavaud, R., Floc'h, E., Fabri, M., Sarradin, P., et al. (2012). Biological data extraction from imagery - How far can we go? A case study from the Mid-Atlantic Ridge. *Mar. Environ. Res.* 82, 15–27. doi: 10.1016/j.marenvres.2012.09.001

Cuvelier, D., Sarradin, P., Sarrazin, J., Colaço, A., Copley, J., Desbruyères, D., et al. (2011a). Hydrothermal faunal assemblages and habitat characterisation at the Eiffel Tower edifice (Lucky Strike, Mid-Atlantic Ridge). *Mar. Ecol.* 32, 243–255. doi: 10.1111/j.1439-0485.2010.00431.x

Cuvelier, D., Sarrazin, J., Colaço, A., Copley, J., Glover, A., Tyler, P., et al. (2011b). Community dynamics over 14 years at the Eiffel Tower hydrothermal edifice on the Mid-Atlantic Ridge. *Limnol. Oceanogr.* 56, 1624–1640. doi: 10.4319/lo.2011.56.5.1624

Cuvelier, D., Sarrazin, J., Colaço, A., Copley, J., Desbruyères, D., Glover, A., et al. (2009). Distribution and spatial variation of hydrothermal faunal assemblages at LuckyStrike (Mid-AtlanticRidge) revealed by high-resolution video image analysis. *Deep Sea Res. Part I Oceanogr. Res. Pap.* 56, 2026–2040. doi: 10.1016/j.dsr.2009.06.006

Dayrat, B. (2005). Towards integrative taxonomy. *Biol. J. Linn. Soc.* 85, 407–415. doi: 10.1111/j.1095-8312.2005.00503.x

De Barba, M., Miquel, C., Boyer, F., Mercier, C., Rioux, D., Coissac, E., et al. (2014). DNA metabarcoding multiplexing and validation of data accuracy for diet assessment: application to omnivorous diet. *Mol. Ecol. Resour.* 14, 306–323. doi: 10.1111/1755-0998.12188

De Ley, P., De Ley, I., Morris, K., Abebe, E., Mundo-Ocampo, M., Yoder, M., et al. (2005). An integrated approach to fast and informative morphological vouchering of nematodes for applications in molecular barcoding. *Philos. Trans. R. Soc. B Biol. Sci.* 360, 1945–1958. doi: 10.1098/rstb.2005.1726

De Ley, P., Félix, M., Frisse, L., Nadler, S., Sternberg, P., and Thomas, W. (1999). Molecular and morphological characterisation of two reproductively isolated species with mirror-image anatomy (Nematoda: Cephalobidae). *Nematology* 1, 591–612. doi: 10.1163/156854199508559

Deagle, B., Jarman, S., Coissac, E., Pompanon, F., and Taberlet, P. (2014). DNA metabarcoding and the cytochrome c oxidase subunit I marker: not a perfect match. *Biol. Lett.* 10:20140562. doi: 10.1098/rsbl.2014.0562

Dejean, T., Valentini, A., Duparc, A., Pellier-Cuit, S., Pompanon, F., Taberlet, P., et al. (2011). Persistence of environmental DNA in freshwater ecosystems. *PLoS One* 6:e23398. doi: 10.1371/journal.pone.0023398

Desbruyères, D., Almeida, A., Biscoito, M., Comtet, T., Khripounoff, A., Le Bris, N., et al. (2000). A review of the distribution of hydrothermal vent communities

along the northern Mid-Atlantic Ridge: dispersal vs. environmental controls. *Hydrobiologia* 440, 201–216. doi: 10.1007/978-94-017-1982-7_19

Doi, H., Inui, R., Akamatsu, Y., Kanno, K., Yamanaka, H., Takahara, T., et al. (2017). Environmental DNA analysis for estimating the abundance and biomass of stream fish. *Freshw. Biol.* 62, 30–39. doi: 10.1371/journal.pone.0218823

Doyle, J. (1991). "DNA protocols for plants," in *Molecular Techniques in Taxonomy*, eds G. M. Hewitt, A. W. B. Johnston, and J. P. W. Young, (Berlin: Springer), 283–293. doi: 10.1007/978-3-642-83962-7_18

Dupuis, J., Roe, A., and Sperling, F. (2012). Multi-locus species delimitation in closely related animals and fungi: one marker is not enough. *Mol. Ecol.* 21, 4422–4436. doi: 10.1111/j.1365-294X.2012.05642.x

Epp, L., Boessenkool, S., Bellemain, E., Haile, J., Esposito, A., Riaz, T., et al. (2012). New environmental metabarcodes for analysing soil DNA: potential for studying past and present ecosystems. *Mol. Ecol.* 21, 1821–1833. doi: 10.1111/j.1365-294X.2012.05537.x

Escudié, F., Auer, L., Bernard, M., Mariadassou, M., Cauquil, L., Vidal, K., et al. (2017). FROGS: find, rapidly, OTUs with galaxy solution. *Bioinfomatics* 34, 1287–1294. doi: 10.1093/bioinformatics/btx791

Ficetola, G., Pansu, J., Bonin, A., Coissac, E., Giguet-Covex, C., De Barba, M., et al. (2015). Replication levels, false presences and the estimation of the presence/absence from eDNA metabarcoding data. *Mol. Ecol. Resour.* 15, 543–556. doi: 10.1111/1755-0998.12338

Fisher, C., Takai, K., and Le Bris, N. (2007). Hydrothermal vent ecosystems. *Oceanography* 20, 14–23. doi: 10.5670/oceanog.2007.75

Folmer, O., Black, M., Hoeh, W., Lutz, R., and Vrijenhoek, R. (1994). DNA primers for amplification of mitochondrial cytochrome c oxidase subunit I from diverse metazoan invertebrates. *Mol. Mar. Biol. Biotechnol.* 3, 294–299.

Frézal, L., and Leblois, R. (2008). Four years of DNA barcoding: current advances and prospects. *Infect. Genet. Evol.* 8, 727–736. doi: 10.1016/j.meegid.2008.05.005

Gaudron, S., Pradillon, F., Pailleret, M., Duperron, S., Le Bris, N., and Gaill, F. (2010). Colonization of organic substrates deployed in deep-sea reducing habitats by symbiotic species and associated fauna. *Mar. Environ. Res.* 70, 1–12. doi: 10.1016/j.marenvres.2010.02.002

Gauthier, O., Sarrazin, J., and Desbruyères, D. (2010). Measure and mis-measure of species diversity in deep-sea chemosynthetic communities. *Mar. Ecol. Prog. Ser.* 402, 285–302. doi: 10.3354/meps08395

Goldberg, C., Turner, C., Deiner, K., Klymus, K., Thomsen, P., Mruphy, M., et al. (2016). Critical considerations for the application of environmental DNA methods to detect aquatic species. *Methods Ecol. Evol.* 7, 1299–1307. doi: 10.1111/2041-210x.12595

Gollner, S., Kaiser, S., Menzel, L., Jones, D., Brown, A., Mestre, N., et al. (2017). Resilience of benthic deep-sea fauna to mining activities. *Mar. Environ. Res.* 129, 76–101. doi: 10.1016/j.marenvres.2017.04.010

Guillera-Arroita, G., Lahoz-Monfort, J., van Rooyen, A., Weeks, A., and Tingley, R. (2017). Dealing with false-positive and false-negative errors about species occurrence at multiple levels. *Methods Ecol. Evol.* 8, 1081–1091. doi: 10.1111/2041-210x.12743

Günther, B., Knebelsberger, T., Neumann, H., Laakmann, S., and Martínez Arbizu, P. (2018). Metabarcoding of marine environmental DNA based on mitochondrial and nuclear genes. *Sci. Rep.* 8:14822.

Hajibabaei, M., Singer, G., Hebert, P., and Hickey, D. (2007). DNA barcoding: how it complements taxonomy, molecular phylogenetics and population genetics. *Trends Genet.* 23, 167–172. doi: 10.1016/j.tig.2007.02.001

Hammer, Ø., Harper, D., and Ryan, P. (2001). PAST: paleontological statistics software package for education and data analysis. *Palaeontol. Electronica* 4, 1–9.

Hänfling, B., Lawson Handley, L., Read, D., Hahn, C., Li, J., Nichols, P., et al. (2016). Environmental DNA metabarcoding of lake fish communities reflects long-term data from established survey methods. *Mol. Ecol.* 25, 3101–3119. doi: 10.1111/mec.13660

Hannington, M., Jamieson, J., Monecke, T., Petersen, S., and Beaulieu, S. (2011). The abundance of seafloor massive sulfide deposits. *Geology* 39, 1155–1158. doi: 10.1128/mBio.00279-11

Hebert, P., Cywinska, A., Ball, S., and Dewaard, J. (2003). Biological identifications through DNA barcodes. *Proc. R. Soc. Lond. Ser. B Biol. Sci.* 270, 313–321. doi: 10.1098/rspb.2002.2218

Hoagland, P., Beaulieu, S., Trivey, M., Eggert, R., German, C., Glowka, L., et al. (2010). Deep-sea mining of seafloor massive sulfides. *Mar. Policy* 34, 728–732. doi: 10.1016/j.marenvres.2016.02.005

Humphris, S., Fornari, D., Scheirer, D., German, C., and Parson, L. (2002). Geotectonic setting of hydrothermal activity on the summit of Lucky Strike Seamount (37 17'N, Mid-Atlantic Ridge). *Geochem. Geophys. Geosyst.* 3, 1–24.

Hunt, H., Metaxas, A., Jennings, R., Halanych, K., and Mullineaux, L. (2004). Testing biological control of colonization by vestimentiferan tubeworms at deep-sea hydrothermal vents (East Pacific Rise, 9 50'N). *Deep Sea Res. Part Oceanogr. Res. Pap.* 1, 225–234. doi: 10.1016/j.dsr.2003.10.008

ISA, (2010). *Polymetallic Sulphides [Online]*. Available at: https://ran-s3.s3.amazonaws.com/isa.org.jm/s3fs-public/documents/EN/Brochures/ENG8.pdf doi: 10.1016/j.dsr.2003.10.008 (accessed November 8, 2018).

Ji, Y., Ashton, L., Pedley, S., Edwards, D., Tang, Y., Nakamura, A., et al. (2013). Reliable, verifiable and efficient monitoring of biodiversity via metabarcoding. *Ecol. Lett.* 16, 1245–1257. doi: 10.1111/ele.12162

Johnson, K., Childress, J., and Beehler, C. (1988). Short-term temperature variability in the Rose Garden hydrothermal vent field: an unstable deep-sea environment. *Deep Sea Res. Part A Oceanogr. Res. Pap.* 35, 1711–1721. doi: 10.1016/0198-0149(88)90045-3

Johnson, M., Zaretskaya, I., Raytselis, Y., Merezhuk, Y., Mcginnis, S., and Madden, T. (2008). NCBI Blast: a better web interface. *Nucleic Acids Res.* 36, W5–W9. doi: 10.1093/nar/gkn201

Juniper, S. (2002). "Impact of the development of seafloor massive sulphides on the vent ecosystem," in *Polymetallic Massive Sulphides and Cobalt-Rich Ferromanganese Crusts: Status and Prospects*, (Kingston: International Seabed Authority).

Karl, D., Wirsen, C., and Jannasch, H. (1980). Deep-sea primary production at the Galapagos hydrothermal vents. *Science* 207, 1345–1347. doi: 10.1126/science.207.4437.1345

Kearse, M., Moir, R., Wilson, A., Stones-Havas, S., Cheung, M., Sturrock, S., et al. (2012). Geneious Basic: an integrated and extendable desktop software platform for the organization and analysis of sequence data. *Bioinfomatics* 28, 1647–1649. doi: 10.1093/bioinformatics/bts199

Kelly, N., Metaxas, A., and Butterfield, D. (2007). Spatial and temporal patterns of colonization by deep-sea hydrothermal vent invertebrates on the Juan de Fuca Ridge, NE Pacific. *Aquat. Biol.* 1, 1–16. doi: 10.3354/ab00001

Krasnov, S., Cherkashev, G., Stepanova, T., Batuyev, B., Krotov, A., Malin, B., et al. (1995). Detailed geological studies of hydrothermal fields in the North Atlantic. Hydrothermal vents and processes. *Geol. Soc.* 87, 43–64.

Kvist, S. (2013). Barcoding in the dark?: a critical view of the sufficiency of zoological DNA barcoding databases and a plea for broader integration of taxonomic knowledge. *Mol. Phylogenet. Evol.* 69, 39–45. doi: 10.1016/j.ympev.2013.05.012

Lacoursière-Roussel, A., Rosabal, M., and Bernatchez, L. (2016). Estimating fish abundance and biomass from eDNA concentrations: variability among capture methods and environmental conditions. *Mol. Ecol. Resour.* 16, 1401–1414. doi: 10.1111/1755-0998.12522

Lahoz-Monfort, J., Guillera-Arroita, G., and Tingley, R. (2016). Statistical approaches to account for false positive errors in environmental DNA samples. *Mol. Ecol. Resour.* 16, 673–685. doi: 10.1111/1755-0998.12486

Langmuir, C., Humphris, S., Fornari, D., Van Dover, C., Von Damm, K., Tivey, M., et al. (1997). Hydrothermal vents near a mantle hot spot: the Lucky Strike vent field at 37°N on the Mid-Atlantic Ridge. *Earth Planet. Sci. Lett.* 148, 69–91. doi: 10.1016/s0012-821x(97)00027-7

Laroche, O., Wood, S., Tremblay, L., Ellis, J., Lear, G., and Pochon, X. (2018). A cross-taxa study using environmental DNA/RNA metabarcoding to measure biological impacts of offshore oil and gas drilling and production operations. *Mar. Pollut. Bull.* 127, 97–107. doi: 10.1016/j.marpolbul.2017.11.042

Laroche, O., Wood, S., Tremblay, L., Lear, G., Ellis, J., and Pochon, X. (2017). Metabarcoding monitoring analysis: the pros and cons of using co-extracted environmental DNA and RNA data to assess offshore oil production impacts on benthic communities. *PeerJ* 5:e3347. doi: 10.7717/peerj.3347

Lear, G., Dickie, I., Banks, J., Boyer, S., Buckley, H., Tr, B., et al. (2018). Methods for the extraction, storage, amplification and sequencing of DNA from environmental samples. *N. Z. J. Ecol.* 42, 10–50.

Lecroq, B., Gooday, A., Cedhagen, T., Sabbatini, A., and Pawlowski, J. (2009). Molecular analyses reveal high levels of eukaryotic richness associated with enigmatic deep-sea protists (Komokiacea). *Mar. Biodivers.* 39, 45–55. doi: 10.1007/s12526-009-0006-7

Lennon, J., Muscarella, M., Placella, S., and Lehmkuhl, B. (2018). How, when, and where relic DNA affects microbial diversity. *mBio* 9:e00637-18. doi: 10.1128/mBio.00637-18

Leray, M., and Knowlton, N. (2015). DNA barcoding and metabarcoding of standardized samples reveal patterns of marine benthic diversity. *Proc. Natl. Acad. Sci. U.S.A.* 112, 2076–2081. doi: 10.1073/pnas.1424997112

Leray, M., Yang, J., Meyer, C., Mills, S., Agudelo, N., Ranwez, V., et al. (2013). A new versatile primer set targeting a short fragment of the mitochondrial COI region for metabarcoding metazoan diversity: application for characterizing coral reef fish gut contents. *Front. Zool.* 10:34. doi: 10.1186/1742-9994-10-34

Levin, L. (1991). Interactions between metazoans and large, agglutinating protozoans: implications for the community structure of deep-sea benthos. *Am. Zool.* 31, 886–900. doi: 10.1093/icb/31.6.886

Levin, L., Baco, A., Bowden, D., Colaco, A., Cordes, E., Cunha, M., et al. (2016). Hydrothermal vents and methane seeps: rethinking the sphere of influence. *Front. Mar. Sci.* 3:72. doi: 10.3389/fmars.2016.00072

Levin, L., Mendoza, G., Konotchick, T., and Lee, R. (2009). Macrobenthos community structure and trophic relationships within active and inactive Pacific hydrothermal sediments. *Deep Sea Res. II Top. Stud. Oceanogr.* 56, 1632–1648. doi: 10.1016/j.dsr2.2009.05.010

Lindeque, P., Parry, H., Harmer, R., Somerfield, P., and Atkinson, A. (2013). Next generation sequencing reveals the hidden diversity of zooplankton assemblages. *PLoS One* 8:e81327. doi: 10.1371/journal.pone.0081327

Lotze, H., Coll, M., Magera, A., Ward-Paige, C., and Airoldi, L. (2011). Recovery of marine animal populations and ecosystems. *Trends Ecol. Evol.* 26, 595–605. doi: 10.1016/j.tree.2011.07.008

Lutz, R., and Kennish, M. (1993). Ecology of deep-sea hydrothermal vent communities: a review. *Rev. Geophys.* 31, 211–242.

Machida, R., and Knowlton, N. (2012). PCR primers for metazoan nuclear 18S and 28S ribosomal DNA sequences. *PLoS One* 7:e46180. doi: 10.1371/journal.pone.0046180

MacKenzie, D., Nichols, J., Lachman, G., Droege, S., Royle, A., and Langtimm, C. (2002). Estimating site occupancy rates when detection probabilities are less than one. *Ecology* 38, 2248–2255. doi: 10.1890/0012-9658(2002)083%5B2248:esorwd%5D2.0.co;2

Mahé, F., Rognes, T., Quince, C., de Vargas, C., and Dunthorn, M. (2014). Swarm: robust and fast clustering method for amplicon-based studies. *PeerJ* 2:e593. doi: 10.7717/peerj.593

McMurdie, P., and Holmes, S. (2013). phyloseq: an R package for reproducible interactive analysis and graphics of microbiome census data. *PLoS One* 8:e61217. doi: 10.1371/journal.pone.0061217

Mengerink, K., Van Dover, C., Ardron, J., Baker, M., Escobar-Briones, E., Gjerde, K., et al. (2014). A call for deep-ocean stewardship. *Science* 344, 696–698. doi: 10.1126/science.1251458

Meusnier, I., Singer, G., Landry, J.-F., Hickey, D., Hebert, P., and Hajibabaei, M. (2008). A universal DNA mini-barcode for biodiversity analysis. *BMC Genomics* 9:214. doi: 10.1186/1471-2164-9-214

Micheli, F., Peterson, C., Mullineaux, L., Fisher, C., Mills, S., Sancho, G., et al. (2002). Predation structures communities at deep-sea hydrothermal vents. *Ecol. Monogr.* 72, 365–382. doi: 10.1890/0012-9615(2002)072%5B0365:pscads%5D2.0.co;2

Monecke, T., Petersen, S., Hannington, M., and Grant, H. (2015). *The Global Rare Element Endowment of Seafloor Massive Sulfide Deposits*. Kiel: Helmholtz Centre for Ocean Research.

Mullineaux, L. (2000). Tubeworm succession at hydrothermal vents: use of biogenic cues to reduce habitat selection error? *Oecologia* 123, 275–284. doi: 10.1007/s004420051014

Mullineaux, L. (2014). "Deep-sea hydrothermal vent communities," in *Marine Community Ecology and Conservation*, eds M. D. Bertness, J. F. Bruno, B. R. Silliman, and J. J. Stachowicz, (Sunderland, MA: Sinauer Associates Inc), 383–400.

Mullineaux, L., Adams, D., Mills, S., and Beaulieu, S. (2010). Larvae from afar colonize deep-sea hydrothermal vents after a catastrophic eruption. *Proc. Natl. Acad. Sci. U.S.A.* 107, 7829–7834. doi: 10.1073/pnas.0913187107

Mullineaux, L., Metaxas, A., Beaulieu, S., Bright, M., Gollner, S., Grupe, B., et al. (2018). Exploring the ecology of deep-sea hydrothermal vents in a metacommunity framework. *Front. Mar. Sci.* 5:49. doi: 10.3389/fmars.2018.00049

Mullineaux, L., Peterson, C., Micheli, F., and Mills, S. (2003). Successional mechanism varies along a gradient in hydrothermal fluid flux at deep-sea vents. *Ecol. Monogr.* 73, 523–542. doi: 10.1890/02-0674

Oksanen, J. (2015). Multivariate analysis of ecological communities in R: vegan tutorial. *R. Doc.* 43, 11–12.

Olu-Le Roy, K., Von Cosel, R., Hourdez, S., Carney, S. L., and Jollivet, D. (2007). Amphi-Atlantic cold-seep Bathymodiolus species complexes across the equatorial belt. *Deep Sea Res. Part I Oceanogr. Res. Pap.* 54, 1890–1911. doi: 10.1016/j.dsr.2007.07.004

Ondréas, H., Cannat, M., Fouquet, Y., Normand, A., Sarradin, P., and Sarrazin, J. (2009). Recent volcanic events and the distribution of hydrothermal venting at the Lucky Strike hydrothermal field, Mid-Atlantic Ridge. *Geochem. Geophys. Geosyst.* 10:Q02006.

Pietramellara, G., Ascher, J., Borgogni, F., Ceccherini, M., Guerri, G., and Nannipieri, P. (2009). Extracellular DNA in soil and sediment: fate and ecological relavance. *Biol. Fertil. Soils* 45, 219–235. doi: 10.1007/s00374-008-0345-8

Plum, C., Pradillon, F., Yoshihiro, F., and Sarrazin, J. (2017). Copepod colonization of organic and inorganic substrata at a deep-sea hydrothermal vent site on the Mid-Atlantic Ridge. *Deep Sea Res. Part II Top. Stud. Oceanogr.* 137, 335–348. doi: 10.1016/j.dsr2.2016.06.008

Pochon, X., Bott, N., Smith, K., and Wood, S. (2013). Evaluating detection limits of next-generation sequencing for the surveillance and monitoring of international marine pests. *PLoS One* 8:e73935. doi: 10.1371/journal.pone.0073935

Pochon, X., Zaiko, A., Fletcher, L., Laroche, O., and Wood, S. (2017). Wanted dead or alive? Using metabarcoding of environmental DNA and RNA to distinguish living assemblages for biosecurity applications. *PLoS One* 12:e0187636. doi: 10.1371/journal.pone.0187636

Porter, T., and Hajibabaei, M. (2018). Over 2.5 million COI sequences in GenBank and growing. *PLoS One* 13:e0200177. doi: 10.1371/journal.pone.0200177

Quast, C., Pruesse, E., Yilmaz, P., Gerken, J., Schweer, T., Yarza, P., et al. (2012). The SILVA ribosomal RNA gene database project: improved data processing and web-based tools. *Nucleic Acids Res.* 41, D590–D596. doi: 10.1093/nar/gks1219

Ramirez-Llodra, E., Tyler, P., Baker, M., Bergstad, O., Clark, M., Escobar, E., et al. (2011). Man and the last great wilderness: human impact on the deep sea. *PLoS One* 6:e22588. doi: 10.1371/journal.pone.0022588

Rees, H., Maddison, B., Middleditch, D., Patmore, J., and Gough, K. (2014). The detection of aquatic animal species using environmental DNA - a review of eDNA as a survey tool in ecology. *J. Appl. Ecol.* 51, 1450–1459. doi: 10.1111/1365-2664.12306

Rognes, T., Flouri, T., Nichols, B., Quince, C., and Mahé, F. (2016). VSEARCH: a versatile open source tool for metagenomics. *PeerJ*. 4:e2584. doi: 10.7717/peerj.2584

Rona, P. (2008). The changing vision of marine minerals. *Ore Geol. Rev.* 33, 618–666. doi: 10.1016/j.oregeorev.2007.03.006

Sancho, G., Fisher, C., Mills, S., Micheli, F., Johnson, G., Lenihan, H., et al. (2005). Selective predation by zoarcid fish *Thermarces cerberus* at hydrothermal vents. *Deep Sea Res. I Oceanogr. Res. Pap.* 52, 837–844. doi: 10.1016/j.dsr.2004.12.002

Sarrazin, J., and Juniper, S. (1999). Biological characteristics of a hydrothermal edifice mosaic community. *Mar. Ecol. Prog. Ser.* 185, 1–19. doi: 10.3354/meps185001

Sarrazin, J., Legendre, P., De Busserolles, F., Fabri, M., Guilini, K., Ivanenko, V., et al. (2015). Biodiversity patterns, environmental drivers and indicator species on a high-temperature hydrothermal edifice, Mid-Atlantic Ridge. *Deep Sea Res. II Top. Stud. Oceanogr.* 121, 177–192. doi: 10.1016/j.dsr2.2015.04.013

Sarrazin, J., Robigou, V., Juniper, S., and Delaney, J. (1997). Biological and geological dynamics over four years on a high-temperature sulfide structure at the Juan de Fuca Ridge hydrothermal observatory. *Mar. Ecol. Prog. Ser.* 153, 5–24. doi: 10.3354/meps153005

Seidel, L., Strathmann, M., and Nocker, A. (2017). The feasibility of improved live-dead distinction in qPCR-based microbial source tracking. *J. Microb. Methods* 140, 23–31. doi: 10.1016/j.mimet.2017.06.013

Shank, T., Fornari, D., Von Damm, K., Lilley, M., Haymon, R., and Lutz, R. (1998). Temporal and spatial patterns of biological community development at nascent deep-sea hydrothermal vents (9 50'N, East Pacific Rise). *Deep Sea Res. Part II Top. Stud. Oceanogr.* 45, 465–515. doi: 10.1016/s0967-0645(97)00089-1

Sigsgaard, E., Carl, H., Møller, P., and Thomsen, P. (2015). Monitoring the near-extinct European weather loach in Denmark based on environmental DNA from water samples. *Biol. Conserv.* 183, 46–52. doi: 10.1016/j.biocon.2014.11.023

Sinniger, F., Pawlowski, J., Harii, S., Gooday, A., Yamamoto, H., Chevaldonné, P., et al. (2016). Worldwide analysis of sedimentary DNA reveals major gaps in taxonomic knowledge of deep-sea benthos. *Front. Mar. Sci.* 3:92. doi: 10.3389/fmars.2016.00092

Stoeck, T., Bass, D., Nebel, M., Christen, R., Jones, M., Breiner, H., et al. (2010). Multiple marker parallel tag environmental DNA sequencing reveals a highly complex eukaryotic community in marine anoxic waters. *Mol. Ecol.* 19, 21–31. doi: 10.1111/j.1365-294X.2009.04480.x

Taberlet, P., Coissac, E., Hajibabaei, M., and Riesenberg, L. (2012a). Environmental DNA. *Mol. Ecol.* 21, 1789–1793.

Taberlet, P., Prud'Homme, S., Campione, E., Roy, J., Miquel, C., Shehzad, W., et al. (2012b). Soil sampling and isolation of extracellular DNA from large amount of starting material suitable for metabarcoding studies. *Mol. Ecol.* 21, 1816–1820. doi: 10.1111/j.1365-294X.2011.05317.x

Tang, C., Leasi, F., Obertegger, U., Kieneke, A., Barraclough, T., and Fontaneto, D. (2012). The widely used small subunit 18S rDNA molecule greatly underestimates true diversity in biodiversity surveys of the meiofauna. *Proc. Natl. Acad. Sci. U.S.A.* 109, 16208–16212. doi: 10.1073/pnas.1209160109

Ter Braak, C., and Verdonschot, P. (1995). Canonical correspondence analysis and related multivariate methods in aquatic ecology. *Aquat. Sci.* 57, 255–289. doi: 10.1007/bf00877430

Thomsen, P., Møller, P., Sigsgaard, E., Knudsen, W., Jørgensen, O., and Willerslev, E. (2016). Environmental DNA from seawater samples correlate with trawl catches of subarctic, deepwater fishes. *PLoS One* 11:e0165252. doi: 10.1371/journal.pone.0165252

Thomsen, P., and Willerslev, E. (2015). Environmental DNA - An emerging tool in conservation for monitoring past and present biodiversity. *Biol. Conserv.* 183, 4–18. doi: 10.1016/j.biocon.2014.11.019

Torti, A., Jørgensen, B., and Lever, M. (2018). Preservation of microbial DNA in marine sediments: insights from extracellular DNA pools. *Environ. Microbiol.* 20, 4526–4542. doi: 10.1111/1462-2920.14401

Tsurumi, M. (2003). Diversity at hydrothermal vents. *Glob. Ecol. Biogeogr.* 12, 181–190. doi: 10.1046/j.1466-822x.2003.00016.x

Tunnicliffe, V. (1991). The biology of hydrothermal vents: ecology and evolution. *Oceanogr. Mar. Biol. Annu. Rev.* 29, 319–407.

Tunnicliffe, V. (1992). Hydrothermal-vent communities of the deep sea. *Am. Sci.* 80, 336–349.

Tunnicliffe, V., Embley, R., Holden, J., Butterfield, D., Massoth, G., and Juniper, S. (1997). Biological colonization of new hydrothermal vents following an eruption on Juan de Fuca Ridge. *Deep Sea Res. Part I Oceanogr. Res. Pap.* 44, 1627–1644. doi: 10.1016/s0967-0637(97)00041-1

Tunnicliffe, V., and Juniper, S. (1990). Dynamic character of the hydrothermal vent habitat and the nature of sulphide chimney fauna. *Prog. Oceanogr.* 24, 1–13. doi: 10.1016/0079-6611(90)90015-t

Valentini, A., Taberlet, P., Miaud, C., Civade, R., Herder, J., Thomsen, P., et al. (2016). Next-generation monitoring of aquatic biodiversity using environmental DNA metabarcoding. *Mol. Ecol.* 25, 929–942. doi: 10.1111/mec.13428

Van Dover, C. (2011). Mining seafloor massive sulphides and biodiversity: what is at risk? *ICES J. Mar. Sci.* 68, 341–348. doi: 10.1093/icesjms/fsq086

Van Dover, C. (2014). Impacts of anthropogenic disturbances at deep-sea hydrothermal vent ecosystems: a review. *Mar. Environ. Res.* 102, 59–72. doi: 10.1016/j.marenvres.2014.03.008

Van Dover, C., German, C., Speer, K., Parson, L., and Vrijenhoek, R. (2002). Evolution and biogeography of deep-sea vent and seep invertebrates. *Science* 295, 1253–1257. doi: 10.1126/science.1067361

Vanreusel, A., Van Den Bossche, I., and Thiermann, F. (1997). Free-living marine nematodes from hydrothermal vent sediments: similarities with communities from diverse reduced habitats. *Mar. Ecol. Prog. Ser.* 157, 207–219. doi: 10.3354/meps157207

Veraart, A., Ej, F., Dakos, V., Van Nes, E., Lürling, M., and Scheffer, M. (2012). Recovery rates reflect distance to a tipping point in a living system. *Nature* 481, 357–360. doi: 10.1038/nature10723

Wagner, A., Malin, C., Knapp, B., and Illmer, P. (2008). Removal of free extracellular DNA from environmental samples by ethnidium monoazide and propidium monoazide. *Appl. Environ. Microbiol.* 74, 2537–2539. doi: 10.1128/AEM.02288-07

Wei, N., Nakajima, F., and Tobino, T. (2018). Effects of treated sample weight and DNA marker length on sediment eDNA based detection of a benthic invertebrate. *Ecol. Indic.* 93, 267–273. doi: 10.1016/j.ecolind.2018.04.063

Wu, S., Xiong, J., and Yu, Y. (2015). Taxonomic resolutions based on 18S rRNA genes: a case study of subclass Copepoda. *PLoS One* 10:e0131498. doi: 10.1371/journal.pone.0131498

Yamamoto, S., Minami, K., Fukaya, K., Takahashi, K., Sawada, H., Murakami, H., et al. (2016). Environmental DNA as a 'Snapshot' of fish distribution: a case study of Japanese jack mackerel in Maizuru Bay, Sea of Japan. *PLoS One* 11:e0149786. doi: 10.1371/journal.pone.0149786

Yu, D., Ji, Y., Emerson, B., Wang, X., Ye, C., Yang, C., et al. (2012). Biodiversity soup: metabarcoding of arthropods for rapid biodiversity assessment and biomonitoring. *Methods Ecol. Evol.* 3, 613–623. doi: 10.1111/j.2041-210x.2012.00198.x

Zeppilli, D., Vanreusel, A., Pradillon, F., Fuchs, S., Mandon, P., James, T., et al. (2015). Rapid colonisation by nematodes on organic and substrata deployed at the deep-sea Lucky Strike hydrothermal vent field (Mid-Atlantic Ridge). *Mar. Biodivers.* 45, 489–504. doi: 10.1007/s12526-015-0348-2

Conflict of Interest: The authors declare that the research was conducted in the absence of any commercial or financial relationships that could be construed as a potential conflict of interest.

Annexe 3 Article récupération de la diversité

Version finale de l'article publié dans la revue Marine Environmental Research après la soutenance de thèse et modifié par rapport au Chapitre 1 en tenant compte des suggestions des révisseurs choisis par l'éditeur du journal.

Recovery of hydrothermal vent communities in response to an induced disturbance at the Lucky Strike vent field (Mid-Atlantic Ridge)

Marticorena J.[1]*, Matabos M.[1]*, Ramirez-Llodra E.[2,3], Cathalot, C.[4], Laes-Huon, A.[5], Leroux R.[6], Hourdez S. [7], Donval J-P. [4], Sarrazin J.[1]*

[1] *Ifremer, REM/EEP, F-29280 Plouzané, France*

[2] *Norwegian Institute for Water Research, Gaustadalleen 21, 0349 Oslo, Norway*

[3] *REV Ocean, Oksenøyveien 10, 1366 Lysaker, Norway*

[4] *Ifremer, REM/GM/LCG, F-29280 Plouzané, France*

[5] *Ifremer, REM/RDT/LDCM, F-29280 Plouzané, France*

[6] *Research Centre for Watershed-Aquatic Ecosystem Interactions, Université du Québec à Trois-Rivières, Trois-Rivières, QC G9A 5H7, Canada*

[7] *Observatoire Océanologique de Banyuls-sur-Mer, UMR 8222 CNRS-SU, 1 avenue Pierre Fabre, 66650, Banyuls-sur-Mer, France.*

*Corresponding authors : Julien Marticorena (julienmarticorena@gmail.fr), Marjolaine Matabos (Marjolaine.matabos@ifremer.fr), Jozée Sarrazin (Jozee.sarrazin@ifremer.fr),

Abstract

So far, the natural recovery of vent communities at large scales has only been evaluated at fast spreading centres, by monitoring faunal recolonisation after volcanic eruptions. However, at slow spreading ridges, opportunities to observe natural disturbances are rare, the overall hydrothermal system being more stable. In this study, we implemented a novel experimental approach by inducing a small-scale disturbance to assess the recovery potential of vent communities along the slow-spreading northern Mid-Atlantic Ridge (nMAR). We followed the recovery patterns of thirteen Bathymodiolus azoricus mussel assemblages colonising an active vent edifice at the Lucky Strike vent field, in relation to environmental conditions and assessed the role of biotic interactions in recolonisation dynamics. Within 2 years after the disturbance, almost all taxonomic richness had recovered, with the exception of a few low occurrence species. However, we observed only a partial recovery of faunal densities and a major change in faunal composition characterised by an increase in abundance of gastropod species, which are hypothesised to be the pioneer colonists of these habitats. Although not significant, our results suggest a potential role of mobile predators in early-colonisation stages. A model of post-disturbance succession for nMAR vent communities from habitat opening to climax assemblages is proposed, also highlighting numerous knowledge gaps. This type of experimental approach, combined with dispersal and connectivity analyses, will contribute to fully assess the resilience of active vent communities after a major disturbance, especially along slow spreading centres targeted for seafloor massive sulphide extraction.

Key words: Hydrothermal vent; *Bathymodiolus azoricus*; Disturbance; Colonisation; Recovery; Deep-sea mining; Ecological succession; Benthic ecology; Mid-Atlantic Ridge

1. Introduction

Deep-sea hydrothermal vents are mainly distributed along mid-ocean ridges and back-arc basins. Vent communities are considered as productivity hotspots with a high level of endemic fauna (Tunnicliffe, 1991) that thrives mainly on chemoautotrophic primary production (Childress and Fisher, 1992). Faunal assemblages are often dominated by symbiotic foundation species such as siboglinid tubeworms, mytilid mussels, large provannid gastropods or alvinocaridid shrimps, which promote local diversity by providing 3D structures and enhancing habitat heterogeneity (Dreyer et al., 2005; Govenar and Fisher, 2007). At the edifice scale, faunal distribution consists in a mosaic of assemblages mainly influenced by environmental conditions and patchiness of fluid emissions (Sarrazin et al., 1997; Sarrazin and Juniper, 1999; Luther et al., 2001; Gollner et al., 2010; Marsh et al., 2012; Husson et al. 2017). Indeed, species colonise the mixing gradient depending on their physiological tolerance to environmental conditions, nutritional requirements and biotic interactions (e.g. predation, facilitation; Levesque et al. 2003, Mullineaux et al. 2003, Sancho et al. 2005). Biotic interactions were suggested to prevail in high diffuse-flow areas where the resources are not limited, while facilitation will predominate in habitats with lower fluid input (Mullineaux et al. 2003). As observed in coastal hard substrate communities, mosaics are highly dynamic and patche's size and boundaries amongst the patched may change through time (Connell and Keough, 1985). At large spatial scale, the patchiness of vent habitat results in a network of metacommunities and population connectivity is insured by dispersal of planktonic larvae (Mullineaux et al., 2018).

Hydrothermal vents are naturally subject to stochastic major disturbance such as volcanic eruptions that may eradicate faunal assemblages at the vent-field scale. On the other hand, since the first discovery of hydrothermal vents and associated seafloor massive sulphide (SMS) deposits, more than 40 years ago, the interest of mining companies for commercial exploitation of their high metal content has been increasing (Corliss et al., 1979; Spiess et al., 1980; Van Dover, 2011). These industrial activitiy has not yet started, but it is predicted that they may induce different levels of impacts (Boschen et al., 2013; Cuvelier et al., 2018; Orcutt et al., 2020), including physical destruction of habitats and the complete eradication of their faunal communities within the mining site (Van Dover 2007). The creation of a sediment plume may also affect different biological processes, such as reproduction, dispersal, mobility

and feeding strategies at larger scale (Van Dover, 2010; Boschen et al., 2013; Gollner et al., 2017; Suzuki et al., 2018; Washburn et al., 2019). However, there are still many uncertainties about community resilience, and the time-scale needed for a possible recovery of the impacted ecosystems (Cuvelier et al., 2018).

Disturbance in mosaic habitats such as active vents may play an important role in initiating, maintaining or enlarging patches within established assemblages (Sousa 1985; Denny 1987). The fundamental question of recolonisation and recovery of vent assemblages after a disturbance can be studied in a metacommunity framework, using a patch dynamics approach in which the colonisation and persistence of impacted area is highly dependent on dispersal across vent fields and local disturbance regimes (Leibold et al., 2004; Mullineaux et al., 2018). At local scale, the settlement of post-larvae is influenced by environmental conditions and habitat suitability and recolonisation dynamics are also dependent on biotic interactions that may induce facilitation or competitive exclusion (Mullineaux et al., 2003; Sancho et al., 2005). Understanding processes acting at small scales are paramount in evaluating mechanisms controlling successional dynamics after recolonisation by species from afar.

At active vents, the few examples of recovery are based on studies linked to large-scale natural disturbances caused by volcanic and tectonic activities (Butterfield et al., 1997; Tunnicliffe et al., 1997; Shank et al., 1998; Marcus et al., 2009; Gollner et al., 2015a). The frequency of such disturbances is highly variable among vent systems, depending on their geological settings. At fast-spreading ridges, where vent sites are separated by a few kilometers, volcanic eruptions occurs with time intervals of a decade (Tolstoy et al. 2006) and macrofaunal communities show a fairly good recovery of diversity and densities within few years following the various eruptions (Tunnicliffe et al. 1997; Shank et al. 1998; Marcus et al. 2009; Gollner et al. 2015a, 2017, 2020). However, differences in the sampling methodology between these studies (e.g. some used visual surveys while others sampled faunal assemblages) and the faunal compartment considered lead to differences in the estimation of recovery rates. Moreover, little information about the pre-disturbed baseline communities was available, making the comparison with post-disturbance communities difficult. Differences in community composition after re-colonisation were also observed (Mullineaux et al., 2020, 2012) and the prolonged monitoring of diversity showed that community composition was still changing ten years after the disturbance, suggesting that the disturbed

assemblages did not reach a climax stage during this time period (Mullineaux et al., 2020). Conversely, at slow spreading ridges, vent sites are separated by hundreds of kilometers (Beaulieu et al., 2015) and opportunities to observe natural disturbances are rare. Therefore, assessing the recovery ability of communities requires the use of alternative indirect approaches. One way is to use population connectivity data to estimate the recolonisation potential of key species, and thus infer vent community recovery rates (Baco et al., 2016; Breusing et al., 2016) as it was done by Suzuki et al. (2018). Their dispersal network analysis on species from 131 vent fields of the western Pacific Ocean estimated that a full recovery to original communities would take from 6 to 130 years. The slow recovery rate estimated in comparison to fast-spreading centers may notably be due in part to differences in topography that may reduce horizontal dispersal and connectivity (Mullineaux et al. 2018). However, this approach based on dispersal ability does not take into account the local factors influencing faunal establishment and many uncertainties remain regarding the role of biotic and abiotic conditions in recolonisation dynamics and ecological succession once the larvae reach the disturbed area.

In the present study, we provide an early evaluation of the recovery potential of active vent communities to a small-scale (< 1 m^2) disturbance experiment initiated in 2017 on the Lucky Strike (LS) vent field, northern Mid-Atlantic Ridge (nMAR). After removing the fauna, we followed during 2 years the recolonisation dynamics of *Bathymodiolus azoricus* mussel assemblages and their habitats on a series of experimental quadrats. This experimental setting allowed us to describe the pre-disturbed structure of vent communities on the Montségur edifice (LS) and to monitor the recolonisation of benthic communities after the disturbance. The main objective of this work is to identify the role of biotic and abiotic conditions on recolonisation dynamics at the edifice scale, through the use of cages and measurements of environmental conditions. We expected that microbial communities would first colonise the bare substratum, followed by grazers (including several species of gastropods) that may feed on microbial mats. The engineer species *B. azoricus* would take more time to fully occupy the space, its presence facilitating the establishment of associated taxa and contributing to increasing diversity. We anticipated that mobile predators (e.g. shrimps, crabs or fishes) would play a major role in patch colonisation, influencing the first step of recovery. Although the scale and target of this experiment strongly differ from large-scale disturbance, our results

provide fundamental knowledge on recolonisation patterns of active hydrothermal vent habitats at the edifice scale.

2. Material and methods

2.1. Study site

The Lucky Strike (LS) vent field is a basalt-hosted vent field situated close to the Azores Triple Junction on the northern part of the Mid Atlantic Ridge (MAR) (Langmuir et al., 1997) (Fig. 1A). LS contains over twenty active hydrothermal edifices distributed around a circular fossilised lava lake at an average depth of 1700 m (Ondreas et al., 2009). Montségur is a small active sulphide edifice that extends over a surface of 24 m x 16 m. It is located on a flat hydrothermal slab at the south-east of LS (Fig. 1B). At least seven black smokers have been identified on the edifice, in addition to the extensive diffuse low-temperature discharges through cracks at its base and on its flanks (Barreyre et al., 2014). Montségur is covered by dense mussel assemblages of the engineer species *Bathymodiolus azoricus*. Vent faunal communities inhabiting diffuse flow areas on and around the edifice are characterised by high-density populations of gastropods (*Protolira valvatoides, Lepetodrilus atlanticus, Pseudorimula midatlantica*), polychaetes (*Branchipolynoe seepensis, Amphisamytha lutzi*) and shrimps (*Mirocaris fortunata*) (Sarrazin et al. 2020).

2.2. Experimental setup

In July 2017, an experimental setup was deployed during the Momarsat cruise on board the R/V "*Pourquoi pas ?*" using the Remotely Operated Vehicle (ROV) *Victor6000*. Thirteen stainless steel quadrats (50 x 50 cm), equipped with pyramidal structures on top, were installed over *Bathymodiolus azoricus* assemblages (Fig. 2), on the steep walls of the Montségur edifice or in cracks at its base (Fig. 1C), to account for spatial variability of vent assemblages. Eight of them, named "experimental quadrats", were devoted to the study of recolonisation processes following faunal clearance after 1 (C1) and 2 (C2) years (August 2018 and June 2019 respectively). Replicate samples for each year were denoted as "a" or "b" (Fig. 1C). In addition to the experimental quadrats, five "reference" quadrats (R) were deployed and sampled in 2017 (R0a, R0b), 2018 (R1) and 2019 (R2, R2cg) to characterise the natural dynamics of faunal communities on Montségur throughout the experiment. The role of large mobile predators (crabs, shrimp or fish) on local recolonisation was examined by covering

some of the pyramidal structures with a 1 cm plastic mesh. These specific quadrats were denoted as “cg'' for caged (Fig. 2C). This experimental design is summarised in Figure 3.

2.3. Environmental characterisation

Temperature and key chemical parameters were assessed from *in situ* measurements on all quadrats before and after faunal sampling and this, for each year of the study (2017 to 2019). Our objectives were to identify the spatial and temporal variability of these factors and evaluate their role in the recolonisation processes. The *in situ* chemical analysers CHEMINI (Vuillemin et al., 2009) were used on three replicate points in each quadrat to measure dissolved concentration of total sulphides [TdS : $H_2S+HS^-+S_2$] and total dissolved iron [TdFe : Fe (II)]. To complete the chemical characterisation, water samples were collected with the PEPITO water sampler at each quadrat prior to faunal sampling (Sarradin et al., 2009). Oxygen concentrations were measured using an Aanderaa optode probe (Tengberg et al. 2006) connected to the outlet of the PEPITO sampler. Methane [CH_4], was analysed back in the laboratory by GC-FID and HID (Donval et al. 2008). In addition to this one-time yearly characterisation, temperature was monitored every 2 hours over the deployment period using two iButtons^{TM} probes attached to each quadrat and deployed directly on the mussel assemblages with a measurement resolution of 0.5 °C.

2.4. Faunal sampling and identification

During the Momarsat 2017 cruise, eight experimental quadrats -noted “C”- were cleared of their fauna using both the suction sampler and the claw of the ROV *Victor6000* mechanical arm (Fig. 2A, 2B). The same year, R0a and R0b reference quadrats were also sampled, leading to a total of 10 quadrats used to describe the pre-disturbed vent community of Montségur (Fig. 3). During Momarsat 2018, the four experimental quadrats dedicated to the “one-year after disturbance recolonisation study” -noted “C1”- and reference quadrat R1 were sampled (5 quadrats in total; Fig. 3). During the Momarsat 2019 cruise, the four experimental quadrats dedicated to the “two-year after disturbance recolonisation study” noted “C2”-and reference quadrats R2 and R2-cg were sampled (6 quadrats, Fig. 3). The surface area of each quadrat was filmed before and after faunal sampling with the ROV high definition cameras to estimate

the sampled surfaces using imagery analysis (Fig. 2A, 2B). A target with 7 mm checkerboard squares was fixed on each quadrat, providing scaling in the field of view (Fig. 2B).

In this study, fauna will include macrofauna and any meiofauna taxa larger than 250 µm (nematodes, copepods and ostracods). We also include species often considered as megafauna (shrimp, mussels) recovered within the quadrats. The faunal samples were preserved in 96% ethanol. All individuals collected were identified to the lowest possible taxonomic level under a stereomicroscope and counted.

2.5. Population size structure

Size-frequency distributions of the six most dominant species were analysed for each sample of the Montségur edifice. Each individual was measured, using different measurements depending on the species (see details in Table S1). The biggest individuals were measured using a caliper while small individuals were measured on screen to the nearest 0.001 mm, using the Leica Application Suite software. Measurement error was calculated as the maximum difference among 10 measurements of the same individual on 10 specimens comprising a range of all sizes for each species (Table S1). For each assemblage sampled, length-frequency distribution was plotted for the six species. Size class intervals were chosen according to three criteria: i) most size-classes must have at least five individuals; ii) the number of adjacent empty classes must be minimised; and iii) the interval has to be greater than the measurement error (see Jollivet et al. 2000). Size-frequency distributions were compared to a normal distribution using a one-sample Kolmogorov-Smirnov test and differences between the pre-disturbed and post-disturbance communities were identified using a pairwise Kolmogorov-Smirnov test. Non-parametric Wilcoxon-Mann-Whitney tests were performed to identify differences in mean individual size between the pre-disturbed community and the novel one, after the recolonisation processes in each location.

2.6. Data analyses

All analyses were computed in R environment (R Core Team, 2018). Species rarefaction curves were computed for each sample, habitat and year to verify the robustness of the sampling effort and characterise the overall diversity. Local diversity was estimated for each assemblage by computing α-diversity indices such as species richness (S), Shannon entropy (H) and the Pielou's evenness index (J') using the vegan package in R (Oksanen et al., 2019). Contingency

tables were weighted by the sampling surface for each quadrat for comparison purposes. The resulting density data were used for all subsequent analyses.

Environmental conditions – The temperatures measured by the iButtons^{TM} probes were used to characterise each assemblage/quadrat. Four temperature parameters were compiled, including the average (T.avg), minimum (T.min), maximum (T.max) and standard deviation (T.sd). In addition, average concentrations of oxygen (O_2), methane (CH_4), total dissolved iron (TdFe) and sulphides (TdS) as well as standard deviations of TdFe and TdS were used to characterise the spatial variability of abiotic factors among the different Montségur quadrats. A principal component analysis (PCA) was built with all environmental variables (packages FactoMineR and factoextra - Kassambara and Mundt 2019) to identify patterns in environmental conditions among quadrats and determine which variables accounted for most of the observed variance. Finally, Whittaker-Robinson periodograms, programmed in the R package adespatial (Dray et al., 2020) were used to screen for significant periodicities in temperature time series.

Community structure – A canonical redundancy analysis (RDA) was performed on Hellinger-transformed densities and environmental variables retained by a forward selection (vegan package - Oksanen et al. 2019) to evaluate the spatial variability of community composition in relation to abiotic factors in the baseline communities on the Montségur edifice. This allows us to evaluate the representativeness of baseline communities in Montségur in comparison with faunal assemblages already described on other active edifices of the Lucky Strike vent field.

Recovery patterns – Faunal recovery patterns were assessed from experimental quadrats. Differences in faunal composition among quadrats along the recolonisation processes were tested using a non-parametric analysis of similarity (ANOSIM; Anderson 2001). The ANOSIM R value is based on differences in average ranking of dissimilarity indices (i.e. Bray-Curtis dissimilarity matrix) between and within the different predefined groups (here each recovery stage, i.e.: pre-disturbed state, one year and two years after disturbance). A RDA on Hellinger-transformed densities data was also used to identify the role of environmental conditions and biotic interactions (i.e. by testing the cage effect) on the structure of macrofaunal assemblages during the recolonisation processes. A variable named “quadrat” was used to evaluate the independence of the samples from the same quadrat over the years in the explanatory

environmental matrix. Moreover, to test for the effect of time after disturbance, we coded a quantitative variable named "Yr-aft-dist" (i.e. year after disturbance). In this framework, pre-disturbed reference samples were considered as baseline communities at an equilibrium state and thus were coded with a value greater than 2 years. As the age of the natural community is unknown, analyses were run with different values [3 years, 10 years and 100 years] but they all yielded to similar results. Based on previous studies about the temporal stability of these communities (more than 14 years on Eiffel Tower, Cuvelier et al. 2011b) and data about recovery time in other vent system after a major disturbance (4-5 years, Gollner et al. 2017), we considered 10 years as a good compromise to be used for the analysis.

3. Results

3.1. Environmental conditions

Mean temperature among the different quadrats of Montségur varied between 5.2 °C and 9.5 °C (Table 1). R1 and C2a exhibited the highest maximum temperatures (with maximum of 16.1 °C and 22.1 °C respectively), but also higher concentrations in TdFe and CH_4 associated with a more acidic pH (Table 1, Fig. S1).

The two temperature probes separated by ~ 10 cm deployed on each quadrat were used to characterise the spatial variability of abiotic conditions at fine scales. While homogeneous temperatures are observed within some quadrats (e.g. C1a, C1bcg, C2b, C2bcg), others showed a high variability of temperatures in the narrow spatial gradient (few centimetres, e.g. C1b, C2acg); (Fig. S2).

Notable differences in temperature on single quadrats between the two years were observed. C1b, C1acg and C2a quadrats showed a sharp decrease in mean and variability of temperatures at different times during the first year of deployment (Fig. S2). Periodogram analyses carried out on temperature time series revealed significant periods of 12 h for most quadrats. In addition, significant periods of 24 h were also identified on all quadrats except C1acg. Additional periodic signals, possibly harmonics related to the tidal signal, with periods of 36 h and 48 h, were also revealed for C1a, C1acg and C1bcg.

3.2. Pre-disturbed communities

The rarefaction curves built for each pre-disturbed sample of Montségur (Fig. S3) nearly reached an asymptote showing that the sampling effort was sufficient to capture the overall taxonomic diversity of macrofaunal benthic communities of active vent habitats. In total, 43 taxa were identified among a total of 34 158 individuals in the different samples. Most assemblages were characterised by a taxonomic richness varying between 19 and 28 (Table S2). The C1a sample, which is the only quadrat located on the west side of the edifice, displayed the highest taxonomic richness with the occurrence of 32 taxa, while R2 showed only 12 taxa among 133 identified specimens (Fig. 4; Table S2). Macrofaunal communities were dominated by six taxa: the engineer species *Bathymodiolus azoricus* and its commensal worm *Branchipolynoe seepensis*, the polychaete *Amphisamytha lutzi* and three species of gastropods *Lepetodrilus atlanticus*, *Protolira valvatoides* and *Pseudorimula midatlantica*. Together, they accounted for 68.3 ± 15.7% of the total abundance. The nematode *Oncholaimus dyvae* and copepod *Aphotopontius sp*., which are typical meiofaunal species, were also abundant in the > 250 µm fraction of most samples. In the pre-disturbed community, ~74% of taxa (e.g. 29 taxa over 43) showed low occurrence and abundance (i.e. below 1% frequency) in the different samples (Table S3).

A RDA has been performed to identify the role of environmental conditions on faunal distribution and verify the temporal stability of baseline communities. The RDA model performed on Hellinger-transformed species densities accounted for 49.6% (adjusted R^2: 25.1%, p = 0.008) of the total inertia in macrofaunal species assemblage structure (Fig. 5). The overall RDA model was significant (*p-value* = 0.004) and only the first axis was significant (p = 0.05), accounting for 20% of the variation in community structure. Maximum temperature (T.max) and total dissolved sulphide concentrations (TdS) were the significant environmental factors influencing macrofaunal composition (p = 0.009 and 0.021, respectively). The years at which the samples were collected did not explain the differences between quadrats. R2cg sample stood out from the other sampling locations and was characterised by a high relative density of the gastropod *Lurifax vitreus*, contrasting with a low density of *B. azoricus* (Fig. 5). Moreover, the C2acg and R0b samples, characterised by a high density of amphipods (*Luckia striki*), formed a distinct group (Fig. 5). All other samples showed a quite homogeneous faunal composition.

3.3. Recovery patterns of benthic communities

Recolonisation dynamics of the foundation species – The recovery rate of *Bathymodiolus azoricus*, in terms of density, varied between 9.7% and 37.6% on the different quadrats one year after disturbance, and from 1.9% to 33% two years after disturbance (Fig. 6). No significant difference can be noticed between the mean recovery rate after 1 year (19.8 ± 13%) and 2 years of recolonisation (14.4 ± 13.5%) (Student test: t = 0.59, *p-value* = 0.58). However, with the exception of the C2bcg quadrat, the percentage of recovery was slightly higher in the quadrats that were caged during the recolonisation process (>20%) compared to the uncaged quadrats (<15%) (Fig. 6). The size population structure analyses of *B. azoricus* showed individuals ranging from 251 µm to 8.5 cm length within the different assemblages (Fig. 6). The pre-disturbed structure of the population on Montségur showed a polymodal size distribution dominated by a large proportion (i.e. 52% of the overall population) of small individuals below 5 mm in shell-length and a tail of distribution in larger sizes containing several cohorts (Fig. 6). Pairwise Kolmogorov-Smirnov distribution tests showed significant differences in population size structure between the pre-disturbed and post-disturbance communities in all samples (*p-value* < 0.001), except C2b (D = 0.10, *p-value* = 0.13) (Fig. 6). Furthermore, Wilcoxon-Mann-Whitney tests highlighted that the mean shell length of *B. azoricus* was smaller 1 and 2 years after the disturbance compared to that of the pre-disturbed community for all samples except C1a and C2b (Fig. 6). Furthermore, the proportion of juveniles of *B. azoricus* (< 5 mm) in the overall population was higher in assemblages sampled 1 year (67%) and two years (70%) after the disturbance in comparison to pre-disturbed populations (52%) (Table S3).

Recolonisation dynamics of active vent communities – The rarefaction curves did not level off for most of the post-disturbance samples on Montségur, but they show similar trends than that of pre-disturbed communities (Fig. S3). The shape of the curves indicate that they should reach a plateau earlier, highlighting a higher evenness in the recovering communities. Species richness (S) is lower (from 1 to 6 less species) in the post-disturbance assemblages compared to the pre-disturbed communities 1 year after the induced disturbance (Fig. 4A, Table S2). On the other hand, two years after, the C2a and C2acg quadrats showed a higher species richness than pre-disturbed quadrats, while C2b and C2bcg exhibited lower values after the disturbance (Fig. 4A, Table S2). Overall, species richness was homogeneous between all samples and was not significantly different along the recolonisation process (Kruskal-Wallis

352 test: P= 1.17, *p-value* = 0.56, Fig. 4A). However, macrofaunal densities were significantly lower
353 after 1 year (15 768 ± 12 487 ind.m^{-2}) and 2 years (11 190 ± 8 270 ind.m^{-2}) after the
354 disturbance, in comparison to the pre-disturbed community (34 402 ± 7 590 ind.m^{-2}) (Kruskal-
355 Wallis test: P= 7.65, *p-value* = 0.021 and Post hoc Dunn test: *p-value* < 0.05, Fig. 4A) with a
356 density recovery rate ranging from 15.7% on C1b after 1 year to 79.6% on C2acg 2 years after
357 the disturbance (Fig. 6, Table S2). The Shannon index and Pielou's evenness were highly
358 variable across samples in the pre-disturbed communities, but higher 1 year and 2 years after
359 the disturbance (Fig. 4C and 4D, Table S2). Overall Pielou's evenness index is significantly
360 higher in post-disturbance communities compared to pre-disturbed communities (Kruskal-
361 Wallis test: P= 7.34, *p-value* = 0.026 and Post hoc Dunn test: *p-value* < 0.05, Fig. 4D). In the
362 same way, the proportion of low occurrence species is lower in post-disturbance communities
363 (60% after 1 year and 58% after 2 years) than prior to the induced disturbance (74%) (Table
364 S2).

365 The output of the RDA computed on Hellinger-transformed densities of the different species
366 along the recolonisation process showed a significant difference in faunal composition
367 between the pre-disturbed communities and post-disturbance communities at Montségur
368 (Fig. 7). The RDA model explained 42% (Adjusted R^2 = 20.5%) of the total inertia in species
369 assemblage structure (*p-value* = 0.006). The main driver of this observed difference is time
370 after the induced disturbance (*p-value* = 0.001), whereas no significant cage effect or
371 dependence between sites were observed (p-values = 0.300 and 0.262, respectively). The
372 analysis of similarity (ANOSIM) on Bray-Curtis dissimilarity matrix suggests a major change in
373 macrofaunal composition between pre-disturbed communities and those after 1 and 2 years
374 of recolonisation (R = 0.712, *p-value* = 0.001). However, no significant difference in faunal
375 composition was identified between the assemblages collected 1 year and those collected 2
376 years after the disturbance.

377 Some species appeared to play a major role in the observed differences along the
378 recolonisation process (Fig. 8). Indeed, a decrease in the abundance of the typical vent species
379 (*Bathymodiolus azoricus*, *Branchipolynoe seepensis*, *Amphisamytha lutzi* and *Lepetodrilus*
380 *atlanticus)* was observed in the post-disturbance communities, while small gastropod species
381 (i.e. *Lurifax vitreus*, *Protolira valvatoides*, *Laeviphitus desbruyeresi*, *Xylodiscula analoga*) and
382 nematodes (*Oncholaimus dyvae*) showed a significant increase in the post-disturbance

communities (Fig. 8, Fig. S4). *Pseudorimula midatlantica* and the copepod *Aphotopontius sp.* displayed higher relative abundances in the first year after the disturbance in comparison to the pre-disturbed community and returned to lower values 2 years after the disturbance. As observed for *B. azoricus,* the other dominant species displayed a polymodal structure of size distribution and differences have been identified between the pre-disturbed community and post disturbance state (pairwise Kolmogorov-Smirnov test) (Fig. S4). Furthermore, individuals of *A. lutzi*, *B. seepensis, L. lepetodrilus* and *P. valvatoides* were overall smaller within the communities after disturbance in comparison to those of the pre-disturbed community in most quadrats (Fig. S4). For *P. midatlantica*, only 1 quadrat showed significant differences in population size structure (Fig. S4).

4. Discussion

In this study, we provide an early evaluation of the recovery of deep-sea benthic communities to a small-scale (<1 m²) disturbance experiment at an active hydrothermal edifice located on the Lucky Strike vent field. The structure of pre-disturbed communities and their recovery patterns were characterised through the analysis of faunal composition, diversity, population size structure in relation to biotic and abiotic factors at the Montségur edifice. This experimental design represents an innovative approach to assess the recovery of vent communities in areas where opportunities to observe natural disturbances are rare. It provides useful insights about local recolonisation drivers at hydrothermal vents, data that can contribute to the elaboration of conservation strategies in the context of potential deep-sea mining activities on seafloor massive sulphides.

4.1. Habitat characterisation

In active vent ecosystems, environmental factors are strongly linked to the output flux and chemistry of hydrothermal fluids and the resulting physico-chemical conditions along the mixing gradient between vent fluids and surrounding sea water. Within the active habitats sampled in this study, mean temperature among *Bathymodiolus azoricus* faunal assemblages varied from 5.2 to 9.5 °C with a maximum of 22.1 °C, which corresponds to the temperature ranges of Eiffel Tower habitats (Husson et al. 2017, Sarrazin et al. 2020). We identified two microhabitats hosting *B. azoricus* assemblages, which have previously been described as cold and warm habitats in Sarrazin et al. (2015). However, while in our study these habitats are

colonised by mussels, in the previous study warm habitats were rather reported to be associated with shrimp assemblages. This discrepancy could be related to temperature measurements: in the present study, temperature was measured using iButtons^{TM} deployed on or within the mussels while most measurements reported previously were conducted using the ROV probe placed a few millimeters above the faunal assemblages (Cuvelier et al. 2014a, Husson et al. 2017, Sarrazin et al. 2015, 2020). The rapid mixing of the warm fluids with the above cold seawater can account for these differences. Similar to previous studies, most samples belonging to the cold habitat showed small variability in environmental conditions and were associated with low temperature, low concentrations of iron and sulphides, high pH and high concentrations of dissolved oxygen (Cuvelier et al. 2011a; Sarrazin et al. 2015). However, a few quadrats (R1, C2a and R0b) were characterised by higher temperatures, total dissolved sulphide and iron concentrations as well as lower dissolved oxygen concentrations with acidic pH, which are more representative of warm habitats.

The continuous bi-hourly monitoring of temperature revealed a high spatial variability in temperature regime (up to 3°C across 10 cm), suggesting the occurrence of multiple microhabitats within a single quadrat. This was supported by high standard deviation values of replicate measurements for sulphides and iron concentrations performed every year. This small-scale temporal variability of temperature can be a result of several processes, including the interplay between sulphide and oxygen biological uptake (Johnson et al., 1988), the formation of diffuse fluids in the subsurface, the chemical reactivity of the mixing zone, the porosity of the substratum in active habitats on the East Pacific Rise (Butterfield et al. 1990; Sarrazin et al. 2002, Le Bris et al. 2006) or tidal oscillations (Barreyre et al. 2014). Our results show significant semi-diurnal and diurnal periods and harmonics, supporting the presence of periodic oscillations related to tidal processes. Tidal modulation of diffused-flow has been reported in many vent systems (Cuvelier et al., 2014b; Sarrazin et al., 2014; Scheirer et al., 2006). These variations are mainly caused by tidally induced currents (Barreyre et al., 2014; Khripounoff et al., 2008) and changes in hydrostatic pressure on the seafloor (Davis and Becker, 1999). This periodicity could be beneficial for symbiotic sessile species that need alternative inputs of reduced compounds and oxygen to ensure chemosynthesis (Scheirer et al. 2006, Mat et al. 2020) but can also influence the behaviour of mobile species (Lelièvre et al., 2017).

4.2. Pre-disturbed communities and natural variability

On the active Montségur edifice, all experimental quadrats were visually dominated by medium-sized *B. azoricus* mussels from 5.2 ± 8.8 mm to 24.4 ± 14.3 mm. These sizes are consistent with the mean lengths reported by Comtet and Desbruyères (1998) on different edifices of Lucky Strike (between 5.63 ± 5.67 mm and 49.63 ± 31.41 mm), but smaller than those measured by Sarrazin et al. (2015) on the nearby Eiffel Tower edifice (between 22.7 ± 18.07 and 74.7 ± 2.57 mm). Indeed, we observed a high proportion (between 52 and 96%) of very small individuals -below 3 mm- in each sample, sizes that correspond to post larval and juvenile stages. The presence of several successive cohorts suggests the occurrence of a massive recruitment event around June, just before sampling. These results are consistent with the lifecycle of *B. azoricus*, with an annual spawning event in January followed by a planktotrophic larval development and the settlement of post-larvae in May-June (Colaço et al., 2006; Comtet and Desbruyères, 1998; Dixon et al., 2006). Furthermore, differences in mean shell length of *B. azoricus* observed among samples on pre-disturbed communities may be due to spatial segregation of sizes related to environmental factors (Sarrazin et al., 2015; Husson et al., 2017) or to biotic interactions (e.g. competition, predation) that may play an important role in recruitment success and survival of post-larvae (Lenihan et al., 2008; Sancho et al., 2005).

All samples collected at the active Montségur edifice were dominated by the same macrofaunal species (e.g. *B. azoricus*, *B. seepensis*, *A. lutzi*, *P. valvatoides* and *L. atlanticus*), which have been previously described as indicator species of cold microhabitats on the Eiffel Tower edifice situated ~ 50 m from Montségur (Sarrazin et al., 2015b). The high similarity between the fauna from the two edifices may be related to their belonging to the same chemistry domain (Chavagnac et al. 2018, Sarrazin et al. 2020). Among the 43 macrofaunal species identified on Montségur, approximately 74% exhibit a low frequency of abundance (<1%). Total densities of organisms in the pre-disturbed communities ranged from 3 330 to 68 960 ind.m^{-2} across the different samples, and is much lower than the values reported by Sarrazin et al. (2020) on the same edifice (between 62 253 and 126 437 ind.m-2). In several studies, small mussel assemblages, inhabiting cold microhabitats, harbour higher density and

diversity of associated species than large mussel assemblages, found in warmer microhabitats (Cuvelier et al., 2009; Dreyer et al., 2005; Sarrazin et al., 2015). Surprisingly, in this study the highest densities of organisms have been observed in the warmest and more variable habitats. This result may be linked to the differences in the method for assessing temperature as mentioned above. Indeed, temperature values obtained by probes deployed directly on the substratum are expected to be higher than the ones obtained with the ROV probe a few millimeters above faunal assemblages.

As expected, macrofaunal distribution was significantly influenced by environmental conditions, especially by mean temperature and mean concentrations in total sulphides and methane, in addition to slightly acidic conditions (pH <7.3). However, biotic factors such as competition for space and food resource, but also predation or facilitation, may also play an important role in faunal distribution in diffuse flow habitats (Sarrazin et al. 1997, Sen et al. 2013; Gollner et al. 2015b; Husson et al. 2017). On the other hand, faunal composition within reference quadrats did not differ over the three years of the experiment, suggesting a relative stability of the community over time. This supports the observed high stability of mussel communities on the nearby Eiffel Tower edifice, which led to the assumption that *B. azoricus* assemblages at Lucky Strike can be considered as a "climax" community (Cuvelier et al., 2011b). The absence of natural changes in faunal assemblages, at the edifice scale, during the experiment allows us to use them as a baseline to test the effect of the induced disturbance on benthic communities.

4.3. Recolonisation processes and recovery

In Figure 9, we propose a succession model of nMAR vent communities based on the present experiment at the Lucky Strike vent field and from previous studies conducted after natural disturbances at vents. The first step after the disturbance relies on the release of an ecological niche induced by the removing of faunal assemblages. Then, the stabilisation of environmental conditions, especially of temperature and reduced compounds, would allow chemoautotrophic primary production and proliferation of microbial mats, as observed in studies from vents in the Pacific Ocean (Marcus et al., 2009; Shank et al., 1998; Tunnicliffe et al., 1997). This is followed, within one year, by the arrival of mobile opportunistic species,

including shrimps and copepod species. Although not significant, our results suggest that these predator species may slow down the settlement of associated species, resulting in a poor recovery of faunal densities despite a good species richness recovery. Two years after the disturbance, the settlement of several gastropod species grazing on free-living microbial mats have been observed. At this stage, the higher Pielou's evenness compared to baseline communities suggests that biotic interactions are not yet fully effective within assemblages. Gastropods have already been described as main pioneer colonists at 9°N EPR after the 2006 volcanic eruption (Mullineaux et al., 2012, 2010). Indeed, despite contrasting reproductive characteristics, some of them are able to maintain an important effective population size and support high abundances, especially through an early maturity and continuous gametogenesis (Marticorena et al., 2020). Thereafter, we hypothesise a later settlement of the foundation species *B. azoricus* due to its seasonal reproduction, which leads to a single recruitment event in June (Colaço et al., 2006; Dixon et al., 2006). The recolonisation of *B. azoricus* can occur through recruitment events and settlement of post-larvae and juveniles or by immigration of mobile adults from nearby assemblages (Comtet and Desbruyères, 1998). Indeed, observations made on imagery on the Eiffel Tower edifice showed that *B. azoricus* is able to move several centimetres a day (Matabos, Sarrazin, unpublished data). Since the growth rate of B. azoricus juveniles has been estimated to reach ~ 2 mm per year on the Eiffel Tower edifice (from imagery analysis, Sarrazin and Matabos unpublished data), we can assume that the presence of mussels larger than 1 cm after 1 and 2 years of recolonisation is most probably a result of adult migration. On the other hand, the mean shell length of *B. azoricus* was significantly lower and a higher proportion of juveniles were observed on post-disturbance assemblages compared to pre-disturbed communities. This suggests that within our study, the recruitment and settlement of young mussels were the main drivers of recolonisation after the disturbance, rather than migration. Moreover, the results of the predator exclusion experiment suggest that the recruitment success of *B. azoricus* might depend on predation pressure on post-larval individuals by large mobile predators (e.g. shrimp, crabs, fishes). The impact of predation on the entire benthic community could be even more significant when predators specifically feed on taxa that play a key role in the community and interact widely with other species (Paine, 1966). We also observed that the cages led to the formation of thick microbial mats on their surfaces, implying that the presence of the plastic mesh and its size may have modified the input of hydrothermal fluids. The deployment of additional "true" cage

control quadrats would be necessary to dissociate the role of predator exclusion and potentially other effects of the mesh such as hydrodynamic modifications. The establishment and growth of *B. azoricus* may then promote the settlement of low occurrence species and a rapid recovery of faunal densities through the creation of a three dimensional habitat that contributes to reduce fluid flux, making the habitat more suitable for other species (Johnson et al. 1988; Sarrazin et al. 1997, Shank et al. 1998). Finally, biotic interactions including predation, competition for space and nutritional resources and facilitation may lead to changes in faunal relative abundance and dominance before reaching an equilibrium. All these mechanisms contribute to reducing the evenness among assemblages and enhance the dominance of a few taxa (Fig. 9). Once this equilibrium is achieved, we can consider that these assemblages reach their climax. The climax community of Montségur appears to be similar to that of the neighbouring Eiffel Tower edifice (Cuvelier et al., 2011a) and some other active edifices of the Lucky Strike vent field (Sarrazin et al. 2020). These communities are characterised by the dominance of a few vent taxa and a high proportion of low occurrence species. Natural or anthropogenic disturbance events, which can occur at each step of this successional model, may lead to significant changes in faunal assemblages and even provoke community collapse, depending on their spatial breadth as proposed in different vent successional models (Sarrazin et al. 1997, Shank et al. 1998).

Several factors can come into play in recolonisation and ecological succession following a disturbance, and their relative importance changes according to the scale of disturbance (Zajac et al. 1998, Benedetti 2000). After a small-scale disturbance, recovery of vent assemblages are strongly affected by the spatio-temporal variability of environmental conditions, which may lead to local extinction or creation of new suitable habitats (Sarrazin et al. 1997; Shank et al. 1998, Marcus et al. 2009; Sen et al. 2014). Feeding strategies (Lelièvre et al. 2018; Van Audenhaege et al., 2019) and biotic interactions (i.e. competition for space, facilitation or predation) have also been identified as important drivers of faunal succession at the edifice scale (Sarrazin et al. 1997, Micheli et al. 2002; Hunt et al. 2004; Govenar and Fisher 2007; Cuvelier et al. 2014a). In this study, we showed that, at this small-scale, biological interactions are more likely to play a predominant role in faunal succession rather than environmental conditions. The same observations have been noticed on vents at back-arc basins and may be due to the high stability of environmental conditions, typical of slow-spreading centers (Sen et al., 2014). Furthermore, in mosaic habitats, the diversity and species

574 composition at the boundary of disturbed patches might modulate biotic interactions and
575 migrations of individuals, influencing early stages of recovery (Bulleri et al. 2006). However,
576 diversity descriptors and faunal composition were relatively homogeneous between the
577 different quadrats at each step of the recolonisation process, suggesting that succession after
578 small-scale disturbance at Lucky Strike can be described as a deterministic sequence of species
579 replacement. As observed on rocky-shore habitats, the timing of disturbance might also affect
580 recolonisation patterns (Sousa 1985, Benedetti and Cinelli 1996). For example, *B. azoricus*
581 have been described to recruit seasonally around the month of June (Dixon et al. 2006; Colaço
582 et al. 2006) and the occurrence of disturbance in spring might result in a faster recovery of
583 assemblages and less importance of gastropods in the first stage of recolonisation.
584

585 ## 5. Conclusion

586 We designed a novel *in situ* experimental approach to identify biotic and abiotic factors driving
587 the recolonisation and succession of vent communities after a small-scale disturbance.
588 Recolonisation dynamics was strongly affected by species composition of the neighbouring
589 faunal assemblages. Biotic interactions were predominant and highly influenced the slow
590 recovery of vent assemblages, while environmental factors remained stable. Our results,
591 coupled with observations from literature data, lead to a first conceptual model of
592 colonisation and ecological succession for northern Mid-Atlantic communities.
593

594 At regional scales (i.e. vent field), life-history traits including reproduction (Kelly and Metaxas,
595 2007), larval dispersal modes and recruitment abilities (Levin et al., 1996; Levin, 2006;
596 Mullineaux et al., 2003, 2012) constitute additional key factors that influence faunal
597 colonisation processes and subsequent successional patterns (Zajac et al., 1998; Adams et al.,
598 2012; Nakamura et al., 2014). While the recolonisation of areas following large-scale
599 disturbance relies on dispersal across vent fields, at local scale the successful settlement of
600 post-larvae depends on habitat suitability, environmental conditions and biotic interactions.
601 Understanding the processes acting at small scales are paramount in evaluating mechanisms
602 controlling successional dynamics after recolonisation by species from afar. In addition, recent
603 workshops and working groups, emerging from the development of mining regulations and
604 the necessity to inform industries and policy makers, stressed the urgent need to address

knowledge gaps in vent species biology and ecology (Collins et al. 2013; Levin et al. 2016; Dunn et al. 2018, ISA REMPS, SEMPIA). This study is one of the first to assess natural recovery of communities on a slow-spreading ridge and provide data that are essential to elaborate and develop conservation strategies and mitigate long-term harmful effects of anthropogenic activities on hydrothermal vent ecosystems.

DOI of cruises involved

SARRADIN Pierre-Marie, CANNAT Mathilde (2017) MOMARSAT2017 cruise, RV Pourquoi pas ?, https://doi.org/10.17600/17000500

CANNAT Mathilde (2018) MOMARSAT2018 cruise, RV L'Atalante, https://doi.org/10.17600/18000514

SARRADIN Pierre-Marie, LEGRAND Julien (2019) MOMARSAT2019 cruise, RV Pourquoi pas ?, https://doi.org/10.17600/18001110

Acknowledgements

We would like to thank the captains and crews of the oceanographic cruises Momarsat 2017, 2018 and 2019 aboard the vessels N/O Pourquoi pas? and L'Atalante, as well as the ROV Victor6000 and Nautile team. We are particularly grateful to Pierre-Marie Sarradin and Mathilde Cannat, chief scientists of the cruises who greatly supported our sampling program. We are also sincerely thankful to Philippe Rodier for instrumental design of pyramidal structure and cage experiment but also for the deployment of the reversing thermometer and the data acquisition of bottom sea water temperature. We would like to offer our special thanks to Sandra Fuchs and Fanny Girard for sample collection during the cruise and Julie Tourolle for providing the map captions. We are particularly grateful for the assistance given by Thomas Day, Mathilde Le Pans, Maureen Lapalme and Fanny Volage in sorting and morphometrical measurements. Finally, we wish to acknowledge the help provided for specimen identification by the taxonomists Dr Paulo Bonifácio and Dr Maurício Shimabukuro for polychaetes, Dr Anders Warén for gastropods, Dr Inmaculada Frutos for isopods, Dr Magdalena Błażewicz for tanaids, Dr Laure Corbari for amphipods and Dr Hayato Tanaka for ostracods. This research was supported by the European H2020 MERCES (Project ID 689518) and the eCOREF project funded by Equinor (Norway). Julien Marticorena PhD project was funded by Ifremer and Equinor. This project is part of the EMSO-Azores (https://www.emso-fr.org) regional node and EMSO ERIC Research Infrastructure (https://emso.eu/). ERLL was supported by the European H2020 MERCES (Project ID 689518).

References

Adams, D.K., Arellano, S.M., Govenar, B., 2012. Larval dispersal : vent life in the water column. https://doi.org/10.5670/oceanog.2012.24

Anderson, M.J., 2001. A new method for non-parametric multivariate analysis of variance. Austral Ecol. 26, 32–46. https://doi.org/10.1111/j.1442-9993.2001.01070.pp.x

643 Baco, A.R., Etter, R.J., Ribeiro, P.A., Heyden, S. von der, Beerli, P., Kinlan, B.P., 2016. A synthesis of
644 genetic connectivity in deep-sea fauna and implications for marine reserve design. Mol. Ecol. 25, 3276–
645 3298. https://doi.org/10.1111/mec.13689

646 Barreyre, T., Escartín, J., Sohn, R.A., Cannat, M., Ballu, V., Crawford, W.C., 2014. Temporal variability
647 and tidal modulation of hydrothermal exit-fluid temperatures at the Lucky Strike deep-sea vent field,
648 Mid-Atlantic Ridge. J. Geophys. Res. Solid Earth 119, 2543–2566.
649 https://doi.org/10.1002/2013JB010478

650 Beaulieu, S.E., Baker, E.T., German, C.R., 2015. Where are the undiscovered hydrothermal vents on
651 oceanic spreading ridges? Deep Sea Res. Part II Top. Stud. Oceanogr., Exploring New Frontiers in Deep-
652 Sea Research: In Honor and Memory of Peter A. Rona 121, 202–212.
653 https://doi.org/10.1016/j.dsr2.2015.05.001

654 Benedetti-Cecchi, L., Cinelli, F., 1996. Patterns of disturbance and recovery in littoral rock pools:
655 nonhierarchical competition and spatial variability in secondary succession. Marine Ecology Progress
656 Series 135, 145–161. https://doi.org/10.3354/meps135145

657 Benedetti-Cecchi, L., 2000. Predicting Direct and Indirect Interactions During Succession in a Mid-
658 Littoral Rocky Shore Assemblage. Ecological Monographs 70, 45–72. https://doi.org/10.1890/0012-
659 9615(2000)070[0045:PDAIID]2.0.CO;2

660 Boschen, R.E., Rowden, A.A., Clark, M.R., Gardner, J.P.A., 2013. Mining of deep-sea seafloor massive
661 sulfides: A review of the deposits, their benthic communities, impacts from mining, regulatory
662 frameworks and management strategies. Ocean Coast. Manag. 84, 54–67.
663 https://doi.org/10.1016/j.ocecoaman.2013.07.005

664 Breusing, C., Biastoch, A., Drews, A., Metaxas, A., Jollivet, D., Vrijenhoek, R.C., Bayer, T., Melzner, F.,
665 Sayavedra, L., Petersen, J.M., Dubilier, N., Schilhabel, M.B., Rosenstiel, P., Reusch, T.B.H., 2016.
666 Biophysical and Population Genetic Models Predict the Presence of “Phantom” Stepping Stones
667 Connecting Mid-Atlantic Ridge Vent Ecosystems. Curr. Biol. CB 26, 2257–2267.
668 https://doi.org/10.1016/j.cub.2016.06.062

669 Bulleri, F., Benedetti-Cecchi, L., 2006. Mechanisms of recovery and resilience of different components
670 of mosaics of habitats on shallow rocky reefs. Oecologia 149. https://doi.org/10.1007/s00442-006-
671 0459-3

672 Butterfield, D.A., Jonasson, I.R., Massoth, G.J., Feely, R.A., Roe, K.K., Embley, R.E., Holden, J.F., McDuff,
673 R.E., Lilley, M.D., Delaney, J.R., 1997. Seafloor eruptions and evolution of hydrothermal fluid chemistry.
674 Philos. Trans. R. Soc. Lond. Ser. Math. Phys. Eng. Sci. 355, 369–386.
675 https://doi.org/10.1098/rsta.1997.0013

676 Butterfield, D.A., Massoth, G.J., McDuff, R.E., Lupton, J.E., Lilley, M.D., 1990. Geochemistry of
677 hydrothermal fluids from Axial Seamount hydrothermal emissions study vent field, Juan de Fuca Ridge:
678 Subseafloor boiling and subsequent fluid-rock interaction. J. Geophys. Res. Solid Earth 95, 12895–
679 12921. https://doi.org/10.1029/JB095iB08p12895

680 Chavagnac, V., Leleu, T., Fontaine, F., Cannat, M., Ceuleneer, G., Castillo, A., 2018. Spatial Variations in
681 Vent Chemistry at the Lucky Strike Hydrothermal Field, Mid-Atlantic Ridge (37°N): Updates for
682 Subseafloor Flow Geometry From the Newly Discovered Capelinhos Vent. Geochemistry, Geophysics,
683 Geosystems 19, 4444–4458. https://doi.org/10.1029/2018GC007765

Childress, J.J., Fisher, C.R., 1992. The biology of hydrothermal vent animals: physiology, biochemistry, and autotrophic symbioses. Unkn. J. 337–441.

Colaço, A., Martins, I., Laranjo, M., Pires, L., Leal, C., Prieto, C., Costa, V., Lopes, H., Rosa, D., Dando, P.R., Serrão-Santos, R., 2006. Annual spawning of the hydrothermal vent mussel, Bathymodiolus azoricus, under controlled aquarium, conditions at atmospheric pressure. J. Exp. Mar. Biol. Ecol. 333, 166–171. https://doi.org/10.1016/j.jembe.2005.12.005

Collins, P.C., Kennedy, R., Van Dover, C.L., 2012. A biological survey method applied to seafloor massive sulphides (sms) with contagiously distributed hydrothermal-vent fauna. https://doi.org/10.3354/meps09646

Comtet, T., Desbruyères, D., 1998. Population structure and recruitment in mytilid bivalves from the Lucky Strike and Menez Gwen hydrothermal vent fields (37°17\'N and 37°50\'N on the Mid-Atlantic Ridge). Mar. Ecol. Prog. Ser. 163, 165–177. https://doi.org/10.3354/meps163165

Connell, J.H., Keough, M.J., 1985. Disturbance and patch dynamics of subtidal marine animals on hard substrata.

Corliss, J.B., Dymond, J., Gordon, L.I., Edmond, J.M., Herzen, R.P. von, Ballard, R.D., Green, K., Williams, D., Bainbridge, A., Crane, K., Andel, T.H. van, 1979. Submarine Thermal Springs on the Galápagos Rift. Science 203, 1073–1083. https://doi.org/10.1126/science.203.4385.1073

Cuvelier, D., Beesau, J., Ivanenko, V.N., Zeppilli, D., Sarradin, P.-M., Sarrazin, J., 2014a. First insights into macro- and meiofaunal colonisation patterns on paired wood/slate substrata at Atlantic deep-sea hydrothermal vents. Deep Sea Res. Part Oceanogr. Res. Pap. 87, 70–81. https://doi.org/10.1016/j.dsr.2014.02.008

Cuvelier, D., Gollner, S., Jones, D.O.B., Kaiser, S., Arbizu, P.M., Menzel, L., Mestre, N.C., Morato, T., Pham, C., Pradillon, F., Purser, A., Raschka, U., Sarrazin, J., Simon-Lledó, E., Stewart, I.M., Stuckas, H., Sweetman, A.K., Colaço, A., 2018. Potential Mitigation and Restoration Actions in Ecosystems Impacted by Seabed Mining. Front. Mar. Sci. 5. https://doi.org/10.3389/fmars.2018.00467

Cuvelier, D., Legendre, P., Laes, A., Sarradin, P.-M., Sarrazin, J., 2014b. Rhythms and Community Dynamics of a Hydrothermal Tubeworm Assemblage at Main Endeavour Field – A Multidisciplinary Deep-Sea Observatory Approach. PLOS ONE 9, e96924. https://doi.org/10.1371/journal.pone.0096924

Cuvelier, D., Sarradin, P.-M., Sarrazin, J., Colaço, A., Copley, J.T., Desbruyères, D., Glover, A.G., Santos, R.S., Tyler, P.A., 2011a. Hydrothermal faunal assemblages and habitat characterisation at the Eiffel Tower edifice (Lucky Strike, Mid-Atlantic Ridge). Mar. Ecol. 32, 243–255. https://doi.org/10.1111/j.1439-0485.2010.00431.x

Cuvelier, D., Sarrazin, J., Colaço, A., Copley, J., Desbruyères, D., Glover, A.G., Tyler, P., Serrão Santos, R., 2009. Distribution and spatial variation of hydrothermal faunal assemblages at Lucky Strike (Mid-Atlantic Ridge) revealed by high-resolution video image analysis. Deep Sea Res. Part Oceanogr. Res. Pap. 56, 2026–2040. https://doi.org/10.1016/j.dsr.2009.06.006

Cuvelier, D., Sarrazin, J., Colaço, A., Copley, J.T., Glover, A.G., Tyler, P.A., Santos, R.S., Desbruyères, D., 2011b. Community dynamics over 14 years at the Eiffel Tower hydrothermal edifice on the Mid-Atlantic Ridge. Limnol. Oceanogr. 56, 1624–1640. https://doi.org/10.4319/lo.2011.56.5.1624

Davis, E., Becker, K., 1999. Tidal pumping of fluids within and from the oceanic crust: New observations and opportunities for sampling the crustal hydrosphere. Earth Planet. Sci. Lett. 172, 141–149. https://doi.org/10.1016/S0012-821X(99)00197-1

Denny, M.W., 1987. Lift as a mechanism of patch initiation in mussel beds. Journal of Experimental Marine Biology and Ecology 113, 231–245. https://doi.org/10.1016/0022-0981(87)90103-1

Dixon, D.R., Lowe, D.M., Miller, P.I., Villemin, G.R., Colaço, A., Serrão-Santos, R., Dixon, L.R.J., 2006. Evidence of seasonal reproduction in the Atlantic vent mussel Bathymodiolus azoricus, and an apparent link with the timing of photosynthetic primary production. J. Mar. Biol. Assoc. U. K. 86, 1363–1371. https://doi.org/10.1017/S0025315406014391

Donval, J.-P., Charlou, J.-L., Lucas, L., 2008. Analysis of light hydrocarbons in marine sediments by headspace technique: Optimization using design of experiments. Chemometrics and Intelligent Laboratory Systems 94, 89–94. https://doi.org/10.1016/j.chemolab.2008.06.010

Dray, S., Bauman, D., Blanchet, G., Borcard, D., Clappe, S., Guenard, G., Jombart, T., Larocque, G., Legendre, P., Madi, N., Wagner, H.H., 2020. adespatial: Multivariate Multiscale Spatial Analysis.

Dreyer, J.C., Knick, K.E., Flickinger, W.B., Dover, C.L.V., 2005. Development of macrofaunal community structure in mussel beds on the northern East Pacific Rise. Mar. Ecol. Prog. Ser. 302, 121–134. https://doi.org/10.3354/meps302121

Dunn, D.C., Dover, C.L.V., Etter, R.J., Smith, C.R., Levin, L.A., Morato, T., Colaço, A., Dale, A.C., Gebruk, A.V., Gjerde, K.M., Halpin, P.N., Howell, K.L., Johnson, D., Perez, J.A.A., Ribeiro, M.C., Stuckas, H., Weaver, P., Participants, S.W., 2018. A strategy for the conservation of biodiversity on mid-ocean ridges from deep-sea mining. Science Advances 4, eaar4313. https://doi.org/10.1126/sciadv.aar4313

Kassambara and Mundt, 2009. Factoextra: Extract and Visualize the Results of Multivariate Data Analyses, 2019. , R package.

Gollner, S., Govenar, B., Arbizu, P.M., Mills, S., Le Bris, N., Weinbauer, M., Shank, T.M., Bright, M., 2015a. Differences in recovery between deep-sea hydrothermal vent and vent-proximate communities after a volcanic eruption. Deep Sea Res. Part Oceanogr. Res. Pap. 106, 167–182. https://doi.org/10.1016/j.dsr.2015.10.008

Gollner, S., Riemer, B., Arbizu, P.M., Bris, N.L., Bright, M., 2010. Diversity of Meiofauna from the 9°50'N East Pacific Rise across a Gradient of Hydrothermal Fluid Emissions. PLOS ONE 5, e12321. https://doi.org/10.1371/journal.pone.0012321

Gollner, S., Govenar, B., Fisher, C.R., Bright, M., 2015b. Size matters at deep-sea hydrothermal vents: different diversity and habitat fidelity patterns of meio- and macrofauna. Mar. Ecol. Prog. Ser. 520, 57–66. https://doi.org/10.3354/meps11078

Gollner, S., Kaiser, S., Menzel, L., Jones, D.O.B., Brown, A., Mestre, N.C., van Oevelen, D., Menot, L., Colaço, A., Canals, M., Cuvelier, D., Durden, J.M., Gebruk, A., Egho, G.A., Haeckel, M., Marcon, Y., Mevenkamp, L., Morato, T., Pham, C.K., Purser, A., Sanchez-Vidal, A., Vanreusel, A., Vink, A., Martinez Arbizu, P., 2017. Resilience of benthic deep-sea fauna to mining activities. Mar. Environ. Res. 129, 76–101. https://doi.org/10.1016/j.marenvres.2017.04.010

Gollner, S., Govenar, B., Martinez Arbizu, P., Mullineaux, L.S., Mills, S., Le Bris, N., Weinbauer, M., Shank, T.M., Bright, M., 2020. Animal Community Dynamics at Senescent and Active Vents at the 9°N

East Pacific Rise After a Volcanic Eruption. Front. Mar. Sci. 6. https://doi.org/10.3389/fmars.2019.00832

Govenar, B., Fisher, C.R., 2007. Experimental evidence of habitat provision by aggregations of Riftia pachyptila at hydrothermal vents on the East Pacific Rise. Mar. Ecol. 28, 3–14. https://doi.org/10.1111/j.1439-0485.2007.00148.x

Hunt, H.L., Metaxas, A., Jennings, R.M., Halanych, K.M., Mullineaux, L.S., 2004. Testing biological control of colonization by vestimentiferan tubeworms at deep-sea hydrothermal vents (East Pacific Rise, 9°50'N). Deep Sea Res. Part Oceanogr. Res. Pap. 51, 225–234. https://doi.org/10.1016/j.dsr.2003.10.008

Husson, B., Sarradin, P.-M., Zeppilli, D., Sarrazin, J., 2017. Picturing thermal niches and biomass of hydrothermal vent species. Deep Sea Res. Part II Top. Stud. Oceanogr., Advances in deep-sea biology: biodiversity, ecosystem functioning and conservation 137, 6–25. https://doi.org/10.1016/j.dsr2.2016.05.028

Johnson, K.S., Childress, J.J., Beehler, C.L., 1988. Short-term temperature variability in the Rose Garden hydrothermal vent field: an unstable deep-sea environment. Deep Sea Res. Part Oceanogr. Res. Pap. 35, 1711–1721. https://doi.org/10.1016/0198-0149(88)90045-3

Jollivet, D., Empis, A., Baker, M.C., Hourdez, S., Comtet, T., Jouin-Toulmond, C., Desbruyères, D., Tyler, P.A., 2000. Reproductive biology, sexual dimorphism, and population structure of the deep sea hydrothermal vent scale-worm, Branchipolynoe seepensis (Polychaeta: Polynoidae). Journal of the Marine Biological Association of the United Kingdom 80, 55–68. https://doi.org/10.1017/S0025315499001563

Kelly, N.E., Metaxas, A., 2007. Influence of habitat on the reproductive biology of the deep-sea hydrothermal vent limpet Lepetodrilus fucensis (Vetigastropoda: Mollusca) from the Northeast Pacific. Mar. Biol. 151, 649–662. https://doi.org/10.1007/s00227-006-0505-z

Khripounoff, A., Vangriesheim, A., Crassous, P., Segonzac, M., Lafon, V., Warén, A., 2008. Temporal variation of currents, particulate flux and organism supply at two deep-sea hydrothermal fields of the Azores Triple Junction. Deep Sea Res. Part Oceanogr. Res. Pap. 55, 532–551. https://doi.org/10.1016/j.dsr.2008.01.001

Langmuir, C., Humphris, S., Fornari, D., Van Dover, C., Von Damm, K., Tivey, M.K., Colodner, D., Charlou, J.-L., Desonie, D., Wilson, C., Fouquet, Y., Klinkhammer, G., Bougault, H., 1997. Hydrothermal vents near a mantle hot spot: the Lucky Strike vent field at 37°N on the Mid-Atlantic Ridge. Earth Planet. Sci. Lett. 148, 69–91. https://doi.org/10.1016/S0012-821X(97)00027-7

Le Bris, N., Govenar, B., Le Gall, C., Fisher, C.R., 2006. Variability of physico-chemical conditions in 9°50'N EPR diffuse flow vent habitats. Mar. Chem. 98, 167–182. https://doi.org/10.1016/j.marchem.2005.08.008

Leibold, M.A., Holyoak, M., Mouquet, N., Amarasekare, P., Chase, J.M., Hoopes, M.F., Holt, R.D., Shurin, J.B., Law, R., Tilman, D., Loreau, M., Gonzalez, A., 2004. The metacommunity concept: a framework for multi-scale community ecology. Ecology Letters 7, 601–613. https://doi.org/10.1111/j.1461-0248.2004.00608.x

Lelièvre, Y., Legendre, P., Matabos, M., Mihály, S., Lee, R.W., Sarradin, P.-M., Arango, C.P., Sarrazin, J., 2017. Astronomical and atmospheric impacts on deep-sea hydrothermal vent invertebrates. Proc. R. Soc. B Biol. Sci. 284, 319–407. https://doi.org/10.1098/rspb.2016.2123

Lenihan, H.S., Mills, S.W., Mullineaux, L.S., Peterson, C.H., Fisher, C.R., Micheli, F., 2008. Biotic interactions at hydrothermal vents: Recruitment inhibition by the mussel Bathymodiolus thermophilus. Deep Sea Res. Part Oceanogr. Res. Pap. 55, 1707–1717. https://doi.org/10.1016/j.dsr.2008.07.007

Levin, L.A., 2006. Recent progress in understanding larval dispersal: new directions and digressions. Integr. Comp. Biol. 46, 282–297. https://doi.org/10.1093/icb/icj024

Levin, L.A., Baco, A.R., Bowden, D.A., Colaco, A., Cordes, E.E., Cunha, M.R., Demopoulos, A.W.J., Gobin, J., Grupe, B.M., Le, J., Metaxas, A., Netburn, A.N., Rouse, G.W., Thurber, A.R., Tunnicliffe, V., Van Dover, C.L., Vanreusel, A., Watling, L., 2016a. Hydrothermal Vents and Methane Seeps: Rethinking the Sphere of Influence. Front. Mar. Sci. 3. https://doi.org/10.3389/fmars.2016.00072

Levin, L.A., D, T., G, T., 1996. Succession of macrobenthos in a created salt marsh. Mar. Ecol. Prog. Ser. 141, 67–82. https://doi.org/10.3354/meps141067

Levin, L.A., Mengerink, K., Gjerde, K.M., Rowden, A.A., Van Dover, C.L., Clark, M.R., Ramirez-Llodra, E., Currie, B., Smith, C.R., Sato, K.N., Gallo, N., Sweetman, A.K., Lily, H., Armstrong, C.W., Brider, J., 2016b. Defining “serious harm” to the marine environment in the context of deep-seabed mining. Mar. Policy 74, 245–259. https://doi.org/10.1016/j.marpol.2016.09.032

Luther, G.W., Rozan, T.F., Taillefert, M., Nuzzio, D.B., Di Meo, C., Shank, T.M., Lutz, R.A., Cary, S.C., 2001. Chemical speciation drives hydrothermal vent ecology. Nature 410, 813–816. https://doi.org/10.1038/35071069

Marcus, J., Tunnicliffe, V., Butterfield, D.A., 2009. Post-eruption succession of macrofaunal communities at diffuse flow hydrothermal vents on Axial Volcano, Juan de Fuca Ridge, Northeast Pacific. Deep Sea Res. Part II Top. Stud. Oceanogr., Marine Benthic Ecology and Biodiversity: A Compilation of Recent Advances in Honor of J. Frederick Grassle 56, 1586–1598. https://doi.org/10.1016/j.dsr2.2009.05.004

Marsh, L., Copley, J.T., Huvenne, V.A.I., Linse, K., Reid, W.D.K., Rogers, A.D., Sweeting, C.J., Tyler, P.A., 2012. Microdistribution of Faunal Assemblages at Deep-Sea Hydrothermal Vents in the Southern Ocean. PLoS One 7. https://doi.org/10.1371/journal.pone.0048348

Marticorena, J., Matabos, M., Sarrazin, J., Ramirez-Llodra, E., 2020. Contrasting reproductive biology of two hydrothermal gastropods from the Mid-Atlantic Ridge: implications for resilience of vent communities. Mar. Biol. 167, 109. https://doi.org/10.1007/s00227-020-03721-x

Mat, A.M., Sarrazin, J., Markov, G.V., Apremont, V., Dubreuil, C., Eché, C., Fabioux, C., Klopp, C., Sarradin, P.-M., Tanguy, A., Huvet, A., Matabos, M., 2020. Biological rhythms in the deep-sea hydrothermal mussel Bathymodiolus azoricus. Nature Communications 11, 3454. https://doi.org/10.1038/s41467-020-17284-4

Micheli, F., Peterson, C.H., Mullineaux, L.S., Fisher, C.R., Mills, S.W., Sancho, G., Johnson, G.A., Lenihan, H.S., 2002. Predation Structures Communities at Deep-Sea Hydrothermal Vents. Ecol. Monogr. 72, 365–382. https://doi.org/10.1890/0012-9615(2002)072[0365:PSCADS]2.0.CO;2

Mullineaux, L.S., Adams, D.K., Mills, S.W., Beaulieu, S.E., 2010. Larvae from afar colonize deep-sea hydrothermal vents after a catastrophic eruption. Proc. Natl. Acad. Sci. 107, 7829–7834. https://doi.org/10.1073/pnas.0913187107

Mullineaux, L.S., Metaxas, A., Beaulieu, S.E., Bright, M., Gollner, S., Grupe, B.M., Herrera, S., Kellner, J.B., Levin, L.A., Mitarai, S., Neubert, M.G., Thurnherr, A.M., Tunnicliffe, V., Watanabe, H.K., Won, Y.-J., 2018. Exploring the Ecology of Deep-Sea Hydrothermal Vents in a Metacommunity Framework. Front. Mar. Sci. 5. https://doi.org/10.3389/fmars.2018.00049

Mullineaux, L.S., Bris, N.L., Mills, S.W., Henri, P., Bayer, S.R., Secrist, R.G., Siu, N., 2012. Detecting the Influence of Initial Pioneers on Succession at Deep-Sea Vents. PLOS ONE 7, e50015. https://doi.org/10.1371/journal.pone.0050015

Mullineaux, L.S., Peterson, C.H., Micheli, F., Mills, S.W., 2003. Successional Mechanism Varies Along a Gradient in Hydrothermal Fluid Flux at Deep-Sea Vents. Ecol. Monogr. 73, 523–542. https://doi.org/10.1890/02-0674

Nakamura, M., Watanabe, H., Sasaki, T., Ishibashi, J., Fujikura, K., Mitarai, S., 2014. Life history traits of Lepetodrilus nux in the Okinawa Trough, based upon gametogenesis, shell size, and genetic variability. Mar. Ecol. Prog. Ser. 505, 119–130. https://doi.org/10.3354/meps10779

Oksanen, J., Blanchet, F.G., Friendly, M., Kindt, R., Legendre, P., McGlinn, D., Minchin, P.R., O'Hara, R.B., Simpson, G.L., Solymos, P., Stevens, M.H.H., Szoecs, E., Wagner, H., 2019. vegan: Community Ecology Package.

Ondreas, H., Cannat, M., Fouquet, Y., Normand, A., Sarradin, P., Sarrazin, J., 2009. Recent volcanic events and the distribution of hydrothermal venting at the Lucky Strike hydrothermal field, Mid-Atlantic Ridge. Geochem. Geophys. Geosystems 10. https://doi.org/10.1029/2008gc002171

Orcutt, B.N., Bradley, J.A., Brazelton, W.J., Estes, E.R., Goordial, J.M., Huber, J.A., Jones, R.M., Mahmoudi, N., Marlow, J.J., Murdock, S., Pachiadaki, M., 2020. Impacts of deep-sea mining on microbial ecosystem services. Limnol. Oceanogr. n/a. https://doi.org/10.1002/lno.11403

Paine, R.T., 1966. Food Web Complexity and Species Diversity. Am. Nat. 100, 65–75.

Sancho, G., Fisher, C.R., Mills, S., Micheli, F., Johnson, G.A., Lenihan, H.S., Peterson, C.H., Mullineaux, L.S., 2005. Selective predation by the zoarcid fish Thermarces cerberus at hydrothermal vents. Deep Sea Res. Part Oceanogr. Res. Pap. 52, 837–844. https://doi.org/10.1016/j.dsr.2004.12.002

Sarradin, P.-M., Waeles, M., Bernagout, S., Le Gall, C., Sarrazin, J., Riso, R., 2009. Speciation of dissolved copper within an active hydrothermal edifice on the Lucky Strike vent field (MAR, 37°N). Sci. Total Environ. 407, 869–878. https://doi.org/10.1016/j.scitotenv.2008.09.056

Sarrazin, J., Cuvelier, D., Peton, L., Legendre, P., Sarradin, P.M., 2014. High-resolution dynamics of a deep-sea hydrothermal mussel assemblage monitored by the EMSO-Açores MoMAR observatory. Deep Sea Res. Part Oceanogr. Res. Pap. 90, 62–75. https://doi.org/10.1016/j.dsr.2014.04.004

Sarrazin, J., Levesque, C., Juniper, S., Tivey, M., 2002. Mosaic community dynamics on Juan de Fuca Ridge sulphide edifices: substratum, temperature and implications for trophic structure. CBM - Cahiers de Biologie Marine 43, 275–279.

Sarrazin, J., Juniper, S.K., Massoth, G., Legendre, P., 1999. Physical and chemical factors influencing species distributions on hydrothermal sulfide edifices of the Juan de Fuca Ridge, northeast Pacific. Mar. Ecol. Prog. Ser. 190, 89–112. https://doi.org/10.3354/meps190089

Sarrazin, J., Legendre, P., de Busserolles, F., Fabri, M.-C., Guilini, K., Ivanenko, V.N., Morineaux, M., Vanreusel, A., Sarradin, P.-M., 2015a. Biodiversity patterns, environmental drivers and indicator species on a high-temperature hydrothermal edifice, Mid-Atlantic Ridge. Deep Sea Res. Part II Top.

Stud. Oceanogr., Exploring New Frontiers in Deep-Sea Research: In Honor and Memory of Peter A. Rona 121, 177–192. https://doi.org/10.1016/j.dsr2.2015.04.013

Sarrazin, J., Portail, M., Legrand, E., Cathalot, C., Laes, A., Lahaye, N., Sarradin, P.M., Husson, B., 2020. Endogenous versus exogenous factors: What matters for vent mussel communities? Deep Sea Res. Part Oceanogr. Res. Pap. 103260. https://doi.org/10.1016/j.dsr.2020.103260

Sarrazin, J., V, R., Sk, J., Jr, D., 1997. Biological and geological dynamics over four years on a high-temperature sulfide structure at the Juan de Fuca Ridge hydrothermal observatory. Mar. Ecol. Prog. Ser. 153, 5–24. https://doi.org/10.3354/meps153005

Scheirer, D.S., Shank, T.M., Fornari, D.J., 2006. Temperature variations at diffuse and focused flow hydrothermal vent sites along the northern East Pacific Rise. Geochem. Geophys. Geosystems 7. https://doi.org/10.1029/2005GC001094

Sen, A., Becker, E.L., Podowski, E.L., Wickes, L.N., Ma, S., Mullaugh, K.M., Hourdez, S., Luther, G.W., Fisher, C.R., 2013. Distribution of mega fauna on sulfide edifices on the Eastern Lau Spreading Center and Valu Fa Ridge. Deep Sea Res. Part Oceanogr. Res. 72, 48–60. https://doi.org/10.1016/j.dsr.2012.11.003

Sen, A., Podowski, E.L., Becker, E.L., Shearer, E.A., Gartman, A., Yücel, M., Hourdez, S., Luther, G.W., III, Fisher, C.R., 2014. Community succession in hydrothermal vent habitats of the Eastern Lau Spreading Center and Valu Fa Ridge, Tonga. Limnol. Oceanogr. 59, 1510–1528. https://doi.org/10.4319/lo.2014.59.5.1510

Shank, T.M., Fornari, D.J., Von Damm, K.L., Lilley, M.D., Haymon, R.M., Lutz, R.A., 1998. Temporal and spatial patterns of biological community development at nascent deep-sea hydrothermal vents (9°50′N, East Pacific Rise). Deep Sea Res. Part II Top. Stud. Oceanogr. 45, 465–515. https://doi.org/10.1016/S0967-0645(97)00089-1

Sousa, W.P., 1985. Disturbance and patch dynamics on rocky intertidal shores. The ecology of natural disturbance and patch dynamics.

Spiess, F.N., Macdonald, K.C., Atwater, T., Ballard, R., Carranza, A., Cordoba, D., Cox, C., Garcia, V.M., Francheteau, J., Guerrero, J., Hawkins, J., Haymon, R., Hessler, R., Juteau, T., Kastner, M., Larson, R., Luyendyk, B., Macdougall, J.D., Miller, S., Normark, W., Orcutt, J., Rangin, C., 1980. East pacific rise: hot springs and geophysical experiments. Science 207, 1421–1433. https://doi.org/10.1126/science.207.4438.1421

Suzuki, K., Yoshida, K., Watanabe, H., Yamamoto, H., 2018. Mapping the resilience of chemosynthetic communities in hydrothermal vent fields. Sci. Rep. 8, 9364. https://doi.org/10.1038/s41598-018-27596-7

Tengberg, A., Hovdenes, J., Andersson, H.J., Brocandel, O., Diaz, R., Hebert, D., Arnerich, T., Huber, C., Körtzinger, A., Khripounoff, A., Rey, F., Rönning, C., Schimanski, J., Sommer, S., Stangelmayer, A., 2006. Evaluation of a lifetime-based optode to measure oxygen in aquatic systems. Limnology and Oceanography: Methods 4, 7–17. https://doi.org/10.4319/lom.2006.4.7

Tolstoy, M., Cowen, J.P., Baker, E.T., Fornari, D.J., Rubin, K.H., Shank, T.M., Waldhauser, F., Bohnenstiehl, D.R., Forsyth, D.W., Holmes, R.C., Love, B., Perfit, M.R., Weekly, R.T., Soule, S.A., Glazer, B., 2006. A Sea-Floor Spreading Event Captured by Seismometers. Science 314, 1920–1922. https://doi.org/10.1126/science.1133950

928 Tunnicliffe, V., 1991. The biology of hydrothermal vents : ecology and evolution. Biol. Hydrothermal
929 Vents Ecol. Evol. 29, 319–407.

930 Tunnicliffe, V., Embley, R.W., Holden, J.F., Butterfield, D.A., Massoth, G.J., Juniper, S.K., 1997. Biological
931 colonization of new hydrothermal vents following an eruption on Juan de Fuca Ridge. Deep Sea Res.
932 Part Oceanogr. Res. Pap. 44, 1627–1644. https://doi.org/10.1016/S0967-0637(97)00041-1

933 Van Audenhaege, L., Fariñas-Bermejo, A., Schultz, T., Lee Van Dover, C., 2019. An environmental
934 baseline for food webs at deep-sea hydrothermal vents in Manus Basin (Papua New Guinea). Deep Sea
935 Res. Part Oceanogr. Res. Pap. 148, 88–99. https://doi.org/10.1016/j.dsr.2019.04.018

936 Van Dover, C.L., 2007. The biological environment of polymetallic sulphides deposits, the potential
937 impact of exploration and mining on this environment, and data required to establish environmental
938 baselines in exploration areas. In: Polymetallic Sulphides and Cobalt-rich Ferromanganese Crusts
939 Deposits: Establishment of Environmental Baselines and an Associated Monitoring Programme during
940 Exploration. Proceedings of the International Seabed Authority's Workshop held in Kingston, Jamaica,
941 6e10 September 2004. Prepared by Offices of Resources and Environmental Monitoring (OREM), pp.
942 169e190. International Seabed Authority, Kingston, Jamaica: http://www.isa.org.jm/files/
943 documents/EN/Workshops/2004/Proceedings-ae.pdf. (accessed 13.06.13.).

944 Van Dover, C.L., 2011. Mining seafloor massive sulphides and biodiversity: what is at risk? ICES J. Mar.
945 Sci. 68, 341–348. https://doi.org/10.1093/icesjms/fsq086

946 Van Dover, C.L., 2010. Mining seafloor massive sulphides and biodiversity: what is at risk? ICES J. Mar.
947 Sci. 68, 341–348. https://doi.org/10.1093/icesjms/fsq086

948 Vuillemin, R., Le Roux, D., Dorval, P., Bucas, K., Sudreau, J.P., Hamon, M., Le Gall, C., Sarradin, P.M.,
949 2009. CHEMINI: A new in situ CHEmical MINIaturized analyzer. Deep Sea Res. Part Oceanogr. Res. Pap.
950 56, 1391–1399. https://doi.org/10.1016/j.dsr.2009.02.002

951 Washburn, T.W., Turner, P.J., Durden, J.M., Jones, D.O.B., Weaver, P., Van Dover, C.L., 2019. Ecological
952 risk assessment for deep-sea mining. Ocean Coast. Manag. 176, 24–39.
953 https://doi.org/10.1016/j.ocecoaman.2019.04.014

954 Zajac, R.N., Whitlatch, R.B., Thrush, S.F., 1998. Recolonization and succession in soft-sediment infaunal
955 communities: the spatial scale of controlling factors. Hydrobiologia 375, 227–240.
956 https://doi.org/10.1023/A:1017032200173

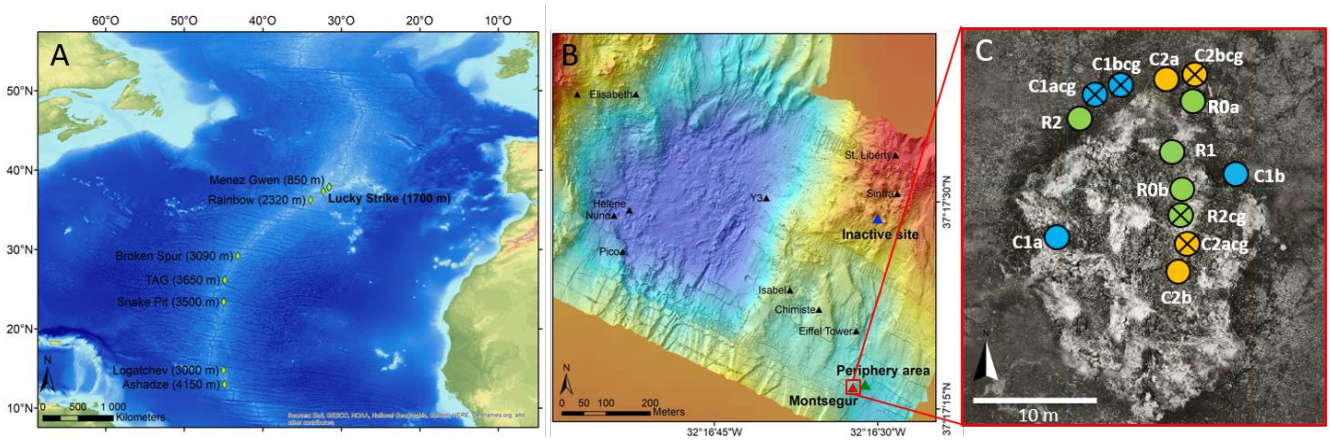

Figure 1. A. Location of the Lucky Strike (LS) vent field along the Mid-Atlantic Ridge. **B**. Bathymetric chart of LS and location of the Montségur edifice **C**. Position of the experimental and reference quadrats on and around the Montségur edifice. Green circles represent the reference quadrats, blue circles represent the experimental quadrats used to study the recolonisation 1 year after the disturbance, and orange circles represent the experimental quadrats used to study the recolonisation 2 years after the disturbance. Crossed off circles represent "caged" quadrats while empty circles represent quadrats without a cage.

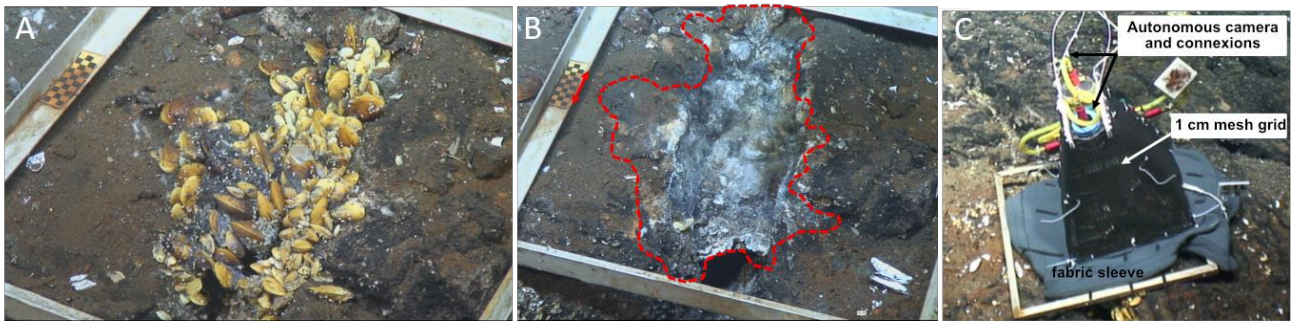

Figure 2. The C1a-cg experimental quadrat in 2017, (**A**) before faunal clearance (baseline community) and ; (**B**) after the induced disturbance. Red arrow highlights the check-board used to calibrate imagery analysis and estimate the sampling surface area (red dotted line). (**C**) The C1bcg "caged" experimental quadrat used to exclude large mobile predators. A 1 cm mesh grid was adjusted on the pyramidal structure on top of the quadrat (in black on the picture) and a grey fabric sleeve was attached to the edge of the caged quadrat to avoid colonisation of crawlers. A camera was deployed at the top of the pyramidal structure and connected to a battery on the side (yellow cables).

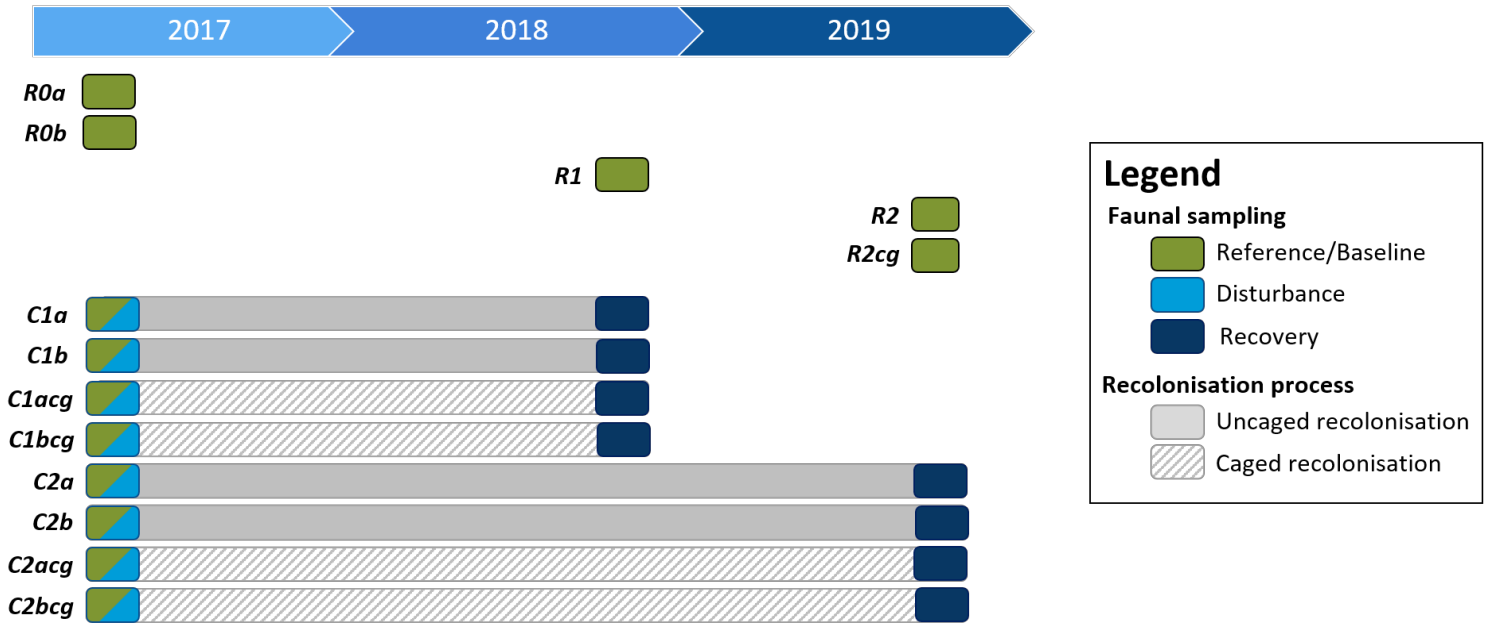

Figure 3. Experimental design of the disturbance experiment deployed between 2017 and 2019 on the Montségur edifice, Lucky Strike vent field (Mid-Atlantic Ridge). Small rectangles represent faunal sampling and their color indicates the nature of the operation: green, sampling of baseline communities; light blue, induction of disturbance by clearing faunal assemblages; dark blue, sampling after recolonisation to evaluate the recovery. Grey segments represent the recolonisation period studied for each quadrat. Hatched segments indicate the presence of caged during the recolonisation period.

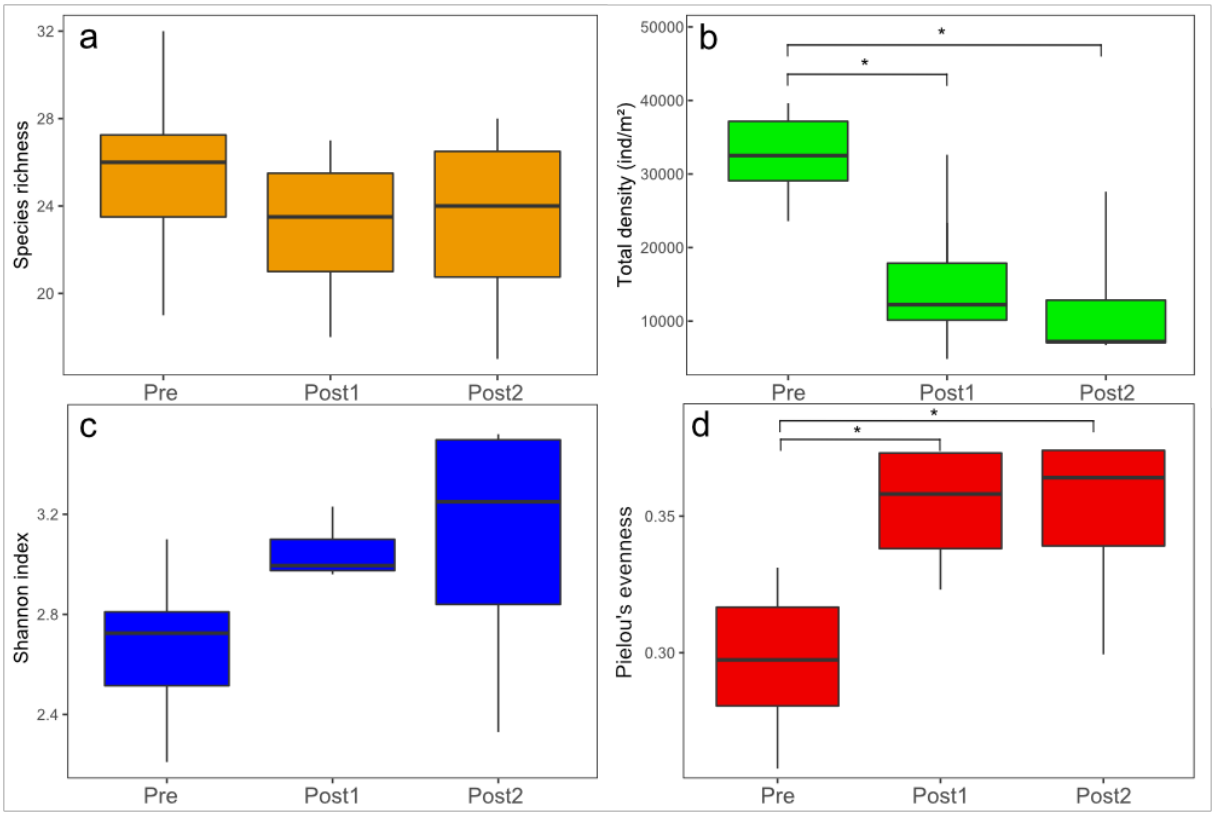

Figure 4. Species richness (**a**), total density (**b**), Shannon index (**c**) and Pielou's evenness index (**d**) of macrofaunal communities on the baseline communities and during the recolonisation process on the active Montségur edifice. Pre: assemblages sampled before the disturbance; Post1: assemblages sampled 1 year after the disturbance; Post2: assemblages sampled 2 years after the disturbance. Significance of Kruskall-Wallis multisample tests and post-hoc Dunn's tests are represented on the top of the boxplots.

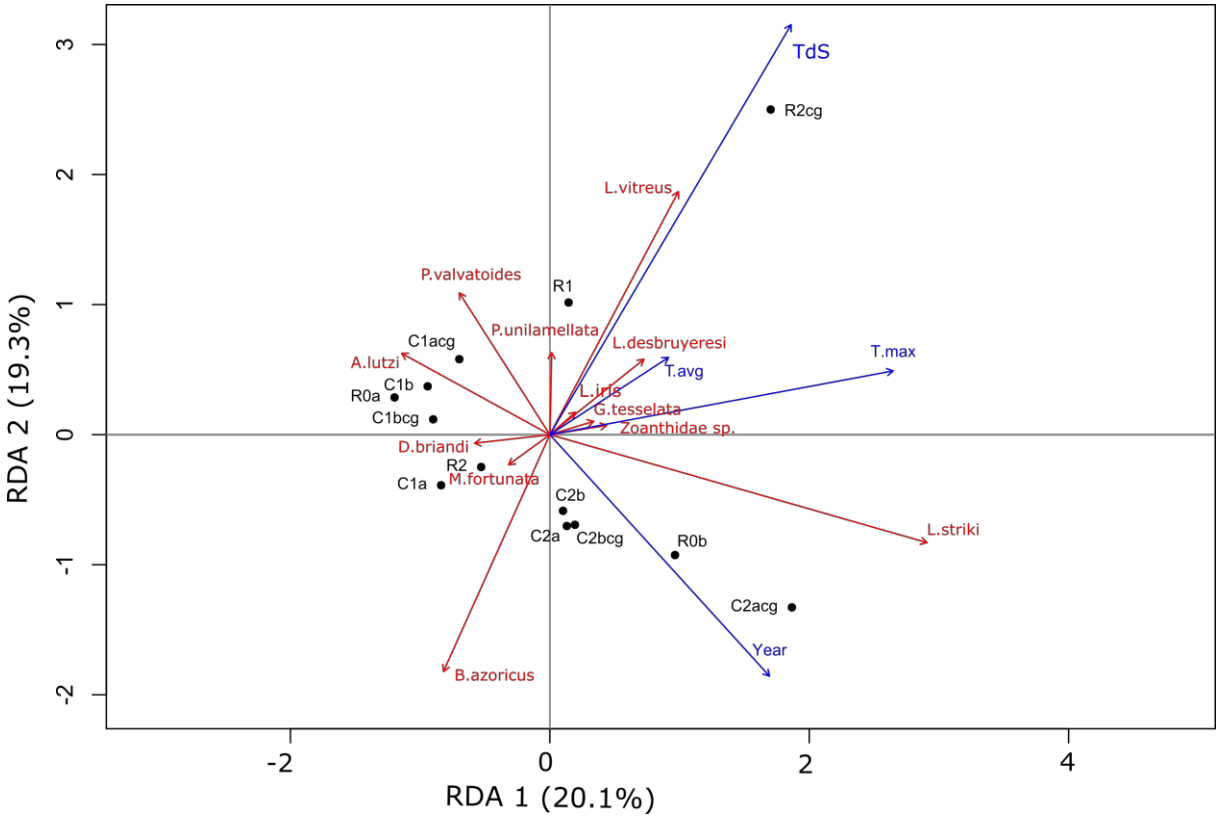

Figure 5. Canonical redundancy analysis (RDA, scaling 2) of Hellinger-transformed macrofaunal densities observed in the baseline community of the Montségur active edifice at the Lucky Strike vent field (Mid-Atlantic Ridge). The first canonical axis represents 20.1 % of the total variance in macrofaunal densities while the second axis represents 19.3% (adj R^2 = 25.1%, p = 0.004). The first axis is significant (p = 0.05). Only species that accounted for more than 50% of cumulative inertia on the two first axes are represented.

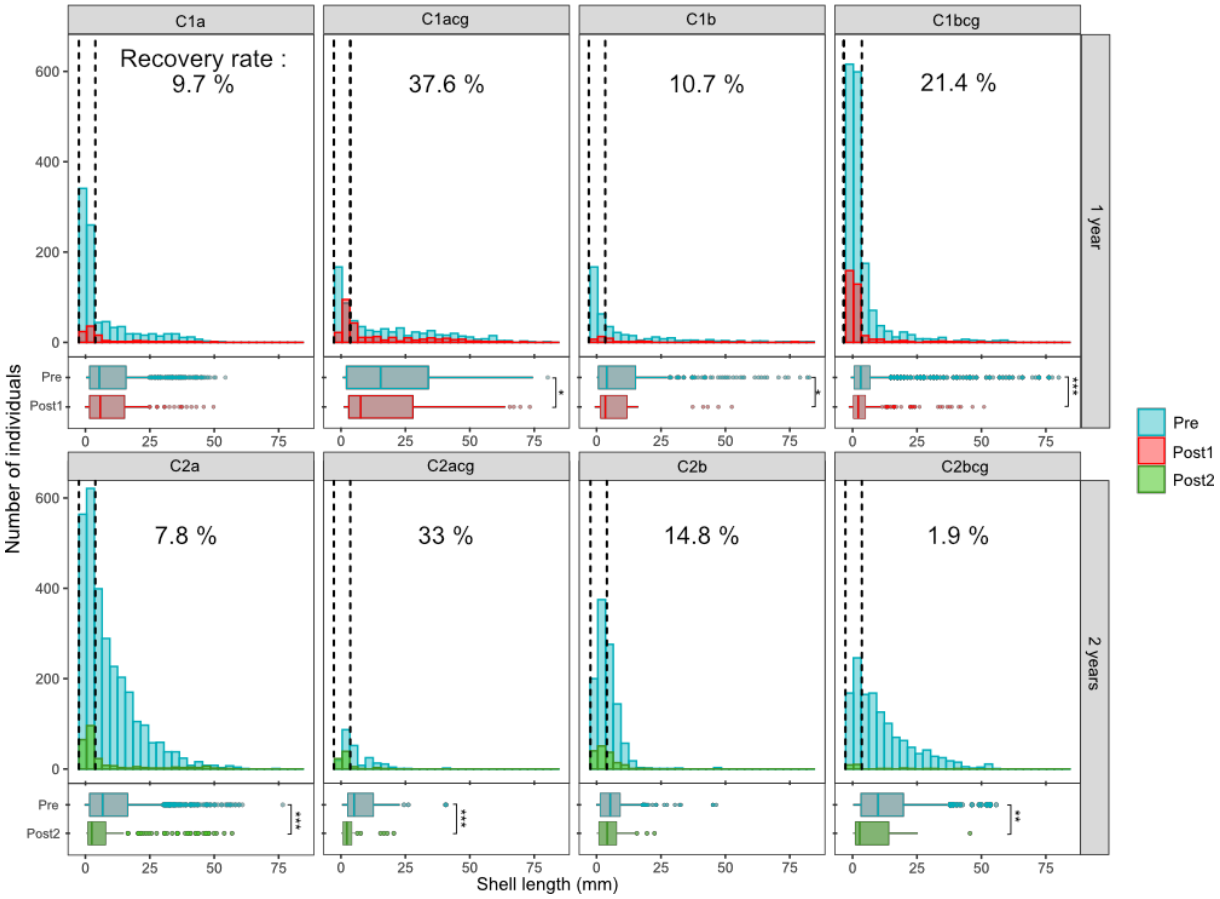

Figure 6. Histograms and boxplots of size frequency distribution of *Bathymodiolus azoricus* for each quadrat sampled at the Montségur edifice at the Lucky Strike vent field (Mid-Atlantic Ridge) including the pre-disturbed community (blue) and the communities one (red) and 2 (green) years after disturbance. Wilcoxon-Mann-Whitney tests were performed to identify differences in mean individual size between the baseline and post-disturbance communities. Asterisks indicate significant differences in mean shell length (*p-value<0.05; ** p-value <0.01; *** p-value <0.001). The interval between dotted lines represents the range of size at recruitment. The percentages represent the proportion of *B. azoricus* density which recovered in comparison of the pre-disturbed value in each quadrat.

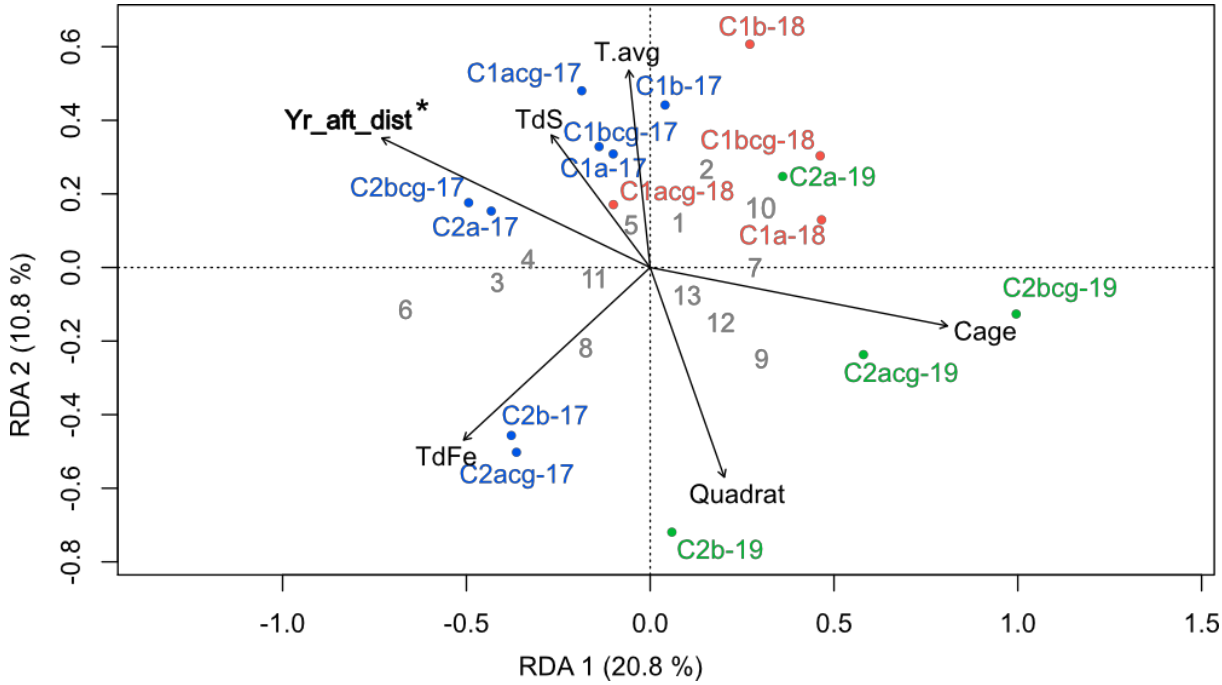

Figure 7. Canonical redundancy analysis (RDA, scaling 2) of Hellinger-transformed macrofaunal densities observed in the different assemblages during the recolonization process at the Montségur active edifice (Lucky Strike vent field, Mid-Atlantic Ridge). The first canonical axis represents 20.8% of the total variance in macrofaunal densities while the second axis represents 10.8% (with an adjusted R^2 of 20.5%). The RDA and the first axis are significant (p-values =0.006 and 0.023, respectively). Only species showing good fit with the first two canonical axes are represented. Colors refer to the time after disturbance: baseline communities (blue); 1 year after disturbance (red); two years after disturbance (green). Explanatory variables: Years after disturbance (*Yr_aft_dist*), average temperature measured before sampling (*T.avg*), mean concentration of total dissolved sulphides (*TdS*), mean concentration of total dissolved iron (*TdFe*), if quadrats are caged or uncaged (*Cage*), identification of quadrats to test the dependence of the same location over the time of the experiment (*Quadrat*). Response variables, each species is designated by a number: 1 – *Amphisamytha lutzi*; 2 – *Aphotopontius sp.*; 3 – *Bathymodiolus azoricus*; 4 – *Branchipolynoe seepensis*; 5 – *Lepetodrilus atlanticus*; 6 – *Lirapex costellata*; 7 – *Laeviphitus desbruyeresi*; 8 – *Luckia striki*; 9 – *Lurifax vitreus*; 10 – *Oncholaimus dyvae*; 11 – *Paralepetopsis ferrugivora*; 12 – *Protolira valvatoides*; 13 – *Xylodiscula analoga*.

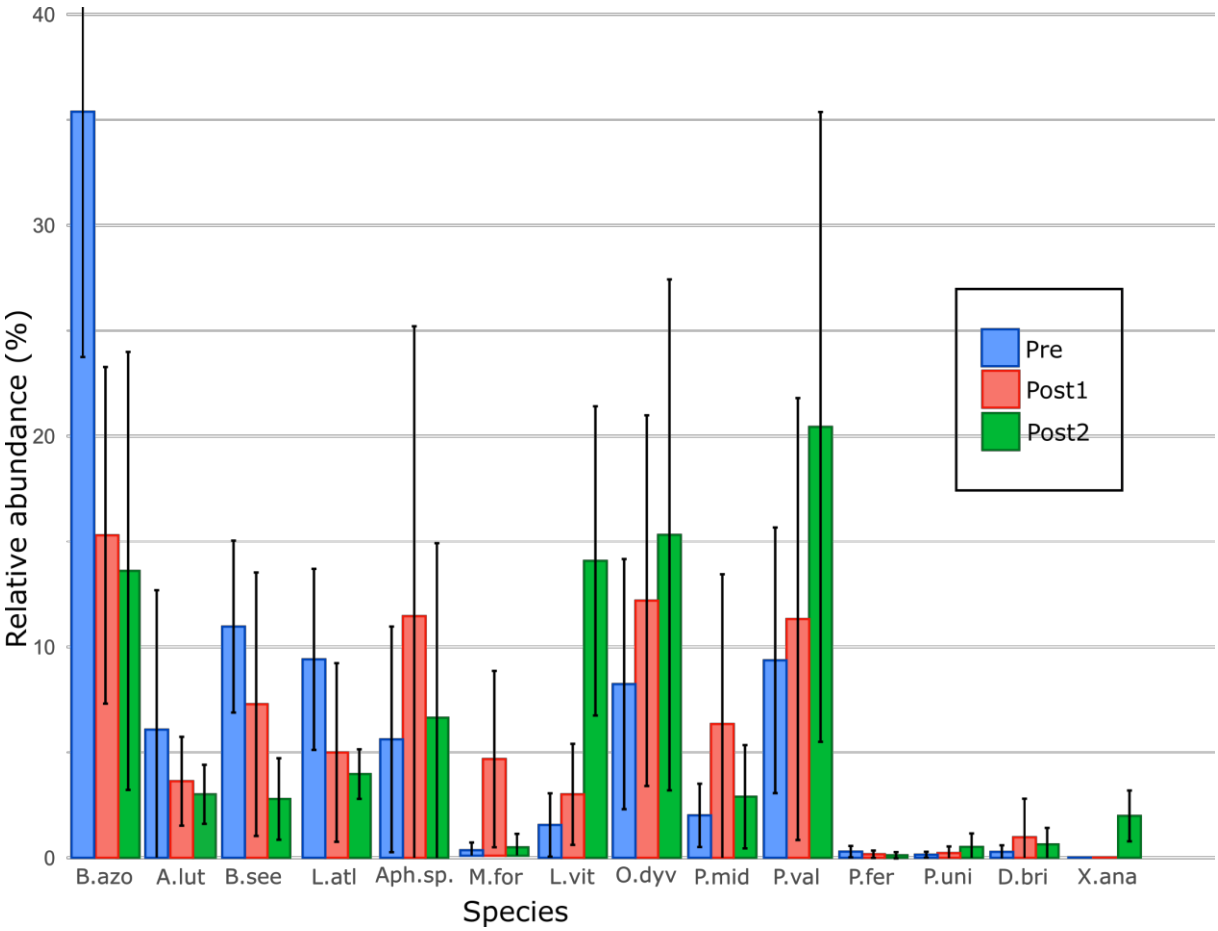

Figure 8. Mean and standard deviations of densities for the most abundant species among the experimental quadrats on the active Montségur edifice before the disturbance (Pre) and one/two years after the disturbance (Post1 and Post2). Species acronyms: B.azo – *Bathymodiolus azoricus*, A.lut – *Amphisamytha lutzi*; B.see – *Branchipolynoe seepensis*; L.atl – *Lepetodrilus atlanticus*; Aph.sp. – *Aphotopontius sp.*; M.for – *Mirocaris fortunata*; L.vit – *Lurifax vitreus*; O.dyv – *Oncholaimus dyvae*; P.mid – *Pseudorimula midatlantica*; P.val – *Protolira valvatoides*; P.uni – *Prionospio unilamellata*; D.bri – *Divia briandi*; X.ana – *Xylodiscula analoga*.

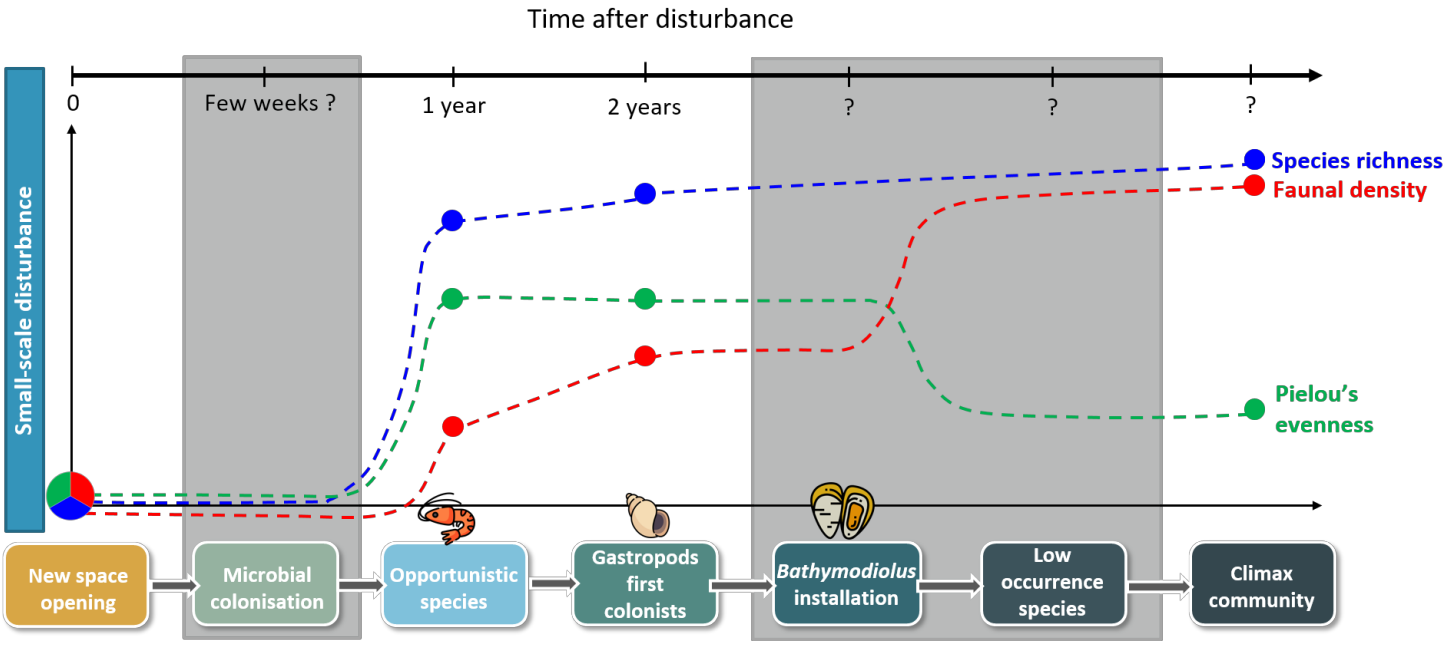

Figure 9. Conceptual model of colonisation and ecological succession until climax after a small-scale disturbance on the Lucky Strike vent assemblages (MAR). Evolution of species richness, faunal densities and Pielou's evenness index during the recovery process, based on the main results of our disturbance experiment (solid dots) and inferred from the literature (grey boxes).

Table 1. Environmental conditions on the baseline communities of the different quadrats deployed on the Montségur edifice (Lucky Strike vent field, Mid-Atlantic Ridge). Temperature: average: T.avg., standard deviation: T.std. maximum: T.max and minimum: T.min. from iButtons™. Oxygen (O_2). Total dissolved sulphide (TdS) and Total dissolved iron (TdFe) measured with the *in situ* analysers CHEMINI. Methane (CH_4) and pH were measured through quantitative analyses from samples collected with the PEPITO water sampler (Sarradin et al. 2009). Highest values are highlighted in bold and lowest values in grey.

Quadrat	T.avg	T.std	T.min	T.max	O_2 (µM)	TdS (µM)	TdFe (µM)	CH_4 (µM)	pH
					Mean ± SD				
Montségur									
R0a	*5.2*	*0.2*	*4.6*	*6.1*	*208.2 ± 0.1*	2.7 ± 0.2	0.2 ± 0.1	0.4	**7.8**
R0b	6.9	0.8	5.1	11.5	207.2 ± 0.4	3.1 ± 1.0	1.1 ± 0.3	0.5	7.6
R1	**9.5**	**2.7**	**6.1**	**22.1**	206.1 ± 1.1	2.3 ± 0.2	**2.2 ± 0.2**	**2.1**	7.2
R2	5.5	0.4	5.1	11.4	206.9 ± 1.3	3.2 ± 2.7	0.2 ± 0.1	0.9	7.5
R2cg	5.3	0.2	4.6	7.1	205.6 ± 0.6	0.9 ± 0.2	0.6 ± 1.1	*0.2*	7.9
C1a	6.1	0.3	5.1	7.1	207.4 ± 0.1	3.2 ± 0.8	0.2 ± 0.1	0.7	7.6
C1acg	5.8	1.2	4.6	12.1	204.3 ± 1.5	3.9 ± 2.6	0.3 ± 0.1	**2.1**	7.2
C1b	6.4	0.4	4.6	10.6	206.2 ± 1	**10.8 ± 14.7**	0.3 ± 0.3	1.1	7.4
C1bcg	5.7	0.42	4.6	8.1	207.9 ± 0.4	2.5 ± 0.6	0.2 ± 0.1	0.8	7.7
C2a	**7.6**	**1.12**	**6.1**	**16.1**	203.8 ± 2.1	**23.2 ± 26.3**	1.1 ± 0.3	**15.2**	6.1
C2acg	6.3	0.5	5	8.6	207.4 ± 0.8	1.3 ± 0.1	0.9 ± 0.8	0.7	7.7
C2b	5.3	0.2	5	*6.1*	205.2 ± 0.5	3.8 ± 3.8	0.9 ± 0.4	0.4	7.8
C2bcg	5.3	0.3	4.6	6.6	206.6 ± 0.3	5.6 ± 1.2	0.2 ± 0.1	**2.0**	7.2

DOCTORAT SCIENCES BRETAGNE DE LA MER LOIRE ET DU LITTORAL

UBO Université de Bretagne Occidentale

Titre : Résilience des écosystèmes hydrothermaux : résultats d'une expérience de perturbation au sein du champ hydrothermal Lucky Strike (dorsale médio-Atlantique)

Mots clés : sources hydrothermales, perturbation, rétablissement, dynamique de recolonisation, structure des communautés, réseau trophique, traits reproducteurs

Résumé : Les écosystèmes hydrothermaux peuvent être naturellement soumis à des perturbations liés à l'activité tectonique et volcanique. Quarante ans après leur découverte, alors que nous commençons à avoir une bonne connaissance des facteurs structurant leur biodiversité, notre compréhension de la dynamique de recolonisation est parcellaire et limite grandement notre capacité à prédire leur résilience en réponse à des perturbations, qu'elles soient naturelles ou anthropiques. Face à l'augmentation de l'intérêt des compagnies minières pour l'exploitation des ressources minérales profondes, il devient impératif de multiplier nos efforts pour mieux appréhender les mécanismes impliqués dans le rétablissement des communautés impactées. Cette thèse a donc pour principal objectif de décrire la dynamique de recolonisation d'assemblages de macrofaune à la suite d'une perturbation à petite échelle, induite au sein du champ hydrothermal Lucky Strike (1700 m de profondeur, dorsale médio-Atlantique). Pour cela, nous avons mis en place une expérimentation de défaunation *in situ* et suivi l'évolution de la composition et de la diversité de la faune ainsi que de la structure du réseau trophique au cours des deux années consécutives à la perturbation. Malgré un rapide retour de la richesse taxonomique et de la structure du réseau trophique, nos résultats ont mis en évidence un rétablissement incomplet des densités d'organismes et d'importantes modifications de la structure des communautés en comparaison aux assemblages de référence. Combinées aux facteurs environnementaux, les interactions biotiques semblent jouer un rôle majeur sur la colonisation et la succession écologique des assemblages étudiés. L'utilisation d'une approche expérimentale, couplée à l'analyse des traits reproducteurs des espèces dominantes, permet d'apporter des informations cruciales sur la capacité des communautés à maintenir leur structure et fonctions à la suite d'une perturbation, mais également de rendre compte de leur aptitude à disperser à grande échelle pour recoloniser des habitats impactés.

Title : Resilience of deep-sea hydrothermal vent communities: results of a disturbance experiment implemented on the Lucky Strike vent field (Mid-Atlantic ridge)

Keywords : Hydrothermal vent, disturbance, recovery, recolonisation dynamic, community structure, food-web, reproductive traits

Abstract: Hydrothermal ecosystems can be naturally subject to disturbances linked to tectonic and volcanic activities. Forty years after their discovery, we now have a fair knowledge of the factors structuring their biodiversity. However, our understanding of recolonisation dynamics is restricted and greatly limits our ability to predict their resilience in response to disturbances, whether natural or anthropogenic. With the increasing interest of mining companies for the exploitation of deep-sea minerals, it becomes urgent that we increase our efforts to better understand the mechanisms involved in the recovery of impacted communities. The main objective of this thesis is therefore to describe the recolonisation dynamics of macrofaunal assemblages following a small-scale disturbance induced within the Lucky Strike hydrothermal field (1700 m depth, Mid-Atlantic Ridge). We thus implemented an in situ defaunation experiment and monitored the composition, diversity as well as the food-web structure of vent communities during the two years following the disturbance. Despite a rapid return of the taxonomic richness and food-web structure, our results suggest an incomplete recovery of organism densities and significant changes in community structure compared to reference assemblages. In addition to environmental factors, biotic interactions appear to play a major role in the colonisation and ecological succession of the studied assemblages. The use of an experimental approach, coupled with reproductive trait analysis for the dominant species, provide crucial information on the ability of hydrothermal communities to maintain their overall structure and functions in face of a disturbance, and infer their dispersal abilities to recolonise impacted habitats.